U.PORTO

DOURORAMENTO

CIÊNCIAS BIOMÉDICAS

Study of Bioactive SecondaryMetabolites from the Marine Sponges and Marine Sponge-Associated Fungi

Chadaporn Prompanya

D

2018

U.PORTO

Chadaporn Prompanya. Study of Bioactive Secondary Metabolites from the Marine Sponges and Marine Sponge-Associated Fungi

Study of Bioactive Secondary Metabolites from the Marine Sponges and Marine Sponge-Associated Fungi
Chadaporn Prompanya

INSTITUTO DE CIÊNCIAS BIOMÉDICAS ABEL SALAZAR

D.ICBAS **2018**

CHADAPORN PROMPANYA

STUDY OF BIOACTIVE SECONDARY METABOLITES FROM THE MARINE SPONGES AND MARINE SPONGE-ASSOCIATED FUNGI

Thesis submitted to Instituto de Ciências Biomédicas Abel Salazar, Universidade do Porto to obtain the degree of Doctor in Biomedical Sciences.

Adviser - Dr. Anake Kijjoa
Category - Full Professor
Affiliation - Instituto de Ciências Biomédicas Abel Salazar da Universidade do Porto

Co-adviser - Dr. Madalena Maria de Magalhães Pinto
Category - Full Professor
Affiliation - Faculdade de Farmácia da Universidade do Porto

The experimental work of this thesis has been carried out in the Departamento de Química, Instituto de Ciências Biomédicas Abel Salazar (ICBAS) da Universidade do Porto. The candidate performed this work with the PhD's scholarship provided by Faculty of Pharmaceutical Sciences of Burapha University, Thailand. This work was partially supported through national funds provided by FCT/MCTES - Foundation for Science and Technology from the Minister of Science, Technology and Higher Education (PIDDAC) and European Regional Development Fund (ERDF) through the COMPETE – Programa Operacional Factores de Competitividade (POFC) programme, under the project PTDC/MAR-BIO/4694/2014 (reference POCI-01-0145-FEDER-016790; Project 3599 – Promover a Produção Científica e Desenvolvimento Tecnológico e a Constituição de Redes Temáticas (3599-PPCDT) in the framework of the programme PT2020 as well as by the project INNOVMAR - Innovation and Sustainability in the Management and Exploitation of Marine Resources (reference NORTE-01-0145-FEDER-000035, within Research Line NOVELMAR), supported by North Portugal Regional Operational Programme (NORTE 2020), under the PORTUGAL 2020 Partnership Agreement, through the European Regional Development Fund (ERDF).

STATUS THESIS

The results of the work of this thesis have been published, as original articles, in the following journals.

LIST OF PUBLICATIONS

1. **Prompanya, C.**, Dethoup, T., Bessa, L. J., Pinto, M. M., Gales, L., Costa, P. M., Silva, A. M., Kijjoa, A. (2014). New isocoumarin derivatives and meroterpenoids from the marine sponge-associated fungus *Aspergillus similanensis* sp. nov. KUFA 0013. *Mar. Drugs, 12*, 5160 – 5173. Doi:10.3390/md12105160

2. **Prompanya, C.**, Fernandes, C., Cravo, S., Pinto, M. M., Dethoup, T., Silva, A. M., Kijjoa, A. (2015). A new cyclic hexapeptide and a new isocoumarin derivative from the marine sponge-associated fungus *Aspergillus similanensis* KUFA 0013. *Mar. Drugs, 13*, 1432 – 1450. Doi:10.3390/md13031432

3. **Prompanya, C.**, Dethoup, T., Gales, L., Lee, M., Pereira, J. A., Silva, A. M., Pinto, M. M., Kijjoa, A. (2016). New polyketides and new benzoic acid derivatives from the marine sponge-associated fungus *Neosartorya quadricincta* KUFA 0081. *Mar. Drugs, 14*, 134 – 159. Doi:10.3390/md14070134

COMMUNICATIONS

Poster presentations

1. **Prompanya, C**., Keokitichai, S., Pinto, M., Kijjoa, A. Bromoindoles from *Iotrochota baculifera*. Trends in natural products research: young scientists meeting of PSE and ÖphG. University Centre Obergurgl/Tyrol, Austria, July 21-25, 2013.

2. **Prompanya, C**., Dethoup, T., Pinto, M., Kijjoa, A. Isocoumarins and cyclic hexapeptide from the sponge-associated fungus *Aspergillus similanensis* sp. nov. KUFA 0013. 9th European Conference on Marine Natural Products. The University of Strathclyde, Glasgow, Scotland, August 30 – September 2, 2015.

INDEX

Chapter III. Chemistry of the Fungi of the Genera *Aspergillus* and *Neosartorya*

Chapter IV. Results and Discussion

FIGURES INDEX

TABLES INDEX

SCHEMES INDEX

ACKNOWLEDGEMENTS

I would like to express my deepest gratitude to my adviser, Professor Dr. Anake Kijjoa who gave me the precious opportunity to pursue my doctoral study in Biomedical Sciences at the Instituto de Ciências Biomédicas Abel Salazar (ICBAS) of the University of Porto, for the continuous support, motivation, recommendation, immense knowledge and for his patience. Without his guidance, I surely could not succeed in doing research and writing this thesis. I am really proud to be a PhD student under his supervision.

Besides my adviser, I would also like to give my sincere appreciation to my co-adviser, Professor Dr. Madalena Maria de Magalhães Pinto of the Faculdade de Farmácia, Universidade do Porto, for her kindness and support.

I am thankful to Dr. Sumaitt Putchakarn, Bangsaen Institute of Marine Science, Burapha University, for collection and identification of the marine sponge, and also to Assistant Professor Dr. Tida Dethoup of the Department of Plant Pathology, Kasetsart University, Bangkok, Thailand, and to Dr. Jamrearn Buaruang of the Division of Environmental Science, Faculty of Science, Ramkhamhaeng University, Bangkok, Thailand, for collection of the marine animals, isolation, identification and culture of the marine-derived fungi, as well as for preparation of the extracts for my research work.

I am grateful to Professor Dr. Artur Manuel Soares Silva of the Departamento de Quimica, Universidade de Aveiro, for providing all the 1D and 2D NMR spectra, to Professor Dr. Luís Gales of Instituto de Ciências Biomédicas Abel Salazar (ICBAS), Universidade do Porto, for the X-ray crystallography analysis, to Dr. Michael Lee of the Department of Chemistry, Leicester University (UK), for providing High Resolution Mass spectra, to Professor Dr. Carla Sofia Garcia Fernandes of Faculdade de Farmácia, Universidade do Porto, for her guidance to make HPLC analyses of amino acids by chiral column and their interpretation, and to Professor Dr. José Augusto Caldeira Pereira of Instituto de Ciências Biomédicas Abel Salazar (ICBAS), Universidade do Porto, for performing and interpretation of molecular mechanics conformation analysis.

I would like to thank Professor Dr. Paulo Costa of Instituto de Ciências Biomédicas Abel Salazar (ICBAS), Universidade do Porto, and Dr. Lucinda Bessa of CIIMAR – Centro Interdisciplinar de Investigação Marinha e Ambiental, Universidade do Porto, for

antibacterial assay, to Professor Dr. Eugénia Pinto, Faculdade de Farmácia, /Universidade do Porto, for antifungal assay, and to Professor Dr. Madalena Pedro, Instituto Superior de Ciências da Saúde do Norte (CESPU), for cytotoxic activity assay.

My sincere thank goes to Mrs. Júlia Bessa, Ms. Sonia Pereira and Mrs. Isabel Silva not only for their technical assistance, but also for mental support and friendship, and to Ms. Sara Cravo for technical support of HPLC analysis of amino acids.

I also thank my lab mates, Dr. Suradet Buttachon, Dr. War War May Zin, Madalena Silva, Decha Kumla, Jidapa Noinart, Renato Pereira, Ângela Ferreira and Tin Shine Aung for helping me in TLC plate preparation, providing an unforgettable friendship and a good atmosphere of working. It was great sharing laboratory with all of you.

I would like to express my sincere appreciation to the former Dean, Associate Professor Dr. Sindhchai Keokitichai, and the current Dean, Associate Professor Dr. Ekarin Saifa, of the Faculty of Pharmaceutical Sciences, Burapha University, for the scholarship, and also to my colleagues and friends in Thailand, especially Associate Professor Dr. Mayuree Tantisira, Dr. Nuttinee Teerakulkittipong, Dr. Anusorn Thampithak, Dr. Naphatson Chanthathamrongsiri, and Dr. Thunchanok Sirirak, for all helps and supports during these years.

Finally, I would like to express my gratitude and love to my beloved parents, Mr. Manit and Mrs. Piyatida Prompanya, and my dear brother, Mr. Thanatad Prompanya, for all the love and supports.

ABSTRACT

This thesis describes isolation, structure elucidation and biological activity evaluation of secondary metabolites of the marine sponge ***Iotrochota baculifera***, collected from the Gulf of Thailand, as well as those produced by the cultures of the marine-derived fungi, ***Aspergillus similanensis* KUFA 0013**, isolated from the marine sponge *Rhabdermia* sp., and ***Neosartorya quadricincta* KUFA 0081**, isolated from the marine sponge *Clathria reinwardti*. The structures of the isolated compounds were established based on extensive analyses of their 1D and 2D NMR, High Resolution Mass and Infrared spectra. The absolute configurations of the chiral compounds were determined by X-ray crystallographic analysis for chevalone E (**348**), quadricinctone A (**381**), quadricinctapyran A (**382**), quadricinctone B (**386**), quadricinctone C (**387**), quadricinctafuran A (**388**) and quadricinctone D (**390**). In the case of the cyclohexapeptide, similanamide (**380**), the configurations of its amino acid constituents were determined by HPLC analysis of its hydrolysate by a Chirobiotic T column using the amino acid standards as controls.

From the ethyl acetate extract of the marine sponge *I. baculifera*, two previously described bromoindoles, 6-bromo-1*H*-indole-3-carbaldehyde (**40**) and methyl (2*E*)-3-(6-bromo-1*H*-indol-3-yl)-prop-2-enoate (**370**), were isolated.

The ethyl acetate extract of the culture of *A. similanensis* KUFA 0013 furnished three previously undescribed isocoumarin derivatives, similanpyrones A (**375**), B (**373**) and C (**376**), one previously undescribed chevalone derivative, chevalone E (**356**), two previously undescribed pyripyropene derivatives, pyripyropene S (**378**) and T (**379**), and one previously unreported cyclohexapeptide, similanamide (**380**), together with seven previously reported 6,8-dihydroxy-3-methylisocoumarin (**372**), reticulol (**374**), *p*-hydroxy-benzaldehyde (**371**), chevalones B (**348**) and C (**349**), S14-95 (**377**) and pyripyropene E (**154**). Compounds **154**, **357**, **373** – **376** and **378** – **380** were evaluated for their antimicrobial activity against reference strains of Gram-positive and Gram-negative bacteria and the multidrug-resistant isolates (MRS and VRE) from the environment as well as *Candida albicans* ATCC 10231. None of the tested compounds exhibited any activity at the highest concentration tested (256 µg/mL). Furthermore, these compounds

were also evaluated for their synergistic capacity with antibiotics against the multidrug-resistant isolates from the environment. However, only chevalone E (**356**) was found to show synergism with oxacillin against methicillin resistant *Staphylococcus aureus* (MRSA). In addition, pyripyropene T (**379**) and similanamide (**380**) were tested for their *in vitro* growth inhibitory activity against MCF-7 (breast adenocarcinoma), NCI-H460 (non-small cell lung cancer) and A373 (melanoma) cancer cell lines. Only similanamide (**380**) showed weak activity against the three tested cell lines.

From the ethyl acetate extract of the culture of *N. quadricincta* KUFA 0081, two previously undescribed pentaketides, quadricinctones A (**381**) and C (**387**), and seven previously unreported benzoic acid derivatives, quadricinctapyrans A (**382**) and B (**383**), quadricinctoxepine (**384**), quadricinctones B (**386**) and D (**390**), and quadricinctofurans A (**389**) and B (**389**), were isolated, together with the previously reported 6-hydroxy-2,2-dimethyl-2,3-dihydro-4*H*-chromen-4-one (**385**). The isolated compounds were evaluated for their antibacterial activity against reference strains of Gram-positive and Gram-negative bacteria and the multidrug-resistant isolates from the environment, and antifungal activity against reference strains of yeast, filamentous fungi and dermatophyte, as well as the *in vitro* growth inhibitory activity against the MCF-7, NCI-H460 and A375-C5 cancer cell lines by the protein binding dye SRB method, however none of the tested compounds were active in all these assays.

Keywords: *Iotrochota baculifera; Aspergillus similanensis* KUFA 0013; *Neosartorya quadricincta* KUFA 0081; bromoindoles; similanpyrones; isocoumarins; pyripyropenes; chevalones; cyclic hexapeptide; similanamide; pentaketides; benzoic acid derivatives

RESUMO

Nesta tese é descrito o isolamento, a elucidação estrutural e a avaliação da atividade biológica de metabolitos secundários da esponja marinha ***Iotrochota baculifera***, coletada no Golfo da Tailândia, e também produzidos por culturas dos fungos marinhos ***Aspergillus similanensis* KUFA 0013**, isolado da esponja marinha *Rhabdermia* sp., e ***Neosartorya quadricincta* KUFA 0081**, isolado da esponja marinha *Clathria reinwardti*. As estruturas dos compostos isolados foram estabelecidas por análise de espectros de RMN (1D e 2D), massa de alta resolução e espectrometria no infravermelho. A configuração absoluta dos compostos quirais foi determinada por cristalografia de raios X para chevalona E (**348**), quadricinctona A (**381**), quadricinctapirano A (**382**), quadricinctona B (**386**), quadricinctona C (**387**), quadricinctafurano A (**388**) e quadricinctona D (**390**). No caso do ciclo-hexapeptideo similanamida (**380**), as configurações dos aminoácidos constituintes foram determinadas por análise cromatográfica (HPLC) do respetivo hidrolisado, usando uma coluna Chirobiotic T e aminoácidos padrão como controlo.

Do extrato de acetato de etilo da esponja marinha *I. baculifera*, foram isolados dois bromoindolos já descritos, 6-bromo-1*H*-indole-3-carbaldeído (**40**) e metil-(2*E*)-3-(6-bromo-1*H*-indole-3-il)-prop-2-enoato (**370**).

O extrato de acetato de etilo da cultura de *A. similanensis* KUFA 0013 forneceu três derivados isocumarínicos já descritos, similanpironas A (**375**), B (**373**) e C (**376**), um derivado já descrito de chevalona, chevalona E (**356**), dois derivados não descritos de pyripyropeno, o pyripyropenos S (**378**) e o T (**379**), e um derivado ciclo-hexapeptideo não descrito, similanamida (**380**), juntamente com sete outros compostos já descritos, 6,8-di-hidroxi-3-metillisocumarina (**372**), reticulol (**374**), *p*-hidroxibenzaldeído (**371**), chevalonas B (**348**) e C (**349**), S14-95 (**377**) e pyripyropeno E (**154**). Os compostos **154**, **357**, **373**-**376** e **378**- **380** foram avaliados para atividade antimicrobiana em estipes de referência de bactérias de Gram-positivo e de Gram-negativo e isolados resistentes a múltiplos fármacos (SRM and ERV) de ambiente, assim como *Candida albicans* ATCC 10231. Nenhum dos compostos testados exibiu atividade mesmo a alta concentração (256 µg/mL). Estes compostos foram também avaliados para capacidade sinergista com

antibióticos contra isolados resistentes a múltiplos fármacos de ambiente. Somente chevalona E (**356**) manifestou sinergismo com oxacilina contra *Staphylococcus aureus* resistentes à meticilina (SARM).

Adicionalmente pyripyropeno T (**379**) e similanamida (**380**) foram testados *in vitro* para avaliação da atividade inibidora do crescimento das linhas celulares tumorais MCF-7 (adenocarcinoma da mama), NCI-H460 (cancro do pulmão de células não pequenas) e A373 (melanoma).Somente similanamida (**380**) mostrou fraca atividade contra estas linhas celulares.

Do extrato de acetato de etilo da cultura de *N. quadricincta* KUFA 0081, foram isolados dois pentacetideos ainda não descritos, quadricinctonas A (**381**) e C (**387**), sete derivados do ácido benzóico ainda não descritos, quadricinctapiranos A (**382**) e B (**383**), quadricinctoxepina (**384**), quadricinctonas B (**386**) e D (**390**) equadricinctofuranos A (**389**) and B (**389**), e a já descrita 6-hidroxi-2,2-dimetil-2,3-di-hidro-4*H*-chromen-4-ona (**385**).

Os compostos isolados foram avaliados para atividade antibacteriana em estipes de referência de bactérias de Gram-positivo e de Gram-negativo e isolados resistentes a múltiplos fármacos de ambiente e também atividade antifúngica contra estirpes de referência de leveduras, fungos filamentosos e dermatófitos, assim como para avaliação da atividade inibidora do crescimento da linhas celulares tumorais MCF-7, NCI-H460 e A373, pelo método de SRB. Nenhum dos compostos testados manifestou atividade.

Palavras-chave: *Iotrochota baculifera; Aspergillus similanensis* KUFA 0013; *Neosartorya quadricincta* KUFA 0081; bromoindolos; similanpironas; isocumarínicos; pyripyropenos; chevalonas; cyclo-hexapeptideo; pentacetideos; derivados do ácido benzóico

LIST OF ABBREVIATIONS AND SYMBOLS

$[^3H]$EBOB	$[^3H]$ Ethynylbicycloorthobenzoate
$[M+H]^+$	Pseudo-molecular ion (Positive ion mode)
$[\alpha]^{20}_D$	Specific optical rotation at 20 °C for D (sodium) line
®	Register or Trademark
°C	Degree Celsius
^{13}C NMR	Carbon-13 Nuclear Magnetic Resonance
^{1}H NMR	Proton Nuclear Magnetic Resonance
Å	Angstrom
A2780	Human ovarian carcinoma cell line
A375-C5	Human melanoma cell line
A549	Human lung carcinoma cell line
Ac	Acetyl
ADC	Antibody drug conjugate
AMP	Ampicillin
amu	Atomic mass unit
Ara-A	Arabino furanosyladenine
Ara-C	Arabinosyl cytosine
ASCT	Autologous stem cell transplant
ATCC	American Type Culture Collection
ATP	Adenosine triphosphate
B.C.	Before Christ
B16F10	Mouse melanoma cell line
BCMA	B-cell maturation antigen
BEL-7402	Human hepatocellular carcinoma cell line
BGC-823	Human gastric cancer cell line
brd	Broad doublet
brs	Broad singlet
CAM	Chick Chorioallantoic Membrane
cAMP	Cyclic adenosine monophosphate

CCDC	Cambridge Crystallographic Data Centre
CD	Cluster of differentiation
CD4	Cluster of differentiation 4
CDK2	Cyclin-dependent kinase-2
CFU	Colony-forming unit
CIP	Ciprofloxacin
CLSI	The Clinical and Laboratory Standards Institute
cm	Centimeter
c-Met	Tyrosine-protein kinase Met
CoA	Coenzyme A
COSY	Correlated spectroscopy
CRPC	Castration-resistant prostate cancer
CTX	Cefotaxime
d	Doublet
dd	Double doublet
ddd	Double double doublet
DEPT	Distortionless Enhancement by Polarization Transfer
dL	Deciliter
DLBCL	Diffuse large B-cell lymphoma
DMAPP	Dimethylallyl diphosphate
DMSO	Dimethyl sulfoxide
DMSO-d_6	Deuterated dimethyl sulfoxide
DMXBA	3-(2,4-Dimethoxybenzylidene)-Anabaseine
DNA	Deoxyribonucleic acid
DPPH	2,2-Diphenylpicrylhydrazyl
DU145	Human prostate cancer cell line
E	Erythromycin
e.g.	For example
EC_{50}	Half maximal effective concentration
ECACC	European Collection of Authenticated Cell Cultures
ED_{100}	One hundred percent effective dose

ED_{50}	Median effective dose
EGFR	Epidermal growth factor receptor
EMBRACE	Efficacy and Safety of Belimumab in Black Race Patients with Systemic Lupus Erythematosus
ENPP3	Ectonucleotide pyrophosphatase/phosphodiesterase family member 3
et al.	And others
ET	Ecteinascidin
EtOAc	Ethyl acetate
EtOH	Ethanol
FBS	Fetal bovine serum
FDA	Food and Drug Administration
FIC	Fractional inhibitory concentration
Fr	Fraction
g	Gram
GABA	Gamma-aminobutyric acid
GCC	Guanylyl cyclase C
GC-MS	Gas chromatography – mass spectrometry
GI_{50}	Half maximal growth inhibitory concentration
GluPY	Glucose-peptone-yeast extract
GPNMB	Glycoprotein nonmetastatic melanoma protein b
h	Hour
H1299	Human non-small cell lung cancer cell line
hCMEC/D3	Human brain microvascular endothelial cell line
HCT-116	Human colon cancer cell line
HCT-8	Human colon cancer cell line
HEK293	Human embryonic kidney cancer cell line
HeLa	Human cervical cancer cell line
HepG2	Human hepatocellular carcinoma cell line
HIV-1	Human immunodeficiency virus type-1
HL-60	Human promyelocytic leukemia cell line

HMBC	Heteronuclear Multiple Bond Correlation
hNFAP	Heterologous *Neosartorya ficheri* antimicrobial protein
HPLC	High-performance liquid chromatography
HRESIMS	High-resolution electrospray ionization mass spectrometry
Hs683	Human glioblastoma cell line
HSQC	Heteronuclear Single Quantum Coherence
HuCCA-1	Human lung cholangiocarcinoma cell line
HUVEC	Human umbilical vein endothelial cell
Hz	Hertz
I.D.	Inside diameter
IC_{50}	Half maximal inhibitory concentration
IL-2	Interleukin 2
IL-8	Interleukin 8
Inc.	Incorporation
IPP	Isopentenyl pyrophosphate
IR	Infrared
IT	Intrathecal
ITS	Internal Transcribed Spacer
J	Coupling constant in Hz
JNK	c-Jun N-terminal protein kinase
K562	Human chronic myeloid leukemia cell line
KB	Human nasopharyngeal epidermoid cell line
Ki	The inhibitor constant
L	Liter
L1210	Mouse lymphocytic leukemia cell line
L5178Y	Mouse lymphoma cell line
LCK	Lymphocyte-specific protein tyrosine kinase
LC-MS	Liquid chromatography – mass spectrometry
LIV-1	Zinc transporter SLC39A6
LRRC15	Leucine-rich repeat-containing protein 15
LY6E	Lymphocyte antigen 6 complex, Locus E

m	Meter
m	Multiplet
m/z	Mass per charge
MA	Massachusetts
MAGI	HeLa CD4+ HIV-1 LTR-β-gal cell
MCF-7	Human breast adenocarcinoma cell line
MD	Maryland
MDA-MB-231	Human breast adenocarcinoma cell line
Me_2CO	Acetone
MEA	Malt Extract Agar
MeOH	Methanol
MetAP2	Methionine aminopeptidase-2
mg	Milligram
MH	Mueller-Hinton agar
MHB	Mueller-Hinton broth
MHz	Mega hertz
Mia PaCa-2	Human pancreas cancer cell
MIC	Minimum inhibitory concentration
min	Minute
mL	Milliliter
mm	Millimeter
MM418c5	Human melanoma cell line
MMAE	Monomethyl auristatin E
MMAF	Monomethyl auristatin F
mmol	Millimole
MO	Missouri
MOLT-3	Human acute lymphoblastic leukemia cell line
mp	Melting point in °C
MRSA	Methicillin-resistant *Staphylococcus aureus*
MSS31	Mouse spleen stromal cell
MTT	3-(4,5-Dimethylthiazol-2-yl)-2,5-diphenyltetrazolium bromide

N	Normality
NA	Not available
NADH	Reduced Nicotinamide adenine dinucleotide
NaPi2b	Sodium-dependent phosphate transport protein 2b
NCI	National Cancer Institute
NCI-H187	Human small cell lung cancer cell line
NCI-H460	Human non-small cell lung cancer cell line
NFAP	*Neosartorya fishceri* antifungal protein
NFRD	NADH-fumarate reductase
ng	Nanogram
NJ	New Jersey
NK-1	Neurokinin 1
NKT cell	Natural killer T cell
nm	Nanometer
NMR	Nuclear Magnetic Resonance
NOESY	Nuclear Overhauser Effect Spectroscopy
NSCLC	Human non-small cell lung cancer cell line
NSCLC-N6L16	Human non-small cell lung cancer cell line
OAc	Acetoxy
OE21	Human esophageal cancer cell line
ORTEP	Oak Ridge Thermal Ellipsoid Plot
OX	Oxacillin
P388	Murine leukemia cell line
PANC-1	Human pancreas ductal adenocarcinoma cell line
PC12	Rat pheochromocytoma cell line
PC-3	Human prostate cancer cell line
PDA	Potato Dextrose Agar
PLK1	Serine/threonine-protein kinase-1
ppm	Part per million
PSMA	Prostate-specific membrane antigen
Rac1	Ras-related C3 botulinum toxin substrate 1

RAW264.7	Mouse macrophage cell line
RNA	Ribonucleic acid
s	Singlet
S	Streptomycin
SAB	Sabouraud dextrose agar
SAM	S-Adenosyl methionine
SCCHN	Squamous cell carcinoma of the head and neck
SCLC	Small cell lung cancer
SEM	Standard error of the mean
Sfr	Sub-fraction
SGC-7901	Human gastric cancer cell
SK-MEL-28	Human melanoma cell line
SLITRK6	SLIT and NTRK-like protein 6
SMMC-7721	Human hepatoma cell line
sp.	Species
SRB	Sulforhodamine B
SW1990	Human pancreatic cancer cell line
t	Triplet
T47D	Human breast cancer cell line
TLC	Thin Layer Chromatography
TMV	Tobacco mosaic virus
U-373 MG	Human astrocytoma cell line
UK	United Kingdom
USA	United States of America
UV	Ultraviolet
UV/VIS	Ultraviolet – visible spectroscopy
VA	Vancomycin
VEGF	Vascular endothelial growth factor
VRE	Vancomycin-resistant enterococci
WE-1990	Human pancreatic cancer cell line
WI-38	Normal human lung fibroblast cell

XDE	Xanthocillin dimethylether
XTE	Methoxy-xanthocillin dimethylether
δ	Chemical shift value in ppm
ΔFIC	FIC index
λ	Wavelength
µg	Microgram
µL	Microliter
µM	Micromolar
ε	Molar absorptivity (molar extinction coefficient)

CHAPTER I

INTRODUCTION

1.1) General Introduction

Nature is the source of the pharmaceuticals for treatment many human diseases since ancient time. The discovery of clay tablets revealed that plants have been used as medicines in Mesopotamia since 2400 B.C. Initially, apothecaries have been used medicinal plants in a form of crude extracts, then it was developed to partially purified natural products, and later, to single molecule drugs. Until the late 1980s, the improvement of technologies and techniques moved the focus of drug discovery from nature to chemical synthesis in the laboratory. However, nature is still the valuable source of lead compounds for drug development due to the high diversity of organisms. This is reflected by the number of approved drugs derived from nature. From 1981 to 2010, there were 1,135 approved drugs, and 50 % of these drugs were from natural product origin (David *et al*., 2015). The examples of well-known drugs which derived from nature are penicillin G (**1**), an antibiotic isolated from fungus *Penicillium notatum*; paclitaxel (**2**), a drug for treatment breast cancer obtained from the bark of *Taxus brevifolia*; the last example is cytarabine or ara-C (**3**) (Figure 1), an anticancer drug which was modified from the C-nucleoside isolated from marine sponge *Cryptotethya crypta* (Jaspars *et al*., 2016).

1.2) Marine Organisms as a Treasure Source of New Compounds

Not only terrestrial organisms can produce bioactive chemicals that provide the lead compounds in drug discovery process, but marine organisms are also the rich source of bioactive compounds. About 70 % of the earth's surface is the ocean. The biodiversity of the marine environment is high; thus, the ocean became an interesting source for drug discovery. However, there were only a few studies about marine organisms before 1970 due to low technology in that time. Since the SCUBA diving technologies and deep-sea vehicles (e.g., submarine) were improved, the discovery of marine organisms was raised. Moreover, the laboratory techniques were also developed, leading to the discovery and evaluation of the huge number of marine-derived secondary metabolites (Gerwick & Fenner, 2013; David *et al*., 2015).

The secondary metabolites obtained from marine organisms have unique chemical structures and high bioactivities compared to the secondary metabolites derived from terrestrial source (Hu *et al.,* 2015). These are because the extreme conditions under the sea, including temperature, pressure, nutrients, light, salinity and competition (Hasan *et al*., 2015; Jaspars *et al*., 2016).

Hundreds of new marine-derived compounds are reported every year. The report from Hu *et al.* (2015) showed that from 1985 to 2005, the number of new compounds reported annually was less than 600 compounds, but since 2006 the number were increased to more than 800 compounds, and more than 1,000 compounds in 2008 to 2012, as shown in Figure 2. The total number of new marine-derived compounds which were reported from 1985 to 2012 is 16,616 compounds. Among these compounds, 4,196 compounds (25.25 %) are bioactive compounds.

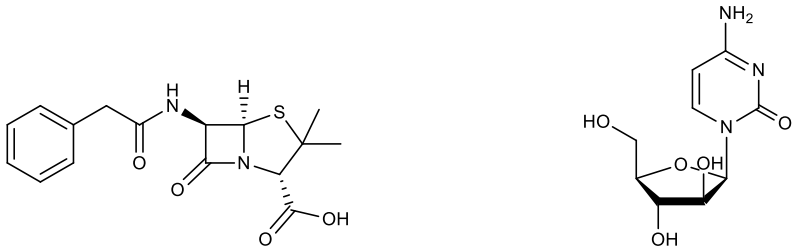

1

3

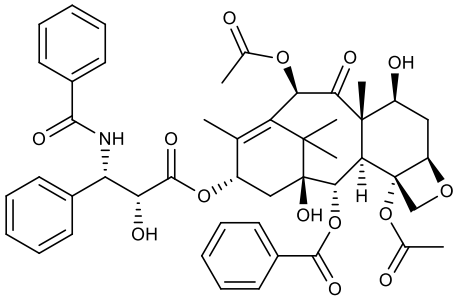

2

Figure 1. Structures of penicillin G (**1**), paclitaxel (**2**) and cytarabine (**3**).

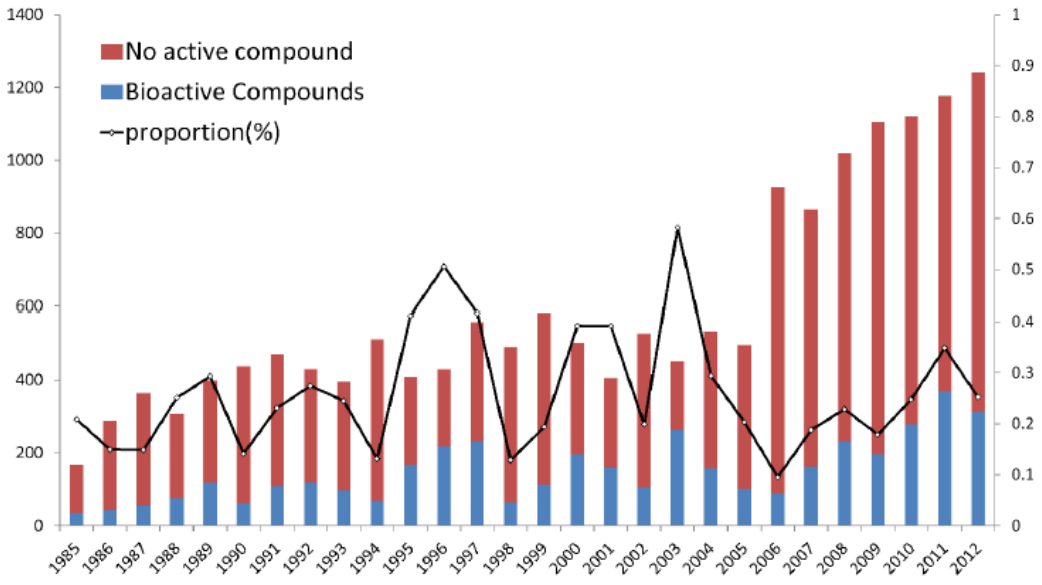

Figure 2. Variation in number of new marine natural products for 1985 – 2012 (Hu *et al*., 2015).

The new compounds were divided into eight categories by chemical structure, including alkaloids, terpenes, ethers and ketals, steroids, lactones, hydroxybenzene and quinones, peptides, and others. As shown in Figure 3, the highest number of new compounds belongs to terpenes, followed by alkaloids, but the highest proportion of bioactive compounds is peptides with 40.85 %, followed by lactones, alkaloids, and hydroxybenzene and quinones with 32.61, 31.49 and 31.36 %, respectively. The major bioactivity of these new compounds is anticancer activity (2,225 compounds; 56 % of the total bioactive compounds), followed by antibacterial activity (521 compounds; 13%) (Hu *et al*., 2015).

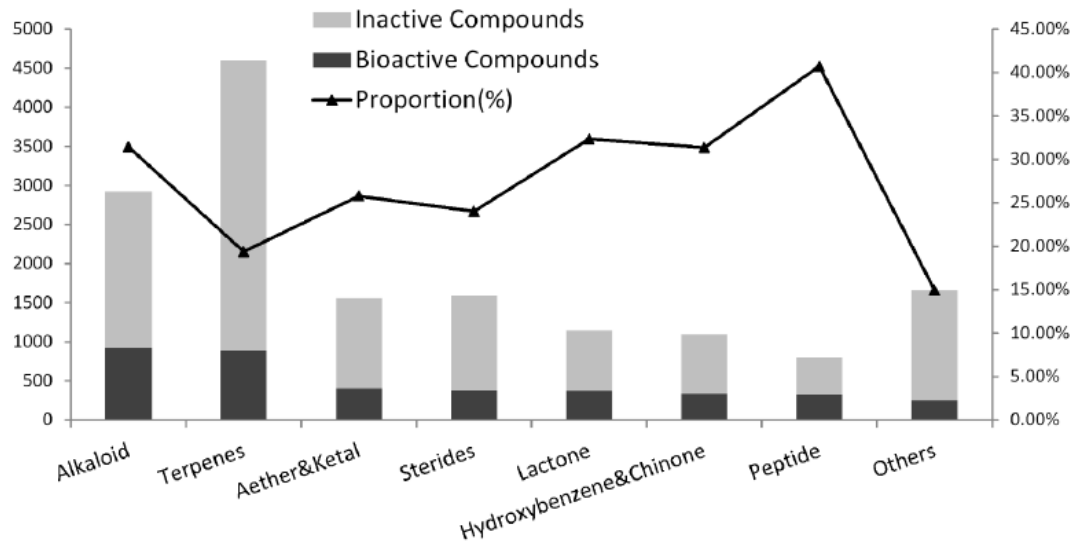

Figure 3. The quantity and proportion of bioactive compounds in each category of chemical compounds (Hu *et al.,* 2015).

1.3) Marine Sponges are a Potential Source of Novel Compounds

Marine invertebrates, mainly sponges, tunicates, bryozoans and mollusks provided the majority of marine natural products. Among these organisms, sponges (phylum Porifera) have been recognized as a rich source of novel compounds for drug discovery and development (Laport *et al*., 2009 and Mehbub *et al*., 2014; Hu *et al*., 2015). In the early 1950s, the nucleosides spongothymidine (**4**) and spongouridine (**5**) were discovered, and the first marine-derived anticancer drug, cytarabine (ara-C; **3**), and antiviral drug used against *Herpes simplex*, vidarabine (ara-A; **6**) (Figure 4), were developed from these nucleosides. Since then, the bioactive compounds from sponges became interesting (Laport *et al*., 2009). Till now, more than 5,300 metabolites have been isolated from marine sponges, and more than 200 compounds are being discovery each year (Agrawal *et al*., 2016). Metabolites isolated from marine sponges showed many interesting biological activities such as anticancer, antimicrobial and anti-inflammatory activities, as shown in Table 1 (Laport *et al*., 2009 and Sipkema *et al*., 2005).

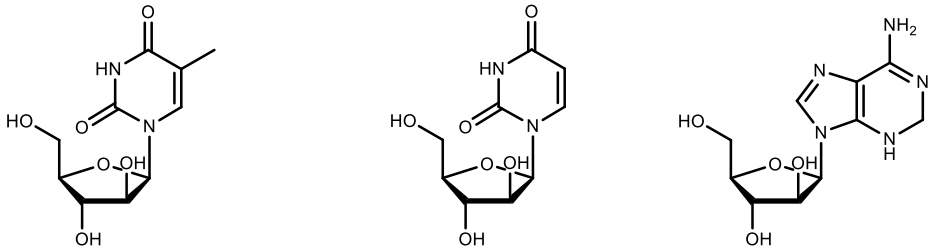

4 **5** **6**

Figure 4. Structures of spongothymidine (**4**), spongouridine (**5**) and vidarabine (**6**).

Table 1. Examples of secondary metabolites derived from sponges with different bioactivities.

Compound	Compound class	Mode of action	Species	References
Anticancer activity				
BRS1	Diamino-dihydroxy polyunsaturated lipid	Protein kinase C inhibitor	Calcareous sponge	Sipkema *et al,* 2005
Adociasulfates	Triterpenoid hydroquinones	Kinesin motor protein inhibitors	*Haliclona (aka Adocia)* sp.	
Discodermolide	Linear tetraene lactone	Stabilization of microtubules	*Discodermia dissolute*	
Spongistatin 1	Bis(spiroacetal) macrolide	Tubulin polymerization inhibitor	*Spongia* sp.	
Latrunculin A	Thiazole macrolide	Actin-depolymerization	*Latrunculia magnifica*	
Neoamphimedine	Pyridoacridine alkaloid	Topoisomerase II inhibitor	*Xestospongia* cf *carbonaria*	
Namine D	Imidazole alkaloid	Nitic oxide synthetase inhibitor	*Leucetta* cf *chagosensis*	
Agelasphin (KRN7000)	α-Galactosylceramide	NKT cell activator	*Agelas mauritianus*	
Salicylihalamide A	Salicylate macrolide	v-ATPase inhibitor	*Haliclona* sp.	

6-Hydroximino-4-en-3-one steroids	Oximated steroid	Aromatase inhibitor	*Cinachyrella* sp.	
Crambescidins 1-4	Pentacyclic guanidine derivatives	Ca^{2+} channel blocker	*Crambe crambe*	

Antimicrobial activity

Discodermins B, C and D	Cyclic peptides	Antibacterial	*Discodermia kiiensis*	Laport *et al*., 2009
Acanthosterol I and J	Sulfated sterols	Antifungal	*Acanthodendrilla* sp.	
Axinellamines B-D	Imidazo-azoloimidazole alkaloids	Antibacterial	*Axinella* sp.	
Spongistatin	Polyether macrolide lactone	Antifungal	*Hyrtios erecta*	Sipkema *et al*., 2005

Antiviral activity

Dragmacidin F	Indole alkaloid	Antiviral	*Halicortex* sp.	Laport *et al*., 2009
Papuamides C and D	Cyclic peptide	Antiviral (HIV-1)	*Theonella mirabilis*	
Haplosamates A and B	Sulfamated steroids	Antiviral (HIV-1 integrase inhibitor)	*Xestospongia* sp.	Sipkema *et al*., 2005
Hamigeran B	Phenolic macrolide	Antiviral (herpes and polio)	*Hamigera tarangaensis*	Laport *et al*., 2009
2-5A	2',5' linked oligonucleotide	Interferon mediator	Many sponges	Sipkema *et al*., 2005

Anti-inflammatory activity

Manoalide	Cyclohexane sesterterpenoid	Phospholipase A_2 inhibitor	*Luffariella variabilis*	Sipkema *et al*., 2005
Spongidines A-D	Pyridinium alkaloids	Phospholipase A_2 inhibitor	*Spongia* sp.	
Jaspaquinol	Diterpene benzenoid	Lipoxygenase inhibitor	*Jaspis splendens*	

Subersic acid	Diterpene benzenoid	Lipoxygenase inhibitor	*Suberea* sp.	

Immunosuppressive activity

Simplexides	Glycolipids	Inhibitor of T-cell proliferation	*Plakortis simplex*	Sipkema *et al*., 2005
Polyoxygenated sterols	Sterols	IL-8 inhibitor	*Dysidea* sp.	
Contignasterol	Oxygenated sterol	Histamine release inhibitor	*Petrosia contignata*	
Pateamine A	Thiazole macrolide	IL-2 inhibitor	*Mycale* sp.	

1.4) Marine Microbes are the True Treasure Source of Secondary Metabolites

At initial studies of marine organisms, researchers were focusing on macroorganisms such as sponges, tunicates and mollusks. Later, there has been a perception that the isolated secondary metabolites might be produced by the symbiotic or associated microorganisms, and this hypothesis are supported in several cases by experimental and circumstantial evidences.

Zhang *et al.* (2005) reported marine natural products in clinical trial, which revealed that sponges are an important source of bioactive compounds. However, investigation of the microbes isolated from sponges and other marine invertebrates revealed that they produced the same compounds as their host animals.

Gerwick and Fenner (2013) reported the data of marine-derived agents in the preclinical or clinical trial. At that time, there were nine approved drugs and twelve compounds in clinical trial. These twenty-one agents were isolated from different marine sources, majority from mollusks and sponges. However, these compounds were also reported from symbiotic or associated microorganisms.

In addition, Schofield *et al*. (2015) have been recently confirmed that ecteinascidin 743 (ET-743) or trabectedin (**7**) (Figure 5), an anticancer drug which was isolated from the tunicate *Ecteinascidia turbinata*, was truly produced by

bacteria *Candidatus* Endoecteinascidia frumentensis, by sequencing and assembling the genome of this bacterium.

These data support the hypothesis that the original producer of many marine secondary metabolites might be the associated microbes in marine invertebrates because of the same chemicals were found from both marine sources.

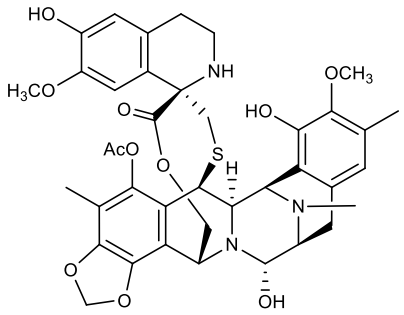

7

Figure 5. Structure of trabectedin (**7**).

1.5) Marine Pharmaceuticals: Approved Drugs and a Current Pipeline Perspective

1.5.1) FDA-approved drugs

To date, there are seven drugs which have been approved by the Food and Drug Administration (FDA) (Table 2). Among them, four drugs are anticancer (Mayer *et al*., 2010). The indication of the marine-derived drugs, which will be discussed in the next section, reveal that they have potential activity to treat patients in severe state or patients who failed with the prior treatment.

The proportion of approved drugs from marine source is higher than another source. The current rate is seven approved drugs from 28,175 discovered molecular entities, e.g. one drug per 4,025 natural products described. Thus, it is approximately 1.2 to 2.5 – fold higher than the average (one in 5,000 – 10,000 tested compounds) (Jaspars *et al*., 2016).

Table 2. The marine-derived compounds which have been approved by FDA for treatment human diseases (http://marinepharmacology.midwestern.edu/clinPipeline.htm).

Compound name	Trademark (approved year)	Marine organism origin	Chemical class	Molecular target	Disease Area
Cytarabine (Ara-C)	Cytosar-U® (1969)	Sponge	Nucleoside	DNA polymerase	Cancer: Leukemia
Vidarabin (Ara-A)	Vira-A® (1976)	Sponge	Nucleoside	Viral DNA polymerase	Antiviral: Herpes simplex virus
Omega-3-acid ethyl esters	Lovaza® (2004)	Fish	Omega-3 fatty acids	Triglyceride-synthesizing enzymes	Hypertriglyceridemia
Ziconotide	Prialt® (2004)	Cone snail	Peptide	DNA polymerase	Pain: severe chronic pain
Trabectedin	Yondelis® (2005)	Tunicate	Alkaloid	Minor groove of DNA	Cancer: soft tissue sarcoma and ovarian cancer
Eribulin mesylate	Halaven® (2010)	Sponge	Macrolide	Microtubules	Cancer: metastatic breast cancer
Brentuximab vedotin	Adcetris® (2011)	Mollusk/ cyano-bacterium	ADC (MMAE)	CD30 & microtubules	Cancer: anaplastic large T-cell systemic malignant lymphoma and Hodgkin's disease

Approved marine-derived drugs

Cytarabine (Ara-C; Cytosar-U®)

Cytarabine (arabinosyl cytosine; cytosine arabinoside; ara-C; **3**) is a synthetic analogue of spongothymidine (**4**), a nucleoside originally isolated from the Caribbean sponge *Cryptotethya crypta* (Jaspars *et al*., 2016; Mayer *et al*., 2010). The FDA has approved cytarabine to be used with other drugs for treatment of patients with acute lymphoblastic leukemia, acute myeloid leukemia and chronic myelogenous leukemia, and to be used alone to prevent and treat patients with meningeal leukemia (https://www.cancer.gov/about-cancer/treatment/drugs/cytarabine).

Vidarabine (Ara-A; Vira-A®)

Vidarabine (**6**) (arabinofuranosyl adenine or adenine arabinoside, Ara-A) is a synthetic purine nucleoside analogue of spongouridine (**5**), a nucleoside originally isolated from the Caribbean sponge *Tethya crypta*. Currently, this compound was obtained from fermentation cultures of the bacterium *Streptomyces antibioticus.* Vidarabine has been approved by the FDA for treatment of Herpes simplex virus infection (Jaspars *et al*., 2016; Mayer *et al*., 2010).

Omega-3-acid ethyl esters (Lovasa®)

Omega-3-acid ethyl esters are marine products obtained from fish oils, typically from oily fish such as mackerel and anchovy. The FDA approved Lovaza® on October 11, 2004, as a lipid-regulating agent to reduce triglyceride levels in adult patients with severe (≥500 mg/dL) hypertriglyceridemia (Jaspars *et al*., 2016; http://www.accessdata.fda.gov/drugsatfda_docs/label/2014/021654s041lbl.pdf).

Ziconotide (Prialt®)

Ziconotide (**8**) (Figure 6) is a synthetic *N*-type calcium-channel blocker equivalent of conotoxin from the Magician's cone snail, *Conus magus.* The FDA has approved ziconotide intrathecal (IT) infusion for management of intractable patients with severe chronic pain who neither respond to nor tolerate other treatment (Jaspars *et al*., 2016).

Trabectedin (Yondelis®)

Trabectedin (**7**) (Figure 5) is a tetrahydroisoquinoline alkaloid, which was isolated from the tunicate *Ecteinascidia turbinata* found in the Caribbean and Mediterranean Sea (Mayer *et al*., 2010). On October 23, 2015, the FDA approved trabectedin for the treatment of patients with unresectable or metastatic liposarcoma or leiomyosarcoma who have already been treated with anthracycline-based chemotherapy (https://www.cancer.gov/news-events/cancer-currents-blog/2015/fda-trabectedin-sarcoma and www.yondelis.com).

Eribulin mesylate (Halaven®)

A pharmacophore of halichondrin B (**9**), a polyether metabolite isolated from the Japanese sea sponge *Halichondria okadai,* obtained synthetically gave rise to eribulin (**10**) (Figure 6) (McBride & Butler, 2012; Jaspars *et al*., 2016). Due to the results from the phase III clinical trial called EMBRACE, which revealed that eribulin improved survival of women with metastatic breast cancer, the FDA approved this drug, on November 15, 2010, for treatment of patients with metastatic breast cancer after at least two treatment regimens with an anthracycline and a taxane (https://www.cancer.gov/about-cancer/treatment/drugs/fda-eribulinmesylate).

Brentuximab vedotin (Adcetris®)

Brentuximab vedotin (**11**) (Figure 6) is an anti-CD30 antibody conjugated via a protease-cleavable linker to the potent anti-microtubule agent monomethyl auristatin E (MMAE) (van de Donk & Dhimolea, 2012). This drug was approved by the FDA on August 19, 2011, for treatment of patients with Hodgkin lymphoma after autologous stem cell transplant (ASCT) failure or after failure of at least two prior multi-agent chemotherapy regiments in patients who are not candidates for ASCT and patients with systemic anaplastic large cell lymphoma after failure of at least one prior multi-agent chemotherapy regimen (https://www.cancer.gov/about-cancer/treatment/drugs/fda-brentuximabvedotin).

1.5.2) Current Marine Pharmaceutical Clinical Pipeline

Currently, there are twenty-four marine-derived compounds in clinical development (phase I to phase III clinical trials), twenty-one as anti-cancer agents, one for neovascular disease, one for chronic pain and one for schizophrenia and Alzheimer's disease, as shown in Table 3 (Mayer *et al*., 2010; http://marinepharmacology.midwestern.edu/clinPipeline.htm).

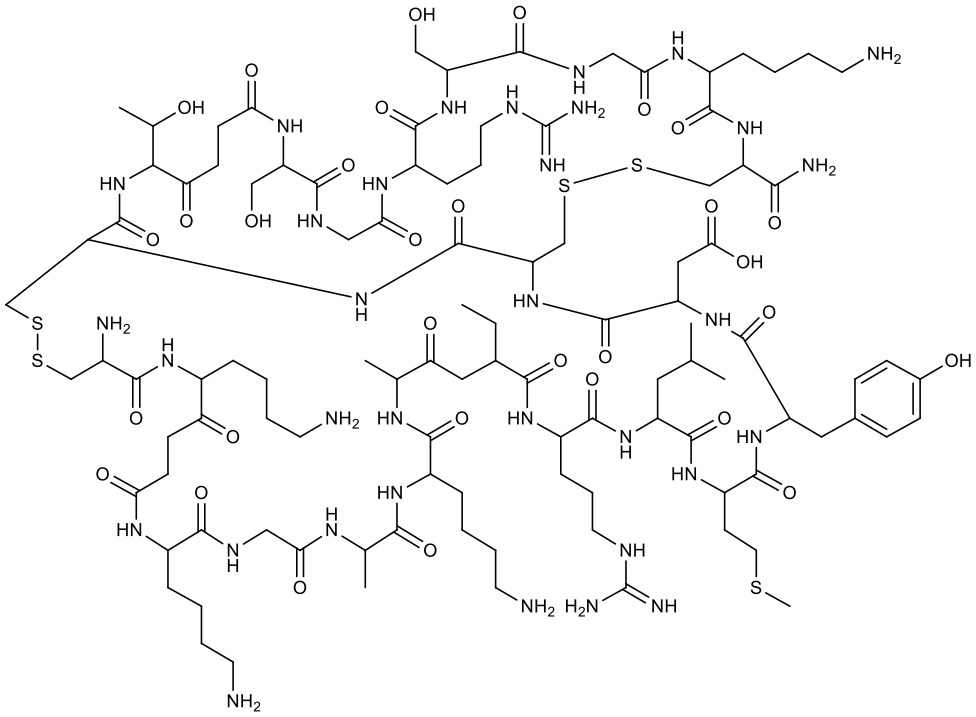

8

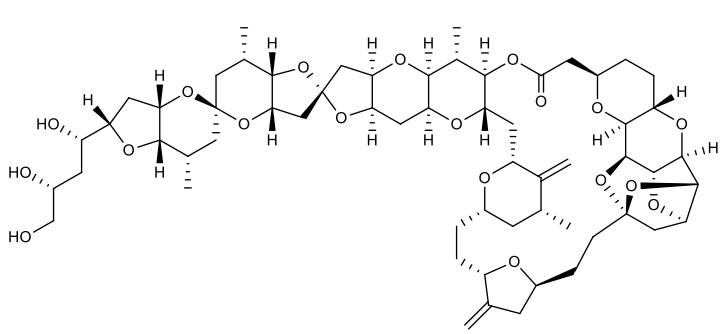

9

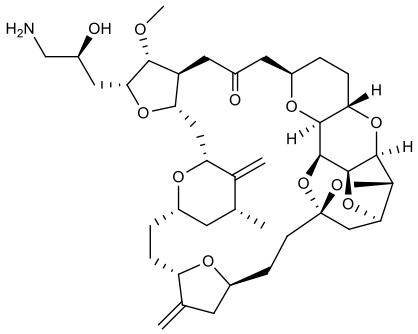

10

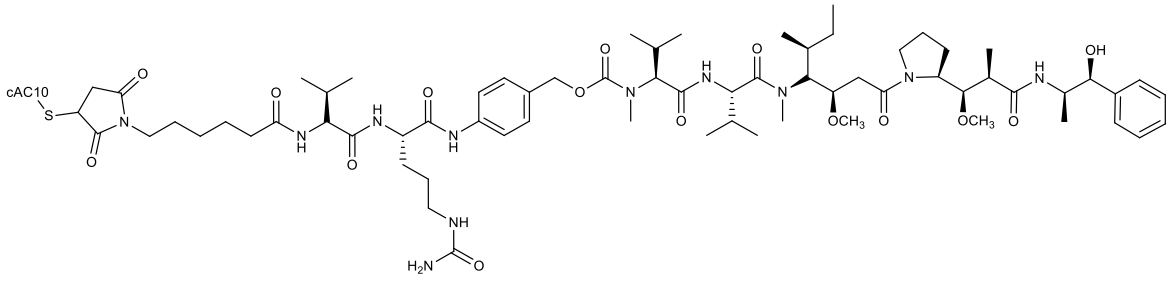

11

Figure 6. Amino acid sequence of ziconotide (**8**), and structures of halichondrin B (**9**), eribulin (**10**) and brentuximab vedotin (**11**).

Table 3. The marine-derived compounds in a current pipeline perspective.

Clinical status	Compound name	Marine organism	Chemical class	Molecular target	Disease area	Company/ Institution
Phase III	Plinabulin (NPI-2358)	Fungus *Aspergillus* sp. (Singh *et al*., 2011)	Diketopiperazine	Microtubules	Cancer: NSCLC, brain tumor	BeyondSpring Pharmaceuticals
	Plitidepsin	Tunicate *Aplidium albicans* (Alonso-Álvarez *et al*., 2017)	Depsipeptide	Rac1 & JNK activation	Cancer: multiple myeloma, leukemia, lymphoma	Pharmamar
	Squalamine lactate (OHR-102)	Dogfish shark *Squalus acanthias* (Moore *et al*., 1993)	Aminosterol	Growth factors of neovascularization	Neovascular disease: macular degeneration	Ohr Pharmaceutical Inc.
	Tetrodotoxin	Pufferfish family Tetradontidae (Lago *et al*., 2015)	Guanidinium alkaloid	Sodium channel	Pain: chronic pain	Wex Pharmaceutical Inc.
	Glembatumumab vendotin (CDX-011)	Mollusk/cyanobacterium	ADC (MMAE)	GPNMB & microtubules	Cancer: metastatic breast cancer, melanoma, triple negative breast cancer	Celldex Therapeutics
	Lurbinectedin (PM01183)	Tunicate *Ecteinascidia turbinata* (Romano *et al*., 2013)	Alkaloid	RAN polymerase II	Cancer: ovarian cancer, breast cancer, SCLC	Pharmamar

Phase II	Depatuxizumab mafodotin (ABT-414)	Mollusk/cyanobacterium	ADC (MMAF)	EGFR & microtubules	Cancer: glioblastoma, pediatric brain tumors	AbbVie
	GTS-21 (DMXBA)	Worms of Phylum Nemertiea (Kem *et al*., 2006)	Alkaloid	α7 nicotinic acetylcholine receptor	Schizophrenia, Alzheimer disease, attention deficit hyperactivity disorder, endotoxemia, sepsis, vagal activity	
	Denintuzumab mafodotin (SGN-CD19A)	Mollusk/cyanobacterium	ADC (MMAF)	CD19 & microtubules	Cancer: relapsed/refractory and frontline DLBCL	Seattle Genetics
	AGS-16C3F	Mollusk/cyanobacterium	ADC (MMAF)	ENPP3 & microtubules	Cancer: renal cell carcinoma	Agensys & Astellas Pharma
	Polatuzumab vendotin (DCDS-4501A)	Mollusk/cyanobacterium	ADC (MMAE)	CD19b & microtubules	Cancer: non-Hodgkin lymphoma, chronic lymphocytic leukemia, lymphoma, B-cell lymphoma, follicular	Genentech/Roche
	PM060184	Sponge *Lithoplocamia lithistoides* (Martín *et al.,* 2013)	Polyketide	Minor groove of DNA	Cancer: solid tumors	Pharmamar

	Tisotumab vendotin	Mollusk/cyanobacterium	ADC (MMAE)	Tissue factor & microtubules	Cancer: Ovary cancer, cervix cancer, endometrium cancer, bladder cancer, prostate cancer (CRPC), cancer of head and neck (SCCHN), esophargus cancer, lung cancer (NSCLC)	GenMab
	Enfortumab vendotin (ASG-22ME)	Mollusk/cyanobacterium	ADC (MMAE)	Nectin-4 & microtubules	Cancer: tumors; medical oncology; neoplasm; metastatic urothelial cancer	Seattle Genetics
Phase I	GSK2857916	Mollusk/cyanobacterium	ADC (MMAF)	BCMA	Cancer: multiple myeloma	GlaxoSmithKline
	ABBV-085	Mollusk/cyanobacterium	ADC (MMAE)	LRRC15	Cancer: solid tumors	Abbvie
	ABBV-399	Mollusk/cyanobacterium	ADC (MMAE)	c-Met	Cancer: solid tumors	Abbvie
	ABBV-221	Mollusk/cyanobacterium	ADC (MMAE)	EGFR & microtubules	Caner: solid tumors	Abbvie
	ASG-67E	Mollusk/cyanobacterium	ADC (MMAE)	CD37 & microtubules	Cancer: refractory lymphoid malignancy;	Agensys & Astellas Pharma

					relapsed lymphoid malignancy	
	ASG-15ME	Mollusk/cyanobacterium	ADC (MMAE)	SLITRK6 & microtubules	Cancer: metastatic urothelial cancer	Seattle Genetics
	Bryostatin	Bryozoan *Bugula neritina* (Manning *et al*., 2005)	Macrolide lactone	Protein kinase C	Cancer: melanoma, renal cell cancer, lymphoma, pancreatic cancer, fallopian tube cancer, gastric cancer, prostate cancer kidney cancer, lung cancer	Neurotrope BioScience
	Marizomib (Salinosporamide A; NPI-0052)	Bacterium *Salinispora tropica* (Kale *et al*.,, 2011)	Beta-lactone-gamma lactam	20S proteasome	Cancer: NSCLC, pancreatic cancer, melanoma, lymphoma, multiple myeloma	Triphase
	SGN-LIV1A	Mollusk/cyanobacterium	ADC (MMAE)	LIV-1 & microtubules	Cancer: breast cancer	Seattle Genetics

1.6) Aim and Scope of the Study

The aim of this study is to investigate the secondary metabolites of the marine sponge *Iotrochota baculifera,* collected from the Gulf of Thailand, as well as the secondary metabolites produced by the cultures of the marine sponge-associated fungi, *Aspergillus similanensis* KUFA 0013, isolated the marine sponge *Rhabdermia* sp., and *Neosartorya quadricincta* KUFA 0081, isolated from the marine sponge *Clathria reinwardti.*

1.6.1) Isolation and Chemical Investigation of Selected Sponge and Fungal Strains

In order to isolate the secondary metabolites, the crude extracts of the marine sponge and of the cultures of the sponge-associated fungi were fractionated by column chromatography. The fractions were further isolated and purified by various chromatographic techniques and also by crystallization. The structures of the isolated compounds were elucidated by 1D and 2D NMR, IR and HRMS. In case that the compounds were obtained as suitable crystals, the X-ray crystallography were used to determine the absolute configuration of the stereogenic carbons otherwise the molecular mechanics conformation analysis or chiral HPLC were used.

1.6.2) Biological Evaluation of the Isolated Compounds

The isolated compounds were evaluated for their biological activities by various bioassays. Antibacterial and antifungal activities were evaluated by a broth microdilution technique. While antibacterial assay was performed using Gram-positive and Gram-negative bacteria and the multidrug-resistant isolates from the environment, antifungal assay was performed using yeast, filamentous fungus and dermatophyte. In order to evaluate the *in vitro* growth inhibitory activity, the compounds were tested against three human cancer cell lines by SRB method

CHAPTER II

CHEMISTRY OF THE MARINE SPONGES OF THE GENUS *IOTROCHOTA*

2.1) The Marine Sponges of the Genus *Iotrochota*

Sponges are one of marine invertebrates in the oldest metazoan group which still exist on the planet. There are about 5,000 to 10,000 species reported and most of them are found in the Oceans. Sponges belong to the Phylum Porifera which are divided into 3 major classes: Demospongiae, Hexactineliida and Calcarea (Van Soest *et al*., 2012), based on the morphological characteristics of their spicule and texture.

The marine sponges of the genus *Iotrochota* belong to the class Demospongiae, subclass Heteroscleromorpha, order Poecilosclerida and family Iotrochotidae. There are several reports on chemical constituents from members of this genus, including *I. baculifera, I. birotulata, I. purpurea* and some unidentified species. Herein, the chemical constituents and their biological activities are reviewed covering the period of 1981 to 2016.

2.1.1) *Iotrochota baculifera*

Iotroridoside-B (**12**), a glycosphingolipid, together with **sphingolipid** (**13**) and a four-component mixture of **sphingolipid homologues** (**14a – d**) (Figure 7) were isolated from the sponge *Iotrochota baculifera*, collected from the coast near Tuticorin, India. In order to determine the length of the fatty acid and spingosine chains of **14**, methanolysis was carried out. From the NMR, HPLC and GC-MS data, **14** was a mixture of spingolipids containing 1,3,4-trihydroxy-2-docosanoylamino-nonadecane (**14a**), 1,3,4-trihydroxy-2-docosanoylamino-eicosane (**14b**), 1,3,4-trihydroxy-2-docosanoylamino-heneicosane (**14c**) and 1,3,4-trihydroxy-2-docosanoylamino-docosane (**14d**). Compounds **14a** and **14c** were reported as new metabolites while **14b** and **14d** were previously reported (Muralidhar *et al*., 2003).

Baculiferins A – **O** (**16** – **30**), the DOPA-derived pyrrole alkaloids, and two alkaloids, **purpurone** (**15**) and **ningalin A** (**31**) (Figure 7), were isolated from the marine sponge *I. baculifera* which was collected from the coral reef at Hainan Island, China. All isolated compounds were evaluated for their antitumor activity against HCT-8, BEL-7402,

BGC-823, A549 and A2780 human cancer cell lines, and anti-HIV-1 IIIB activity. Compounds **22**, **28** and **30** showed moderate inhibitory activity against the tested cell lines, whereas other compounds were only weakly active. Compounds **18**, **20 – 23**, **26 – 29** exhibited potent inhibitory activity against the HIV-1 IIIB virus in both, MT4 and MAGI cells (Fan *et al*., 2010).

2.1.2) *Iotrochota birotulata*

A ecdysteroid, named **2β,3β,14α,20β-tetrahydroxy-22α-(2-hydroxyacetiloxy)-5β-colest-7-en-6-one** (**32**), together with **ponasterone A** (**33**), **(2β,3β,5β,22*R*)-2,3,14,20,24-pentahydroxy-6-oxocholest-7-pen-22-yl-glycolate** (**34**)**, (2β,3β,5β,-22*R*)-2,3,14,20,24-pentahydroxy-6-oxocholest-7-pen-22-yl-acetate** (**35**) and **ecdysterone** (**36**) (Figure 8), were isolated from the Caribbean sponge *I. birotulata,* collected from the coast of Little San Salvador Island (Costantino *et al*., 2000).

The tyrosine derivative **1,3-dibromo-5-(2-[(*p*-hydroxyphenyl)-acetamido] ethyl)-2-[3-(methyl-2-butenamido)propoxy] benzene** (**37**) and **β-sitosterol** (**38**) (Figure 8) were isolated from the marine sponge *I. birotulata*, collected from the coast of Port Royal, Jamaica. The hexane, dichloromethane and methanol crude extracts of *I. Birotulata* were evaluated for their insecticidal activity against *Cylas formicarius elegantulus*. The hexane and dichloromethane extracts exhibited 100% mortality at concentration of 2 µg/mL after 72 hours whereas the methanol extract was inactive (Thompson & Gallimore, 2016).

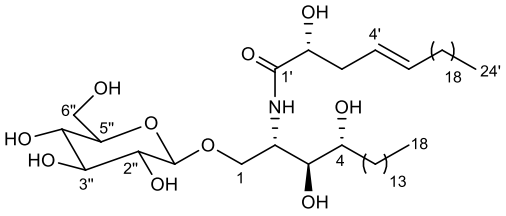

12

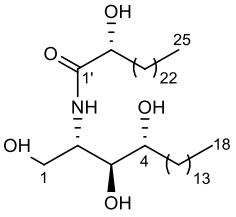

13

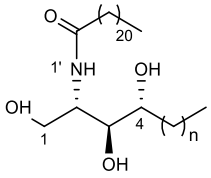

14a, n = 14; **14b**, n = 15;
14c, n = 16; **14d**, n = 17

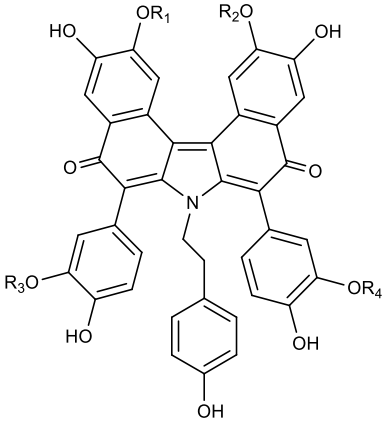

15 $R_1 = R_2 = R_3 = R_4 = H$
16 $R_1 = SO_3H$, $R_2 = R_3 = R_4 = H$
17 $R_3 = SO_3H$, $R_1 = R_2 = R_4 = H$
18 $R_3 = R_4 = SO_3H$, $R_1 = R_2 = H$
19 $R_1 = R_2 = SO_3H$, $R_3 = R_4 = H$
20 $R_1 = R_3 = SO_3H$, $R_2 = R_4 = H$
21 $R_1 = R_4 = SO_3H$, $R_2 = R_3 = H$
22 $R_1 = R_3 = R_4 = SO_3H$, $R_2 = H$
23 $R_1 = R_2 = R_3 = SO_3H$, $R_4 = H$

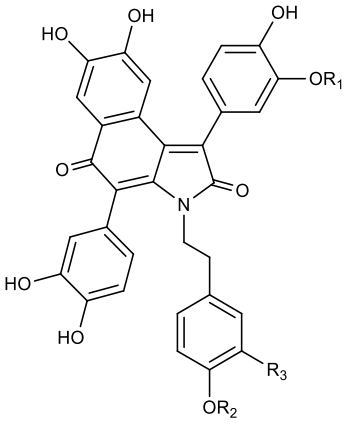

24 $R_1 = SO_3H$, $R_2 = R_3 = H$
25 $R_1 = R_3 = H$, $R_2 = SO_3H$
26 $R_1 = R_2 = R_3 = H$

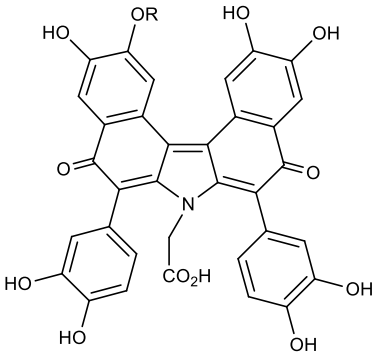

27 R = H
28 R = SO_3H

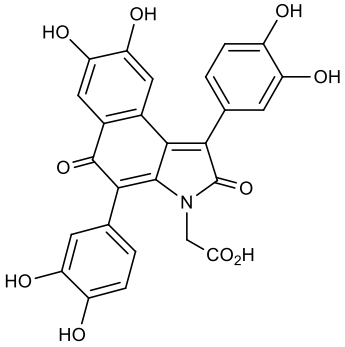

29

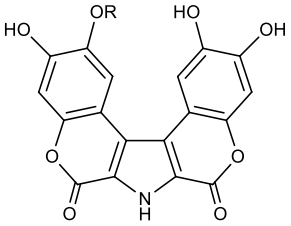

30 R = SO_3H
31 R = H

Figure 7. Structures of iotroridoside-B (**12**), sphingolipid (**13**), sphingolipid homologues (**14a** – **d**), purpurone (**15**), baculiferins A – O (**16** – **30**) and ningalin A (**31**).

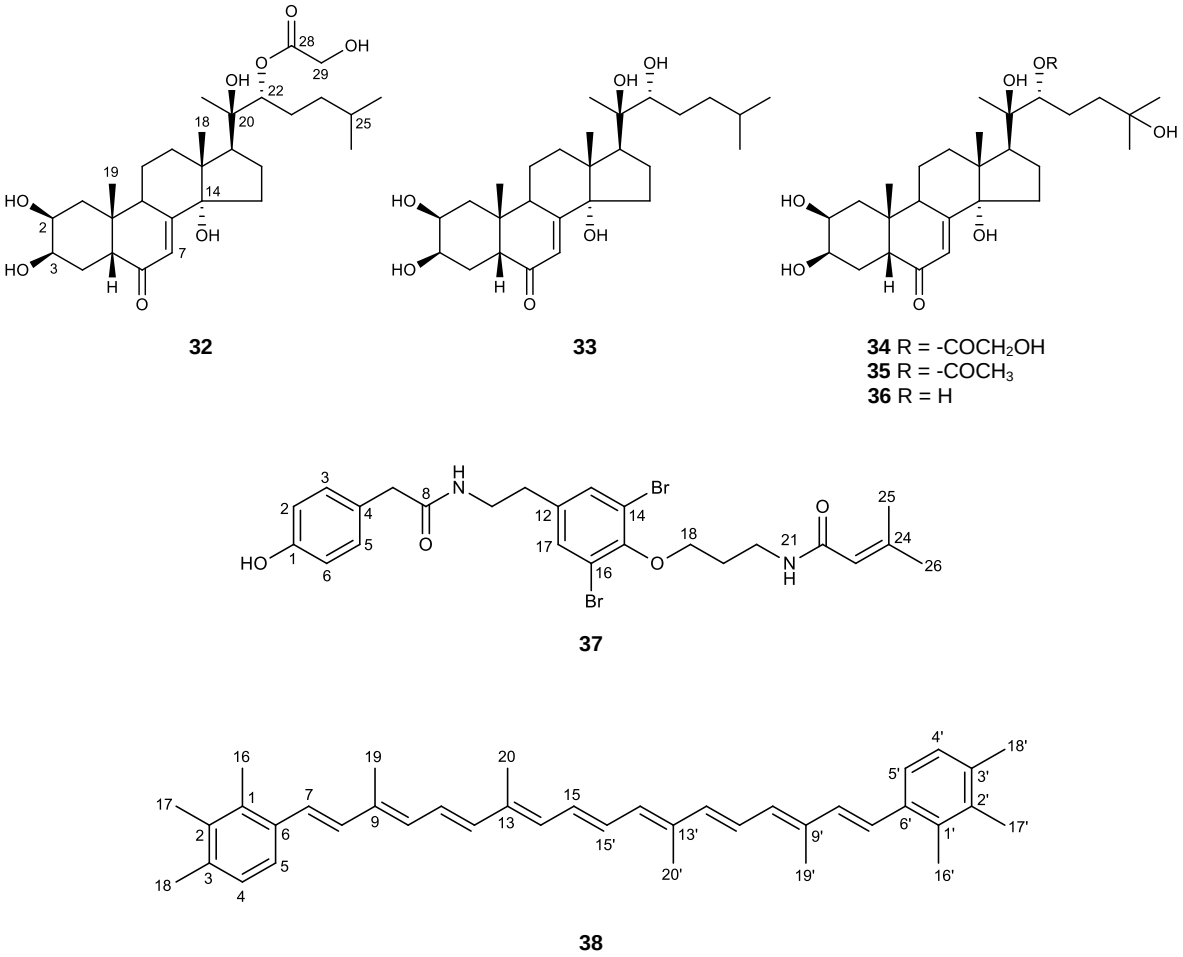

32 **33** **34** R = -$COCH_2OH$; **35** R = -$COCH_3$; **36** R = H

37

38

Figure 8. Structures of 2β,3β,14α,20β-tetrahydroxy-22α-(2-hydroxyacetyloxy)-5β-colest-7-en-6-one (**32**), ponasterone A (**33**), (2β,3β,5β,22*R*)-2,3,14,20,24-pentahydroxy-6-oxocholest-7-pen-22-yl-glycolate (**34**), (2β,3β,5β,22*R*)-2,3,14,20,24-pentahydroxy-6-oxocholest-7-pen-22-yl-acetate (**35**), ecdysterone (**36**), 1,3-dibromo-5-(2-[(*p*-hydroxyphenyl)acetamido]ethyl)-2-[3-(methyl-2-butenamido)propoxyl]benzene (**37**) and β-sitosterol (**38**).

2.1.3) *Iotrochota purpurea*

A bromine-containing oxindole alkaloid, named **matemone** (**39**) was isolated along with **6-bromoindole-3-carbaldehyde** (**40**) (Figure 9), from the Indian Ocean sponge *I. purpurea,* collected from the Matemo Island. Compound **39** was evaluated for its antimicrobial activity against *Staphylococcus aureus* (IPC 53146) and *Candida albicans* (IPC 1283) by the paper-disk agar diffusion method. At 50, 100 and 200 µg/disk

concentrations, **39** weakly inhibited the growth of *S. aureus* with inhibitory zones of 7, 9 and 11 mm, respectively while it was inactive against *C. albicans* at the highest concentration tested (200 µg/disk). It also exhibited a mild cytotoxicity against NSCLC-N6 L16, Mia PaCa-2 and Du145 cancer cell lines, and sea urchin egg with IC_{50} values of 30, 24, 27 and 35 µg/mL, respectively. DNA intercalant assay, using HPLC analysis, showed significant binding ability of DNA (40-50%; ethidium bromide (control), 100%) (Carletti *et al*., 2000).

Two brominated tyrosine derivatives, **itampolins A** (**41**) and **B** (**42**) (Figure 9), were isolated from the marine sponge *I. purpurea* which was collected from Itampolo, Madagascar (Sorek *et al*., 2006).

Two ceramides, named **iotrochotamide I** (**43**) and **iotrochotamide II** (**44**), were isolated from the Indonesian sponge *I. purpurea*, together with three 6-bromoindoles, including **6-bromo-1*H*-indole-3-carbaldehyde** (**40**), **6-bromo-1*H*-indole-3-carboxylic acid methyl ester** (**45**) and **6-bromo-1*H*-indole-3-carboxylic acid ethyl ester** (**46**) (Figure 9) (Ibrahim *et al*., 2009).

Ten halogenated alkaloids, **purpuroines A – J** (**47** – **56**), together with the previously described ***O*-methyl-*N*-trimethyl-3,5-dibromotyrosine** (**57**) (Figure 9), were isolated from the marine sponge *I. purpurea*, collected from the inner coral reef in Sanya Bay, Hainan Island, China. Compounds **47** – **50**, **53** – **55** and **57** were tested for their antimicrobial activity against human disease-related bacteria (*Staphylococcus aureus, S. pneumoniae, Escherichia coli* and *Pseudomonas aeruginosa*) and fungi (*Candida albicans, Saccharomyces cerevisiae, Aspergillus fumigatus*, *A. flavus* and *Fusarium oxysporum*). Compounds **47** and **49** selectively inhibited the growth of *A. fumigatus* with IC_{50} values of 28.58 ± 0.52 and 26.07 ± 0.55 mg/mL, respectively, while **50** exhibited inhibitory activity against *A. fumigatus* and *C. albicans* with IC_{50} values of 25.56 ± 0.44 and 19.03 ± 0.12 mg/mL, respectively. Compound **55** inhibited the growth of *S. pneumoniae* with IC_{50} value of 18.06 ± 0.76 mg/mL. Furthermore, **47** – **50**, **52** – **55** and **57** were selected for kinase-targeted bioassay. Compound **50** showed potent inhibition

against lymphocyte-specific protein tyrosine kinase (LCK) and serine/threonine-protein kinase-1 (PLK1) with IC_{50} values of 0.94 and 1.45 µg/mL, respectively. Compound **47** selectively inhibited LCK with IC_{50} value of 2.35 µg/mL. Compounds **49**, **52** and **54** exhibited moderate inhibition against LCK and PLK1 with IC_{50} values less than 8.0 µg/mL. Moreover, all tested compounds weakly inhibited cyclin-dependent kinase-2 (CDK2) (Shen *et al*., 2012).

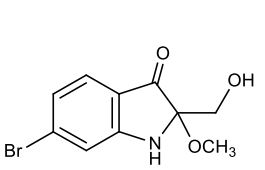

39

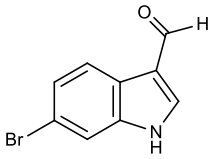

40

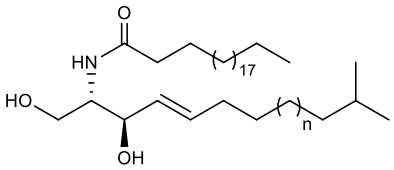

43 n = 10
44 n = 14

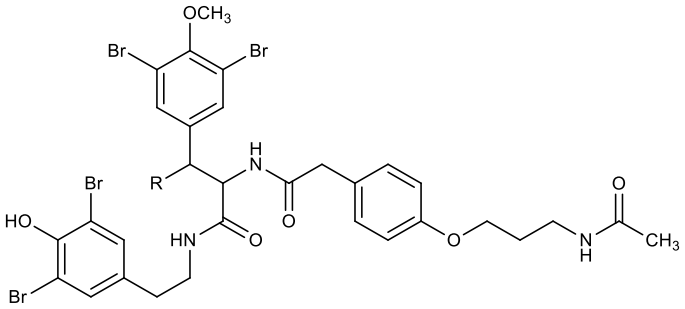

41 R = H
42 R = OH

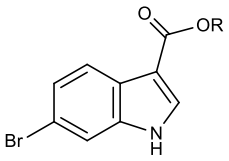

45 R = CH_3
46 R = CH_2CH_3

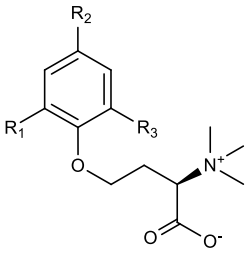

47 $R_1 = R_2 = R_3 = Br$
48 $R_1 = R_2 = Br$, $R_3 = H$
49 $R_1 = R_3 = Cl$, $R_2 = Br$
50 $R_1 = R_2 = Br$, $R_3 = I$
51 $R_1 = R_2 = Br$, $R_3 = Cl$

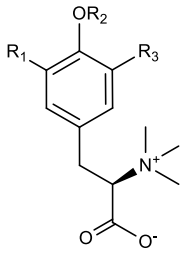

52 $R_1 = R_3 = I$, $R_2 = CH_3$
53 $R_1 = R_3 = I$, $R_2 = H$
54 $R_1 = Br$, $R_2 = CH_3$, $R_3 = I$
55 $R_1 = Br$, $R_2 = H$, $R_3 = I$
56 $R_1 = R_3 = Br$, $R_2 = CH_3$

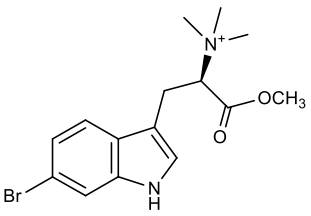

57

Figure 9. Structures of matemone (**39**), 6-bromoindole-3-carbaldehyde (**40**), itampolins A (**41**) and B (**42**), iotrochotamide I (**43**), iotrochotamide II (**44**), 6-bromo-1*H*-indole-3-carboxylic acid methyl ester (**45**), 6-bromo-1*H*-indole-3-carboxylic acid ethyl ester (**46**), purpuroines A-J (**47**-**56**) and *O*-methyl-*N*-trimethyl-3,5-dibromotyrosine (**57**).

2.1.4) *Iotrochota* sp.

A bromoindole, named **methyl (*E*)-3-(6-bromoindol-3-yl)prop-2-enoate** (**58**) (Figure 10), was isolated from a marine sponge *Iotrochota* sp. Its structure was assigned on the basis of spectroscopic analysis, and then confirmed by synthesis (Dellar *et al*., 1981).

Two cinnamoyl amino acids, **iotrochamides A** (**59**) and **B** (**60**) (Figure 10), were isolated from the CH_2Cl_2/MeOH extract of the Australian marine sponge *Iotrochota* sp., collected from Curacao Island, Queensland. The isolated compounds were evaluated for their cytotoxicity against *Trypanosoma brucei brucei* and HEK293 human cancer cell line. Compounds **59** and **60** moderately inhibited the growth of *T. b. brucei* with IC_{50} values of 4.7 ± 2.5 and 3.4 ± 1.9 µM, respectively, while exhibited 85 ± 14% the growth inhibition of HEK293 cell at 50 µM and 100 ± 0% at 70 µM, respectively. The results revealed that both compounds exhibited selectively moderate inhibition against *T. b. brucei* (Feng *et al*., 2012).

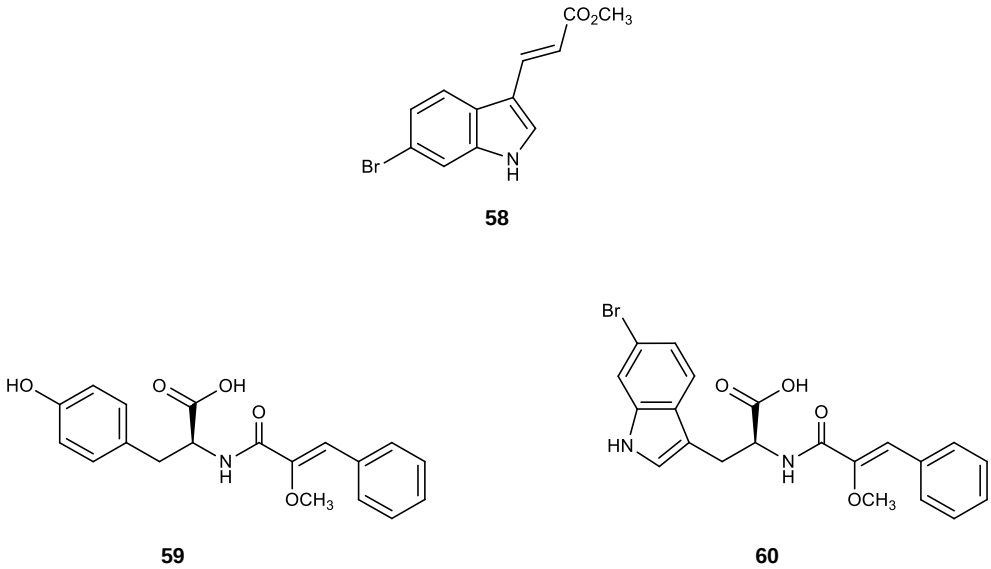

Figure 10. Structures of methyl (*E*)-3-(6-bromoindol-3-yl)prop-2-enoate (**58**) and iotrochamides A (**59**) and B (**60**).

CHAPTER III

CHEMISTRY OF THE FUNGI OF THE GENERA *ASPERGILLUS* AND *NEOSARTORYA*

3.1) The Fungi of the Genus *Aspergillus*

3.1.1) *Aspergillus aculeatus*

Aspergillusol A (**61**), a tyrosine-derived metabolite, together with **4-hydroxyphenylpyruvic acid oxime** (**62**) and **secalonic acid A** (**63**) (Figure 11), were isolated from the fungus *Aspergillus aculeatus* CRI323-04 which was isolated from the marine sponge *Xestospongia testudinaria,* collected from Phi Phi Islands, Thailand. Compound **61** exhibited α-glucosidase inhibitory activity toward α-glucosidases from *Saccharomyces cerevisiae* and *Bacillus stearothermophilus* with IC_{50} values of 465 ± 2 and 1060 ± 20 μM, respectively. Moreover, **61** also exhibited weak cytotoxicity with IC_{50} values of 50, 74 and 19 μM, against HuCCA-1, A549 and MOLT-3 human cancer cell lines, respectively, while it did not show any activity toward HepG2 cancer cell line at the concentration of 105 μM (Ingavat *et al*., 2009).

Later on, Ingavat *et al*. (2011) isolated a sesquiterpenoid, **Asperaculin A** (**64**) (Figure 11), from the same fungus. Compound **64** was evaluated for its cytotoxicity against four human cancer cell lines: HepG2, MOLT-3, A549 and HuCCA-1. Compound **64** was inactive at the highest concentration tested (50 μg/mL) (Ingavat *et al*., 2011).

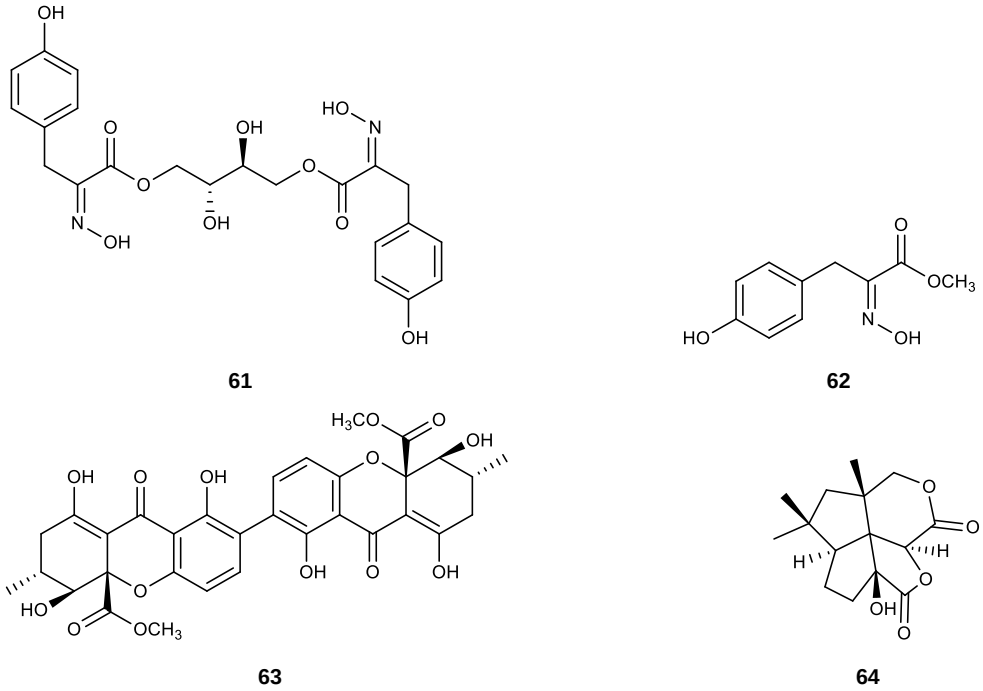

Figure 11. Structures of aspergillusol A (**61**), 4-hydroxyphenylpyruvic acid oxime (**62**), secalonic acid A (**63**) and asperaculin A (**64**).

3.1.2) *Aspergillus clavatus*

Two coumarin derivatives, **4,4'-dimethoxy-5,5'-dimethyl-7,7'-oxydicoumarin** (**65**) and **7-(γ,γ-dimethylallyloxy)-5-methoxy-4-methylcoumarin** (**66**), a chromone derivative, **(*S*)-5-hydroxy-2,6-dimethyl-4*H*-furo[3,4-g]benzopyran-4,8(6*H*)-dione** (**69**) and a bicoumarin, **24-hydroxylergosta-4,6,8(14),22-tetraen-3-one** (**70**), together with two previously described **kotanin** (**67**) and **orlandin** (**68**) (Figure 12), were isolated from the marine-derived fungus *Aspergillus clavatus* R7 which was isolated from a mangrove tree *Myoporum bontioides,* collected from China. The isolated compounds were evaluated for their antifungal activity against three plant pathogens: *Fusarium oxysporum, Colletotrichum musae* and *Penicillium italicum,* using the broth dilution method. All tested compounds exhibited antifungal activity against these three fungal strains, except for **66** which was inactive against *P. italicum*. Compound **70** showed the most potent activity

towards three fungal strains with MIC values of 44.73, 195.79 and 61.18 μM, respectively (Li *et al*., 2017).

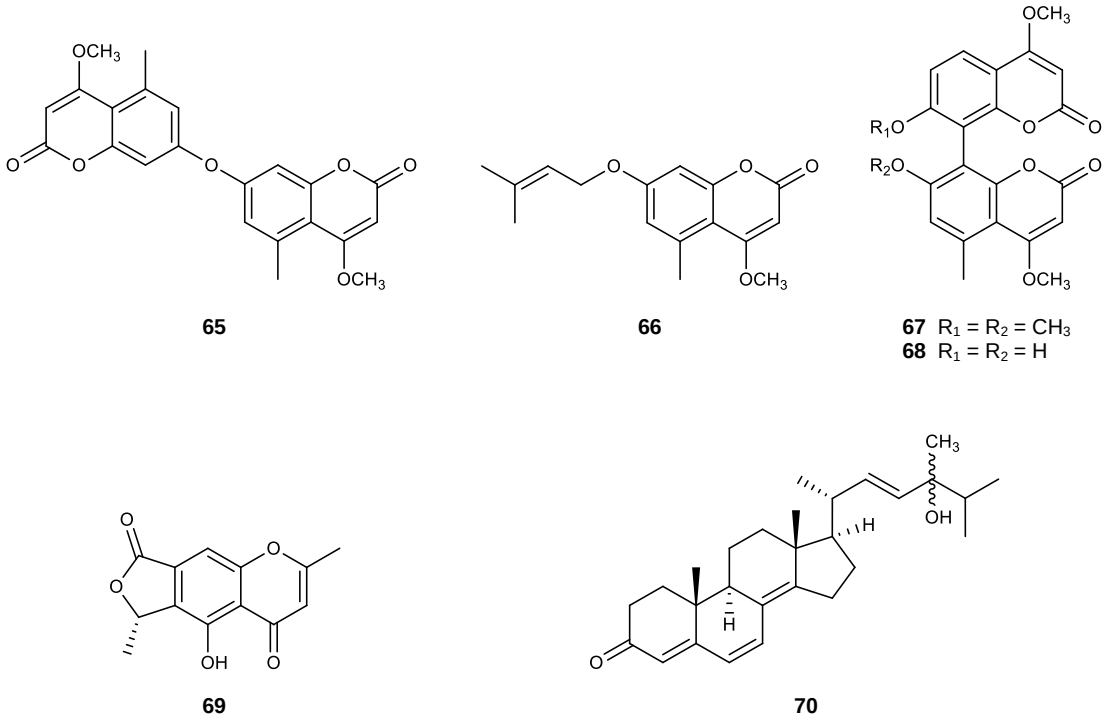

Figure 12. Structures of 4,4'-dimethoxy-5,5'-dimethyl-7,7'-oxydicoumarin (**65**), 7-(γ,γ-dimethylallyloxy)-5-methoxy-4-methylcoumarin (**66**), kotanin (**67**), orlandin (**68**), (*S*)-5-hydroxy-2,6-dimethyl-4*H*-furo[3,4-g]benzopyran-4,8(6*H*)-dione (**69**) and 24-hydroxylergosta-4,6,8(14),22-tetraen-3-one (**70**).

3.1.3) *Aspergillus fumigatus*

Two alkaloids, **9-deacetylfumigaclavine C** (**71**) and **9-deacetoxyfumigaclavine C** (**72**), together with twelve previously reported **fumigaclavine C** (**73**), **14-norpseurotin** (**74**), **pseurotin A** (**75**), **spirotryprostatin A** (**76**), **6-methoxyspirotryprostatin B** (**77**), **fumitremorgin F** (**78**), **dimethylgliotoxin** (**79**), **12α-fumitremorgin C** (**80**), **demethoxyfumitremorgin C** (**81**), **verruculogen** (**82**), and **tryprostatins A** (**83**) and **B** (**84**) (Figure 13), were isolated from the fungus *Aspergillus fumigatus* CY018, which was

isolated from the healthy stem of *Cynodon dactylon,* collected from Jiangsu Province, China. Compounds **71** and **72** were evaluated for their cytotoxicity against three human cancer cell lines: KB, MCF-7 and K562, using MTT method. Compounds **71** and **72** exhibited activity against K562 cell line with IC_{50} values of 41.0 ± 4.6 and 3.1 ± 0.9 μM, respectively. Furthermore, **74** significantly exhibited nerite outgrowth induction activity of PC12 cancer cell line at the concentration of 10.0 μM (Ge *et al*., 2009).

3.1.4) *Aspergillus glaucus*

An anthraquinone derivative with naphtho[1,2,3-*de*]chromene-2,7-dione skeleton, **aspergiolide A** (**85**) (Figure 14), was isolated from the marine fungus *Aspergillus glaucus* HB1-19 which was isolated from the sediment around the mangrove roots, collected from Fujian Province, China. Compound **85** was evaluated for its cytotoxicity against four cancer cell lines: P388, HL-60, BEL-7402 and A-549, using MTT method. Compound **85** exhibited selective activity to four cell lines with IC_{50} values of 35.0, 0.28, 7.5 and 0.13 μM, respectively (Du *et al*., 2007).

Eight aromatic polyketides: **aspergiolide B** (**86**), **isotorachrysone-6-*O*-α-D-ribofuranoside** (**88**), **8-methoxy-3-methyl-1-naphthalenol-6-*O*-α-D-ribofuranoside** (**89**), **8-methoxy-1-naphthalenol-6-*O*-α-D-ribofuranoside** (**90**), **isoasperflavin** (**92**), **(+)-variecolorquinones A** (**98**) and **(*trans*)-** and **(*cis*)-emodinphyscion bianthrone** (**100** and **101**), along with eight previous reported metabolites: **isotorachrysone** (**87**), **asperflavin** (**91**), **emodin** (**93**), **physcion** (**94**), **questin** (**95**), **catenarin** (**96**), **rubrocristin** (**97**) and **physcion bianthrones** (**99**) (Figure 14), were isolated from the same fungus. Compounds **86**-**90**, **92**, **98**, **100** and **101** were tested for their cytotoxicity against two human cancer cell lines: HL-60 and A-549. Compound **86** exhibited potent cytotoxicity against both cell lines with IC_{50} values of 0.51 and 0.24 μM, respectively. Compound **100** exhibited moderate activity with IC_{50} values of 7.8 and 9.2 μM, respectively, while its *cis*-isomer (**101**), showed cytotoxicity with IC_{50} values of 44.0 and 14.2 μM, respectively. On the contrary, all other tested compounds were inactive at the highest concentration tested of 100 μM (Du *et al*., 2008).

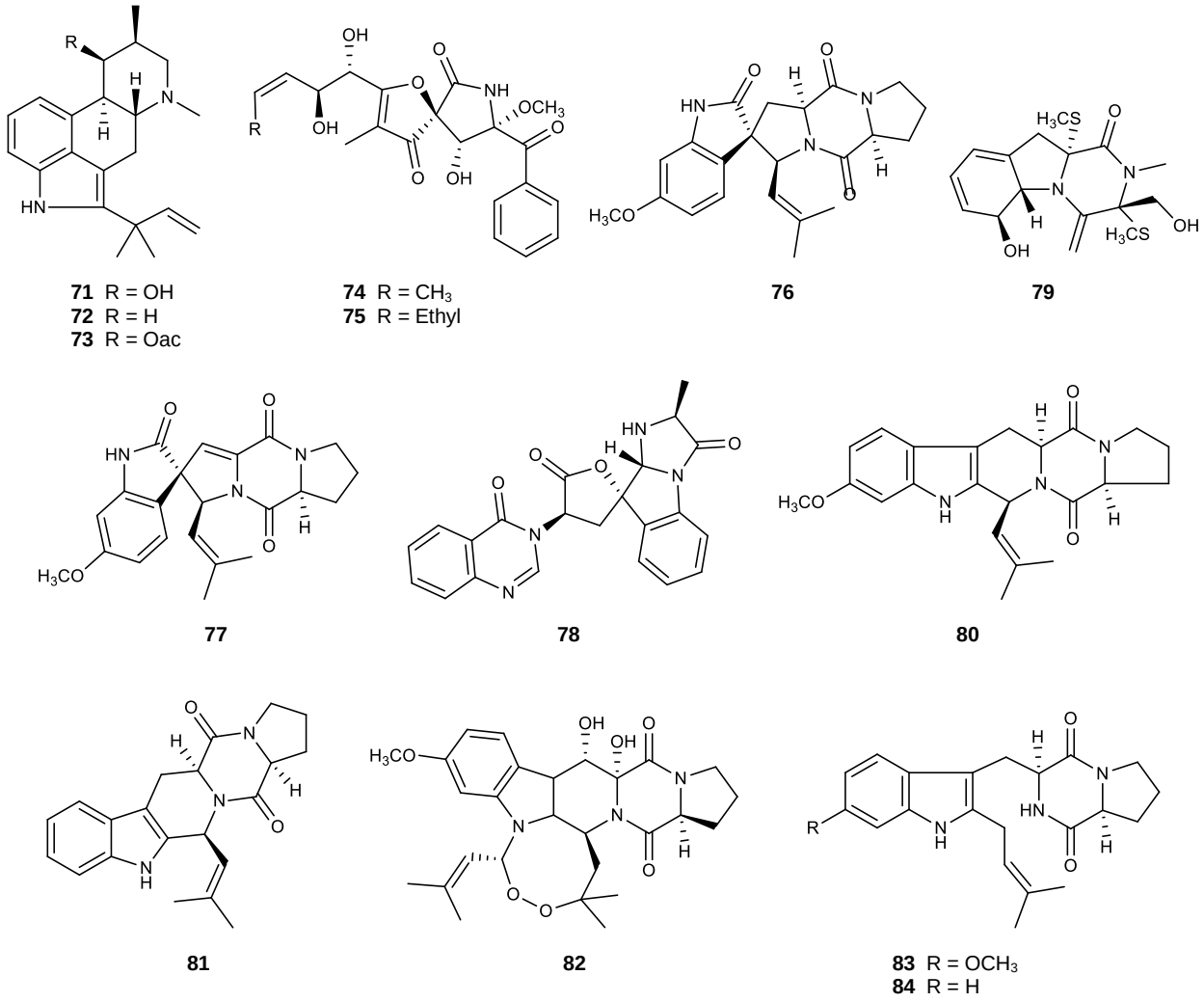

71 R = OH
72 R = H
73 R = Oac

74 R = CH_3
75 R = Ethyl

76

79

77

78

80

81

82

83 R = OCH_3
84 R = H

Figure 13. Structures of 9-deacetylfumigaclavine C (**71**), 9-deacetoxyfumigaclavine C (**72**), fumigaclavine C (**73**), 14-norpseurotin (**74**), pseurotin A (**75**), spirotryprostatin A (**76**), 6-methoxyspirotryprostatin B (**77**), fumitremorgin F (**78**), dimethylgliotoxin (**79**), 12α-fumitremorgin C (**80**), demethoxyfumitremorgin C (**81**), verruculogen (**82**), and tryprostatins A (**83**) and B (**84**).

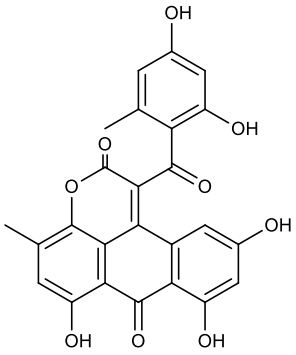

85

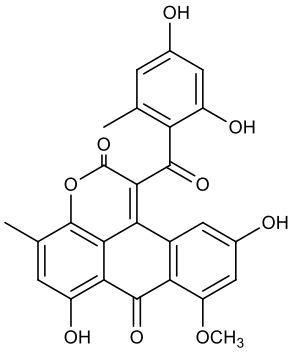

86

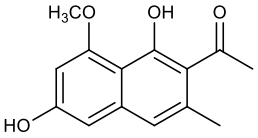

87

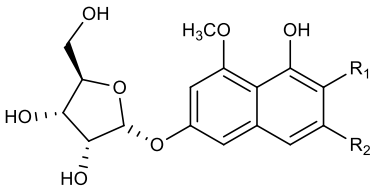

88 $R_1 = OCH_3$, $R_2 = CH_3$
89 $R_1 = H$, $R_2 = CH_3$
90 $R_1 = R_2 = H$

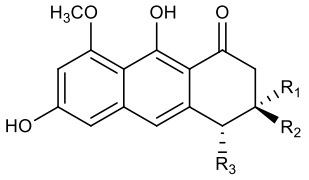

91 $R_1 = CH_3$, $R_2 = OH$, $R_3 = OH$
92 $R_1 = H$, $R_2 = CH_3$, $R_3 = OH$

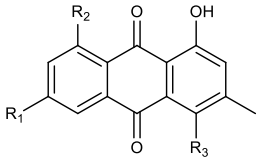

93 $R_1 = OH$, $R_2 = OH$, $R_3 = H$
94 $R_1 = OCH_3$, $R_2 = OH$, $R_3 = H$
95 $R_1 = OH$, $R_2 = OCH_3$, $R_3 = H$
96 $R_1 = R_2 = R_3 = OH$
97 $R_1 = OH$, $R_2 = OCH_3$, $R_3 = OH$

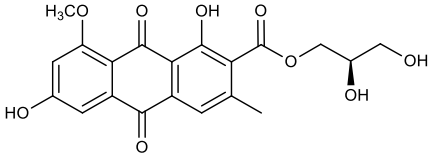

98

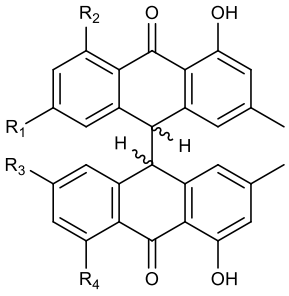

99 $R_1 = R_3 = OCH_3$, $R_2 = R_4 = OH$, *meso* and (±)-racemic C-10/C-10'
100 $R_1 = R_2 = R_4 = OH$, $R_3 = OCH_3$, *trans* H-10/H-10
101 $R_1 = R_2 = R_4 = OH$, $R_3 = OCH_3$, *cis* H-10/H-10'

Figure 14. Structures of aspergiolide A (**85**), aspergiolide B (**86**), isotorachrysone (**87**), isotorachrysone-6-*O*-α-D-ribofuranoside (**88**), 8-methoxy-3-methyl-1-naphthalenol-6-*O*-α-D-ribofuranoside (**89**), 8-methoxy-1-naphthalenol-6-*O*-α-D-ribofuranoside (**90**), asperflavin (**91**), isoasperflavin (**92**), emodin (**93**), physcion (**94**), questin (**95**), catenarin (**96**), rubrocristin (**97**), (+)-variecolorquinones A (**98**) physcion bianthrones (**99**) and (*trans*)- and (*cis*)-emodinphyscion bianthrone (**100** and **101**).

3.1.5) *Aspergillus insuetus*

The meroterpene derivatives, **terretonins E** (**102**) and **F** (**103**), along with **aurantiamine** (**104**) (Figure 15), **linoleic acid** and **uridine**, were isolated from the marine-derived fungus *Aspergillus insuetus,* which was isolated from surface of the marine sponge *Petrosia ficiformis,* collected from Punta de Santa Ana in the Mediterranean Sea, Spain. Compounds **102** – **104** inhibited the mammalian mitochondrial respiratory chain by inhibiting NADH oxidase activity with IC_{50} values of 3.90 ± 0.4, 2.97 ± 1.2 and 15.1 ± 1.8 μM, respectively (López-Gresa *et al*., 2009).

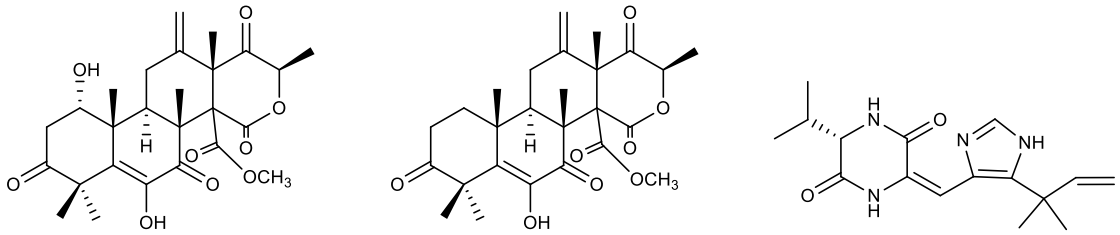

102 **103** **104**

Figure 15. Structures of terretonins E (**102**) and F (**103**), and aurantiamine (**104**).

3.1.6) *Aspergillus insulicola*

Five strains of the marine-derived fungus *Aspergillus insulicola* were isolated from various marine sources, including an unidentified green alga, collected from Acklins Island; a decaying leaf of *Rhizophora mangle,* collected from red mangrove, Little San Salvador; a green alga *Penicillus* sp., collected from black mangrove, Grand Bahama; a green alga *Batophora* sp., collected from Eleuthera. The investigation of these strains led to a discovery of a new nitrobenzoyloxy-substitued sesquiterpene, **insulicolide A** (**105**) and the previously reported **asteltoxin** (**106**) (Figure 16) (Rahbæk *et al*., 1997).

Azonazine (**107**) (Figure 16), a hexacyclic dipeptide, was isolated from the marine-derived fungus *Aspergillus insulicola* which was isolated from a Hawaiian shallow water

sediment. The cytotoxicity assay revealed that **107** was inactive at the concentration of 1 mg/mL in the disk diffusion assay and was also inactive at the concentration of 100 μM in MTT method, against two human cancer cell lines: PC3 and MCF-7, and a murine macrophage cell: RAW 264.7 (Wu *et al*., 2010).

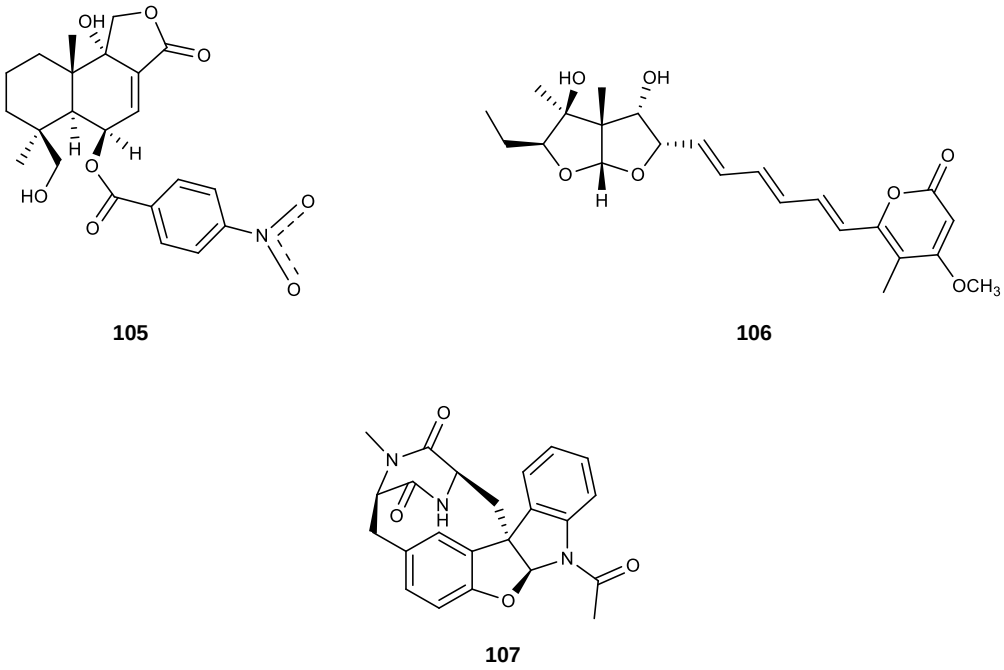

105 **106**

107

Figure 16. Structures of insulicolide A (**105**), asteltoxin (**106**) and azonazine (**107**).

3.1.7) *Aspergillus karnatakaensis*

Two dibenzofurans, **karnatakafurans A** (**108**) and **B** (**109**) (Figure 17), were isolated from the fungus *Aspergillus karnatakaensis* (IBT 22154) which was obtained from the IBT Culture Collection at BioCentrum-DTU, the Technical University of Denmark. Compounds **108** and **109** were evaluated for their antimicrobial activity against four bacterial strains: *Bacillus subtilis, Staphylococcus aureus, Escherichia coli* and *Pseudomonas aeruginosa*, together with various fungal strains, including *Alternaria infectoria, Cladosporium* sp., *Penicillium italicum, Penicillium digitatum, Penicillium expansum, Aspergillus fumigatus, Fusarium avenaceum, Fusarium culmorum, Fusarium solani, Fusarium sporotrichioides, Fusarium oxysporum* and *Botrytis cinerea.* Both

compounds did not exhibit antimicrobial activity at the highest concentration tested (100 µg/disk), except for *P. aeruginosa.* Moreover, **108** and **109** were also tested for their antimalarial activity against chloroquine-sensitive *Plasmodium falciparum* 3D7 parasite, using chloroquine as a positive control. Chloroquine exhibited antimalarial activity with IC_{50} value of 0.012 µg/mL while **108** and **109** showed activity with IC_{50} values of 3.9 and 3.6 µg/mL, respectively (Manniche *et al*., 2004).

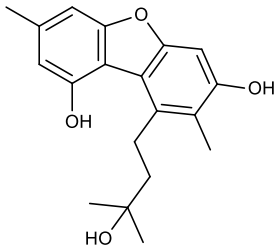

108

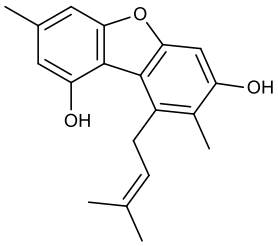

109

Figure 17. Structures of karnatakafurans A (**108**) and B (**109**).

3.1.8) *Aspergillus niger*

Bicoumanigrin (**111**), **aspernigrins A** (**112**) and **B** (**113**), and **pyranonigrins A – D** (**114** – **117**), together with a fungal pigment **cycloleucomelone** (**110**) (Figure 18), were isolated from the marine-derived fungus *Aspergillus niger* which was isolated from the sponge *Axinella damicornis,* collected in the south of Elba, Italy. All isolated compounds, except for **117** which was isolated in a very small quantity, were evaluated for insecticidal property against *Spodoptera littoralis*, lethality toward eggs of *Artemia salina* in brine shrimp assay, antimicrobial activity using agar diffusion assay, and cytotoxicity against ten different human leukemia and carcinoma cell lines. All tested compounds exhibited neither antimicrobial activity nor toxicity to brine shrimp. Compound **111** displayed moderate effect on the growth inhibition of tumor cells (Hiort *et al*., 2004).

Liu *et al*. (2011) described isolation of eight α-pyrone derivatives, **nigerapyrones A – E** (**118 – 122**) and **nigerapyrones F – H** (**125** – **127**), together with the previously reported **asnipyrones B** (**123**) and **A** (**124**) (Figure 18), from the marine-

derived fungus *Aspergillus niger* MA-132 which was isolated from the mangrove plant *Avicennia marina,* collected from Hainan, China. All isolated compounds were evaluated for their cytotoxicity against eight human tumor cell lines: DU145, HeLa, HepG2, MCF-7, NCI-H460, MDA-MB-231, SW1990 and A549. Compound **122** exhibited strong cytotoxicity against SW1990, A549 and MDA-MB-231 cell lines with IC_{50} values of 38, 43 and 48 μM, respectively, which was more potent than fluorouracil (positive control). This compound also showed weak or moderate activity against HepG2, Du145 and MCF-7 cell lines with IC_{50} values of 86, 86 and 105 μM, respectively. Compounds **119** and **121** exhibited cytotoxicity against HepG2 cell with IC_{50} values of 62 and 81 μM, respectively, while compounds **121** and **124** showed activity toward A549 cell with IC_{50} values of 81 and 62 μM, respectively. Compound **121** also displayed weak activity against MCF-7 cell line with IC_{50} value of 121 μM. Moreover, all isolated compounds were also tested for antimicrobial activity against six microbial strains: two bacterial isolates (*Staphylococcus aureus* and *Escherichia coli)* and four plant-pathogenic fungal isolates (*Alternaria brassicae, Fusarium oxysporum, Coniella diplodiella* and *Physalospora piricola)*. The results revealed that none of the tested compounds exhibited antimicrobial activity.

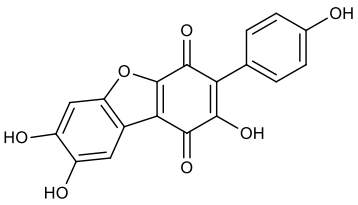

110

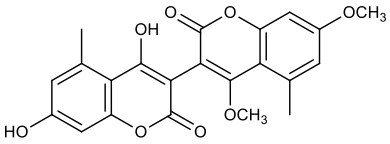

111

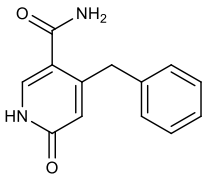

112

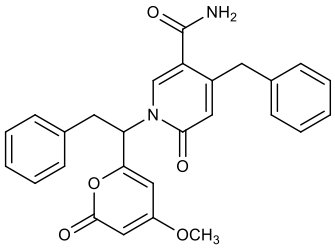

113

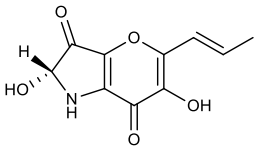

114

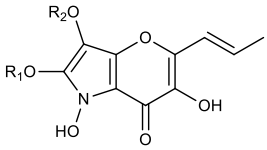

115 R_1 = H, R_2 = CH
116 R_1 = CH_3, R_2 = H

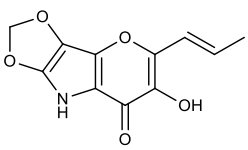

117

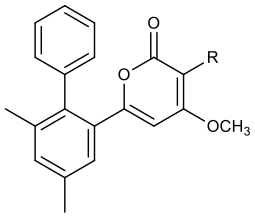

118 R = H
119 R = CH_3

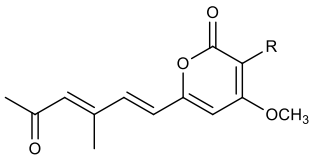

120 R = H
121 R = CH_3

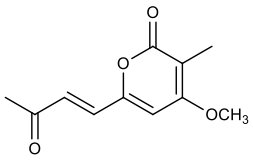

122

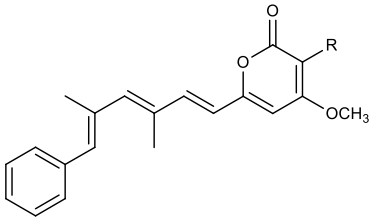

123 R = H
124 R = CH_3

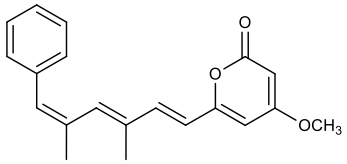

125

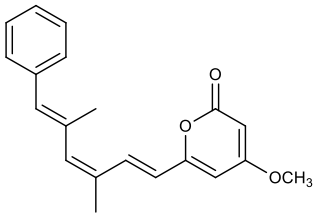

126

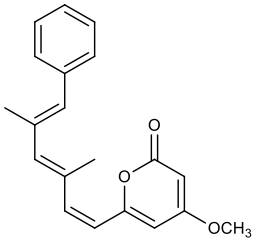

127

Figure 18. Structures of cycloleucomelone (**110**), bicoumanigrin (**111**), aspernigrins A (**112**) and B (**113**) and pyranonigrins A – D (**114** – **117**), nigerapyrones A – E (**118** – **122**), asnipyrones B (**123**) and A (**124**) and nigerapyrones F – H (**125** – **127**).

3.1.9) *Aspergillus ochraceus*

Three benzodiazepine alkaloids, **circumdatins A – C** (**128** – **130**) (Figure 19) were isolated from the terrestrial fungus *Aspergillus ochraceus* (IBT 12704), which was obtained from sterilized milo sorghum seed buried in the soil for 1 – 4 months at Sevilleta National Wildlife Refuge, New Mexico (Rahbæk *et al*., 1999). Later on, Rahbæk and Breinholt (1999) further investigated the secondary metabolites from this fungus, leading to the discovery of another three circumdatin analogues, **circumdatins D – F** (**131** – **133**) (Figure 19).

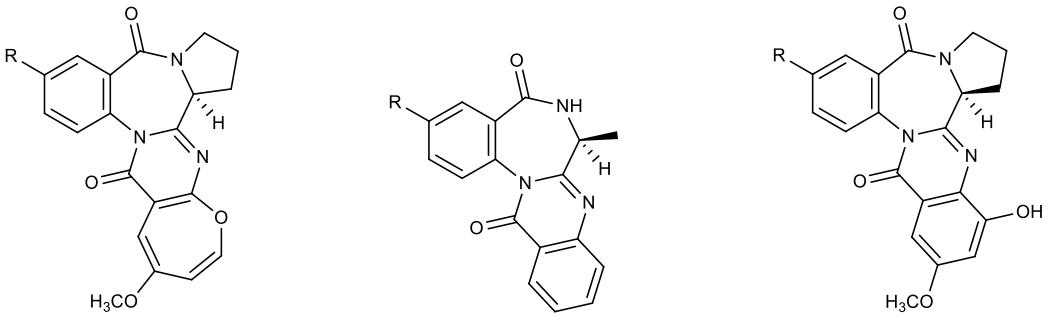

128 R = OCH_3
129 R = H

130 R = OH
133 R = H

131 R = OCH_3
132 R = H

Figure 19. Structures of circumdatins A – F (**128** – **133**).

3.1.10) *Aspergillus ostianus*

Three pentaketides, **aspinotriols A** (**134**) and **B** (**135**), and **aspinonediol** (**136**), together with the previously described **aspinonene** (**137**) and **dihydroaspyrone** (**138**) (Figure 20), were isolated from the marine fungus *Aspergillus ostianus* strain 01F313 which was isolated from an unidentified marine sponge, collected in Pohnpei, the Federated States of Micronesia. Compounds **134** – **138** were evaluated for their antibacterial activity against methicillin-resistant *Staphylococcus aureus* (MRSA), and none of them exhibited antibacterial activity at 100 µg/disk concentration. Compounds **134**, **137** and **138** were also tested for their cytotoxicity against L1210 mouse cancer cell line. However, only **137** exhibited cytotoxicity at 25 ppm concentration (27% inhibition) (Kito *et al*., 2007).

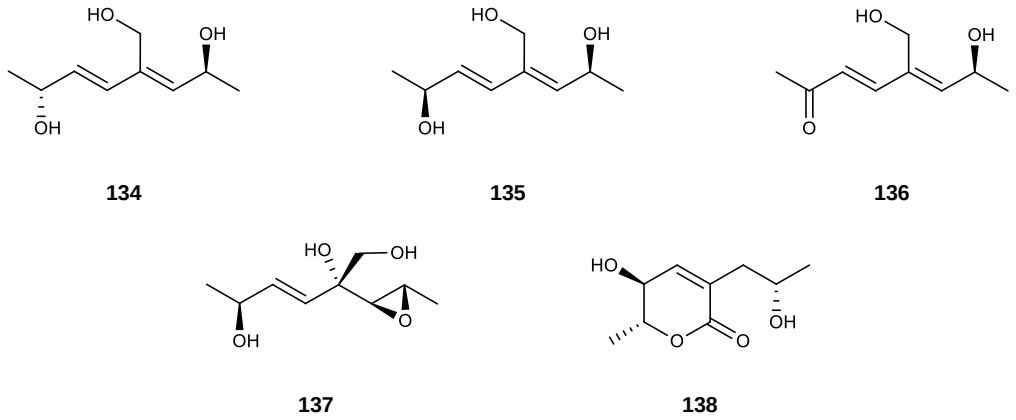

Figure 20. Structures of aspinotriols A (**134**) and B (**135**), aspinonediol (**136**), aspinonene (**137**) and dihydroaspyrone (**138**).

3.1.11) *Aspergillus parasiticus*

A gabosine derivative, **parasitenone** (**139**), was isolated, together with **3-chloro-4,5-dihydroxybenzyl alcohol** (**140**) and **gentisyl alcohol** (**141**) (Figure 21), from a marine fungus *Aspergillus parasiticus* MFA153 which was obtained from the red alga *Carpopeltis cornea,* collected in Ulsan, South Korea. Compound **139** exhibited weak scavenging activity against DPPH and peroxy nitrite ($ONOO^-$) with IC_{50} values of 57.0 and 52.6 µM, respectively, while **140** and **141** showed potent activity toward DPPH (IC_{50} = 0.6 and 1.4 µM, respectively) and $ONOO^-$ (IC_{50} = 3.1 and 2.2 µM, respectively). Moreover, **140** also exhibited strong activity toward superoxide and nitric oxide radicals with IC_{50} values of 11.0 and 0.5 µM, respectively, while **141** showed activity toward only nitric oxide radical with IC_{50} value of 0.4 µM (Son *et al*., 2002).

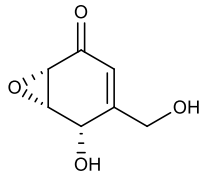

139

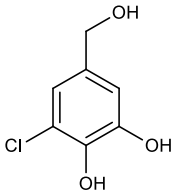

140

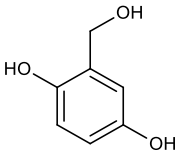

141

Figure 21. Structures of parasitenone (**139**), 3-chloro-4,5-dihydroxybenzyl alcohol (**140**) and gentisyl alcohol (**141**).

3.1.12) *Aspergillus sydowii*

Three diketopiperazine alkaloids, **6-methoxyspirotryprostatin B** (**142**), **18-oxotryprostatin A** (**143**) and **14-hydroxyterezine D** (**144**), an oxaspiro[4.4]lactam, **14-norpseurotin A** (**74**), and a 29-nordammarane triterpenoid, **(4*S*,5*S*,6*S*,8*S*,9*S*,10*R*,13*R*,-14*S*,16*S*,17*Z*)-6,16-diacetoxy-25-hydroxy-3,7-dioxy-29-nordammara-1,17(20)-dien-21-oic acid** (**145**) were isolated, together with twelve previously described compounds: **terezine D** (**146**), **pseustin A** (**147**), **helvolic acid** (**148**), **spirotryprostatin A** (**76**), **12,13-dihydroxyfumitremorgin C** (**149**), **fumitremorgin C** (**150**), **didehydro-besdethiobis(methylthio)gliotoxin** (**151**), **verruculogen** (**82**), **fumigaclavine C** (**73**), **fumigaclavine B** (**152**), and **pyripyropenes A** (**153**) and **E** (**154**) (Figure 22), from the marine fungus *Aspergillus sydowii* PFW1-13 which was obtained from a driftwood sample, collected from the beach of Baishamen, Hainan, China. Compounds **142** – **144** weakly inhibited the growth of A-549 human cancer cell line with IC_{50} values of 8.29, 1.28 and 7.31 μM, respectively. Compound **142** also exhibited cytotoxic activity against HL-60 human cancer cell line with IC_{50} value of 9.71 μM. Moreover **74**, **145**, **146** and **148** were evaluated for their antibacterial activity against *Escherichia coli, Bacillus subtilis* and *Micrococcus lysodeikticus,* using disk diffusion method. Compounds **145** and **146** exhibited antibacterial activity against the tested bacterial strains more potent than **74** and **148** with MIC values of 3.74, 14.97, 7.49 μM and 10.65, 5.33, 10.65 μM, respectively,

while the MIC values of **74** and **148** were 14.49, 14.49, 7.24 µM and 87.92, 21.98, 10.99 µM, respectively (Zhang *et al*, 2008).

Three sesquiterpenes: **aspergillusenes A** (**155**) and **B** (**156**), and **(+)-(7*S*)-7-*O*-methylsydonic acid** (**157**), and two tetrahydroxanthone derivatives: **aspergillusones A** (**158**) and **B** (**159**) were isolated, together with six previously described compounds: **(+)-(7*S*)-sydonic acid** (**160**), **(7*R*,8*R*)-AGI-B4** (**161**), **(7*R*,8*R*)-α-diversonolic ester** (**162**), **methyl 8-hydroxy-6-methyl-9-oxo-9*H*-xanthene-1-carboxylate** (**163**), and **sydowinins A** (**164**) and **B** (**165**) (Figure 22), from the marine fungus *Aspergillus sydowii* PSU-F154 which was isolated from the sea fan *Annella* sp., collected from the coastal area in Suratthani Province, Thailand. Compounds **155** – **157** and **161** – **165** were tested for their antioxidant activity using DPPH assay. Only **161** exhibited antioxidant activity with IC_{50} value of 17 µM while other tested compounds were inactive (Trisuwan *et al*., 2011).

3.1.13) *Aspergillus terreus*

The marine-derived fungus *Aspergillus terreus* PT06-2 which was isolated from the sediment, collected from Putian Sea Saltern, Fujian, China, was culture under a high salinity condition. The investigation of this fungus led to the isolation of **terremides A** (**166**) and **B** (**167**), and **terrelactone A** (**168**), together with twelve previously reported compounds: **3,4,5-trimethoxy-2-(2-(nicotinamido)benzamido)benzoate** (**169**), **(+)-butyrolactones I – III** (**170**-**172**), **3-hydroxy-5-[[4-hydroxy-3-(3-methyl-2-buten-1-yl)phenyl]methyl]-4-)4-hydroxyphenyl)-2(5*H*)-furanone** (**173**), **aspernolide A** (**174**), **5-[(3,4-dihydro-2,2-dimethyl-2*H*-1-benzopyran-6-yl)-methyl]-3-hydroxy-4-(4-hydroxyphenyl)-2(5*H*)-furanone** (**175**), **territrem B** (**176**), **(-)-(1*R*,4*R*)-1,4-(2,3)-indomethane-1-methyl-2,4-dihydro-1*H*-pyrazino[2,1-*b*]quinazoline-3,6-dione** (**177**), ***R*-(-)-6-hydroxymellein** (**178**), ***trans*-4,6-dihydroxymellein** (**179**) and **(+)-terrein** (**180**) (Figure 23). Compounds **166** – **175** and **180** were tested for their cytotoxicity against two human cancer cell lines: HL-60 and BEL-7402 using MTT assay. Only **170** exhibited weak cytotoxicity against HL-60 cell line with IC_{50} values of 57.5 µM. Furthermore, **166** – **175**

and **180** were also evaluated for their antimicrobial activity against *Enterobacter aerogenes, Pseudomonas aeruginosa, Staphylococcus aureus* and *Candida albicans* by agar dilution method, and antiviral activity against influenza virus using CPE inhibition assay. Compounds **166** and **169** exhibited weak antibacterial activity against *S. aureus* with MIC values of 63.9 and 52.4 µM, respectively while **167** showed weak antibacterial activity against *E. aerugenes* with MIC value of 33.5 µM. All other tested compounds showed neither cytotoxicity nor antimicrobial activity at the highest concentration tested (100 µM). Only **166** exhibited anti-H1N1 activity with IC_{50} and CC_{50} (50% cytotoxicity concentration) values of 143.1 and 976.4 µM, respectively (Wang *et al*., 2011).

Two sesterterpenoids, **aspterpenacids A** (**181**) and **B** (**182**) (Figure 23), were isolated from the marine-derived fungus *Aspergillus terreus* H010 which was isolated from the mangrove plant *Kandelia obovata*. Compounds **181** and **182** were evaluated for their antibacterial activity against three Gram-positive (*Staphylococcus aureus, S. epidermidis* and *Bacillus subtilis*) and three Gram-negative (*Escherichia coli, Klebsiella pneumoniae* and *Acinetobacter calcoaceticus*) bacterial strains. Both compounds were inactive at the highest concentration tested (50 µM). Moreover, these two compounds were also inactive in cytotoxicity assay against two human cancer cell lines: HeLa and MCF-7 by MTT method (Liu *et al.,* 2016).

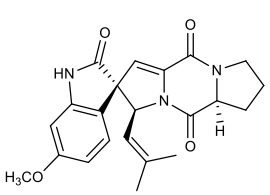

142

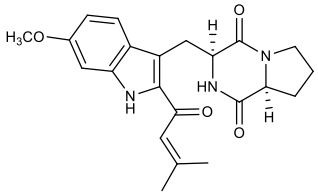

143

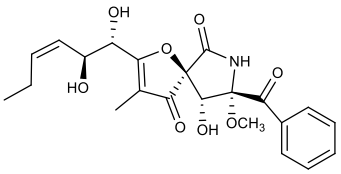

147

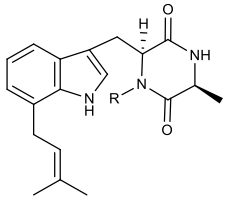

144 R = OH

146 R = H

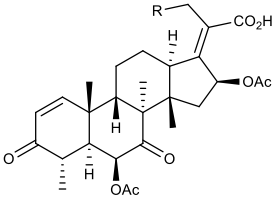

145 R = 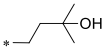

148 R = 

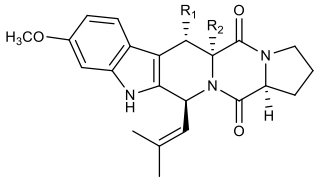

149 R1 = R2 = OH

150 R1 = R2 = H

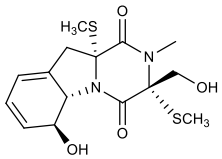

151

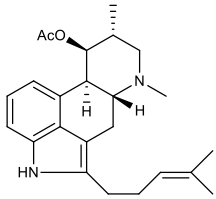

152

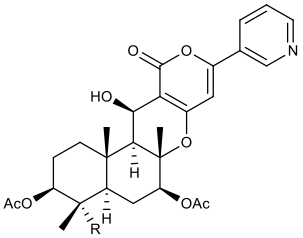

153 R = CH3
154 R = OAc

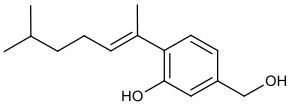

155

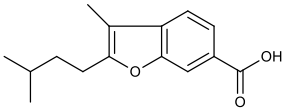

156

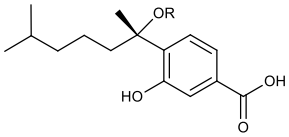

157 R = CH
160 R = H

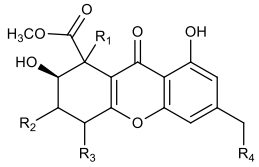

158 R_1 = β-H, R_2 = R_3 = double bond, R_4 = H
159 R_1 = α-OH, R_2 = R_3 = H, R_4 = OH
161 R_1 = β-H, R_2 = R_3 = double bond, R_4 = OH
162 R_1 = α-OH, R_2 = R_3 = R_4 = H

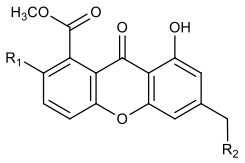

163 R_1 = R_2 =H
164 R_1 = H, R_2 = OH
165 R_1 = R_2 = OH

Figure 22. Structures of 6-methoxyspirotryprostatin B (**142**), 18-oxotryprostatin A (**143**) and 14-hydroxyterezine D (**144**), (4*S*,5*S*,6*S*,8*S*,9*S*,10*R*,13*R*,14*S*,16*S*,17*Z*)-6,16-diacetoxy-25-hydroxy-3,7-dioxy-29-nordammara-1,17(20)-dien-21-oic acid (**145**), terezine D (**146**), pseustin A (**147**), helvolic acid (**148**), 12,13-dihydroxyfumitremorgin C (**149**), fumitremorgin C (**150**), didehydrobesdethiobis(methylthio)gliotoxin (**151**), fumigaclavine B (**152**), pyripyropene A (**153**), pyripyropene E (**154**), aspergillusenes A (**155**) and B (**156**), (+)-(7*S*)-7-*O*-methylsydonic acid (**157**), aspergillusones A (**158**) and B (**159**), (+)-(7*S*)-sydonic acid (**160**), (7*R*,8*R*)-AGI-B4 (**161**), (7*R*,8*R*)-α-diversonolic ester (**162**), methyl 8-hydroxy-6-methyl-9-oxo-9*H*-xanthene-1-carboxylate (**163**), and sydowinins A (**164**) and B (**165**).

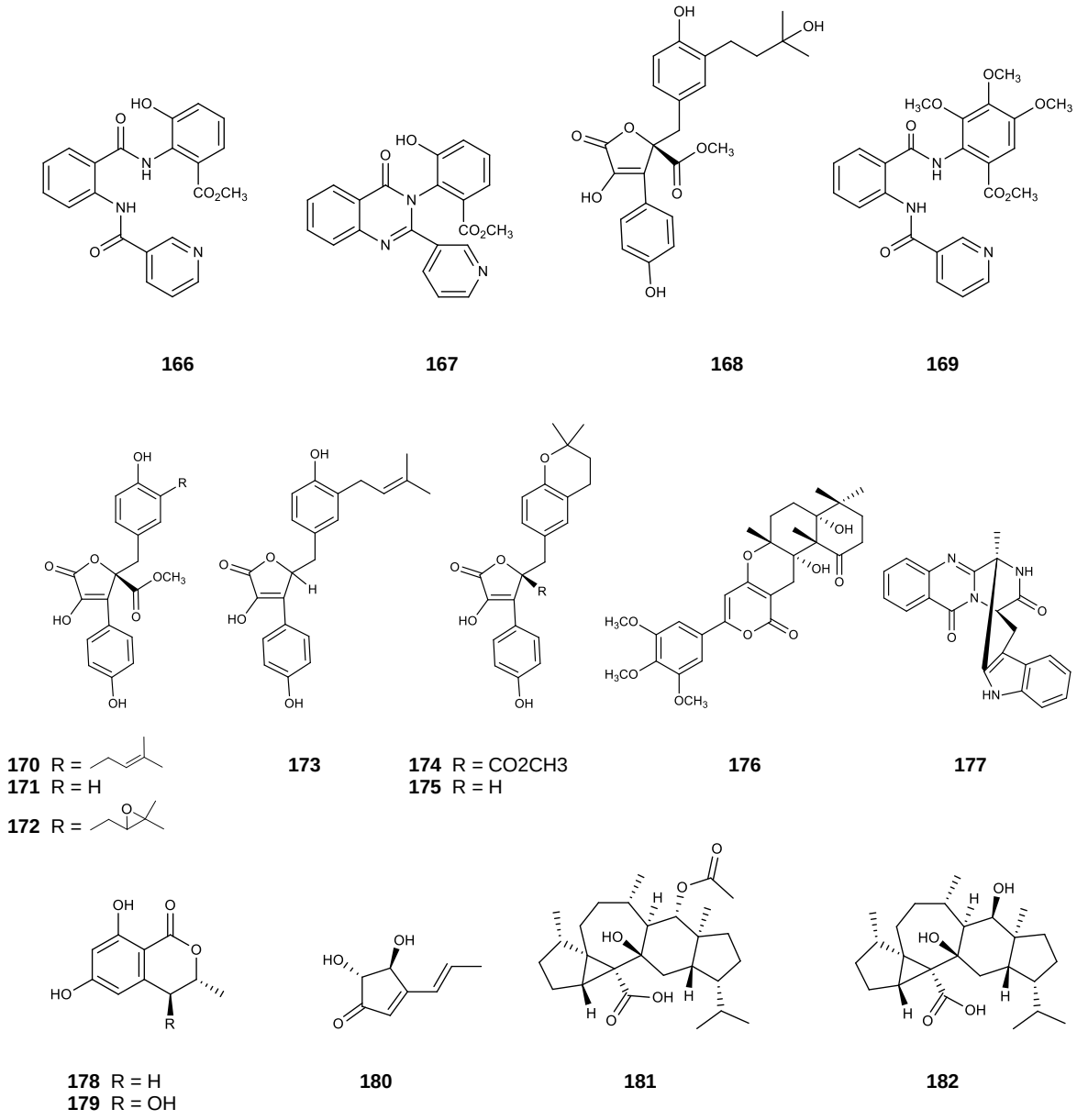

Figure 23. Structures of terremides A (**166**) and B (**167**), terrelactone A (**168**), 3,4,5-trimethoxy-2-(2-(nicotinamido)benzamido)benzoate (**169**), (+)-butyrolactones I – III (**170** – **172**), 3-hydroxy-5-[[4-hydroxy-3-(3-methyl-2-buten-1-yl)phenyl]methyl]-4-)4-hydroxyphenyl)-2(5*H*)-furanone (**173**), aspernolide A (**174**), 5-[(3,4-dihydro-2,2-dimethyl-2*H*-1-benzopyran-6-yl)-methyl]-3-hydroxy-4-(4-hydroxyphenyl)-2(5*H*)-furanone (**175**), territrem B (**176**), (-)-(1*R*,4*R*)-1,4-(2,3)-indomethane-1-methyl-2,4-dihydro-1*H*-pyrazino[2,1-*b*]quinazoline-3,6-dione (**177**), *R*(-)-6-hydroxymellein (**178**), *trans*-4,6-dihydroxymellein (**179**), (+)-terrein (**180**), aspterpenacids A (**181**) and B (**182**).

3.1.14) *Aspergillus ustus*

Seven drimane sesquiterpenoids, **3β,9α,11-trihydroxy-6-oxodrim-7-ene** (**183**), **2α,9α,11-trihydroxy-6-oxodrim-7-ene** (**184**), **2α,11-dihydroxy-6-oxodrim-7-ene** (**185**), **mono(6-strobilactone-B) ester of (*E*,*E*)-2,4-hexadienen-dioic acid** (**188**), **(6-strobilactone-B) ester of (*E*,*E*)-6-oxo-2,4-hexadienoic acid** (**189**), **(6-strobilactone-B) ester of (*E*,*E*)-6,7-dihydroxy-2,4-octadienoic acid** (**190**) and **(6-strobilactone-B) ester of (*E*,*E*)-6,7-dihydroxy-2,4-octadienoic acid** (**191**), together with three previously described **deoxyuvidin B** (**186**), **strobilactone B** (**187**) and **RES-1149-2** (**192**) (Figure 24), were isolated from the marine-derived fungus *Aspergillus ustus* 8009 which was isolated from the marine sponge *Suberites domuncula,* collected from the Adriatic Sea. The crude extract of *A. ustus* and all isolated compounds were evaluated for their cytotoxicity against L5178Y, PC12 and HeLa cancer cell lines using the MTT assay. The crude extract exhibited cytotoxicity against L5178Y at the concentration of 10 µg/mL, while **188**, **189** and **192** displayed activity against this cell line with EC_{50} of 5.3, 0.6 and 1.9 µg/mL, respectively. All other compounds were inactive at the highest concentration tested (10 µg/mL) (Liu *et al*., 2009).

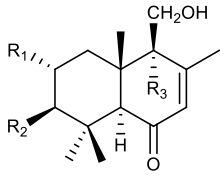

183 R_1 = H, R_2 = OH, R_3 = OH
184 R_1 = OH, R_2 = H, R_3 = OH
185 R_1 = OH, R_2 = H, R_3 = H
186 R_1 = H, R_2 = OH, R_3 = H

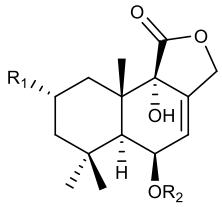

187 R_1 = OH, R_2 = H

188 R_1 = H, R_2 = 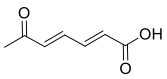

189 R_1 = H, R_2 = 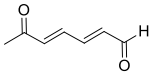

190,191 R_1 = H, R_2 = 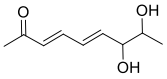

192 R_1 = H, R_2 = 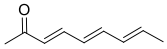

Figure 24. Structures of 3β,9α,11-trihydroxy-6-oxodrim-7-ene (**183**), 2α,9α,11-trihydroxy-6-oxodrim-7-ene (**184**), 2α,11-dihydroxy-6-oxodrim-7-ene (**185**), deoxyuvidin B (**186**), strobilactone B (**187**), mono(6-strobilactone-B) ester of (*E*,*E*)-2,4-hexadienendioic acid (**188**), (6-strobilactone-B) ester of (*E*,*E*)-6-oxo-2,4-hexadienoic acid (**189**), (6-strobilactone-B) ester of (*E*,*E*)-6,7-dihydroxy-2,4-octadienoic acid (**190**), (6-strobilactone-B) ester of (*E*,*E*)-6,7-dihydroxy-2,4-octadienoic acid (**191**) and RES-1149-2 (**192**).

3.1.15) *Aspergillus versicolor*

A alkaloid, **cottoquinazoline A** (**193**), and two cyclopentapeptides, **cotteslosins A** (**194**) and **B** (**195**), were isolated, together with **sterigmatocystin** (**196**), **violaceol I** (**197**), **violaceol II** (**198**), **diorcinol** (**199**), **(-)-cyclopenol** (**200**) and **viridicatol** (**201**) (Figure 25), from the marine-derived fungus *Aspergillus versicolor* (MST-MF495) which was isolated from a beach sand sample collected from Cottesloe, Western Australia. Compound **194** showed weak cytotoxicity against three human cancer cell lines: MM418c5, DU145 and T47D, with EC_{50} values of 66, 90 and 94 µg/mL, respectively (Fremlin *et al*., 2009).

Eight prenylated indole diketopiperazines, **versicamides A** – **H** (**202** – **209**), and **(-)-enamide** (**210**), **notoamide E** (**211**) and **brevianamide F** (**212**) (Figure 25), were isolated from another strain (HDN08-60) of the marine-derived fungus *Aspergillus versicolor* which was isolated from the sediments, collected from the South China Sea. Compounds **202** – **209** were tested for their cytotoxicity against four human cancer cell lines: HeLa, HCT-116, HL-60 and K562, however only **209** showed moderate cytotoxicity with IC_{50} values of 19.4, 17.7, 8.7 and 22.4 µM, respectively. All other compounds were inactive at the highest concentration tested (50 µM) (Peng, Gao, Li, *et al*., 2014).

3.1.16) *Aspergillus wentii*

Three tetranorlabdane diterpenoids, **asperolides A – C** (**213** – **215**), and five previously reported **a tetranorditerpenoid derivative** (**216**), **wentilactones A** (**217**) and **B** (**218**), **botryosphaerin B** (**219**) and **LL-Z1271-β** (**220**) (Figure 26) were isolated from the endophytic fungus *Aspergillus wentii* EN-48 which was isolated from a marine brown alga *Sargassum* sp. All isolated compounds were tested for their cytotoxicity against seven human cancer cell lines: HeLa, HepG2, MCF-7, MDA-MB-231, NCI-H460, SMMC-7721 and WE1990. All tested compounds did not exhibit significant activity against any cell lines at the concentration of 10 µM. Moreover, **213**, **216** – **218** and **220** were further evaluated for their antimicrobial activity against the methicillin-resistant *Staphylococcus aureus* (MRSA)*, Pseudomonas aeruginosa, P. fluorescens, Bacillus subtilis* and *Candida albicans.* Compound **216** exhibited antifungal activity against *C. albicans* with MIC value of 16 µg/mL while other tested compounds showed only weak activity (H. F. Sun *et al*., 2012).

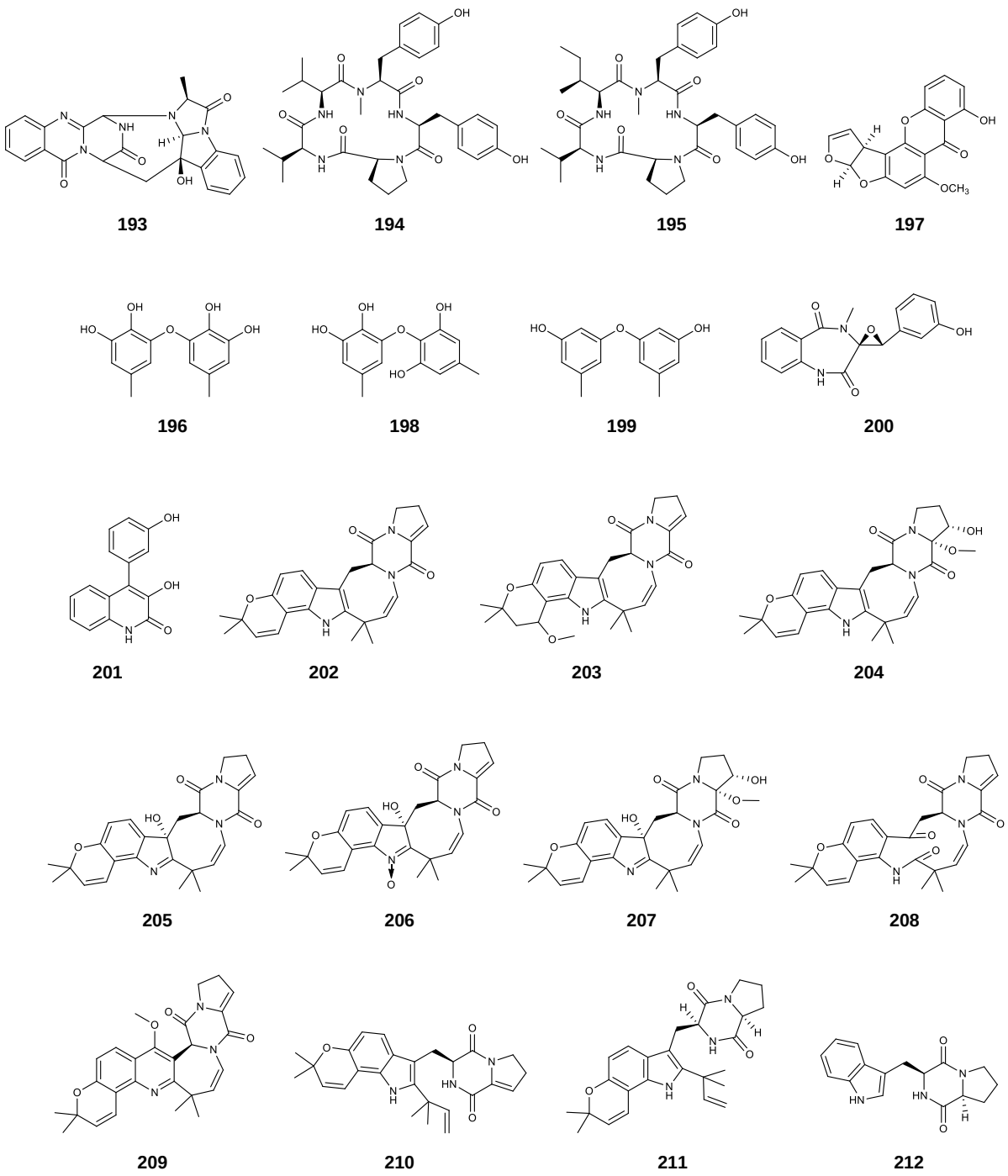

Figure 25. Structures of cottoquinazoline A (**193**), cotteslosins A (**194**) and B (**195**), sterigmatocystin (**196**), violaceols I (**197**) and II (**198**), diorcinol (**199**), (-)-cyclopenol (**200**), viridicatol (**201**), versicamides A – H (**202** – **209**), (-)-enamide (**210**), notoamide E (**211**) and brevianamide F (**212**).

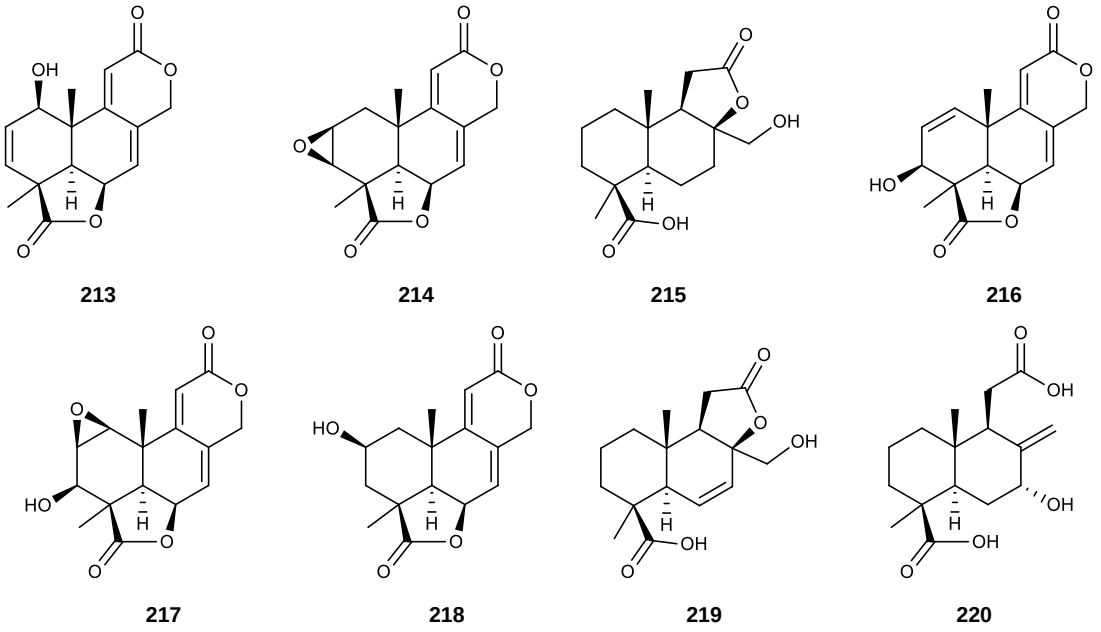

Figure 26. Structures of asperolides A – C (**213** – **215**), a tetranorditerpenoid derivative (**216**), wentilactones A (**217**) and B (**218**), botryosphaerin B (**219**) and LL-Z1271-β (**220**).

3.1.17) *Aspergillus westerdijkiae*

Two benzodiazepine alkaloids: **circumdatins K** (**221**) and **L** (**222**), two prenylated indole alkaloids: **5-chlorosclerotiamide** (**223**) and **10-*epi*-sclerotiamide** (**224**), and **aspergilliamide B** (**225**) were isolated, along with six previously described alkaloids: **(+)-circumdatin F** (**226**), **circumdatin G** (**227**), **sclerotiamide** (**228**), **notoamide C** (**229**), **notoamide I** (**230**) (Figure 27) and **cyclo-L-tryptophanyl-L-proline** (**212**), from the marine-derived fungus *Aspergillus westerdijkiae* DFFSCS013 which was isolated from a marine sediment sample, collected from the South China Sea. All isolated compounds were investigated for their cytotoxicity against A549, HL-60, K562 and MCF-7 cancer cell lines. All tested compounds were inactive at the highest concentration tested (10 μm) (Peng *et al*., 2013).

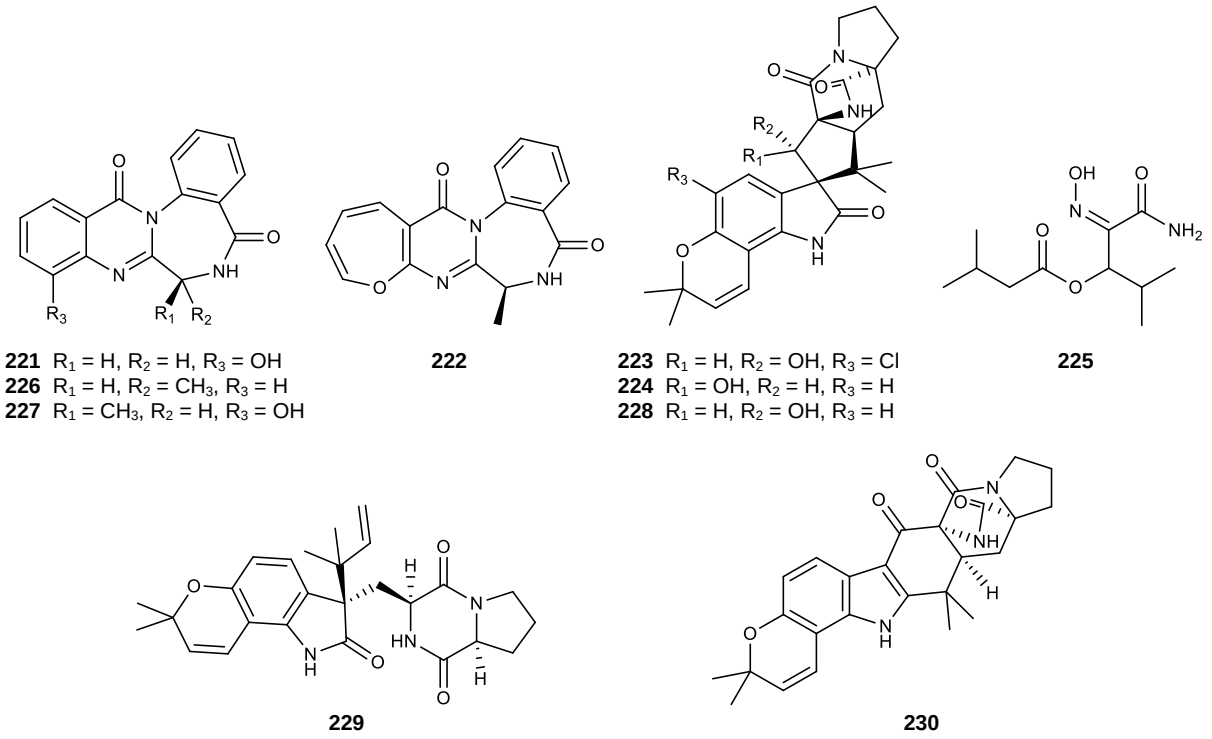

Figure 27. Structures of circumdatins K (**221**) and L (**222**), 5-chlorosclerotiamide (**223**), 10-*epi*-sclerotiamide (**224**), aspergilliamide B (**225**), (+)-circumdatin F (**226**), circumdatin G (**227**), sclerotiamide (**228**), notoamide C (**229**) and notoamide I (**230**).

3.2) The Fungi of the Genus *Neosartorya*

3.2.1) *Neosartorya fischeri*

Neosartorya fischeri is the most studied species among the members of the genus *Neosartorya*. Several strains of this species have been investigated for their capacity to produce bioactive secondary metabolites.

Fiscalins A – C (**231 – 233**) (Figure 28) were isolated from the culture broth of the soil fungus *Neosartorya fischeri* which was isolated from a plant rhizosphere, collected in Taiwan. The isolated compoudns were examined for their substance P inhibitory activity using I-Bolton-Hunter-substance P binding assay. Compound **231** – **233** exhibited the binding inhibition of substance P ligand to the neurokinin (NK-1) receptor of U-373 MG cancer cell line with K_i values of 57, 174 and 68 µM, respectively (Wong *et al*., 1993).

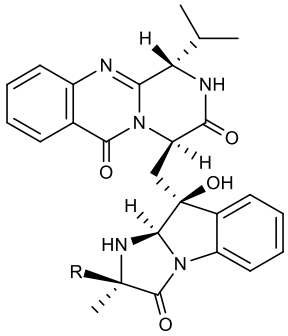

231 R = H
233 R = CH_3

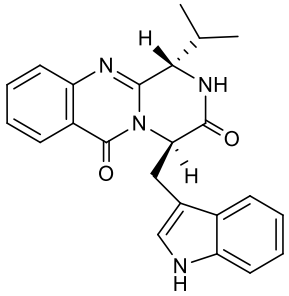

232

Figure 28. Structures of fiscalins A (**231**), B (**232**) and C (**233**).

Three congeners of the dihydrogenated form of the xanthocillin group, **NK372135s A – C** (**234** – **236**) (Figure 29), were isolated from the culture broth of the fungus *N. fischeri* var. *glabra* IF09857. These three compounds exhibited the growth inhibitory activity against *Candida albicans* TIMM0144 with IC_{50} values of 2.12, 0.53 and 0.27 µg/mL, respectively. Compounds **234** – **236** showed stronger activity than xanthocillin dimethylether (XDE) and methoxy-xanthocillin dimethylether (XTE) which had IC_{50} values

of 12.1 and 8.2 µg/mL, respectively. From these results, it could be suggested that C_2-C_3 bond of NK372135s must be related to potent inhibitory activity of these three compounds (Morino *et al*., 1994).

A yellow pigment N**eosartorin** (**237**) (Figure 29) was isolated from the soil fungus *N. fischeri* which was isolated from the river Vah sediment in Slovakia. This was the first report of ergochrome isolation from this fungus (Proksa *et al*., 1998).

The cyclopentenone derivatives, **isoterrein** (**238**) and **terrein** (**239**), were isolated, together with **nortryptoquivalone** (**240**) and **aszonalenin** (**241**) (Figure 29), from *N. fischeri* IFM52672 (Wakana *et al*., 2006).

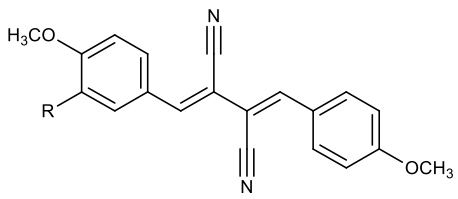

XDE; R = H
XTE; R = OCH_3

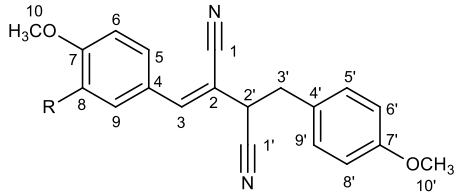

234 R = H
235 R = OCH_3
236 R = OH

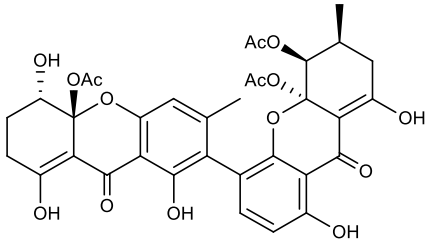

237

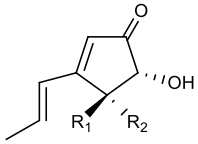

238 R_1 = H, R_2 = OH
239 R_1 = OH, R_2 =H

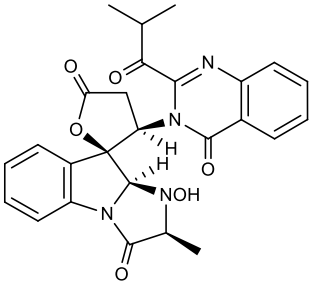

240

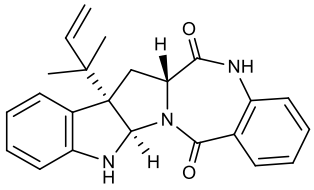

241

Figure 29. Structures of xanthocillins, NK372135s A – C (**234 – 236**), neosartorin (**237**), isoterrein (**238**), terrein (**239**), nortryptoquivalone (**240**) and aszonalenin (**241**).

The antifungal peptide (**NFAP**; *N. fischeri* antimicrobial protein), a small, basic and cysteine-rich protein consisting of 57 amino acid residues, was isolated from the culture supernatant of *N. fischeri* NRRL 181. **NFAP** was evaluated for its antifungal activity against five asco- and five zygomycetous fungal isolates, including *Aspergillus nidulans* SZMC 0307, *Aspergillus niger* SZMC 601, *Botrytis cinerea* NCAIM F00751, *Fusarium graminearum* SZMC 11030, *Trichoderma longibrachiatum* UAMH 7955, *Absidia corymbifera* SZMC 95033, *Mucor piriformis* SZMC 12078, *Rhizomucor miehei* CBS 360.92, *Rhizopus microsporus* var. *rhizopodiformis* CBS 102.277 and *Mortierella wolfii* CBS 651.93, using 96-well microtiter plate bioassay. **NFAP** exhibited growth inhibitory activity against filamentous fungi in a dose-dependent manner. This compound completely inhibited the growth of *A. niger* after 48 h of incubation at the concentration of 200 µg/mL and partially inhibited at the concentration of 12.5 µg/mL with 32 ± 5% growth inhibition. **NFAP** exhibited the growth inhibitory activity of fungi within broad pH and temperature ranges, and the highest activity was at pH 8.4-8.6 (Kovács *et al*., 2011). In 2014, Virágh *et al*. investigated the heterologous expression of NFAP in the yeast *Pichia pastoris* KM71H and evaluated the growth inhibitory activity of this heterologous NFAP (**hNFAP**), and compared to the native **NFAP** by a 96-well microtiter plate bioassay, against human pathogenic filamentous fungal strains, including five zygomycetous (*Absidia corymbifera* SZMC 95033, *R. miehei* CBS 360.92, *Rhizomucor pusillus* ETH M4920, *R. mocrosporus* var. *rhizopodifomis* CBS 102.277 and *Rhizopus oryzae* CBS 146.90) and fourteen ascomycetous (*Aspergillus awamori* SZMC 2390, *Aspergillus flavus* SZMC 2521, *Aspergillus fumigatus* SZMC 2394, *A. niger* SZMC 2402, *Aspergillus nomius* SZMC 2441, *Aspergillus tamarii* SZMC 2482, *Aspergillus terreus* SZMC 2535, *Aspergillus tubingensis* SZMC 2503, *Fusarium incarnatum* SZMC 11403, *Fusarium solani* SZMC 11412, *F. solani* SZMC 11427, *Fusarium sporotrichioides* SZMC 11421, *T. longibrachiatum* UAMH 7955, *T. longibrachiatum* UAMH 9515) fungal isolates. The antifungal activity of **hNFAP** was not different from that of **NFAP**. Both compounds exhibited the growth inhibitory activity against only eight ascomycetous fungal isolates: *A. awamori* SZMC 2390, *A. fumigatus* SZMC 2394, *A. niger* SZMC 2402, *A. nomius* SZMC 2441, *A. tamarii* SZMC 2482, *A. tubingensis* SZMC 2503, *F. incarnatum* SZMC 11403 and *F. solani* SZMC 11412. At 200 µg/mL concentration, **NFAP** and **hNFAP**

inhibited the growth of these eight fungal isolates about fifty percent, and the most sensitive fungal isolate was *A. tubingensis* which showed the growth percentage 31 ± 4.6 and 20 ± 3.6% for **NFAP** and **hNFAP**, respectively. In 2015, Virágh *et al*. studied the mechanism of antifungal activity of **NFAP** by investigating a reduced cellular metabolism using FUN1 viability staining, apoptosis induction by Annexin V-FITC Apoptosis Detection Kit, membrane disruption using PI staining, changes in the actin distribution and chitin deposition at the hyphal tip in NFAP-sensitive *Aspergillus nidulans.* NFAP did not exhibit a direct membrane disruption, but it induced apoptosis by activating the cAMP/protein kinase A pathway via G-protein.

Norfumiquinazoline derivatives, **Cottoquinazolines E** (**242**) and **F** (**243**) (Figure 30), were isolated, together with **pyripyropene A** (**153**), from the fungus *N. fischeri* NRRL 181, which was purchased from DSMZ (DE-Braunschweig) (Shan *et al*., 2015).

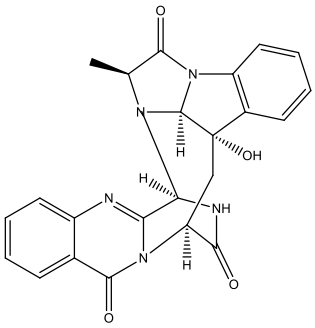

242

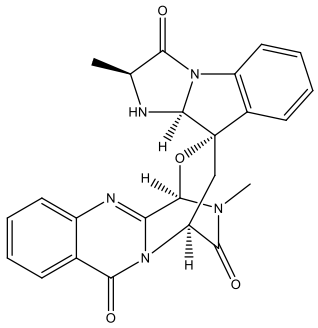

243

Figure 30. Structures of cottoquinazolines E (**242**) and F (**243**).

Fischeacid (**244**) and **fischexanthone** (**245**) were isolated, together with **sydowinins A** (**164**) and **B** (**165**), **AGI-B4** (**246**), **chrysophanol** (**247**), **emodin** (**93**), **5'-deoxy-5'-methylamino-adenosine** (**248**), **adenosine** (**249**) and **3,4-dihydroxybenzoic acid** (**250**) (Figure 31), from the marine-derived fungus *N. fischeri* strain 1008F$_1$. All isolated compounds were examined for their cytotoxicity on SGC-7901 and BEL-7404 cancer cell lines, by MTT assay, and antiphytoviral activity against tobacco mosaic virus

(TMV) by the leaf-disc method. The results showed that **246** exhibited a potent inhibition of the proliferation of SGC-7901 and BEL-7404 cells with IC_{50} values of 0.29 ± 0.005 and 0.31 ± 0.004 mmol L^{-1}, respectively. Moreover, **246** and **250** exhibited inhibition of replication of TMV with IC_{50} values of 0.26 ± 0.006 and 0.63 ± 0.008 mmol L^{-1}, respectively (Tan *et al*., 2012).

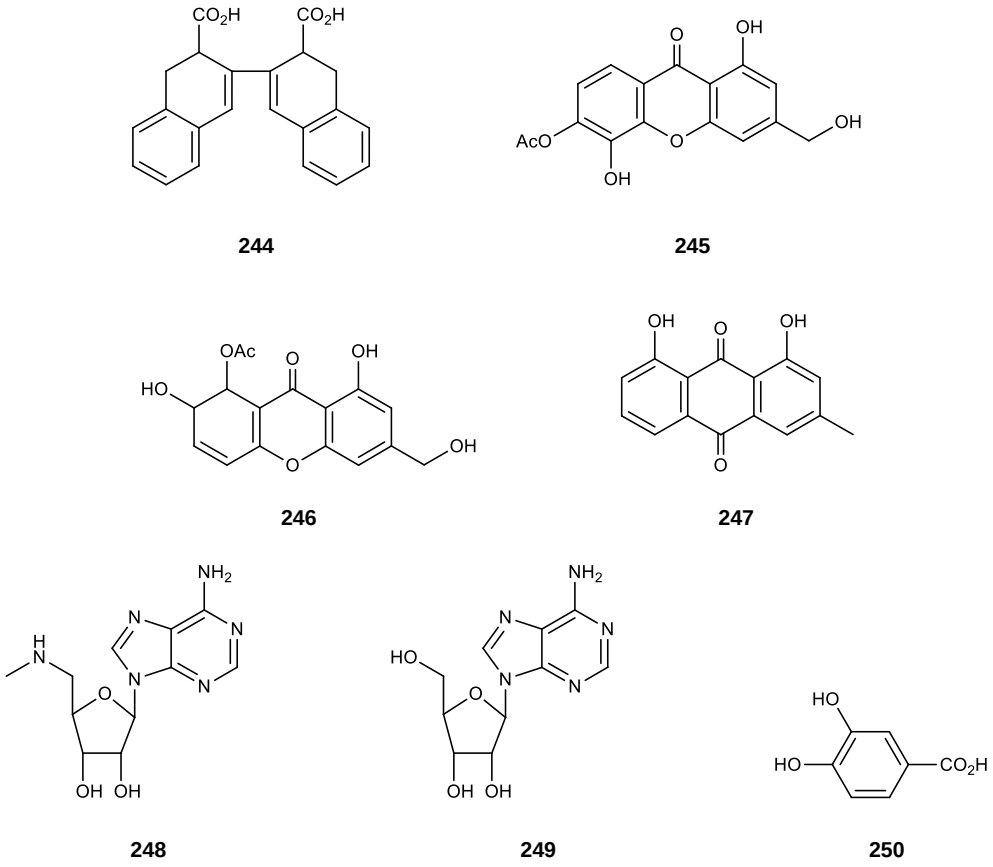

Figure 31. Structures of fischeacid (**244**), fischexanthone (**245**), AGI-B4 (**246**), chrysophanol (**247**), 5'-deoxy-5'-methylamino-adenosine (**248**), adenosine (**249**) and 3,4-dihydroxybenzoic acid (**250**).

1-formyl-5-hydroxyaszonalenin (**251**) and **sartorypyrone A** (**253**) were isolated, together with **aszonalenin** (**241**), **acetylaszonalenin** (**252**), **13-oxofumitremorgin B** (**255**), **aszonapyrone A** (**256**) and **helvolic acid** (**148**) (Figure 32), from the soil fungus *N. fischeri* KUFC 6344 which was isolated from the coastal forest soil, collected from Samaersarn Island, Thailand, by Eamvijarn *et al*. (2013). Compounds **241**, **251 – 253** and

255 – 256 were tested for their cytotoxicity against MCF-7, NCI-H460 and A375-C5 cancer cell lines. The results showed that **256** potently inhibited the growth of MCF-7, NCI-H460 and A375-C5 cells with GI_{50} values of 13.6 ± 0.9 μM, 11.6 ± 1.5 μM and 10.2 ± 1.2 μM, respectively. Compound **253** also displayed strong growth inhibitory activity against A375-C5 cell with GI_{50} value of 21.5 ± 1.9 μM, but less active against MCF-7 and NCI-H460 cells with GI_{50} values of 46.3 ± 7.6 and 37.3 ± 4.0 μM, respectively. Compound **255** exhibited weak growth inhibitory activity against all tested cell lines with GI_{50} values of 115.0 ± 20.0, 123.3 ± 11.5 and 68.6 ± 12.9 μM, for MCF-7, NCI-H460 and A375-C5 cell lines, respectively. In contrast, all three aszonalenin derivatives (**241**, **251** and **252**) were inactive against all tested cell lines at the highest concentration tested (150 μM).

The antibacterial activity of **sartorypyrone A** (**253**), which was previously isolated from the soil fungus *N. fischeri* KUFC 6344 (Eamvijarn *et al*., 2013), was evaluated against four bacterial isolates, including *Staphylococcus aureus* ATCC 25923, *Bacillus subtilis* ATCC 6633, *Escherichia coli* ATCC 25922 and *Pseudomonas aeruginosa* ATCC 27853, and the multidrug-resistant bacterial isolates from the environment, including *S. aureus* B1 and B2, *Enterococcus faecalis* W1, *Enterococcus faecium* W5 and *E. coli* G1, as well as its potential synergism with antibiotic against the methicillin-resistant *S. aureus* (MRSA) and vancomycin-resistant *Enterococci* (VRE) (Gomes *et al*., 2014). Compound **253** inhibited the growth of *S. aureus* and *B. subtilis* with the MIC values of 32 and 64 μg/mL, respectively, however it was inactive against the multidrug-resistant bacterial isolates at the highest concentration tested (256 μg/mL). The combination of **253** and oxacillin, and ampicillin exhibited no synergism against MRSA isolate. Compound **253** was also found to completely inhibited biofilm formation of *S. aureus* ATCC 25923, *B. subtilis* ATCC 6633 and *S. aureus* B1 at the concentrations of 2 x MIC and MIC. However, at the sub-inhibitory concentration (1/2 × MIC), *S. aureus* and *S. aureus* B1 showed more biofilm formation.

Sartorypyrone D (**254**), **sartorypyrone A** (**253**), **aszonapyrone A** (**256**) and **aszonapyrone B** (**257**) (Figure 32) were isolated from the soil fungus *N. fischeri* FO-5897 which was isolated from the soil sample, collected in Chiba, Japan. All isolated

compounds were tested for their inhibitory activity against NADH-fumarate reductase (NFRD) and NADH oxidase. Compounds **253** and **254** exhibited potent inhibitory activity toward NFRD with IC_{50} values of 1.7 and 0.6 μM, respectively, while compound **256** and **257** exhibited moderate activity, but the selectivity toward NADH oxidase was higher than compound **253** and **254** (Kaifuchi *et al*., 2015).

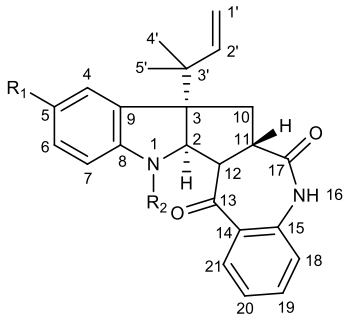

251 R_1 = OH, R_2 = CHO
252 R_1 = H, R_2 = Oac

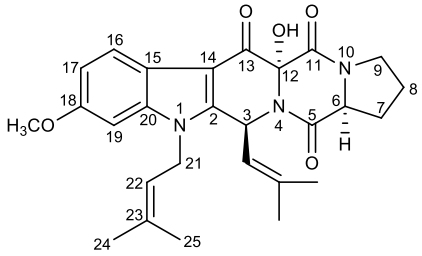

255

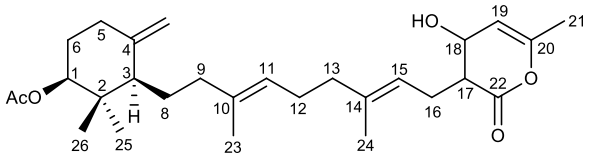

253

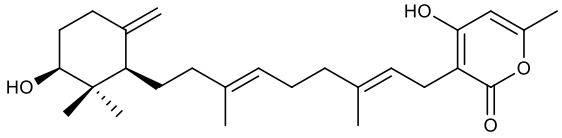

254

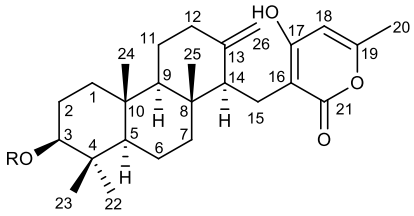

256 R = Ac
257 R = H

Figure 32. Structures of 1-formyl-5-hydroxyaszonalenin (**251**), acetylaszonalenin (**252**), sartorypyrone A (**253**), sartorypyrone D (**254**), 13-oxofumitremorgin B (**255**), aszonapyrone A (**256**) and aszonapyrone B (**257**).

6-Hydroxyaszonalenin (**258**) and six previously described compounds, **acetylaszonalenin** (**252**), **aszonalenin** (**241**), **fumitremorgin B** (**259**) (Figure 33), **verruculogen** (**82**), **aszonapyrone A** (**256**) and **aszonapyrone B** (**257**), were isolated from the fungus *N. fischeri* CGMCC 3.5378, which was obtained from the Chinese Academy of Science (Shan *et al*., 2014).

Later on, Zheng *et al*. (2014) reported the isolation of prenylated 2,5-diketopiperazines, **Neofipiperazines A – C** (**260 – 262**), together with **verruculogen** (**82**), **verruculogen TR-2** (**263**), **12α,13α-dihydroxyfumitremorgin C** (**149**), **fumitremorgin C** (**150**), **cyclotryprostatin** (**264**) and ***rel*-(8S)-19,20-dihydro-9,20-dihydroxy-8-methoxy-9,18-diepifumitremorgin C** (**265**) (Figure 33), from the same fungus.

From the same fungus, Chen *et al*. (2014) isolated a prenylated indole alkaloid, **neofipiperazine D** (**266**), together with **fumitremorgin C** (**150**), **ergosterol** (**267**) and **(1*S*,2*R*,5*R*,6*R*,9*R*,10*R*,13*S*,15*S*)-5-[2*R*,3*E*,5*S*)-5,6-dimehtyl-3-hepten-2-yl]-6,10-dimethyl-16,17-dioxapentacyclo[12.2.2.0^{1,9}.0^{2,6}.0^{10,15}]nonadec-18-en-13-ol** (**268**) (Figure 33). Compound **266** was evaluated for its cytotoxicity against four human cancer cell lines: MCF-7, H1299, HUVEC and MDA-MB-231, but it was inactive against all tested cell lines at a concentration of 20 µM.

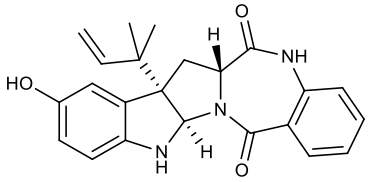

258

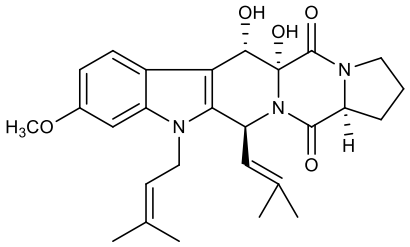

259

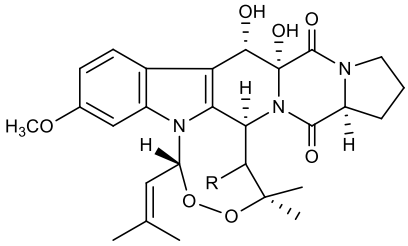

260 R = *α*-OH
261 R = *β*-OH

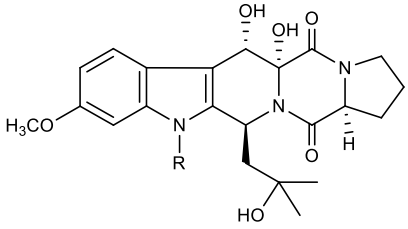

262 R = $(CH_3)_2C{=}CHCH_2$
263 R = H

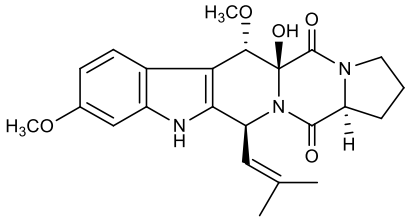

264

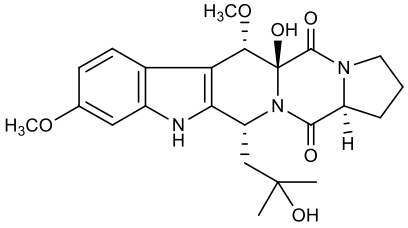

265

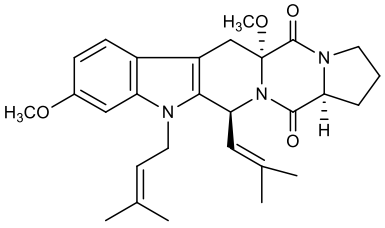

266

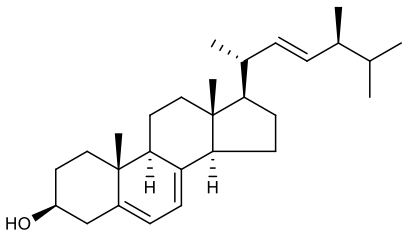

267

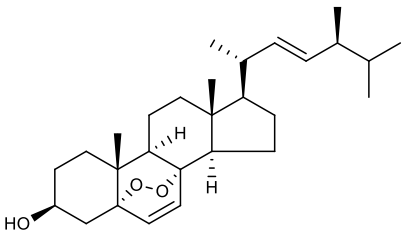

268

Figure 33. Structures of 6-hydroxyaszonalenin (**258**), fumitremorgin B (**259**), neofipiperazines A – C (**260 – 262**), verruculogen TR-2 (**263**), cyclotryprostatin (**264**), *rel*-(8*S*)-19,20-dihydro-9,20-dihydroxy-8-methoxy-9,18-diepifumitremorgin C (**265)**, neofipiperazine D (**266**), ergosterol (**267**) and (1*S*,2*R*,5*R*,6*R*,9*R*,10*R*,13*S*,15*S*)-5-[2*R*,3*E*,5*S*)-5,6-dimehtyl-3-hepten-2-yl]-6,10-dimethyl-16,17-dioxapentacyclo[12.2.2.$0^{1,9}$.$0^{2,6}$.$0^{10,15}$]nonadec-18-en-13-ol (**268**).

Two tryptoquivaline derivatives, **tryptoquivalines T** (**269**) and **U** (**270**) (Figure 34), together with **fiscalin B** (**232**), were isolated from the fermentation broth of the marine-derived fungus *N. fischeri* which was isolated from marine mud, collected in the intertidal zone of Hainan, China. The isolated compounds were evaluated for their cytotoxicity against HL-60 cell line. Compounds **232**, **269** and **270** exhibited the growth inhibitory activity toward HL-60 cell with IC_{50} values of 8.88, 82.3 and 90.0 µM, respectively (Wu *et al*., 2015).

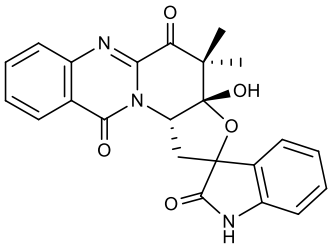

269

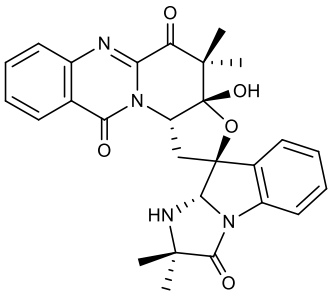

270

Figure 34. Structures of tryptoquivalines T (**269**) and U (**270**).

3.2.2) *Neosartorya glabra*

Three bicyclic lactones, **glabramycins A – C** (**271 – 273**) (Figure 35), were isolated from the soil fungus *N. glabra* (MF7030, F-155,700) which was isolated from the soil sample, collected from Candamia, Spain. All isolated compounds were evaluated for their antimicrobial activity against *Staphylococcus aureus* ATCC 29213, *S. aureus* MB2865, *Streptococcus pneumoniae* CL2883, *Enterococcus faecalis* CL8516, *Bacillus subtilis* MB964, *Haemophilus influenza* MB4572, *Escherichia coli* MB2884 and *Candida albicans* MY1055. The results showed that compound **273** exhibited better activity by inhibiting the growth of *Streptococcus pneumoniae, S. aureus* and *B. subtilis* with MIC values of 2, 16 and 16 µg/mL, respectively. None of the tested compounds exhibited the growth inhibitory activity against Gram-negative bacteria or *C. albicans* (Jayasuriya *et al*., 2009).

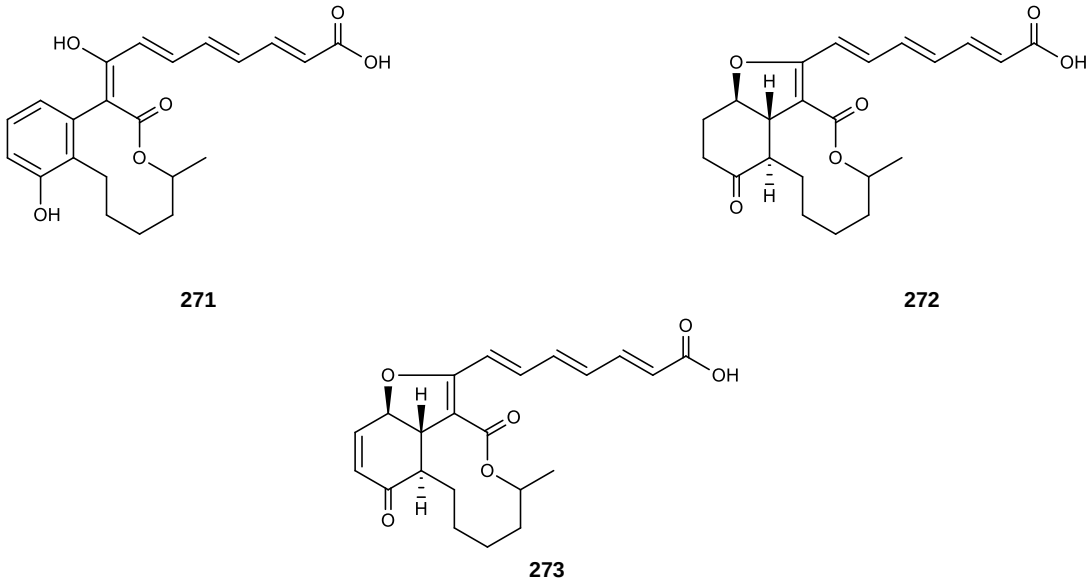

271 **272** **273**

Figure 35. Structures of glabramycins A – C (**271 – 273**).

Sartoryglabins A – C (**274** – **276**) (Figure 36), the analogs of (-) ardeemins, were isolated from the soil-derived fungus *N. glabra* which was isolated from the soil sample, collected in Thailand. All isolated compounds were evaluated for their *in vitro* growth inhibitory activity on three human tumor cell lines: MCF-7, NCI-H460 and A375-C5. Compound **274** exhibited strong growth inhibitory activity against MCF-7 cell line with GI_{50} value at 27.0 ± 0.57 μM while **275** and **276** exhibited moderate activity with GI_{50} values of 53.0 ± 4.7 and 44.0 ± 7.2 μM, respectively. It was found that **274** and **276** showed weak activity against NCI-H460 cell line (GI_{50} 84.0 ± 2.1 and 82.3 ± 5.6 μM, respectively) while **275** did not show any activity at the highest concentration tested (150 μM). Moreover, **276** exhibited weak activity against A375-C5 cell line with GI_{50} value of 108.0 ± 7.7 μM while **274** and **275** were inactive (Kijjoa *et al*., 2011).

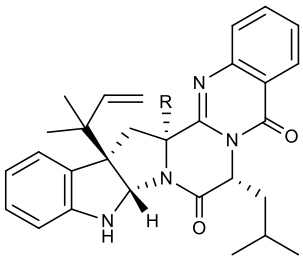

274 R = H
275 R = OH

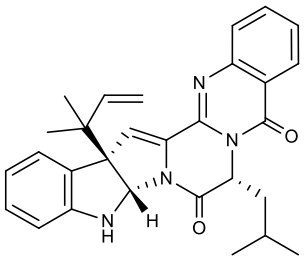

276

Figure 36. Structures of sartoryglabrins A – C (**274 – 276**).

Neosarphenols A (**277**) and **B** (**278**) were isolated, together with **methoxyvermistatin** (**279**), **6-demethylvermistatin** (**280**), **vermistatin** (**281**), **penicillide** (**282**), **purpactin A** (**283**), **phialophoriol** (**284**) and **chrodrimanins A** (**285**) and **B** (**286**) (Figure 37), from the fungus *N. glabra* CGMCC 32286 which was obtained from the Chinese Academy of Science. All isolated compounds were tested for their cytotoxicity against three human tumor cell lines: MDA-MB-231, MFC-7 and PANC-1. Compound **277** and **282** exhibited selective and moderate growth inhibitory activity against PANC-1 cell line with IC_{50} values of 14.38 and 10.93 μM, respectively. On the contrary, other compounds were inactive for all three cell lines (Liu *et al*., 2015).

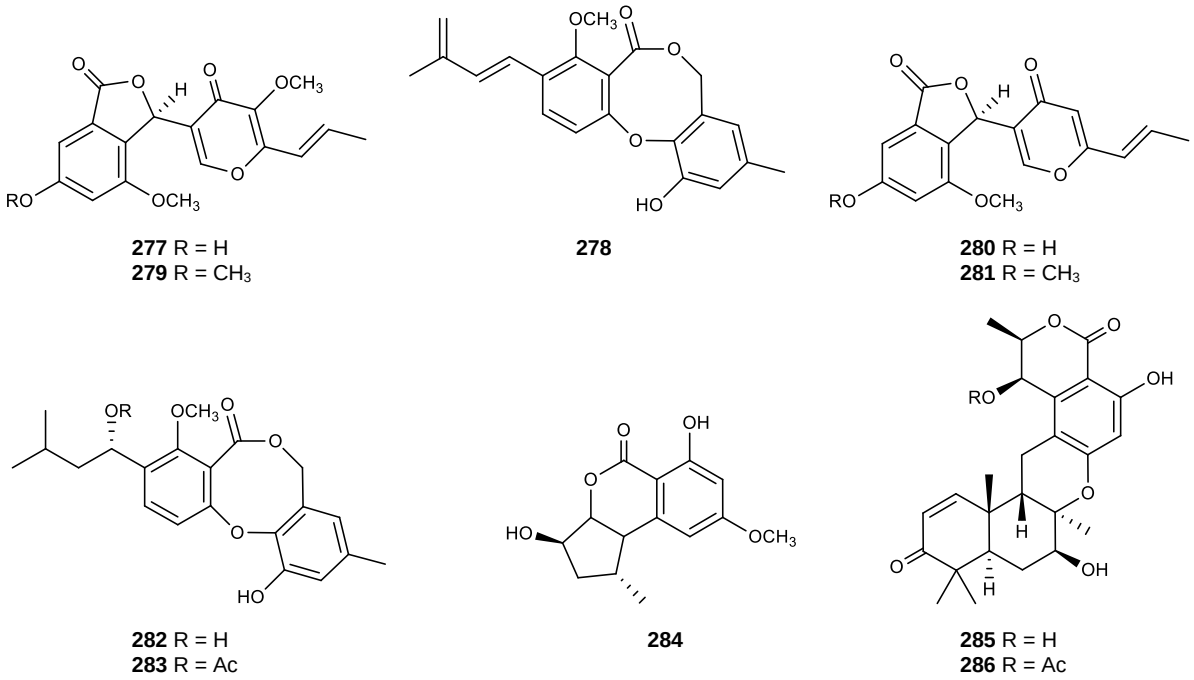

277 R = H
279 R = CH_3

278

280 R = H
281 R = CH_3

282 R = H
283 R = Ac

284

285 R = H
286 R = Ac

Figure 37. Structures of neosarphenols A (**277**) and B (**278**), methoxyvermistatin (**279**), 6-demethylvermistatin (**280**), vermistatin (**281**), penicillide (**282**), purpactin A (**283**), phialophoriol (**284**), and chrodrimanins A (**285**) and B (**286**).

Two cyclic tetrapeptides, **sartoryglabramides A** (**290**) and **B** (**291**), and a *bis*-indolylmethyldiketopiperazine, **fellutanine A epoxide** (**293**), together with **aszonalenin** (**241**), **(3*R*)-3-(1*H*-indol-3-ylmethyl)-3,4-dihydro-1*H*-1,4-benzodiazepine-2,5-dione** (**287**), **takakiamide** (**288**), **(11a*R*)-2,3-dihydro-1*H*-pyrrolo[2,1-*c*] [1,4]benzodiazepine-5,11(10*H*,11a*H*)-dione** (**289**) and **fellutanine A** (**292**) (Figure 38), were isolated from the marine-derived fungus *N. glabra* KUFA 0702 which was isolated from the marine sponge *Mycale* sp., collected from the coral reef at Samaesarn Island, Thailand. All isolated compounds were evaluated for their antimicrobial activity against two bacterial isolates: *Staphylococcus aureus* ATCC 46645 and *Escherichia coli* ATCC 25922, and three fungal isolates: *Aspergillus fumigatus* ATCC 46645, *Trichophyton rubrum* ATCC FF5 and *Candida albicans* ATCC 10231. The results revealed that all tested compounds were inactive at the highest concentration tested (256 µg/mL for antibacterial assay and 512 µg/mL for antifungal assay) (May Zin *et al*., 2016).

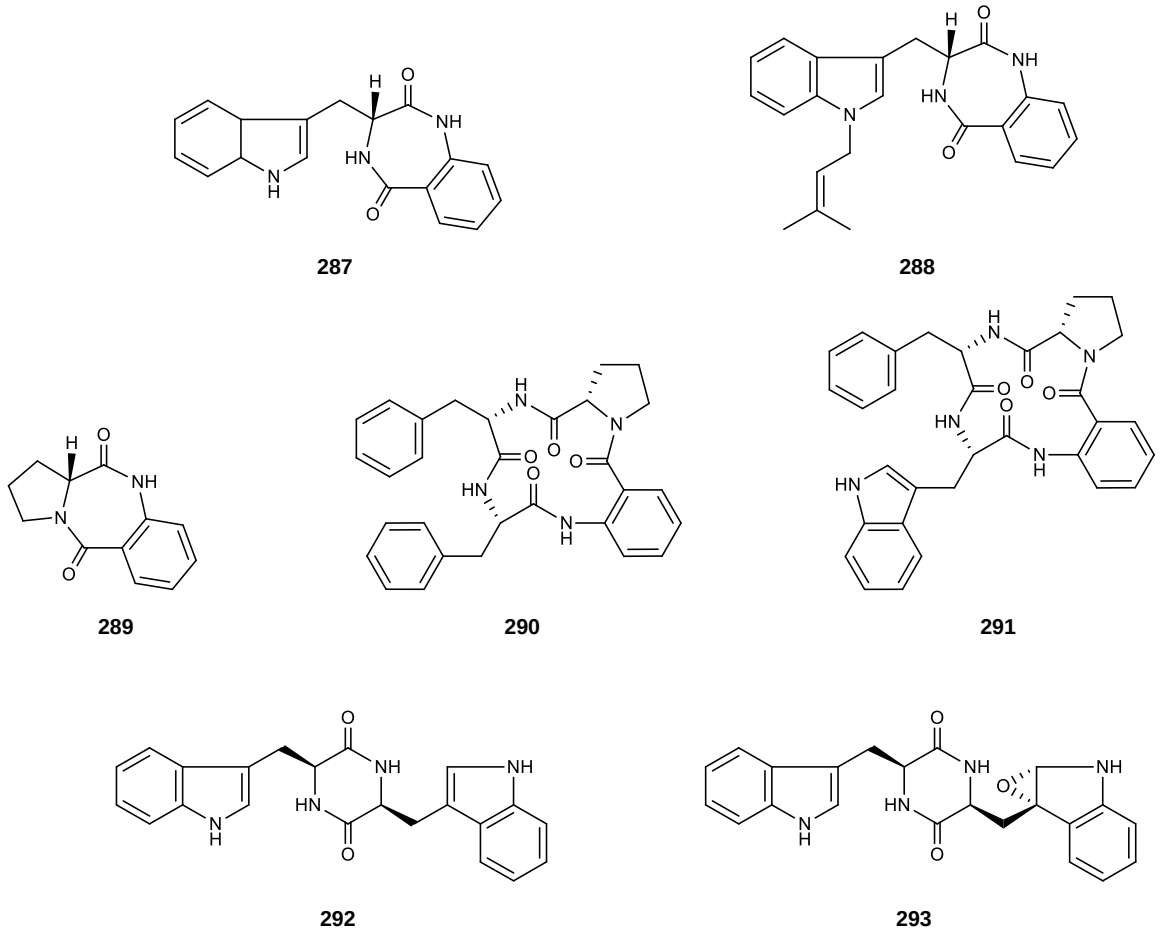

Figure 38. Structures of (3*R*)-3-(1*H*-indol-3-ylmethyl)-3,4-dihydro-1*H*-1,4-benzodiazepine-2,5-dione (**287**), takakiamide (**288**), (11a*R*)-2,3-dihydro-1*H*-pyrrolo[2,1-*c*][1,4] benzodiazepine-5,11(10*H*,11a*H*)-dione (**289**), sartoryglabramides A (**290**) and B (**291**), fellutanine A (**292**) and fellutamine A epoxide (**293**).

3.2.3) *Neosartorya laciniosa*

Eamvijarn *et al.* (2013) reported the isolation of **aszonapyrones A** (**256**) and **B** (**257**), **tryptoquivaline L** (**295**) and **3'-(4'oxoquinazoline-3-yl)spiro[1*H*-indole-3,5'-oxolane]-2,2'-dione** (**294**) (Figure 39) from the marine-derived fungus *N. laciniosa* (KUFC 7896) which was isolated from a diseased coral *Porites lutea,* collected from the Gulf of Thailand. Compounds **256** and **257** were evaluated for their *in vitro* growth inhibitory activity on three human cancer cell lines: MCF-7, NCI-H460 and A375-C5, using sulforhodamine B (SRB) assay. While **aszonapyrone A** (**256**) was found to exhibit potent activity with GI_{50} values of 13.6 ± 0.9, 11.6 ± 1.5 and 10.2 ± 1.2

µM, respectively, **aszonapyrone B** (**257**) which is a 3-deacetyl aszonapyrone A, did not exhibit any growth inhibitory activity against all tested cell lines. Later on, **tryptoquivaline T** (**296**), a new tryptoquivaline analogue (Figure 39), was also isolated from the same extract (Gomes *et al.,* 2014). All isolated compounds were evaluated for their antibacterial activity against Gram-positive (*Staphylococcus aureus* ATCC 25923 and *Bacillus subtilis* ATCC 6633) and Gram-negative (*Escherichia coli* ATCC 25922 and *Pseudomonas aeruginosa* ATCC 27853) bacteria and the multidrug-resistant isolates from the environment (*S. aureus* B1, *S. aureus* B2, *Enterococcus faecalis* W1 and *E. faecium* W5), and the synergistic effect with antibiotics, as well as antibiofilm activity. Only, **256** exhibited significant antibacterial activity with MIC value of 8 µg/mL against both *S. aureus* and *B. subtilis,* and also showed activity against both methicillin-resistant *S. aureus* (MRSA) and vancomycin-resistant *Enterococci* (VRE) isolates. Moreover, **256** also exhibited the synergistic effect with antibiotics against both Gram-negative reference strains and the multidrug-resistant isolates from the environment. Therefore, its biofilm formation inhibitory activity was evaluated. The results of antibiofilm assay of **256** revealed that this compound completely inhibited the biofilm formation at the concentrations of 2 × MIC and MIC, but it increased the production of biofilm at the sub-inhibitory concentration (1/2 MIC) (Gomes *et al*., 2014).

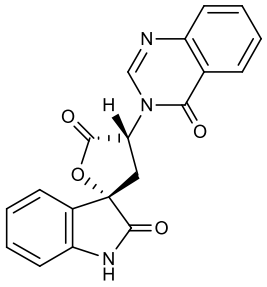

294

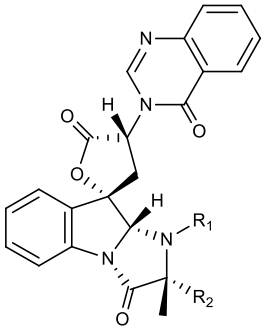

295 R_1 = OH, R_2 = CH_3

296 R_1 = CHO, R_2 = CH_3

Figure 39. Structures of 3'-(4'oxoquinazoline-3-yl)spiro[1*H*-indole-3,5'-oxolane]-2,2'-dione (**294**), and tryptoquivalines L (**295**) and T (**296**).

3.2.4) *Neosartorya paulistensis*

The meroditerpene, **sartorypyrone C** (**298**), was isolated, together with the previously described **tryptoquivalines L** (**295**), **H** (**299**), **F** (**300**), **3'-(4'oxoquinazolin-3-yl)spiro[1*H*-indole-3,5'-oxolane]-2,2'-dione** (**294**) and **4(3*H*)-quinazolinone** (**297**) (Figure 40), from the marine-derived fungus *N. paulistensis* KUFC 7897 which was isolated from the sponge *Chondrilla australiensis*, collected from Mu Kho Lan Beach, Chonburi Province, Thailand (Gomes *et al*., 2014).

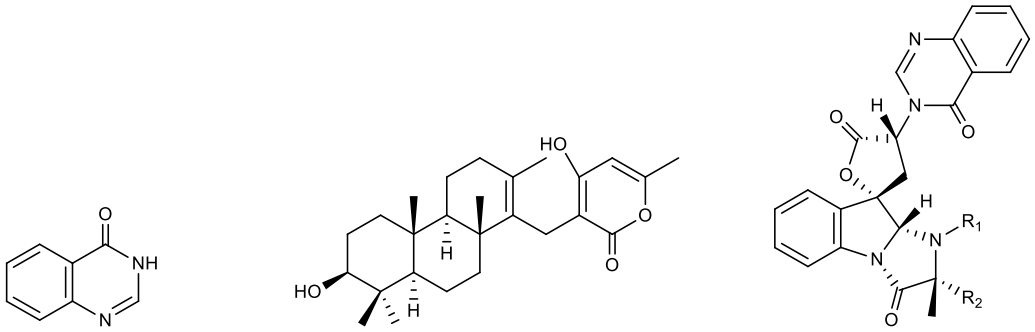

297 **298** **299** R_1 = OH, R_2 = H; **300** R_1 = H, R_2 = H

Figure 40. Structures of 4(3*H*)-quinazolinone (**297**), sartorypyrone C (**298**), and tryptoquivalines H (**299**) and F (**300**).

3.2.5) *Neosartorya pseudofischeri*

Two rotamers of debenzilpiperazine derivatives: **3,8-diacetyl-4-(3-methoxy-4,5-methylene-dioxy)benzyl-6-oxa-3,8-diazebicyclo[3.2.1]octane** (**301a** and **301b**), an indole alkaloid: **pseudofischerine** (**302**) ,and **3-hydroxy-5-methylphenyl-2,4-dihydroxy-6-methylbenzoate** (**303**), together with previously reported **cadinene** (**304**), **euroche-valierine** (**305**), **brasiliamide B** (**306**) (Figure 41) and **pyripyropene A** (**153**), were isolated from the soil-derived fungus *N. pseudofischeri*, collected from an agricultural soil sample in Thailand. All isolated compounds, except for **306**, were evaluated for their *in vitro* growth inhibitory activity on the human U373 and Hs683, A549, MCF-7, SKMEL-28 and OE21 cancer cell lines using etoposide and carboplatin as

reference compounds. Compound **305** exhibited anticancer activity in the range displayed by etoposide and carboplatin. Although **304** was less active than **305,** its activity was similar to that of carboplatin. Other compounds did not show any activity on all tested cell lines at the highest concentration tested (Eamvijarn *et al*., 2012).

The pyrroloindole terpenoid, **fischerindoline** (**307**), together with **eurochevalierine** (**305**), **pyripyropenes A** (**153**) and **E** (**154**), **sequiterpene** (**308**), **gliotoxin** (**309**) and **bis(dethio)bis(methylthio)gliotoxin** (**310**) (Figure 41), were isolated from the fungus *N. pseudofischeri* which was obtained from Centraalbureau voor Schimmelcultures of Baarn. All these compounds were evaluated for their *in vitro* growth inhibitory activity against five human cancer cell lines: A549, Hs683, MCF-7, SKMEL28 and U373, and a mouse cancer cell line: B16F10. Compound **309** exhibited the most potent activity with the median IC_{50} value for all cell lines < 0.05 μM. The growth inhibitory activity of **307** (the median IC_{50} 30 ± 2 μM) was similar to that displayed by **154** and **305** which exhibited the median IC_{50} values of 27.5 ± 1.6 and 38 ± 11 μM, respectively (Masi *et al*., 2013).

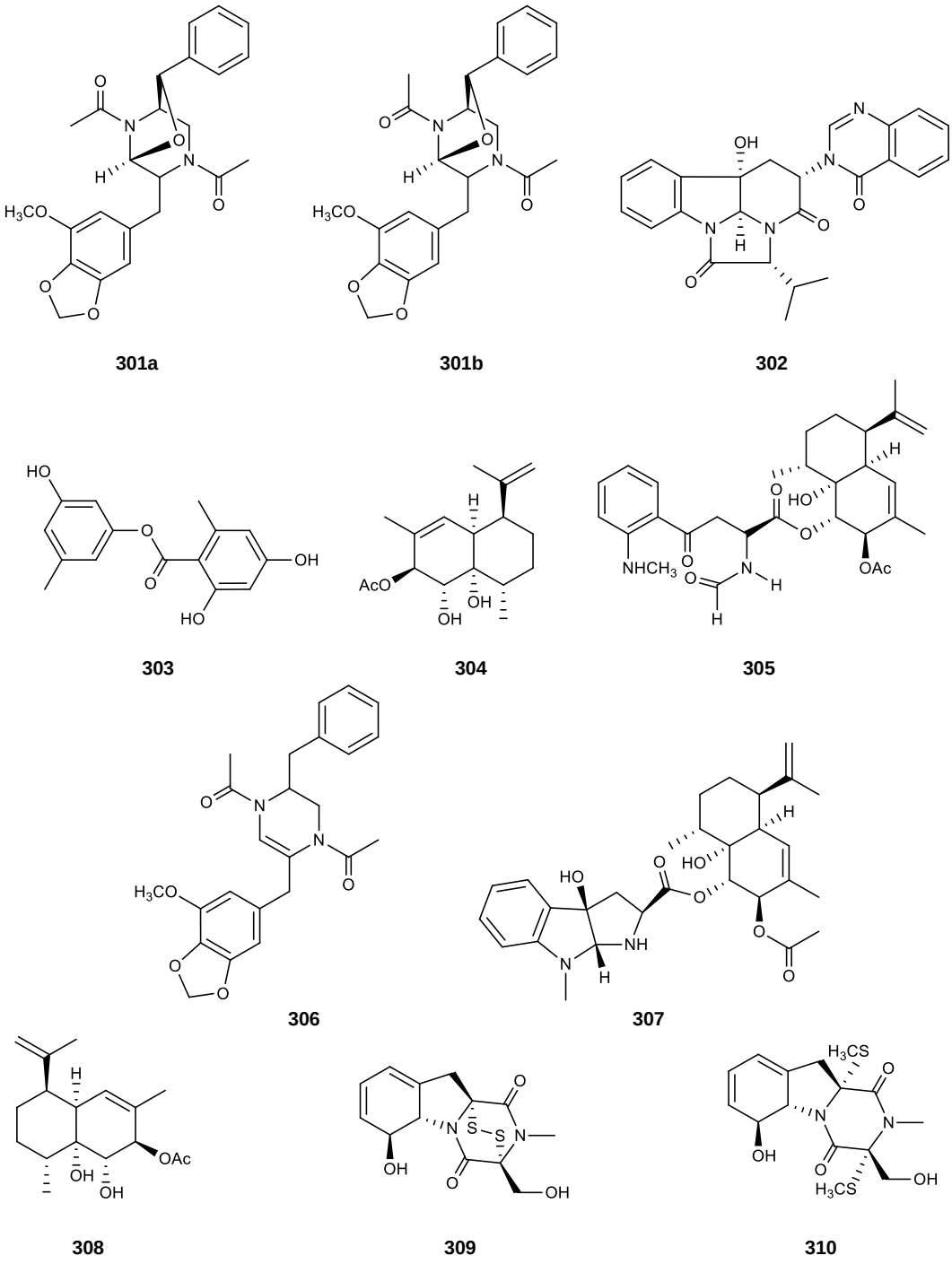

Figure 41. Structures of 3,8-diacetyl-4-(3-methoxy-4,5-methylenedioxy)benzyl-7-phenyl-6-oxa-3,8-diazabicyclo[3.2.1]octane (**301a, 301b**), pseudofischerine (**302**), 3-hydroxy-5-methyl-phenyl-2,4-dihydroxy-6-methylbenzoate (**303**), cadinene (**304**), eurochevalierine (**305**), brasiliamide B (**306**), fischerindoline (**307**), sequiterpene (**308**), gliotoxin (**309**) and bis(dethio)bis (methylthio)gliotoxin (**310**).

By using the glycerol-peptone-yeast extract (GlyPY) medium, Liang *et al*. (2014) was able to isolated **neosartins A** (**311**) and **B** (**312**), as well as **1,2,3,4-tetrahydro-2,3-dimethyl-1,4-dioxopyrazino[1,2-a]indole** (**313**), **1,2,3,4-tetrahydro-2-methyl-1,2,3-trioxopyrazino[1,2-a]indole** (**314**), **1,2,3,4-tetrahydro-2-methyl-1,3,4-trioxopyrazino [1,2-a]indole** (**315**), ***N*-methyl-*1H*-indole-2-carboxamide** (**316**), ***6*-acetylbis(methyl-thio)gliotoxin** (**319**), **bisdethiobis(methylthio)gliotoxin** (**320**), **didehydrobisdethio-bis(methylthio)gliotoxin** (**321**), from the culture of the marine-derived fungus *N. pseudofischeri* which was isolated from the inner tissue of the starfish *Acanthaster planci,* collected from Hainan Sanya National Coral Reef Reserve, China. However, when the fungus was cultured in the glucose-peptone-yeast extract (GluPY) medium, **neosartin C** (**323**), **pyripyropene A** (**153**), **gliotoxin** (**309**), **acetylgliotoxin** (**317**), **reduced gliotoxin** (**318**), **6-acetylbis(methylthio)gliotoxin** (**319**), **bisdethiobis(methylthio) gliotoxin** (**320**) and **bis-*N*-norgliovictin** (**322**) (Figure 42) were isolated. All isolated compounds, except for **153** and **311**, were tested for their antibacterial activity against *Staphylococcus aureus* ATCC 29213, methicillin-resistant *S. aureus* R3708 and *Escherichia coli* ATCC 25922. Compound **153** exhibited significant antibacterial activity against these three bacteria with MIC values of 12.20, 1.53 and 24.53 µM, respectively. Compound **318** also showed antibacterial activity, but less potent than **153**, with MIC values of 48.78, 1.52 and 97.56 µM, respectively. Other tested compounds were inactive for all bacterial strains at the highest concentration tested (256 µg/mL) (Liang *et al*., 2014).

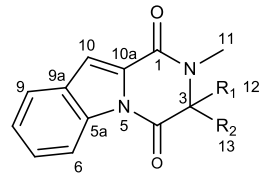

311 $R_1 = CH_3$, $R_2 = OCH_3$
312 $R_1 = CH_2OH$, $R_2 = OCH_3$
313 $R_1 = CH_3$, $R_2 = H$

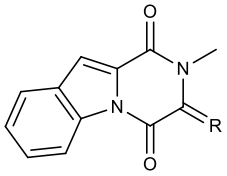

314 R = CH_2
315 R = O

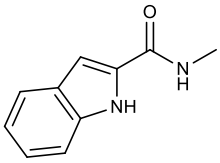

316

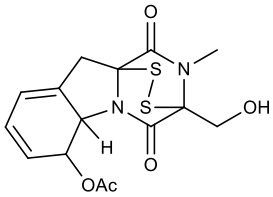

317

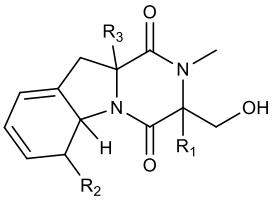

318 $R_1=R_3=SH$, $R_2 = OH$
319 $R_1=R_3=SCH_3$, $R_2 = Oac$
320 $R_1=R_3=SH$, $R_2 = OH$

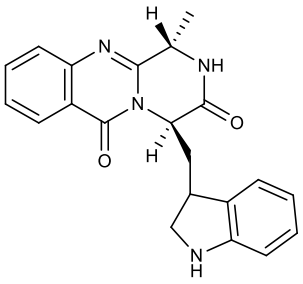

321

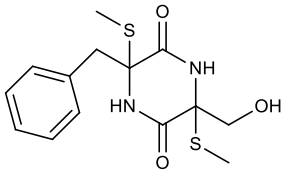

322

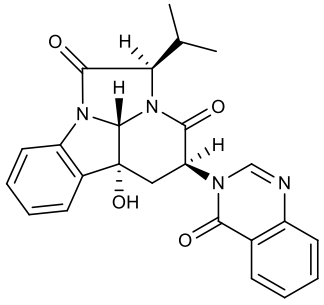

323

Figure 42. Stuctures of neosartins A (**311**) and B (**312**), 1,2,3,4-tetrahydro-2,3-dimethyl-1,4-dioxopyrazino[1,2-a]indole (**313**), 1,2,3,4-tetrahydro-2-methyl-1,2,3-trioxopyrazino[1,2-a]indole (**314**), 1,2,3,4-tetrahydro-2-methyl-1,3,4-trioxopyrazino[1,2-a]indole (**315**), *N*-methyl-*1H*-indole-2-carboxamide (**316**), acetylgliotoxin (**317**), reduced gliotoxin (**318**), 6-acetylbis(methylthio) gliotoxin (**319**), bisdethiobis(methylthio)gliotoxin (**320**), didehydrobisdethiobis(methylthio)gliotoxin (**321**), bis-*N*-norgliovictin (**322**) and neosartin C (**323**).

Recently, Lan *et al*. (2016) reported the isolation of **5-olefin phenylpyropene A** (**324**), **13-dehydroxylpyripyropene A** (**327**), **deacetylsesquiterpene** (**329**), **5-formyl-6-hydroxy-8-isopropyl-2-naphthoic acid** (**331**), **6,8-dihydroxyl-3-((1*E*,3*E*)-penta-1,3-dien-1-yl)isochroman-1-one** (**332**), **phenylpyropenes A** (**325**) and **C** (**326**), **pyripyropene A** (**153**), **7-deacetylpyripyropene A** (**328**), **(1*S*,2*R*,4a*R*,5*R*,8*R*,8a*R*)-1,8a-dihydroxy-2-acetoxy-3,8-dimethyl-5-(prop-1-en-2-yl)-1,2,4a,5,6,7,8,8a-octahydro-naphthalene** (**330**), **isochaetominine C** (**333**), **trichodermamide A** (**334**), **indolyl-3-acetic acid methyl ester** (**335**), **1-acetyl-β-carboline** (**336**), **1,2,3,4-tetrahydro-6-hydroxyl-2-methyl-1,3,4-trioxopyrazina[1,2-a]-indole** (**337**) and **fumiquinazoline F** (**338**) (Figure 43), from the same fungus. All isolated compounds, except for **334** – **336** and **338,** were evaluated for their cytotoxicity against the insect cell line Sf9 from *Spodoptera frugiperda.* All tested compounds exhibited significant cytotoxicity activity, especially **153, 325**, **326**, **329**-**331** and **337** which inhibited the cell growth rate more than 90% after 48 hours of treatment at 50 mg/L concentration.

3.2.6) *Neosartorya quadricincta*

Ozoe *et al*. (2004) reported the isolation of a dihydroisocoumarin derivative, **PF1223** (**339**) (Figure 44), from the culture of *N. quadricincta*. Compound **339** was investigated for its inhibitory activity of the specific binding of the noncompetitive antagonist [^{3}H]EBOB to housefly head membranes. At the concentration of 2.2 μM, this compound inhibited the [^{3}H]EBOB binding by 65%. The result suggested that **339** might prove to be a lead compound for insecticides acting at the insect GABA receptor.

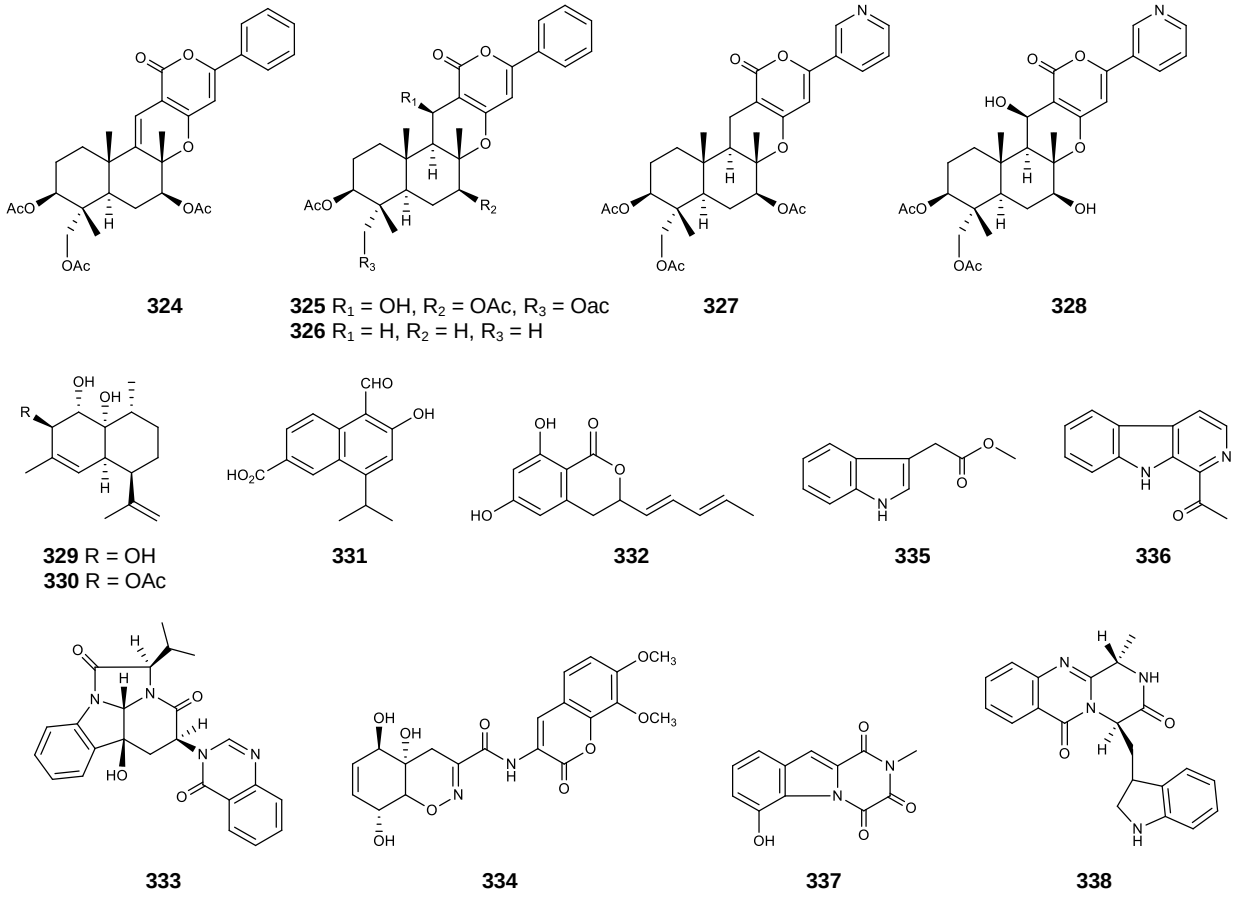

Figure 43. Structures of 5-olefin phenylpyropene A (**324**), phenylpyropenes A (**325**) and C (**326**), 13-dehydroxylpyripyropene A (**327**), 7-deacetylpyripyropene A (**328**), deacetylsesquiterpene (**329**), (1*S*,2*R*,4a*R*,5*R*,8*R*,8a*R*)-1,8a-dihydroxy-2-acetoxy-3,8-dimethyl-5-(prop-1-en-2-yl)-1,2,-4a,5,6,7,8,8a-octahydronaphthalene (**330**), 5-formyl-6-hydroxy-8-isopropyl-2-naphthoic acid (**331**), 6,8-dihydroxyl-3-((1*E*,3*E*)-penta-1,3-dien-1-yl)isochroman-1-one (**332**), isochaetominine C (**333**), trichodermamide A (**334**), indolyl-3-acetic acid methyl ester (**335**), 1-acetyl-β-carboline (**336**), 1,2,3,4-tetrahydro-6-hydroxyl-2-methyl-1,3,4-trioxopyrazina[1,2-a]-indole (**337**) and fumiquinazoline F (**338**).

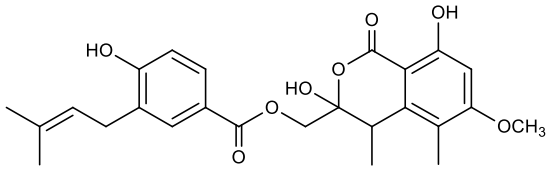

339

Figure 44. Structure of PF1223 (**339**).

3.2.7) *Neosartorya siamensis*

The culture of the soil-derived fungus *N. siemensis* (KUFC 6349), isolated from forest soil sample, collected at Sameasarn Island, Thailand, furnished **sartorymensin** (**341**), **tryptoquivaline O** (**343**), **3'-(4-oxoquinazolin-3-yl)spiro[1*H*-indole-3,5'-oxolane]-2,2'-dione** (**294**), **epi-fiscalin C** (**344**), **epi-fiscalin A** (**345**), **neofiscalin A** (**346**) and **epi-neofiscalin A** (**347**), together with seven previously reported compounds: **2,4-dihydroxy-3-methylactophenone** (**340**), **tryptoquivaline** (**342**), **tryptoquivalines L** (**295**), **H** (**299**) and **F** (**300**) (Figure 45), and **fiscalins A** (**231**) and **C** (**233**). Compounds **294** – **295**, **299** – **300**, **341** – **343** and **345** were examined for their growth inhibitory activity against the human U373, Hs683, A549, MCF-7 and SKMEL-28 cell lines, by MTT colorimetric assay. However, only **341** exhibited moderate growth inhibitory activity against five tested cell lines with IC_{50} values of 44, 50, 39, 43 and 73 μM, respectively (Buttachon *et al*., 2012)

Reexamined the nonpolar fractions from the column chromatography of this fungus led to the isolation of **chevalones B** (**348**) and **C** (**349**) (Figure 45) (Gomes *et al.,* 2014).

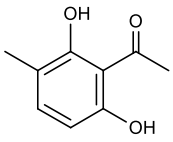

340

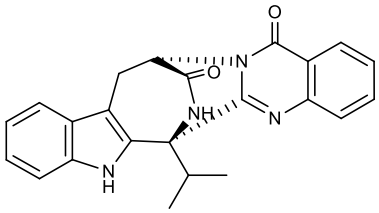

341

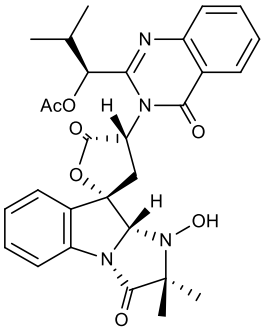

342

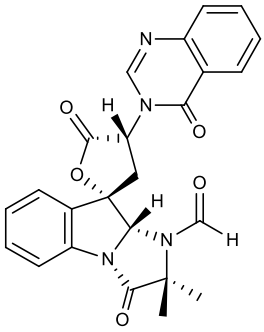

343

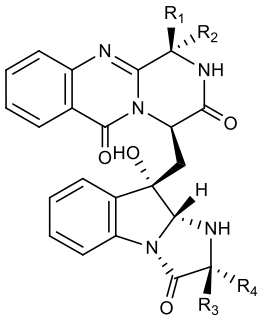

344 $R_1 = CH(CH_3)_2$, $R_2 = H$, $R_3 = R_4 = CH_3$
345 $R_1 = CH(CH_3)_2$, $R_2 = R_4 = H$, $R_3 = CH_3$
346 $R_1 = R_3 = H$, $R_2 = CH(CH_3)_2$, $R_4 = CH_3$
347 $R_1 = CH(CH_3)_2$, $R_2 = R_3 = H$, $R_4 = CH_3$

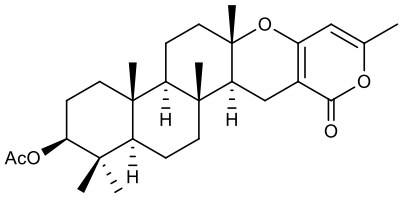

438

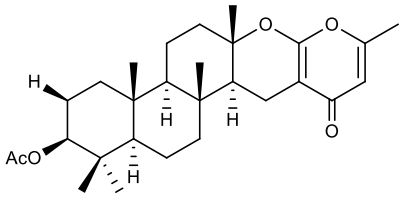

339

Figure 45. Structures of 2,4-dihydroxy-3-methylacetophenone (**340**), sartorymensin (**341**), tryptoquivaline (**342**), tryptoquivaline O (**343**), epi-fiscalin C (**344**), epi-fiscalin A (**345**), neofiscalin A (**346**), epi-neofiscalin A (**347**), and chevalones B (**348**) and C (**349**).

Chromatographic fractionation of the ethyl acetate extract of the culture of the marine-derived fungus *N. siamensis* (KUFA 0017) which was isolated from the sea fan *Rumphella* sp., collected from Similan Island, led to the isolation of **2,4-dihydroxy-3-methylacetophenone** (**340**), **chevalone C** (**349**), **tryptoquivaline** (**342**), **nortryptoquivaline** (**240**), **tryptoquivalines L** (**295**), **H** (**299**) and **F** (**300**), **fiscalin A** (**231**), ***epi*-fiscalin A** (**345**), **neofiscalin A** (**346**), ***epi*-neofiscaline A** (**347**), **fiscalin C** (**233**), ***epi*-fiscalin C** (**344**) and **3'-(4-oxoquinazolin-3-yl)spiro[1*H*-indole-3,5'-**

oxolane]-2,2'-dione (**294**). Compounds **231, 240, 299 – 300, 340**, **344 – 345**, **347** and **349** were evaluated for their anti-proliferative activity, DNA damage induction, and induction of cell death. Compounds **231**, **240**, **344, 345**, **347** and **349** exhibited the anti-proliferative activity with IC_{50} values ranging from 24 to 153 µM in HepG2, HCT116 and HT29 cancer cell lines. Compounds **231, 240** and **349** induced cell death in HCT116 cell line while **231**, **240**, **345** and **347** induced significant cell death in HepG2. Since none of the compounds induced significant DNA damage, this induction of cell death is possibly not related to genotoxicity (Prata-Sena *et al*., 2016).

3'-(4-oxoquinazolin-3-yl)spiro[1*H*-indole-3,5'-oxolane]-2,2'-dione (**294**), **nortryptoquivaline** (**240**), **tryptoquivalines L** (**295**), **H** (**299**) and **F** (**300**), **fiscalin A** (**231**), ***epi*-fiscalin A** (**345**), **neofiscalin A** (**346**), ***epi*-neofiscalin A** (**347**) and ***epi*-fiscalin C** (**344**) which were isolated from the marine-derived fungus *N. siamensis* KUFA 0017 (Prata-Sena *et al.,* 2016), together with **tryptoquivaline O** (**343**), **fiscalin C** (**223**) and **sartorymensin** (**341**) which were previously isolated from the soil-derived fungus *N. siamensis* KUFC 6349 (Buttachon et al., 2012), were evaluated for their antibacterial activity against Gram-positive (*Staphylococcus aureus* ATCC 25923, *Enterococcus faecalis* ATCC 29212) and Gram-negative (*Escherichia coli* ATCC 25922 and *Pseudomonas aeruginosa* ATCC 27853) bacteria, as well as the multidrug-resistant isolates from environment (*S. aureus* B1 and *E. faecalis* W1). All tested compounds were inactive at the highest concentration tested (256 µg/mL), except for **neofiscalin A** (**346**) which exhibited antibacterial activity against all strains of *S. aureus* and *E. faecalis* with MIC 8 µg/mL. Based on the results of a screening susceptibility test for synergistic effect of the compounds and antibiotics against *S. aureus* B1 and *E. faecalis* W1, the synergy of **fiscalin C** (**233**) and oxacillin or ampicillin were evaluated against the methicillin-resistant *S. aureus* (*S. aureus* B1) using a broth microdilution checkerboard method. The results revealed that there was the synergy between **233** and oxacillin (FIC index < 0.5), while the combination of **233** and ampicillin did not show any synergistic effect (0.5 < FIC index ≤ 4). Moreover, **neofiscalin A** (**346**) was tested for antibiofilm activity against *S. aurues* B1 and *E. faecalis* W1, and cytotoxicity toward a human brain microvascular endothelial cell line (hCMEC/D3). Compound **346** completely inhibited the biofilm

formation at the concentration of 2 x MIC and MIC, and did not exhibit cytotoxicity against hCMEC/D3 cell line at concentrations of 5, 10 and 20 µg/mL (Bessa *et al*., 2016).

3.2.8) *Neosartorya spatulata*

Besides the production of secondary metabolites, the fungi of the genus *Neosartorya* have been also investigated for their capacity to transform other compounds to interesting metabolites. For example, **α-Mangostin** (**350**), a prenylated xanthone isolated from the fruit hull of *Garcinia mangostana* L., was metabolized by fungus *N. spatulata* (EYR042) to give **mangostin-3-sulfate** (**351**) (Figure 46). Compounds **350** and **351** exhibited significant anti-mycobacterial activity against *Mycobacterium tuberculosis* with MIC values of 15.24 and 6.75 µM, respectively. (Arunrattiyakorn *et al*., 2011).

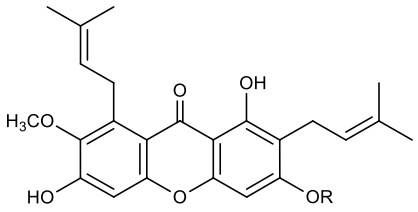

350 R = H
351 R = SO_3H

Figure 46. Structures of α-mangostin (**350**) and mangostin-3-sulfate (**351**).

3.2.9) *Neosartorya spinosa*

Four chevalone C analogues: **1-hydroxychevalone C** (**352**), **1-acetoxy-chevalone C** (**353**), **1,11-dihydroxychevalone C** (**354**) and **11-hydroxychevalone C** (**355**), together with **2*S*,4*S*-spinosate** (**357**) and **2*S*,4*R*-spinosate** (**358**), **chevalones B** (**348**), **C** (**349**), **E** (**356**), **tryptoquivaline** (**342**), **nortryptoquivaline** (**240**), **tryptoquivaline L** (**295**) and **quinadoline A** (**359**) (Figure 47), were isolated from the soil fungus *N. spinosa* which was isolated from a forest soil, collected around the Pha Nok Kao Silvicultural station, Chon Kaen Province, Thailand. Compound **342** and **353**

exhibited weak antimalarial activity against *Plasmodium falciparum* with IC_{50} values of 6.67 and 2.65 μM, respectively, while **352** showed antimycobacterial activity against *Mycobacterium tuberculosis* with MIC value of 26.4 μM. Moreover, **352**-**354** and **359** exhibited also cytotoxicity against two human cancer cell lines, KB and NCI-H187 with IC_{50} values ranging from 32.7 to 103.3 μM (Rajachan *et al*., 2016).

3.2.10) *Neosartorya takakii*

A meroditerpene, **sartorenol** (**360**), **tryptoquivaline U** (**361**) (Figure 48), and **takakiamide** (**288**) were isolated, together with the previously described compounds, including **aszonalenin** (**241**), **acetylaszonalenin** (**252**), **aszonapyrone A** (**256**), **tryptoquivalines L** (**295**), **H** (**299**), **F** (**300**), **3'-(4-oxoquinazolin-3-yl)spiro[1*H*-indole-3,5'-oxolane]-2,2'-dione** (**294**), **chevalone B** (**348**) and **6-hydroxymellein**, from the algicolous fungus *N. takakii* KUFC 7898 which was obtained from the alga *Amphiroa* sp., collected from Samaesarn Island, Thailand. Compounds **241**, **288** and **360** were tested for their antimicrobial activity against Gram-positive (*Staphylococcus aureus* ATCC 25923 and *Bacillus subtilis* ATCC 6633) and Gram-negative (*Escherichia coli* ATCC 25922 and *Pseudomonas aeruginosa* ATCC 27853) bacteria, as well as the multidrug-resistant isolates from environment. All tested compounds were inactive at the highest concentration tested (256 μg/mL). Furthermore, these three compounds were also evaluated for antiquorum sensing activity toward *Chromobacterium violaceum* ATCC 31532, however none of them exhibited the activity (May Zin *et al*., 2015).

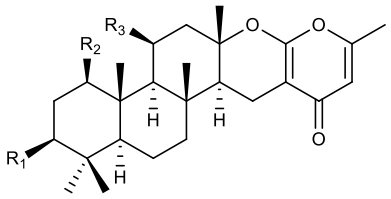

352 R_1 = OAc, R_2 = OH, R_3 = H
353 R_1 = OAc, R_2 = OAc, R_3 = H
354 R_1 = OAc, R_2 = OH, R_3 = OH
355 R_1 = OAc, R_2 = H, R_3 = OH
356 R_1 = OH, R_2 = H, R_3 = H

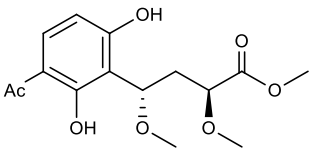

357

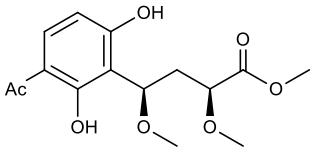

358

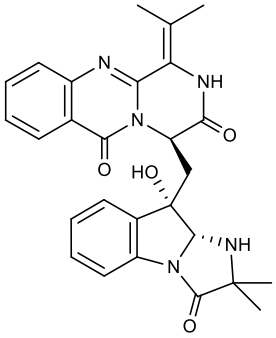

359

Figure 47. Structures of 1-hydroxychevalone C (**352**), 1-acetoxychevalone C (**353**), 1,11-dihydroxychevalone C (**354**), 11-hydroxychevalone C (**355**), chevalone E (**356**), 2*S*,4*S*-spinosate (**357**), 2*S*,4*R*-spinosate (**358**) and quinadoline A (**359**).

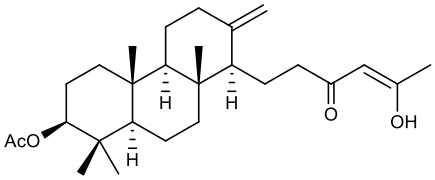

360

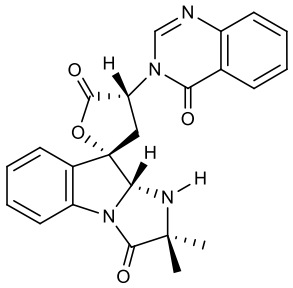

361

Figure 48. Structures of sartorenol (**360**) and tryptoquivaline U (**361**).

3.2.11) *Neosartorya tatenoi*

A meroditerpene, **tatenoic acid** (**362**) (Figure 49), **aszonapyrones A** (**256**) and **B** (**257**), **aszonalenin** (**241**), **ergosterol** (**267**) and **D-mannitol**, were isolated from the soil fungus *Neosartorya tatenoi* KUU-2NK23 which was isolated from the forest soil, collected around the Pha Nok Kao Silvicultural Station, Khon Kaen Province, Thailand. Compounds **241**, **256** and **257** were evaluated for their antimalarial and cytotoxic activities. Compound **256** exhibited antimalarial activity against *Plasmodium falciparum* with IC_{50} value of 1.34 µg/mL, and displayed cytotoxicity against NCI-H187 and KB cancer cell lines, with IC_{50} values of 4.62 and 48.18 µg/mL, respectively, while compounds **241** and **257** were found to be inactive for all tests (Yim *et al*., 2014).

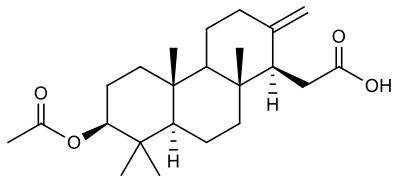

362

Figure 49. Structure of tatenoic acid (**362**).

3.2.12) *Neosartorya tsunodae*

The marine-derived fungus *N. tsunodae* (KUFC 9213) which was isolated from the marine sponge *Aka coralliphaga,* collected in the Similan Islands, Thailand, furnished a meroditerpene **sartorypyrone B** (**363**) (Figure 50) and **helvolic acid** (**148**). Compound **363** was found to exhibit potent growth inhibitory activity against MCF-7, NCI-H460 and A375-C5 cancer cell lines with GI_{50} valeus of 17.8 ± 7.4, 20.5 ± 2.4 and 25.0 ± 4.4 µM, respectively (Eamvijarn *et al*., 2013).

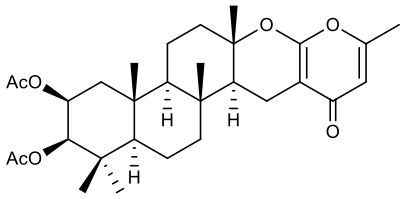

363

Figure 50. Structure of sartorypyrone B (**363**).

3.2.13) Unspecified *Neosartorya* species

3.2.13.1) *Neosartorya sp.*

Asami *et al*. (2002) reported a new angiogenesis inhibitor, **azaspirene** (**364**) (Figure 51), which contains a 1-oxa-7-azaspiro[4.4]non-2-ene-4,6-dione skeleton. This compound was isolated from the soil fungus *Neosartorya* sp. Compound **364** completely inhibited the migration of human umbilical vein endothelial cells (HUVECs) induced by vascular endothelial growth factor (VEGF) at concentration of 27.1 μM (ED_{100} = 27.1 μM) without any significant cell toxicity. Later on, Asami *et al*. (2008) continued investigating the *in vivo* antiangiogenic activity of **364**, using *in vivo* tumor-induced angiogenesis in a renal carcinoma xenograft model and chicken chorioallantoic membrane assay. The results showed that the number of blood vessels oriented toward tumor was decreased with azaspirene (**364**) treatment, and administration of azaspirene (**364**) at 30 μg/egg resulted in the inhibition of angiogenesis (23.6-45.3 % maximum inhibition relative to the controls) in the chick embryo without any sign of thrombosis or hemorrhage in a chicken CAM assay. The mechanism of this compound was evaluated on VEGF-induced activation of the mitogen-activated protein kinase signaling pathway in HVEC, resulting in the suppression of Raf-1 activation without affecting the activation of kinase insert domain-containing receptor/fetal liver kinase 1 (VEGF receptor 2). In addition, **364** inhibited the growth of HUVEC, but not of NIH3T3, MSS31, HeLa and MCF-7.

Later on, Asami *et al*. (2004) also discovered another angiogenesis inhibitor, **RK-805** (**365**) (Figure 51), from the fermentation broth of the fungus *Neosartory sp.*

Compound **365**, which was identified as 6-oxo-6-deoxyfumagillol, was tested for the growth inhibitory activity in both HUVECs and normal human lung fibroblast (WI-38) cells. Compound **365** inhibited the growth of HUVECs in a dose-dependent manner with IC_{50} value of 0.03 ng/mL, but did not exhibited inhibitory activity toward WI-38 cells. Compound **365** also showed the inhibitory activity against the cell migration induced by VEGF in a dose-dependent manner without showing significant cell toxicity, with ED_{50} value of 10 ng/mL. Moreover, this compound selectively inhibited on methionine aminopeptidase-2 (MetAP2).

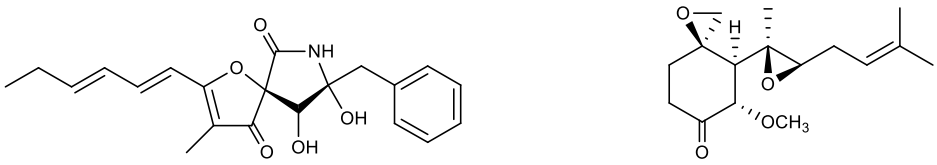

364 **365**

Figure 51. Structures of azaspirene (**364**) and RK-805 (**365**).

3.2.13.2) *Neosartorya* sp. HN-M-3

F. Y. Sun *et al*., (2012) reported the isolation of **tryptoquivalines P** (**366**) and **Q** (**367**) (Figure 52) from the marine-derived fungus *Neosartorya* sp. HN-M-3 which was isolated from mud, collected from the intertidal zone of Hainan Province, China.

Later on, Xu *et al*., (2013) reported other two tryptoquivaline analogues, **tryptoquivalines R** (**368**) and **S** (**369**) (Figure 52), from the same fungus. Both compounds did not exhibit cytotoxicity against HL-60 cell line at the highest concentration tested (100 μM).

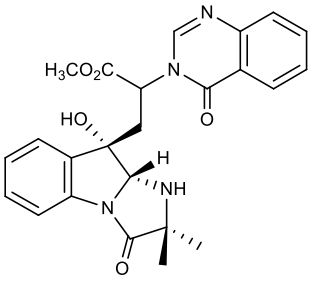

366

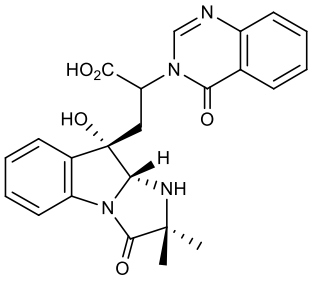

367

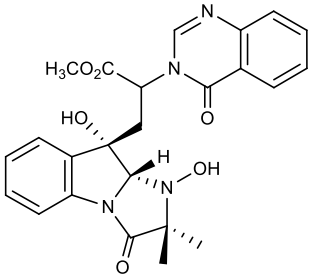

368

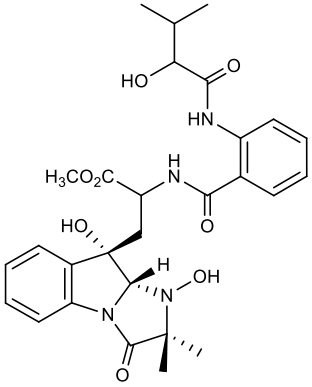

369

Figure 52. Structures of tryptoquivalines P – S (**366 – 369**).

CHAPTER IV

RESULTS AND DISCUSSION

4.1) The Marine Sponge *Iotrochota baculifera*

Chromatographic fractionation and further purification of the ethyl acetate (EtOAc) crude extract of the marine sponge *Iotrochota baculifera,* collected from the Gulf of Thailand, Chonburi Province, Thailand, resulted in isolation of two previously reported, 6-bromo-1*H*-indole-3-carbaldehyde (**40**) and methyl (2*E*)-3-(6-bromo-1*H*-indol-3-yl)-prop-2-enoate (**370**) (figure 53).

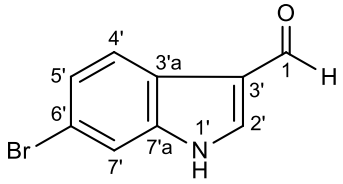

40

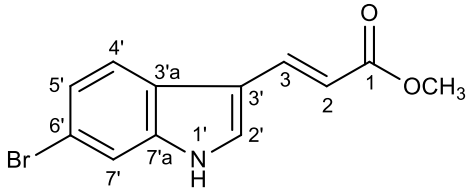

370

Figure 53. Structures of 6-bromo-1*H*-indole-3-carbaldehyde (**40**) and methyl (2*E*)-3-(6-bromo-1*H*-indol-3-yl)-prop-2-enoate (**370**).

4.1.1) 6-Bromo-1*H*-indole-3-carbaldehyde (40)

Compound **40** was isolated as a white crystal (mp, 205 – 206 °C). Its molecular formula, C_9H_6NOBr, was determined on the basis of (+)-HRESIMS *m/z* 223.9704 $[M+H]^+$, indicating seven degrees of unsaturation.

The ^{13}C NMR spectrum exhibited nine carbon signals which, in conjunction with the DEPTs and HSQC spectra, can be classified to one conjugated aldehyde carbonyl (δ_C 185.2), four quaternary sp^2 (δ_C 138.0, 123.1, 118.0 and 116.0), and four methine sp^2 (δ_C 139.2, 125.1, 122.5 and 115.2) carbons (Table 4).

The ^{1}H NMR spectrum (Table 4) exhibited, three doublet aromatic protons at δ_H 8.02, *J* = 8.4 Hz (δ_C 122.5); δ_H 7.71, *J* = 1.1 Hz (δ_C 115.2); δ_H 7.37, brd, *J* = 8.4 Hz (δ_C 125.1), one singlet of an amine proton at δ_H 12.23 which was evidenced by the chemical shift value and HRMS data, one doublet of aldehyde proton at δ_H 9.93, *J* = 0.6 Hz (δ_C 185.2), and one double doublet of olefinic proton at δ_H 8.33, *J* = 3.5, 0.7 Hz (δ_C 139.2).

Analysis of the coupling constant values of the three aromatic protons, together with the COSY correlation (Table 4), indicated the presence of the 1,2,4-trisubstitued benzene ring which confirmed by the HMBC correlations from H-4' to the carbons at δ_C 116.0 (C-6') and δ_C 138.0 (C-7'a), from H-5' to the carbons at δ_C 123.1 (C-3'a) and δ_C 115.2 (C-7'), and from H-7' to C-3'a and C-6'. The bromine atom was placed on C-6' since its chemical shift value (δ_C 116.0) indicated that it was substituted by an electron withdrawing group.

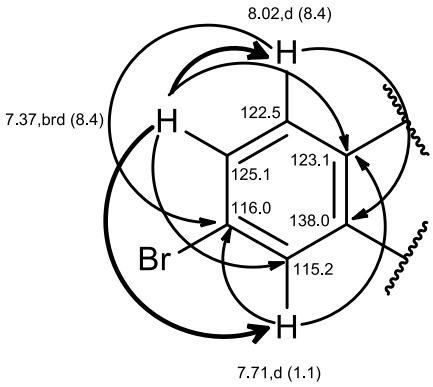

The COSY spectrum displayed cross peak from the amine proton at δ_H 12.23, s (H-1') to the olefinic proton at δ_H 8.33, dd, *J* = 3.5, 0.7 Hz (H-2'), together with the HMBC correlations from the proton at δ_H 9.93, d, *J* = 0.6 Hz (H-1) to the carbon at δ_C 118.0 (C-3') and C-3'a, and from H-2' to the carbon at δ_C 185.2 (C-1), C-3', C-3'a, and C-7'a. Combining the (+)-HRESIMS and NMR data, the structure of **40** was 6-bromo-1*H*-indole-3-carbaldehyde.

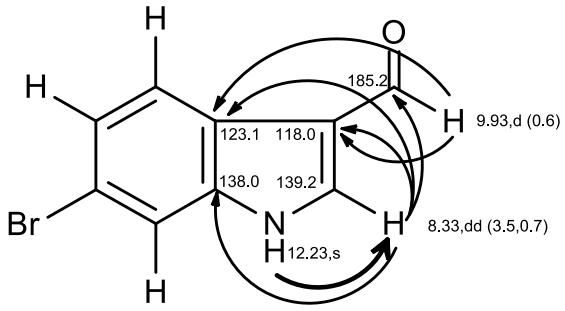

Table 4. ^{1}H and ^{13}C NMR (DMSO, 300.13 MHz and 75.4 MHz), and HMBC assignment for 6-bromo-1*H*-indole-3-carbaldehyde (**40**).

Position	δ_C, type	δ_H, (*J* in Hz)	COSY	HMBC
1	185.2, CHO	9.93, d (0.6)	-	C-3', 3'a
2'	139.2, CH	8.33, dd (3.5, 0.7)	H-1'	C-1, 3', 3'a, 7'a
3'	118.0, C	-	-	-
3'a	123.1, C	-	-	-
4'	122.5, CH	8.02, d (8.4)	H-5'	C-6', 7'a
5'	125.1, CH	7.37, brd (8.4)	H-4', 7'	C-3'a, 7'
6'	116.0, C	-	-	-
7'	115.2, CH	7.71, d (1.1)	H-5'	C-3'a, 6'
7'a	138.0, C	-	-	-
NH	-	12.23, s	H-2'	-

The literature search revealed that **40** was previously isolated from several marine sponges, including *Pseudosuberites hyalinus* (Rasmussen *et al*., 1993), *Halichondria* sp. (Li *et al*., 1994), *Iotrochota purpurea* (Carletti *et al*., 2000; Ibrahim *et al*., 2009), *Smenospongia* sp. (McKay *et al*., 2002), and *Rhopaloeides odorabile* (Longeon *et al*., 2011). Interestingly, this compound was also isolated from several bacteria, such as *Pseudomonad* sp. (Wratten *et al*., 1977) and *Acinetobacter* sp. (Olguin-Uribe *et al*., 1997), as well as from a brown alga *Laminaria japonica* Aresch. (Wang *et al*., 2013). The bioactivities of 6-bromo-1*H*-3-carbaldehyde were reported as antifungal activity against *Mortierella ramannianus* (Li *et al*., 1994) and antifouling activity by inhibiting the settlement of barnacle larvae. (Olguin-Uribe *et al*., 1997).

4.1.2) Methyl (2*E*)-3-(6-bromo-1*H*-indol-3-yl)-prop-2-enoate (370)

Compound **370** was isolated as a white crystal (mp, 212 – 214 °C), and its molecular formula $C_{12}H_{10}NO_2Br$ was established based on the (+)-HRESIMS *m/z* 279.9973 $[M+H]^+$, indicating eight degrees of unsaturation.

The general features of the ^1H and ^{13}C of **370** resembled those of **40**. The ^{13}C NMR spectrum exhibited twelve carbon signals which can be classified as one conjugated ester carbonyl (δ_C 167.6), four quaternary sp^2 (δ_C 138.2, 124.0, 115.1 and 111.8), six methine sp^2 (δ_C 138.4, 132.6, 123.7, 121.7, 115.0 and 111.6), and one methoxy (δ_C 51.1) carbons, based on the data from the DEPTs and HSQC experiments (Table 5)

The ^1H NMR spectrum, in combination with the HSQC spectrum (Table 5) of **370**, also exhibited signals of the protons of the 3',6'-substituted indole nucleus: one amine proton at δ_H 11.89, s, one olefinic proton at δ_H 7.99, d, *J* = 2.8 Hz (δ_C 132.6), and three aromatic protons at δ_H 7.85, d, *J* = 8.5 Hz (δ_C 121.7); δ_H 7.66, d, *J* = 1.8 Hz (δ_C 115.0); δ_H 7.28, dd, *J* = 8.5, 1.8 Hz (δ_C 123.7). This was also confirmed by the COSY correlations (Table 5) from H-5' to H-4' and H-7', as well as by the HMBC correlations (Table 5) from H-2' to the carbons at δ_C 111.8 (C-3'), δ_C 124.0 (C-3'a) and δ_C 138.2 (C-7'a), from H-4' to C-3'a, the carbon at δ_C 115.1 (C-6') and C-7'a, from H-5' to C-3'a and the carbon at δ_C 115.0 (C-7'), from H-7' to C-3'a and C-6', and from the amine proton at δ_H 11.89, s (H-1') to the carbon at δ_C 132.6 (C-2'), C-3', C-3'a and C-7'a.

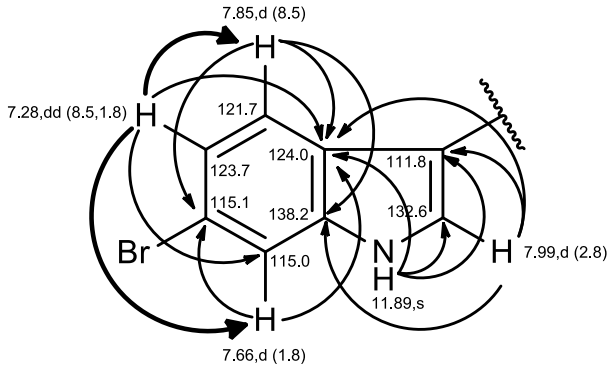

Compound **370** differed from **40** only in the sidechain of the bromoindole nucleus. Instead of the presence of the aldehydic group, the side chain of **40** was methyl (2*E*)-prop-2-enoate. This was supported by the presence of the *trans* double bond (δ_H 7.87, d, J = 16.1 Hz/ δ_C 138.4; δ_H 6.39, d, J = 16.0 Hz/ δ_C 111.6), a conjugated ester carbonyl (δ_C 167.6) and a methoxyl group (δ_H 3.71, s, δ_C 51.1). Since the olefinic proton at δ_H 7.87, d, J = 16.1 Hz (H-3) exhibited the HMBC correlations to the ester carbonyl at δ_C 167.6 (C-1), C-2 and C-3, **370** was identified as methyl (2*E*)-3-(6-bromo-1*H*-indol-3-yl)-prop-2-enoate. Literature survey revealed that this compound has been previously isolated from the sponge *Iotrochota* sp. (Dellar *et al*., 1981).

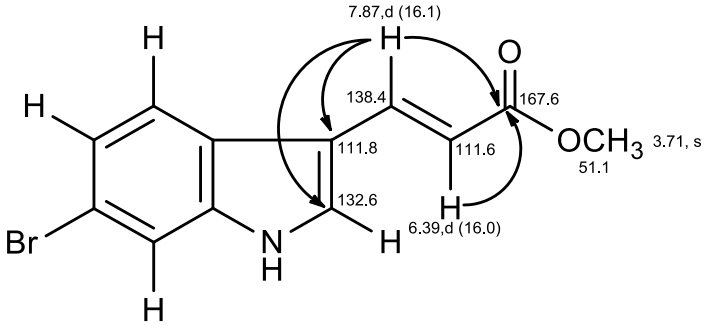

Table 5. ^{1}H and ^{13}C NMR (DMSO, 300.13 MHz and 75.4 MHz), and HMBC assignment for methyl (2*E*)-3-(6-bromo-1*H*-indol-3-yl)-prop-2-enoate (**370**).

Position	δ_C, type	δ_H, (J in Hz)	COSY	HMBC
1	167.6, CO	-	-	-
2	111.6, CH	6.39, d (16.0)	H-3	C-1
3	138.4, CH	7.87, d (16.1)	H-2	C-1, 2', 3'
2'	132.6, CH	7.99, d (2.8)	-	C-3', 3'a, 7'a
3'	111.8, C	-	-	-
3'a	124.0, C	-	-	-
4'	121.7, CH	7.85, d (8.5)	H-5'	C-3'a, 6', 7'a
5'	123.7, CH	7.28, dd (8.5, 1.8)	H-4', 7'	C-3'a, 7'
6'	115.1, C	-	-	-
7'	115.0, CH	7.66 d (1.8)	H-5'	C-3'a, 6'
7'a	138.2, C	-	-	-
OCH_3	51.1, CH_3	3.71, s	-	-
NH	-	11.89, s	-	C-2', 3', 3'a, 7'a

4.2) The Marine-Derived Fungus *Aspergillus similanensis* KUFA 0013

Chromatographic fractionation and further purification of the ethyl acetate extract of the marine-derived fungus *Aspergillus similanensis* KUFA 0013, which was isolated from the marine sponge *Rhabdermia* sp., collected from the coral reef of the Similan Islands, Thailand, resulted in discovering seven previously unreported similanpyrones A (**375**), B (**373**) and C (**376**), chevalone E (**356**), pyripyropenes S (**378**) and T (**379**), and similanamide (**380**), together with the previously described *p*-hydroxybenzaldehyde (**371**), 6,8-dihydroxy-3-methylisocoumarin (**372**), reticulol (**374**), chevalones B (**348**) and C (**349**), S14-95 (**377**) and pyripyropene E (**154**). The structures of the isolated metabolites were shown in figure 54.

4.2.1) *p*-Hydroxybenzaldehyde (371)

Compound **371** was isolated as a white solid (mp 117 – 118 °C). The ^{13}C NMR spectrum (Table 6) exhibited five carbon signals which can be classified as one aldehydic (δ_C 191.9), one oxyquaternary sp^2 (δ_C 162.4), one quaternary sp^2 (δ_C 129.3), and two methine sp^2 (δ_C 132.7 and 116.1) carbons based on the DEPTs spectra.

The ^{1}H NMR spectrum, in combination with the HSQC spectrum (Table 6), showed one singlet of an aldehydic proton at δ_H 9.85 (δ_C 191.9), one broad singlet of hydroxyl proton at δ_H 7.06, and two doublets of four aromatic protons at δ_H 7.82, J = 8.7 Hz (2H; δ_C 132.7) and δ_H 6.99, J = 8.6 Hz (2H; δ_C 116.1).

The COSY spectrum showed correlations between the doublet at δ_H 7.82 and δ_H 6.99, indicating that these four aromatic protons belong to the 1,4-disubstituted benzene ring with substituted of different electronegativity.

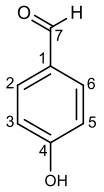

371

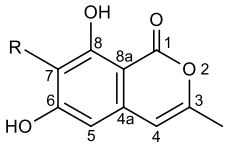

372 R = H
373 R = CH_3
374 R =OCH_3

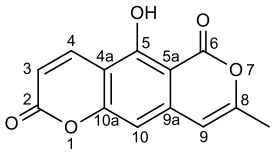

375

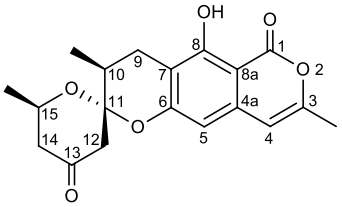

376

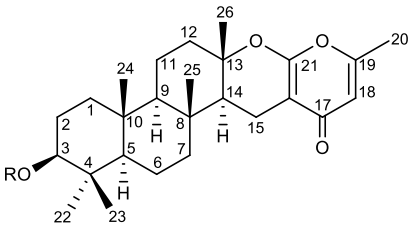

349 R = Ac
356 R = H

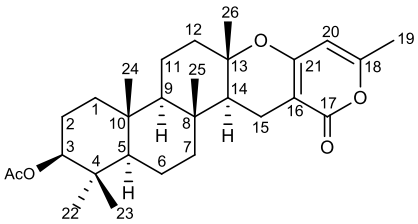

348

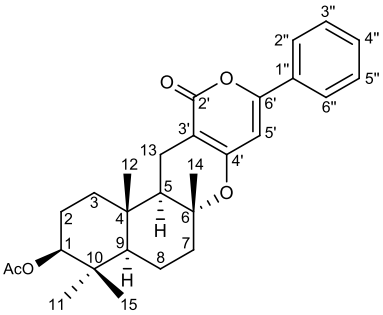

377

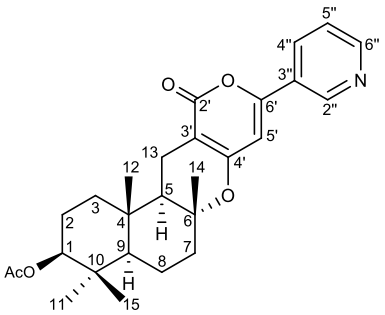

154

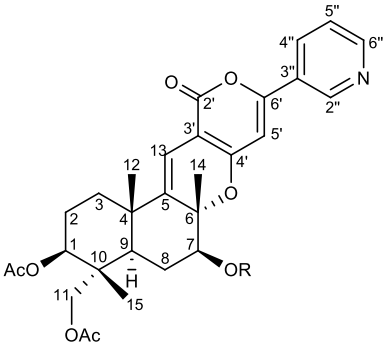

378 R = Ac
379 R = H

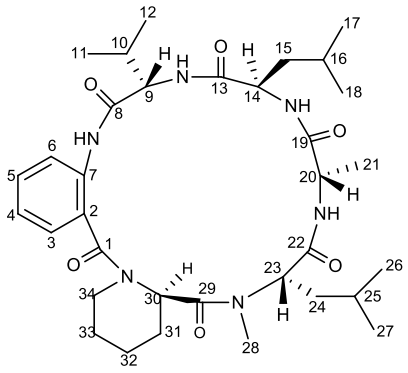

380

Figure 54. Structures of the isolated metabolites from the marine sponge-associated fungus *Aspergillus similanensis* KUFA 0013.

This hypothesis was also confirmed by the HMBC correlations from the doublet at δ_H 7.82, *J* = 8.7 Hz (H-2 and H-6) to the carbons at δ_C 132.7 (C-2 and C-6) and δ_C 162.4 (C-4), and from the doublet at δ_H 6.99, *J* = 8.6 Hz (H-3 and H-5) to the carbons at δ_C 129.3 (C-1), δ_C 116.1 (C-3 and C-5) and C-4.

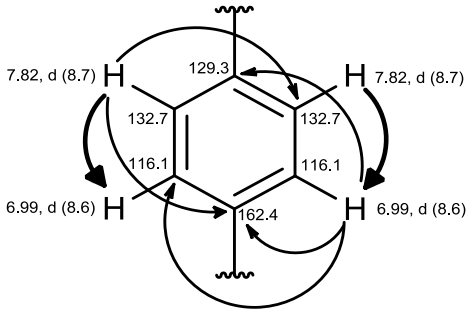

That the aldehyde group was placed on C-7 was evidenced by the HMBC correlations from H-2 and H-6 to the aldehydic carbon at δ_C 191.9 (C-7), and from the aldehydic proton to C-1, C-2 and C-6. Therefore, the hydroxyl group was on the carbon at δ_C 162.4 (C-4). The ^{1}H and ^{13}C NMR of **371** correspond to those of *p*-hydroxybenzaldehyde.

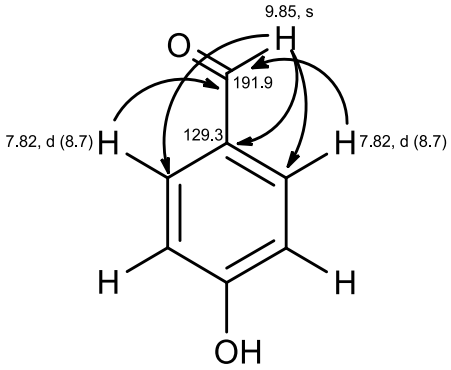

p-Hydroxybenzaldehyde (**371**) has been previously isolated from several plant species, including *Sorghum bicolor* (Woodhead, 1983), *Anoectochilus roxburghii* (He *et al*., 2005) and *Vanilla planifolia* (Shyamala *et al*., 2007), as well as from fungi, *Phaeoacremonium chlamydosporum, Phaeoacremonium aleophilum,* and *Fomitiporia punctata* (Tabacchi *et al*., 2000), marine sponge, *Tedania anhelans* (Parameswara *et al*.,

1997), marine algae, *Laurencia papillosa* (Wright and König, 1996), *Corallina pilulifera, Porphyra tenera* and *Undaria pinnatifida* (Onofrejová *et al*., 2010), and also from freshwater algae, *Spongiochloris spongiosa* and *Anabaena doliolum* (Onofrejová *et al*., 2010).

Table 6. ^{1}H and ^{13}C NMR ($CDCl_3$, 300.13 MHz and 75.4 MHz), and HMBC assignment for *p*-hydroxybenzaldehyde (**371**).

Position	δ_C, Type	δ_H, (*J* in Hz)	COSY	HMBC
1	129.3, C	-	-	-
2	132.7, CH	7.82, d (8.7)	H-3	C-4, 6, 7
3	116.1, CH	6.99, d (8.6)	H-2	C-1, 4, 5
4	162.4, C	-	-	-
5	116.1, CH	6.99, d (8.6)	H-6	C-1, 3, 4
6	132.7, CH	7.82, d (8.7)	H-3	C-2, 4, 7
7	191.9, CHO	9.85, s	-	C-1, 2, 6
OH-4		7.06, brs	-	-

4.2.2) 6,8-Dihydroxy-3-methylisocoumarin (372)

Compound **372** was isolated as a yellow solid (mp 252 – 253 °C), and its molecular formula $C_{10}H_9O_4$ was established on the basis of the (+)-HRESIMS *m/z* 194.0496 $[M+H]^+$, indicating seven degrees of unsaturation.

The ^{13}C NMR spectrum (Table 7) exhibited ten carbon signals which can be classified, according to the DEPTs and HSQC spectra, into one conjugated carbonyl (δ_C 165.7), three oxyquaternary sp^2 (δ_C 165.5, 162.7 and 154.1), two quaternary sp^2 (δ_C 139.7 and 97.9), three methine sp^2 (δ_C 104.2, 102.4, and 101.4) and one methyl (δ_C 18.9) carbons.

The ^{1}H NMR spectrum, together with the HSQC spectrum (Table 7), displayed one singlet of an olefinic proton at δ_H 6.43 (δ_C 104.2), two doublets of two *meta*-coupled aromatic protons at δ_H 6.31, d, J = 2.0 Hz (δ_C 102.4) and δ_H 6.29, d, J = 2.0 Hz (δ_C 101.4), and one methyl singlet at δ_H 2.18 (δ_C 18.9), besides a singlet of the hydrogen-bonded hydroxyl proton at δ_H 10.95.

The presence of two *meta*-coupled aromatic protons at δ_H 6.31, d, *J* = 2.0 Hz (H-5) and δ_H 6.29, d, *J* = 2.0 Hz (H-7), together with the HMBC correlations (Table 7) from the hydroxyl proton at δ_H 10.95, s (OH-8) to the carbons at δ_C 101.4 (C-7), δ_C 162.7 (C-8) and δ_C 97.9 (C-8a), from H-5 to the carbon at δ_C 165.5 (C-6), C-7 and C-8a, and from H-7 to the carbon at δ_C 102.4 (C-5), C-8 and C-8a, suggested the presence of 1,2-disubstituted 3,5-dihydroxybenzene ring. This was also supported by the low frequencies of the aromatic protons and the high frequencies of two quaternary sp^2 carbons (δ_C 165.5; C-6 and 162.7; C-8).

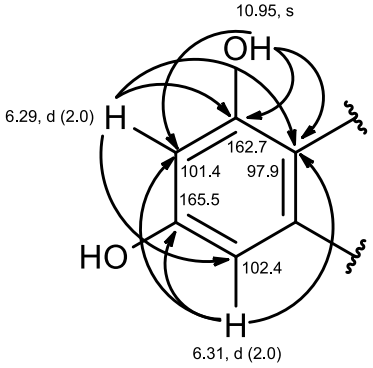

The COSY spectrum (Table 7) exhibited cross peak between the olefinic proton at δ_H 6.43, s (H-4) and the methyl singlet at δ_H 2.18 (H_3-3), suggesting that they were allylic coupled. The HMBC correlations from H-4 to the carbon at δ_C 154.1 (C-3), C-5, C-8a and the carbon at δ_C 18.9 (CH_3-3), from H-5 to the carbon at δ_C 104.2 (C-4), and from the methyl singlet (H_3-3) to C-3 and C-4, together with the presence of the carbonyl carbon (δ_C 165.7), suggested that **372** was 6,8-dihydroxy-3-methyl-1*H*-isochromen-1-one.

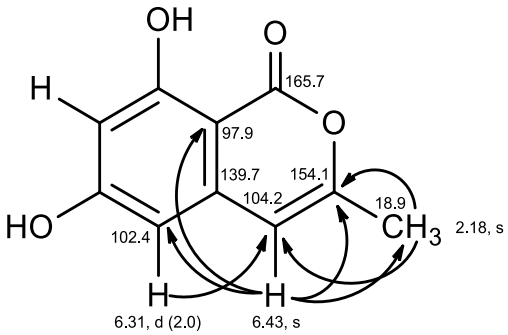

Table 7. ^{1}H and ^{13}C NMR (DMSO, 500.13 MHz and 125.8 MHz), and HMBC assignment for 6,8-dihydroxy-3-methylisocoumarin (**372**).

Position	δ_C, Type	δ_H, (*J* in Hz)	COSY	HMBC
1	165.7, CO	-	-	-
3	154.1, C	-	-	-
4	104.2, CH	6.43, s	H_3-3	C-3, 5, 8a, CH_3-3
4a	139.7, C	-	-	-
5	102.4, CH	6.31, d (2.0)	-	C-4, 7, 8a
6	165.5, C	-	-	-
7	101.4, CH	6.29, d (2.0)	-	C-5, 8, 8a
8	162.7, C	-	-	-
8a	97.9, C	-	-	-
CH_3-3	18.9, CH_3	2.18, s	H-4	C-3, 4
OH-8	-	10.95, s	-	C-7, 8, 8a

The ^{1}H and ^{13}C NMR data of compound **372** were compatible with those previously reported for 6,8-dihydroxy-3-methylisocoumarin isolated from several microorganisms, such as *Streptomyces* sp. (Tang *et al*., 2000; Ben Ameur Mehdi *et al*., 2006; Zinad *et al*., 2011), the marine filamentous fungus *Keissleriella* sp. (Lui *et al*., 2002), the scale insect pathogenic fungus *Torrubiella tenuis* (Kornsakulkarn *et al*., 2009), and the endophytic fungi *Cephalosporium* sp. (Shao *et al*., 2009) and *Papulaspora immersa* (Gallo *et al*., 2010). Moreover, this compound was also found to inhibit the antifungal activity against *Verticullium dahliae* with inhibition zone of 12 mm (Mehdi *et al*., 2006) and zoosporicidal activity against a phytopathogenic oomycete, *Plasmopara viticola*, at concentration of 5 µg/mL (Zinad *et al*., 2011).

4.2.3) Similanpyrone B (373)

Compound **373** was isolated as a white solid (mp, 162 – 163 ˚C), and its molecular formula $C_{11}H_{10}O_4$ was established on the basis of the (+)-HRESIMS *m/z* 207.0658, indicating to seven degrees of unsaturation. The IR spectrum displayed absorption bands for hydroxyl (3243, 3160 cm^{-1}), conjugated ester carbonyl (1677 cm^{-1}), olefin (1635 cm^{-1}) and aromatic (1617 cm^{-1}) groups.

The general features of the ^{1}H and ^{13}C NMR spectra of **373** closely resembled to those of **372.** The ^{13}C NMR spectrum (Table 8) exhibited eleven carbon signals which can be classified, based on the DEPTs and HSQC spectra, into one conjugated ester carbonyl (δ_C 166.1) , three oxyquaternary sp^2 (δ_C 163.7, 160.0 and 153.3), three quaternary sp^2 (δ_C 136.5, 109.6 and 97.5), two methine sp^2 (δ_C 104.2 and 101.4) and two methyl (δ_C 18.8 and 8.0) carbons.

Besides a singlet of the hydrogen-bonded hydroxyl proton at δ_H 11.27 and a broad singlet of another hydroxyl proton at δ_H 3.45, the ^{1}H NMR spectrum, in combination with the HSQC spectrum (Table 8), showed one singlet of olefinic proton at δ_H 6.46 (δ_C 104.2), one singlet of aromatic proton at δ_H 6.40 (δ_C 101.2), and two methyl singlets at δ_H 2.20 (δ_C 18.8) and δ_H 2.00 (δ_C 8.0).

Similar to **372**, the COSY spectrum of **373** showed correlation from the proton at δ_H 6.46, s (H-4) to the the methyl singlet at δ_H 2.20 (H_3-9) while the HMBC spectrum exhibited the cross peaks from the hydrogen-bonded hydroxyl proton at δ_H 11.27, s (OH-8) to the carbons at δ_C 109.6 (C-7), δ_C 160.0 (C-8) and δ_C 97.5 (C-8a), from H-4 to the carbon at δ_C 101.4 (C-5) and C-8a, from the proton at δ_H 6.40, s (H-5) to the carbons at δ_C 104.2 (C-4), δ_C 163.7 (C-6), C-7 and C-8a, from H_3-9 to the carbon at δ_C 153.3 (C-3) and C-4, and from the methyl singlet at δ_H 2.00 (H_3-10) to C-6, C-7 and C-8.

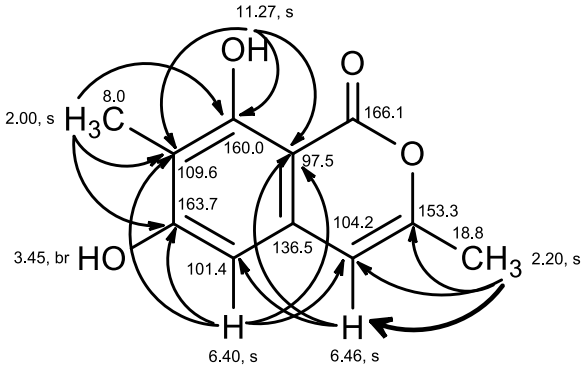

Therefore, the structure of **373** was identified as 6,8-dihydroxy-3,7-dimethyl-1*H*-isochromen-1-one. Exhaustive literature search revealed that **373** has never been previously reported, and it was named similanpyrone B.

Table 8. ^{1}H and ^{13}C NMR ($CDCl_3$, 500.13 MHz and 125.8 MHz), and HMBC assignment for similanpyrone B (**373**).

Position	δ_C, Type	δ_H, (*J* in Hz)	COSY	HMBC
1	166.1, CO	-	-	-
3	153.3, C	-	-	-
4	104.2, CH	6.46, s	H_3-9	C-5, 8a
4a	136.5, C	-	-	-
5	101.4, CH	6.40, s	-	C-4, 6, 7, 8a
6	163.7, C	-	-	-
7	109.6, C	-	-	-
8	160.0, C	-	-	-
8a	97.5, C	-	-	-
9	18.8, CH_3	2.20, s	H-4	C-3, 4
10	8.0, CH_3	2.00, s	-	C-6, 7, 8
OH-6	-	3.45, brs	-	-
OH-8	-	11.27, s	-	C-7, 8, 8a

4.2.4) Reticulol (374)

Compound **374** was isolated as a white solid (mp 172 – 175 °C) and its molecular formula $C_{11}H_{10}O_5$ was established on the basis of the (+)-HRESIMS *m/z* 223.0606 $[M+H]^+$, indicating seven degrees of unsaturation.

The general features of the ^{1}H and ^{13}C NMR spectra of **374** also closely resembled to those of 6,8-dihydroxy-3-methyisocoumarin (**372)**. In contrast to **372**, the ^{1}H NMR spectrum of **374** displayed only one aromatic proton singlet at δ_H 6.40 and a singlet of a methoxy group at δ_H 4.02, instead of two *meta*-coupled aromatic protons.

The ^{13}C NMR spectrum (Table 9) displayed eleven carbon signals which can be classified, according to the DEPTs and HSQC spectra, as one conjugated ester carbonyl (δ_C 166.7), four oxyquaternary sp^2 (δ_C 156.3, 153.8, 153.3, and 132.7), two quaternary sp^2 (δ_C 134.5 and 100.3), two methine sp^2 (δ_C 104.3 and 101.2), one methoxy (δ_C 60.9), and one methyl (δ_C 19.3) carbons.

The ^{1}H NMR spectrum, together with the HSQC spectrum (Table 9), displayed, besides one singlet of the hydrogen-bonded hydroxyl proton at δ_H 11.31 and one singlet of another hydroxyl proton at δ_H 6.49, one singlet of aromatic proton at δ_H 6.40 (δ_C 101.2), one doublet of olefinic proton at δ_H 6.16, J = 0.9 Hz (δ_C 104.3), one methoxyl singlet at δ_H 4.03 (δ_C 60.9) and one methyl doublet at δ_H 2.25, J = 0.9 Hz (δ_C 19.3).

Like **372** and **373**, the COSY spectrum of **374** displayed the correlation from the proton at δ_H 6.16, d, J = 0.9 Hz (H-4) to the methyl doublet at δ_H 2.25, J = 0.9 Hz (H_3-9). The HMBC spectrum exhibited the correlations from the hydroxyl proton at δ_H 6.49, s (OH-6) to the carbons at δ_C 101.2 (C-5) and δ_C 156.3 (C-6), from the hydrogen-bonded hydroxyl proton at δ_H 11.31, s (OH-8) to the carbons at δ_C 132.7 (C-7), δ_C 153.8 (C-8) and δ_C 100.3 (C-8a), from H-4 to the carbon at δ_C 153.3 (C-3), from the proton at δ_H 6.40, s (H-5) to the carbon at δ_C 104.3 (C-4), C-7 and C-8a, and from H_3-9 to C-3 and C-4.

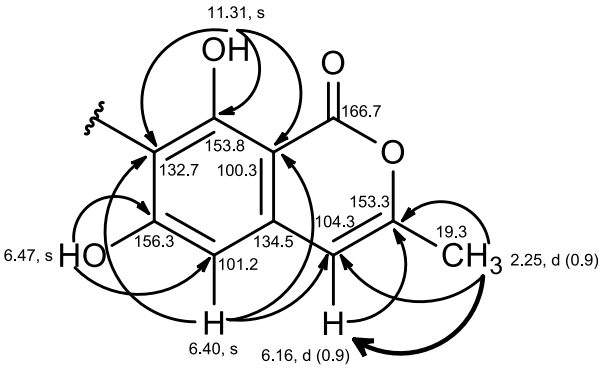

That the methoxy group was on C-7 was confirmed by the HMBC correlation from the methoxyl singlet at δ_H 4.03 (H_3-10) to C-7.

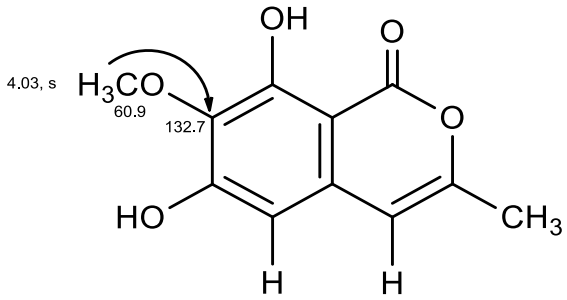

Compound **374** was therefore identified as 6,8-dihydroxy-7-methoxy-3-methyl-1*H*-isochromen-1-one which was known as reticulol. Compound **374** was first reported by Mitscher *et al.* (1964) as a constituent of *Streptomyces rubrireliculae*, and was also reported as a cyclic adenosine 3',5'-monophosphate phosphodiesterase (cAMP PDE) inhibitor with IC_{50} value of 4.1×10^{-5} M (Furutani *et al*., 1977). This compound also exhibited a free radical scavenging activity on ABTS and DPPH radicals (Ryoo *et al*., 2009) and a cytotoxic activity. It exhibited a potent *in vitro* cytotoxicity against A427 (a human lung cancer cell line) and B16F1 (a mouse melanoma cell line) (Lim, Kwak, Kim, *et al*., 2003) by inactivating topoisomerase (topo) I (Lim, Kwak, Lee, *et al*., 2003). The *in vivo* assay for the lung metastasis-blocking effect in mouse model revealed that when **374** was injected intravenously, it exhibited more metastasis inhibition than when it was administered via the peritoneum (Lim, Kwak, Kim, *et al*., 2003). In addition, treating B16F10 melanoma with the mixture of retuculol and adriamycin showed more cytotoxic efficacy than treating with adriamycin alone (Lim, Kwak, Lee, *et al*., 2003).

Table 9. ^{1}H and ^{13}C NMR ($CDCl_3$, 500.13 MHz and 125.8 MHz), and HMBC assignment for reticulol (**374**).

Position	δ_C, Type	δ_H, (*J* = Hz)	COSY	HMBC
1	166.7, CO	-	-	-
3	153.3, C	-	-	-
4	104.3, CH	6.16, d (0.9)	H_3-9	C-3
4a	134.5, C	-	-	-
5	101.2, CH	6.40, s	-	C-4, 7, 8a
6	156.3, C	-	-	-
7	132.7, C	-	-	-
8	153.8, C	-	-	-
8a	100.3, C	-	-	-
9	19.3, CH_3	2.25, d (0.9)	H-4	C-3, 4
10	60.9, OCH_3	4.03, s	-	C-7
OH-6	-	6.49, s	-	C-5, 6
OH-8	-	11.31, s	-	C-7, 8, 8a

4.2.5) Similanpyrone A (375)

Compound **375** was isolated as a white solid (mp, 322 – 323 °C). Based on the HRESIMS, *m/z* 245.0450 $[M+H]^+$, the molecular formula was deduced to be $C_{13}H_8O_5$, indicating ten degrees of unsaturation. The IR spectrum exhibited absorption bands for hydroxyl (3446 cm^{-1}), conjugated lactone carbonyl (1748, 1698 cm^{-1}), aromatic (1658 cm^{-1}) and olefin (1634, 1464 cm^{-1}) groups.

The ^{13}C NMR spectrum (Table 10) exhibited thirteen carbon signals which can be categorized, base on the DEPTs and HSQC spectra, into two conjugated ester carbonyl (δ_C 166.3 and 159.7), six quaternary sp^2 (δ_C 160.3, 156.2, 140.1, 130.0, 107.3 and 101.3), four methine sp^2 (δ_C 137.8, 114.1, 104.6 and 102.7) and one methyl (δ_C 19.6) carbons.

The ^1H NMR spectrum (Table 10) revealed the presence of two doublets of the *cis*-olefinic protons at δ_H 8.13, J = 9.8 Hz (δ_C 137.8) and 6.36, J = 9.8 Hz (δ_C 114.1). This was supported by the COSY correlation and the coupling constant values. Moreover, the ^1H NMR spectrum, together with the HSQC spectrum, also exhibited one singlet of aromatic proton at δ_H 6.70 (δ_C 102.7), one singlet of an olefinic proton at δ_H 6.33 (δ_C 104.6) and one methyl singlet at δ_H 2.33 (δ_C 19.6), besides a singlet of the hydrogen-bonded hydroxyl proton at δ_H 11.90.

The COSY correlation (Table 10) of the proton at δ_H 6.33, s (H-9) to the methyl singlet at δ_H 2.33 (H_3-8) suggested that they were an allylic coupled. The HMBC spectrum (Table 10) displayed cross peaks from the hydrogen-bonded hydroxyl proton at δ_H 11.90, s (OH-5) to the carbons at δ_C 107.3 (C-4a), δ_C 160.3 (C-5) and δ_C 101.3 (C-5a), from H_3-8 to the carbons at δ_C 156.2 (C-8) and δ_C 104.6 (C-9), from H-9 to C-5a, C-8 and the carbons at δ_C 102.7 (C-10) and δ_C 19.6 (CH_3-8), and from the proton at δ_H 6.70, s (H-10) to C-4a, C-5a and the carbons at δ_C 130.0 (C-9a) and δ_C 140.1 (C-10a). Taken together the ^1H and ^{13}C chemical values and the HMBC correlations, **375** should have the 4a,10a-disubstituted-5-hydroxy-8-methylisochromen-6-one as its partial structure.

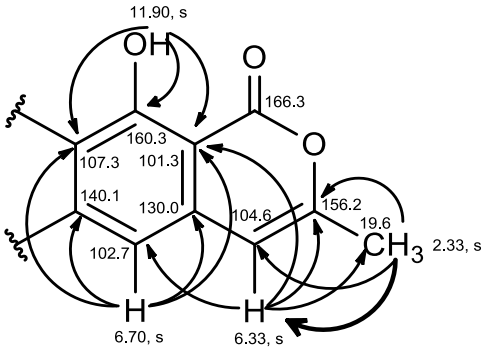

Since the proton at δ_H 8.13, d, *J* = 9.8 Hz (H-4) exhibited the HMBC correlations to the conjugated ester carbonyl carbon at δ_C 159.7 (C-2) and C-4a whereas the proton at δ_H 6.36, d, *J* = 9.8 Hz (H-3) showed the HMBC correlation to C-10a, the 4a,10a-disubstituted-5-hydroxy-8-methylisochromen-6-one nucleus was fused with the pyran-2-one moiety. Therefore, **375** was identified as 5-hydroxy-8-methyl-2*H*,6*H*-pyrano[3,4-g]chromene-2,6-dione. To the best of our knowledge, this compound has not been previously described, and therefore it was named similanpyrone A.

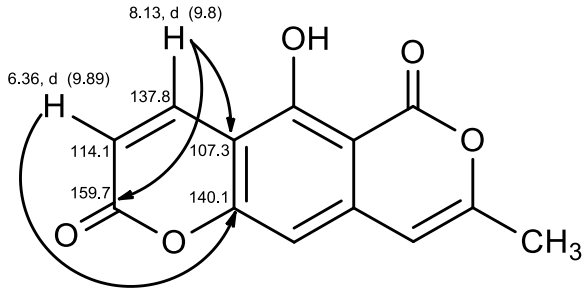

Table 10. ^{1}H and ^{13}C NMR data ($CDCl_3$, 500.13 MHz and 125.8 MHz), and HMBC assignment for similanpyrone A (**375**).

Position	δ_C, Type	δ_H, (*J* in Hz)	COSY	HMBC
2	159.7, CO	-	-	-
3	114.1, CH	6.36, d (9.8)	H-4	C-10a
4	137.8, CH	8.13, d (9.8)	H-3	C-2, 4a
4a	107.3, C	-	-	-
5	160.3, C	-	-	-
5a	101.3, C	-	-	-
6	166.3, CO	-	-	-
8	156.2, C	-	-	-
9	104.6, CH	6.33, s	H_3-8	C-5a, 8, 10, CH_3-8
9a	130.0, C	-	-	-
10	102.7, CH	6.70, s	-	C-4a, 5a, 9a, 10a
10a	140.1, C	-	-	-
CH_3-8	19.6, CH_3	2.33, s	H-9	C-8, 9
OH-5	-	11.90, s	-	C-4a, 5, 5a

4.2.6) Similanpyrone C (376)

Compound **376** was isolated as a pale yellow viscous mass. The molecular formula, $C_{19}H_{20}O_6$, was determined by (+)-HRESIMS (*m/z* 345.1342 $[M+H]^+$), indicating ten degrees of unsaturation. The IR spectrum displayed absorption bands for hydroxyl (3443 cm^{-1}), ketone carbonyl (1730 cm^{-1}), conjugated lactone carbonyl (1683 cm^{-1}), olefin (1647 cm^{-1}) and aromatic (1625, 1572 cm^{-1}) groups.

The general features of ^{1}H and ^{13}C NMR spectra of **376** also assembled to those of **375**, suggesting that it is also an isocoumarin derivative. The ^{13}C NMR spectrum (Table 11) exhibited nineteen carbon signals which can be categorized, according to the DEPTs and HSQC spectra, as one ketone carbonyl (δ_C 205.3) and one conjugated ester carbonyl (δ_C 166.8), six quaternary sp^2 (δ_C 160.0, 158.3, 153.4, 136.7, 110.0 and 99.6), two methine sp^2 (δ_C 104.4 and 103.0), one ketal (δ_C 102.9), two methine sp^3 (δ_C 67.2 and 33.9), three methylene sp^3 (δ_C 48.3, 47.2 and 23.6) and three methyl (δ_C 21.6, 19.4 and 15.9) carbons.

The ^{1}H NMR spectrum, in combination with the HSQC spectrum (Table 11), exhibited one doublet of an olefinic proton at δ_H 6.13, *J* = 0.9 Hz (δ_C 104.4), one singlet of aromatic proton at δ_H 6.26 (δ_C 103.0), two multiplets of two methine protons at δ_H 4.15 (δ_C 67.2) and 1.98 (δ_C 33.9), two broad doublets of two methylene protons at δ_H 2.81, *J* = 14.0 Hz (δ_C 47.2) and δ_H 2.57, *J* = 16.8 Hz (δ_C 23.6), two double doublets of two methylene protons at δ_H 2.81, *J* = 16.8, 5.6 Hz (δ_C 23.6) and δ_H 2.55, *J* = 14.0, 1.9 Hz (δ_C 47.2), two double double doublets of two methylene protons at δ_H 2.48, *J* = 14.7, 2.9, 1.9 Hz (δ_C 48.3) and δ_H 2.28, *J* = 14.7, 11.3, 0.7 Hz (δ_C 48.3), one methyl singlet at δ_H 2.24 (δ_C 19.4) and two methyl doublets at δ_H 1.23, *J* = 6.2 Hz (δ_C 15.9) and 1.21, *J* = 6.2 Hz (δ_C 21.6), besides a singlet of the hydrogen-bonded hydroxyl proton at δ_H 11.35.

That **376** also consisted of a 6,7-disubstituted 8-hydroxy-3-methyliso-chromene-1-one nucleus was substantiated by the COSY correlation from the olefinic proton at δ_H 6.13, d, *J* = 0.9 Hz (H-4) to the methyl singlet at δ_H 2.24 (H_3-3), as well as by the HMBC correlations from the hydrogen-boned hydroxyl proton at δ_H 11.35, s (OH-8) to the carbons at δ_C 110.0 (C-7), δ_C 160.0 (C-8) and δ_C 99.6 (C-8a), from the methyl singlet (H_3-3) to the carbons at δ_C 153.4 (C-3) and δ_C 104.4 (C-4), from H-4 to C-3, the carbon at δ_C 103.0 (C-5) and C-8a, and from the aromatic proton at δ_H 6.26, s (H-5) to C-4, the carbon at δ_C 158.3 (C-6), C-7 and C-8a.

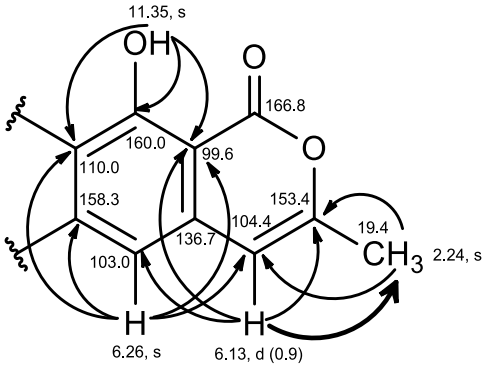

Another portion of the molecule comprised one ketone carbonyl carbon (δ_C 205.3), one ketal (δ_C 102.9), one oxymethine sp^3 (δ_C 67.2, δ_H 4.15, m), three methylene sp^3 (δ_C 48.3; δ_H 2.48, ddd, *J* = 14.7, 2.9, 1.9 Hz/2.28, ddd, *J* = 14.7, 11.3, 0.7 Hz, δ_C 47.2; δ_H 2.81, brd, *J* = 14.0 Hz/2.55, dd, *J* = 14.0, 1.9 Hz and δ_C 23.6; δ_H 2.81, dd, *J* = 16.8, 5.6

Hz/2.57 brd, *J* = 16.8 Hz), one methine sp^3 (δ_C 33.9; δ_H 1.98, m) and two secondary methyl (δ_C 21.6; δ_H 1.21, d, *J* = 6.2 Hz and δ_C 15.9; δ_H 1.23, d, *J* = 6.2 Hz) groups.

The COSY spectrum exhibited correlations from the mutually coupled methylene protons at δ_H 2.81, dd, *J* = 16.8, 5.6 Hz (H-9α) and δ_H 2.57, brd, *J* = 16.8 Hz (H-9β) to the methine proton at δ_H 1.98, m (H-10). In turn, H-10 was also correlated to the methyl doublet at δ_H 1.23, *J* = 6.2 Hz (H_3-10). Moreover, the HMBC spectrum exhibited cross peaks from H-9α and H-9β to C-6, C-7, the carbon at δ_C 33.9 (C-10) and the ketal carbon at δ_C 102.9 (C-11), and from the methyl singlet of H_3-10 to the carbon at δ_C 23.6 (C-9), C-10 and C-11. These COSY and HMBC correlations suggested that the 3-mehtyl-3,4-dihydro-2*H*-pyran was fused, through C-6 and C-7, with the 8-hydroxy-3-methylisochromene-1-one nucleus.

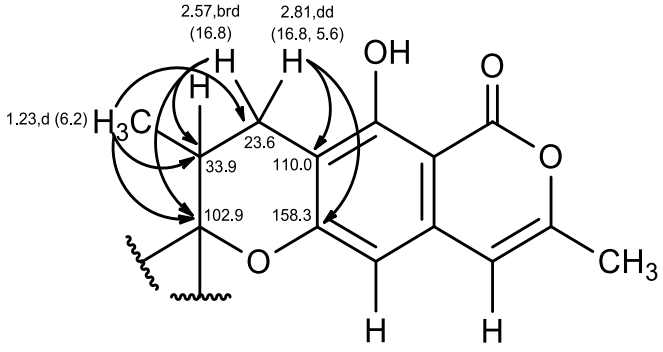

Another coupling system was revealed by the COSY correlations from the proton at δ_H 4.15, m (H-15) to the mutually coupled methylene protons at δ_H 2.28, ddd, *J* = 14.7, 11.3, 0.7 Hz (H-14α) and δ_H 2.48, ddd, *J* = 14.7, 2.9, 1.9 Hz (H-14β) and the methyl doublet at δ_H 1.21, *J* = 6.2 Hz (H_3-15). Since the HMBC spectrum exhibited correlations from the mutually coupled methylene protons at δ_H 2.55, dd, *J* = 14.0, 1.9 Hz (H-12α) and δ_H 2.81, brd, *J* = 14.0 Hz (H-12β) to the ketone carbonyl carbon at δ_C 205.3 (C-13), from H-14α and H-14β to C-13 and the carbon at δ_C 67.2 (C-15), and from H_3-15 to the carbon at δ_C 48.3 (C-14) and C-15, the 2-mehtyltetrahydro-4*H*-pyran-4-one and the 3-mehtyl-3,4-dihydro-2*H*-pyran were connected through C-11 of the spiroketal.

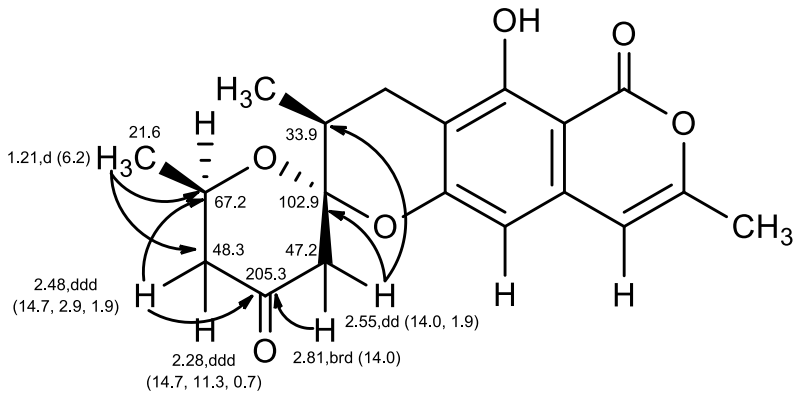

Literature survey revealed that **376** is a new compound, thus it was named similanpyrone C. Since **376** was isolated as a viscous mass, it was impossible to obtain suitable crystals for the X-ray analysis. Consequently, the relative configurations of C-10, C-11 and C-15 were tentatively established using proton coupling constant values and the NOESY correlations.

One of H_2-9 appeared as a double doublet at δ_H 2.81 with coupling constant values of 16.8 Hz, typical for the geminal coupling, and 5.6 Hz, typical for the axial-equatorial coupling, while another appeared as a broad doublet at δ_H 2.57 with a geminal coupling constant of 16.8 Hz. Moreover, the NOESY spectrum exhibited cross peaks from H-10, which was in α-equatorial position, to both H-9α (δ_H 2.81, dd, *J* = 16.8, 5.6 Hz) and H-9β (δ_H 2.57, brd, *J* = 16.8 Hz). Therefore, CH_3-10 was in the β-axial position of the half-chair conformation of the tetrahydropyran ring.

On the other hand, both H_2-14 appeared as double double doublet. One of them appeared at δ_H 2.28 with a geminal coupling of 14.7 Hz, a diaxial coupling of 11.3 Hz and a long-range coupling of 0.7 Hz, while another appeared at δ_H 2.48 with a geminal coupling of 14.7 Hz, an axial-equatorial coupling of 2.9 Hz and a long-range coupling of 1.9 Hz. These patterns of couplings indicated that CH_3-15 was in α-equatorial position of the half-chair conformation of the tetrahydro-4*H*-pyran-4-one ring. This hypothesis was corroborated by the NOESY correlation from H-15 to only H-14β (δ_H 2.48, ddd, *J* = 14.7, 2.9, 1.9 Hz), but not to H-14α (δ_H 2.28, ddd, *J* = 14.7, 11.3, 0.7 Hz), as well as the higher chemical shift value of H-14β than that of H-14α since the former was under the anisotropic deshielding effect of the carbonyl group (C-13). Based on the same reasoning, the double doublet at δ_H 2.55, *J* = 14.0, 1.9 Hz and the broad doublet at δ_H 2.81, *J* = 14.0

Hz was assigned as H-12α and H-12β, respectively. Consequently, the relative configuration of C-10 and C-15 was tentatively assigned as 10*S** and 15*R**. As the NOESY spectrum did not show the correlation between H-10 and H-15, the configuration of C-11 was assigned as 11*S**.

Table 11. ^{1}H and ^{13}C NMR ($CDCl_3$, 500.13 MHz and 125.8 MHz), and HMBC assignment for similanpyrone C (**376)**.

Position	δ_C, Type	δ_H, (*J* in Hz)	COSY	HMBC	NOESY
1	166.8, CO	-	-	-	-
3	153.4, C	-	-	-	-
4	104.4, CH	6.13, d (0.9)	H_3-3	C-3, 5, 8a	CH_3-3
4a	136.7, C	-	-	-	-
5	103.0, CH	6.26, s	-	C-4, 6, 7, 8a	-
6	158.3, C	-	-	-	-
7	110.0, C	-	-	-	-
8	160.0, C	-	-	-	-
8a	99.6, C	-	-	-	-
9α	23.6, CH_2	2.81, dd (16.8, 5.6)	H-9β, 10	C-6, 7,10, 11	H-9β,10, CH_3-10
9β		2.57, brd (16.8)	H-9α, 10	C-7,10, 11	H-9α,10, CH_3-10
10	33.9, CH	1.98, m	H-9α, 9β, H_3-10	-	H-9α,9β,CH_3-10
11	102.9, C	-	-	-	-
12α	47.2, CH_2	2.55, dd (14.0, 1.9)	H-12β	C-10, 11, 13	H-12β
12β		2.81, brd (14.0)	H-12α	C-10, 11, 13	H-12α
13	205.3, CO	-	-	-	-
14α	48.3, CH_2	2.28, ddd (14.7, 11.3, 0.7)	H-14β, 15	C-13, 15	H-14β, CH_3-15
14β		2.48, ddd (14.7, 2.9, 1.9)	H-14α, 15	C-13	H-14β, CH_3-15
15	67.2, CH	4.15, m	H-14α, 14β, H_3-15	-	H-14β, CH_3-15
CH_3-3	19.4, CH_3	2.24, s	H-4	C-3, 4	H-4
CH_3-10	15.9, CH_3	1.23, d (6.2)	H-10	C-9, 10, 11	H-9β, 10, 12α, 12β
CH_3-15	21.6, CH_3	1.21, d (6.2)	H-15	C-14,15	H-14α, 14β, 15
OH-8	-	11.35, s	-	C-7, 8, 8a	-

Similanpyrone C (**376**) can be assumed to be derived from the acetate-malonate pathway (Scheme 1). Cyclization and enolization of the pentaketide (**I**), which is derived from malonyl-CoA and acetyl-CoA, give rise to 6,8-dihydroxy-3-methyl-isocoumarin (**II**). Claisen condensation of **II** with the tetraketide (**III**) leads to the formation of **IV**. Enolization of the side chain of **IV**, and a formation of the hemiketal by the phenolic hydroxyl group on C-6 of the isocoumarin nucleus and the ketone carbonyl of the side chain of **IV**, gives rise to the hemiketal (**V**). Formation of the ketal (**VI**) by hydroxyl group on C-11 and the ketone carbonyl of the side chain of **V** followed by methylation by *S*-adenosylmethionine (SAM) of **VI** finally leads to the formation of similanpyrone C (**376**).

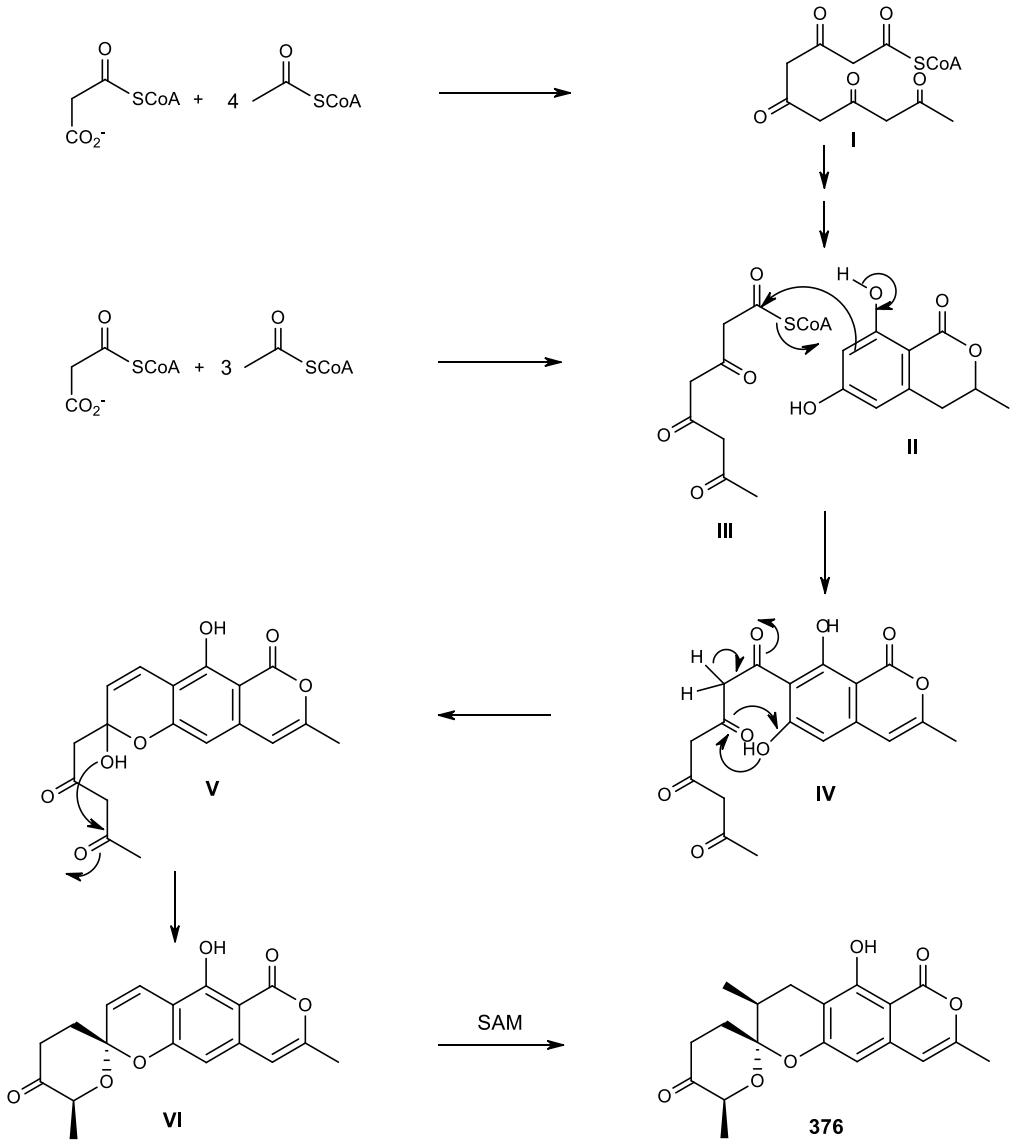

Scheme 1. Proposed biogenesis of similanpyrone C (**376**).

4.2.7) Chevalone C (349)

Compound **349** was isolated as a white solid (mp 201 – 202 °C). The ^{13}C NMR spectrum exhibited twenty-eight carbon signals which can be classified, according to the DEPTs and HSQC spectra, as one ester carbonyl (δ_C 170.7), one ketone carbonyl (δ_C 180.4), two oxyquaternary sp^2 (δ_C 162.4 and 160.3), one quaternary sp^2 (δ_C 98.2), one oxyquaternary sp^3 (δ_C 84.0), three quaternary sp^3 (δ_C 37.5, 37.1 and 36.8), one oxymethine sp^3 (δ_C 80.4), one methine sp^2 (δ_C 111.6), three methine sp^3 (δ_C 59.9, 55.2 and 52.0), seven methylene sp^3 (δ_C 40.7, 39.8, 37.8, 23.3, 18.4, 17.6, and 15.1) and seven methyl (δ_C 27.7, 21.1, 20.3, 19.0, 16.2, 16.1 and 15.9) carbons.

The ^1H NMR spectrum (Table 12), together with the HSQC spectrum, exhibited one singlet of an olefinic proton at δ_H 5.93 (δ_C 111.6), two double doublets of two methine protons at δ_H 4.41, *J* = 10.8, 5.2 Hz (δ_C 80.4) and δ_H 1.46, *J* = 12.7, 5.0 Hz (δ_C 52.0), two doublets of two methine protons at δ_H 0.90, *J* = 11.5 Hz (δ_C 59.9) and δ_H 0.82, *J* = 7.3 Hz (δ_C 55.2), one double double doublet of methylene proton at δ_H 1.84, *J* = 12.9, 3.0, 3.0 Hz (δ_C 40.7), four double doublets of four methylene protons at δ_H 2.48, *J* = 16.4, 4.8 Hz (δ_C 15.0), δ_H 2.06, *J* = 12.4, 5.1 Hz (δ_C 39.8), δ_H 1.53, *J* = 13.8, 2.6 Hz (δ_C 17.6) and δ_H 1.30, *J* = 11.6, 3.2 Hz (δ_C 18.4), three doublets of three methylene protons at δ_H 1.67, *J* = 9.9 Hz (δ_C 18.4), δ_H 1.64, *J* = 16.4 Hz (δ_C 37.8) and δ_H 1.41, *J* = 13.2 Hz (δ_C 17.6), six multiplets of six methylene protons at δ_H 2.10 (δ_C 15.1), δ_H 1.65 (δ_C 39.8), δ_H 1.63 (δ_C 23.3), δ_H 1.55 (δ_C 23.3), δ_H 1.01 (δ_C 37.8) and δ_H 1.00 (δ_C 40.7), and seven methyl singets at δ_H 2.15 (δ_C 19.0), δ_H 1.99 (δ_C 21.1), δ_H 1.23 (δ_C 20.3), δ_H 0.83 (δ_C 16.1), δ_H 0.83 (δ_C 15.9), δ_H 0.81 (δ_C 16.2) and δ_H 0.80 (δ_C 27.7).

The COSY correlation (Table 12) from the mutually coupled methylene protons at δ_H 1.63, m (H-2α) and δ_H 1.55, m (H-2β) to the proton at δ_H 4.41, dd, *J* = 10.8, 5.2 Hz (H-3), together with the HMBC correlations from H-3 to the carbons at δ_C 170.7 (CO; OAc-3), δ_C 37.5 (C-4), δ_C 16.1 (C-22) and δ_C 27.7 (CH_3-23), from the proton at δ_H 0.90, d, *J* = 11.5 Hz (H-9) to the carbon at δ_C 15.9 (CH_3-24), from the methyl singlet at δ_H 0.83 (H_3-22) to the carbon at δ_C 55.2 (C-5) and CH_3-23, from the methyl singlet at δ_H 0.80 (H_3-23) to the carbon at δ_C 80.4 (C-3), C-4, C-5 and C-22, from the methyl singlet at δ_H 0.83 (H_3-24) to C-5 and the carbon at δ_C 59.9 (C-9), from the methyl singlet at δ_H 0.81 (H_3-25) to

C-9, and from the methyl singlet at δ_H 1.99 (OAc-3) to the ester carbonyl carbon (CO; OAc-3), suggesting the presence of the 1,1,4a,6-tetramethyldecahydronaphthalen-2-yl acetate moiety.

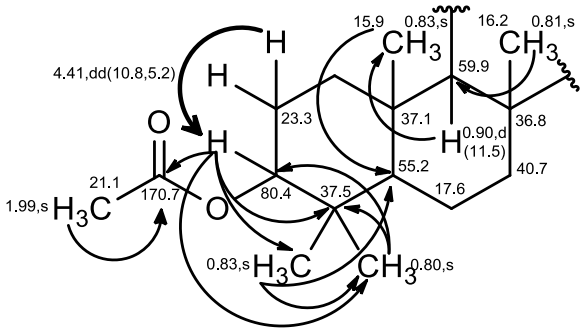

Since there were the COSY correlation between H-14 and H_2-15, as well as the HMBC correlations from the proton at δ_H 1.46, dd, *J* = 12.7, 5.0 Hz (H-14) to the carbons at δ_C 36.8 (C-8), δ_C 84.0 (C-13), δ_C 15.1 (C-15) and δ_C 20.3 (C-26), from the proton at δ_H 2.48, dd, *J* = 16.4, 4.8 Hz (H-15α) to C-13 and the carbon at δ_C 52.0 (C-14), and from the proton at δ_H 2.10, m (H-15β) to the carbons at δ_C 39.8 (C-12) and δ_C 16.2 (C-25), the presence of the substituted tetradecahydrophenanthrene partial structure was proposed.

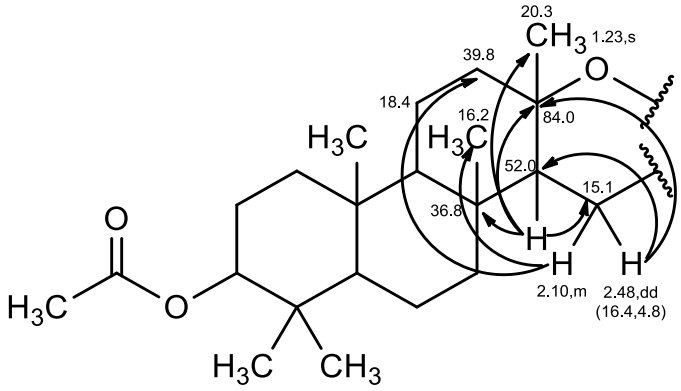

The presence of the 5,6-disubstituted 2-methyl-4*H*-pyran-2-one was substantiated by the COSY correlation from the methine proton at δ_H 5.93, s (H-18) to the methyl singlet at δ_H 2.15 (H_3-20), as well as by the HMBC correlations from H-18 to C-16, the carbons at δ_C 160.3 (C-19) and δ_C 19.0 (C-20), and from H_3-20 to the carbon at δ_C 111.6 (C-18)

and C-19. That the 2-methyl-4*H*-pyran-2-one moiety was connected to the tetradecahydrophenanthrene portion through the ethereal bridge between C-21 of the former and C-13 of the latter as well as by the methylene bridge between C-16 of the former and C-14 of the latter was supported by HMBC correlations from H-15α to the carbons at δ_C 98.2 (C-16), δ_C 180.4 (C-17) and δ_C 162.4 (C-21). Therefore, the structure of **349** was identified as (4a*R*,4b*R*,6a*S*,12a*S*,12b*R*,14a*R*)-1,1,4a,6a,9,12b-hexamethyl-11-oxo-1,2,3,4,4a,4b,5,6,6a,11,12,12a,12b,13,14,14a-hexadecahydrophaphtho[2,1-*f*]pyrano[2,3-*b*]chromen-2-yl acetate.

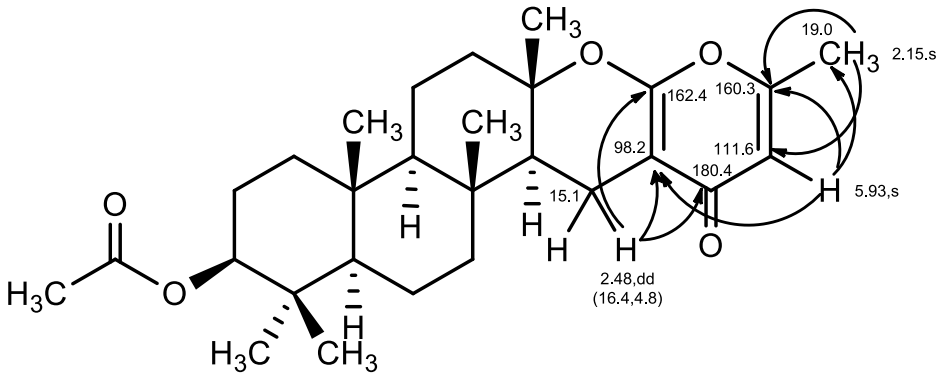

Literature survey revealed that the structure of **349** corresponds to chevalone C, which was first isolated from the fungus *Eurotium chevalieri* by Kanokmedhakul *et al.* (2011) and later from the fungus *Neosartoyra tsunodae* (Eamvijarn et al., 2013) and *Neosartorya siamensis* (Gomes *et al*., 2014). Chevalone C exhibited antimycobacterial activity against *Mycobacterium tuberculosis* with MIC value of 6.3 µg/mL and anticancer activity against BC1 (human breast) cancer cell with IC_{50} value of 8.7 µg/mL (Kanokmedhakul *et al*., 2011). For the antibacterial activity assay, chevalone C did not show any activities on Gram-positive and Gram-negative bacteria at the highest concentration tested (MIC > 256 mg/mL). However, it exhibited a synergism effect with antibiotics against multidrug-resistant isolates of *Escherichia coli, Enterococcus faecium* and *Staphylococcus aureus* (Gomes *et al*., 2014). Furthermore, this compound also exhibited an antimalarial activity with IC_{50} value of 25.0 µg/mL (Sawadsitang *et al*., 2015).

Table 12. ^{1}H and ^{13}C NMR ($CDCl_3$, 300.13 MHz and 75.4 MHz), and HMBC assignment for chevalone C (**349**).

Position	δ_C, Type	δ_H, (*J* in Hz)	COSY	HMBC
1α	37.8, CH_2	1.64, d (16.4)	-	-
1β		1.01, m	-	-
2α	23.3, CH_2	1.63, m	H-3	-
2β		1.55, m	H-3	-
3	80.4, CH	4.41, dd (10.8, 5.2)	H_2-2	C-4, 22, 23, CO (OAc-3)
4	37.5, C	-	-	-
5	55.2, CH	0.82, d (7.3)	-	-
6α	17.6, CH_2	1.53, dd (13.8, 2.6)	-	-
6β		1.41, d (13.2)	-	-
7α	40.7, CH_2	1.84, ddd (12.9, 3.0, 3.0)	-	-
7β		1.00, m	-	-
8	36.8, C	-	-	-
9	59.9, CH	0.90, d (11.5)	-	C-24
10	37.1, C	-	-	-
11α	18.4, CH_2	1.67, d (9.9)	-	-
11β		1.30, dd (11.6, 3.2)	-	-
12α	39.8, CH_2	2.06, dd (12.4, 5.1)	-	-
12β		1.65, m	-	-
13	84.0, C	-	-	-
14	52.0, CH	1.46, dd (12.7, 5.0)	H_2-15	C-8, 13, 15, 26
15α	15.1, CH_2	2.48, dd (16.4, 4.8)	H-14	C-13, 14, 16, 17, 21
15β		2.10, m	H-14	C-12, 16, 25
16	98.2, C	-	-	-
17	180.4, CO	-	-	-
18	111.6, CH	5.93, s	H_3-20	C-16, 19, 20
19	160.3, C	-	-	-
20	19.0, CH_3	2.15, s	H-18	C-18, 19
21	162.4, C	-	-	-
22	16.1, CH_3	0.83, s	-	C-5, 23
23	27.7, CH_3	0.80, s	-	C-3, 4, 5, 22
24	15.9, CH_3	0.83, s	-	C-5, 9
25	16.2, CH_3	0.81, s	-	C-9
26	20.3, CH_3	1.23, s	-	-
OAc-3	170.7, CO	-	-	-
	21.1, CH_3	1.99, s	-	CO (OAc-3)

4.2.8) Chevalone E (356)

Compound **356** was isolated as a white crystal (mp, 262 – 263 °C), and its molecular formula $C_{26}H_{38}O_4$ was established on the basis of the (+)-HRESIMS *m/z* 415.2851 $[M+H]^+$, indicating eight degrees of unsaturation. The IR spectrum exhibited absorption bands for hydroxyl (3300 cm^{-1}), conjugated carbonyl (1664 cm^{-1}) and olefin (1607, 1570 cm^{-1}) groups.

The general features of ^1H and ^{13}C NMR spectra of **356** closely resembled to those of **349.** The ^{13}C NMR spectrum (Table 13) displayed twenty-six carbon signals which can be categorized, based on the DEPTs and HSQC spectra, as one conjugated ketone carbonyl (δ_C 180.6), two oxyquaternary sp^2 (δ_C 162.6 and 160.5), one methine sp^2 (δ_C 111.9), one quaternary sp^2 (δ_C 98.5), one oxyquaternary sp^3 (δ_C 84.3), three quaternary sp^3 (δ_C 38.9, 37.3 and 37.1), one oxymethine sp^3 (δ_C 78.7), three methine sp^3 (δ_C 60.3, 55.3 and 52.3), seven methylene sp^3 (δ_C 41.1, 40.1, 38.4, 27.2, 18.7, 17.9 and 15.2) and six methyl (δ_C 28.0, 20.5, 19.2, 16.4, 16.1 and 15.4) carbons.

The ^1H NMR spectrum (Table 13), together with the HSQC spectrum, revealed the presence of one olefinic proton (δ_H 5.99, s, δ_C 111.9), four methine protons (δ_H 3.21, dd, *J* = 11.1, 5.1 Hz/δ_C 78.7; δ_H 1.50, dd, *J* = 12.5, 4.7 Hz/δ_C 52.3; δ_H 0.93, brd,*J* = 13.0 Hz/ δ_C 60.3; δ_H 0.79, dd, *J* = 11.6, 2.3 Hz/δ_C 55.3), fourteen methylene protons (δ_H 2.55, dd, *J* = 16.4, 4.9 Hz/δ_C 15.2; δ_H 2.15, m/δ_C 15.2; δ_H 2.11, dd, *J* = 12.9, 3.1 Hz/δ_C 40.1; δ_H 1.90, ddd, *J* = 12.7, 3.0, 3.0 Hz/δ_C 41.1; δ_H 1,74, m/δ_C 18.7; δ_H 1.73, m/δ_C 38.4; δ_H 1.64, m (2H)/δ_C 27.2; δ_H 1.61, dd, *J* = 19.8, 3.1 Hz/δ_C 40.1; δ_H 1.59, m/δ_C 17.9; δ_H 1.45, m/δ_C 17.9; δ_H 1.35, dd, *J* = 12.3, 3.0 Hz/δ_C 18.7; δ_H 1.04, ddd, *J* = 12.4, 12.4, 3.6 Hz/δ_C 41.1; δ_H 1.00, ddd, *J* = 10.6, 10.6, 3.5 Hz/δ_C 38.4) and six methyl singlets (δ_H 2.20/δ_C 19.2; δ_H 1.28/δ_C 20.5; δ_H 0.98/δ_C 28.0; δ_H 0.89/δ_C 16.1; δ_H 0.84/δ_C 16.4 and δ_H 0.78/δ_C 15.2).

The COSY and HMBC correlations shown inTable 13 are the same as those observed for chevalone C (**349**). The molecular formula and the lack of the ^1H and ^{13}C signals of the acetyl group led to the conclusion that **356** is a deacetyl analog of **349**. Since H-5 appeared as a double doublet with a diaxial coupling of 11.1 Hz and an axial-equatorial coupling of 5.1 Hz, H-5 was in the α-axial position. Consequently, the hydroxyl group (OH-3) was in β-equatorial position.

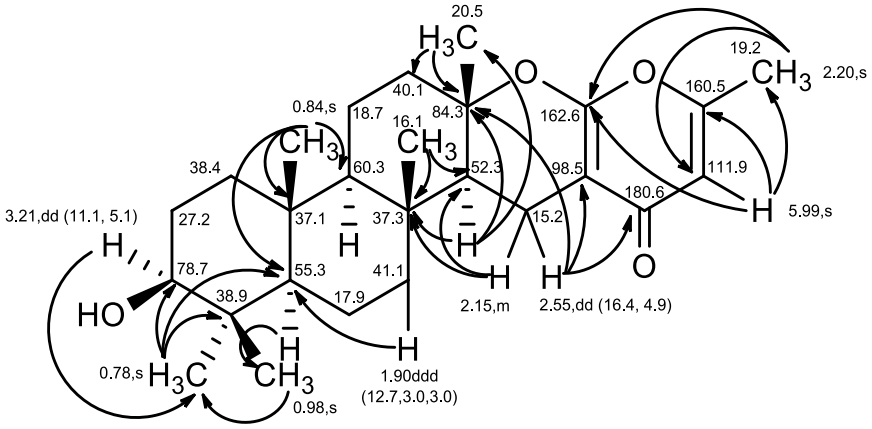
20.5
H3C
O
O
19.2
CH3
2.20,s
160.5
40.1
84.3
162.6
0.84,s
18.7
16.1
CH3
CH3
38.4
60.3
52.3
98.5
111.9
180.6
H
5.99,s
3.21,dd (11.1, 5.1)
27.2
37.1
37.3
15.2
H
H
H
H
O
78.7
55.3
41.1
38.9
17.9
HO
2.15,m
2.55,dd (16.4, 4.9)
H
H
0.78,s
H3C
CH3
1.90ddd
(12.7,3.0,3.0)
0.98,s

Table 13. ^{1}H and ^{13}C NMR ($CDCl_3$, 500.13 MHz and 125.8 MHz) and HMBC assignment for chevalone E (**356**).

Position	δ_C, Type	δ_H, (*J* in Hz)	COSY	HMBC
1α	38.4, CH_2	1.73, m	-	-
1β		1.00, ddd (10.6, 10.6, 3.5)	-	-
2	27.2, CH_2	1.64, m	H-3	-
3	78.7, CH	3.21, dd (11.1, 5.1)	H_2-2	C-22
4	38.9, C	-	-	-
5	55.3, CH	0.79, dd (11.6, 2.3)	-	C-23
6α	17.9, CH_2	1.59, m	-	-
6β		1.45, m	-	-
7α	41.1, CH_2	1.90, ddd (12.7, 3.0, 3.0)	-	C-5
7β		1.04, ddd (12.4, 12.4, 3.6)	-	-
8	37.3, C	-	-	-
9	60.3, CH	0.93, brd (13.0)	H-11	-
10	37.1, C	-	-	-
11α	18.7, CH_2	1.74, m	H-9	-
11β		1.35, dd (12.3, 3.0)	-	-
12α	40.1, CH_2	2.11, dd (12.9, 3.1)	-	C-14
12β		1.61, dd (19.8, 3.1)	-	-
13	84.3, C	-	-	-
14	52.3, CH	1.50, dd (12.5, 4.7)	H_2-15	C-8, 13, 26
15α	15.2, CH_2	2.55, dd (16.4, 4.9)	H-14	C-13, 14, 16, 17
15β		2.15, m	H-14	C-8, 14, 16
16	98.5, C	-	-	-
17	180.6, CO	-	-	-
18	111.9, CH	5.99, s	-	C-19, 20, 21
19	160.5, C	-	-	-
20	19.2, CH_3	2.20, s	-	C-18, 21
21	162.6, C	-	-	-
22	15.2, CH_3	0.78, s	H_3-23	C-3, 4, 5
23	28.0, CH_3	0.98, s	H_3-22	C-3, 4, 5, 22
24	16.4, CH_3	0.84, s	-	C-5, 9, 10
25	16.1, CH_3	0.89, s	-	C-7, 8, 9, 14
26	20.5, CH_3	1.28, s	-	C-12, 13, 14

Since **356** was obtained as a suitable crystal, the X-ray analysis was performed, and its ORTEP view was shown in Figure 55. Since the diffraction data were collected with a Gemini PX Ultra equipped with CuKα radiation, the absolute configurations of C-3, C-5, C-8, C-9, C-10, C-13 and C-14 were established as 3*S*, 5*R*, 8*R*, 9*R*, 10*R*, 13*S* and 14*S*, respectively. Since this is the first report of this chevalone analog, it was named chevalone E.

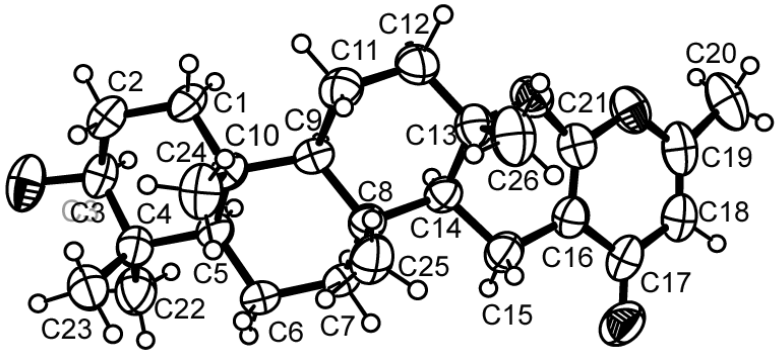

Figure 55. ORTEP diagram of chevalone E (**356**).

4.2.9) Chevalone B (348)

Compound **348** was isolated as a white solid (mp 161 – 163 °C). The general feature of ^{1}H and ^{13}C NMR spectra of **348** closely resemble those of **349**, except for the chemical shift value of conjugated carbonyl carbon (C-17; δ_C 165.4) of **348** appeared at lower frequency than that of chevalone C (δ_C 180.4).

The ^{13}C NMR spectrum (Table 14) exhibited twenty-eight carbon signals which can be classified, according to the DEPTs and HSQC spectra, as two ester carbonyl (δ_C 171.0 and 165.4), three quaternary sp^2 (δ_C 163.3, 159.7 and 97.7), one methine sp^2 (δ_C 100.6), four quaternary sp^3 (δ_C 80.4, 37.7, 37.2 and 37.0), four methine sp^3 (δ_C 80.6, 60.2, 55.4 and 51.8), seven methylene sp^3 (δ_C 40.8, 40.2, 37.9, 23.4, 18.6, 17.7 and 16.7) and seven methyl (δ_C 27.9, 21.2, 20.5, 19.6, 16.4, 16.3 and 16.0) carbons.

The ^{1}H NMR spectrum (Table 14), together with the HSQC spectrum, exhibited one doublet of olefinic proton at δ_H 5.70, J = 0.5 Hz (δ_C 100.6), three double doublets of

three methine protons at δ_H 4.46, *J* = 11.0, 5.1 Hz (δ_C 80.6), δ_H 1.45, *J* = 12.8, 4.8 Hz (δ_C 51.8) and δ_H 0.93, *J* = 12.0, 1.6 Hz (δ_C 60.2), one doublet of methine proton at δ_H 0.86, *J* = 2.8 Hz (δ_C 55.4), one double double doublet of methylene proton at δ_H 1.85, *J* = 12.7, 3.1, 3.1 Hz (δ_C 40.8), one double doublet of methylene proton at δ_H 2.43, *J* = 16.9, 4.9 Hz (δ_C 16.7), twelve multiplets of twelve methylene protons at δ_H 2.14 (δ_C 16.7), δ_H 2.06 (δ_C 40.2), δ_H 1.71 (δ_C 37.9), δ_H 1.70 (δ_C 18.6), δ_H 1.68 (δ_C 23.4), δ_H 1.61 (δ_C 23.4), δ_H 1.61 (δ_C 40.2), δ_H 1.57 (δ_C 17.7), δ_H 1.43 (δ_C 17.7), δ_H 1.32 (δ_C 18.6), δ_H 1.06 (δ_C 37.9) and δ_H 1.03 (δ_C 40.8), and seven methyl singlets at δ_H 2.18 (δ_C 19.6), δ_H 2.05 (δ_C 21.2), δ_H 1.20 (δ_C 20.5), δ_H 0.88 (δ_C 16.0), δ_H 0.87 (δ_C 16.3), δ_H 0.87 (δ_C 16.4) and δ_H 0.86 (δ_C 27.9).

The similarity of the ^{1}H and ^{13}C chemical shift values of **348** (Table 14) to those of chevalone C (**349**), as well as the COSY and HMBC correlations observed for **348**, indicated the presence of the 3-acetoxy-4,4,8,10,13-pentamethyltetradecahydro-phenanthrene moiety.

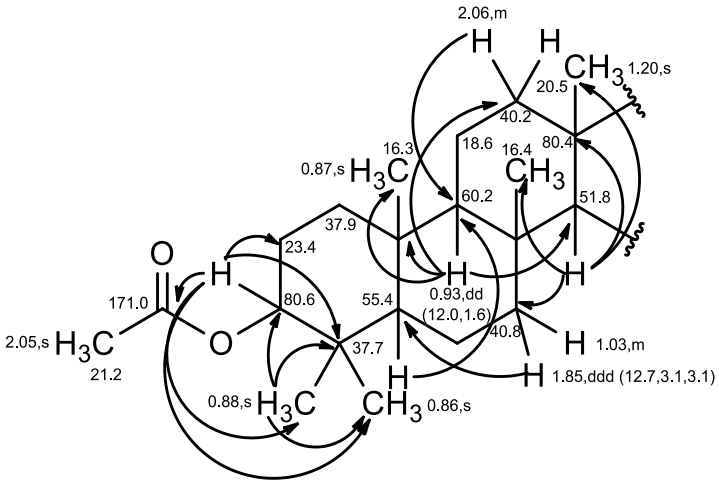

However, instead of the presence of the 5,6-disubstituted 2-methyl-4*H*-pyran-4-one, another moiety of **348** was 3,4-disubstituted 6-methyl-2*H*-pyran-2-one. This was confirmed by the COSY correlations from the olefinic proton at δ_H 5.70, d, *J* = 0.5 Hz (H-20) to the protons of the methyl singlet at δ_H 2.18 (H_3-19), indicating that they were allylic coupled, as well as by the HMBC correlations from the protons at δ_H 2.43, dd, *J* = 16.9, 4.9 Hz (H-15α) to the carbons at δ_C 80.4 (C-13), δ_C 51.8 (C-14), δ_C 97.7 (C-16), δ_C 165.4 (C-17) and δ_C 163.3 (C-21), from the proton at at δ_H 2.14, m (H-15β) to the carbon at δ_C

37.2 (C-8), C-14 and C-21, from H_3-19 to the carbons at δ_C 159.7 (C-18) and δ_C 100.6 (C-20), and from H-20 to C-16, C-18, the methyl carbon at δ_C 19.6 (C-19) and C-21.

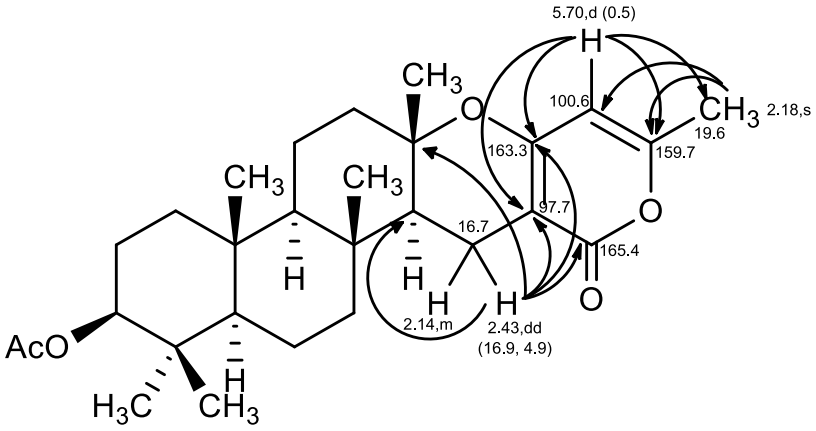

Literature survey revealed that **348** is a known compound, chevalone B, which was first isolated from the fungus *Eurotium chevalieri* (Kanokmedhakul *et al*., 2011) and later from *Neosartorya siamensis* (Gomes *et al*., 2014) and *Neosartorya takakii* (May Zin *et al*., 2015). Chevalone B exhibited cytotoxicity against KB (human epidermoid carcinoma in the mouth) and NCI-H187 (small cell lung cancer) cell lines with IC_{50} values of 2.9 and 3.9 µg/mL, respectively (Kanokmedhakul *et al*., 2011).

Table 14. ^{1}H and ^{13}C NMR ($CDCl_3$, 300.13 MHz and 75.4 MHz), and HMBC assignment for chevalone B (**348**).

Position	δ_C, Type	δ_H, (*J* in Hz)	COSY	HMBC
1α	37.9, CH_2	1.71, m	-	-
1β		1.06, m	-	-
2α	23.4, CH_2	1.68, m	H-3	-
2β		1,61, m	H-3	-
3	80.6, CH	4.46, dd (11.0, 5.1)	H_2-2	C-2, 4, 22, 23, CO (OAc-3)
4	37.7, C	-	-	-
5	55.4, CH	0.86, d (2.8)	-	C-9
6α	17.7, CH_2	1.57, m	-	-
6β		1.43, m	-	-
7α	40.8, CH_2	1.85, ddd (12.7, 3.1, 3.1)	-	C-5, 6, 9, 14
7β		1.03, m	-	-
8	37.2, C	-	-	-
9	60.2, CH	0.93, dd (12.0, 1.6)	H-11	C-10, 12, 14, 24
10	37.0, C	-	-	-
11α	18.6, CH_2	1.70, m	-	-
11β		1.32, m	H-9	-
12α	40.2, CH_2	2.06, m	-	C-9, 13, 14
12β		1.61, m	-	
13	80.4, C	-	-	-
14	51.8, CH	1.45, dd (12.8, 4.8)	H_2-15	C-7, 8, 9, 12, 13, 25, 26
15α	16.7, CH_2	2.43, dd (16.9, 4.9)	H-14	C-13, 14, 16, 17, 21
15β		2.14, m	H-14	C-8, 14, 21
16	97.7, C	-	-	-
17	165.4, CO	-	-	-
18	159.7, C	-	-	-
19	19.6, CH_3	2.18, s	H-20	C-18, 20
20	100.6, CH	5.70, d (0.5)	H_3-19	C-16, 18, 19, 21
21	163.3, C	-	-	-
22	16.0, CH_3	0.88, s	-	C-3, 4, 5, 23
23	27.9, CH_3	0.86, s	-	-
24	16.3, CH_3	0.87, s	-	C-10
25	16.4, CH_3	0.87, s	-	C-8, 14
26	20.5, CH_3	1.20, s	-	C-12, 13, 14
OAc-3	171.0, CO	-	-	-
	21.2, CH_3	2.05, s	-	CO (OAc-3)

4.2.10) S14-95 (377)

Compound **377** was isolated as a pale yellow viscous mass and its molecular formula $C_{28}H_{34}O_5$, was established on the basis of the (+)-HRESIMS *m/z* 451.2484 $[M+H]^+$, indicating twelve degrees of unsaturation.

The ^{13}C NMR spectrum (Table 15) exhibited twenty-eight carbon signals which can be categorized, according to the DEPTs and HSQC spectrum, as two ester carbonyl (δ_C 170.9 and 164.5), two oxyquaternary sp^2 (δ_C 163.2 and 152.8), two quaternary sp^2 (δ_C 131.4 and 99.3), six methine sp^2 (δ_C 130.5, 128.8, 128.8, 125.4, 125.4 and 98.3), one oxyquaternary sp^3 (δ_C 80.5), one oxymethine sp^3 (δ_C 80.1), two methine sp^3 (δ_C 55.0 and 51.4), five methylene sp^3 (δ_C 40.2, 37.1, 23.5, 19.2 and 17.2), two quaternary sp^3 (δ_C 37.7 and 36.7) and five methyl (δ_C 28.1, 21.3, 20.7, 16.6 and 15.1) carbons.

The ^1H NMR spectrum (Table 15), together with the HSQC spectrum, displayed five aromatic protons (δ_H 7.40 - δ_H 7.80), one olefinic proton (δ_H 6.37, s/δ_C 98.3), one oxymethine proton (δ_H 4.51, dd, *J* = 11.3, 5.0 Hz/δ_C 80.1), two methine protons (δ_H 1.51, dd, *J* = 12.8, 5.0 Hz/δ_C 51.4; δ_H 1.09, dd, *J* = 12.0, 2.0 Hz/δ_C 55.0), ten methylene protons (δ_H 2.52, dd, *J* = 17.4, 49 Hz/δ_C 17.2; δ_H 2.24, ddd, *J* = 16.9, 16.9, 4.0 Hz/δ_C 17.2; δ_H 2.14, ddd, *J* = 12.3, 2.9, 2.9 Hz/δ_C 40.2; δ_H 1.82, m/δ_C 37.1; δ_H 1.81, m (2H)/δ_C 19.2; δ_H 1.71, ddd, *J* = 14.1, 4.1, 4.1 Hz/δ_C 23.5; δ_H 1.71, m/δ_C 40.2; δ_H 1.65, m/δ_C 23.5; δ_H 1.18, ddd, *J* = 12.8, 12.8, 4.4 Hz/δ_C 37.1) and five methyl singlets (δ_H 2.06/δ_C 21.3; δ_H 1.27/δ_C 20.7; δ_H 0.94/δ_C 15.1; δ_H 0.91/δ_C 28.1; δ_H 0.89/δ_C 16.6).

Analysis of the ^1H and ^{13}C NMR, HSQC and HMBC spectra (Table 15) revealed the presence of the pentasubstituted decahydronaphthalene ring system with the acetoxyl group on C-3, one methyl group on C-4, one methyl group on C-6 and two methyl groups on C-10, similar to that of chevalone C (**349**). This hypothesis was supported by the HMBC correlations from the proton at δ_H 4.51, dd, *J* = 11.3, 5.0 Hz (H-1) to the carbons at δ_C 37.7 (C-10), δ_C 16.6 (C-11), δ_C 28.1 (C-15) and δ_C 170.9 (CO; OAc-1), from the methyl singlet at δ_H 0.89 (H_3-11) to the carbons at δ_C 80.1 (C-1) and δ_C 55.0 (C-9), from the methyl singlet at δ_H 1.27 (H_3-12) to C-9, from the methyl singlet at δ_H 0.94 (H_3-14) to the carbons at δ_C 51.4 (C-5), δ_C 80.5 (C-6) and the δ_C 37.1 (C-7), and from the methyl singlet at δ_H 0.91 (H_3-15) to C-1 and C-9.

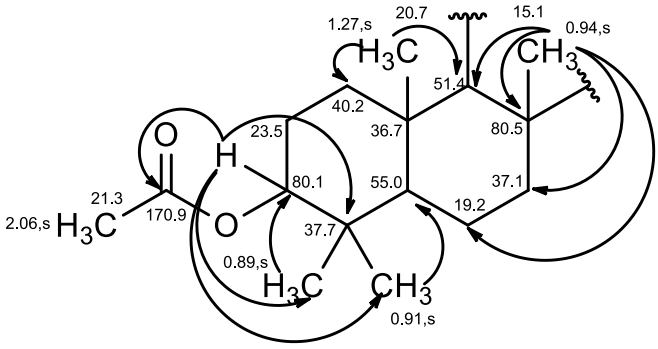

The COSY spectrum exhibited cross peaks from the mutually coupled methylene protons at δ_H 2.52, dd, *J* = 17.0, 4.9 Hz (H-13α) and δ_H 2.24, ddd, *J* = 16.9, 16.9, 4.0 Hz (H-13β)/δ_C 17.2 to the double doublet at δ_H 1.51, *J* = 12.8, 5.0 Hz (H-5). Furthermore, the HMBC spectrum showed cross peaks from H-13α to the carbons at δ_C 36.7 (C-4), C-5 and δ_C 99.3 (C-3'), from H-13β to C-5, C-6 and C-3' and from the proton at δ_H 6.37, s (H-5') to C-3' and the carbons at δ_C 163.2 (C-4') and δ_C 152.8 (C-6'). These data suggested that the decahydronaphthalene ring system was fused with the 3,4-dihydro-2*H*,5*H*-pyrano[4,3-*b*]pyran-5-one ring system through C-5 and C-6.

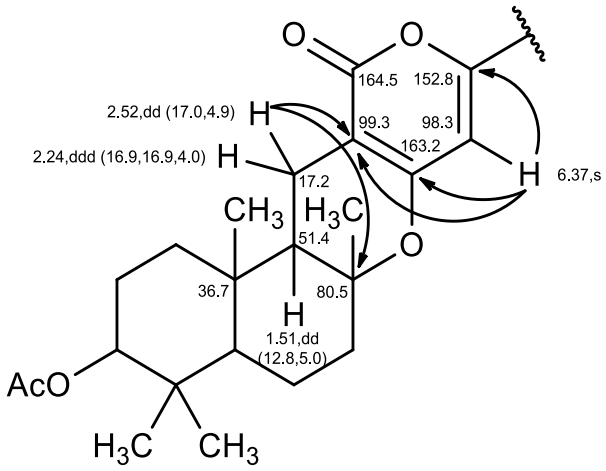

The presence of the phenyl group was corroborated by the presence of the multiplets of aromatic protons (δ_H 7.40 – 7.80) together with five methine sp^2 carbons at δ_C 125.4 (2C), δ_C 128.8 (2C), δ_C 130.5 and one quaternary sp^2 carbon at δ_C 131.4. That the benzene ring was connected to the pyran-2-one ring through the quaternary sp^2 carbon at δ_C 131.4 (C-1'') of the former and the C-6' of the later was supported by the HMBC correlation from H-5' to C-1''. Therefore, the structure of **377** was establisted as:

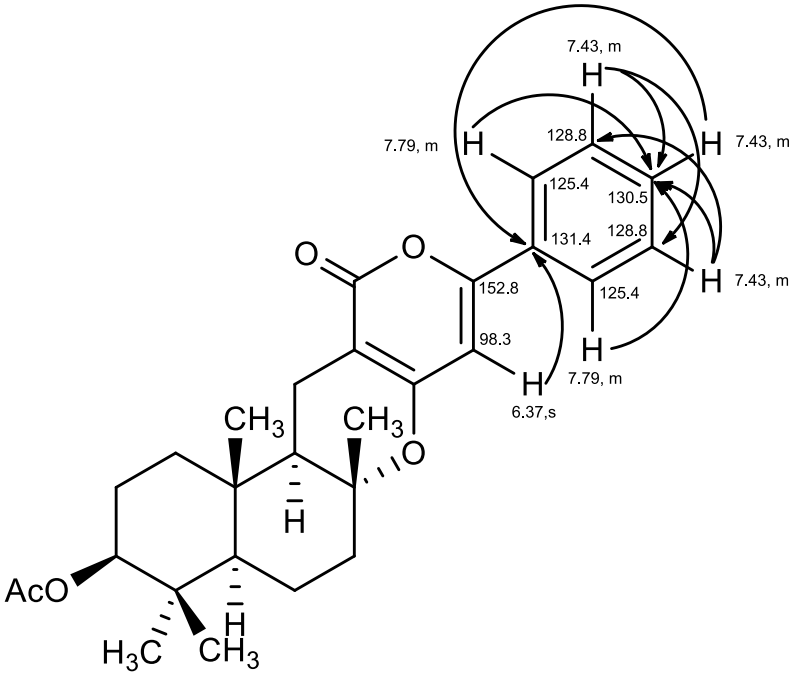

The ^{1}H and ^{13}C NMR and other physical data including optical rotation of **377** were compatible with those reported for S14-95, a meroterpenoid previously isolated from fermentation of *Penicillium* sp. (Erkel *et al*., 2003; Yao *et al.,* 2003). S14-95 exhibited inflammatory activity by inhibiting the IFN-γ mediated expression of the reporter genes, the proinflammatory enzymes COX-2 and NOS II and p38 MAP kinase (Erkel *et al*., 2003). In addition, this compound also inhibited cytokine-induced activation of STAT1α (Erkel *et al*., 2003; Yao *et al*., 2003) and iNOS-dependent NO production (Yao *et al*., 2003).

Table 15. ^{1}H and ^{13}C NMR ($CDCl_3$, 300.13 MHz and 75.4 MHz), and HMBC assignment for S14-95 (**377**).

Position	δ_C, Type	δ_H, (*J* = Hz)	COSY	HMBC
1	80.1, CH	4.51, dd (11.3, 5.0)	H-2	C-10, 11, 15, CO (OAc-1)
2α	23.5, CH_2	1.71, ddd (14.1, 4.1, 4.1)	-	-
2β		1.65, m	H-1	-
3α	40.2, CH_2	2.14, ddd (12.3, 2.9, 2.9)	-	-
3β		1.71, m	-	-
4	36.7, C	-	-	-
5	51.4, CH	1.51, dd (12.8, 5.0)	H_2-13	C-4, 6, 7, 13, 14
6	80.5, C	-	-	-
7α	37.1, CH_2	1.82, m	-	-
7β		1.18, ddd (12.8, 12.8, 4.4)	-	-
8	19.2, CH_2	1.81, m	-	-
9	55.0, CH	1.09, dd (12.0, 2.0)	-	C-7, 11, 12, 15
10	37.7, C	-	-	-
11	16.6, CH_3	0.89, s	-	C-1, 9
12	20.7, CH_3	1.27, s	-	C-9
13α	17.2, CH_2	2.52, dd (17.0, 4.9)	H-5	C-4, 5, 3’
13β		2.24, ddd (16.9, 16.9, 4.0)	H-5	C-5, 6, 3’
14	15.1, CH_3	0.94, s	-	C-5, 6, 7
15	28.1, CH_3	0.91, s	-	C-1,9
2’	164.5, C	-	-	-
3’	99.3, C	-	-	-
4’	163.2, C	-	-	-
5’	98.3, CH	6.37, s	-	C-3’, 4’, 6’, 1’’
6’	152.8, C	-	-	-
1’’	131.4, C	-	-	-
2’’	125.4, CH	7.79, m	-	-
3’’	128.8, CH	7.43, m	-	-
4’’	130.5, CH	7.43, m	-	-
5’’	128.8, CH	7.43, m	-	-
6’’	125.4, CH	7.79, m	-	-
OAc-1	170.9, CO	-	-	-
	21.3, CH_3	2.06, s	-	CO (OAc-1)

4.2.11) Pyripyropene E (154)

Compound **154** was isolated as a white solid (mp 240 – 244 °C). The general feature of ^{1}H and ^{13}C NMR of **154** closely resembled those of S14-95 (**377**), except for the absence of one aromatic carbon and one aromatic proton. Furthermore, the chemical shift values of aromatic carbons and protons of **154** appeared at higher frequencies than those of S14-95.

The ^{13}C NMR spectrum (Table 16) displayed twenty-seven carbon signals which can be categorized, based on the DEPTs and HMBC spectra, as two ester carbonyl (δ_C 170.6 and 163.7), two oxyquaternary sp^2 (δ_C 162.6 and 155.3), five methine sp^2 (δ_C 150.8, 146.4, 132.5, 123.4 and 99.2), two quaternary sp^2 (δ_C 127.3 and 100.0), one oxyquaternary sp^3 (δ_C 80.6), one oxymethine sp^3 (δ_C 79.9), two methine sp^3 (54.8 and 51.1), five methylene sp^3 (δ_C 39.9, 36.9, 23.2, 19.0 and 17.0), two quaternary sp^3 (δ_C 37.5 and 36.5) and five methyl (δ_C 27.8, 21.0, 20.4, 16.4 and 14.9) carbons.

The ^{1}H NMR spectrum (Table 16), together with the HSQC spectra, revealed the presence of four aromatic protons at δ_H 8.90, d, *J* = 2.3 Hz (δ_C 146.4), δ_H 8.55, dd, *J* = 4.8, 1.5 Hz (δ_C 150.8), δ_H 8.00, ddd, *J* = 8.1, 2.0, 2.0 Hz (δ_C 132.5) and δ_H 7.30, dd, *J* = 8.1, 4.8 Hz (δ_C 123.4), one olefinic proton at δ_H 6.35, s (δ_C 99.2), one oxymethine proton at δ_H 4.41, dd, *J* = 11.2, 4.9 Hz (δ_C 79.9), two methine protons at δ_H 1.42, dd, *J* = 12.7, 4.8 Hz (δ_C 51.1) and δ_H 1.00, dd, *J* = 12.0, 1.7 Hz (δ_C 54.8), ten methylene protons at δ_H 2.42, dd, *J* = 17.2, 48 Hz (δ_C 17.0), δ_H 2.14, m (δ_C 17.0), δ_H 2.05, m (δ_C 39.9), δ_H 1.72, m (δ_C 19.0), δ_H 1.71, m (δ_C 36.9), δ_H 1.64, m (2H; δ_C 23.3), δ_H 1.61, m (δ_C 39.9), δ_H 1.36, dd, *J* = 12.8, 2.9 Hz(δ_C 19.0) and δ_H 1.09, ddd, *J* = 12.9, 12.9, 4.6 Hz (δ_C 36.9), and five methyl singlets at δ_H 1.97 (δ_C 21.0), δ_H 1.18 (δ_C 20.4), δ_H 0.85 (δ_C 14.9), δ_H 0.82 (δ_C 27.8) and δ_H 0.80 (δ_C 16.4).

Like S14-95 (**377**), the decahydronaphthalene ring system was fused with the 3,4-dihydro-2*H*,5*H*-pyrano[4,3-*b*]pyran-5-one ring system through C-5 and C-6.

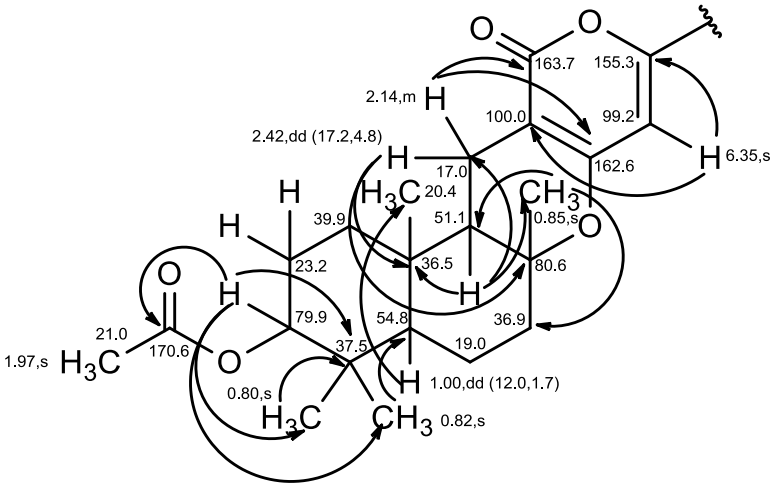

However, the substituent on C-6 of **154** was the 3-substituted pyridine ring. The presence of the 3-substituted pyridine ring instead of the phenyl ring in **377.** The presence of the 3-substituted pyridine ring was supported by the COSY correlations from the proton at δ_H 8.00, ddd, *J* = 8.1, 2.0, 2.0 Hz (H-4'') to the protons at δ_H 8.90, d, *J* = 2.3 Hz (H-2'') and δ_H 7.30, dd, *J* = 8.1, 4.8 Hz (H-5''), and from H-5'' to the proton at δ_H 8.55, dd, *J* = 4.8, 1.5 Hz (H-6''), as well as by the HMBC correlations from H-2'' to the carbons at δ_C 127.3 (C-3''), δ_C 132.5 (C-4'') and δ_C 150.8 (C-6''), from H-4'' to the carbon at δ_C 146.4 (C-2'') and C-6'', from H-5'' to C-3'' and C-6'', and from H-6'' to C-2'', C-4'' and the carbon at δ_C 123.4 (C-5''). Since the HMBC spectrum showed cross peaks from H-2'' and H-4'' to the oxyquaternary sp^2 carbon at δ_C 155.3 (C-6'), the 3-substituted pyridine ring was connected to C-6' of the pyran-2-one ring.

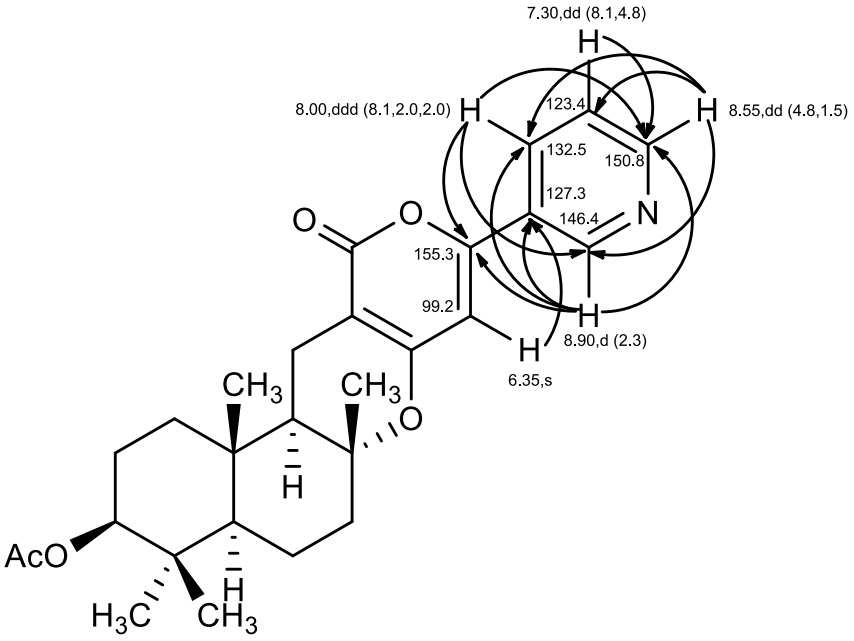

The ^{1}H, ^{13}C and other physical data of **154** allowed us to identify it as pyripyropene E. This commpound has been previously reported by Tomoda *et al*. (1995) and Masi *et al*. (2013) from the fungi *Aspergillus fumigatus* and *Neosartorya pseudofischeri*, respectively. Pyripyropene E exhibited weak inhibitory activity against acyl-CoA:cholesterol acyltransferase (ACAT) activity with an IC_{50} value of 399 μM (Tomoda *et al*.,1995) and *in vitro* growth inhibitory activity in five human cancer cell lines, including A549, Hs683, MCF7, SKMEL28 and U373, and one mouse cancer cell line, B16F1, with IC_{50} values of 37, 36, 22, 33, 87 and 13 μM, respectively (Masi *et al*., 2013).

Table 16. ^{1}H and ^{13}C NMR ($CDCl_3$, 300.13 MHz and 75.4 MHz), and HMBC assignment for pyripyropene E (**154**).

Position	δ_C, Type	δ_H, (*J* in Hz)	COSY	HMBC
1	79.9, CH	4.41, dd (11.2, 4.9)	H-2	C-10, 11, 15, CO (OAc-1)
2	23.2, CH_2	1.64, m	H-1	-
3α	39.9, CH_2	2.05, m	-	-
3β		1.61, m	-	-
4	36.5, C	-	-	-
5	51.1, CH	1.42, dd (12.7, 4.8)	H_2-13	C-4, 6, 12, 13, 14
6	80.6, C	-	-	-
7α	36.9, CH_2	1.71, m	-	-
7β		1.09, ddd (12.9, 12.9, 4.6)	-	-
8α	19.0, CH_2	1.72, m	H-9	-
8β		1.36, dd (12.8, 2.9)	-	-
9	54.8, CH	1.00, dd (12.0, 1.7)	H-8α	C-10, 12, 15
10	37.5, C	-	-	-
11	16.4, CH_3	0.80, s	-	C-9, 10
12	20.4, CH_3	1.18, s	-	C-3, 4
13α	17.0, CH_2	2.42, dd (17.2, 4.8)	H-5	C-4, 5, 2', 3', 4'
13β		2.14, m	H-5	C-6, 3', 4'
14	14.9, CH_3	0.85, s	-	C-5, 7
15	27.8, CH_3	0.82, s	-	C-9, 10
2'	163.7, C	-	-	-
3'	100.0, C	-	-	-
4'	162.6, C	-	-	-
5'	99.2, CH	6.35, s	-	C-3', 4', 6', 3''
6'	155.3, C	-	-	-
2''	146.4, CH	8.90, d (2.0)	H-4''	C-6', 3'', 4'', 6''
3''	127.3, C	-	-	-
4''	132.5, CH	8.00, ddd (8.1, 2.0, 2.0)	H-2'', 5''	C-6', 2'', 6''
5''	123.4, CH	7.30, dd (8.1, 4.8)	H-4'', 6''	C-3'', 6''
6''	150.8, CH	8.55, dd (4.8, 2.0)	H-5''	C-2'', 4'', 5''
OAc-1	170.6, CO	-	-	-
	21.0, CH_3	1.97, s	-	CO (OAc-1)

4.2.12) Pyripyropene S (378)

Compound **378** was isolated as pale yellow viscous mass, the (+)-HRESIMS of **378** indicated the $[M+H]^+$ peak at *m/z* 566.2416, corresponding to $C_{31}H_{36}NO_9$. Thus, the molecular formula of **378** is $C_{31}H_{35}NO_9$, indicating fifteen degrees of unsaturation. The IR spectrum showed absorption bands for ester carbonyl (1742 cm^{-1}), conjugated carbonyl (1671 cm^{-1}), aromatic (1586, 1508, 1465 cm^{-1}) and olefin (1625 cm^{-1}) groups.

The general feature of the ^1H and ^{13}C NMR spectra of **378** resembled to those of pyripyropene E (**154**). The ^{13}C NMR spectrum (Table 17) exhibited thirsty-one carbon signals which can be categorized, based on the DEPTs and HMBC spectra, as three ester carbonyl (δ_C 171.0, 170.4 and 169.8), one conjugated carbonyl (δ_C 161.3), five quaternary sp^2 (δ_C 161.2, 157.2, 144.5, 127.4 and 101.1), six methine sp^2 (δ_C 152.1, 146.6, 133.1, 123.8, 111.2 and 98.6), one oxyquaternary sp^3 (δ_C 83.9), two oxymethine sp^3 (δ_C 77.7 and 73.2), one oxymethylene sp^3 (δ_C 64.7), tone methine sp^3 (δ_C 41.1), two quaternary sp^3 (δ_C 40.6 and 38.8), hree methylene sp^3 (δ_C 35.5, 24.3 and 23.2) and six methyl (δ_C 24.2, 21.3, 21.2, 21.2, 20.8 and 13.3) carbons.

The ^1H NMR spectrum (Table 17), together with the HSQC spectra, exhibited four aromatic protons (δ_H 9.02, brs/δ_C 146.6; δ_H 8.68, brd, *J* = 4.0 Hz/δ_C 151.2; δ_H 8.14, ddd, *J* = 7.8, 1.4, 1.4 Hz/δ_C 133.1; δ_H 7.42, dd, *J* = 8.0, 4.9 Hz/δ_C 123.8), two olefinic protons (δ_H 6.54, s/δ_C 98.6; δ_H 6.36, s/δ_C 111.2), two oxymethine protons (δ_H 5.23, dd, *J* = 11.9, 5.4 Hz/δ_C 77.7; δ_H 4.79, dd, *J* = 11.7, 4.6 Hz/δ_C 73.2), one methine proton (δ_H 1.73, brd, *J* = 12.5 Hz/δ_C 41.1), two oxymethylene protons (δ_H 3.79, d, *J* = 11.9 Hz/δ_C 64.7; δ_H 3.75, d, *J* = 11.9 Hz/δ_C 64.7), six methylene protons (δ_H 2.09, m (2H)/δ_C 35.5; δ_H 1.99, m/δ_C 23.2; δ_H 1,82, ddd, *J* = 12.8, 5.1, 1.4 Hz/δ_C 24.3; δ_H 1.76, m/δ_C 23.2; δ_H 1.61, m/δ_C 24.3) and six methyl singlets (δ_H 2.17/δ_C 21.2; δ_H 2.10/δ_C 20.8; δ_H 2.05/δ_C 21.2; δ_H 1.59/δ_C 21.3; δ_H 1.26/δ_C 24.2; δ_H 0.88/δ_C 13.3).

Analysis of the ^1H, ^{13}C, HSQC and HMBC spectra (Table 17) revealed the presence of three acetoxyl groups (δ_C 170.4 and δ_C 21.2/δ_H 2.05s; δ_C 171.0 and δ_C 20.8/ δ_H 2.10, s; δ_C 169.8 and δ_C 21.2/ δ_H 2.17, s) and a hexasubstituted decahydronaphthalene ring system. That the three acetoxyl groups were on C-1, C-7 and C-11, was substantiated by the HMBC correlations from the proton at δ_H 3.75, d, *J* = 11.9 Hz (H-

11β) to the carbons at δ_C 73.2 (C-1), δ_C 41.1 (C-9) and δ_C 171.0 (CO; OAc-11), from the methyl singlet at δ_H 2.05 (H_3; OAc-1) to the carbon at δ_C 170.4 (CO; OAc-1), from the methyl singlet at δ_H 2.17 (H_3; OAc-7) to the carbon at δ_C 169.8 (CO; OAc-7), and from the methyl singlet at δ_H 2.10 (H_3; OAc-11) to CO (OAc-11). Like other pyripyropenes, the two methyl groups were on C-4 and C-6 was supported by the HMBC correlations from the methyl singlet at δ_H 1.26 (H_3-12) to the carbons at δ_C 35.5 (C-3), δ_C 38.8 (C-4) and C-9, and from the methyl singlet at δ_H 1.59 (H_3-14) to the carbons at δ_C 144.5 (C-5), δ_C 83.9 (C-6) and δ_C 77.7 (C-7). On the other hand, only one methyl group (δ_H 0.88, s, δ_C 13.3) was on C-10, was evidenced by the HMBC correlations from the methyl singlet at δ_H 0.88 (H_3-15) to C-1 and the carbon at δ_C 40.6 (C-10) and δ_C 64.7 (C-11).

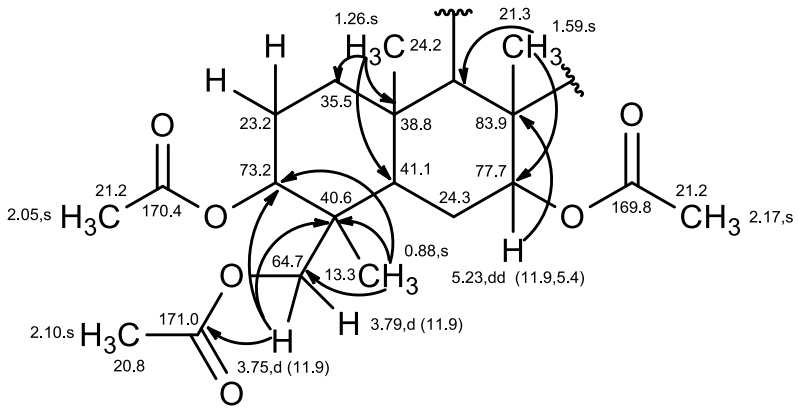

Since the HMBC spectrum exhibited cross peaks from H_3-14 to the carbons at δ_C 144.5 (C-5) and δ_C 83.9 (C-6), C-6 was linked to an oxygen atom and the double bond was on C-5. This was supported by the HMBC correlations from the proton at δ_H 6.36, s (H-13) to C-4 and C-6. On the other hand, the HMBC spectrum also displayed cross peaks from H-13 to the carbons at δ_C 161.3 (C-2') and δ_C 161.2 (C-4'), and from the singlet at δ_H 6.54 (H-5') to C-4' and the carbons at δ_C 101.1 (C-3') and δ_C 157.2 (C-6'), indicating the decahydronaphthalene ring system was fused with 2*H*,5*H*-pyrano[4,3-*b*]pyran-5-one ring system through C-5 and C-6.

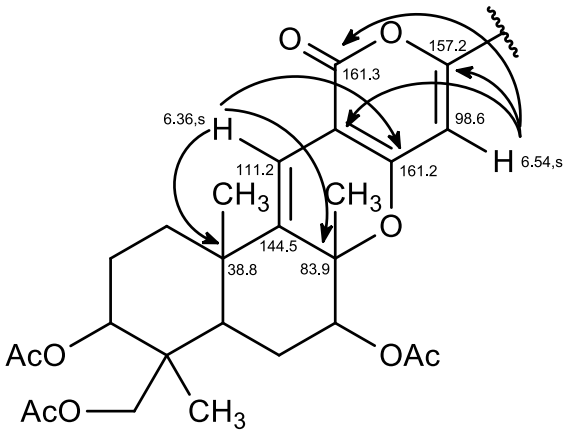

The COSY and HMBC spectra (Table 17) also indicated the presence of the 3-substitued pyridine ring. Like pyripyropene E (**154**), the 3-substituted pyridine ring was connected to the 2-pyranone ring through C-6' and C-3'' since H-5' (δ_H 6.54, s) showed HMBC cross peak to C-3'' (δ_C 127.4).

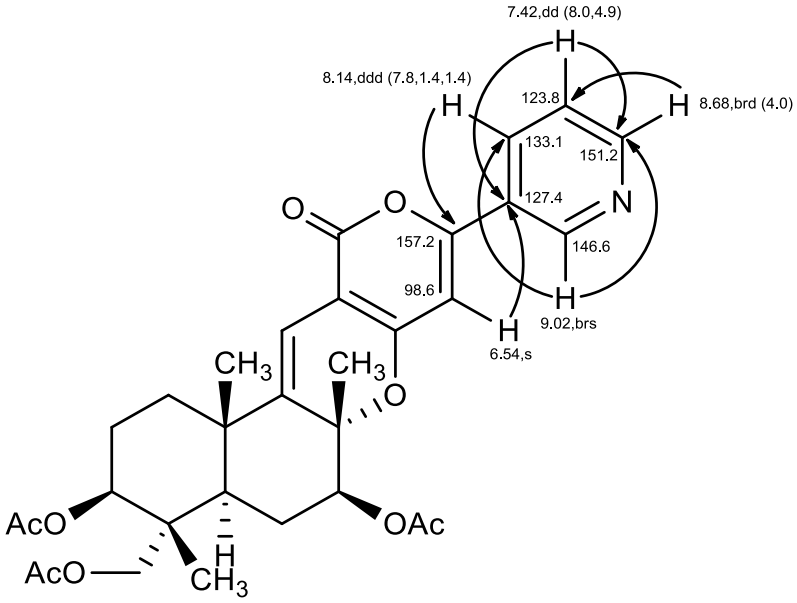

Literature survey revealed that **378** was previously obtained by treatment of pyripyropene A with HCl under anhydrous condition (Obata *et al*., 1995). However, the ^{1}H and ^{13}C NMR data and other description of this compound have not been reported. Since **379** is a new natural product, it was named pyripyropene S.

Table 17. ^{1}H and ^{13}C NMR ($CDCl_3$, 500.13 MHz and 125.8 MHz), and HMBC assignment for pyripyropene S (**378**).

Position	δ_C, Type	δ_H, (*J* in Hz)	COSY	HMBC
1	73.2, CH	4.79, dd (11.7, 4.6)	H-2	-
2α	23.2, CH_2	1.99, m	H-1	-
2β		1.76, m	-	-
3	35.5, CH_2	2.09, m	-	-
4	38.8, C	-	-	-
5	144.5, C	-	-	-
6	83.9, C	-	-	-
7	77.7, CH	5.23, dd (11.9, 5.4)	H-8	C-6
8α	24.3, CH_2	1.82, ddd (12.8, 5.1, 1.4)	H-7, 9	-
8β		1.61, m	-	-
9	41.1, CH	1.73, brd (12.5)	H-8	-
10	40.6, C	-	-	-
11α	64.7, CH_2	3.79, d (11.9)	-	-
11β		3.75, d (11.9)	-	C-1, 9, CO (OAc-11)
12	24.2, CH_3	1.26, s	-	C-3, 4, 9
13	111.2, CH	6.36, s	-	C-4, 6, 2', 4'
14	21.3, CH_3	1.59, s	-	C-5, 6, 7
15	13.3, CH_3	0.88, s	-	C-1, 10, 11
2'	161.3, C	-	-	-
3'	101.1, C	-	-	-
4'	161.2, C	-	-	-
5'	98.6, CH	6.54, s	-	C-2', 3', 6', 3''
6'	157.2, C	-	-	-
2''	146.6, CH	9.02, brs	H-4''	C-3'', 4'', 6''
3''	127.4, C	-	-	-
4''	133.1, CH	8.14, ddd (7.8, 1.4, 1.4)	H-2'', 5''	C-6', 2''
5''	123.8, CH	7.42, dd (8.0, 4.9)	H-4'', 6''	C-3'', 6''
6''	151.2, CH	8.68, brd (4.0)	H-5''	C-5''
OAc-1	170.4, CO	-	-	-
	21.2, CH_3	2.05, s	-	CO (OAc-1)
OAc-7	169.8, CO	-	-	-
	21.2, CH_3	2.17, s	-	CO (OAc-7)
OAc-11	171.0, CO	-	-	-
	20.8, CH_3	2.10, s	-	CO (OAc-11)

4.2.13) Pyripyropene T (379)

Compound **379** was isolated as a pale yellow viscous mass and its molecular formula $C_{29}H_{33}NO_8$ was established on the basis of (+)-HRESIMS *m/z* 524.2284 $[M+H]^+$, indicating fourteen degrees of unsaturation. The IR spectrum showed absorption bands for hydroxyl (3418 cm^{-1}), ester carbonyl (1732 cm^{-1}), conjugated ester carbonyl (1667 cm^{-1}), olefin (1643 cm^{-1}), aromatic (1557, 1507 cm^{-1}).

The general feature of ^{1}H and ^{13}C of **379** closely resembled those of pyripyropene S (**378**). The ^{13}C NMR spectra (Table 18) exhibited twenty-nine carbon signals which can be categorized, based on DEPTs and HSQC spectra, as two ester carbonyl (δ_C 170.1 and 169.8), one conjugated carbonyl (δ_C 161.6), five quaternary sp^2 (δ_C 160.2, 156.8, 146.1, 126.9 and 100.3), methine sp^2 (δ_C 151.3, 146.5, 132.8, 123.9, 109.4 and 98.7), one oxyquaternary sp^3 (δ_C 85.9), two oxymethine sp^3 (δ_C 75.7 and 72.8), six one oxymethylene sp^3 (δ_C 64.4), one methine sp^3 (δ_C 40.7), two quaternary sp^3 (δ_C 40.3 and 38.4), three methylene sp^3 (δ_C 35.2, 27.3 and 22.9) and five methyl (δ_C 23.8, 20.5, 20.8, 20.1 and 12.7) carbons.

The ^{1}H NMR and HSQC spectra (Table 18) revealed the presence of four aromatic protons (δ_H 9.00, d, *J* = 1.7 Hz/δ_C 146.5; δ_H 8.68, dd, *J* = 4.8, 1.5 Hz/δ_C 151.3; δ_H 8.25, dd, *J* = 8.7, 2.2 Hz/δ_C 132.8; δ_H 7.54, dd, *J* = 7.9, 4.8 Hz/δ_C 123.9), two olefinic protons (δ_H 7.11, s/δ_C 98.7; δ_H 6.16, s/δ_C 109.4), one oxymethine proton (δ_H 4.64, t, *J* = 8.5 Hz/ δ_C 72.8), two methine protons (δ_H 3.85, dd, *J* = 10.6, 4.2 Hz/δ_C 75.7; δ_H 1.48, m/δ_C 40.7), two oxymethylene protons (δ_H 3.75, s (2H)/δ_C 64.4), six methylene protons (δ_H 1.98, m (2H)/δ_C 35.2; δ_H 1.79, m (2H)/δ_C 22.9; δ_H 1.70, m (2H)/δ_C 27.3) and five methyl singlets (δ_H 2.00/δ_C 20.8; δ_H 2.00/δ_C 20.5; δ_H 1.45/δ_C 20.1; δ_H 1.19/δ_C 23.8; δ_H 0.84/δ_C 12.7).

Analysis of the ^{1}H, ^{13}C, HSQC and HMBC data (Table 18) revealed the presence of the decahydronaphthalene ring system, which was fused with the 2*H*,5*H*-pyrano[4,3-*b*]pyran-5-one through C-5 (δ_C 146.1) and C-6 (δ_C 85.9) whereas the 3-monosubstituted pyridine ring was also connected to the pyranone ring through C-6' (δ_C 156.8) of the former and C-3'' (δ_C 126.9) of the later, similar to pyripyropene S.

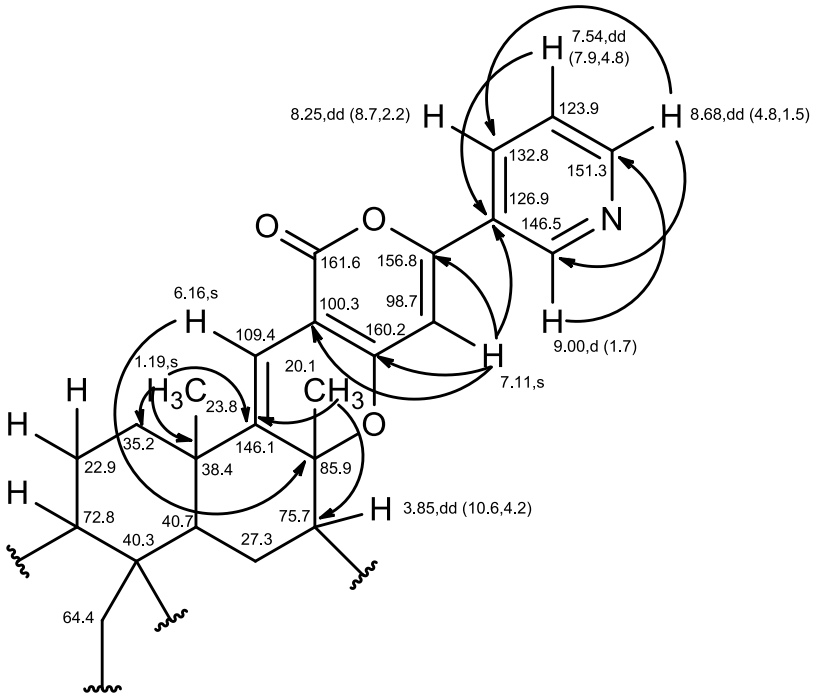

On the other hand, there were only two acetoxyl groups (δ_C 170.1; CO, δ_C 20.5; CH_3/ δ_H 2.00, s and δ_C 169.8; CO, δ_C 20.8; CH_3/ δ_H 2.00, s) in **379**. That the acetoxyl groups were on C-1 and C-11 was supported by the similarity of the chemical shift values of H-1 (δ_H 4.64, t, *J* = 8.5 Hz) and H-11 (δ_H 3.75, s) to those of pyripyropene S. That the substituent on C-7 of **379** was a hydroxyl group instead of an acetoxyl group was evidenced by the chemical shift value of H-7 (δ_H 3.85, dd, *J* = 10.6, 4.2 Hz), which was about 1.4 ppm less than that of pyripyropene S, as well as by the chemical shift value of C-7 (δ_C 75.5), which was 2.00 ppm lower than that of C-7 of pyripyropene S. Moreover, the chemical shift values of C-6 (δ_C 85.9) and C-8 (δ_C 27.3) of **379** were *ca*. 2.00 and 3.00 ppm, respectively, higher than those of pyripyropene S. As H-7 appeared as a double doublet with a diaxial coupling constant of 10.6 Hz and an axial-equatorial coupling constant of 4.2 Hz, the position of the hydroxyl group on C-7 was β. Therefore, **379** is 7-deacetylpyripyropene S. The stereochemistry of **379** was confirmed by the NOESY experiments, which exhibited correlations from CH_3-15 to CH_3-12, but not to H-1 and H-9, from CH_3-12 to CH_3-14 and CH_3-15, and from CH_3-14 to CH_3-12, but not to H-7 (Table 18). Thus, the stereochemistry of **379** is the same as that of pyripyropene S (**378**), i.e.

1*S**, 4*R**, 6*S**, 7*S**, 9*R**, 10*R**. Since **379** is a new compound, it was named pyripyropene T.

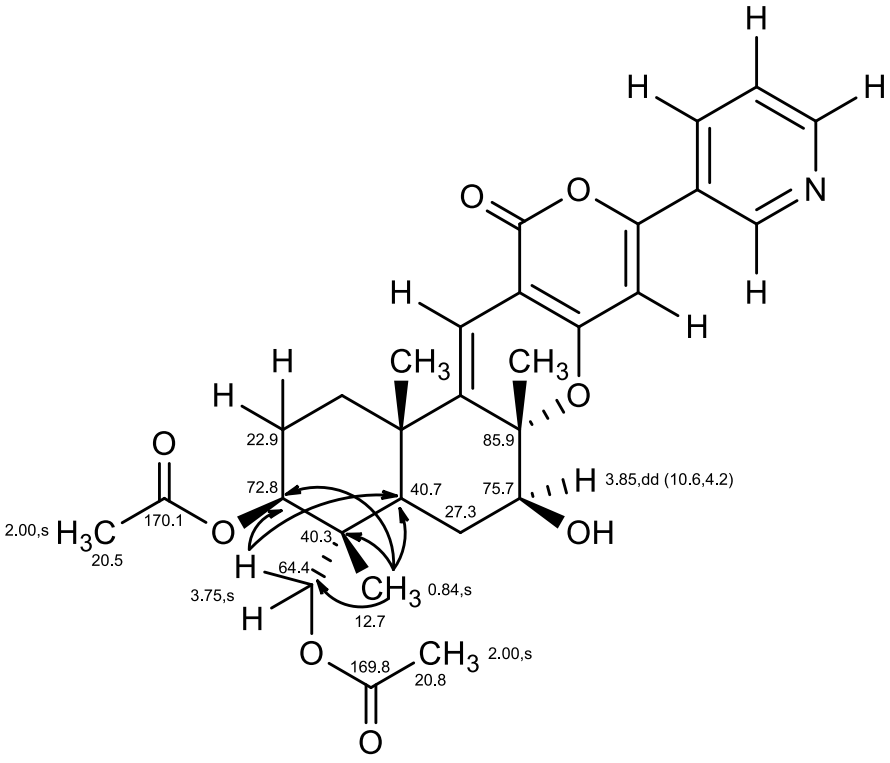

Table 18. ^{1}H and ^{13}C NMR ($CDCl_3$, 500.13 MHz and 125.8 MHz), and HMBC assignment for pyripyropene T (**379**).

Position	δ_C, Type	δ_H, (*J* in Hz)	COSY	HMBC	NOESY
1	72.8, CH	4.64, t (8.5)	H-2	-	-
2	22.9, CH_2	1.79, m	H-1, 3	-	-
3	35.2, CH_2	1.98, m	H-2	-	-
4	38.4, C	-	-	-	-
5	146.1, C	-	-	-	-
6	85.9, C	-	-	-	-
7	75.7, CH	3.85, dd (10.6, 4.2)	H-8	-	-
8	27.3, CH_2	1.70, m	H-7, 9	-	-
9	40.7, CH	1.48, m	H-8	-	-
10	40.3, C	-	-	-	-
11	64.4, CH_2	3.75, s	-	C-1, 9	C-12
12	23.8, CH_3	1.19, s	-	C-3, 4, 5	H-14, 15
13	109.4, CH	6.16, s	-	C-4, 6	-
14	20.1, CH_3	1.45, s	-	C-5, 6, 7	C-13
15	12.7, CH_3	0.84, s	-	C-1, 9, 10, 11	H-11, 12
2’	161.6, C	-	-	-	-
3’	100.3, C	-	-	-	-
4’	160.2, C	-	-	-	-
5’	98.7, CH	7.11, s	-	C-3’, 4’, 6’, 3’’	-
6’	156.8, C	-	-	-	-
2’’	146.5, CH	9.00, d (1.7)	H-4’’, 6’’	C-3’’, 6’’	H-5’
3’’	126.9, C	-	-	-	-
4’’	132.8, CH	8.25, dd (8.7, 2.2)	H-2’’, 5’’	-	H-5’, 5’’
5’’	123.9, CH	7.54, dd (7.9, 4.8)	H-4’’, 6’’	C-3’’	H-4’’, 6’’
6’’	151.3, CH	8.68, dd (4.8, 1.5)	H-2’’, 5’’	C-2’’, 4’’	H-5’’
OAc-1	170.1, CO	-	-	-	-
	20.5, CH_3	2.00, s	-	CO (OAc-1)	-
OAc-11	169.8, CO	-	-	-	-
	20.8, CH_3	2.00, s	-	CO (OAc-11)	-

4.2.14) Similanamide (380)

Compound **380** was isolated as pale yellow viscous mass and its molecular formula $C_{34}H_{52}N_6O_6$ was deduced from the (+)-HRESIMS *m/z* 641.4053 $[M+H]^+$, indicating twelve degrees of unsaturation. The IR spectrum exhibited absorption bands for amine (3335 cm^{-1}), ketone carbonyl (1682, 1644 cm^{-1}) and aromatic (1594, 1519 cm^{-1}).

The ^{13}C NMR spectrum (Table 19) exhibited thirty-four carbon signals which can be classified, according to DEPTs and HSQC spectra, as six amide carbonyls (δ_C 174.3, 174.2, 170.7, 170.2, 169.3 and 168.9), two quaternary sp^2 (δ_C 137.0 and 122.7), four methine sp^2 (δ_C 131.7, 127.1, 123.9 and 123.4), eight methine sp^3 (δ_C 65.1, 61.4, 59.3, 50.9, 47.9, 29.9, 25.5 and 24.4), six methylene sp^3 (δ_C 52.5, 37.8, 36.2, 28.1, 27.4 and 24.5) and eight methyl (δ_C 37.9, 23.3, 23.2, 22.1, 21.7, 19.8, 18.4 and 16.2) carbons.

The ^1H NMR spectrum (Table 19), together with the HSQC spectrum, displayed the presence of, besides four amide protons at δ_H 9.41, brs; 8.02, d, *J* = 7.9 Hz; 7.64, d, *J* = 9.7 Hz; 7.43, d, *J* = 7.5 Hz, and four aromatic protons of the 1,2-disubstitued benzene ring at δ_H 8.29, d, *J* = 8.3 Hz (δ_C 123.9); δ_H 7.20, dd, *J* = 7.7, 1.5 Hz (δ_C 127.1); δ_H 7.47, ddd, *J* = 7.9, 7.9, 1.6 Hz (δ_C 131.7); δ_H 7.13, ddd, *J* = 7.9, 7.9, 1.0 Hz (23.4), eight methine protons at δ_H 4.82, dd, *J* = 7.4, 3.3 Hz (δ_C 47.9); δ_H 4.57, m (δ_C 50.9); δ_H 3.71, dd, *J* = 11.3, 2.5 Hz (δ_C 61.4); δ_H 3.49, dd, *J* = 9.0, 4.7 Hz (δ_C 65.1); δ_H 2.68, m (δ_C 29.9); δ_H 1.77, m (δ_C 24.4); δ_H 1.65, m (δ_C 25.5), twelve methylene protons at δ_H 4.14, dd, *J* = 14.4, 2.4 Hz (δ_C 52.5); δ_H 3.16, dd, *J* = 13.2, 2.3 Hz(δ_C 52.5); δ_H 2.20, m (δ_C 37.8); δ_H 2.07, m (2H; δ_C 24.5); δ_H 2.05, m (2H; δ_C 28.1); δ_H 2.02, m (δ_C 36.2); δ_H 1.95, m (δ_C 37.8); δ_H 1.77, m (δ_C 36.2); δ_H 1.56, m (2H; δ_C 27.4), one methyl singlet at δ_H 3.20 (δ_C 37.9), and seven methyl doublets at δ_H 1.29, *J* = 7.3 Hz (δ_C 18.4); δ_H 1.06, *J* = 6.9 Hz (δ_C 19.8); δ_H 0.99, *J* = 6.5 Hz (δ_C 22.1); δ_H 0.97, *J* = 6.5 Hz (δ_C 23.2); δ_H 0.97, *J* = 6.5 Hz (δ_C 23.3); δ_H 0.94, *J* = 7.0 Hz (δ_C 16.2); δ_H 0.88, *J* = 6.4 Hz (δ_C 21.7).

The COSY and HMBC spectra (Table 19) indicated the presence of a 1,2-disubstituted benzene ring. The HMBC spectrum exhibited the correlations from the aromatic proton at δ_H 7.20, dd, *J* = 7.7, 1.5 Hz (H-3) to the amide carbonyl at δ_C 170.2 (C-1), and from the amide proton at δ_H 9.41, brs (NH) to the carbons at δ_C 123.9 (C-6) and

δ_C 137.0 (C-7), indicating therefore the presence of the anthranilic acid residue was corroborated.

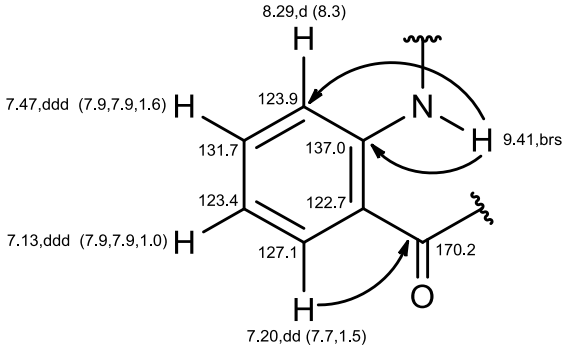

The presence of the valine residue was evidenced by the COSY correlations from the methine proton at δ_H 4.32, dd, *J* = 7.4, 3.3 Hz (H-9; δ_C 59.3) to the methine proton at δ_H 2.68, m (H-10; δ_C 29.9) and the amide proton at δ_H 7.43, d, *J* = 7.5 Hz (NH), and from H-10 to the methyl doublets at δ_H 1.06, *J* = 6.9 Hz (H_3-11; δ_C 19.8) and δ_H 0.94, *J* = 7.0 Hz (H_3-12; δ_C 16.2), as well as by the HMBC correlations from H-9 to the amide carbonyl at δ_C 170.7 (C-8), the carbons at δ_C 29.9 (C-10), δ_C 19.8 (C-11) and δ_C 16.2 (C-12), from H_3-11 to the carbon at δ_C 59.3 (C-9), C-10 and C-12, from H_3-12 to C-9, C-10 and C-11, and from NH to C-9 and C-10.

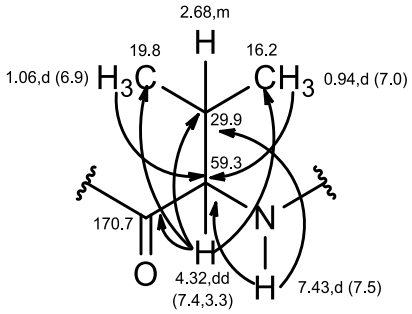

That the valine residue was linked to the anthranilic acid residue through the carbonyl group of the former and the amino group of the latter was corroborated by the HMBC correlation from the *brs* at δ_H 9.42 to the carbonyl at δ_C 170.7 (C-8).

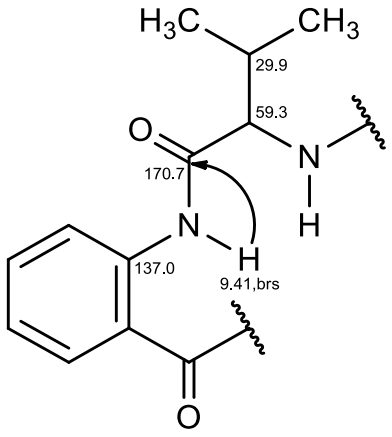

The COSY correlations from the methine proton at δ_H 4.57, m (H-14; δ_C 50.9) to the methylene protons at δ_H 2.20, m and 1.77, m (H_2-15; δ_C 36.2), the methine proton at δ_H 1.77, m (H-16; δ_C 24.4), the methyl doublets at δ_H 0.97, d, J = 6.5 Hz (H_3-17; δ_C 23.3) and 0.88, d, J = 6.4 Hz (H_3-18; δ_C 21.7) and the amide proton at δ_H 8.02, d, J = 7.9 Hz (NH), together with the HMBC correlations from H_3-17 to the carbons at δ_C 36.2 (C-15), δ_C 24.4 (C-16) and δ_C 21.7 (C-18), from H_3-18 to C-15, C-16 and the methyl carbon at δ_C 23.3 (C-17), and from NH (δ_H 8.02, d, J = 7.9 Hz) to the amide carbonyl at δ_C 174.2 (C-13), indicated the presence of the leucine residue.

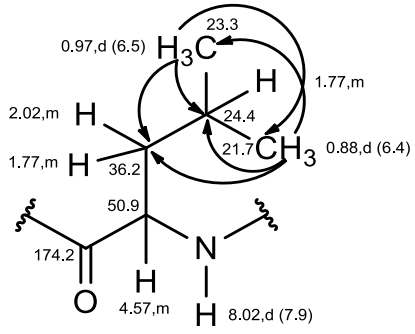

That the leucine residue was linked to the valine residue through the carbonyl group of the former and the amino group of the latter was supported by the HMBC correlation from NH (δ_H 7.43, d, J = 7.5 Hz) to C-13 (δ_C 174.2).

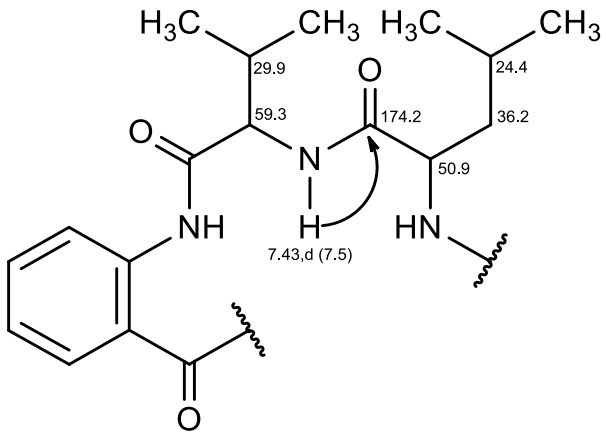

The presence of the alanine residue was substantiated by the COSY correlations from the methine proton at δ_H 4.82, dd, *J* = 9.7, 7.3 Hz (H-20; δ_C 47.9) to the methyl doublet at δ_H 1.29, *J* = 7.3 Hz (H_3-21; δ_C 18.4) and the amide proton at δ_H 7.64, d, *J* = 7.9 Hz (NH), as well as by the HMBC correlations from H-20 to the amide carbonyl at δ_C 174.3 (C-19) and the methyl carbon at δ_C 18.4 (C-21), and from H_3-21 to C-19 and the carbon at δ_C 47.9 (C-20).

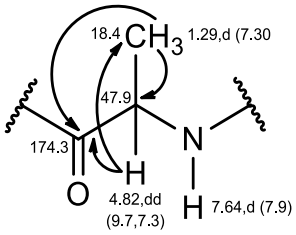

That the alanine residue was linked to the leucine residue through the carbonyl group of the former and the amino group of the latter was evidenced by the HMBC correlation from the NH (δ_H 8.02, d, *J* = 7.9 Hz) to C-19.

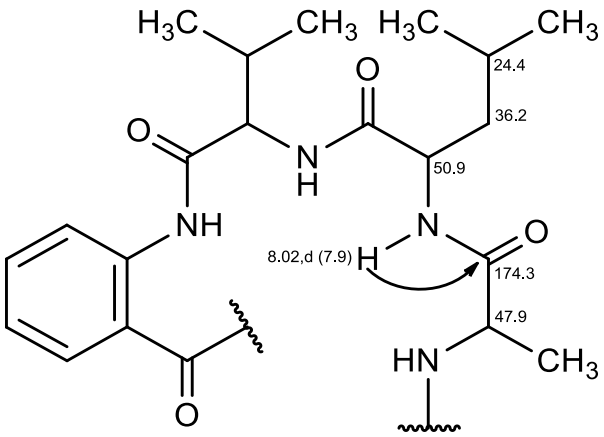

As the COSY spectrum displayed the correlations of the methylene protons at δ_H 2.20, m and 1.95, m (H_2-24; δ_C 37.8) to two methine protons at δ_H 3.49, dd, *J* = 9.0, 4.7 Hz (H-23; δ_C 65.1) and 1.65, m (H-25; δ_C 25.5). In turn, H-25 was also correlated to the methyl doublets at δ_H 0.97, *J* = 6.5 Hz (H_3-26; δ_C 23.2) and 0.99, *J* = 6.5 Hz (H_3-27; δ_C 22.1), the presence of a 2-methylbutyl moiety was suggested. This was confirmed by the HMBC correlations from H-23 to the carbon at δ_C 37.8 (C-24), from H_3-26 to C-24, the carbons at δ_C 25.5 (C-25) and δ_C 22.1 (C-27), and from H_3-27 to C-24, C-25 and the methyl carbon at δ_C 23.2 (C-26).

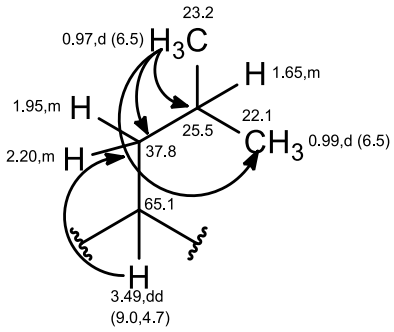

The HMBC spectrum also exhibited the correlations from H-23 to the amide carbonyl at δ_C 169.3 (C-22) and the methyl carbon at δ_C 37.9 (C-28), and from the methyl singlet at δ_H 3.20 (H_3-28) to the carbon at δ_C 65.1 (C-23), suggesting the presence of the *N*-methyl leucine moiety.

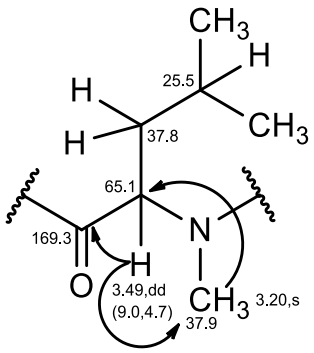

The HMBC spectrum displayed cross peak from the NH at δ_H 7,64, d, *J* = 7.9 Hz to C-22, indicating that the alanine residue was linked to the *N*-methyl leucine residue through the amino group of the former and the carbonyl group of the latter.

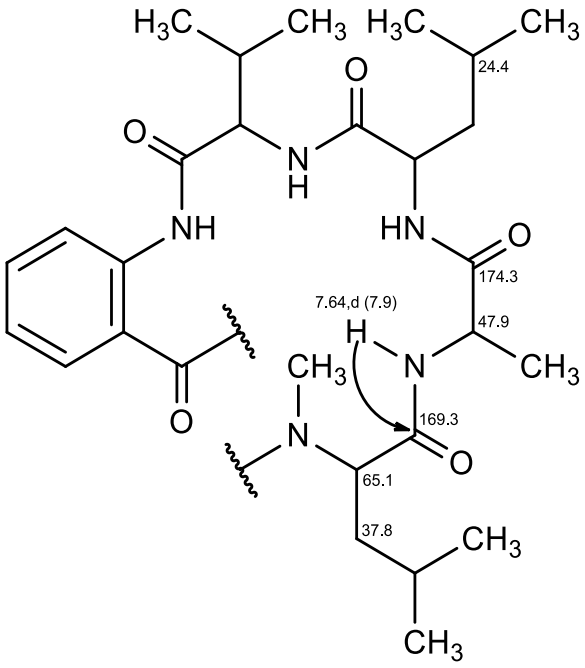

Finally, the presence of pipercolic acid was corroborated by the COSY correlations from the methylene protons at δ_H 2.05, m (H_2-31/δ_C 28.1) to the methine proton at δ_H 3.71, dd, *J* = 11.3, 2.5 Hz (H-30/δ_C 61.4) and the methylene protons at δ_H 2.07, m (H_2-32/ δ_C 24.5), from H_2-32 to the methylene protons at δ_H 1.56, m (H_2-33/δ_C 27.4), from H_2-33 to H-34α (δ_H 3.16, dd, *J* = 13.2, 2.3 Hz), and from H-34α to H-34β (δ_H 4.14, dd, *J* = 14.4,

2.4 Hz). This was supported by the HMBC correlation from H-30 to the carbonyl at δ_C 168.9 (C-29).

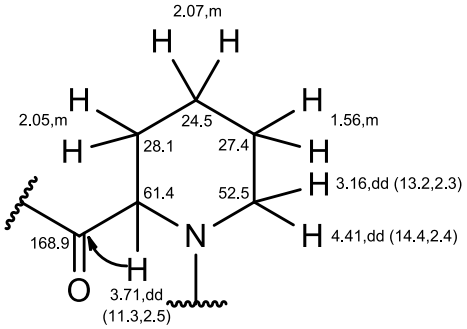

The HMBC correlation from H_3-28 to C-29 indicated that the pipercolic acid was linked to the *N*-methyl leucine through the carbonyl group (δ_C 168.9) of the former and the amino group (δ_H 3.20, s) of the latter.

Since **380** presents twelve degrees of unsaturation, the nitrogen atom of the piperidine ring of the pipecolic acid moiety must link to the carbonyl carbon of the anthranilic acid residue, forming a cyclic structure. This hypothesis was also supported by the HMBC correlation from H-30 to the carbonyl of the anthranilic acid residue (C-1), as well as by the NOESY correlations from the NH at δ_H 9.41, brs (NH; anthranilic acid) to H-9 and H_3-12, from NH at δ_H 7.43, d, *J* = 7.5 Hz (NH; Val) to H-9, H_3-11, H_3-12 and H-14, from NH at δ_H 8.02, d, *J* = 7.9 Hz (NH; Leu) to H-14, H-15 and H_3-17, from NH at δ_H 7.64, d, *J* = 7.9 Hz (NH; Ala) to H_3-21, H-23, H_3-28, from H-3 to H-34β (δ_H 4.14, dd, *J* = 14.4, 2.4 Hz), and from H-30 to H_3-28. Therefore, compound **380** was identified as cyclo (anthranilic acid-Val-Leu-Ala-*N*-methyl-Leu-pipecolic acid).

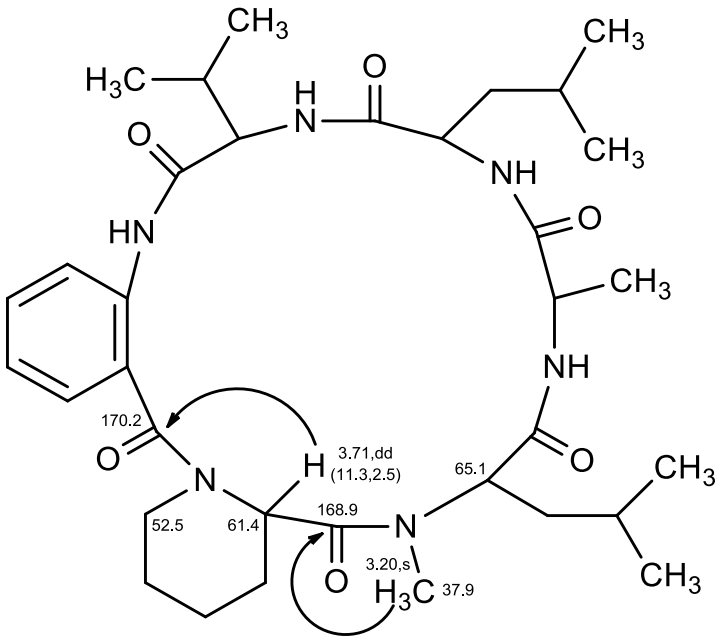

Extensive literature search revealed that the ^{1}H and ^{13}C NMR data of **380** were similar to those of the cyclic hexapeptide PF1171C, previously isolated from the fermentation of okara by the unidentified ascomycete OK-128 by Kai *et al*. (2010) and later by a total synthesis by Masuda *et al*. (2014). However, some of their physical properties are difference. Compound **380** was isolated as a pale yellow viscous mass while PF1171C was reported as a white solid (mp 138 – 140 °C) (Masuda *et al*., 2014). Moreover, the value of optical rotation of **380** was quite different from that of PF1171C (Kai *et al*., 2010; Masuda *et al*., 2014). This observation suggested that **380** and PF1171C could be diastereomers.

Table 19. ^{1}H and ^{13}C NMR ($CDCl_3$, 500.13 MHz and 125.8 MHz) and HMBC assignment of similanamide (**380**).

	Position	δ_C, Type	δ_H, (*J* in Hz)	COSY	HMBC	NOESY
Anthranilic acid	1	170.2, CO	-	-	-	-
	2	122.7, C	-	-	-	-
	3	127.1, CH	7.20, dd (7.7, 1.5)	H-4	C-1, 5, 7	H-34
	4	123.4, CH	7.13, ddd (7.9, 7.9, 1.0)	H-3, 5	C-2, 6	-
	5	131.7, CH	7.47, ddd (7.9, 7.9, 1.6)	H-4, 6	C-3, 7	-
	6	123.9, CH	8.29, d (8.3)	H-5	C-2, 4	H-12
	7	137.0, C	-	-	-	-
	NH	-	9.41, brs	-	C-6, 7, 8	NH (Val), H-9, 12
Val	8	170.7, CO	-	-	-	-
	9	59.3, CH	4.32, dd (7.4, 3.3)	H-10, NH	C-8, 10, 11, 12	H-10, 11
	10	29.9, CH	2.68, m	H-9, 11, 12	-	H-9, 11, 12
	11	19.8, CH_3	1.06, d (6.9)	H-10	C-9, 10, 12	-
	12	16.2, CH_3	0.94, d (7.0)	H-10	C-9, 10, 11	-
	NH	-	7.43, d (7.5)	H-9	C-9, 10, 13	H-9, 11, 12, 14
Leu	13	174.2, CO	-	-	-	-
	14	50.9, CH	4.57, m	H-15, NH	-	H-15, 18
	15	36.2, CH_2	2.02, m; 1.77, m	H-14, 16	-	-
	16	24.4, CH	1.77, m	H-15, 17, 18	-	-
	17	23.3, CH_3	0.97, d (6.5)	H-16	C-15, 16, 18	-
	18	21.7, CH_3	0.88, d (6.4)	H-16	C-15, 16, 17	-
	NH	-	8.02, d (7.9)	H-14	C-13, 19	NH (Ala), H-14, 15, 17
Ala	19	174.3, CO	-	-	-	-
	20	47.9, CH	4.82, dd (9.7, 7.3)	H-21, NH	C-19, 21	H-21
	21	18.4, CH_3	1.29, d (7.3)	H-20	C-19, 20	-
	NH	-	7.64, d (7.9)	H-20	C-22	H-21, 23, 28
N-Me Leu	22	169.3, CO		-	-	-
	23	65.1, CH	3.49, dd (9.0, 4.7)	H-24	C-22, 24, 28, 29	-
	24	37.8, CH_2	1.95, m; 2.20, m	H-23, 25	-	-
	25	25.5, CH	1.65, m	H-24, 26, 27	-	-
	26	23.2, CH_3	0.97, d (6.5)	H-25	C-24, 25, 27	-
	27	22.1, CH_3	0.99, d (6.5)	H-25	C-24, 25, 26	-
	28	37.9, CH_3	3.20, s	-	C-23, 29	C-23, 30, 32, 34α
Pipecolic acid	29	168.9, CO	-	-	-	-
	30	61.4, CH	3.71, dd (11.3, 2.5)	H-31	C-1, 29	H-34α
	31	28.1, CH_2	2.05, m	H-30, 32	-	-
	32	24.5, CH_2	2.07, m	H-31, 33	-	-
	33	27.4, CH_2	1.56, m	H-32, 34	-	-
	34α	52.5, CH_2	3.16, dd (13.2, 2.3)	H-33	-	H-34β
	34β	-	4.14, dd (14.4, 2.4)	-	-	H-34α

In order to prove this hypothesis, we have attempted to determine the stereochemistry of the amino acid residues of **380** by analysis of its acid hydrolysate, using the appropriated D- and L- amino acids standards, by chiral HPLC analysis. The enantioseparations of the amino acid standards were performed with the Chirobiotic T column under reversed-phase elution conditions. The co-injection of the acidic hydrolysate of **380** and the DL-amino acids standards were performed for HPLC analysis at a flow rate of 1 mL/min. The result revealed that **380** is a cyclo (anthranilic acid-L-Val-D-Leu-L-Ala-*N*-methyl-L-Leu-D-pipercolic acid). The chromatogram and the chiral HPLC analysis of the acidic hydrolysate of **380** were shown in Figure **56** and Table **20**, respectively.

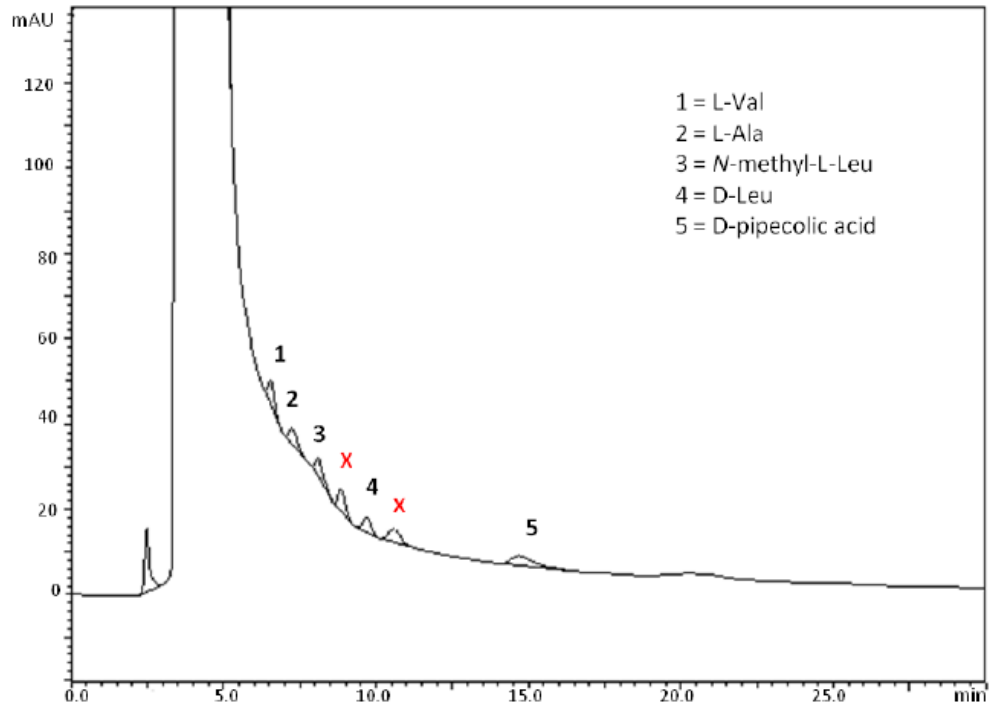

Figure 56. Chromatogram of the acidic hydrolysate of similanamide (**380**). Chromatographic conditions: column, Chirobiotic T; mobile phase, CH_3OH:H_2O:CH_3CO_2H (70:30:0.02 v/v/v); flow rate, 0.5 mL/min; detection, 210 nm.

Table 20. Chiral HPLC analysis of the acidic hydrolysate of similanamide (**380**)*.

	Retention Time (min)
L-valine	6.60
D-valine	8.32
L-alanine	7.16
D-alanine	9.36
L-leucine	6.78
D-leucine	9.67
L-pipecolic acid	8.68
D-pipecolic acid	14.67
N-methyl-L-leucine	8.09
Acidic hydrolysate of similanamide (**380**)	6.59, 7.20, 8.09, 8.83, 9.67, 10.57, 14.69
Acidic hydrolysate of **380** + DL-valine (coinjection)	6.61, 7.31, 8.30, 8.10, 8.84, 9.70, 10.50, 14.95
Acidic hydrolysate of **380** + DL-alanine (coinjection)	6.59, 7.19, 8.04, 8.81, 9.37, 9.70, 10.50, 14.90
Acidic hydrolysate of **380** + DL-leucine (coinjection)	6.60, 6.76, 7.26, 8.04, 8.83, 9.67, 10.54, 15.02
Acidic hydrolysate of **380** + DL-pipecolic acid (coinjection)	6.58, 7.20, 8.09, 8.64, 8.84, 9.77, 10.64, 14.64
Acidic hydrolysate of **380** + *N*-methyl-L-leucine (coinjection)	6.59, 7.20, 8.09, 8.83, 9.67, 10.57, 14.69

* Chromatographic conditions: column, Chirobiotic T; mobile phase, methanol:water:acetic acid (70:30:0.02 v/v/v); flow rate, 0.5 mL/min; detection, 210 nm.

The results showed that although the amino acid sequence of **380** is the same as that of PF1171C, the stereochemistry of its amino acid constituents is different from that of the amino acids constituents of PF1171C. While **380** contains L-Ala, D-Leu, L-Val, and D-pipecolic acid, PF1171C contains D-Ala, L-Leu, D-Val, and L-pipecolic acid. Therefore, compound **380** is a new compound, and was named similanamide.

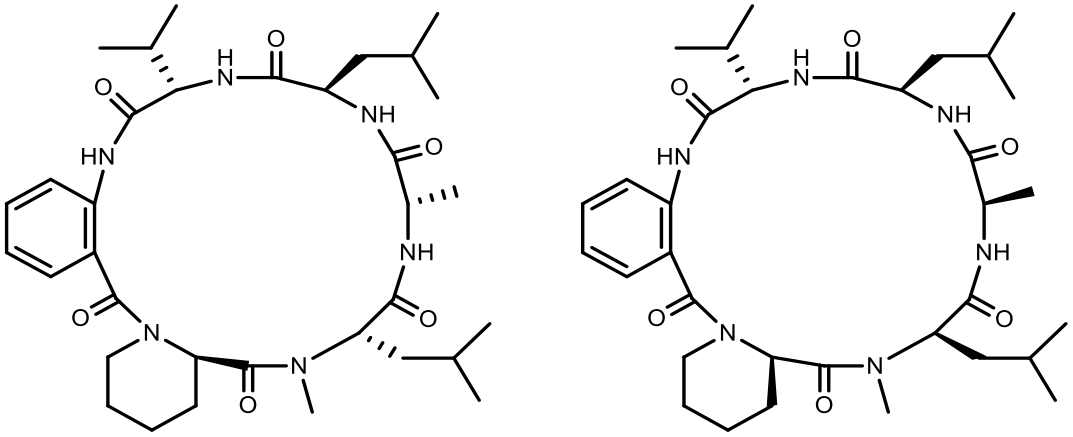

380 PF1171C

Figure 57. Structures of similanamide (**380**) and PF1171C.

So far, only few cyclic hexapeptides have been reported from marine-derived microorganisms. Zheng *et al*. (2009) have isolated two new antifungal cyclo-hexapeptides, sclerotides A and B, from the culture nutrient-limited hypersaline medium of the marine-derived halotolerant *Aspergillus sclerotiorum* PT06-1. Two new cyclic hexapeptides, nocardiamides A and B, were isolated from the culture broth of the marine-derived actinomycete *Nocardiopsis* sp. CNX037 by Wu *et al*. (2013). Cai *et al*. (2013), described isolation of hytramycins A and B, two anti-*Mycobacterium tuberculosis* cyclohexapeptides, from *Streptomyces hygroscopicus* strain ECUM 14046. Desotamides B-D, three new antibacterial cyclohexapeptides, were isolated from the deep South China sea-derived *Streptomyces scopuliridis* SCSIO ZJ46 (Song *et al*., 2014) while Peng, Gao, Zhang, *et al*. (2014) isolated versicotide C, a new and first natural cyclohexapeptide containing two anthranilic acids, from the marine-derived fungus *Aspergillus versicolor* ZLN-60. To the best our knowledge, compound **380** is the first cyclopeptide containing D-pipecolic acid residue ever isolated from marine-derived fungi.

4.3) The Marine-Derived Fungus *Neosartorya quadricincta* KUFA 0081

Fractionation and purification EtOAc extract of the culture of the marine sponge-associated fungus *N. quadricincta* KUFA 0081 resulted in isolation of two new pentaketides, quadricintones A (**381**) and C (**387**), and seven new benzoic acid derivatives, quadricintapyrans A (**382**) and B (**383**), quadricintoxepine (**384**), quadricinctones B (**386**) and D (**390**) and quadricintafurans A (**388**) and B (**389**), together with the previously reported, 2,3-dihydro-6-hydroxy-2,2-dimethyl-4*H*-1-benzopyran-4-one (**385**). The structures of isolated metabolites are shown in Figure 58.

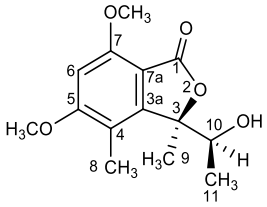

381

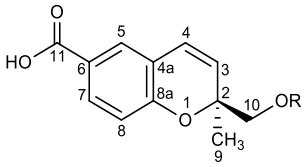

382 R = H
383 R = Ac

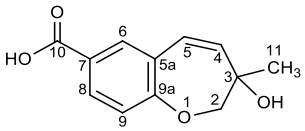

384

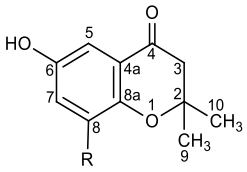

385 R = H
386 R = 

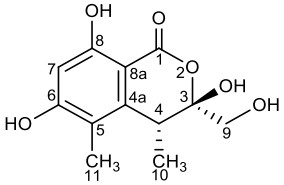

387

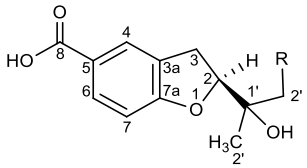

388 R = H

389 R = OH

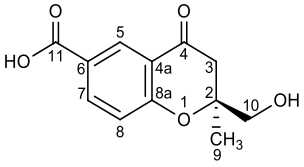

390

Figure 58. Structures of the compounds isolated from the culture of marine sponge-associated fungus *Neosartorya quadricincta* KUFA 0081.

4.3.1) Quadricinctone A (381)

Compound **381** was isolated as a white crystal (mp 176 – 177 °C), and its molecular formula $C_{14}H_{18}O_5$ was determined based on the (+)-HRESIMS *m/z* 267.1332 $[M+H]^+$, indicating six degrees of unsaturation. The IR spectrum showed absorption bands for hydroxyl (3455 cm^{-1}), conjugated ester carbonyl (1723 cm^{-1}) and aromatic (1612, 1596 cm^{-1}) groups.

The ^{13}C NMR spectrum (Table 21) displayed fourteen carbon signals which can be classified, based on DEPTs and HSQC spectra, as one conjugated ester carbonyl (δ_C 168.2), two oxyquaternary sp^2 (δ_C 164.6 and 158.3), three quaternary sp^2 (δ_C 152.8, 111.7 and 105.3), one methine sp^2 (δ_C 94.5), one oxyquaternary sp^3 (δ_C 88.8), one oxymethine sp^3 (δ_C 70.8), two methoxyl (δ_C 56.1 and 56.0), and three methyl (δ_C 21.5, 17.8 and 11.2) carbons.

The ^1H NMR spectrum (Table 21), together with the HSQC spectrum, exhibited, besides a broad singlet of the hydroxyl proton at δ_H 2.15, a singlet of the aromatic proton at δ_H 6.41 (δ_C 94.5), a doublet of methine proton at δ_H 4.22, *J* = 6.4 Hz (δ_C 70.8), two singlets of two methoxy groups at δ_H 3.97 (δ_C 56.0) and 3.92 (δ_C 56.1) , two methyl singlets at δ_H 2.12 (δ_C 11.2) and 1.76 (δ_C 21.5), and one methyl doublet at δ_H 0.87, *J* = 6.4 Hz (δ_C 17.8).

Analysis ^1H and ^{13}C NMR data revealed the presence of a pentasubstitued benzene ring with the methoxyl groups at δ_H 3.92, s (δ_C 56.1) and δ_H 3.97, s (δ_C 56.0), and a methyl group at δ_H 2.12, s (δ_C 11.2) on C-5 (δ_C 164.6), C-7 (δ_C 158.3) and C-4 (δ_C 111.7), respectively, as confirmed by the HMBC correlations from the proton singlet at δ_H 6.41 (H-6) to C-4, C-5 and C-7, from the methyl singlet at δ_H 2.12 (H_3-8) to the carbon at δ_C 152.8 (C-3a), C-4 and C-5, from the methoxyl singlets at δ_H 3.92 (OCH_3-5) and δ_H 3.97, s (OCH_3-7) to C-5 and C-7, respectively, as well as the NOESY correlations from H-6 to OCH_3-5 and OCH_3-7.

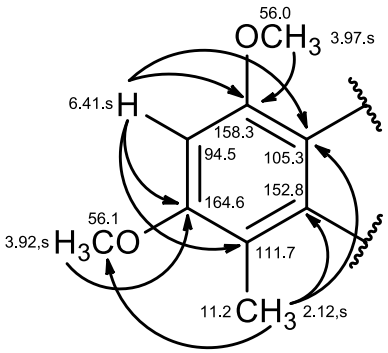

That the 2,4-dimethoxy-1-methylbenzene was fused with 5-methyldihydrofuran-2(3*H*)-one to form a 5,7-dimethoxy-3,4-dimethyl-2-benzofuran-1(3*H*)-one ring system was supported by the HMBC correlation from H-6 to the conjugated carbonyl at δ_C 168.2 (C-1) as well as from the methyl singlet at δ_H 1.76 (H_3-9) to C-3a, the carbons at δ_C 88.8 (C-3) as well as the NOESY correlations between H_3-8 and H_3-9.

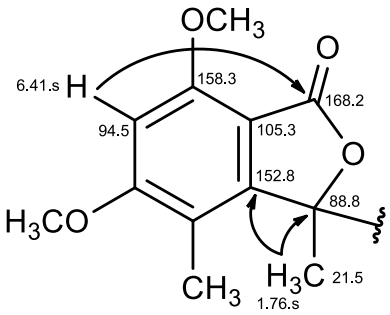

That another substituent on C-3 was 1-hydroxyethyl group was evidenced by the COSY correlations from the doublet at δ_H 4.22 (*J* = 6.4 Hz; H-10) to the methyl doublet at δ_H 0.87 (*J* = 6.4 Hz, H_3-11), as well as by the HMBC correlations from H_3-9 and H_3-11 to C-10 (δ_C 70.8), and from H-10 to C-11 (δ_C 15.8). This was also supported by NOESY correlations from H_3-8 to H_3-9, H-10, from H_3-9 to H-10, and from H_3-11 to H-10 and OH-10 (δ_H 2.15, br). Therefore, the structure of **381** was identified as 3-(1-hydroxyethyl)-5,7-dimethoxy-3,4-dimethyl-2-benzofurn-1(3*H*)-one.

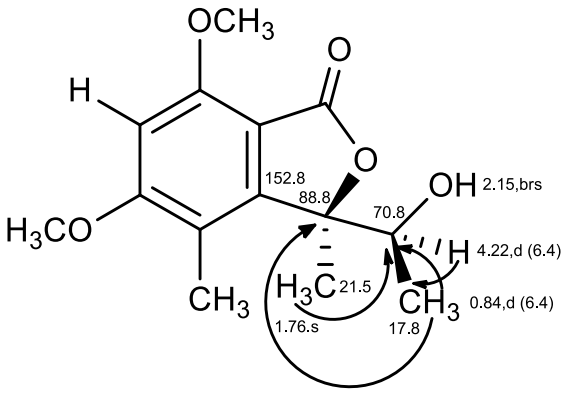

In order to assign stereochemistry of **381**, X-ray analysis was carried out, using a Gemini PX Ultra equipped with CuKα radiation to collect the diffraction data. The ORTEP view of **381** (Figure 59) showed clearly that the absolute configurations of C-3 and C-10 are 3*R* and 10*S*, respectively. The literature survey revealed that **381** is a new compound, so we have named it quadricinctone A.

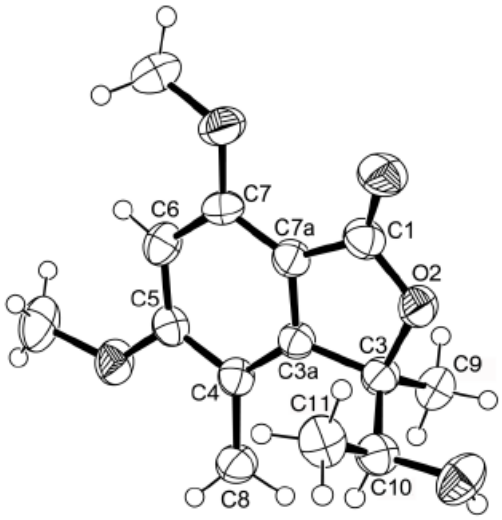

Figure 59. ORTEP diagram of quadricinctone A (**381**).

Table 21. ^{1}H and ^{13}C NMR ($CDCl_3$, 300.13 MHz and 75.4 MHz), HMBC and NOESY assignments for quadricinctone A (**381**).

Position	δ_C, type	δ_H, (*J* in Hz)	COSY	HMBC	NOESY
1	168.2, CO	-	-	-	-
3	88.8, C	-	-	-	-
3a	152.8, C	-	-	-	-
4	111.7, C	-	-	-	-
5	164.6, C	-	-	-	-
6	94.5, CH	6.41, s	CH_3-8, OMe-5, 7	C-1, 4, 5, 7, 7a	OMe-5, 7
7	158.3, C	-	-	-	-
7a	105.3, C	-	-	-	-
8	11.2, CH_3	2.12, s	H-6	C-3a, 4, 5, 7	H-9, 10
9	21.5, CH_3	1.76, s	-	C-3, 3a, 10	H-8, 9, 10
10	70.8, CH	4.22, d (6.4)	CH_3-11	C-11	H-8, 9, 11
11	17.8, CH_3	0.87, d (6.4)	H-10	C-3, 10	H-10
OCH_3-5	56.1 CH_3	3.92, s	H-6	C-5	H-6
OCH_3-7	56.0, CH_3	3.97, s	-	C-7	H-6
OH-10	-	2.15, brs	-	-	H-11

4.3.2) Quadricinctapyran A (382)

Compound **382** was isolated as a white crystal (mp 147 – 148 °C), and its molecular formula $C_{12}H_{12}O_4$ was established on the basis of the (+)-HRESIMS *m/z* 221.0814 $[M+H]^+$, indicating seven degrees of unsaturation. The IR spectrum exhibited absorption bands for hydroxyl (3447 cm^{-1}), conjugated carbonyl (1696 cm-1), aromatic (1609 cm^{-1}) and olefin (1647 cm^{-1}) groups.

The ^{13}C NMR spectrum (Table 22) exhibited twelve carbon signals which can be categorized, based on DEPTs and HSQC spectra, into one conjugated carboxyl carbonyl (δ_C 167.0), one oxyquaternary sp^2 (δ_C 156.8), two quaternary sp^2 (δ_C 123.0 and 120.5), five methine sp^2 (δ_C 139.8, 128.6, 127.9, 122.8 and 115.7), oxyquaternary sp^3 (δ_C 80.5), one one methylene sp^3 (δ_C 67.1) and one methyl (δ_C 23.3) carbons.

The ^{1}H NMR spectrum, in conjunction with the HSQC spectrum (Table 22) exhibited the presence of, besides two broad singlets of the hydroxyl protons at δ_H 12.59 and 5.07, three aromatic protons of 1,2,4-trisubstitued benzene ring at δ_H 7.69, dd, *J* = 8.4, 2.1 Hz (δ_C 139.8), 7.65, d, *J* = 2.1 Hz (δ_C 127.9) and 6.79, d, *J* = 8.4 Hz (δ_C 115.7), two olefinic protons of a *cis*-double bond at δ_H 6.56, d, *J* = 10.0 Hz (δ_C 122.8) and 5.74, d, *J* = 10.0 Hz (δ_C 128.6), a singlet of two methylene protons at δ_H 3.54 (δ_C 67.1), and a methyl singlet at δ_H 1.31 (δ_C 23.3).

The presence of the 1,2,4-trisubstitued benzene ring and the *cis*-double bond were confirmed by the COSY correlations from the olefinic proton at δ_H 5.74, d, *J* = 10.0 Hz (H-3) to another olefinic proton at δ_H 6.56, d, *J* = 10.0 Hz (H-4), and from the aromatic proton at δ_H 7.69, dd, *J* = 8.4, 2.1 Hz (H-7) to the other two aromatic protons at δ_H 7.65, d, *J* = 2.1 Hz (H-5) and δ_H 6.79, d, *J* = 8.4 Hz (H-8). The HMBC spectrum displayed correlations from H-3 to the carbons at δ_C 80.5 (C-2), δ_C 120.5 (C-4a) and δ_C 127.9 (C-5), from H-4 to C-2, C-5 and the carbon at δ_C 156.8 (C-8a), from H-5 to the carbons at δ_C 122.8 (C-4), C-8a and δ_C 167.0 (C-11), from H-7 to C-5, C-8a and C-11, and from H-8 to C-4a, the carbon at δ_C 123.0 (C-6) and C-8a, indicating that the 1,2,4-trisubstitued benzene ring and the *cis*-double bond were part of the 2*H*-chromene-6-carboxylic acid moiety.

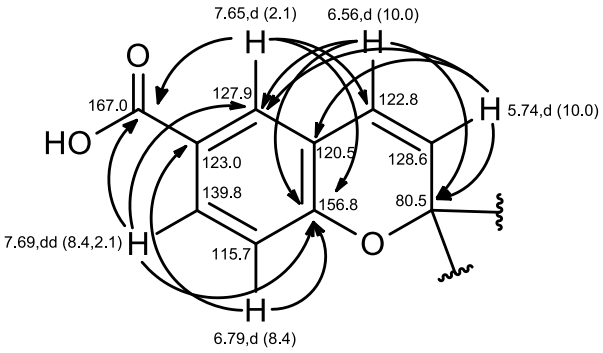

As the HMBC spectrum also showed correlations from H-3 to the carbons at δ_C 23.3 (C-9) and δ_C 67.1 (C-10), from the methyl singlet at δ_H 1.31 (H_3-9) to C-2, the carbon at δ_C 128.6 (C-3) and C-10, and from the methylene singlet at δ_H 3.45 (H_2-10) to C-2, C-3 and C-9, the methyl and hydroxymethyl groups were on C-2. In addition, the NOESY correlations from H-4 to H-3 and H-5, from H-7 to H-8 and H_3-9, and from H_3-9 to H_2-10

confirmed the proposed planar structure. Therefore, **382** was identified as 2-(hydroxymethyl)-2-methyl-2*H*-chromene-6-carboxylic acid.

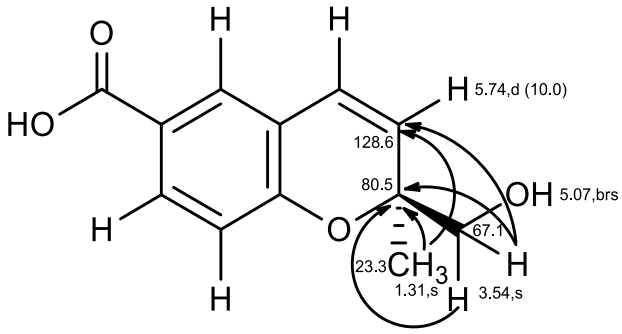

The stereochemistry of this compound was provided by X-ray analysis. The ORTEP view shown in Figure 56 revealed that the absolute configuration of C-2 is *S*. Since **382** has not been previously reported, it was named quadricinctapyran A.

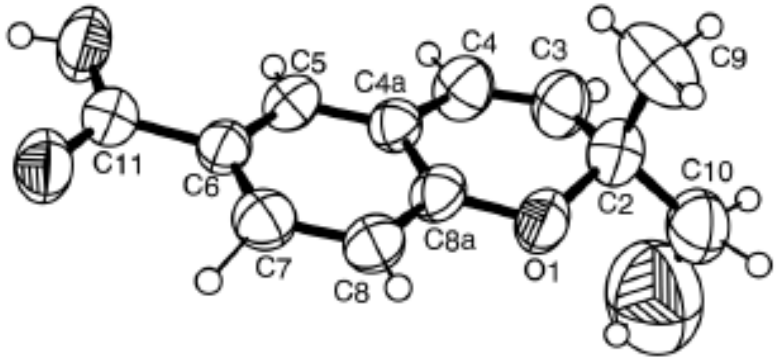

Figure 60. ORTEP diagram of quadricinctapyran A (**382**).

Table 22. ^{1}H and ^{13}C NMR (DMSO, 300.13 MHz and 75.4 MHz), HMBC and NOESY assignments for quadricinctapyran A (**382**).

Position	δ_C, type	δ_H, (*J* in Hz)	COSY	HMBC	NOESY
2	80.5, C	-	-	-	-
3	128.6, CH	5.74, d (10.0)	H-4	C-2, 4a, 5, 9, 10	H-4
4	122.8, CH	6.56, d (10.0)	H-3	C-2, 5, 8a	H-3, 5
4a	120.5, C	-	-	-	-
5	127.9, CH	7.65, d (2.1)	H-7	C-4, 8a, 11	H-4
6	123.0, C	-	-	-	-
7	139.8, CH	7.69, dd (8.4, 2.1)	H-5, 8	C-5, 8a, 11	H-8, H_3-9
8	115.7, CH	6.79, d (8.4)	H-7	C-4a, 6, 8a	H-7
8a	156.8, C	-	-	-	-
9	23.3, CH_3	1.31, s	-	C-2, 3, 10	H-7, H_2-10
10	67.1, CH_2	3.45, s	-	C-2, 3, 9	H_3-9
11	167.0, CO	-	-	-	-
OH-10	-	5.07, brs	-	-	-
OH-11	-	12.59, brs	-	-	-

4.3.3) Quadricinctapyran B (383)

Compound **383** was isolated as a white solid (mp 118 – 119 °C), and its molecular formula $C_{14}H_{14}O_5$ was established based on the (+)-HRESIMS *m/z* 263.0971, indicating eight degrees of unsaturation.

The general feature of the ^{1}H and ^{13}C NMR spectra of **383** closely resembled those of **382**, except for an additional carbonyl carbon at δ_C 170.8 and a methyl singlet at δ_H 1.98 (δ_C 20.7), characteristic of the acetoxyl group. The presence of the acetoxyl was also confirmed by the HMBC correlation from the methyl singlet at δ_H 1.98 to the carbonyl carbon at δ_C 170.8.

The ^{13}C NMR spectrum (Table 23) exhibited fourteen carbon signals which can be categorized, according to DEPTs and HSQC spectra, as one conjugated carboxyl carbonyl (δ_C 171.7), one ester carbonyl (δ_C 170.8), one oxyquaternary sp^2 (δ_C 157.8), two quaternary sp^2 (δ_C 122.0 and 120.2), five methine sp^2 (δ_C 132.2, 128.9, 126.2, 124.3 and

116.1), one oxyquaternary sp^3 (δ_C 78.5), one oxymethylene sp^3 (δ_C 68.8) and two methyl (δ_C 24.0 and 20.7) carbons.

The ^{1}H NMR spectrum, together with the HSQC spectrum (Table 23), revealed the presence of , besides three aromatic protons of 1,2,4-trisubstituted benzene ring at δ_H 7.90, dd, *J* = 8.5, 2.1 Hz (δ_C 132.2), δ_H 7.75, d, *J* = 2.1 Hz (δ_C 128.9) and δ_H 6.83, d, *J* = 8.5 Hz (δ_C 116.1), two doublets of two protons of the *cis*-double bond at δ_H 6.51, *J* = 10.0 Hz (δ_C 124.3) and δ_H 5.59, *J* = 10.0 Hz (δ_C 126.2), two doublets of the mutually coupled methylene protons at δ_H 4.24, *J* = 11.7 Hz and δ_H 4.13, *J* = 11.7 Hz (δ_C 68.8), two methyl singlets at δ_H 1.98 (δ_C 20.7) and δ_H 1.48 (δ_C 24.0), and one broad signal of the hydroxyl proton at δ_H 12.79.

That the acetoxyl group was on C-10 (δ_C 68.8) was corroborated by the HMBC correlations from the mutually coupled oxymethylene protons at δ_H 4.24, d, *J* = 11.7 Hz and δ_H 4.13, d, *J* = 11.7 Hz (H_2-10) to the carbonyl of the acetoxyl group at δ_C 170.8 (CO; OAc-10).This hypothesis was also supported by the chemical shift values of the oxymethylene protons (H_2-10) which were about 0.7 ppm higher than those of H_2-10 in **382**. Therefore, compound **383** was identified as 2-[(acetyloxy)methyl]-2-methyl-2*H*-chromene-6-carboxylic acid.

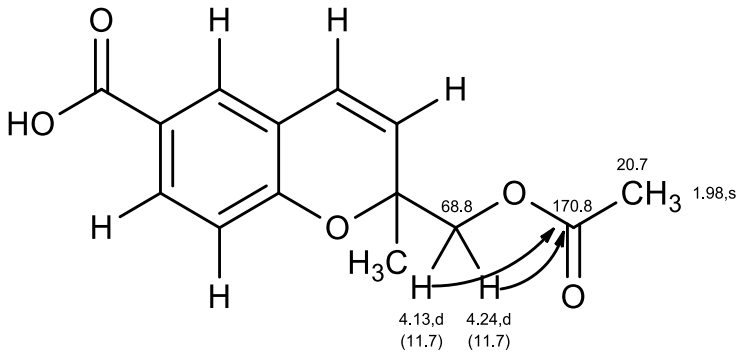

Since **383** could not obtained as a suitable crystal, absoluted configuration of its stereogenic carbon (C-2) cannot be determined by X-ray analysis. However, **383** is the acetate derivative of **382**, it was speculated that the absolute configuration of its C-2 must be the same as that of C-2 of **382**. This hypothesis was also supported by the fact that

H-8 (δ_H 6.38, d, *J* = 8.5 Hz) exhibited the NOESY correlation to CH_3-9 and not to H_2-10, similar to what was observed in **382**. Moreover, acid hydrolysis of **383** also give the product whose ^1H and ^{13}C NMR data and optical rotation are the same as those of **382**. Since it has never been previously reported, it wan named quadricinctapyran B.

Table 23. ^1H and ^{13}C NMR (DMSO, 300.13 MHz and 75.4 MHz), HMBC and NOESY assignments for quadricinctapyran B (**383**).

Position	δ_C, type	δ_H, (*J* in Hz)	COSY	HMBC	NOESY
2	75.8, C	-	-	-	-
3	126.2, CH	5.59, d (10.0)	H-4	C-2, 4a, 10	H-4, H_3-9, H_2-10
4	124.3, CH	6.51, d (10.0)	H-3	C-2, 5, 8a	H-3, 5
4a	120.2, C	-	-	-	-
5	128.9, CH	7.75, d (2.1)	H-7	C-4, 7, 8a, 11	H-4, 7
6	122.0, C	-	-	-	-
7	132.2, CH	7.90, dd (8.5, 2.1)	H-5, 8	C-5, 8a, 11	H-5, 8
8	116.1, CH	6.83, d (8.5)	H-7	C-4a, 6, 8a	H-7, H_3-9
8a	157.8, C	-	-	-	-
9	24.0, CH_3	1.48, s	-	C-2, 3, 10	H-3, 8, H_2-10
10	68.8, CH_2	4.24, d (11.7)	H-10	C-2, 3, 9	H-3, H_3-9,
				CO (OAc-10)	H_3(OAc-10)
		4.13, d (11.7)	H-10	C-2, 3, 9	H-3, H_3-9,
				CO (OAc-10)	H_3(OAc-10)
11	171.7, CO	-	-	-	-
OH-11	-	12.79, br	-	-	-
OAc-10	170.8, CO	-	-	-	-
	20.7, CH_3	1.98, s	-	CO (OAc-10)	H_2-10

4.3.4) Quadricinctoxepine (384)

Compound **384** was isolated as a white solid (mp 189 – 191 °C), and its molecular formula $C_{12}H_{12}O_4$ was determined based on the (+)-HRESIMS 221.0819 $[M+H]^+$, indicating seven degrees of unsaturation.

As the molecular formula of **384** is $C_{12}H_{12}O_4$, it is an isomer of **384**. Moreover, the general features of ^1H and ^{13}C NMR spectra of **384** resembled those of **382**, but the chemical shift values of some of the protons and carbons were slightly different.

The ^{13}C NMR spectrum (Table 24) exhibited twelve carbon signals which can be classified, according to the DEPTs and HSQC spectra, into one conjugated carboxyl carbonyl (δ_C 166.7), one oxyquaternary sp^2 (δ_C 161.2), two quaternary sp^2 (δ_C 125.3 and 125.0), five methine sp^2 (δ_C 139.5, 134.5, 129.8, 123.5 and 119.8), one oxymethylene sp^3 (δ_C 77.0), one oxyquaternary sp^3 (δ_C 70.7) and one methyl (δ_C 26.1) carbons.

The ^1H NMR spectrum, in combination with the HSQC spectrum (Table 24), exhibited, besides two broad singlets of two hydroxyl protons at δ_H 12.79 and 3.39, three aromatic protons of a 1,2,4-trisubstituted benzene ring at δ_H 7.89, d, J = 2.1 Hz (δ_C 134.5), δ_H 7.74, dd, J = 8.4, 2.1 Hz (δ_C 129.8) and δ_H 7.05, d, J = 8.4 Hz (δ_C 119.8), two olefinic protons of a *cis*-double bond at δ_H 6.31, d, J = 12.0 Hz (δ_C 123.5) and δ_H 5.95, dd, J = 12.0, 1.2 Hz (δ_C 139.5), one pair of geminally-coupled methylene protons at δ_H 4.02, dd, J = 11.1, 1.6 Hz and 3.84, d, J = 11.1 Hz (δ_C 77.0) and one methyl singlet at δ_H 1.26 (δ_C 26.1).

The HMBC spectrum exhibited the correlations from the olefinic proton at δ_H 5.59, dd, J = 12.0, 1.2 Hz (H-4) to the carbon at δ_C 125.0 (C-5a), from another olefinic proton at δ_H 6.31, d, J = 12.0 Hz (H-5) to C-5a, the carbons at δ_C 134.5 (C-6) and δ_C 161.2 (C-9a), and from the aromatic proton at δ_H 7.89, d, J = 2.1 Hz (H-6) to C-5, the carbons at δ_C 129.8 (C-8), C-9a and δ_C 166.7 (C-10), indicating that the *cis*-double bond was on C-5a and the carboxylic acid group was on C-7. In contrast to **382**, the HMBC spectrum of **384** displayed the correlations from the mutually coupled methylene protons at δ_H 4.02, dd, J = 11.1, 1.6 Hz and δ_H 3.84, d, J = 11.1 Hz (H_2-2) to not only the carbon at δ_C 139.5 (C-4), but also to C-9a. Consequently, the benzoic acid moiety was fused with the 2,3,6,7-tetrahydrooxepine ring through C-5a and C-9a.

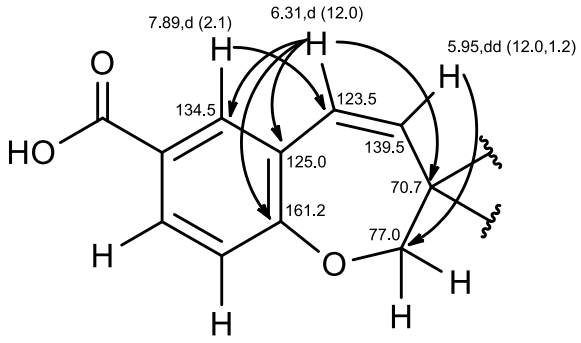

Since the HMBC spectrum showed cross peaks from the methyl singlet at δ_H 1.26 (H_3-11) to the carbons at δ_C 77.0 (C-2), δ_C 70.7 (C-3) and C-4, as well as from H_2-2 to C-3 and the methyl carbon at δ_C 26.1 (C-11), the methyl and hydroxyl groups were on C-3. This was also supported by the NOESY correlations from H_3-11 to the hydroxyl proton at δ_H 3.39, brs (OH-3), H_2-2 and H-4. Thus, **384** was identified as 3-hydroxy-3-methyl-2,3-dihydro-1-benzoxepine-7-carboxylic acid. Literature survey revealed that this compound is a new compound, thus it was named quadricinctoxepine.

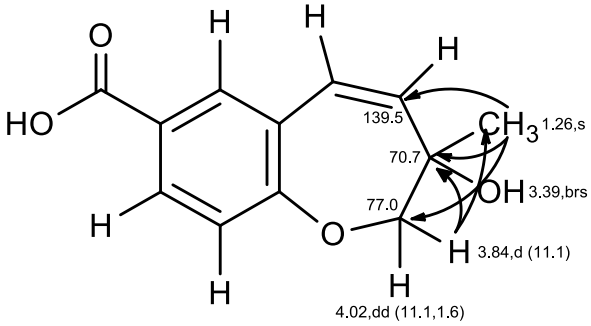

Table 24. ^{1}H and ^{13}C NMR (DMSO, 300.13 MHz and 75.4 MHz), HMBC and NOESY assignments for quadricinctoxepine (**384**).

Position	δ_C, type	δ_H, (*J* in Hz)	COSY	HMBC	NOESY
2α	77.0, CH_2	3.84, d (11.1)	H-2β	C-3, 4, 9a, 11	H-2β, 4 (w), 11 (w)
2β		4.02, dd (11.1, 1.6)	H-2α	C-3, 4, 9a, 11	H-2α, 4 (w), 11 (str)
3	70.7, C	-	-	-	-
4	139.5, CH	5.95, dd (12.0, 1.2)	H-5	C-2, 5a	H-2α(w), 5, 9(w), 11
5	123.5, CH	6.31, d (12.0)	H-4	C-3, 5a, 6, 9a	H-4, 6 (str)
5a	125.0, C	-	-	-	-
6	134.5, CH	7.89, d (2.1)	H-8	C-5, 8, 9a, 10	H-5
7	125.3, C	-	-	-	-
8	129.8, CH	7.74, dd (8.4, 2.1	H-6, 9	C-6, 9a	H-9
9	119.8, CH	7.05, d (8.4)	H-8	C-5a, 7, 9a	H-8
9a	161.2, C	-	-	-	-
10	166.7, CO	-	-	-	-
11	26.1, CH_3	1.26, s	-	C-2, 3, 4	H-2α (w), 2β (str)
OH-3	-	3.39, brs	-	-	H-4, 11
OH-10	-	12.79, brs	-	-	-

Since **384** could not be obtained as a suitable crystal, its stereochemistry could not be determined by X-ray analysis. Therefore, the relative configuration of C-3 of **384** was determined by molecular mechanics conformation analysis and the NOESY experiments. The relative configuration of **384** was assigned as 3*R* configuration with the half-chair conformatin of the seven-membered ring which the methyl group was in axial position. This assignment was supported by the data from molecular mechanics conformation analysis and NOESY experiments. The computer modeling can generate two minimal energy structures of **384** as the methyl group in both axial and equatorial positions (Figure 61). The axial position of the methyl group in **384** was confirmed by the data from the NOESY experiment. The NOE interaction between the protons of methyl group at C-11 and the diastereotopic protons at C-2 can indicate the axial position of methyl group by a weak cross peak of H-2b (δ_H 3.84, d, J = 11.1 Hz) to H_3-11 but the medium cross peak of H-2a (δ_H 4.02, d, J = 11.1 Hz) to H_3-11. Since **384** is a new compound, it was named quadricinctoxepine.

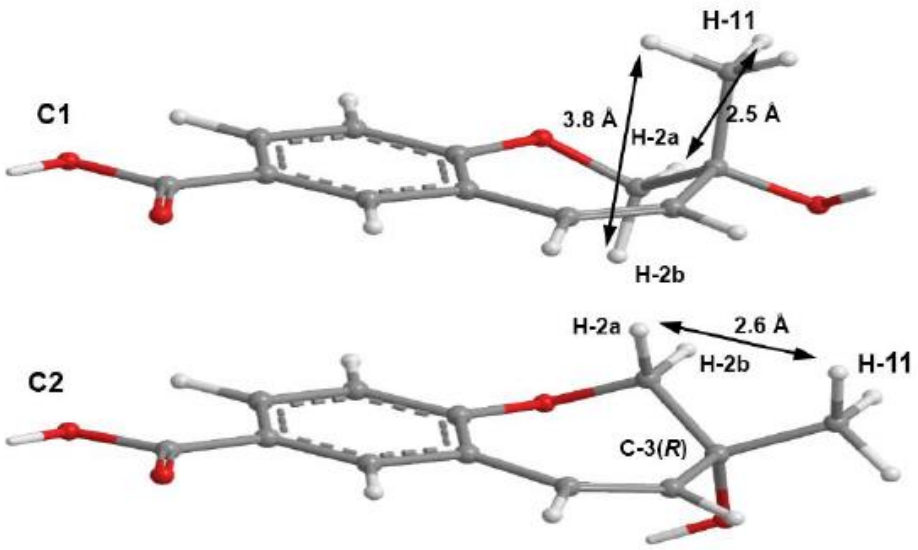

Figure 61. The two minimal energy conformations, C1 and C2, for the structure of quadricinctoxepine (**384)**, with *R* configuration for C-3. All calculated distances and energies are exactly the same for the pairs 3*R*-C1/3*S*-C2 and 3*R*-C2/3*S*-C1. The shorter predicted inter-hydrogen distances H-2/H-11 are presented.

4.3.5) 6-Hydroxy-2,2-dimethyl-2,3-dihydro-4*H*-chromen-4-one (385)

Compound **385** was isolated as a white solid (mp 154-156 °C). The ^{13}C NMR spectrum (Table 25), in combination with the DEPTs and HSQC spectra, exhibited one ketone carbonyl at δ_C 191.6, two oxyquaternary sp^2 carbons at δ_C 162.5 and 157.9, three methine sp^2 carbons at δ_C 136.6, 127.8 and 118.7, one quaternary sp^2 carbon at δ_C 119.3, one oxyquaternary sp^3 carbon at δ_C 80.5, one methylene sp^3 carbon at δ_C 47.6, and two methyl carbons at δ_C 26.0.

The ^{1}H spectrum, together with the HSQC spectrum (Table 25), displayed, besides three aromatic protons of the 1,2,4-trisubstituted benzene ring at δ_H 8.30, d, *J* = 2.1 Hz (δ_C 127.8), δ_H 8.06, dd, *J* = 8.7, 2.2 Hz (δ_C 136.6) and δ_H 7.08, d, *J* = 8.7 Hz (δ_C 118.7), one singlet of two magnetically equivalent methylene protons at δ_H 2.87 (δ_C 47.6), and one singlet of two methyl groups at δ_H 1.42 (δ_C 26.0).

The existence of 1,2,4-trisubstitued benzene ring was confirmed by the COSY correlations from the proton at δ_H 8.06, dd, *J* = 8.7, 2.2 Hz (H-7) to the protons at δ_H 8.30,

d, *J* = 2.1 Hz (H-5) and δ_H 7.08, d, *J* = 8.7 Hz (H-8), as well as by the HMBC correlations from H-5 to the carbons at δ_C 157.9 (C-6) and 136.6 (C-7), from H-7 to the carbon at δ_C 127.8 (C-5) and C-6, and from H-8 to the carbon at δ_C 119.3 (C-4a) and C-6. That C-6 was connected to the hydroxyl group was evidenced by its chemical shift value (δ_C 157.9) which was also similar to that of **quadricinctone B** (**386**; δ_C 151.6).

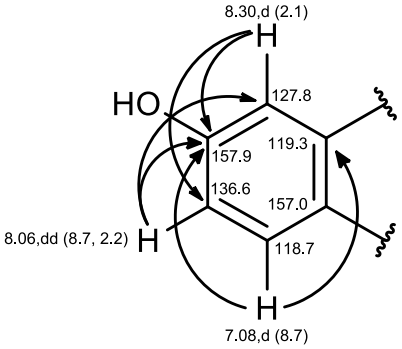

The HMBC spectrum also exhibited correlations from the methylene protons at δ_H 2.87, s (H_2-3) to the carbons at δ_C 70.5 (C-2), 191.6 (C-4), 26.0 (C-9 and C-10) and C-4a, and from the methyl singlet at δ_H 1.42 (H_3-9/ H_3-10) to C-2 and the carbons at δ_C 47.6 (C-3) and 26.0 (C-10/ C-9), suggesting the presence of a 2,2-dimethyl-2,3-dihydro-4*H*-chromen-4-one moiety. Therefore, **385** was identified as 6-hydroxy-2,2-dimethyl-2,3-dihydro-4*H*-chromen-4-one. Extensive literature search revealed that **385** was previously reported from several plants, including *Calea cuneifolia* (Lourenço *et al*., 1981), *Gynura elliptica* (Lin *et al*., 2000) and *Tussilago farfara* (Jang *et al*., 2016), as well as from synthesis (El-Desoky *et al*., 2013). Compound **386** completely inhibited platelet aggregation induced by arachidonic acid at the concentration of 100 µg/mL (Lin *et al*., 2000).

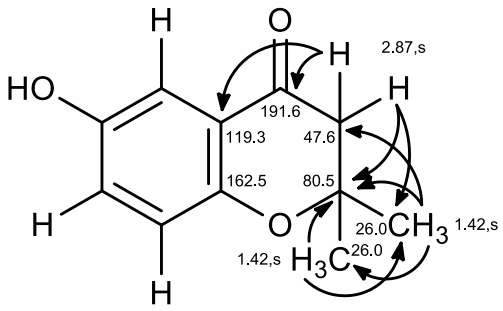

Table 25. ^{1}H and ^{13}C NMR ($CDCl_3$, 300.13 MHz and 75.4 MHz) and HMBC assignment for 6-hydroxy-2,2-dimethyl-2,3-dihydro-4*H*-chromen-4-one (**385**).

Position	δ_C, type	δ_H, (*J* in Hz)	COSY	HMBC
2	80.5, C	-	-	-
3	47.6, CH_2	2.87, s	-	C-2, 4a, 9, 10
4	191.6, CO	-	-	-
4a	119.3, C	-	-	-
5	127.8, CH	8.30, d (2.1)	H-7	C-6, 7
6	162.5, C	-	-	-
7	136.6, CH	8.06, dd (8.7, 2.2)	H-5, 6	C-5, 6
8	118.7, CH	7.08, d (8.7)	H-7	C-4a, 6
8a	157.9, C	-	-	-
9	26.0, CH_3	1.42, s	-	C-2, 3, 10
10	26.0, CH_3	1.42, s	-	C-2, 3, 9

4.3.6) Quadricinctone B (386)

Compound **386** was isolated as white crystals (mp 227 – 228 °C), and its molecular formula $C_{12}H_{14}O_4S$ was determined based on the (+)-HRESIMS *m/z* 255.0694 $[M+H]^+$ (calculated 255.0691), indicating seven degrees of unsaturation. The IR spectrum exhibited absorption bands for hydroxyl (3442 cm^{-1}), conjugated ketone carbonyl (1690 cm^{-1}) and aromatic (1622 cm^{-1}) groups.

The ^{13}C NMR spectrum, together with DEPTs and HSQC spectra (Table 26), exhibited signals of one conjugated ketone carbonyl carbon at δ_C 191.2, two oxyquaternary sp^2 carbons at δ_C 151.6 and 147.4, two quaternary sp^2 carbons at δ_C 135.7

and 120.8, two methine sp^2 carbons at δ_C 118.7 and 112.4, one oxyquaternary sp^3 carbon at δ_C 80.9, one methylene sp^3 carbon at δ_C 48.0, and three methyl carbons at δ_C 40.8, 26.1 and 25.7.

The ^{1}H NMR spectrum (Table 26), together with the HSQC spectra, exhibited one hydroxyl proton at δ_H 9.85, s, two *meta*-coupled aromatic protons at δ_H 7.35, d, *J* = 3.1 Hz (δ_C 118.7) and 7.17, d, *J* = 3.1 Hz (δ_C 112.4), two geminally-coupled methylene protons at δ_H 2.85, d, *J* = 16.6 Hz and 2.80, d, *J* = 16.6 Hz (δ_C 48.0), and three methyl singlets at δ_H 2.77 (δ_C 40.8), 1.38 (δ_C 25.7) and 1.39 (δ_C 26.1).

The presence of the 1,2,3,5-tetrasubstituted benzene ring was substantiated by the COSY correlations (Table 26) between the two *meta*-coupled aromatic protons at δ_H 7.17, d, *J* = 3.1 Hz (H-5) and δ_H 7.35, d, *J* = 3.1 Hz(H-7), as well as by the HMBC correlations (Table 26) from H-5 to the carbons at δ_C 151.6 (C-6), δ_C 147.4 (C-8a) and δ_C 118.7 (C-7), and from H-7 to the carbons at δ_C 112.4 (C-5), C-6, δ_C 135.7 (C-8) and C-8a. That the phenolic hydroxyl group was on C-6 was evidenced by the HMBC correlations from the singlet at δ_H 9.85 (OH-6) to C-5, C-6 and C-7.

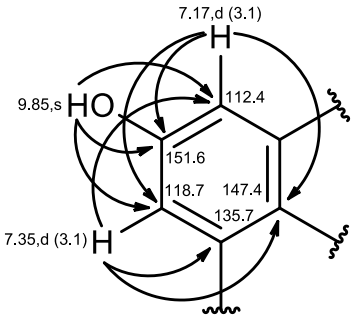

The HMBC spectrum also gave cross peaks from H-5 to the carbon at δ_C 191.2 (C-4), from H_2-3 at δ_H 2.80, d (*J* = 16.6 Hz) and δ_H 3.85, d (*J* = 16.6 Hz) to the carbons at δ_C 80.9 (C-2), C-4, δ_C 26.1 (C-9) and δ_C 25.7 (C-10), from the methyl singlet at δ_H 1.39 (H_3-9) to C-2, the carbon at δ_C 48.0 (C-3) and C-10, and from the methyl singlet at δ_H 1.38 (H_3-10) to C-2, C-3 and C-9, indicating that the 1,2,3,5-tetrasubstituted benzene ring was fused to the 2,2-dimethyl-2,3-dihydro-4*H*-pyran-4-one moiety forming the 6-hydroxyl-2,2-dimethyl-2,3-dihydro-4*H*-1-benzopyran-4-one ring system.

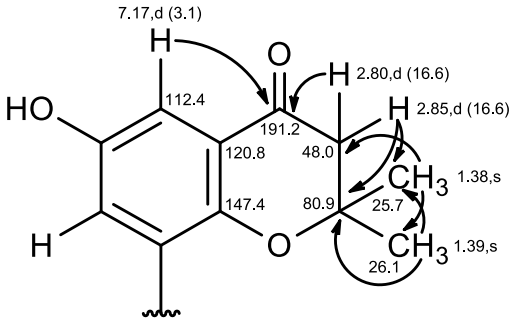

Since this partial structure accounted for only $C_{11}H_{11}O_3$, another part of the molecule must be CH_3SO. Since the HMBC spectrum showed correlation from the methyl singlet at δ_H 2.77 (H_3-11) to C-8, the methyl sulfoxide group was placed on C-8. This hypothesis was also supported by the chemical shift value of CH_3-11 (δ_H 2.77; δ_C 40.8), indicating that it was on the electron-withdrawing group. Therefore, **386** was identified as 6-hydroxy-2,2-dimethyl-8-(methylsulfinyl)-2,3-dihydro-4*H*-chromen-4-one.

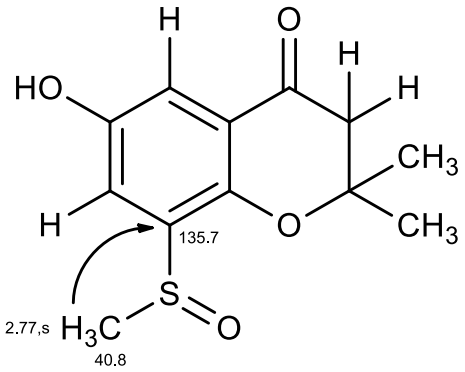

Table 26. ^{1}H and ^{13}C NMR (DMSO, 300.13 MHz and 75.4 MHz) and HMBC assignment for quadricinctone B (**386**).

Position	δ_C, type	δ_H, (*J* in Hz)	COSY	HMBC
2	80.9, C	-	-	-
3	48.0, CH_2	2.80, d (16.6)	H-3	C-2, 4, 9, 10
		2.85, d (16.6)	H-3	C-2, 4, 9, 10
4	191.2, CO	-	-	-
4a	120.8, C	-	-	-
5	112.4, CH	7.17, d (3.1)	H-7	C-4, 6, 7, 8a
6	151.6, C	-	-	-
7	118.7, CH	7.35, d (3.1)	H-5	C-5, 6, 8, 8a
8	135.7, C	-	-	-
8a	147.4, C	-	-	-
9	26.1, CH_3	1.39, s	-	C-2, 3, 10
10	25.7, CH_3	1.38, s	-	C-2, 3, 9
11	40.8, CH_3	2.77, s	-	C-8
OH-6	-	9.85, s	-	C-5, 6, 7

Final proof of the proposed structure and the stereochemistry assigned to **386** was determined by X-ray analysis. The ORTEP view of **386** shown in Figure 62 showed that the absolute configuration of the sulfoxide group is *R*. Since **386** has not been previously reported, it was named quadricinctone B.

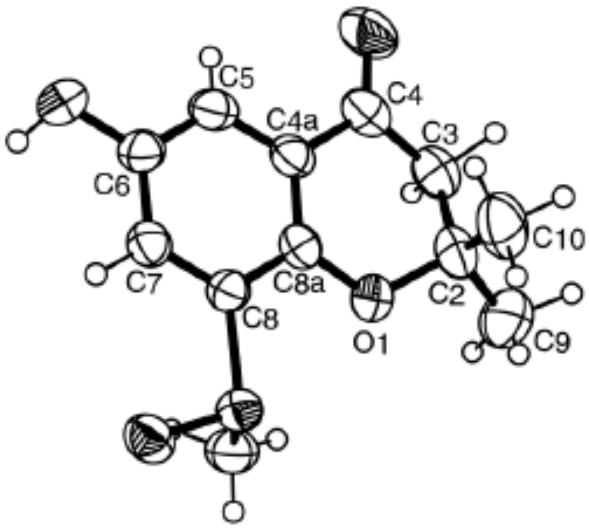

Figure 62. ORTEP diagram of quadricinctone B (**386**).

4.3.7) Quadricinctone C (387)

Compound **387** was isolated as white crystals (mp 223 – 224 °C), and its molecular formula $C_{12}H_{14}O_6$ was established based on the (+)-HRESIMS *m/z* 255.0875 $[M+H]^+$ (calculated 255.0869), indicating six degrees of unsaturation. The IR spectrum showed absorption bands for hydroxyl (3439 cm^{-1}), conjugated ester carbonyl (1660 cm^{-1}) and aromatic (1643 cm^{-1}) groups.

The ^{13}C NMR spectrum (Table 27) displayed twelve carbon signals which can be categorized, according to the DEPTs and HSQC spectra, as one conjugated ester carbonyl (δ_C 168.8), two oxyquaternary sp^2 (δ_C 162.9 and 161.3), three quaternary sp^2 (δ_C 144.6, 113.5 and 98.9), one quaternary sp^3 of a hemiketal (δ_C 104.8), one methine sp^2 (δ_C 99.9), one methine sp^3 (δ_C 34.9), one oxymethylene sp^3 (δ_C 63.7), and two methyl (δ_C 16.3 and 9.8) carbons.

The ^1H NMR spectrum, together with the HSQC spectrum (Table 27), revealed the presence of a singlet of hydrogen-bonded phenolic hydroxyl proton at δ_H 11.24, a broad singlet of phenolic hydroxyl proton at δ_H 10.62, two broad singlets of two hydroxyl protons at δ_H 7.07 and δ_H 5.26, a singlet of an aromatic proton at δ_H 6.27 (δ_C 99.9), a broad doublet of two geminally-coupled methylene protons at δ_H 3.65 (*J* = 16.6 Hz; δ_C 63.7), a multiplet of a methine proton at δ_H 3.26 (δ_C 34.9), a methyl singlet at δ_H 1.98 (δ_C 9.8), and a methyl doublet at δ_H 1.06 (*J* = 7.2 Hz; δ_C 16.3).

The existence of a 3,3,4,5,6,8-hexasubstituted 3,4-dihyro-1*H*-isochromen-1-one ring system was supported by the HMBC correlations from the aromatic proton at δ_H 6.27, s (H-7) to the carbons at δ_C 168.8(C-1), δ_C 113.5 (C-5), δ_C 98.9 (C-8a), δ_C 162.9 (C-6) and δ_C 161.3 (C-8), and from the hydrogen-bonded phenolic hydroxyl at δ_H 11.24, s (OH-8) to the carbon at δ_C 99.9 (C-7), C-8 and C-8a. Since the HMBC spectrum also exhibited the correlations from the methyl singlet at δ_H 1.98 (H_3-11) to the carbon at δ_C 144.6 (C-4a), C-5 and C-6, the methyl group (δ_C 9.8; δ_H 1.98, s) and another phenolic hydroxyl group (δ_H 10.62, brs) were placed on C-5 and C-6, respectively, and the carbon signals at δ_C 144.6 and δ_C 162.9 were assigned for C-4a and C-6, respectively.

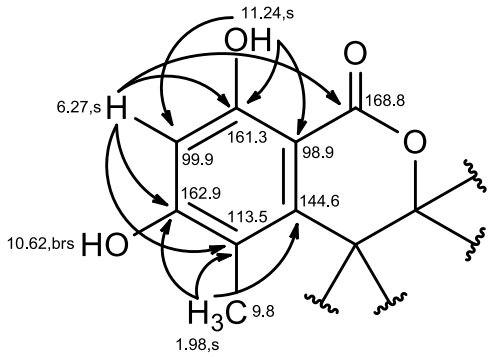

The COSY spectrum exhibited correlations from the multiplet of the methine proton at δ_H 3.26 (H-4) to the methyl doublet at δ_H 1.06 (J = 7.2 Hz; H_3-10), and from the the broad singlet of the hydroxyl proton at δ_H 5.26 (OH-9) to the broad doublet of the methylene protons at δ_H 3.65 (J = 16.6 Hz; H_2-10). The HMBC spectrum also gave cross peaks from H_3-10 to the carbons at δ_C 104.8 (C-3), δ_C 34.9 (C-4) and C-4a. Taken together, the methyl (δ_C 16.3; δ_H 1.06) and the hydroxymethyl (δ_C 63.7; δ_H 3.65, OH; δ_H 5.26) groups were placed on C-4 and C-3, respectively. Thus, another hydroxyl group (δ_H 7.07, brs) was on C-3. This was confirmed by the chemical shift value of C-3 (δ_C 104.8), which is typical for a hemiketal carbon.

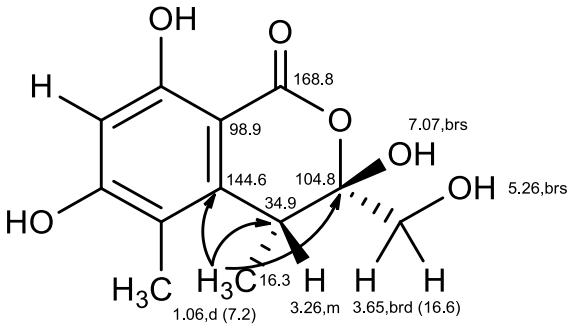

Table 27. ^{1}H and ^{13}C NMR (DMSO, 300.13 MHz and 75.4 MHz) and HMBC assignment for quadricinctone C (**387**).

Position	δ_C, type	δ_H, (*J* in Hz)	COSY	HMBC
1	168.8, CO	-	-	-
3	104.8, C	-	-	-
4	34.9, CH	3.26, m	H_3-10	-
4a	144.6, C	-	-	-
5	113.5, C	-	-	-
6	162.9, C	-	-	-
7	99.9, CH	6.27, s	-	C-1 (w), 5, 6, 8, 8a
8	161.3, C	-	-	-
8a	98.9, C	-	-	-
9	63.7, CH_2	3.65, brd (16.6)	OH-9	-
10	16.3, CH_3	1.06, d (7.2)	H-4	C-3, 4, 4a
11	9.8, CH_3	1.98, s	-	C-4a, 5, 6
OH-3	-	7.07, brs	-	-
OH-6	-	10.62, brs	-	-
OH-8	-	11.24, s	-	C-7, 8, 8a
OH-9	-	5.26, brs	H_2-9	-

Since **387** was obtained as suitable crystal, the X-ray analysis was performed to confirm the proposed structure and to establish the absolute configurations of its stereogenic centers (C-3 and C-4). The ORTEP view shown in Figure 63 revealed that the absolute configurations of C-3 and C-4 are *S* and *R*, respectively. Since **387** is a new compound, we have named it quadricinctone C.

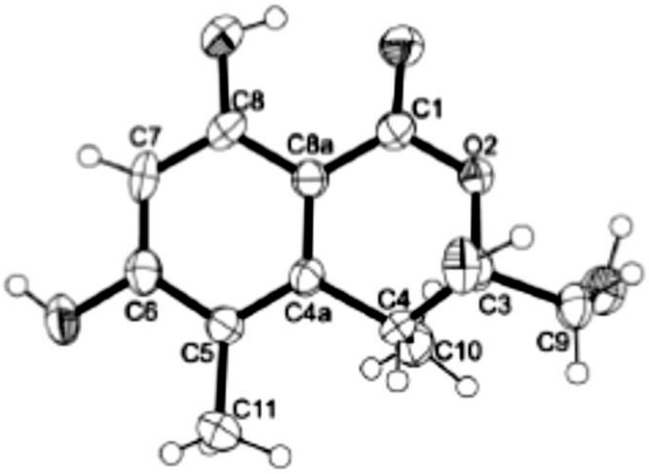

Figure 63. ORTEP diagram of quadricinctone C (**387**).

4.3.8) Quadricinctafuran A (388)

Compound **388** was isolated as white crystals (mp 149 – 150 °C), and its molecular formula $C_{12}H_{14}O_4$ was established based on the (+)-HRESIMS *m/z* 223.9067 $[M+H]^+$, indicating six degrees of unsaturation. The IR spectrum displayed absorption bands for hydroxyl (3417 cm^{-1}), conjugated carbonyl (1681 cm^{-1}) and aromatic (1634 cm^{-1}) groups.

The ^{13}C NMR (Table 28) showed twelve carbon signals which can be classified, based on the DEPTs and HSQC spectra, into one conjugated carboxyl carbonyl (δ_C 167.2), one oxyquaternary sp^2 (δ_C 163.7), two quaternary sp^2 (δ_C 128.2 and 122.6), three methine sp^2 (δ_C 130.4, 126.4 and 108.4), one oxymethine sp^3 (δ_C 90.2), one quaternary sp^3 (δ_C 70.0), one methylene sp^3 (δ_C 29.3) and two methyl (δ_C 25.9 and 24.9) carbons.

The ^1H NMR spectrum, together with the HSQC spectrum (Table 28), exhibited, besides the signals of three aromatic protons of the 1,2,4-trisubstituted benzene ring at δ_H 7.75, d, *J* = 1.8 Hz (δ_C 126.4), 7.72, dd, *J* = 8.3, 1.8 Hz (δ_C 130.4) and 6.80, d, *J* = 8.3 Hz (δ_C 108.4), one broad singlet of the hydroxyl proton at δ_H 12.49, one doublet of two geminally-coupled methylene protons at δ_H 3.17, *J* = 8.9 Hz (δ_C 29.3), one triplet of the methine proton at δ_H 4.64, *J* = 8.9 Hz (δ_C 90.2), and two methyl singlets at δ_H 1.14 (δ_C 24.9) and 1.13 (δ_C 25.9).

That the 1,2,4-trisubstituted benzene ring was part of the 2,5-disubstituted 2,3-dihydro-1-benzofuran moiety was substantiated by the HMBC correlations from the

methylene protons at δ_H 3.17, d, *J* = 8.9 Hz (H_2-3) to the carbons at δ_C 90.2 (C-2), δ_C 128.2 (C-3a) and δ_C 163.7 (C-7a), from the aromatic proton at δ_H 7.75, d, *J* = 1.8 Hz (H-4) to the carbon at δ_C 130.4 (C-6) and C-7a, from the aromatic proton at δ_H 7.72, dd, *J* = 8.3, 1.8 Hz (H-6) to the carbon at δ_C 126.4 (C-4) and C-7a, and from the aromatic proton at δ_H 6.80, d, *J* = 8.3 Hz (H-7) to C-3, the carbon at δ_C 122.6 (C-5) and C-7a, as well as by the COSY correlations from H-6 to H-4 and H-7, and from the methine proton at δ_H 4.64, t, *J* = 8.9 Hz (H-2) to H-3.

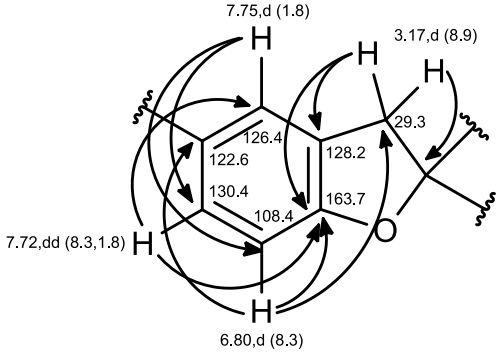

The presence of broad signal at δ_H 12.49, which is typical of a hydroxyl group of carboxylic acid, together with the HMBC correlations from H-4 and H-6 to the carbon at δ_C 167.2 (C-8), indicated that the carboxyl group was on C-5. Since the HMBC spectrum displayed correlations from H-2 to the carbons at δ_C 70.0 (C-1'), δ_C 24.9 (C-2') and δ_C 25.9 (C-3'), the 2-hydroxypropyl group was placed on C-2. This hypothesis also supported by the HMBC correlations from the methyl singlet at δ_H 1.14 (H_3-2') to C-2, C-1' and C-3', and from the methyl singlet at δ_H 1.13 (H_3-3') to C-2, C-1' and C-2', as well as by the NOESY correlations from H-2 to H-3, H_3-2' and H_3-3'.Therefore, **388** was identified as 2-(2-hydroxypropan-2-yl)-2,3-dihydro-1-benzofuran-5-carboxylic acid.

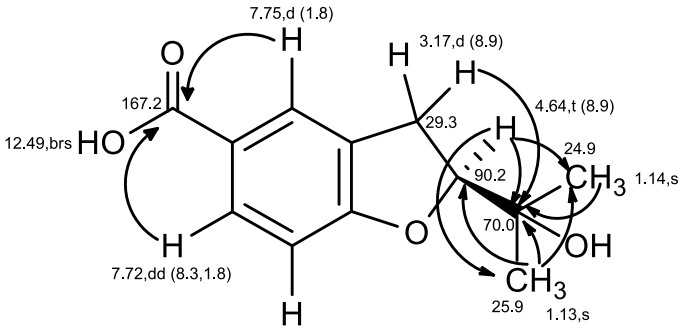

Table 28. ^{1}H and ^{13}C NMR (DMSO, 300.13 MHz and 75.4 MHz) and HMBC assignment for quadricinctafuran A (**388**).

Position	δ_C, type	δ_H, (*J* in Hz)	COSY	HMBC
2	90.2, CH	4.64, t (8.9)	H-3	C-1', 2', 3'
3	29.3, CH_2	3.17, d (8.9)	H-2	C-2, 3a, 7a, 1'
3a	128.2, C	-	-	-
4	126.4, CH	7.75, d (1.8)	H-6	C-6, 7a, 8
5	122.6, C	-	-	-
6	130.4, CH	7.72, dd (8.3, 1.8)	H-4, 7	C-4, 7a, 8
7	108.4, CH	6.80, d (8.3)	H-6	C-3a, 5, 7a
7a	163.7, C	-	-	-
8	167.2, C	-	-	-
1'	70.0, C	-	-	-
2'	24.9, CH_3	1.14, s	-	C-2, 1', 3'
3'	25.9, CH_3	1.13, s	-	C-2, 1', 2'
OH-8	-	12.49, brs	-	-

Literature survey revealed that **388** has the same flat structure as anodendroic acid [2-(1-hydroxy-1-methylethyl)-2,3-dihydrobenzofuran-5-carboxylic acid], which was first isolated from the stem of *Anodendron affine* Durce by Shima *et al*. (1972) and was later synthesized from 2-(1-hydroxy-1-mehylethyl)-2,3-dihydrobenzofuran by Yamaguchi *et al*. (1982). Anodendroic acid was also obtained by hydrolysis of its methyl ester, a constituent of *Eriodictyon sessilifolium* (Arriaga-Giner *et al*., 1988) and by biotransformation of 3-(γ,γ-dimethylallyl)-*p*-coumaric acid (Bisogno *et al*., 2007). However, in all these previous studies, anodendroic acid were identified by comparison of the melting point, ^{1}H NMR

and MS data with those reported by Shima *et al*., and without determination of the stereochemistry of C-2. Since the ^{1}H NMR data of **388** and anodendroic acid reported by Shima *et al*. were obtained in different solvent (**388** was run in DMSO-d_6 while anodendroic acid was run in pyridine-d_6), it was not possible to compare these ^{1}H NMR data. Interestingly, the ^{1}H NMR (DMSO-d_6) data of anodendroic acid reported by Yamaguchi *et al*. were slightly different from those we have obtained for **388**. The obvious differences between anodendroic acid (Shima *et al*., 1972) and **388** are their melting points and optical rotations. The melting points of anodendroic acid and **388** are 212 – 214 °C and 149 – 150 °C, repectively, while the optical rotations are leavorotatory ($[\alpha]_D^{26}$ –19°, *c* 0.7, EtOH) and dextrorotatory ($[\alpha]_D^{20}$ +74°, *c* 0.03, MeOH), repectively. Therefore, we concluded that the structure of **388** is different from the structure of anodendroic acid. Since we were able to obtaine suitable crystal of **388**, its X-ray analysis was carried out to determine the stereochemistry of C-2. The ORTEP view in Figure 64 shows that the absolute configuration of C-2 is *R*. Since it is a new compound, it was named quadricinctafuran A.

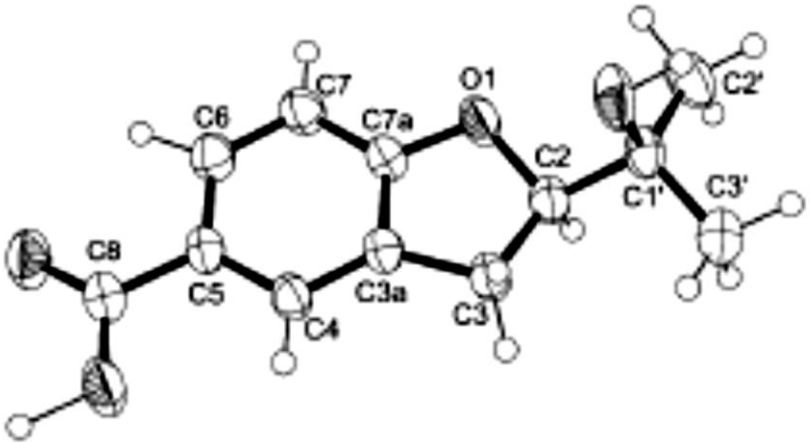

Figure 64. ORTEP diagram of quadricinctafuran A (**388**).

4.3.9) Quadricinctafuran B (389)

Compound **389** was isolated as white solid (mp 209 – 210 °C), and its molecular formula $C_{12}H_{14}O_5$ was determined based on the (+)-HRESIMS *m/z* 239.0919 $[M+H]^+$ (calculated239.0919), indicating six degrees of unsaturation.

The general features of ^1H and ^{13}C NMR spectra of **389** closely resembled those of **388**. The ^{13}C NMR spectrum (Table 29) exhibited twelve carbon signals which can be categorized, according to the DEPTs and HSQC spectra, as one conjugated carboxyl carbonyl (δ_C 167.2), one oxyquaternary sp^2 (δ_C 163.6), two quaternary sp^2 (δ_C 128.4 and 122.6), three methine sp^2 (δ_C 130.8, 126.4 and 108.4), one oxymethine sp^3 (δ_C 86.5), one oxyquaternary sp^3 (δ_C 72.5), one oxymethylene sp^3 (δ_C 66.7), one methylene sp^3 (δ_C 28.7), and one methyl (δ_C 20.0) carbons.

The ^1H NMR spectrum, together with the HSQC spectrum (Table 29), exhibited, besides the signals of three aromatic protons of the 1,2,4-trisubstituted benzene ring at δ_H 7.76, d, *J* = 1.8 Hz (δ_C 126.4), 7.71, dd, *J* = 8.3, 1.8 Hz (δ_C 130.8) and 6.79, d, *J* = 8.3 Hz (δ_C 108.4), a broad singlet of the hydroxyl proton at δ_H 12.47, a singlet of two methylene protons at δ_H 3.33 (δ_C 66.4), a multiplet of another two methylene protons at 3.19 (δ_C 28.7), a double doublet of a methine proton at 4.83 (*J* = 9.7, 8.1 Hz; δ_C 86.5), and a methyl singlet at δ_H 1.09 (δ_C 20.0).

Analysis of ^1H, ^{13}C NMR and COSY spectra led to the conclusion that **389** contained the same 2.3-dihydro-1-benzofuran-5-carboxylic acid nucleus as **388**. However, the ^1H NMR of **389** displayed only one methyl singlet at δ_H 1.09 and one singlet of oxymethylene protons at δ_H 3.33, instead of two methyl singlets. Thus, the difference between **388** and **389** was the substitutions on C-2. That the substitutent on C-2 of **389** was 1,2-dihydroxypropyl group was supported by the molecular formula of **389** ($C_{12}H_{14}O_5$) which has one oxygen atom more than that of **388**, as well as by the presence of the oxymethylene carbon at δ_C 66.7 (C-2') instead of the methyl carbon. Moreover, the chemical shift value of C-2 (δ_C 86.5) was about 4 ppm lower than that of **388**. This hypothesis was also confirmed by the HMBC correlation from the methylene protons at δ_H 3.33, s (H_2-2') to the carbons at δ_C 86.5 (C-2), δ_C 72.5 (C-1') and δ_C 20.0 (C-3'), and from the methyl singlet at δ_H 1.09 (H_3-3') to C-2, C-1' and the carbon at δ_C 66.7 (C-2').

Therefore, compound **389** was identified as 2-(1,2-dihydroxypropan-2-yl)-2,3-dihydro-1-benzofuran-5-carboxylic acid.

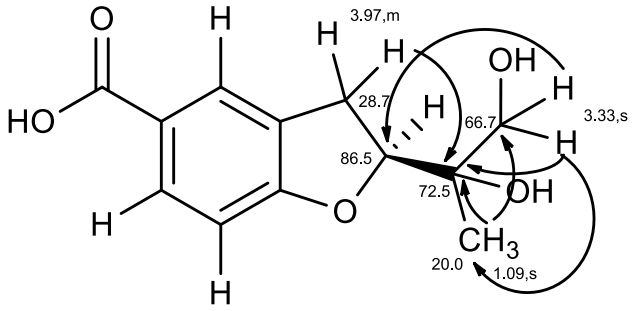

Compound **389** could not be obtained as suitable crystal for X-ray analysis. Furthermore, the absolute configurations of C-2 and C-1' could not be determine by Mosher's NMR method, since C-1' is a tertiary alcohol and C-2' is a primary alcohol. However, since compound **389** is derived from **388**, it was possible to speculate that the absolute configuration of C-2 should be the same as that of C-2 of **388**, i.e. 2*R*. However, it is not yet possible to determine the absolute configuration of C-1'. To the best of our knowledge, **389** has never been previously reported. Therefore, it was named quadricinctafuran B.

Table 29. ^{1}H and ^{13}C NMR (DMSO, 300.13 MHz and 75.4 MHz) and HMBC assignment for quadricinctafuran B (**389**).

Position	δ_C, type	δ_H, (*J* in Hz)	COSY	HMBC
2	86.5, CH	4.83, dd (9.7, 8.1)	H-3	-
3	28.7, CH_2	3.19, m	H-2	C-1', 3[a]
3a	128.4, C	-	-	-
4	126.4, CH	7.76, d (1.8)	H-6	C-3, 6, 7a
5	122.6, C	-	-	-
6	130.8, CH	7.71, dd (8.3, 1.8)	H-4, 7	C-4, 7a, 8
7	108.4, CH	6.79, d (8.3)	H-6	C-3a, 5, 7a
7a	163.6, C	-	-	-
8	167.2, C	-	-	-
1'	72.5, C	-	-	-
2'	66.7, CH_2	3.33, s	-	C-2, 1', 3'
3'	20.0, CH_3	1.09, s	-	C-2, 1', 2'
OH-8	-	12.47, brs	-	-

4.3.10) Quadricinctone D (390)

Compound **390** was isolated as white crystals (mp 196 – 197 °C), and its molecular formula $C_{12}H_{12}O_5$ was determined on the basis of the (+)-HRESIMS *m/z* 237.0792 $[M+H]^+$ (calculated 237.0763), indicating seven degrees of unsaturation. The IR spectrum exhibited absorption bands for hydroxyl (3404 cm^{-1}), conjugated ketone carbonyl (1708 cm^{-1}), conjugated carboxyl carbonyl (1670 cm^{-1}) and aromatic (1558, 1540 cm^{-1}) group.

The ^{13}C NMR spectrum (Table 30) displayed twelve carbon signals which can be classified, based on the DEPTs and HSQC spectra, as one conjugated ketone carbonyl (δ_C 191.0), one conjugated carboxyl carbonyl (δ_C 166.4), one oxyquaternary sp^2 (δ_C 162.9), two quaternary sp^2 (δ_C 123.0 and 119.6), three methine sp^2 (δ_C 136.4, 127.5 and 118.5), one oxyquaternary sp^3 (δ_C 80.3), one oxymethylene sp^3 (δ_C 66.8), one methylene sp^3 (δ_C 43.4) and one methyl (δ_C 21.2) carbons.

The ^{1}H NMR spectrum, together with the HSQC spectrum (Table 30), revealed the presence of , besides two hydroxyl protons at δ_H 12.69, brs and 5.26, brt, *J* = 5.4 Hz,

three aromatic protons of the 1,2,4-trisubstituted benzene ring at δ_H 8.04, dd, *J* = 8.7, 2.3 Hz (δ_C 136.4), 8.26, d, *J* = 2.3 Hz (δ_C 127.5) and 7.07, d, *J* = 8.7 Hz (δ_C 118.5), and two pairs of geminally-coupled protons at δ_H 3.59, dd, *J* = 11.6, 4.2 Hz; δ_H 3.49, dd, *J* = 11.6, 4.5 Hz (δ_C 66.8) and δ_H 3.00, d, *J* = 16.7 Hz; δ_H 2.74, d, *J* = 16.7 Hz (δ_C 43.4).

Since the HMBC spectrum gave cross peaks from the aromatic proton at δ_C 8.26, d, *J* = 2.3 Hz (H-5) to the conjugated ketone carbonyl at δ_C 191.1 (C-4), the carbons at δ_C 136.4 (C-7) and δ_C 162.9 (C-8a), the ketone functionality was connected to C-4a. Moreover, the HMBC spectrum also exhibited correlations from the aromatic proton at δ_H 7.07, d, *J* = 8.7 Hz (H-8) to C-8a and the carbons at δ_C 123.0 and 119.6. Therefore, the carbon signals at δ_C 123.0 and 119.6 were assigned to C-4a and C-6, respectively.

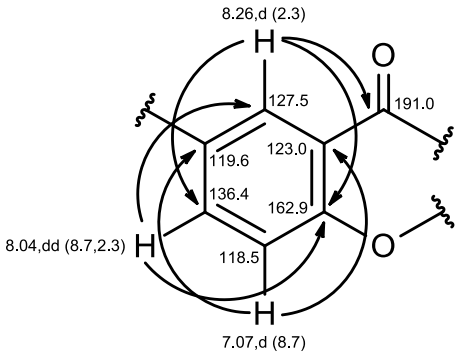

The presence of the 1-hydroxy-2-methyl-2-oxypropyl moiety was evidenced by the COSY correlations from the methylene protons at δ_H 3.49, dd, *J* = 11.6, 4.5 Hz and δ_H 3.59, dd, *J* = 11.6, 4.2 Hz (H_2-10) to the hydroxyl proton at δ_H 5.26, brt, *J* = 5.4 Hz (OH-10), as well as by the HMBC correlations from the methylene protons at δ_H 2.74, d, *J* = 16.7 Hz and δ_H 3.00, d, *J* = 16.7 Hz (H_2-3) to the carbons at δ_C 80.3 (C-2), δ_C 21.2 (C-9) and δ_C 66.8 (C-10), and from the methyl singlet at δ_H 1.30 (H_3-9) to C-2, the carbon at δ_C 43.4 (C-3) and C-10. That the methylene group (CH_2-3) of the 1-hydroxy-2-methyl-2-oxypropyl portion was connected to C-4 was supported by the HMBC correlation from H_2-3 to C-4. Since these two moieties accounted for only $C_{11}H_{12}O_4$, another substituent was the carboxyl group (δ_C 166.4, δ_H 12.69, br).

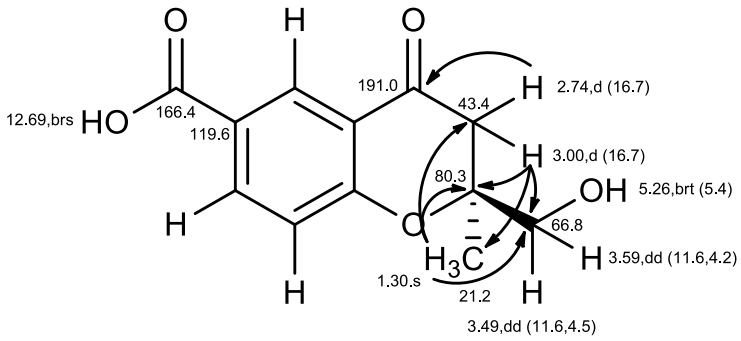

Therefore, **390** was identified as 2-(hydroxymethyl)-2-methyl-4-oxo-3,4-dihydro-2*H*-chromene-6-carboxylic acid. Since **390** was obtained as a suitable crystal, X-ray analysis was carried out to confirm the proposed structure and determine the stereochemistry of this compound. The ORTEP view shown in Figure 65 revealed the absolute configuration of C-2 is 2*S*. Since **390** is a new compound, we named it quadricinctone D.

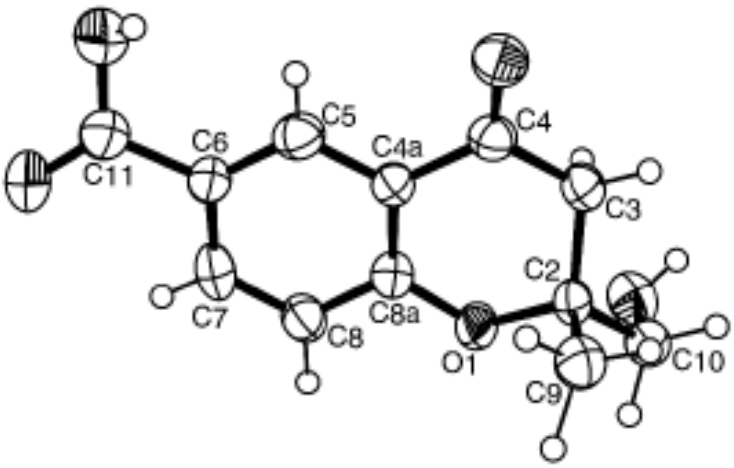

Figure 65. ORTEP diagram of quadricinctone D (**390**).

In order to determine the conformation of the 2,3-dihydro-4*H*-pyran-4-one, analysis of the NOESY correlations was carried out. Since, the NOESY spectrum exhibited strong cross peak from H-7 to H-8, and also weak cross peaks from H_3-9 to H-5 and H-8, H_3-9 is in the α-axial position. Moreover, H_3-9 also gave strong cross peak to the methylene

proton at δ_H 2.47, d, *J* = 16.7 Hz and a weak cross peak to the proton at δ_H 3.00, d, *J* = 16.7 Hz, therefore, they were assigned as H-3α and H-3β, respectively.

Table 30. ^{1}H and ^{13}C NMR ($CDCl_3$, 300.13 MHz and 75.4 MHz), HMBC and NOESY assignments for quadricinctone D (**390**).

Position	δ_C, type	δ_H, (*J* in Hz)	COSY	HMBC	NOESY
2	80.3, C	-	-	-	-
3α	43.4, CH_2	2.74, d (16.7)	H-3	C-2, 4, 9, 10	H_3-11 (str)
3β		3.00, d (16.7)	H-3	C-2, 4, 9, 10	H_3-11 (w)
4	191.1, CO	-	-	-	-
4a	123.0, C	-	-	-	-
5	127.5, CH	8.26, d (2.3)	H-7	C-4, 7, 8a	-
6	119.6, C	-	-	-	-
7	136.4, CH	8.04, dd (8.7, 2.3)	H-5, 8	C-5, 8a	-
8	118.5, CH	7.07, d (8.7)	H-7	C-4a, 6, 8a	-
8a	162.9, C	-	-	-	-
9	21.2, CH_3	1.30, s	-	C-2, 3, 10	H-3α (str), 3β (w), 5, 8 (w)
10	66.8, CH_2	3.49, dd (11.6, 4.5)	OH-10	-	-
		3.59, dd (11.6, 4.2)	OH-10	-	-
11	166.4, CO	-	-	-	-
OH-10	-	5.26, brt (5.4)	H_2-10	-	-
OH-11	-	12.69, br	-	-	-

Compounds **381** and **387** can be hypothesized as originating from the pentaketide intermediate (**I**), which is derived from acetyl-CoA and malonyl-CoA. The intermediated **II**, which is derived by methylation of **I** by SAM, undergoes cyclization and enolization to form the intermediate **III**. Methylation of the α-carbon of the carbonyl ketone and the phenolic hydroxyl groups by SAM gives the intermediate **IV**. Oxidation of the α-carbon of the side chain of **IV** leads to the intermediate **VII**, which was followed by lactonization and reduction of the ketone carbonyl, gives rise to **381**. Alternatively, enolization of the intermediate **IV**, followed by lactonization, arises **V**, which undergoes hydration to give **VI**, and oxidation of one of methyl groups gives rise to **387** (Scheme 2).

The origin of **382**, **383**, **385**, **386**, **388**, **389** and **390** is the intermediates from shikimate (chorismate; **IX**) and mevalonate (DMAPP; **XI**) pathways, similar to that proposed for fomannoxin (Hansson *et al*., 2012). *p*-Hydroxybenzoic acid (**X**), which is derived from the pyruvate elimination of **IX** by chorismate pyruvate-lyase, is prenylated by **XI** leads to the formation of the intermediate **XII**. Epoxidation of **XII** leads to the formation of **XIII** which after cyclization, via Route *a*, orginates the furan ring in **388**. One of the methyl groups of **388** is oxidized to give rise to **389**. On the other hand, cyclization of **XIII**, via Route *b*, originates the pyran ring in **XIV**. Dehydration and oxidation of one of the methyl groups of **XIV** leads to the formation of **382** which after is acetylated of the primary alcohol function of the side chain, leads to the formation of **383**. Alternatively, dehydration and oxidation of the pyran ring of **XIV** originates the ketone function of **390**. Compound **390** undergoes oxidative decarboxylation to give rise to **385** which after is sulfinylated of the benzene ring, leads to the formation of 387 (Scheme 3).

The intermediate **XVII** is also derived from the prenylation of *p*-hydroxybenzoic acid (**X**); however, it is prenylated by IPP (**XVI**) instead of DMAPP (**XI**). Epoxidation of the double bond of the side chain of **XVII** leads to the formation of **XVIII** which after undergoes cyclization to give rise to an oxepin ring in **XIX**. Oxidation and dehydration of the oxepin ring orinates **384** (Scheme 4).

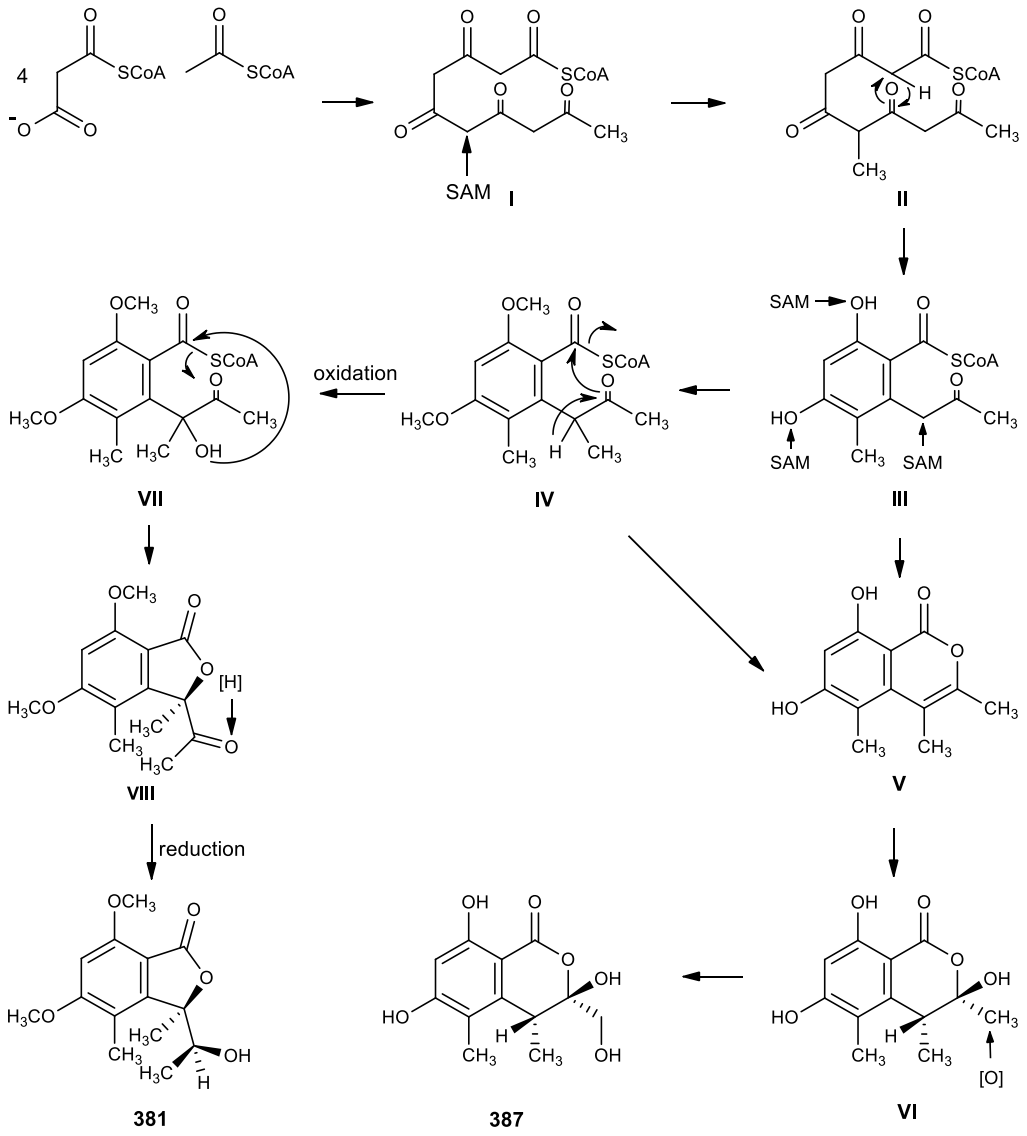

Scheme 2. Proposed biosynthetic pathways for quadricinctones A (**381)** and C (**387)**.

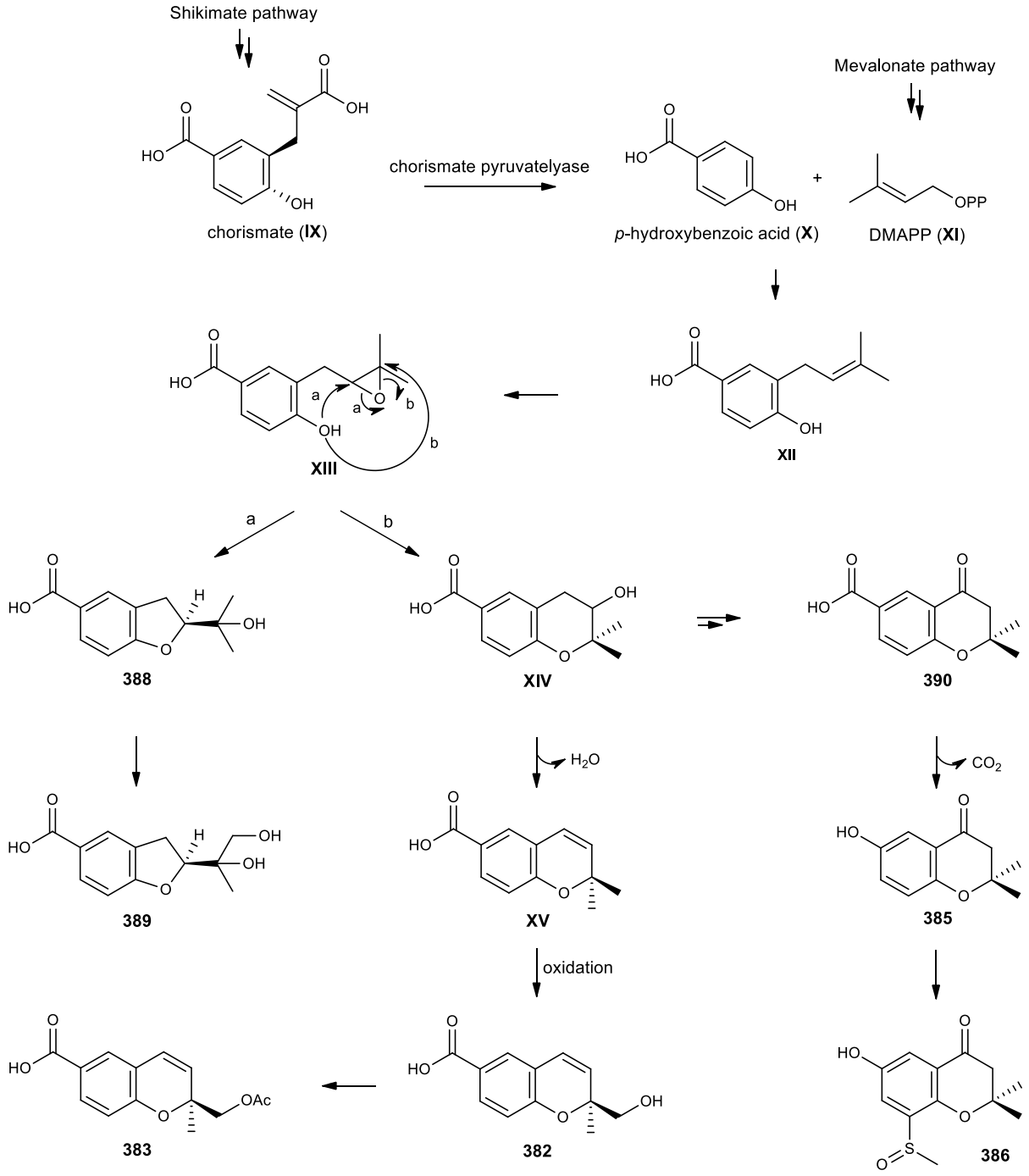

Scheme 3. Proposed biosynthetic pathways for quadricinctapyrans A (**382)**, B (**383)**, 2,3-dihydro-6-hydroxy-2,2-dimethyl-4*H*-1-benzopyran-4-one (**385)**, quadricinctone B (**386**), quadricinctafurans A (**388)**, B (**389)** and quadricinctone D (**390)**.

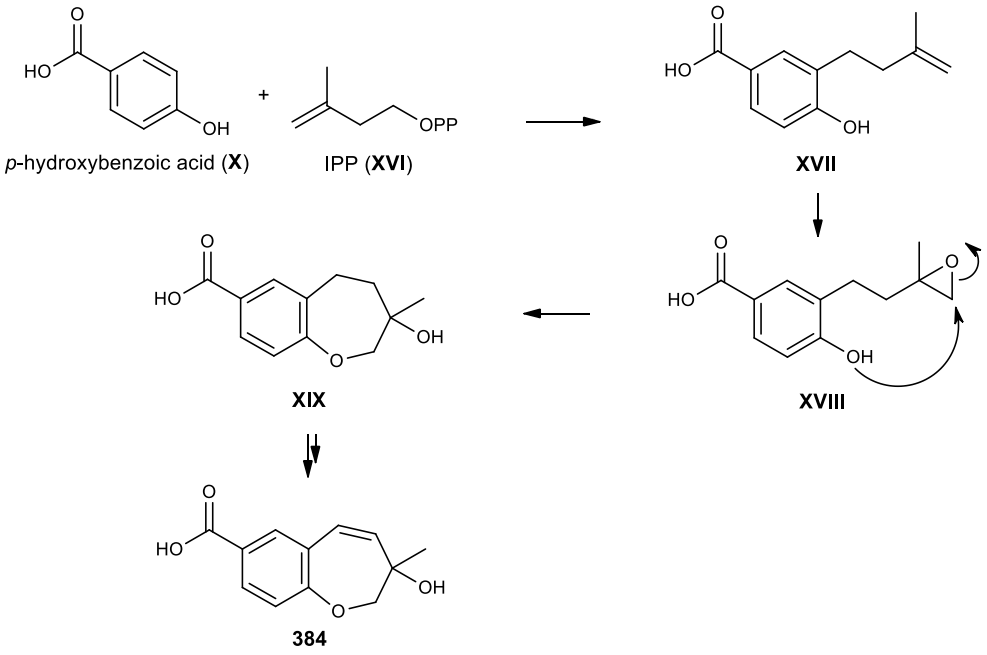

Scheme 4. Proposed biosynthetic pathway for quadricinctoxepine (**384)**.

4.4) Biological Activity Evaluation of the Isolated Compounds from the Marine Sponge *Iotrochota baculifera*, and the Marine-Derived Fungi *Aspergillus similanensis* KUFA 0013 and *Neosartorya quadricincta* KUFA 0081

Cancer is one of world health problems which causes approximately 8.8 million people died in 2015. It is nearly 1 in 6 deaths is from cancer. The first leading type of cancer which causes death is lung cancer with approximately 1.69 million deaths worldwide; the Fifth leading cause of global death in 2015 (http://www.who.int/ mediacentre/factsheets/fs297/en/; http://www.who.int/mediacentre/factsheets/fs310/ en/).

Not only cancer, but infectious diseases are also one of leading causes of global death. From the report of WHO in 2015, lower respiratory tract infection is the third cause of death worldwide, with approximately 3.19 million deaths (http://www.who.int/media-centre/factsheets/fs310/en/). One of important causes of mortality is antimicrobial resistance which leads to decrease the efficacy of antimicrobial agents. The death rate of patients who were infected by MRSA are about 64% higher than non-resistant *S. aureus* infected patients (http://www.who.int/ mediacentre/factsheets/fs194/en/). Nowadays, the problem of antimicrobial resistance is growing higher. WHO has been reported that the world is lack of new antibiotics to treat the antimicrobial-resistant pathogens. Therefore, the priority pathogens list (PPL) that includes 12 families of antibiotic-resistant bacteria was published by WHO to guide researchers for new drug discovery and development (http://www.who.int/mediacentre/news/releases/2017/bacteria-antibiotics-needed/en/).

As described in chapter I (introduction), marine-derived secondary metabolites are a rich source of leading compounds. They exhibit many interesting bioactivities such as anticancer, antimicrobial and anti-inflamatory activities. Therefore, we decided to test the secondary metabolites we have isolated for their antimicrobial and anticancer activities in our studies.

4.4.1) Antibacterial Activity Evaluation

Compounds **154**, **356**, **372** – **375** and **377** – **390** were evaluated for their antibacterial activity against Gram-positive (*Staphylococcus aureus* ATCC 25923 and *Bacillus subtilis* ATCC 6633) and Gram-negative (*Escherichia coli* ATCC 25922 and *Pseudomonas aeruginosa* ATCC 27853) bacteria, as well as the multidrug-resistant isolates from the environment [*S. aureus* B1 (isolated from public bus); *Enterococcus faecalis* W1 (isolated from river water); *E. coli* G1 (isolated from seagull feces)]. None of the tested compounds exhibited antibacterial activity at the highest concentration tested (256 µg/mL). Similar to chevalone C (**349**), the structure of chevalone E (**356**) does not possess the β-acetoxyl group on C-3 and the 4-hydroxy-6-methyl-2*H*-pyran-2-one ring on C-15 which are the structural requirements for the antibacterial activity of this group of meroditerpenes (Gomes *et al*., 2014). Therefore, **356** also did not exhibit the antibacterial activity the same as **349**. However, **349** displayed synergistic effect with antibiotics against the multidrug-resistant isolates (*S. aureus* B1, *E. coli* G1 and *E. faecalis* W1; Gomes *et al*.,2014). According to this fact, **154**, **356**, **372** – **375** and **377** – **378** were also tested for their synergistic effect with antibiotics (ciprofloxacin, ampicillin, cefotaxime, streptomycin, oxacillin, vancomycin and erythromycin) against three multidrug-resistant bacteria isolated from environment, using the disc diffusion method. None of the tested compounds exhibited synergistic effect against the multidrug-resistant *E. coli* and *E. faecalis*. Only chevalone E (**356**) exhibited a good synergistic effect with oxacillin and ampicillin against MRSA (Table 31).

Table 31. Antibacterial efficacy of combined effect of antibiotics with the isolated compounds (15 µg/disc) against three environmental multidrug-resistant isolates, using the disc diffusion method.

Compounds	*E. coli* G1				*S. aureus* B1			*E. faecalis* W1		
	Antibiotics									
	CIP	AMP	CTX	S	OX	AMP	CIP	VA	AMP	E
154	-	-	-	-	-	++	-	-	-	-
356	-	-	-	-	+++	+++	-	-	-	-
372	-	-	-	-	-	++	-	-	-	-
373	-	-	-	-	-	++	-	-	-	-
374				-	-	++	-	-	-	-
375	-	-	-	-	-	-	-	-	-	-
377			-	-		++	-	-	-	-
378	-	-	-	-	-	++	-	-	-	-

(-) noneffective; (+) slight efficacy – halo of inhibition or additional increase in the halo of 1 to 2.5 mm around the disc; (++) moderate efficacy – from > 2.5 to 5 mm; (+++) good efficacy – from > 5 to 8 mm; CIP: ciprofloxacin; AMP: ampicillin; CTX: cefotaxime; S: streptomycin; OX: oxacillin; VA: vancomycin; E: erythromycin.

The checkerboard method was carried out to verify if the synergism occurred with both oxacillin and ampicillin, or with either of them. The results, represented by the fractional inhibitory concentration (FIC) index (Table 32), revealed that only the combination of chevalone E (**356**) and oxacillin exhibited the synergistic effect with FIC index < 0.188.

Table 32. MIC values of chevalone E (**356**) in combination with oxacillin or ampicillin, and the respective FIC index obtained against a MRSA (*S. aureus* B1) using the checkerboard method.

Strain	MIC (µg/mL)				FIC index
S. aureus B1	**356** alone	OX alone	**356** with OX	OX with **356**	< 0.1888
	> 1024	128	64	16	
S. aureus B1	**356** alone	AMP alone	**356** with AMP	AMP with **356**	> 1.5
	> 1024	128	> 512	128	

FIC index ≤ 0.5: synergy; 0.5 < FIC index ≤ 4: no interaction; FIC index > 4: antagonism

4.4.2) Antifungal Activity Evaluation

Compounds **381** – **390** were evaluated for their antifungal activity against three fungi, *Candida albicans* ATCC 10231 (yeast), *Aspergillus fumigatus* ATCC 46645 (filamentous fungus) and *Trichophyton rubrum* FF5 (dermatophyte) while **154**, **356**, **372** – **375** and **377** – **378** were tested against only *C. albicans* ATCC 10231. The results revealed that all the tested compounds did not exhibit antifungal activity at the highest concentration tested (**382** – **391** at the concentration of 512 µg/mL and **154**, **356**, **372** – **375** and **377** – **378** at 256 µg/mL).

4.4.3) Cytotoxicity Evaluation

Compounds **379** – **390** were evaluated for their cytotoxicity against three human cancer cell lines, using SRB assay. While **379** – **380** were tested against MCF-7, NCI-H460 and A373, other compounds were tested against MCF-7, NCI-H460 and A375-C5. All tested compounds, except for **380**, did not show any activity (GI_{50} > 150 mM). Compound **380** weakly inhibited the growth of MCF-7, NCI-H460 and A373 cancer cell lines with GI_{50} values of 125 ± 0, 117.50 ± 3.55 and 115 ± 7.07 mM, respectively.

CHAPTER V

MATERIALS AND METHODS

5.1) General Experimental Procedures

^{1}H and ^{13}C NMR spectra were recorded at ambient temperature in deuterated chloroform ($CDCl_3$) or deuterated dimethylsulfoxide (DMSO-d_6) on a Bruker AMC instrument (Bruker Biosciences Corporation, Billerica, MA, USA) operating at 500.13 and 125.8 MHz or at 300.13 and 75.4 MHz, respectively.

High-resolution mass spectra were measured with a Waters Xevo QToF mass spectrometer (Waters Corporations, Milford, MA, USA) coupled to a Waters Aquity UPLC system.

Infrared spectra were recorded in a KBr microplate in a FTIR spectrophotometer Nicolet iS10 from Thermo Scientific (Waltham, MA, USA) with Smart OMNI-Transmission accessory (Software 188 OMNIC 8.3).

Melting points were determined on a Bock monoscope and are uncorrected.

Optical rotations were determined on an ADP410 Polarimeter (Bellingham + Stanley Ltd., Tunbridge Wells, Kent, UK).

Silica gel 60 (0.2-0.5 mm; 70-230 mesh, Merck), LiChroPrep Si 60 (0.04-0.063 mm, Merck) and Sephadex LH-20 were used for column chromatography. Analytical TLC was performed on Silica gel 60 (GF_{254}, Merck), 0.25 mm thickness (The plates were activated at 110 °C in the oven Binder for 4 hours) and pre-coated silica gel sheets, GF_{254} (Macherey-Nagel), ALUGRAM®, Sil G/UV_{254}, 20 × 20 cm. TLC plates were visualized under UV lamp (254 and 365 nm) or developed with iodine vapor.

The organic solvents (acetone, chloroform, ethyl acetate, methanol, petroleum ether 40-60 °C) were purchased from Merck and Fischer with analytical reagent grade. Solvents were evaporated at reduced pressure, using Büchi Heating Bath B-49, Büchi Ratavapor R-210, Büchi Vacuum Module V-801 EasyVac and Vacuum Pump V-700.

The weight was measured on the analytical balance AND GH-202.

Ultraviolet spectra were recorded on a Shimadzu mini-1240UV-VIS spectrophotometer using 1.000 cm quartz cells.

5.2) Isolation and Identification of the Marine-Derived Fungi

5.2.1) *Aspergillus similanensis* KUFA 0013

The fungus *Aspergillus similanensis* KUFA 0013 was isolated from the marine sponge *Rhabdermia* sp., which was collected, by scuba diving at a depth of 10 m, from the coral reef of the Similan Islands, Phang Nga Province, Thailand, in April 2010. The sponge was identified by Dr. Jamrearn Buaruang (Division of Environmental Science, Faculty of Science, Ramkhamhaeng University, Bangkok, Thailand). Briefly, the sponge was rinsed with sterile sea water and dried on a sterile filter paper, then cut into small pieces (5 × 5 mm). After placing the sponge on the plates containing malt extract agar (MEA) medium with 70% sea water, the plates were incubated at 28 °C under 12 h light/ 12 h dark cycle for 7 days. The MEA medium was prepared by using 30 g of malt extract powder (Himedia, Mumbai, India), 15 g of bacto agar, distilled water 300 mL and sea water 700 mL, and then adjusted to the final pH at 5.5. The fungus was identified by Prof. Dr. Tida Dethoup (Department of Plant Pathology, Faculty of Agriculture, Kasetsart University, Bangkok, Thailand), based on morphological characteristics of ascospores, conidiogenesis and colonies, as well as by DNA sequence analysis of the calmodulin gene (Glass & Donaldson, 1995), and it was deposited at GenBank with Accession No. of KC 920702. However, the strain was not identified at species level due to the sequence was not identical to that deposited at GenBank, therefore the pure cultures were deposited as KUFA 0013 at the Department of Plant Pathology, Faculty of Agriculture, Kasetsart University, Bangkok, Thailand. Later on, this fungus was further studied by Dethoup *et al*. (2016) and was identified as *Aspergillus similanensis* Dethoup.

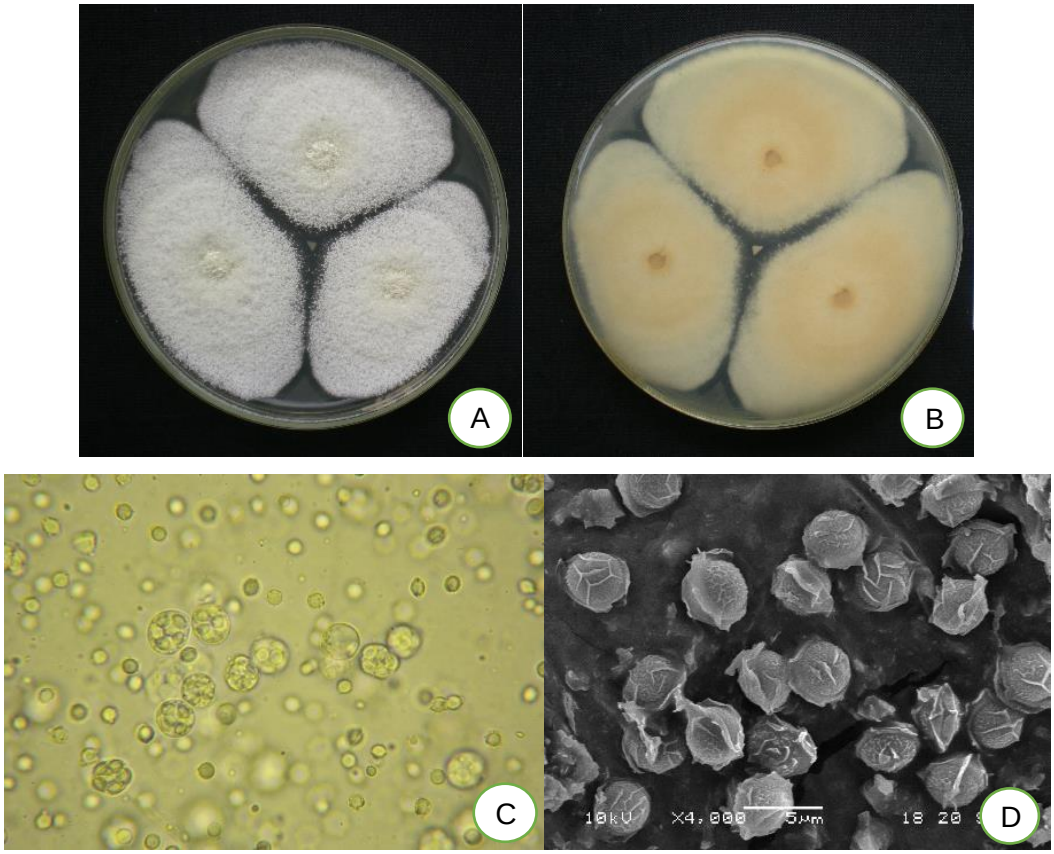

Figure 66. Colony on MEA, 7 days, 28 °C obverse (A), reverse (B), asci and ascospores (C) and scanning electron microscope of ascospores (D) of *Aspergillus similanensis* KUFA 0013.

5.2.2) *Neosartorya quadricincta* KUFA 0081

The fungus *Neosartorya quadricincta* KUFA 0081 was isolated from the marine sponge *Clathria reinwardti*, which was collected from the coral reef at Samae San Island (12°34’ 36.64’’ North 100°56’ 59.69’’ East) in the Gulf of Thailand, Chonburi Province, by scuba diving at 15-20 m depth, in July 2013. After washing with 0.06% sodium hypochlorite solution for 1 min and followed by sterilized sea water 3 times, the sponge was dried on sterile filter paper and cut into small pieces (5 × 5 cm), then placed on the plates containing MEA medium with 70% seawater and 300 mg/L of streptomycin sulphate. The plates were incubated at 28 °C for 7 days, after which the hyphal tips were transferred onto a MEA slant and maintained as pure culture for

further identification. The fungus was identified by Prof. Dr. Tida Dethoup, using morphological features, including characteristics of ascospores and colonies, as well as by sequence analysis of the β-tubulin, calmodulin and actin genes (Matsuzawa *et al*., 2014).

The identification of *N. quadricincta* was also confirmed by the sequence analysis of the internal transcribed spacer (ITS) gene (MayZin *et al*., 2015). The gene sequences were deposited in GenBank (Accession No. KM095492 and KT201525, respectively). The pure culture was deposited as KUFA0081 at Kasetsart University Fungal Collection, Department of Plant Pathology, Faculty of Agriculture, Kasetsart University, Bangkok, Thailand.

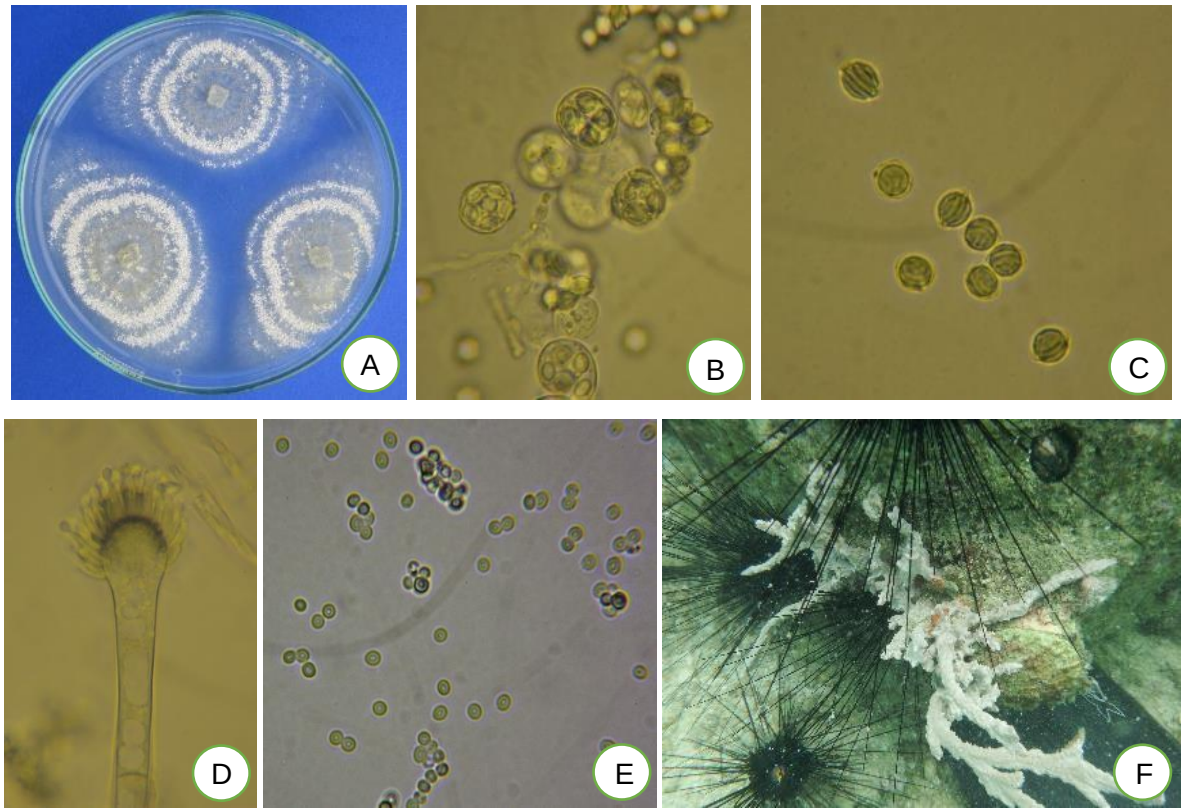

Figure 67. Colony on PDA, 7 days, 28 °C obverse (A), asci (B), ascospores (C), aspergilla (D), spores (E) of *N. quadricincta* KUFA 0081 and *Clathria reinwardti* (F).

5.3) Extraction and Isolation of Metabolites

5.3.1) The marine sponge *Iotrochota baculifera*

The marine sponge *Iotrochota baculifera* was collected from the Gulf of Thailand, Chonburi province, by scuba diving, in March 2012. The sponge was collected and identified by Dr. Sumaitt Putchakarn, Bangsaen Institute of Marine Science, Burapha University. The frozen sponge (1,174 g, wet weight) was thawed and homogenized with EtOH (3 L), allowed to stand for 24 h in a dark chamber and the residue was re-extracted with EtOH (2 × 3 L). The aqueous alcoholic extracts were combined, evaporated under reduced pressure by rotatory evaporator to *ca*. 500 mL and then partitioned with EtOAc (3 × 500 mL). The EtOAc solutions were combined and concentrated under reduced pressure by rotatory evaporator to give the crude EtOAc extract (5.06 g) which was chromatographed over a Silica gel column (42 g) and eluted with mixtures of petroleum ether (petrol) – $CHCl_3$ and $CHCl_3$ – Me_2CO, wherein 150 mL fractions were collected as follows: Frs 1-42 (petrol-$CHCl_3$, 3:7), 43-73 (petrol-$CHCl_3$, 1:9), 74-100 ($CHCl_3$-Me_2CO, 9:1) and 101-130 ($CHCl_3$-Me_2CO, 7:3). Frs 47-58 were combined and recrystallized in a mixture of petrol and $CHCl_3$ to give **370** (10.4 mg). Frs 74-77 were combined and recrystallized in a mixture of petrol and $CHCl_3$ to give **40** (7.8 mg).

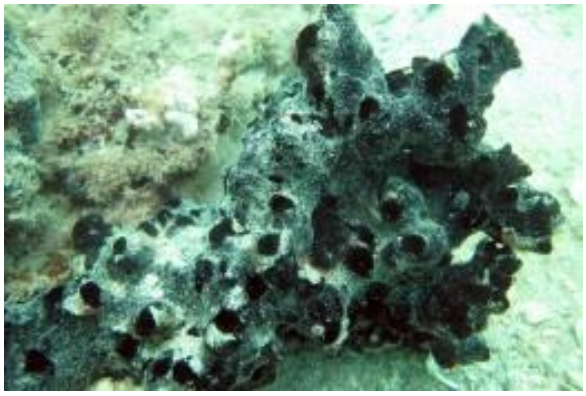

Figure 68. The picture of the marine sponge *Iotrochota baculifera.*

5.3.2) *Aspergillus similanenesis* KUFA 0013

The fungus was cultured for 7 days in 5 Petri dishes (ID 90 mm), which contained 25 mL of MEA with 70% sea water per dish. Thirty 1000 mL Erlenmeyer flasks, containing white rice (200 g), water (30 mL) and sea water (70 mL), were autoclaved at 121 °C for 15 min, inoculated with 10 mycelia plugs of the fungus and then incubated at 28 °C for 30 days. The moldy rice was macerated in EtOAc (7 L total) for 7 days and then filtered by filter paper and a mixture of EtOAc and H_2O in the filtrate was separated by separating funnel. The EtOAc layer was evaporated under reduced pressure using rotary evaporator to yield crude ethyl acetate extract (97 g) that was dissolved in 500 mL of a mixture of EtOAc and $CHCl_3$ (4:1), and then washed twice with 5% aqueous solution of $NaHCO_3$ (300 mL), H_2O (3 x 300 mL). The organic layer was dried using anhydrous Na_2SO_4, filtered by filter paper and the filtrate was evaporated under reduced pressure by rotatory evaporator to give 75 g of crude extract which was applied on a column chromatography of silica gel (640 g) and eluted with mixtures of $CHCl_3$-petrol and $CHCl_3$-Me_2CO, wherein 250 mL fractions were collected as follows: Frs 1-18 ($CHCl_3$-petrol, 3:7), 19-53 ($CHCl_3$-petrol, 1:1), 54-114 ($CHCl_3$-petrol, 7:3), 115-215 ($CHCl_3$-petrol, 9:1), 216-395 ($CHCl_3$-Me_2CO, 9:1), and 396-443 ($CHCl_3$-Me_2CO, 7:3). Frs 185-196 were combined (654.0 mg) and purified by TLC (silica gel G254, $CHCl_3$: Me_2CO: HCO_2H, 97: 3: 0.01) to give 4.0 mg of similanpyrone A (**375**) and 7.4 mg of similanpyrone C (**376**). Frs 197-221 were combined (1.2 g) and crystallized in a mixture of petrol and $CHCl_3$ to give additional 17.6 mg of a yellow solid which was further purified by TLC (silica gel G254, $CHCl_3$: Me_2CO: HCO_2H, 98: 2: 0.01) to give 2.5 mg of similanpyrone A (**375**). Fr 222 (8.1 g) was crystallized in a mixture of $CHCl_3$ and Me_2CO to give 238.0 mg of white precipitate, which was further purified by TLC (silica gel G254, $CHCl_3$: Me_2CO: HCO_2H, 97: 3: 0.01) to give 32.7 mg of similanpyrone B (**373**), 4.6 mg of S14-95 (**377**), and 70.8 mg of chevalone B (**348**). The mother liquor of frs 197-221 and frs 223-224 were combined (9.2 g), applied on the silica gel column (58 g), and eluted with mixtures of $CHCl_3$-petrol and $CHCl_3$-Me_2CO, wherein 100 mL sub-fractions were collected as follows: sfrs 1-59 ($CHCl_3$-petrol, 7:3), 60-69 ($CHCl_3$-petrol, 9:1), and 70-76 ($CHCl_3$-Me_2CO, 9:1). Sfrs 11-22 were combined

(2.0 g) and crystallized in a mixture of petrol and $CHCl_3$ to give additional 16.4 mg of similanpyrone A (**375**). Sfrs 29-42 were combined (468.0 mg) and crystallized in a mixture of petrol and $CHCl_3$ to give additional 92.1 mg of similanpyrone B (**373**). Frs 225-228 were combined (446.0 mg) and crystallized in a mixture of petrol and $CHCl_3$ to give 63.0 mg of a precipitate which was further purified by TLC (silica gel G254, $CHCl_3$: Me_2CO: HCO_2H, 97: 3: 0.01) to give 35.4 mg of 6,8-dihydroxy-3-methylisocoumarin (**372**) and 35.8 mg of similanpyrone B (**373**). The mother liquor of frs 225-228 and frs 229-230 were combined and chromatographed on a silica gel column (33 g) and eluted with mixtures of $CHCl_3$-petrol and $CHCl_3$-Me_2CO, wherein 100 mL sub-fractions were collected as follow: sfrs 1-49 ($CHCl_3$-petrol, 7:3), 50-64 ($CHCl_3$-petrol, 9:1), and 65-77 ($CHCl_3$-Me_2CO, 9:1). Sfrs 4-5 were combined and recrystallized in a mixture of petrol and $CHCl_3$ to give 2.4 mg of similanpyrone A (**375**). Sfrs 6-10 were combined (160.0 mg) and recrystallized in a mixture of petrol and $CHCl_3$ to give 7.6 mg of reticulol (**374**). Sfrs 11-16 were combined (108.0 mg) and recrystallized in a mixture of petrol and $CHCl_3$ to give 5.0 mg of similanpyrone B (**373**). Sfrs 27-33 were combined (206.0 mg) and purified by TLC (silica gel G254, $CHCl_3$: Me_2CO: HCO_2H, 97: 3: 0.01) to give 36.0 mg of *p*-hydroxybenzaldehyde (**371**). Frs 231-247 were combined (6.7 g) and recrystallized in a mixture of petrol and $CHCl_3$ to give 1.4 g of chevalone C (**349**). Frs 272-294 were combined (1.5 g) and crystallized in mixture of petrol and $CHCl_3$ to yield 265 mg of pyripyropene E (**154**). Frs 310-327 were combined (1.2 g), applied on a Sephadex LH-20 column (10 g) and eluted with methanol (MeOH), wherein 10 sub-fractions of 1 mL were collected. Sfrs 1-7 were combined and purified by TLC (silica gel G254, $CHCl_3$: Me_2CO: HCO_2H, 19: 1: 0.01) to give 108.0 mg of similanamide (**380**). Frs 328-335 were combined (296.0 mg) and applied on a column of Sephadex LH-20 (10 g) and eluted with a mixture of $CHCl_3$-MeOH (1:1) to give 11.2 mg of chevalone E (**356**). Frs 336-345 were combined (165.0 mg) and purified by TLC (silica gel G254, $CHCl_3$: Me_2CO: HCO_2H, 17: 3: 0.01) to give additional 60.0 mg of similanamide (**380**). Frs 354-398 were combined (1.1 g), applied on a Sephadex LH-20 column (10 g) and eluted with a mixture of $CHCl_3$-MeOH (1:1), wherein thirty-four sub-fractions of 1mL were collected. Sfrs 7-15 were combined (150.0 mg) and purified by TLC (silica gel G254, $CHCl_3$: MeOH: HCO_2H, 95: 5: 0.01)

to give 67.0 mg of pyripyropene S (**378**). Frs 435-443 were combined (377.0 mg), applied on a Sephadex LH-20 column (10 g) and eluted with a mixture of $CHCl_3$-MeOH (1:1), wherein 14 sub-fractions of 1 mL were collected. Sfrs 8-11 were combined (62.0 mg) and purified by TLC (silica gel G254, $CHCl_3$: MeOH: HCO_2H, 95: 5: 0.01) to give 35.0 mg of pyripyropene T (**379**).

5.3.3) *Neosartorya quadricincta* KUFA 0081

The fungus was cultured for 7 days at 28 °C in ten 90 mm Petri dishes, containing 25 mL of MEA with 70% sea water and 300 mg/L of streptomycin sulphate. In order to obtain the mycelial suspension, the mycelial plugs were transferred to two 500 mL Erlenmeyer flasks containing 200 mL of potato dextrose broth and then incubated on a rotary shaker at 120 rpm at 20 °C for 4 days. Fifty 1000 mL Erlenmeyer flasks, containing 300 g of cooked rice with 70% sea water per flask, were autoclaved at 121 °C for 15 min, inoculated with 20 mL of mycelial suspension of *Neosartorya quadricincta* and then incubated at 28 °C for 30 days, after which the mouldy rice was macerated in EtOAc (25 L total) for 7 days and then filtered with filter paper. The two layers were separated using separating funnel and the EtOAc solution was concentrated under reduced pressure by rotatory evaporator to yield 176.5 g of crude EtOAc extract which was dissolved in 500 mL of $CHCl_3$ and then washed with H_2O (3 x 500 mL). The organic layers were separated, combined and dried with anhydrous Na_2SO_4, then filtered and evaporated under reduced pressure to give 31.1 g of the crude $CHCl_3$ extract, which was applied on a column of silica gel (440 g) and eluted with mixtures of petrol-$CHCl_3$ and $CHCl_3$-Me_2CO, 250 mL fractions were collected as follows: Frs 1-15 (petrol-$CHCl_3$, 1:1), 16-55 (petrol-$CHCl_3$, 3:7), 56-118 (petrol-$CHCl_3$, 1:9), 119-284 ($CHCl_3$-Me_2CO, 9:1), 285-329 ($CHCl_3$-Me_2CO, 7:3), 330-359 ($CHCl_3$-Me_2CO, 1:1). Frs 175-181 were combined (250 mg) and purified by TLC (silica gel G254, $CHCl_3$: Me_2CO: HCO_2H, 3: 2: 0.01) to give 86.6 mg of quadricinctone A (**381**) and 15.0 mg of quadricinctapyran B (**383**). Frs 182-197 were combined (565.1 mg) and purified by TLC (silica gel G254, $CHCl_3$: Me_2CO: HCO_2H, 17: 3: 0.02) to give 35.1 mg of quadricinctone A (**381**) and 14.3 mg of quadricinctapyran B (**383**). Frs 224-235 were

combined (249.3 mg) and purified by TLC (silica gel G254, $CHCl_3$: Me_2CO: HCO_2H, 4: 1: 0.01) to give 11.4 mg of 6-hydroxy-2,2-dimethyl-2,3-dihydro-4*H*-chromen-4-one (**385**). Frs 236-285 were combined (1.2 g), applied over a column chromatography of silica gel (42 g) and eluted with mixtures of petrol-$CHCl_3$ and $CHCl_3$-Me_2CO, wherein 100 mL sub-fractions were collected as follows: sfrs 1-17 (petrol-$CHCl_3$, 1:9), 18-61 ($CHCl_3$-Me_2CO, 9:1). Sfrs 24-33 were combined (432.4 mg) and precipitated in a mixture of $CHCl_3$ and Me_2CO to give a white solid (46.2 mg), which was recrystallized in a mixture of $CHCl_3$ and Me_2CO to give 9.4 mg of quadricinctafuran A (**388**), and the mother liquor which left from recrystallization was purified by TLC (silica gel G254, $CHCl_3$: Me_2CO: HCO_2H, 9: 1: 0.01) to give 23.2 mg of quadricinctafuran A (**388**) and 4.9 mg of quadricinctapyran A (**382**). The mother liquor of sfrs 24-33 from the first crystallization (133.0 mg) was purified by TLC (silica gel G254, $CHCl_3$: Me_2CO: HCO_2H, 7: 3: 0.01) to give 41.1 mg of quadricinctapyran A (**382**) and 12.4 mg of quadricinctapyran B (**383**). Sfrs 34-39 were combined (77.7 mg) and purified with TLC (silica gel G254, $CHCl_3$: Me_2CO: HCO_2H, 3: 1: 0.01) to give 7.9 mg of quadricinctone B (**386**) and 17.1 mg of quadricinctapyran A (**382**). Sfrs 40-61 were combined (496.4 mg) and purified by TLC (silica gel G254, $CHCl_3$: Me_2CO: HCO_2H, 4: 1: 0.01) to give 22.7 mg of quadricinctone C (**387**). Frs 307-315 were combined (291.0 mg), applied over a column chromatography of Sephadex LH-20 (10 g) and eluted with a 1:1 mixture of $CHCl_3$-MeOH to give twelve 1 mL sub-fractions. Sfrs 9-12 were combined and purified by TLC (silica gel G254, $CHCl_3$: Me_2CO: HCO_2H, 3: 2: 0.01) to give 13.4 mg of quadricinctafuran B (**389**) and 9.4 mg of quadricinctone D (**390**). Frs 316-359 were combined (1.2 g), applied over a column chromatography of Sephadex LH-20 (10 g) and eluted with a 1:1 mixture of $CHCl_3$-MeOH to give twenty-one 1 mL sub-fractions. Sfrs 12-21 were combined (645.7 mg), applied over a column chromatography of Sephadex LH-20 (10 g) and eluted with a 1:1 mixture of $CHCl_3$-MeOH to give sixteen 1 mL fractions. Ssfrs 5-16 were combined (597.5 mg), applied over a column chromatography of silica gel (15 g) and eluted with a mixture of petrol-$CHCl_3$ and $CHCl_3$-Me_2CO, wherein 100 mL fractions were collected as follows: frs 1-8 (petrol-$CHCl_3$, 1:9), 9-28 ($CHCl_3$-Me_2CO, 9:1), 29-41 ($CHCl_3$:Me_2CO, 7:3). Frs 17-18 were

combined (47.4 mg) and purified by TLC (silica gel G254, $CHCl_3$: Me_2CO: HCO_2H, 3: 2: 0.01) to give 20.8 mg of quadricinctafuran B (**389**).

5.4) Physical Characteristics and Spectroscopic Data

6-Bromo-1*H*-indole-3-carbaldehyde (**40**): White crystal; mp 205-206 °C; ^1H and ^{13}C NMR see Table 4; HRESIMS *m/z* 223.9704 $[M+H]^+$ (calculated for C_9H_7NOBr, 223.9711).

Methyl (2*E*)-3-(6-bromo-1*H*-indol-3-yl) prop-2-enoate (**370**): White crystal; mp 212-214 °C; ^1H and ^{13}C NMR see Table 5; HRESIMS *m/z* 279.9984 $[M+H]^+$ (calculated for $C_{12}H_{11}NO_2Br$, 279.9973).

***p*-Hydroxybenzaldehyde (371)**: White solid; mp 117-118 °C; ^1H and ^{13}C NMR see Table 6.

6,8-Dihydroxy-3-methylisocoumarin (372): Yellow solid; mp 252-253 °C; ^1H and ^{13}C NMR see Table 7.

Similanpyrone B (373): White crystals, mp 162-163 °C (petrol/$CHCl_3$); UV ($CHCl_3$); λ_{max} (log ϵ) 240 (4.35), 277 (3.51), 330 (3.46) nm; IR (KBr) υ_{max} 3243, 3160, 2923, 2851, 1677, 1634, 1617, 1585, 1571, 1455, 1256, 1154, 1110 cm^{-1}; ^1H and ^{13}C NMR see Table 8; HRESIMS *m/z* 207.0658 $[M+H]^+$ (calculated for $C_{11}H_{11}O_4$, 207.0657).

Reticulol (374): White solid; mp 172-175 °C; ^1H and ^{13}C NMR see Table 9; HRESIMS *m/z* 223.0618 $[M+H]^+$ (calculated for $C_{11}H_{10}O_5$, 223.0606).

Similanpyrone A (375): White solid, mp 322-323 °C (petrol/$CHCl_3$); UV ($CHCl_3$); λ_{max} (log ϵ) 240 (4.31), 269 (4.31), 295 (3.95), 333 (4.23), 358 (4.16) nm; IR (KBr) υ_{max} 3446, 3010, 2923, 2851, 1748, 1698, 1658, 1634, 1464, 1177, 1151 cm^{-1}; ^1H and ^{13}C NMR see Table 10; HRESIMS *m/z* 245.0455 $[M+H]^+$ (calculated for $C_{13}H_9O_5$, 245.0450).

Similanpyrone C (376): Pale yellow viscous mass; $[\alpha]_D^{20}$ = -80.0 (*c* 0.01, $CHCl_3$); UV ($CHCl_3$); λ_{max} (log ϵ) 239 (4.57), 245 (4.59), 332 (2.10) nm; IR (KBr) υ_{max} 3443, 2923, 2852, 1730, 1683, 1647, 1625, 1572, 1508, 1457, 1429, 1352, 1251 cm^{-1}; ^1H and ^{13}C NMR see Table 11; HRESIMS *m/z* 345.1342 $[M+H]^+$ (calculated for $C_{19}H_{21}O_6$, 345.1338).

Chevalone C (349): White solid; mp 201-202 °C; ^1H and ^{13}C NMR see Table 12**.**

Chevalone E (356): White crystals; mp 262-263 °C (petrol/$CHCl_3$); $[\alpha]_D^{20}$ = –146.3° (*c* 0.04, $CHCl_3$); IR (KBr) υ_{max} 3300, 3016, 2979, 2950, 2871, 1664, 1607, 1570, 1444, 1288 cm^{-1}; ^1H and ^{13}C NMR see Table 13; HRESIMS *m/z* 415.2851 $[M+H]^+$ (calculated for $C_{26}H_{39}O_4$, 415.2848).

Chevalone B (348): White crystals; mp 161-163 °C; ^1H and ^{13}C NMR see Table 14.

S14-95 (377): Pale yellow viscous mass; ^1H and ^{13}C NMR see Table 15; HRESIMS *m/z* 451.2488 $[M+H]^+$ (calculated for $C_{28}H_{34}O_5$, 451.2484).

Pyripyropene E (154): White solid; mp 240-244 °C; ^1H and ^{13}C NMR see Table 16.

Pyripyropene S (378): Yellow viscous liquid, $[\alpha]_D^{20}$ = +116.3 (*c* 0.04, $CHCl_3$); IR (KBr) υ_{max} 2923, 2851, 1742, 1671, 1624, 1586, 1508, 1465, 1374, 1242, 1043 cm^{-1}; ^1H and ^{13}C NMR see Table 17; HRESIMS *m/z* 566.2415 $[M+H]^+$ (calculated for $C_{31}H_{36}NO_9$, 566.2390).

Pyripyropene T (379): Pale yellow viscous mass; $[\alpha]_D^{20}$ = +106.0 (*c* 0.03, $CHCl_3$); IR (KBr) υ_{max} 3418, 2949, 1732, 1667, 1643, 1557, 1507, 1480, 1246, 1028 cm^{-1}; ^1H and ^{13}C NMR see Table 18; HRESIMS *m/z* 524.2287 $[M+H]^+$ (calculated for $C_{29}H_{34}NO_8$, 524.2284).

Similanamide (380): Pale yellow viscous mass; $[\alpha]_D^{20}$ = +30.3 (*c* 0.03, $CHCl_3$); IR (KBr) υ_{max} 3335, 3054, 2958, 2870, 1682, 1644, 1594, 1519, 1449, 1292 cm^{-1}; ^1H and ^{13}C NMR see Table 19; HRESIMS *m/z* 641.4053 $[M+H]^+$ (calculated for $C_{34}H_{53}N_6O_6$, 641.4027).

Quadricinctone A (381): White crystals; mp 176-177 °C (petrol/$CHCl_3$); $[\alpha]_D^{20}$ -59° (*c* 0.05, $CHCl_3$); UV (MeOH); λ_{max} (log ϵ) 233 (4.39), 260 (4.03), 298 (3.78) nm; IR (KBr) υ_{max} 3455, 2981, 2490, 1723, 1612, 1596, 1499, 1467, 1432, 1228 cm^{-1}; ^1H and ^{13}C NMR, see Table 21; HRESIMS *m/z* 267.1243 $[M+H]^+$ (calculated for $C_{14}H_{19}O_5$, 267.1332).

Quadricinctapyran A (382): White crystals; mp 147-148 °C ($CHCl_3$/ Me_2CO); $[\alpha]_D^{20}$ +30° (*c* 0.03, MeOH); UV (MeOH); λ_{max} (log ϵ) 237 (4.61) nm; IR (KBr) υ_{max} 3447, 2922, 2359, 2341, 1696, 1647, 1609, 1578, 1490, 1430, 1301, 1267 cm^{-1}; ^1H and ^{13}C NMR, see Table 22; HRESIMS *m/z* 221.0820 $[M+H]^+$ (calculated for $C_{12}H_{13}O_4$, 221.0814).

Quadricinctapyran B (383): White solid; mp 118-119 °C (petrol/$CHCl_3$); $[\alpha]_D^{20}$ +58° (*c* 0.07, $CHCl_3$); UV (MeOH); λ_{max} (log ϵ) 201 (4.13), 237 (4.47) nm; IR (KBr) υ_{max} 3441, 2986, 2943, 1745, 1678, 1640, 1607, 1574, 1453, 1419, 1297, 1264, 1228 cm^{-1}; ^1H and ^{13}C NMR, see Table 23; HRESIMS *m/z* 263.0971 $[M+H]^+$ (calculated for $C_{14}H_{15}O_5$, 263.0919).

Quadricinctoxepine (384): White solid; mp 189-191 °C ($CHCl_3Me_2CO$); $[\alpha]_D^{20}$ +21° (*c* 0.07, MeOH); UV (MeOH); λ_{max} (log ϵ) 234 (4.50) nm; IR (KBr) υ_{max} 3404, 2921, 2359, 2341, 1701, 1606, 1574, 1497, 1384, 1297, 1259, 1117 cm^{-1}; ^1H and ^{13}C NMR, see Table 24; HRESIMS *m/z* 221.0819 $[M+H]^+$ (calculated for $C_{12}H_{13}O_4$, 221.0814).

6-Hydroxy-2,2-dimethyl-2,3-dihydro-4*H*-chromen-4-one (385): ^1H and ^{13}C NMR see Table 25.

Quadricinctone B (386): White crystals; mp 227-228 °C ($CHCl_3/Me_2CO$); $[\alpha]_D^{20}$ +30° (*c* 0.03, MeOH); UV (MeOH); λ_{max} (log ϵ) 205 (4.27), 234 (4.22), 358 (3.64) nm; IR (KBr) υ_{max} 3442, 2975, 2922, 1690, 1622, 1484, 1441, 1417, 1326, 1251, 1177 cm^{-1}; ^1H and ^{13}C NMR, see Table 26; HRESIMS *m/z* 255.0694 $[M+H]^+$ (calculated for $C_{12}H_{15}O_4S$, 255.0691).

Quadricinctone C (387): White crystals; mp 223-224 °C ($CHCl_3/Me_2CO$); $[\alpha]_D^{20}$ +64° (*c* 0.06, MeOH); UV (MeOH); λ_{max} (log ϵ) 214 (4.23), 271 (3.96), 312 (3.70) nm; IR (KBr) υ_{max} 3439, 3006, 2976, 2360, 2342, 1660, 1644, 1600, 1494, 1472, 1448, 1385, 1157 cm^{-1}; ^1H and ^{13}C NMR, see Table 27; HRESIMS *m/z* 255.0875 $[M+H]^+$ (calculated for $C_{12}H_{15}O_6$, 255.0869).

Quadricinctafuran A (388): White crystals; mp 149-150 °C ($CHCl_3/Me_2CO$); $[\alpha]_D^{20}$ +74° (*c* 0.03, MeOH); UV (MeOH); λ_{max} (log ϵ) 203 (3.40), 254 (3.49) nm; IR (KBr) υ_{max} 3417, 2920, 1681, 1634, 1491, 1261 cm^{-1}; ^1H and ^{13}C NMR, see Table 28; HRESIMS *m/z* 223.9067 $[M+H]^+$ (calculated for $C_{12}H_{15}O_4$, 223.0970).

Quadricinctafuran B (389): White solid; mp 209-210 °C ($CHCl_3/Me_2CO$); $[\alpha]_D^{20}$ +20° (*c* 0.05, MeOH); UV (MeOH); λ_{max} (log ϵ) 205 (4.27), 211 (4.03) nm; IR (KBr) υ_{max} 3328, 2984, 2941, 1673, 1610, 1599, 1495, 1362, 1290, 1247 cm^{-1}; ^1H and ^{13}C NMR, see Table 29; HRESIMS *m/z* 239.0919 $[M+H]^+$ (calculated for $C_{12}H_{15}O_5$, 239.0919).

Quadricinctone D (390): White crystals; mp 196-197 °C ($CHCl_3/Me_2CO$); $[\alpha]_D^{20}$ +19° (*c* 0.05, MeOH); UV (MeOH); λ_{max} (log ϵ) 232 (4.21), 254 (3.84) nm; IR (KBr) υ_{max} 3404, 2934, 2360, 2341, 1708, 1670, 1614, 1492, 1466, 1250 cm^{-1}; ^1H and ^{13}C NMR, see Table 30; HRESIMS *m/z* 237.0792 $[M+H]^+$ (calculated for $C_{12}H_{15}O_5$, 237.0763).

5.5) X-Ray Crystallographic Analysis

5.5.1) X-Ray Crystal Structure of Chevalone E (356)

The crystals suitable for X-ray diffraction were obtained by slow evaporation of a solution in petrol/$CHCl_3$. They were orthorhombic, space group $P2_12_12_1$, cell volume 2310.9(1) $Å^3$ and unit cell dimensions *a* = 8.2325(2) Å, *b* = 11.3341(3) Å, and *c* = 24.7665(6) Å. Diffraction data were collected at 293 K with a Gemini PX Ultra equipped with CuK_α radiation (λ = 1.54181 Å). The structures were solved by direct methods using SHELXS-97 and refined with SHELXL-97 (Sheldrick, 2008). Carbon, oxygen, and nitrogen atoms using refined anisotropically. Hydrogen atoms were refined freely with isotropic displacement parameters. The refinement converged to *R* (all data) = 6.38% and wR_2 (all data) = 10.21%. Towards the end of refinement of the absolute structure parameter *x* (Flack *x* parameter) was refined at the same time as all other parameters, using the TWIN instruction with the default matrix R = (-1 0 0, 0 -1 0, 0 0 -1) and BASF with one parameter (*x*), to reach the final value of *x* = 0.0 (3). The inverted structure, obtained with the instruction MOVE 1 1 1 -1, yielded *x* = 1.5 (3). Tables containing the final fractional coordinates, temperature parameters, bond distances, and bond angles were deposited with the Cambridge Crystallographic Data Centre: CCDC reference number 1002416.

5.5.2) X-Ray Crystal Structure of Quadricinctone A (381), Quadricinctapyran A (382), Quadricinctone B (386), Quadricinctone C (387), Quadricinctafuran A (388), and Quadricinctone D (390)

Diffraction data were collected at 293 K with a Gemini PX Ultra equipped with CuK_α radiation (λ = 1.54184 Å). The structures were solved by direct methods using SHELXS-97 and refined with SHELXL-97 (Sheldrick, 2008). Carbon, oxygen and Sulphur atoms were refined anisotropically. Hydrogen atoms were either placed at their idealized positions using appropriate HFIX instructions in SHELXL and included in

subsequent refinement cycles or were directly found from difference Fourier maps and were refined freely with isotropic displacement parameters. Full details of the data collection and refinement and tables of atomic coordinates, bond lengths and angles and torsion angles have been deposited with the Cambridge Crystallographic Data Centre.

Quadricinctone A (381): Crystals were triclinic, space group P1, cell volume 663.27(7) Å^3 and unit cell dimensions *a* = 7.3973(5) Å, *b* = 8.4830(6) Å and *c* = 11.2438(6) Å and angles *α* = 107.541(5)°, *β* = 92.005(5)° and *γ* = 98.365(6)° (uncertainties in parentheses). The refinement converged to *R* (all data) = 3.68% and *w*R$_2$ (all data) = 9.54%. The absolute structure was established with confidence (flack *x* parameter 0.028(18)). CCDC 1465376.

Quadricinctapyran A (382): Crystals were orthorhombic, space group P*bcn*, cell volumn 2189.45(9) Å^3 and unit cell dimension *a* = 21.3981(5) Å, *b* = 14.5017(3) Å and *c* = 7.05561(18) Å. The refinement converged to *R* (all data) = 15.06% and *w*R$_2$ (all data) = 40.39%. CCDC 1468869.

Quadricinctone B (386): Crystals were orthorhombic, space group I*bα2*, cell volume 2469.66(11) Å^3 and unit cell dimension *a* = 8.52510(19) Å, *b* = 30.2340(7) Å and *c* = 9.5817(3) Å. The refinement converged to *R* (all data) = 5.90% and *w*R$_2$ (all data) = 15.62%. The absolute structure was established with confidence (flack *x* parameter -0.04(4)). CCDC 1468868.

Quadricinctone C (387): Crystals were monoclinic, space group P2_1, cell volume 1116.25(5) Å^3 and unit cell dimension *a* = 12.1131(3) Å, *b* = 7.0501(2) Å and *c* = 13.2091(3) Å and *β* = 98.291(2)°. The refinement converged to *R* (all data) = 6.85% and *w*R$_2$ (all data) = 17.04%. CCDC 1468170.

Quadricinctafuran A (388): Crystals were monoclinic, space group P$2_1/n$, cell volume 1066.67(10) Å^3 and unit cell dimension a = 11.6064(7) Å, b = 5.9593(2) Å and c = 15.8588(8) Å and β = 103.481(6)°. The refinement converged to R (all data) = 11.08% and wR_2 (all data) = 24.01%. CCDC 1468171.

Quadricinctone D (390): Crystals were orthorhombic, space group P$ca2_1$, cell volume 1081.35(13) Å^3 and unit cell dimension a = 19.5607(13) Å, b = 7.4646(5) Å and c = 7.4058(5) Å. The refinement converged to R (all data) = 3.81% and wR_2 (all data) = 8.57%. CCDC 1468166.

5.6) Molecular Mechanics Conformation Analysis of Quadricinctoxepine (383) and Quadricinctone D (390)

Molecular simulations for structures **383** and **390** were carried out in ChemBio3D Ultra 14 (Perkin-Elmer). Molecular mechanics energy minimizations used the MM2 and MMFF force fields with the ChemBio3D most recent default parameters and implementation, adequate for small to medium carbon-based models. Ab initio MP2/6-311G and semi-empirical PM3 molecular modelling was done using CS GAMESS interfaced by ChemBio3D. The conformational search was done by stochastic, dihedral driver and molecular dynamics methods. Around 60 conformations were stochastically created and then minimized using the PM3, MMFF and PM3 methods. The resulting models were then grouped under the resultant two seven-membered ring conformations (exemplified in Figure 61 for **384**). A minimal energy for each model set was found by driving by 360° the dihedral angles of the single bonds that attach substituent groups to the rings. Molecular dynamics runs were also applied to the models to confirm the convergence to a minimal energy conformation for each model set.

5.7) Biological Activity Assays

5.7.1) Cytotoxicity Bioassay

5.7.1.1) Samples

Stock solutions of the compounds were prepared in DMSO and kept at -20 °C. Appropriate dilutions of the compounds were freshly prepared just before the assays.

5.7.1.2) Cell cultures

Three human tumor cell lines were used in this study, including MCF-7 (breast adenocarcinoma, NCI, Bethesda, USA), NCI-H460 (non-small cell lung cancer, NSCLC, NCI, Bethesda, USA), and A375-C5 (melanoma, ECACC, UK). Cells were cultured in RPMI-1640 with Ultraglutamine (Lonza) supplemented with 10% FBS (PAA) and maintained in a humidified incubator at 37 °C with 5% CO_2. Cell number and viability were determined with Trypan Blue exclusion assay. All experiments were performed with cells in exponential growth with viabilities over 90% and repeated at least three times.

5.7.1.3) Cell growth inhibitory assay

The screening of fungal metabolites was performed with the Sulforhodamine B (SRB) assay adopted from the National Cancer Institute, USA (Cidade *et al*., 2001). Briefly, 5×10^3 cells of MCF-7 and NCI-H460 cell lines, and 7.5×10^3 cells of the A375-C5 cell line were placed in 96 wells plate and incubated at 37 °C for 24 h. The growing cells were treated with five dilutions of each compound. After 48 h of treatment, cells were fixed with 10% ice-cold trichloroacetic acid, then washed and stained with SRB. After washing with 1% acetic acid, the bound SRB was solubilized with 10 mM Tris Base, and the absorbance was measured at 515 nm in a microplate reader (Biotek Instruments). A dose-response curve was obtained for each compound and the corresponding GI_{50} (the concentration of compound that inhibited 50% of net cell growth) was determined. The effect of the vehicle solvent (DMSO) on the growth of

these cell lines was evaluated by treating cells with the maximum concentration of DMSO used in each assay (0.25%).

5.7.2) Antimicrobial Activity Assays

5.7.2.1) Bacterial and Fungal Strains

For the antimicrobial assays, the compounds were tested against the reference strains, including four strains of bacteria (*Staphylococcus aureus* ATCC 25923, *Bacillus subtilis* ATCC 6633, *Escherichia coli* ATCC 25922, and *Pseudomonas aeruginosa* ATCC 27853), three strains of fungi (yeast; *Candida albicans* ATCC 10231, filamentous fungus; *Aspergillus fumigatus* ATCC 46645, and dermatophyte; *Trichophyton rubrum* FF5), and three strains of multidrug-resistant bacteria isolated from the environment (*S. aureus* B1 isolated from public bus, *Enterococcus faecalis* W1 isolated from river water, and *E. coli* G1 isolated from seagull feces). Bacterial isolates were grown in Mueller-Hinton agar (MH-BioKar diagnostics, Allonne, France) from stock cultures, while *C. albicans* was grown in Sabouraud dextrose agar (SAB-BioDar diagnostics, Allonne, France). MH and SAB plates were incubated at 37 °C prior to obtain fresh cultures for each in vitro bioassay.

5.7.2.2) Determination of Minimum Inhibitory and Bactericidal/Fungal Concentrations

The minimum inhibitory concentrations (MIC) of the compounds were determined using a broth microdilution technique, following the recommendations of the Clinical and Laboratory Standards Institute (Franklin and Cockerill, 2011). Stock solutions of 10 mg/mL, prepared in dimethylsulfoxide (DMSO-Applichem GmbH, Darmstadt, Germany), were serially diluted in Mueller-Hinton broth (MHB-BioKar diagnostics, Allonne, France) to achieve in-test concentrations ranging from 2 to 256 µg/mL. Bacterial inoculums and *C. albicans* inoculum were prepared in MHB and RPMI-1640 with L-glutamine, respectively, with MOPS and without $NaHCO_3$ (Lonza, Walkersville, MD, USA). All inocula were standardized in order to obtain a concentration of 5×10^5 CFU/mL in each inoculated well of the microtiter plate. The

concentration of DMSO in the highest in-test concentration did not affect the microbial growth. The MIC was defined as the lowest concentration of compound that has inhibited the visible growth.

5.7.2.3) Synergistic Studies

5.7.2.3.1) Screening of Combined Effect the Compounds and Antibiotics

A screening susceptibility test to assess the combined effect between the compounds and antibiotics was evaluated using the disc diffusion method on Mueller Hinton (MH) medium. Multidrug-resistant isolates were obtained from overnight cultures in MH, and suspensions were prepared in buffered peptone water (Oxoid, England) by adjusting the turbidity to equal a 0.5 McFarland standard. A set of antibiotic discs (Oxoid, England) was selected based on the resistance of the isolates towards those antibiotics. Antibiotic disc alone (controls) and impregnated with 15 µL of a 1 mg/mL solution (in DMSO) of each metabolite were placed on the agar plate seeded with the respective bacteria. 15 µL of DMSO impregnated in a sterile filter paper disc (6 mm in diameter) (Oxoid, England) was used as the negative control. Inoculated MH plates were incubated overnight at 37 °C. Each compound was tested in duplicate. Potential synergism was recorded when the halo of antibiotic discs impregnated with metabolites was greater than the halo of antibiotic discs or compound-impregnated blank discs alone.

5.7.2.3.2) Synergy Test: Checkerboard Method

Based on the result of the previous assay, potential synergy between chevalone E (**356**) and oxacillin or ampicillin (Sigma-Aldrich, St. Louis, MO, USA) was evaluated using a broth microdilution checkerboard method and tested against MRSA isolate (*S. aureus* B1). Briefly, the stock solutions and serial twofold dilutions of the compound and antibiotic to at least double the MIC were prepared according to the recommendations of CLSI (Franklin and Cockerill, 2011). The metabolite to be tested was serially diluted along the ordinate, while the antibiotic was diluted along the abscissa. A bacterial inoculum equal to a 0.5 McFarland turbidity standard was prepared in MHB. Each microtiter plate well was inoculated with 100 µL of a bacterial

inoculum of 5 × 10^5 CFU/mL, and the plates were inoculated overnight at 37 °C. The fractional inhibitory concentration (FIC) was calculated as follows: FIC of drug A (FIC A) = MIC of drug A in combination/MIC of drug A alone. The FIC index (ΔFIC), calculated as the sum of each FIC, was interpreted as follows: ΔFIC ≥ 0.5, synergy; 0.5 < ΔFIC ≤4, no interaction; ΔFIC > 4, antagonism (Odds, 2003).

5.8) Amino Acids Analysis of Acidic Hydrolysate of Similanamide (380)

5.8.1) Acid Hydrolysis

The stereochemistry of the amino acids was determined by analysis of the acidic hydrolysate from **380**. Five milligrams of **380** was dissolved in 5 mL of 6 N HCl, and heated at 110 °C, in a furnace, for 24 h in a sealed glass tube. After cooling to room temperature, the solution was dried under N_2 for 24 h, reconstituted in methanol for HPLC-MS (200 µL), filtered through a 4 mm PTFE Syringe Filter F2504-4 of 0.2 µm pore size (Thermo Scientific, Mumbai, India), and then analyzed by HPLC equipped with a chiral column.

5.8.2) Chiral HPLC Analysis

The HPLC system consisted of Shimadzu LC-20AD pump, equipped with a Shimadzu DGV-20A5 degasser, a Rheodyne 7725i injector fitted with a 20 µL loop, and an SPD-M20A DAD detector (Kyoto, Japan). Data acquisition was performed using Shimadzu LCMS Lab Solutions software, version 3.50 SP2. The Chiral column used in this study was Chirobiotic T (15 cm × 4.6 mm I.D., particle size 5 µm) manufactured by ASTEC (Whippany, NJ, USA). The mobile phase composition was MeOH: H_2O: CH_3CO_2H, 70: 30: 0.02, v/v/v), all were LC-MS grade solvents obtained from Sigma-Aldrich Co (St. Luis, MO, USA). The flow rate was 0.5 mL/min and the UV detection wavelength was 210 nm. Analyses were performed at room temperature in the isocratic mode.

All standards of racemic amino acids and pure amino acid enantiomers were purchased from Sigma-Aldrich Co (St. Louis, MO, USA). The elution order of the enantiomers of all the standard amino acids was confirmed by injecting the solutions of the racemic or enantiomeric mixtures, and then each enantiomer separately (or only L-amino acid in the case of *N*-methyl leucine) at a flow rate of 1 mL/min or 0.5 mL/min. Working solutions of single enantiomeric amino acids were prepared by dissolution in MeOH at the concentration of 1 mg/mL (10 µL sample injection), while the enantiomeric mixtures were prepared by mixing equal aliquots of each enantiomer (20 µL sample injection). Mix HPLC analyses of the acidic hydrolysate with standard amino acids (co-injection) confirmed the stereochemistry of the amino acid of similanamide (**380**).

CHAPTER VI

CONCLUSIONS

In this study, the marine sponge *Iotrochota baculifera*, collected from the Gulf of Thailand, together with two marine-derived fungi, *Aspergillus similanensis* KUFA 0013, isolated from the marine sponge *Rhabdermia* sp. and *Neosartorya quadricincta* KUFA 0081, isolated from the marine sponge *Clathria reinwardti,* were investigated for their secondary metabolites.

Chemical investigation of the marine sponge *I. baculifera* resulted in isolation of two previously described bromoindoles, 6-bromo-1*H*-indole-3-carbaldehyde (**40**) and methyl (2*E*)-3-(6-bromo-1*H*-indol-3-yl)prop-2-enoate (**370**).

The investigation of the ethyl acetate extract of the culture of the marine sponge-associated fungus *A. similanensis* KUFA 0013 resulted in isolation of three new isocoumarin derivatives: similanpyrones A (**375**), B (**373**) and C (**376**), one new chevalone derivative: chevalone E (**356**), two new pyripyropene derivatives: pyripyropenes S (**378**) and T (**379**), and one new cyclohexapeptide: similanamide (**380**), together with seven previously reported: *p*-hydroxybenzaldehyde (**371**), 6,8-dihydroxy-3-methylisocoumarin (**372**), reticulol (**373**), chevalones B (**348**) and C (**349**), S14-95 (**377**) and pyripyropene E (**154**).

Although several chevalone analogs have been reported from several members of the genera *Aspergillus* and *Neosartorya*, *A. similanensis* KUFA 0013 also produced analogs of chevalone, including chevalone B (**348**), chevalone C (**349**) a new chevalone derivative, chevalone E (**356**). Similanpyrone C (**376**), a new isocoumarin derivative, showed a unique structure, containing an unusual 1,7-dioxaspiro-undecenone moiety. This is the first report of isolation of isocoumarin derivatives from a member of this genus.

Several cyclohexapeptides have been reported from marine-associated microorganisms. However, similanamide is the first cyclohexapeptide which was reported from the marine-associated fungus.

Pyripyropene E (**154)**, chevalone E (**356)**, 6,8-dihydroxy-3-methylisocoumarin (**372**), similanpyrone B (**373**), reticulol (**374**), similanpyrone A (**375**), S14-95 (**377**), pyripyropenes S (**378**) and T (**379**), and similanamide (**380)** were evaluated for their antibacterial activity against Gram-positive (*Staphylococcus aureus* ATCC 25923 and

Bacillus subtilis ATCC 6633) and Gram-negative (*Escherichia coli* ATCC 25922 and *Pseudomonas aeruginosa* ATCC 27853) bacteria, as well as multidrug-resistant isolates from the environment (*S. aureus* B1, *Enterococcus faecalis* W1 and *E. coli* G1). None of the tested compounds exhibited antibacterial activity at the highest concentration tested (256 µg/mL).

Furthermore, pyripyropene E (**154)**, chevalone E (**356)**, 6,8-dihydroxy-3-methylisocoumarin (**372**), similanpyrone B (**373**), reticulol (**374**), similanpyrone A (**375**), S14-95 (**377**) and pyripyropene S (**378**) were further evaluated for synergistic effect with the antibiotics (ciprofloxacin, ampicillin, cefotaxime, streptomycin, oxacillin, vancomycin and erythromycin) against three multidrug-resistant isolates from the environment, using a disc diffusion method. However, none of the tested compounds exhibited any synergistic effects for multidrug-resistant *E. faecalis* and *E. coli*, except for chevalone E (**356**) which demonstrated potential synergistic effect with oxacillin against the MRSA strain. There for, this compound can be considered relevant for anti-infective marine natural products research.

Pyripyropene E (**154)**, chevalone E (**356)**, 6,8-dihydroxy-3-methylisocoumarin (**372**), similanpyrone B (**373**), reticulol (**374**), similanpyrone A (**375**), S14-95 (**377**) and pyripyropene S (**378**) were tested for their antifungal activity against *Candida albicans* ATCC 10231, and all of them were inactive at the highest concentration tested (256 µg/mL).

Moreover, pyripyropene T (**379**) and similanamide (**380**) were evaluated for their cytotoxicity against three human cell lines, including MCF-7 (breast adenocarcinoma), NCI-H460 (non-small cell lung cancer) and A373 (melanoma). Only similanamide (**380)** showed weak *in vitro* growth inhibitory activity against the three cell lines with GI_{50} values of 125 ± 0, 117.50 ± 3.55 and 115 ± 7.07 mM, respectively.

The investigation of the ethyl acetate extract of the culture of the marine sponge-derived fungus *Neosartorya quadricincta* KUFA 0081 resulted in isolation of two new pentaketides: a new benzofuran-1-one derivative, quadricinctone A (**381**), and a new isochromen-1-one derivative, quadricinctone C (**387**), together with seven new benzoic acid derivatives: two new benzopyran derivatives, quadricinctapyrans A (**382**) and B (**383**), a new benzoxepine derivative, quadricinctoxepine (**384**), two new chromen-4-

one derivatives, quadrincinctones B (**386**) and D (**390**), and two new benzofuran derivatives, quadricinctafurans A (**388**) and B (**389**), as well as the previously reported compound, 6-hydroxy,2,2-dimethyl-2,3-dihydro-4*H*-chromen-4-one (**385**).

An isocoumarin derivative, PF1223, was first reported by Ozoe *et al*. (2004), using a GABA receptor ligand as a screening target, from the culture of the fungus *N. quadricincta* PF1223, but the source of the fungus was not revealed. Thus, this is the first report of the secondary metabolites from the culture of a marine-derived *N. quadricincta* (KUFA 0081).

The unique, but related, structures of the isolated metabolites from the fungus *N. quadricincta* KUFA 0081 has allowed us to propose the biosynthetic pathway of these metabolites. Interestingly, the structure of quadricinctone B (**386**), which possesses a methyl sulfinyl group in the benzopyran nucleus, revealed the capacity of this marine-derived fungus to introduce sulphur in to the aromatic ring. Thus, this fungus can have potential for biotechnological transformation.

Quadricinctone A (**381**), quadricinctapyrans A (**382**) and B (**383**), quadricinctoxepine (**384**), 6-hydroxy,2,2-dimethyl-2,3-dihydro-4*H*-chromen-4-one (**385**), quadrincinctones B (**386**) and D (**390**), quadricinctone C (**387**), and quadricinctafurans A (**388**) and B (**389**) were tested for their antimicrobial activity against Gram positive (*S. aureus* and *B. subtilis*) and Gram negative (*E. coli* and *P. aeruginosa*) bacteria, the multidrug-resistant isolates from the environment (*S. aureus* B1, *E. faecalis* W1 and *E. coli* G1), yeast (*C. albicans*), filamentous fungus (*A. fumigatus* ATCC 46645) and dermatophyte (*T. rubrum* FF5). The tested compounds did not show any antimicrobial activity at the highest concentration tested (256 µg/mL for antibacterial assay and 512 µg/mL for antifungal assay).

The isolated metabolites were also evaluated for their *in vitro* growth inhibitory activity against MCF-7, NCI-H460 and A375-C5 cell lines by the protein binding dye SRB method, however, all of them were inactive against the cell lines tested (GI_{50} > 150 mM).

Even though, all the tested compounds, except for chevalone E (**356**) and similanamide (**380**), exhibited neither antimicrobial activity nor growth inhibitory activity against three human cancer cell lines in our assay protocols, it does not mean that

they are devoid of other interesting biological activities. In order to prove this hypothesis, it is necessary to investigate their potential in other target-based assay protocols.

REFERENCES

Agrawal, S., Adholeya, A., Deshmukh, S. K. (2016). The Pharmacological potential of non-ribosomal peptides from marine sponge and tunicates. *Front. Pharmacol., 7,* 333.

Alonso-Álvarez, S., Pardal, E., Sánchez-Nieto, D., Navarro, M., Caballero, M. D., Mateos, M. V., Martín, A. (2017). Plitidepsin: design, development, and potential place in therapy. *Drug Des. Devel. Ther., 11,* 253 – 264.

Arriaga-Giner, F. J., Wollenweber, E., Schober, I., Yatskievych, G. (1988). Three new benzoic acid derivatives from the glandular excretion of *Eriodictyon sessilifolium* (Hydrophyllaceae). *Z. Naturforsch., 43,* 337 – 340.

Arunrattiyakorn, P., Suksamrarn, S., Suwannasai, N., Kanzaki, H. (2011). Microbial metabolism of α-mangostin isolated from *Garcinia mangostana* L. *Phytochemistry, 72,* 730 – 734.

Asami, Y., Kakeya, H., Komi, Y., Kojima, S., Nishikawa, K., Beebe, K., Neckers, L., Osada, H. (2008). Azaspirene, a fungal product, inhibits angiogenesis by blocking Raf-1 activation. *Cancer Sci., 99,* 1853 – 1858.

Asami, Y., Kakeya, H., Onese, R., Yoshida, A., Matsuzaki, H., Osada, H. (2002). Azaspirene: a novel angiogenesis inhibitor containing a 1-oxa-7-azaspiro[4.4]non-2-ene-4,6-dione skeleton produced by the fungus *Neosartorya* sp. *Org. Lett., 4,* 2845 – 2848.

Asami, Y., Kakeya, H., Onose, R., Chang, Y. H., Toi, M., Osada, H. (2004). RK-805, and endothelial-cell-growth inhibitor produced by *Neosartorya* sp., and a docking model with methionine aminopeptidase-2. *Tetrahedron, 60,* 7085 – 7091.

Ben Ameur Mehdi, R., Sioud, S., Fourati Ben Fguira, L., Bejar, S., Mellouli, L. (2006). Purification and structure determination of four bioactive molecules from a newly isolated *Streptomyces* sp. TN97 strain. *Process Biochem., 41,* 1506 – 1513.

Bessa, L. J., Buttachon, S., Dethoup, T., Martins, R., Vasconcelos, V., Kijjoa, A., Martins da Dosta, P. (2016). Neofiscalin A and fiscalin C are potential novel indole alkaloid alternatives for the treatment off multidrug-resistant Gram-positive bacterial infections. *FEMS Microbiol. Lett., 363,* pii: fnw150.

Bisogno, F., Mascoti, L., Sanchez, C., Garibotto, F., Giannini, F., Kurina-Sanz, M., Enriz, R. (2007). Structure – antifungal activity relationship of cinnamic acid derivatives. *J. Agric. Food Chem., 55,* 10635 – 10640.

Buttachon, S., Chandrapatya, A., Manoch, L., Silva, A., Gales, L., Bruyère, C., Kiss, R., Kijjoa, A. (2012). Sartorymensi, a new indole alkaloid, and new analogues of tryptoquivaline and fiscalins produced by *Neosartorya siamensis* (KUFC 6349). *Tetrahedron, 68,* 3253 – 3262.

Cai, G., Napolitano, J. G., McAlpine, J. B., Wang, Y., Jaki, B. U., Suh, J. W., Yang, S. H. Lee, I. A., Franzblau, S. G., Pauli, G. F., Cho, S. (2013). Hytramycins V and I, anti-*Mycobacterium tuberculosis* hexapeptides from a *Streptomyces hydroscopicus* strain. *J. Nat. Prod., 76,* 2009 – 2018.

Carletti, I., Banaigs, B., Amade, P. (2000). Matemone, a new bioactive bromine-containing oxindole alkaloid from the Indian Ocean sponge *Iotrochota purpurea. J. Nat. Prod., 63*(7), 981 – 983.

Carletti, I., Banaigs, B., Amade, P. (2000). Matemone, a new bioactive bromine-containing oxindole alkaloid from the Indian Ocean sponge *Iotrochota purpurea. J. Nat. Prod., 63,* 981 – 983.

Chen, B. Y., Wang, Z., Ying, Y. M., Jiang, L. X., Zhan, Z. J., Wang, J. L., Zhang, W. (2014). Neofipiperzine D, a new prenylated indole alkaloid metabolite of the fungus *Neosartorya fischeri. J. Chem. Res., 38,* 539 – 541.

Cidade, H. M., Nascimento., M. S., Pinto, M. M., Kijjoa, A., Silva, A. M., Herz, W. (2001). Artelastocarpin and carpelastofuran, two new flavones, and cytotoxicities of prenyl flavonoids from *Artocarpus elasticus* against three canceer cell lines. *Planta Med., 67*, 867-870.

Costantino, V., Dell'Aversano, C., Fattorusso, E., Mangoni, A. (2000). Ecdysteroids from the Caribbean sponge *Iotrochota birotulata. Steroids, 65,* 138 – 142.

Cytarabine. *National Cancer Institute.* Retrieved from https://www.cancer.gov/a-cancer/treatment/drugs/cytarabine.

David, B., Wolfender, J. L., Dias, D. A. (2015). The pharmaceutical industry and natural products: historical status and new trends. *Phytochem. Rev., 14,* 299 – 315.

Dellar, G., Djura, P., Sargent, M. V. (1981). Structure and synthesis of a new bromoindole from a marine sponge. *J. Chem. Soc., Perkin 1, 0,* 1679 – 1680.

Dethoup, T., Gomes, N. G., Chaopongpang, S., Kijjoa, A. (2016). *Aspergillus similanensis* sp. nov. from a marine sponge in Thailand. *Mycotaxon, 131,* 7 – 15.

Du, L., Zhu, T., Fang, Y., Liu, H., Gu, Q., Zhu, W. (2007). Aspergiolide A, a novel anthraquinone derivative with naphtho[1,2,3-*de*]chromene-2,7-dione skeleton isolated from a marine-derived fungus *Aspergillus glaucus. Tetrahedron, 63,* 1085 – 1088.

Du, L., Zhu, T., Liu, H., Fang, Y., Zhu, W., Gu, Q. (2008). Cytotoxic polyketides from a marine-derived fungus *Aspergillus glaucus. J. Nat. Prod., 71,* 1837 – 1842.

Eamvijarn, A., Gomes, N. M., Dethoup, T., Buaruang, J., Manoch, L., Silva, A., Pedro, M., Marini, I., Roussis, V., Kijjoa, A. (2013). Bioactive meroditerpenes and indole alkaloids from the soil fungus *Neosartorya fischeri* (KUFC 6344), and the marine-derived fungi *Neosartorya laciniosa* (KUFC 7896) and *Neosartorya tsunodae* (KUFC 9213). *Tetrahedron, 69,* 8583 – 8591.

Eamvijarn, A., Kijjoa, A., Bruyère, C., Mathieu, V., Manoch, L., Lefranc, F., Silva, A., Kiss, R., Herz, W. (2012). Secondary metabolites from a culture of the fungus *Neosartorya pseudofischeri* and their in vitro cytostatic activity in human cancer cells. *Planta Med., 78,* 1767 – 1776.

El-Desoky, S. I., Badria, F. A., Abozeid, M. A., Kandeel, E. A., Abdel-Rahman, A. H. (2013). Synthesis and antitumor studies of novel benzopyrano-1,2,3-selenadiazole and spiro[benzopyrano]-1,3,4-thiadiazoline derivatives. *Med. Chem. Res., 22,* 2105 – 2114.

Erkel, G., Rether, J., Anke, T. (2003). S14-95, a novel inhibitor of the JAK/STAT pathway from a *Penicillium* species. *J. Antibiot., 56,* 337 – 343.

Fan, G., Li, Z., Shen, S., Zeng, Y., Yang, Y., Xu, M., Bruhn, T., Bruhn, H., Morschhäuser, J., Bringmann, G., & Lin, W. (2010). Baculiferins A – O, *O*-sulfated pyrrole alkaloids with anti-HIV-1 activity, from the Chinese marine sponge *Iotrochota baculifera. Bioorg. Med. Chem., 18,* 5466 – 5474.

FDA Approves Trabectedin for Sarcoma. *National Cancer Institute.* Retrieved from https://www.cancer.gov/news-events/ccancer-currents-blog/2015/fda-trabectedin-sarcoma.

Feng, Y., Davis, R. A., Sykes, M. L., Avery, M. V., Quinn, R. J. (2012). Iotrochamides A and B, antitrypanosomal compounds from the Australian marine sponge *Iotrochota* sp. *Bioorg. Med. Chem. Lett., 22,* 4873 – 4876.

Franklin, R., Cockerill, M.D. (2011). III. Performance standards for antimicrobial susceptibility testing. Twenty-first informational supplement M100-S21. *Clinical and Laboratory Standards Institute (CLSI).*

Fremlin, L. J., Piggott, A. M., Lacey, E., Capon, R. J. (2009). Cottoquinazoline A and Cotteslosins A and B, metabolites from an Australian marine-derived strain of *Aspergillus versicolor. J. Nat. Prod., 72,* 666 – 670.

Furutani, Y., Shimada, M., Hamada, M., Takeuchi, T., Umezawa, H. (1977). Reticulol, an inhibitor of cyclic nucleotide phosphodiesterases. *Agric. Biol. Chem., 41*(6), 989 – 993.

Gallo, M. B., Cavalcanti, B. C., Barros, F. W., Odorico de Moraes, M., Costa-Lotufo, L. V., Pessoa, C., Bastos, J. K., Pupo, M. T. (2010). Chemical constituents of *Papulaspora immersa,* an endophyte from *Smallanthus sonchifolius* (Asteraceae), and their cytotoxic activity. *Chem. Biodivers., 7*(12). 2941 – 2950.

Ge, H. M., Yu, Z. G., Zhang, J., Wu, J. H., Tan, R. X. (2009). Bioactive alkaloids from endophytic *Aspergillus fumigatus. J. Nat. Prod., 72,* 753 – 755.

Gerwick, W. H., Fenner, A. M. (2013). Drug discovery from marine microbes. *Microb. Ecol., 65*(4), 800 – 806.

Glass, N. L. Donaldson, G. C. (1995). Development of primer sets designed for use with the PCR to amplify conserved genes from filamentous ascomycetes. *Appl. Environ. Microbiol., 61,* 1323 – 1330.

Gomes, N. M., Bessa, L. J., Buttachon, S., Costa, P. M., Buaruang, J., Dethoup, T., Silva, A. M., Kijjoa, A. (2014). Antibacterial and antibiofilm activities of tryptoquivalines and meroditerpenes isolated from the marine-derived fungi *Neosartorya paulistensis, N. laciniosa, N. tsunodae,* and the soill fungi *N. fischeri* and *N. siamensis. Mar. Drugs, 12,* 822 – 839.

Hansson, D., Menkis, A., Olson, Å., Stenlid, J., Broberg, A., Karlsson, M. (2012). Biosynthesis of fomannoxin in the root rotting pathogen *Heterobasidion occidentale. Phytochemistry, 84,* 31 – 39.

Hasan, S., Ansari, M. I. Ahmad, A., Mishra, M. (2015). Major bioactive metabolites from marine fungi: a review. *Bioinformation, 11*(4), 176 – 181.

He, C. N., Wang, C. L., Guo, S. X., Yang, J. S., Xiao, P. G. (2005). Study on chemical constituents in herbs of *Anoectochilus roxburhii* II [Abstract]. *Zhongguo Zhong Yao Za Zhi, 30*(10), 761 – 763.

Hiort, J., Maksimenka, L., Reichert, M., Perović-Ottstadt, S., Lin, W. H., Wray, V., Steube, K., Schaumann, K., Weber, H., Proksch, P., Ebel, R., Müller, W. E., Bringmann, G. (2004). New natural products from the sponge-derived fungus *Aspergillus niger. J. Nat. Prod., 67,* 1532 – 1543.

Hu, Y., Chen, J., Hu, G., Yu, J., Zhu, X., Lin, Y., Chen, S., Yuan, J. (2015). Statistical research on the bioactivity of new marine natural products discovered during the 28 years from 1985 to 2012. *Mar. Drugs, 13,* 202 – 221.

Ibrahim, S. R., Mohamed, G. A., Fouad, M. A., El-Khayat, E. S., Proksch, P. (2009). Iotrochotamides I and II: new ceramides from the Indonesian sponge *Iotrochota purpurea. Nat. Prod. Res., 23*(1), 86 – 92.

Ingavat, N., Dobereiner, J., Wiyakrutta, S., Mahidol, C., Ruchirawat, S., Kittakoop, P. (2009). Aspergillusol A, an α-glucosidase inhibitor from the marine-derived fungus *Aspergillus aculeatus. J. Nat. Prod., 72,* 2049 – 2052.

Ingavat, N., Mahidol, C., Ruchirawat, S., Kittakoop, P. (2011). Asperaculin A, a sesquiterpenoid from a marine-derived fungus, *Aspergillus aculeatus. J. Nat. Prod., 74,* 1650 – 1652.

Jang, H., Lee, J. W., Lee, C., Jin, Q., Choi, J. Y., Lee, D., Han, S. B., Kim, Y., Hong, J. T., Lee, M. K., Hwang, B. Y. (2016). Sesquiterpenoids from *Tussilago farfara* inhibit LPS-induced nitric oxide production in macrophage RAW 264.7 cells. *Arch. Pharm. Res., 39,* 127 – 132.

Jaspars, M., de Pascale, D., Andersen, J. H., Reyes, F., Crawford, A. D., Ianora, A. (2016). The marine biodiscovery pipeline and ocean medicines of tomorrow. *J. Mar. Biol. Assoc. U. K., 96*(1), 151 – 158.

Jayasuriya, H., Zink, D., Basilio, A., Vicente, FF., Collado, J., Bills, G., Goldman, M. L., Motyl, M., Huber, J., Dezeny, G., Byrne, K., Singh, S. B. (2009). Discovery and antibacterial activity of glabramycin A – C from *Neosartorya glabra* by an antisense strategy*. J. Antibiot., 62,* 265 – 269.

Kai, K., Yoshikawa, H., Kuo, Y. H., Akiyama, K., Hideo, H. (2010). Determination of absolute structures of cyclic peptides, PF1171A and PF1171C, from unidentified *Ascomycete* OK-128. *Biosci. Biotechnol. Biochem., 74,* 1309 – 1311.

Kaifuchi, S., Mori, M., Nonaka, K., Masuma, R., Ōmura, S., Shiomi, K. (2015). Sartorypyrone D: a new NADH-fumarate reductase inhibitor produced by *Neosartorya fischeri* FO-5897. *J. Antibiot., 68,* 403 – 405.

Kale, A. J., McGlinchey, R. P., Lechner, A., Moore, B. S. (2011). Bacterial self-resistance to the natural proteasome inhibitor salinosporamide A. *ACS Chem. Biol., 6,* 1257 – 1264.

Kanokmedhakul, L., Kanokmedhakul, S., Suwannatrai, R., Soytong, K., Prabpai, S., Kongsaeree, P. (2011). Bioactive meroterpenoids and alkaloids from the fungus *Eurotium chevalieri. Tetrahedron, 67,* 5461 – 5468.

Kem, W., Soti, F., Wildeboer, K., LeFrancois, S., MacDougall, K., Wei, D. Q., Chou, K. C., Arias, H. R. (2006). The nemertine toxin anabaseine and its derivative DMXBA (GTS-21): chemical and pharmacological properties. *Mar. Drugs, 4,* 255 – 273.

Kijjoa, A., Santos, S., Dethoup, T., Manoch, L., Almeida, A. P. Vasconcelos, M. H., Silva, A., Gales, L., Herz, W. (2011). Sartoryglabrins, analogs, of ardeemins, from *Neosartorya glabra. Nat. Prod. Commun., 6,* 807 – 812.

Kito, K., Ookura, R., Yoshida, S., Namikoshi, M., Ooi, T., Kusumi, T. (2007). Pentaketides relating to aspinonene and dihydroaspyrone from a marine-derived fungus, *Aspergillus ostianus. J. Nat. Prod., 70,* 2022 – 2025.

Kornsakulkarn, J., Thongpanchang, C., Lapanun, S., Srichomthong, K. (2009). Isocoumarin glucosides from the scale insect fungus *Torrubiella tenuis* BCC 12732. *J. Nat. Prod., 72,* 1341 – 1343.

Kovács, L., Virágh, M., Takó, M., Papp, T., Vágvölgyi, C., Galgóczy, L. (2011). Isolation and characterization of *Neosartorya fischeri* antifungal protein (NFAP). *Peptides, 32,* 1724 – 1731.

Lago, J., Rodríguez, L. P., Blanco, L., Vieites, J. M., Cabado, A. G. (2015). Tetrodotoxin, an extremely potent marine neurotoxin: distribution, toxicity, origin and therapeutical uses. *Mar. Drugs, 13,* 6384 – 6406.

Lan, W. J., Fu, S. J., Xu, M. Y., Liang, W. L., Lam, C. K., Zhong, G. H., Xu, J., Yang, D. P., Li, H. J. (2016). Five new cytotoxic metabolites from the marine fungus *Neosartorya pseudofischeri. Mar. Drugs, 14,* 18 – 30.

Laport, M. S., Santos, O. C., Muricy, G. (2009). Marine sponges: potential sources of new antimicrobial drugs. *Curr. Pharm. Biotechnol., 10,* 86 – 105.

Li, H. Y., Matsunaga, S., Fusetani, N. (1994). Simple antifungal metabolites from a marine sponge, *Halichondria* sp. *Comp. Biochem. Physiol. B Biochem. Mol. Biol.., 107,* 261 – 264.

Li, W., Xiong, P., Zheng, W., Zhu, X., She, Z., Ding, W., Li, C. (2017). Identification and antifungal activity of compounds from the mangrove endophytic fungus *Aspergillus clavatus* R7. *Mar. Drugs, 15,* 259 – 268.

Liang, W. L., Le, X., Li, H. J., Yang, X. L., Chen, J. X., Xu, J., Liu, H. L., Wang, L. Y., Wang, K. T., Hu, K. C., Yang, D. P. Lan, W. J. (2014). Exploring the chemodiversity and biological activities of the secondary metabolites from the marine fungus *Neosartorya pseudofischeri. Mar. Drugs, 12,* 5657 – 5676.

Lim, D. S., Kwak, Y. S., Kim, J. H., Ko, S. H., Yoon, W. H., Kim, C. H. (2003). Antitumor efficacy of reticulol from *Streptoverticullium* against the lung metastasis model B16F10 melanoma. Lung metastasis inhibition by growth inhibition of melanoma. *Chemotherapy, 49*(3), 146 – 153.

Lim, D. S., Kwak, Y. S., Lee, K. H., Ko, S. H., Yoon, W. H., Lee, W. Y., Kim, C. H. (2003). Topoisomerase I inactivation by reticulol and its in vivo cytotoxicity against B16F10 melanoma. *Chemotherapy, 49*(5), 257 – 263.

Lin, W. Y., Teng, C. M., Tsai, I. L., Chen, I. S. (2000). Anti-platelet aggregation constituents from *Gynura elliptica. Phytochemistry, 53,* 833 – 836.

Liu, C. H., Meng, J. C., Zou, W. X., Huang, L. L., Tang, H. Q., Tan, R. X. (2002). Antifungal metabolite with a new carbon skeleton from *Keissleriella* sp. YS41088, a marine filamentous fungus. *Planta Med., 68*(4), 363 – 365.

Liu, D., Li, X. M., Meng, L., Li, C. S., Gao, S. S., Shang, Z., Proksch, P., Huang, C. G., Wang, B. G. (2011). Nigerapyrones A – H, α-pyrone derivatives from the marine mangrove-derived endophytic fungus *Aspergillus niger* MA-132. *J. Nat. Prod., 74,* 1787 – 1791.

Liu, H., Edrada-Ebel, R., Ebel, R., Wang, Y., Schulz, B., Draeger, S., Müller, W. E., Wray, V., Lin, W., Proksch, P. (2009). Drimane sesquiterpenoids, from the fungus *Aspergillus ustus* isolated from the marine sponge *Suberites domuncula. J. Nat. Prod., 72,* 1585 – 1588.

Liu, W. H., Zhao, H., Li, R. Q., Zheng, H. B., Yu, Q. (2015). Polyketides and meroterpenoids from *Neosartorya glabra. Helv. Chim. Acta, 98,* 515 – 519.

Liu, Z., Chen, Y., Chen, S., Liu, Y., Lu, Y., Chen, D., Lin, Y., Huang, X., She, Z. (2016). Aspterpeacids A and B, two sesterterpenoids from a mangrove endophytic fungus *Aspegillus terreus* H010. *Org. Lett., 18,* 1406 – 1409.

Longeon, A., Copp, B. R., Quévrain, E., Roué, M., Kientz, B., Cresteil, T., Petek, S., Debitus, C., Bourguet-Kondracki, M. L. (2011). Bioactive indole derivatives from the South Pacific marine sponges *Rhopaloeides odorabile* and *Hyrtios* sp. *Mar. Drugs, 9,* 879 – 888.

López-Gresa, M. P., Cabedo, N., González-Mas, M. C., Ciavatta, M. L., Avila, C., Primo, J. (2009). Terretonins E and F, inhibitors of the mitochondrial respiratory chain from the marine-derived fungus *Aspergillus insuetus. J. Nat. Prod., 72,* 1348 – 1351.

Lourenço, T. O., Akisue, G., Roque, N. F. (1981). Reduced acetophenone derivatives from *Calea cuneifolia. Phytochemistry, 20,* 773 – 776.

LOVAZA®. *U.S. Food & Drug Administration.* Retrieved from http://www.accessdata.fda.gov/drugsatfda_docs/label/2014/021654s041lbl.pdf.

Manniche, S., Sprogøe, K., Dalsgaard, P. W., Christophersen, C., Larsen, T. O. (2004). Karnatakafurans A and B: two dibenzofurans isolated from the fungus *Aspergillus karnakakaensis. J. Nat. Prod., 67,* 2111 – 2112.

Manning, T. J., Land, M., Rhodes, E., Chamberlin, L., Rudloe, J., Phillips, D., Lam, T. T., Purcell, J., Cooper, H. J., Emmett, M. R., Marshall, A. G. (2005). Identifying bryostatins and potential precursors from the bryozoan *Bugula neritina. Nat. Prod. Res., 19,* 467 – 491.

Marine Pharmacology: Clinical Development. Marinepharmacology.midwestern.edu. Retrieved from http://marinepharmacology.midwestern.edu/clinPipeline.htm.

Martín, M. J., Coello, L., Fernándex, R., Reyes, F., Rodríguez, A., Murcia, C., Garranzo, M., Mateo, C., Sánchez-Sancho, F., Bueno, S., de Eguilior, C., Francesch, A., Munt, S., Cuevas, C. (2013). Isolation and first total synthesis of PM050489 and PM060184, two new marine anticancer compounds. *J. Am. Chem. Soc., 135,* 10164 – 10171.

Masi, M., Andolfi, A., Mathieu, V., Boari, A., Cimmino, A., Banuls, L. A., Vurro, M., Kornienko, A., Kiss, R., Evidente, A. (2013). Fischerindoline, a pyrroloindole sesquiterpenoid isolated from *Neosartorya pseudofischeri,* with in vitro growth inhibitory activity in human cancer cell lines. *Tetrahedron, 69,* 7466 – 7470

Masi, M., Andolfi, A., Mathieu, V., Boari, A., Cimmino, A., Banuls, L. M., Vurro, M., Kornienko, A., Kiss, R., Evidente, A. (2013). Fischerindoline, a pyrroloindole sesquiterpenoid isolated from *Neosartorya pseudofischeri,* with in vitro growth inhibitory activity in human cancer cell lines. *Tetrahedron, 69,* 7466 – 7470.

Masuda, Y., Tanaka, R., Kai, K., Ganesan, A., Doi, T. (2014). Total synthesis and biological evaluation of PF1171A, C, F, and G, cyclic hexapeptides with insecticidal activity. *J. Org. Chem., 79,* 7844 – 7853.

Matsuzawa, T., Horie, Y., Abliz, P., Gonoi, T., Yaguchi, T. (2014). *Aspergillus huiyaniae* sp. nov., a new teleomorphic species in *Aspergillus* section *Fumigati* isolated from desert soil in China, and described using polyphasic approach. *Mycoscience, 55,* 213 – 220.

May Zin, W. W., Buttachon, S., Buaruang, J., Gales, L., Pereira, J. A., Pinto, M. M., Silva, A. M., Kijjoa, A. (2015). A new meroditerpene and a new tryptoquivaline analog from the algicolous fungus *Neosartorya takakii* KUFC 7898. *Mar. Drugs, 13,* 3776 – 3790.

May Zin, W. W., Buttachon, S., Buaruang, J., Gales, L., Pereira, J. A., Pinto, M. M., Silva, A. M., Kijjoa, A. (2015). A new meroditerpene and a new tryptoquivaline analog from the algicolous fungus *Neosartorya takakii* KUFC 7898. *Mar. Drugs, 13,* 3776 – 3790.

May Zin, W. W., Buttachon, S., Dethoup, T., Fernandes, G., Cravo, S., Pinto, M. M., Gales, L., Pereira, J. A., Silva, A. M., Sekeroglu, N., Kijjoa, A. (2016). New cyclotetrapeptides and a new diketopiperzine derivative from the marine sponge-associated fungus *Neosartorya glabra* KUFA 0702. *Mar. Drugs, 14,* 136 – 150.

Mayer, A. M., Glaser, K. B., Cuevas, C., Jacobs, R. S., Kem, W., Little, R. D., McIntosh, J. M., Newman, D. J., Potts, B. C., Shuster, D. E. (2010). The odyssey of marine pharmaceuticals: a current pipeline perspective. *Trends Pharmacol. Sci., 31,* 255 – 265.

McBride, A., Butler, S. K. (2012). Eribulin mesylate: a halichondrin B analogue for the treatment of metastatic breast cancer. *Am. J. Health Syst. Pharm., 69,* 745 – 755.

McKay, M. J., Carroll, A. R., Quinn, R. J., Hooper, J. N. (2002). 1,2-Bis(1*H*-indol-3-yl)ethane-1,2-dione, an indole alkaloid from the marine sponge *Smenospongia* sp. *J. Nat. Prod., 65,* 595 – 597.

Mehbub, M. F., Lei, J., Franco, C., Zhang, W. (2014). Marine sponge derived natural products between 2001 and 2010: trends and opportunities for discovery of bioactives. *Mar. Drugs, 12,* 4539 – 4577.

Mitscher, L. A., Andres, W. W., McCrae, W. (1964). Reticulol, a new metabolic isocoumarin. *Experientia, 20*(5), 258 – 259.

Moore, K. S., Wehrli, S., Roder, H., Rogers, M., Forrest J. N. Jr., McCrimmon, D., Zasloff, M. (1993). Squalamine: an aminosterol antibiotic from the shark. *Proc. Natl. Acad. Sci. U. S. A., 90,* 1354 – 1358.

Morino, T., Nishimoto, M., Itou, N., Nishikiori, T. (1994). NK372135s, novel antifungal agents produced by *Neosartorya fischeri. J. Antibiot., 47,* 1546 – 1548.

Muralidhar, P., Krishna, N., Kumar, M. M., Rao, C. B., Rao, D. V. (2003). New sphingolipids from marine sponge *Iotrochota baculifera, Chem. Pharm. Bull., 51,* 1193 – 1195.

Obata, R., Sunazaka, T., Tomoda, H., Harigaya, Y., Ōmura, S. (1995). Chemical modificatin and structure-activity relationships of pyripyropenes; potent, bioavailable inhibitor of acyl-CoA: Cholesterol *O*-acyltransferase (ACAT). *Bioorg. Med. Chem. Lett., 5,* 2683 – 2688.

Odds, F.C. (2003). Synergy, antagonism, and what the chequerboard puts between them. *J. Antimicrob. Chemother.,* 52, doi:10.1093/jac/dkg301.

Olguin-Uribe, G., Abou-Mansour, E., Boulander, A., Débard, H., Francisco, C., Combaut, G. (1997). 6-Bromoindole-3-carbaldehyde, from an *Acinetobacter* sp. bacterium associated with the ascidian *Stomozoa murrayi, J. Chem. Ecol., 23*(11), 2507 – 2021.

Onofrejová, L., Vašíčková, J., Klejdus, B., Stratil, P., Mišurcová, L., Kráčmar, S., Kopecký, J., Vacek, J. (2010). Bioactive phenols in algae: the application of pressurized-liquid and solid-phase extraction techniques. *J. Pharm. Biomed. Anal., 51,* 464 – 470.

Ozoe, Y., Kuriyama, T., Tachibana, Y., Haarimaya, K., Takahashi, N., Yaguchi, T., Suzuki, E., Imamura, K., Oyama, K. (2014). Isocoumarin derivative as a novel GABA receptor ligand from *Neosartorya quadricincta. J. Pestic. Sci., 29,* 328 – 331.

Parameswaran, P. S., Naik, C. G., Hegde, V. R. (1997). Secondary metabolites from the sponge *Tedania anhelans*: isolation and characterization of two novel pyrazole acids and other metabolites. *J. Nat. Prod., 60,* 802 – 803.

Peng, J., Gao, H., Li, J., Ai, J., Geng, M, Zhang, G., Zhu, T., Gu, Q., Li, D. (2014). Prnylated indole diketopiperazines from the marine-derived fungus *Aspergillus versicolor. J. Org. Chem., 79,* 7895 – 7904.

Peng, J., Gao, H., Zhang, X., Wang, S., Wu, C., Gu, Q., Guo, P., Zhu, T., Li, D. (2014). Psychrophilins E- H and versicotide C, cyclic peptides from the marine-derived fungus *Aspergillus versicolor* ZLN-60. *J. Nat. Prod., 77,* 2218 – 2223.

Peng, J., Zhang, X. Y., Tu, Z. C., Xu, X. Y., Qi, S. H. (2013). Alkaloids from the deep-sea-derived fungus *Aspergillus westerdijkiae* DFFSCS013. *J. Nat. Prod., 76,* 983 – 987.

Prata-Sena, M., Ramos, A. A., Buttachon, S., Castro-Carvalho, B., Marques, P., Dethoup, T., Kijjoa, A., Rocha, E. (2016). Cytotoxic activity of secondary metabolites from marine-derived fungus *Neosartorya siamensis* in human cancer cells. *Phytother. Res., 30,* 1862 – 1871.

Proksa, B., Uhrín, D., Liptaj, T., Šturdíková, M. (1998). Neosartorin, an ergochrome biosynthesized by *Neosartorya fischeri. Phytochemistry, 48,* 1161 – 1164.

Rahbæk, L., Breinholt, J. (1999). Circumdatins D, E, and F: further fungal benzodiazepine analogues from *Aspergillus ochraceus. J. Nat. Prod., 62,* 904 – 905.

Rahbæk, L., Breinholt, J., Frisvad, J. C., Christophersen, C. (1999). Circumdatins A, B, and C: three new benzodiazepine alkaloids isolated from a culture of the fungus *Aspergillus ochraceus. J. Org. Chem., 64,* 1689 – 1692.

Rahbæk, L., Christophersen, C., Frisvad, J., Bengaard, H. S., Larsen, S., Rassing, B. R. (1997). Insulicolide A: a new nitrobenzoyloxy-substituted sesquiterpene from the marine fungus *Aspergillus insulicola. J. Nat. Prod., 60,* 811 – 813.

Rajachan, O., Kanokmedhakul, K., Sanmanoch, W., Boonlue, S., Hannongbua, S., Saparpakorn, P., Kanokmedhakul, S. (2016). Chevalone C analogues and

globoscinic acid derivatives from the fungus *Neosartorya spinosa* KKU-1NK1. *Phytochemistry, 132,* 68 – 75.

Rasmussen, T., Jensen, J., Anthoni, U., Christophersen, C., Nielsen, P. H. (1993). Structure and synthesis of bromoindoles from the marine sponge *Pseudosuberites hyalinus. J. Nat. Prod., 56*(9), 1553 – 1558.

Romano, M., Frapolli, R., Zangarini, M., Bello, E., Porcu, L., Galmarini, C. M., García-Fernández, L. F., Cuevas, C., Allavena, P., Erba, E., D'Incalci, M. (2013). Comparison of *in vitro* and *in vivo* biological effects of trabectedin, lurbinectedin (PM01183) and Zalypsis® (PM00104). *Int. J. Cancer, 133,* 2024 – 2033.

Ryoo, I. J., Xu, G. H., Kim, Y. H., Choo, S. J., Ahn, J. S., Bae, K. H., Yoo, I. D. (2009). Reticulone, a novel free radical scavenger produced by *Aspergillus* sp. *J. Microbiol. Biotechnol., 19*(12), 1573 – 1575.

Sawadsitang, S., Mongkolthanaruk, W., Suwannasai, N., Sodngam, S. (2015). Antimalarial and cytotoxic costituents of *Xylaria* cf. *cubensis* PK108. *Nat. Prod. Res., 29*(21), 2033 – 2036.

Schofield, M. M., Jain, S., Porat, D., Dick, G. J., Sherman, D. H. (2015). Identification and analysis of the bacterial endosymbiont specialized for production of the chemotherapeutic natural product ET-743. *Environ. Microbiol., 17*(10), 3964 – 3975.

Shan, W. G., Wang, S. L., Lang, H. Y., Chen, S. M., Ying, Y. M., Zhan, Z. J. (2015). Cottoquinazolines E and F from *Neosartorya fischeri* NRRL 1811. *Helv. Chim. Acta, 98,* 552 – 556.

Shan, W., Wang, S., Ying, Y., Ma, L., Zhan, Z. (2014). Indole-benzodiazepine-2,5-dione derivatives from *Neosartorya fischeri. J. Chem. Res., 38,* 692 – 694.

Shao, C. L., Han, L., Li, C. Y., Liu, Z., Wang, C. Y. (2009). 6,8-Dihydroxy-3-methylisocoumarin. *Acta Crystallogr. Sect. E Struct. Rep. Online, E65*, o736.

Sheldrick, G. M. (2008). A Short history of SHELX. *Acta Crystallogr. A,* 112 – 122.

Shen, S., Liu, D., Wei, C., Proksch, P., Lin, W. (2012). Purpuroines A – J, halogenated alkaloids from the sponge *Iotrochota purpurea* with antibiotic acitivity and regulation of tyrosine kinases. *Bioorg. Med. Chem., 20,* 6924 – 6928.

Shima, K., Hisada, S., Inagaki, I. (1972). Studies on the constituents of *Anodendron affine* Durce. V. isolation and structure of two new constituents. *Yakugaku Zasshi, 92,* 1410 – 1414.

Shyamala, B. N., Madhava Naidu, M., Sulochanamma, G., Srinivas, P. (2007). Studies on the antioxidant activities of natural vanilla extract and its constituent compounds through *in vitro* models. *J. Agric. Food Chem., 55,* 7738 – 7743.

Singh, A. V., Bandi, M., Raje, N., Richardson, P., Palladino, M. A., Chauhan, D., Anderson, K. C. (2011). A novel vascular disrupting agent plinabulin triggers JNK-mediated apoptosis and inhibits angiogenesis in multiple myeloma cells. *Blood, 117,* 5692 – 5700.

Sipkema, D., Franssen, M. C., Osinga, R., Tramper, J., Wijffels, R. H. (2005). Marine sponges as Pharmacy. *Mar. Biotechnol., 7,* 142 – 162.

Son, B. W., Choi, J. S., Kim, J. C., Nam, K. W., Kim, D. S., Chung, H. Y., Kang, J. S., Choi, H. D. (2002). Parasitenone, a new epoxycyclohexenone related to gabosine from the marine-derived fungus *Aspergillus parasiticus. J. Nat. Prod., 65,* 794 – 795.

Song, Y., Li, Q., Liu, X., Chen, Y., Zhang, Y., Sun, A., Zhang, W., Zhang, J., Ju, J. (2014). Cyclic hexapeptides from the deep South China Sea-derived *Streptomyces scopuliridis* SCSIO ZJ46 active against pathogenic Gram-positive bacteria. *J. Nat. Prod., 77,* 1937 – 1941.

Sorek, H., Rudi, A., Aknin, M., Gaydou, E., Kashman, Y. (2006). Itampolins A and B, new brominated tyrosine derivatives from the sponge *Iotrochota purpurea*. *Tetrahedron Lett., 47,* 7237 – 7239.

Sun, F. Y., Chen, G., Bai, J., Li, W., Pei, Y. H. (2012). Two new alkaloids from a marine-derived fungus *Neosartorya* sp. HN-M-3. *J. Asian Nat. Prod. Res., 14,* 1109 – 1115.

Sun, H. F., Li, X. M., Meng, L., Cui, C. M., Gao, S. S., Li, C. S., Huang, C. G., Wang, B. G. (2012). Asperolides A – C, tetranorlabdane diterpenoids from the marine alga-derived endophytic fungus *Aspergillus wentii* EN-48. *J. Nat. Prod., 75,* 148 – 152.

Tabacchi, R., Fkyerat, A., Poliart, C., Dubin, G. M. (2000). Phytotoxins from fungi of esca of grapevine. *Phytopathol. Mediterr., 39,* 156 – 161.

Tan, Q. W., Ouyang, M. A., Shen, S., Li, W. (2012). Bioactive metabolites from a marine-derived strain of the fungus *Neosartorya fischeri. Nat. Prod. Res., 26,* 1402 – 1407.

Tang, Y. Q., Sattler, I., Thiericke, R., Grabley, S., Feng, X. Z. (2000, September). *Parallel chromatography in natural products chemistry: isolation of new secondary metabolites from Streptomyces sp*. Paper presented at the Fourth International Electronic Conference on Synthetic Organic Chemistry (ECSOC-4). Retrieved from: www.mdpi.org/ecsoc-4.htm.

Thompson, M N., Gallimore, W. A. (2016). Constituents of the Jamaican sponge *Iotrochota birotulata. World Journal of Organic Chemistry, 4,* 13 – 16.

Tomoda, H., Tabata, N., Yang, D. J., Takayanagi, H., Nishida, H., Ōmura, S. (1995). Pyripyropenes, novel ACAT inhibitors produced by *Aspergillus fumigatus* III. structure elucidation of pyripyropenes E to L. *J. Antibiot., 48,* 495 – 503.

Trisuwan, K., Rukachaisirikul, V., Kaewpet, M., Phongpaichit, S., Hutadilok-Towatana, N., Preedanon, S., Sakayaroj, J. (2011). Sesquiterpene and xanthone derivatives from the sea fan-derived fungus *Aspergillus sydowii* PSU-F154. *J. Nat. Prod., 74,* 1663 – 1667.

van de Donk, N. W., Dhimolea, E. (2012). Brentuximab vedotin. *MAbs, 4,* 458 – 465.

Van Soest, R. W., Boury-Esnault, N., Vacelet, J., Dohrmann, M., Erpenbeck, D., De Voogd, N. J., Santodomingo, N., Vanhoorne, B., Kelly, M., Hooper, J. N. (2012). Global diversity of sponges (Porifera). *PLoS ONE, 7,* e35105.

Virágh, M., Maron, A., Vizler, C., Tóth, L., Vágvölgyi, C., Marx, F., Galgóczy, L. (2015). Insight into the antifungal mechanism of *Neosartorya fischeri* antifungal protein. *Protein Cell, 6,* 518 – 528.

Virágh, M., Vörös, D., Kele, Z., Kovács, L, Fizil, Á., Lakatos, G., Maróti, G., Batta, G., Vágvölgyi, C., Galgóczy, L. (2014). Production of a defensin-like antifungal protein NFAP from *Neosartorya fischeri* in *Pichia pastoris* and its antifungal activity against filamentous fungal isolates from human infections. *Protein Expr. Purif., 94,* 79 – 84.

Wakana, D., Hosoe, T., Itabashi, T., Nozawa, K., Okada, K., Takaki, G. M., Yaguchi, T., Fukushima, K., Kawai, K. (2006). Isolation of isoterrein from *Neosartorya fischeri. Mycotoxins, 56,* 3 – 6.

Wang, C., Yang, Y., Mei, Z., Yang, X. (2013). Cytotoxic compounds from *Laminaria japonica. Chem. Nat. Compd., 49*(4), 699 – 701.

Wang, Y., Zheng, J., Liu, P., Wang, W., Zhu, W. (2011). Three new compounds from *Aspergillus terreus* PT06-2 grown in a high salt medium. *Mar. Drugs, 9,* 1368 – 1378.

Wong, S. M., Musza, L. L., Kydd, G. C., Kullnig, R., Gillum, A. M., Cooper, R. (1993). Fiscalins: new substance P inhibitors produced by the fungus *Neosartorya fischeri. J. Antibiot., 46,* 545 – 553.

Woodhead, S. (1983). Surface chemistry of *Sorghum bicolor* and its importance in feeding by *Locusta migratoria. Physiol. Entomol., 8,* 345 – 352.

World Health Organization (27 February 2017). WHO publishes list of bacteria of which new antibiotics are urgently needed. Retrieved from http://www.who.int/mediacentre/news/releases/2017/bacteria-antibiotics-needed/en/.

World Health Organization (February 2018). Cancer. Retrieved from http://www.who.int/mediacentre/factsheets/fs297/en/.

World Health Organization (Updated January 2017). The top 10 causes of death. Retrieved from http://www.who.int/mediacentre/factsheets/fs310/en/.

World Health Organization (Updated January 2018). Antimicrobial resistance. Retrieved from http://www.who.int/mediacentre/factsheets/fs194/en/.

Wratten, S. J., Wolfe, M. S., Andersen, R. J., Faulkner, D. J. (1977). Antibiotic metabolites from a marine *Pseudomonad. Antimicrob. Agents Chemother., 11*(3), 411 – 414.

Wright, A. D., König, G. M. (1996). Antimalarial activity: the search for marine-derived natural products with selective antimalarial activity. *J. Nat. Prod., 59,* 710 – 716.

Wu, B., Chen, G., Liu, Z., Pei, Y. (2015). Two new alkaloids from a marine-derived fungus *Neosartorya fischeri. Rec. Nat. Prod., 9,* 271 – 275.

Wu, Q. X., Crew, M. S., Draskovic, M., Sohn, J., Johnson, T. A., Tenney, K., Valeriote, F. A., Yao, X. J., Bjeldanes, L. F., Crews, P. (2010). Azonazine, a novel dipeptide from a Hawaiian marine sediment-derived fungus, *Aspergillus insulicola. Org. Lett., 12,* 4458 – 4461.

Wu, Z. C., Li, S., Nam, S. J., Liu, Z., Zhang, C. (2013). Nocardiamides A and B, two cyclohexapeptides from the marine-derived *Actinomycete nocardiopsis* sp. CNX037. *J. Nat. Prod., 76,* 694 – 701.

Xu, N., Cao, Y., Wang, L., Chen, G., Pei, Y. H. (2013). New alkaloids from a marine-derived fungus *Neosartorya* sp. HN-M-3. *J. Asian Nat. Prod. Res., 15,* 731 – 736.

Yamaguchi, S., Kondo, S., Shimokawa, K., Inoue, O., Sannomiya, M., Kawase, Y. (1982). The synthesis of racemic fomannoxin, anodendroic acid, and 5-acetyl-2-[1-(hydroxymethyl)vinyl]-2,3-dihydrobenzofuran. *Bull Chem. Soc. Jpn., 55,* 2500 – 2503.

Yao, Y., Huasding, M., Erkel, G., Anke, T., Förstermann, U., Kleinert, H. (2003). Sporogen, S14-95, and *S*-curvularin, three inhibitors of human inducible nitric-oxide synthase expression isolated from fungi. *Mol. Pharmacol., 63,* 383 – 391.

Yim, T., Kanokmedhakul, K., Kanokmedhakul, S., Sanmanoch, W., Boonlue, S. (2014). A new meroterpenoid tatenoic acid from the fungus *Neosartorya tatenoi* KKU-2NK23. *Nat. Prod. Res., 28,* 1847 – 1852.

Zhang, L., An, R., Wang, J., Sun, N., Zhang, S., Hu, J., Kuai, J. (2005). Exploring novel bioactive compounds from marine microbes. *Curr. Opin. Microbiol., 8,* 276 – 281.

Zhang, M., Wang, W. L., Fang, Y. C., Zhu, T. J., Gu, Q. Q., Zhu, W. M. (2008). Cytotoxic alkaloids and antibiotic nordammarane triterpenoids from the marine-derived fungus *Aspergillus sydowi. J. Nat. Prod., 71,* 985 – 989.

Zheng, J., Zhu, H., Hong, K., Wang, Y., Liu, P., Wang, X., Peng, X., Zhu, W. (2009). Novel cyclic hexapeptides from marine-derived fungus, *Aspergillus sclerotiorum* PT06-1. *Org. Lett., 11,* 5262 – 5265.

Zheng, Z. Z., Shan, W. G., Wang, S. L., Ying, Y. M., Ma, L. F., Zhan, Z. J. (2014). Three new prenylated diketopiperazines from *Neosartorya fischeri. Helv. Chim. Acta, 97,* 1020 – 1026.

Zinad, D. S., Shaaban, K. A., Abdalla, M. A., Islam, M. T., Schüffler, A., Laatsch, H. (2011). Bioactive isocoumarins from a terrestrial *Streptomyces* sp. ANK302. *Nat. Prod. Commun., 6*(1), 45 – 48.

APPENDICES

APPENDIX I

NMR SPECTRA OF THE ISOLATED COMPOUNDS

I.1) 6-Bromo-1*H*-indole-3-carbaldehyde (40)

I.1.1) ^{1}H NMR spectrum (300.13 MHz)

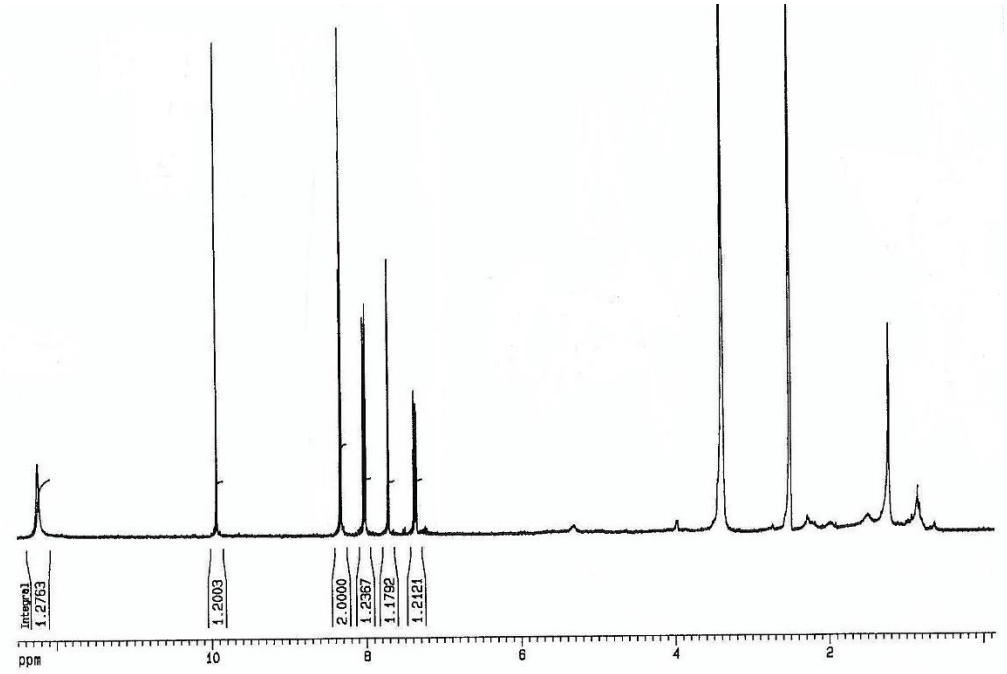

I.1.2) ^{13}C NMR spectrum (75.4 MHz)

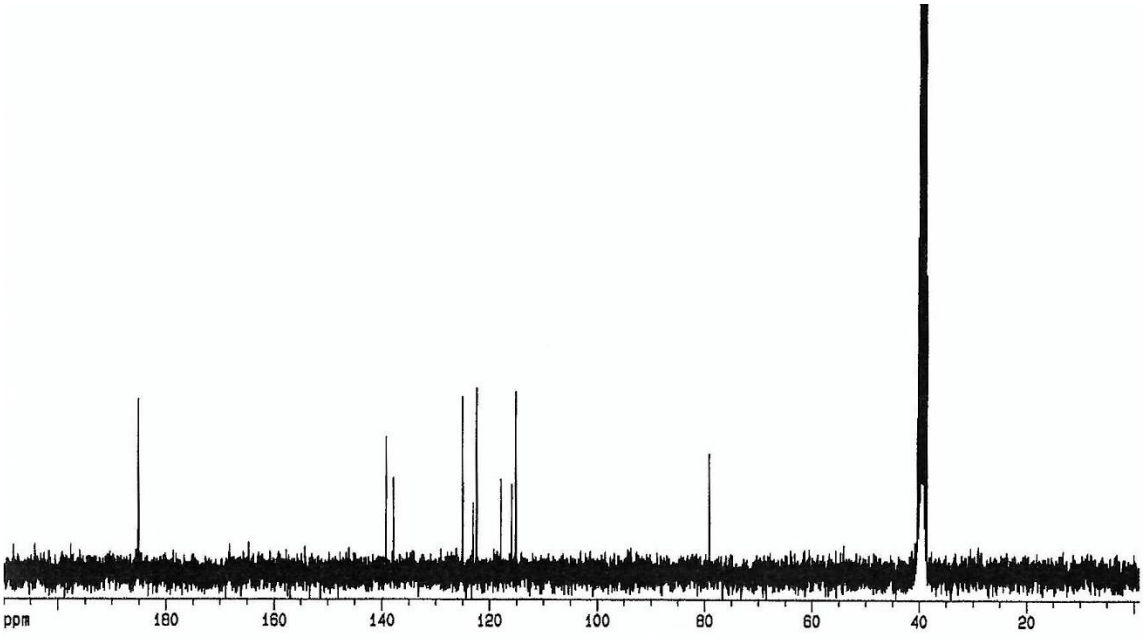

I.2) Methyl (2*E*)-3-(6-bromo-1*H*-indol-3-yl)-prop-2-enoate (370)

I.2.1) ^{1}H NMR spectrum (300.13 MHz)

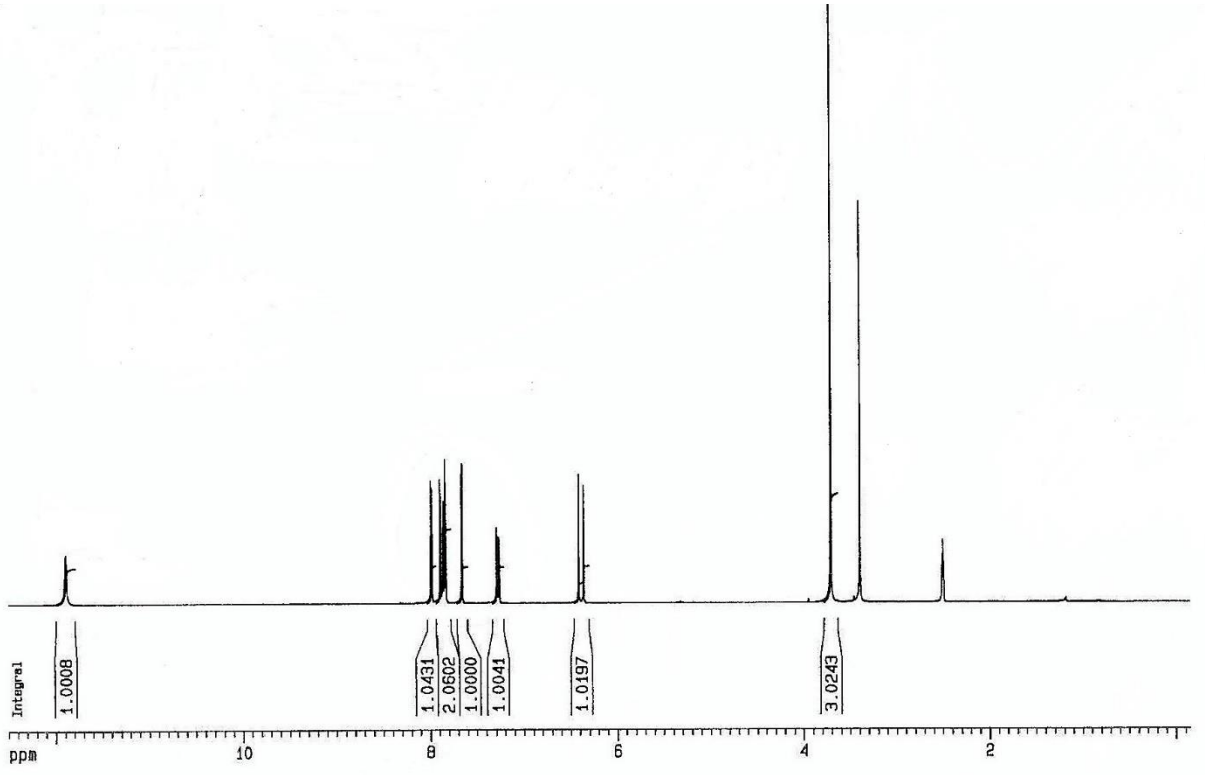

I.2.2) ^{13}C NMR spectrum (75.4 MHz)

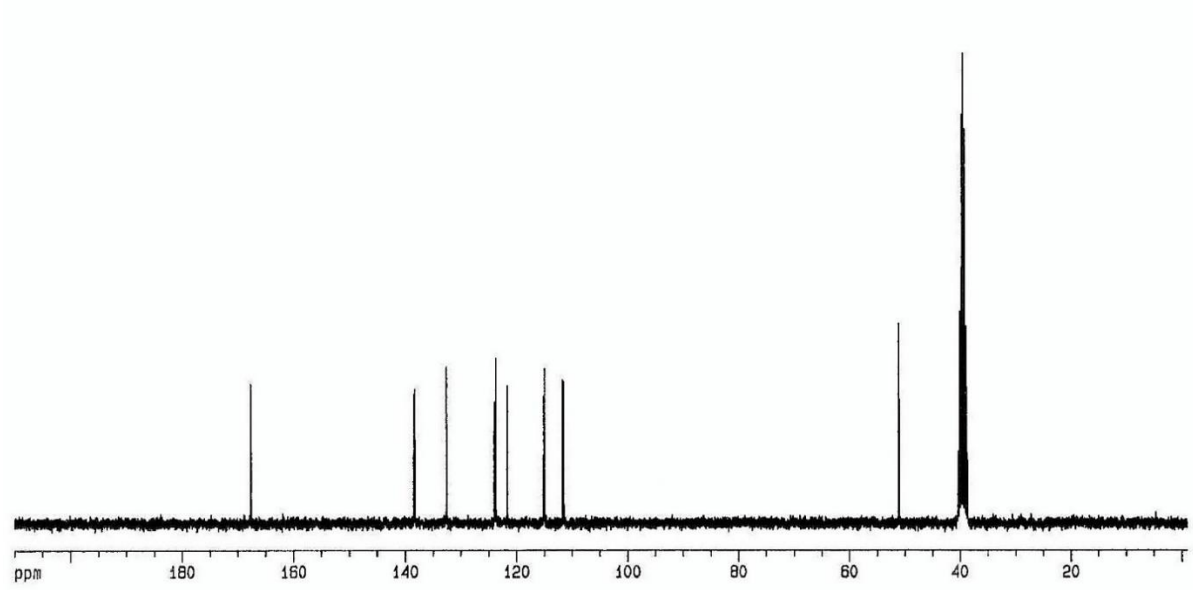

I.3) *p*-Hydroxybenzaldehyde (371)

I.3.1) ^{1}H NMR spectrum (300.13 MHz)

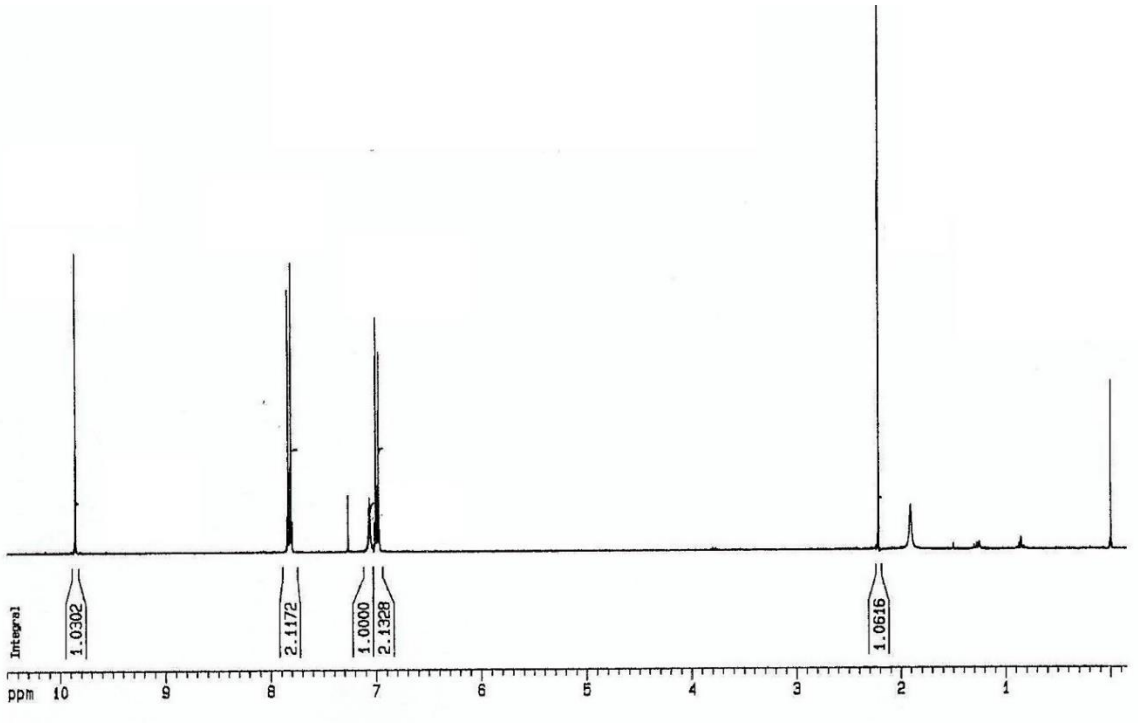

I.3.2) ^{13}C NMR spectrum (75.4 MHz)

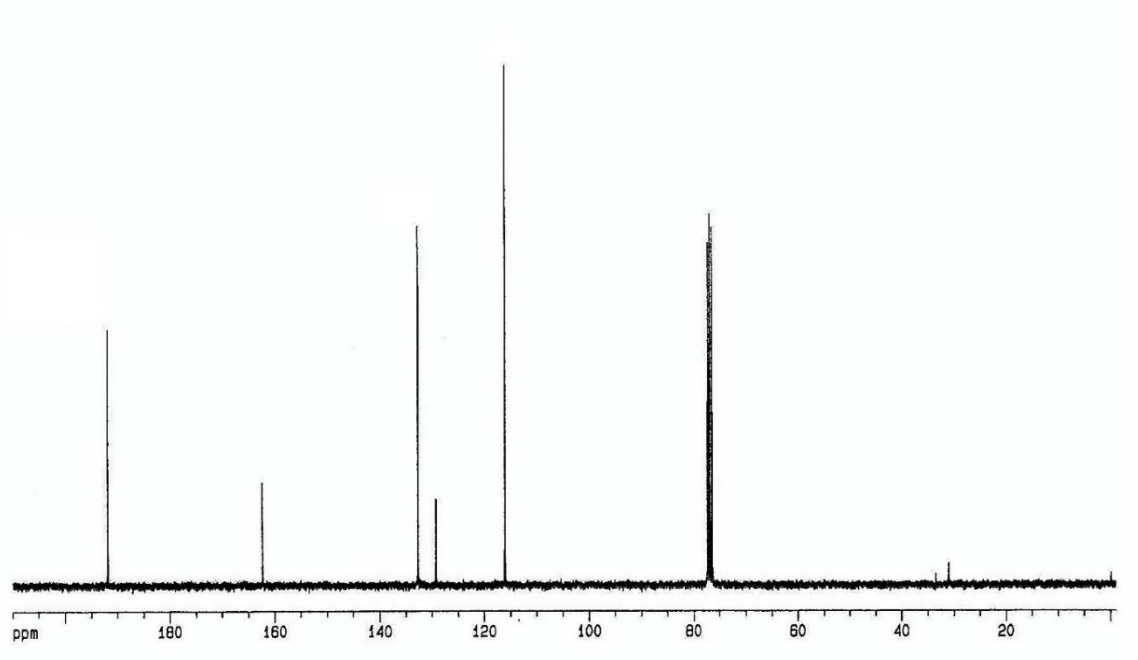

I.4) 6,8-Dihydroxy-3-methylisocoumarin (372)

I.4.1) ^{1}H NMR spectrum (500.13 MHz)

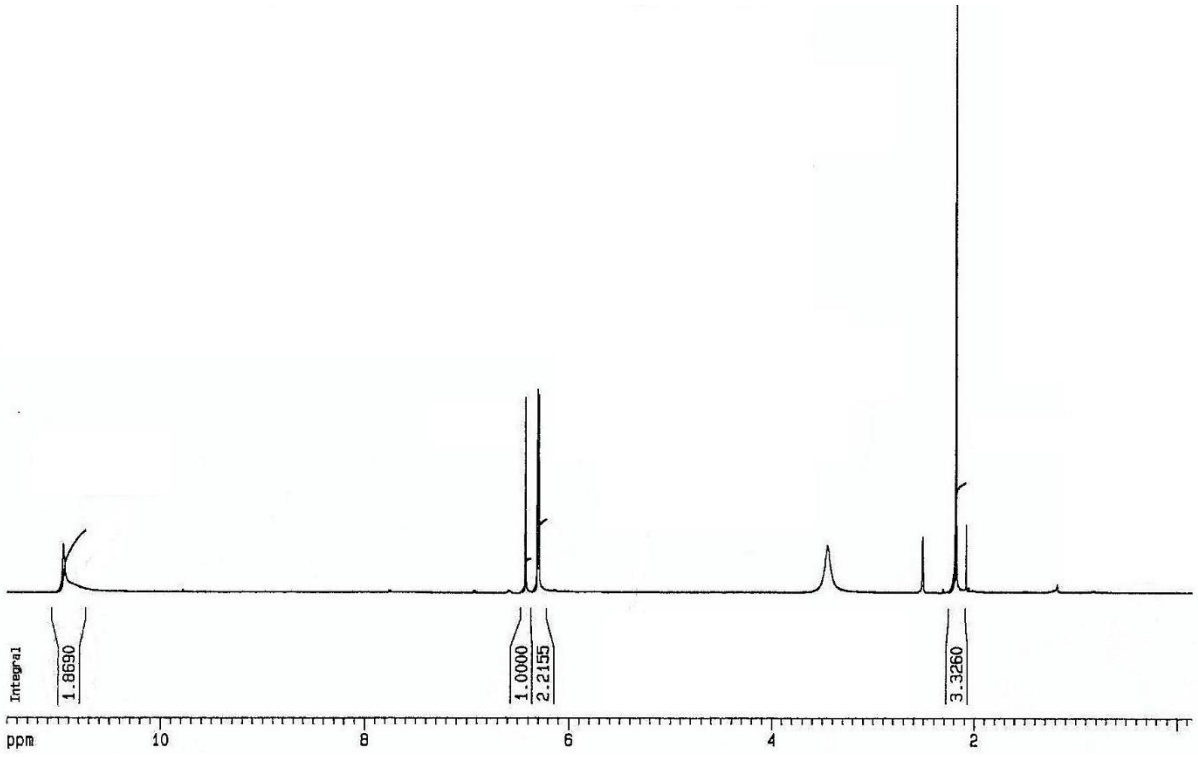

I.4.2) ^{13}C NMR spectrum (125.8 MHz)

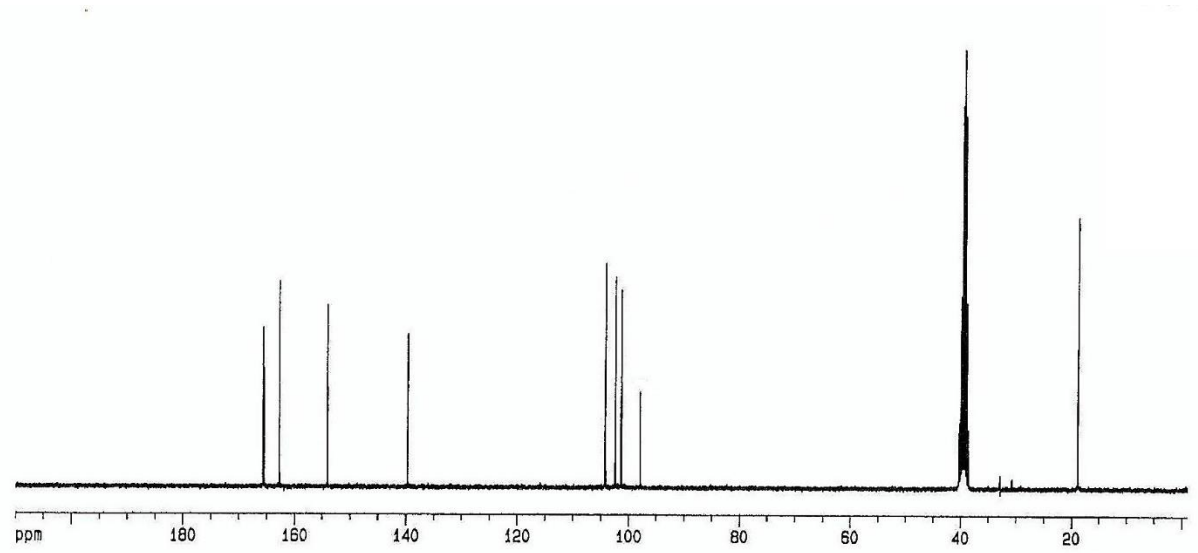

I.5) Similanpyrone B (373)

I.5.1) ^{1}H NMR spectrum (500.13 MHz)

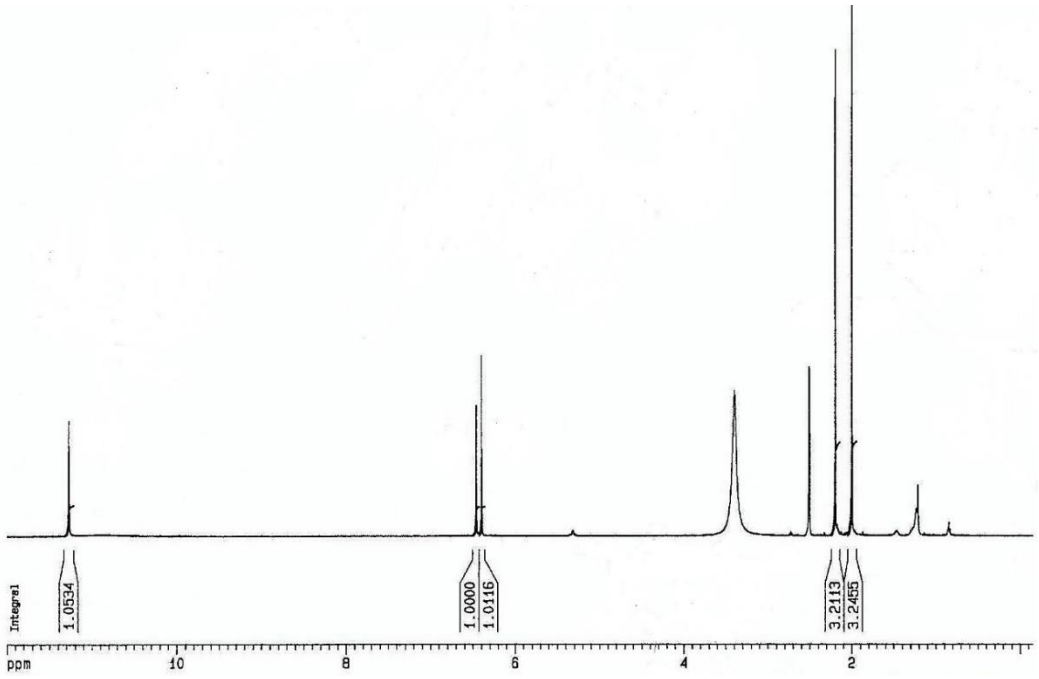

I.5.2) ^{13}C NMR spectrum (125.8 MHz)

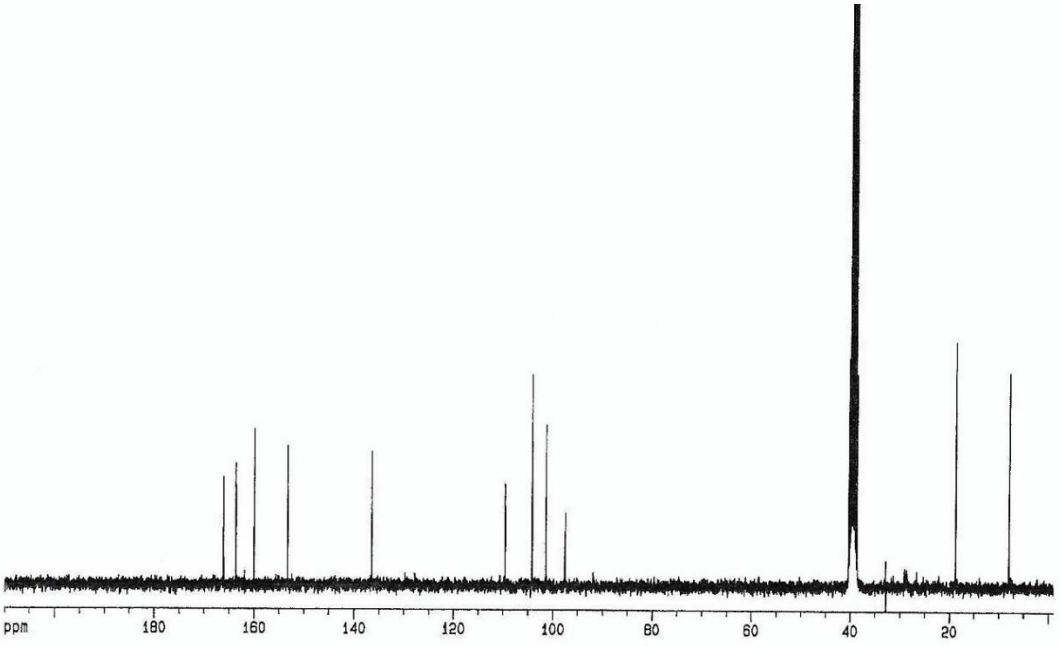

I.6) Reticulol (374)

I.6.1) ^{1}H NMR spectrum (500.13 MHz)

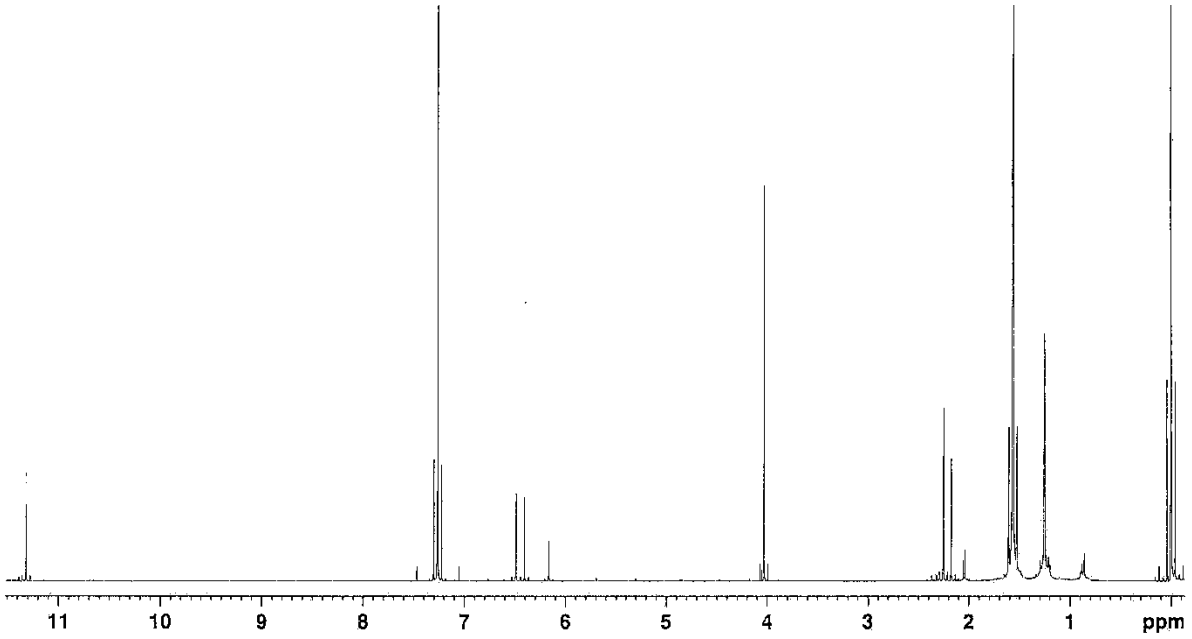

I.6.2) ^{13}C NMR spectrum (125.8 MHz)

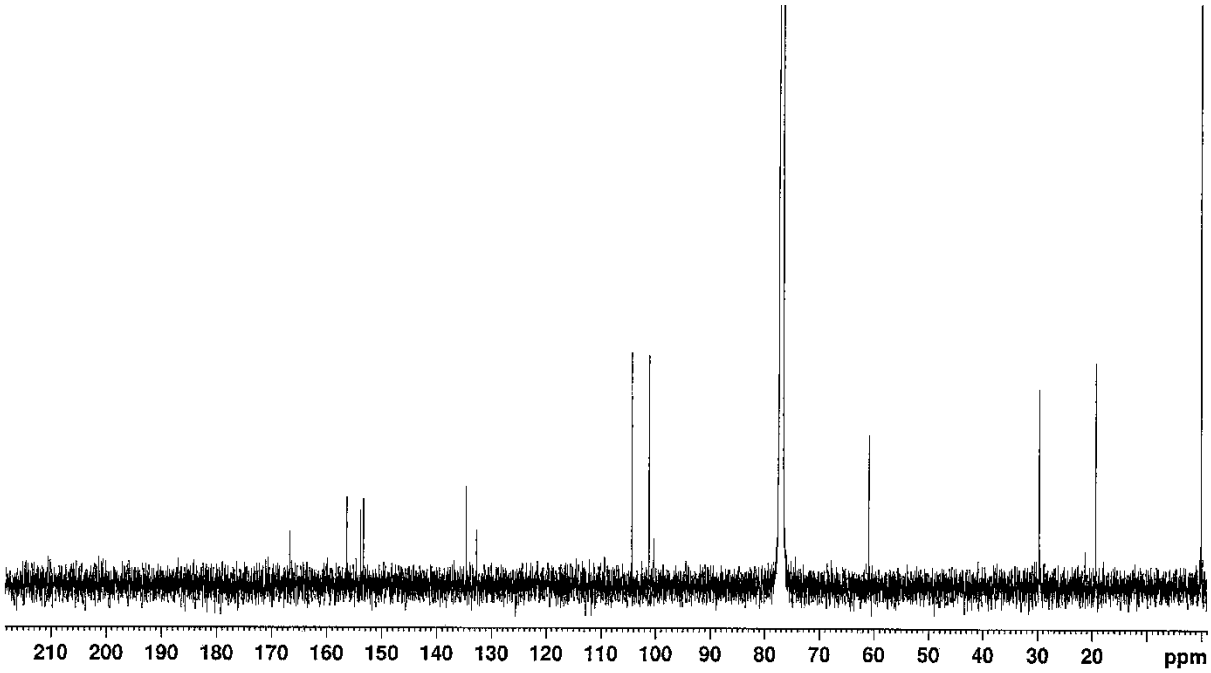

I.7) Similanpyrone A (375)

I.7.1) ^{1}H NMR spectrum (500.13 MHz)

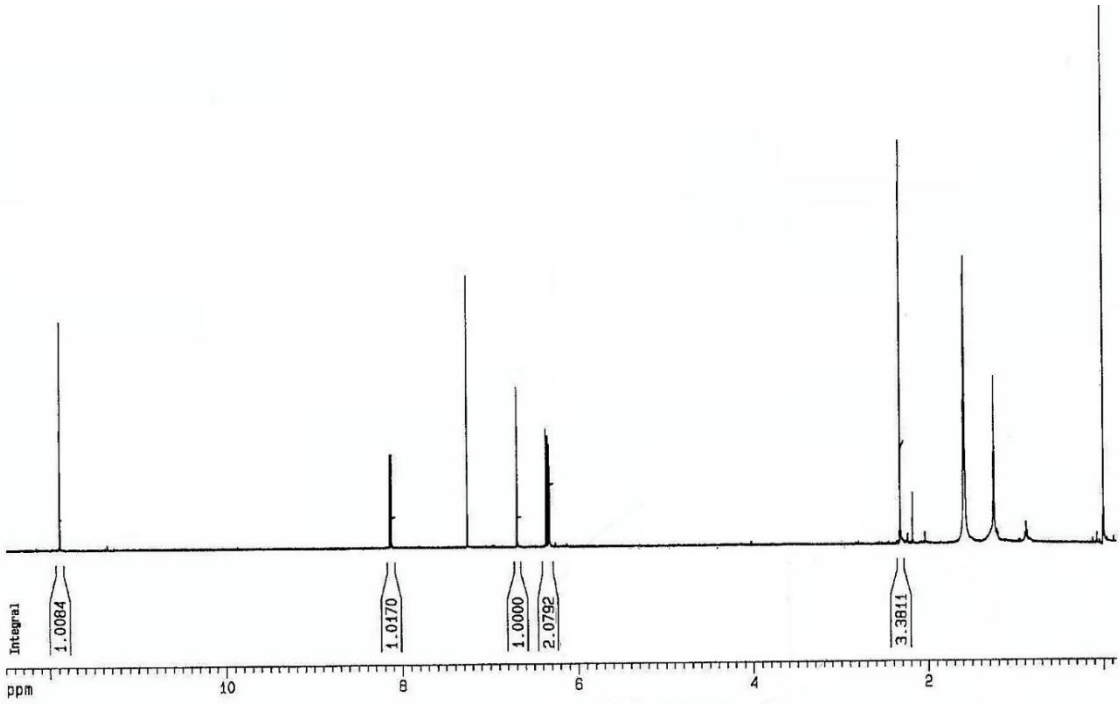

I.7.2) ^{13}C NMR spectrum (125.8 MHz)

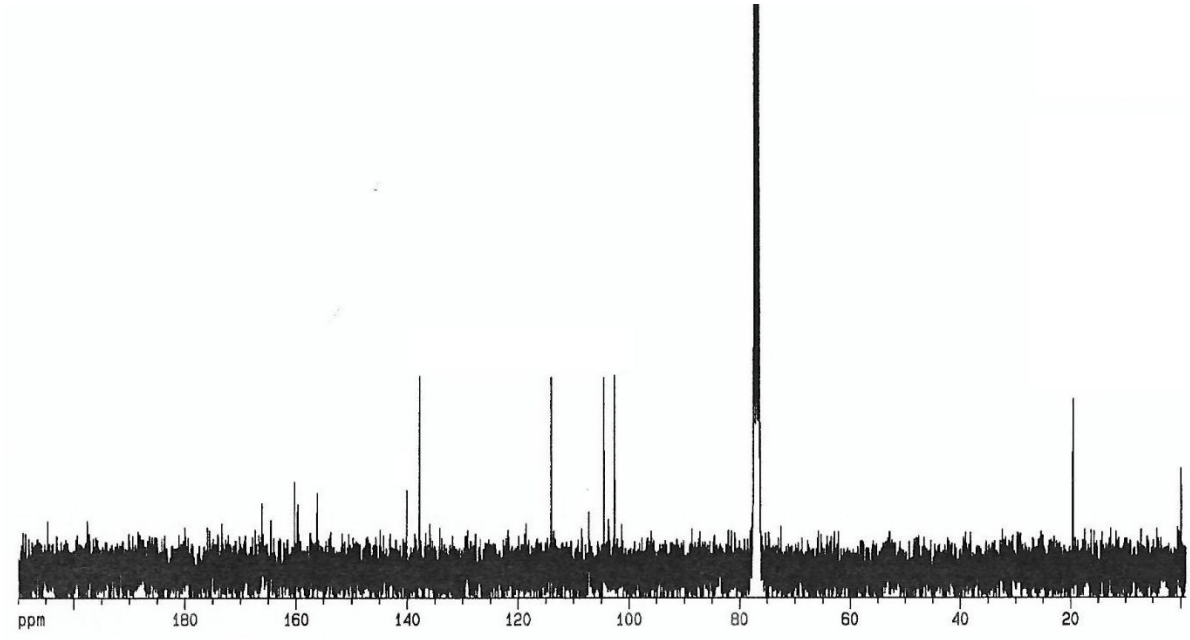

I.8) Similanpyrone C (376)

I.8.1) ^{1}H NMR spectrum (500.13 MHz)

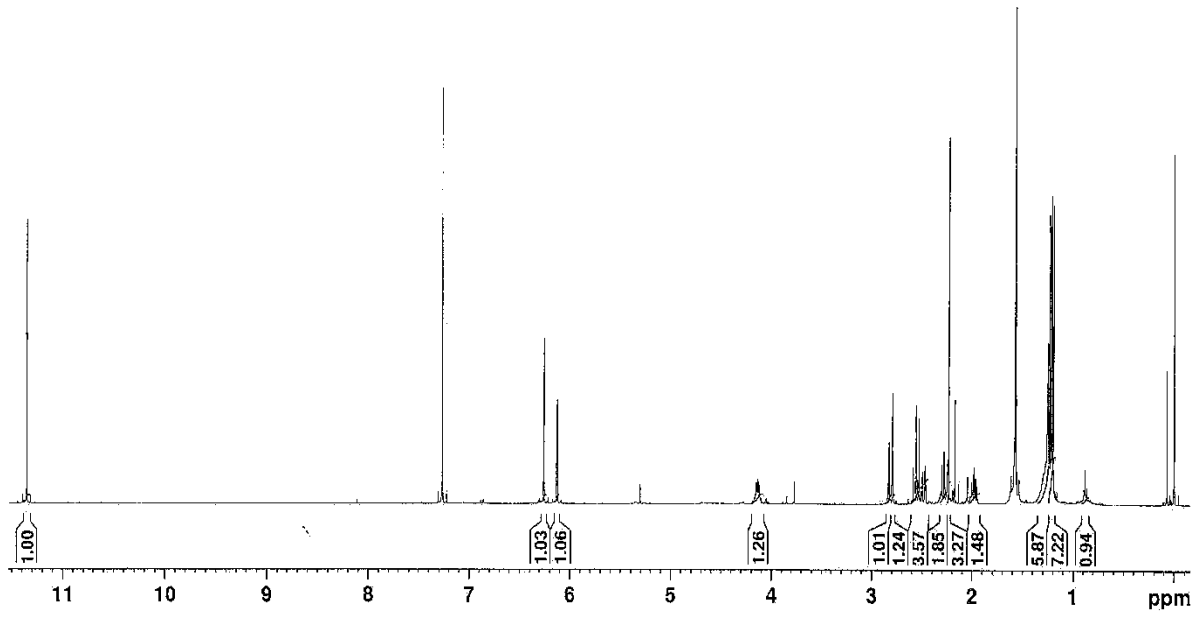

I.8.2) ^{13}C NMR spectrum (125.8 MHz)

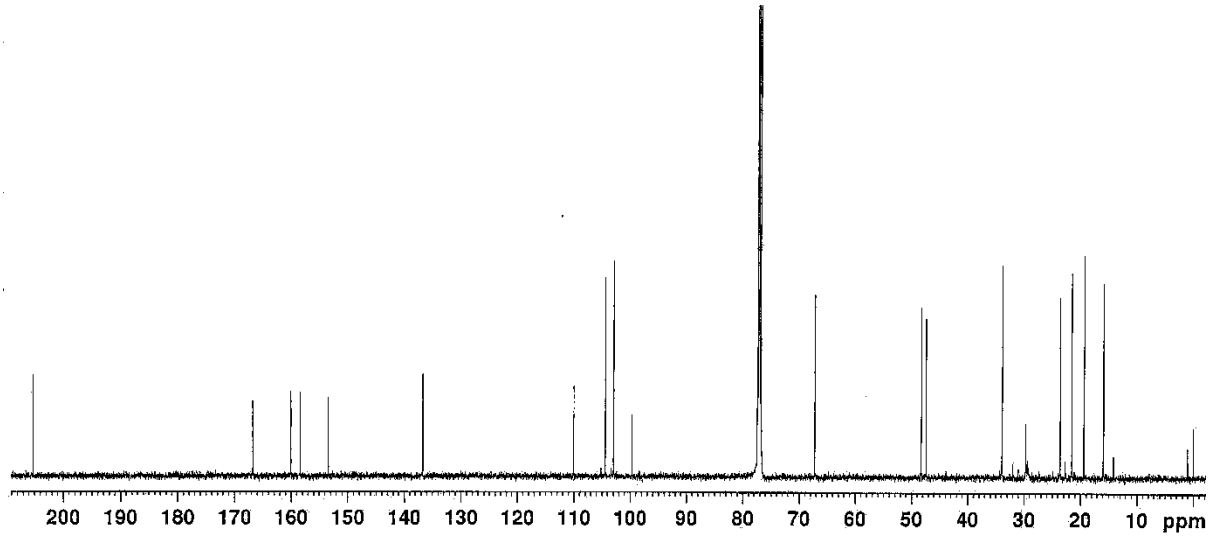

I.9) Chevalone C (349)

I.9.1) ^{1}H NMR spectrum (300.13 MHz)

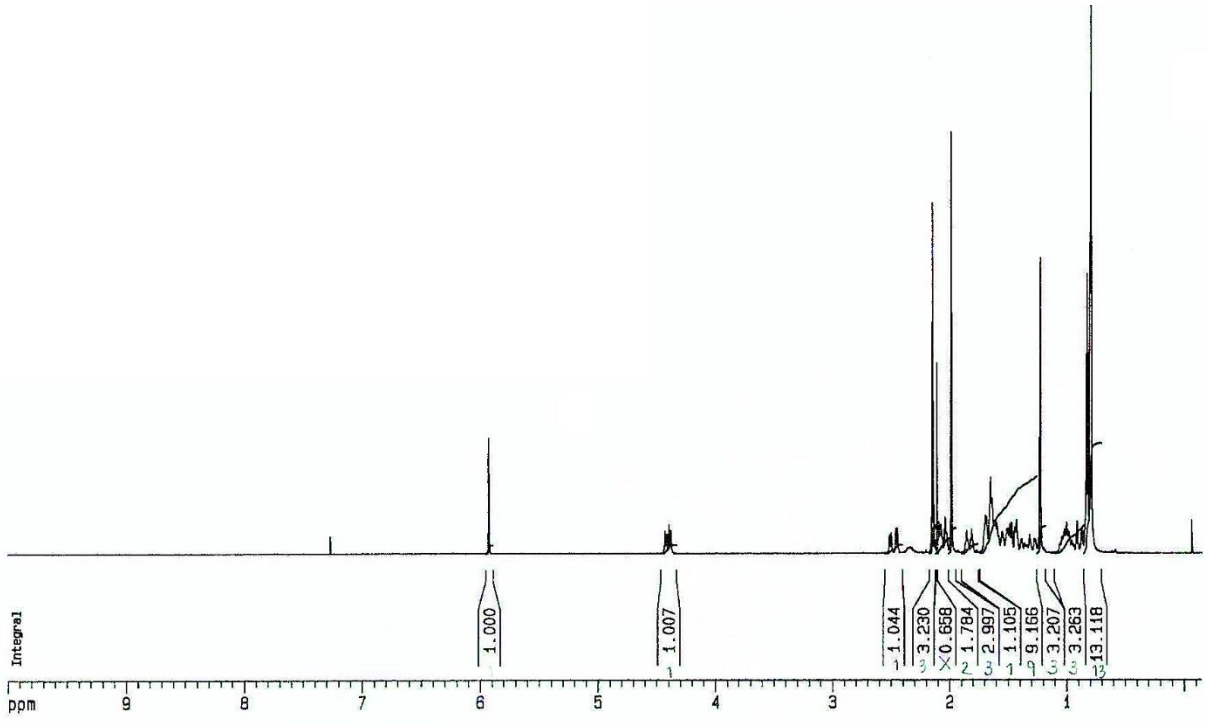

I.9.2) ^{13}C NMR spectrum (75.4 MHz)

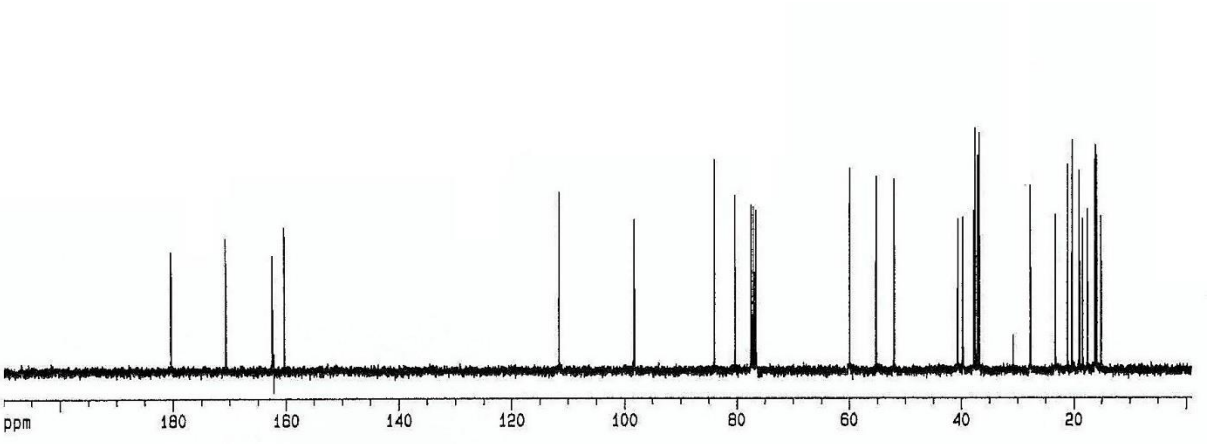

I.10) Chevalone E (356)

I.10.1) ^{1}H NMR spectrum (500.13 MHz)

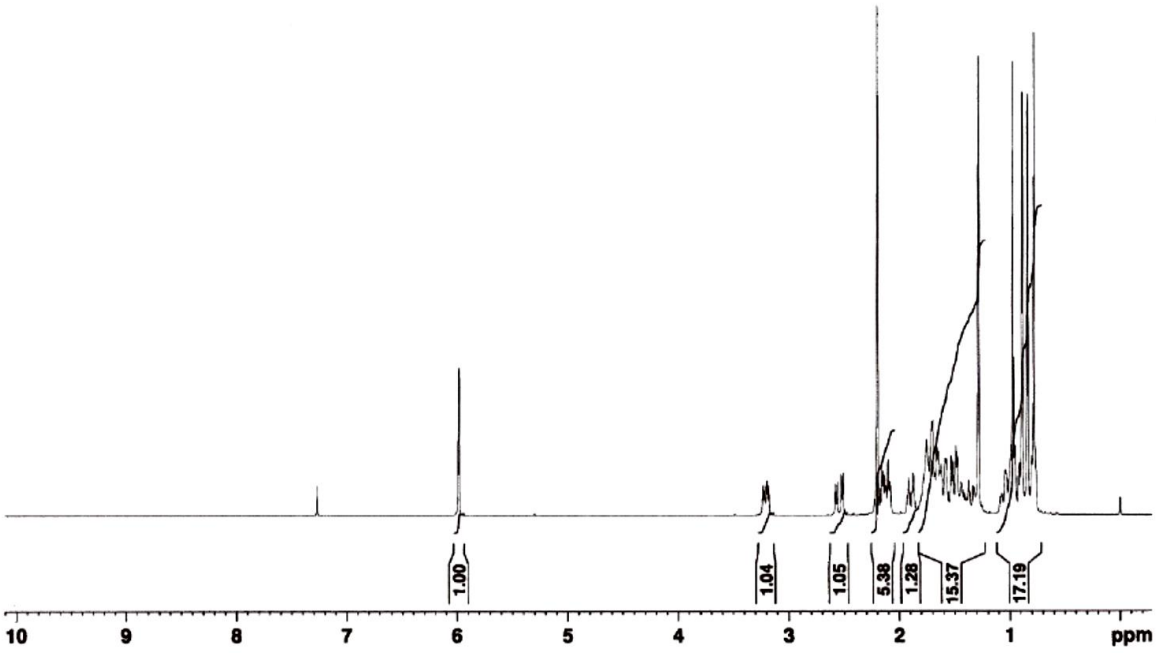

I.10.2) ^{13}C NMR spectrum (125.8 MHz)

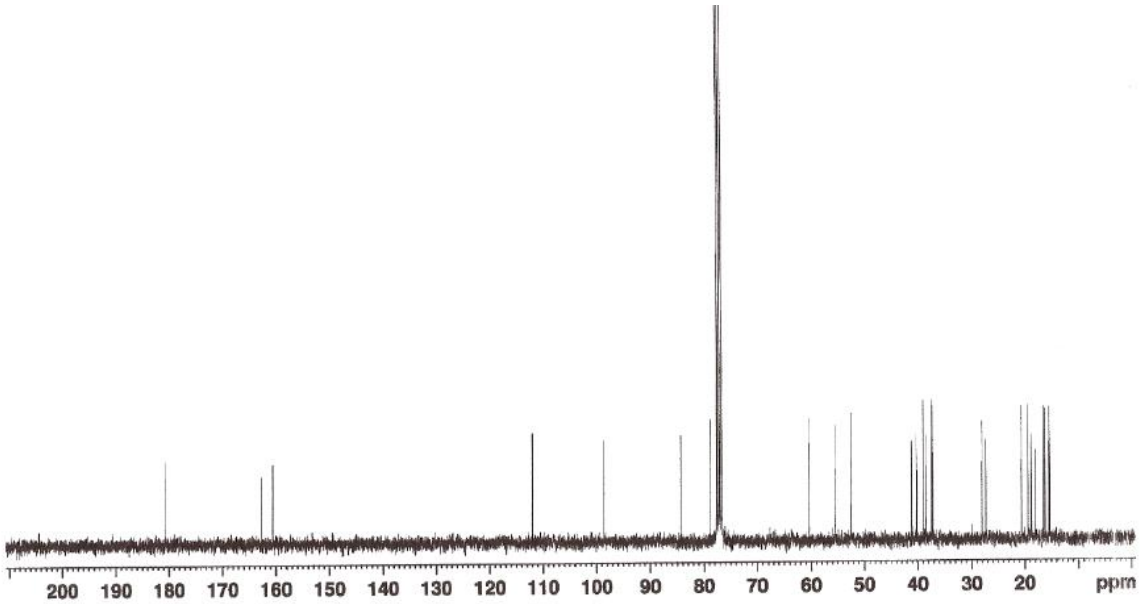

I.11) Chevalone B (348)

I.11.1) ^{1}H NMR spectrum (300.13 MHz)

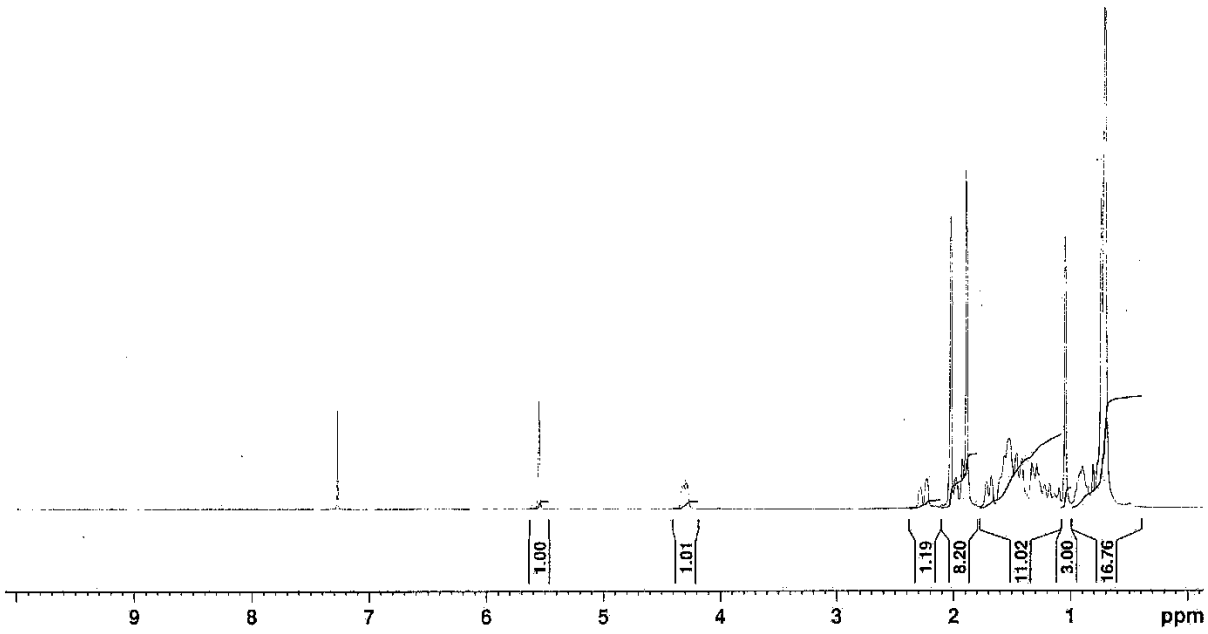

I.11.2) ^{13}C NMR spectrum (75.4 MHz)

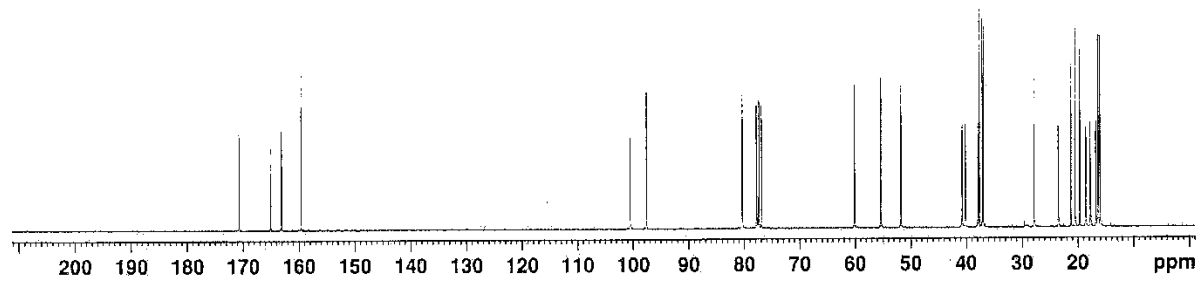

I.12) S14-95 (377)

I.12.1) ^{1}H NMR spectrum (300.13 MHz

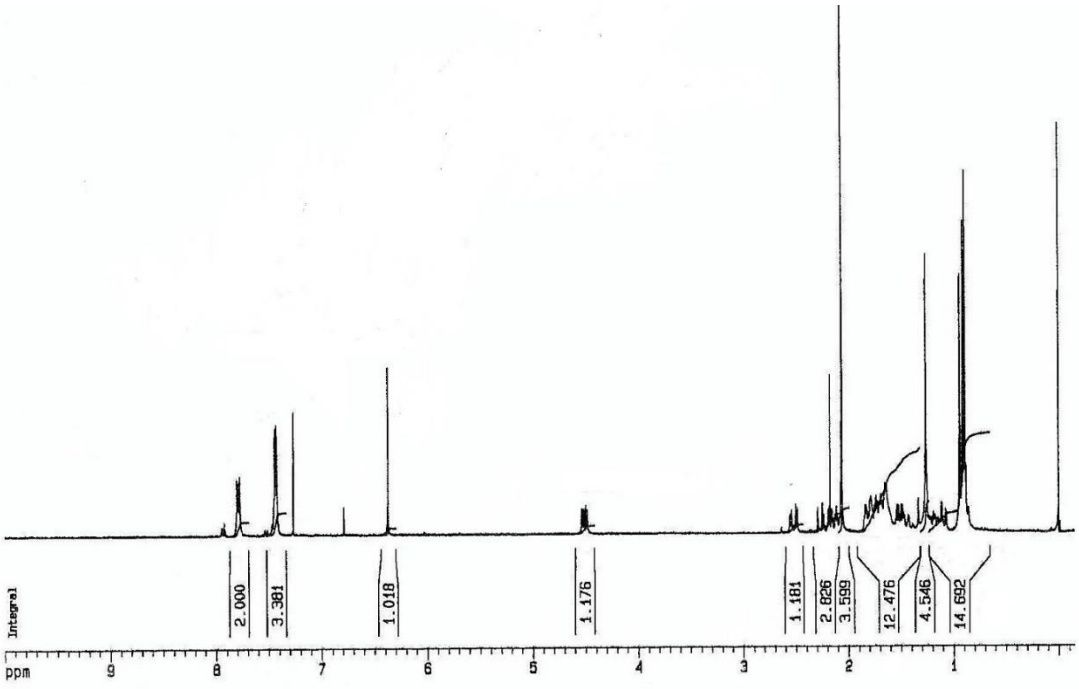

I.12.2) ^{13}C NMR spectrum (75.4 MHz)

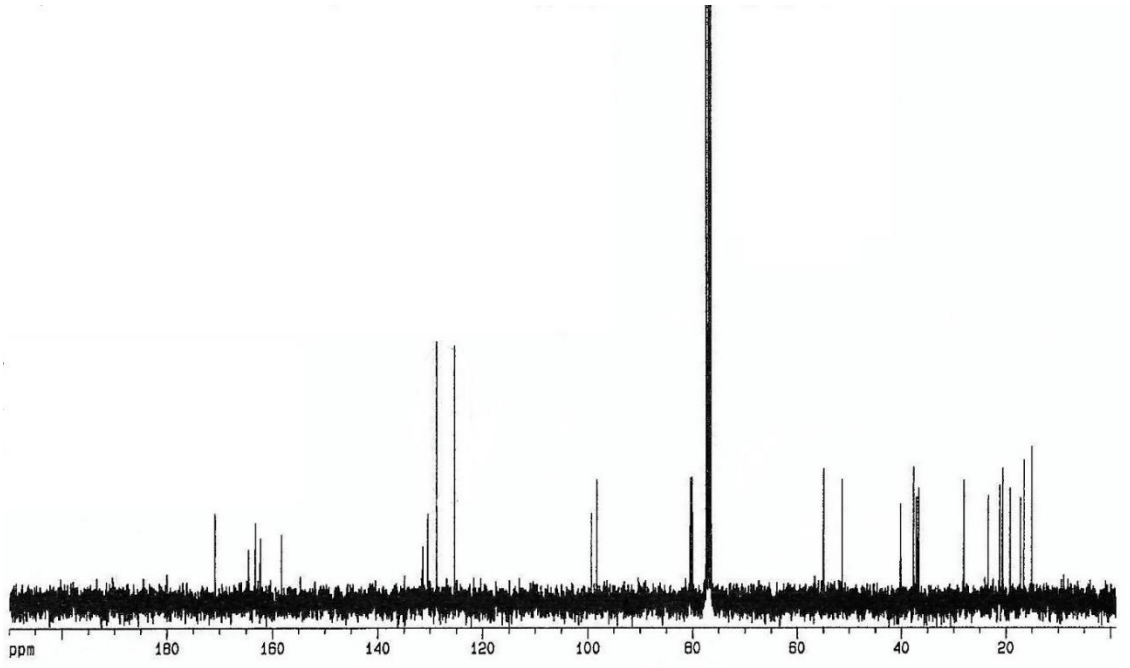

I.13) Pyripyropene E (154)

I.13.1) ^{1}H NMR spectrum (300.13 MHz)

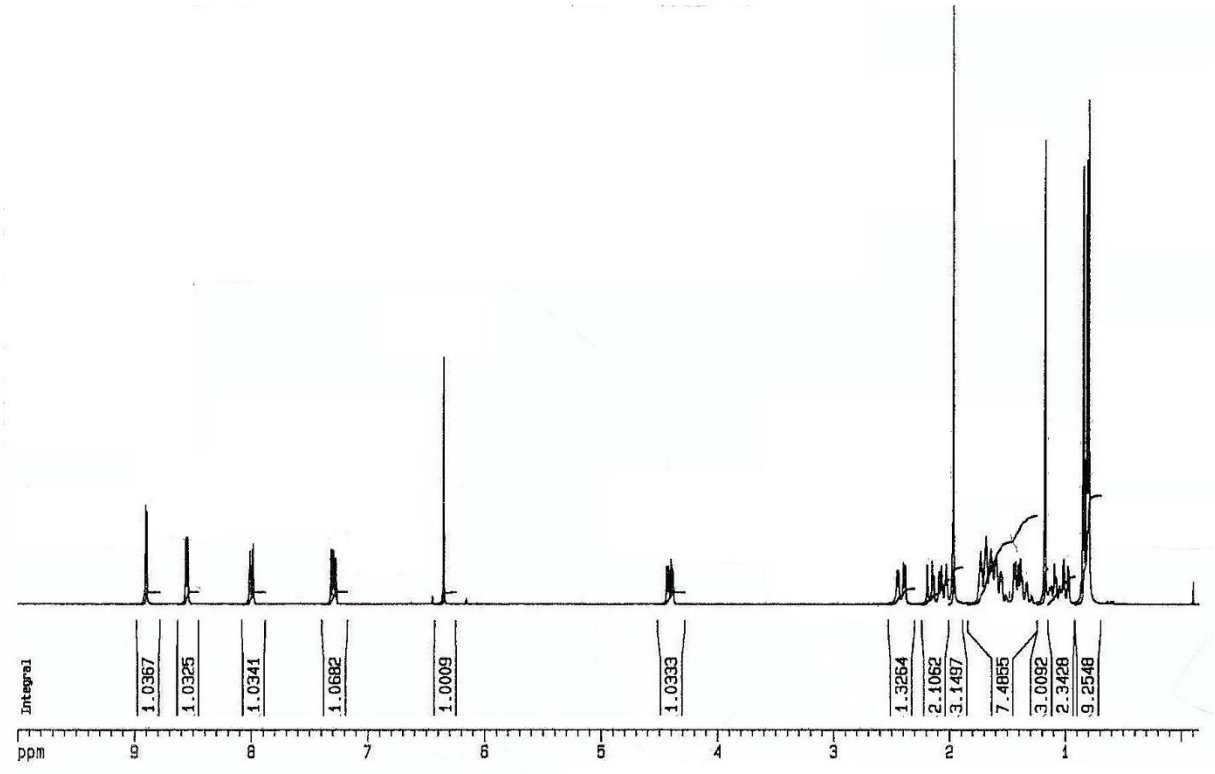

I.13.2) ^{13}C NMR spectrum (75.4 MHz)

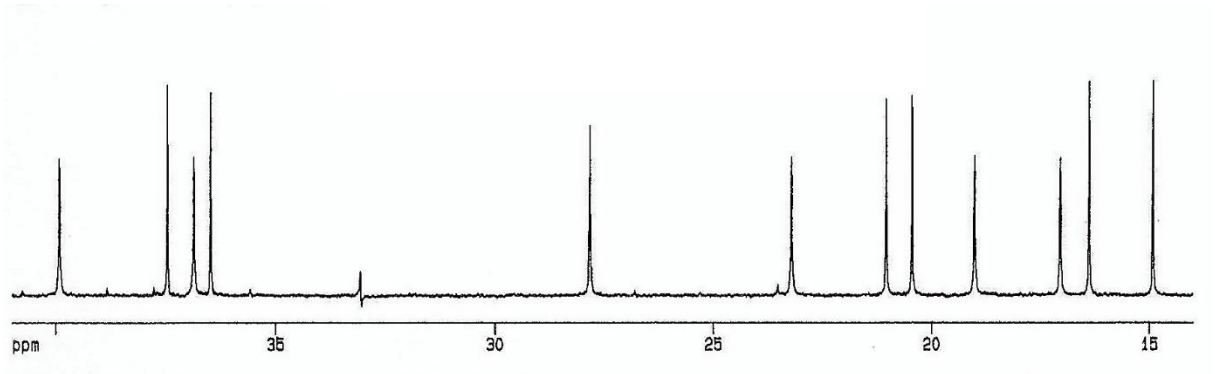

I.14) Pyripyropene S (378)

I.14.1) ^{1}H NMR spectrum (500.13 MHz)

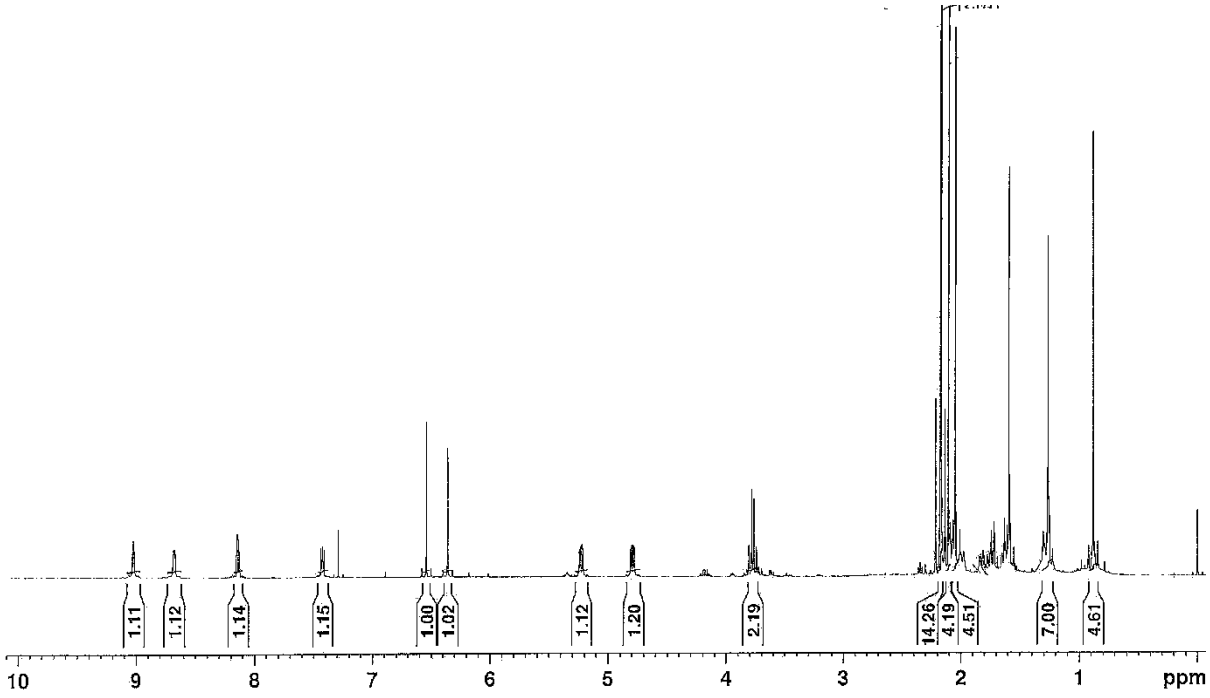

I.14.2) ^{13}C NMR spectrum (125.8 MHz)

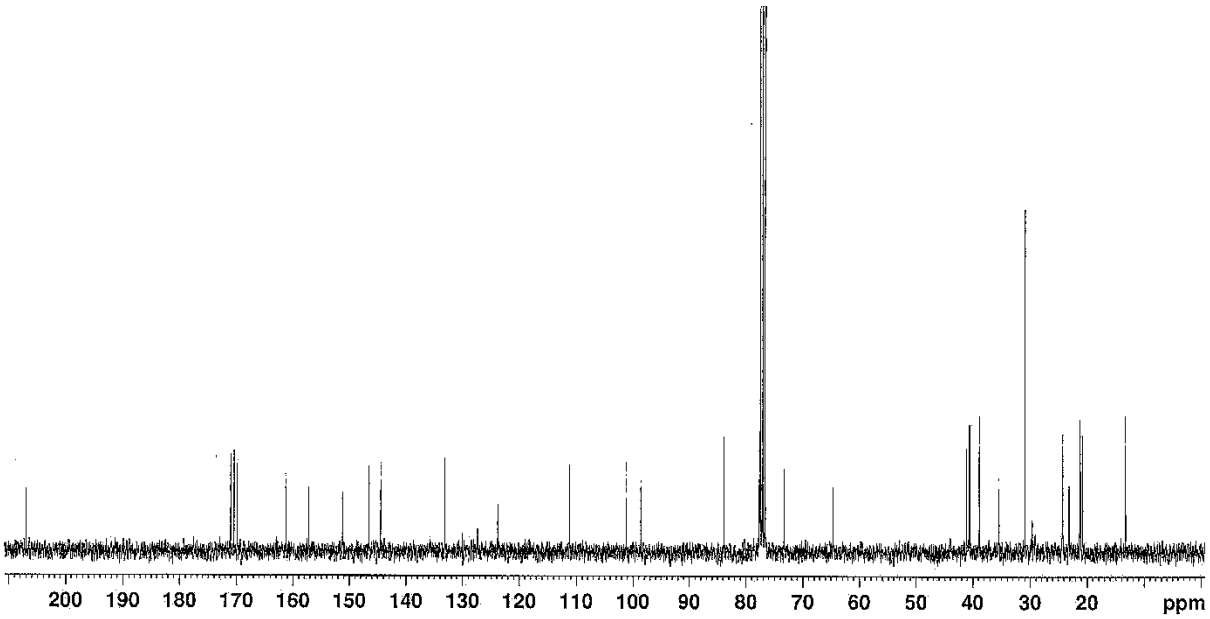

I.15) Pyripyropene T (379)

I.15.1) ^{1}H NMR spectrum (500.13 MHz)

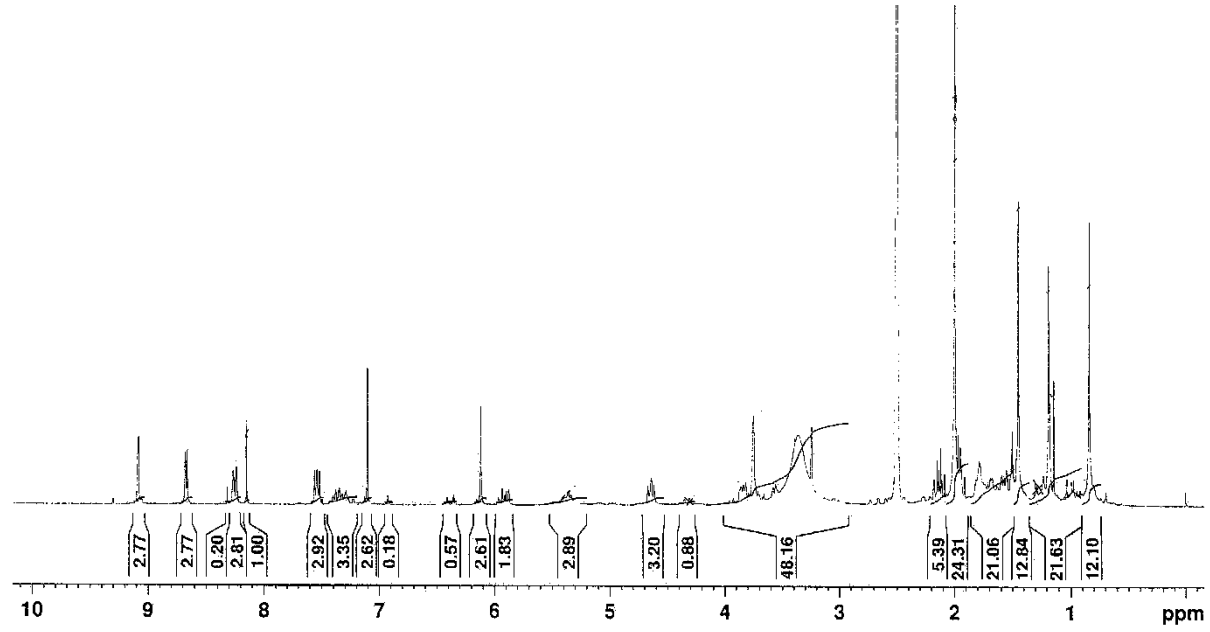

I.15.2) ^{13}C NMR spectrum (125.8 MHz)

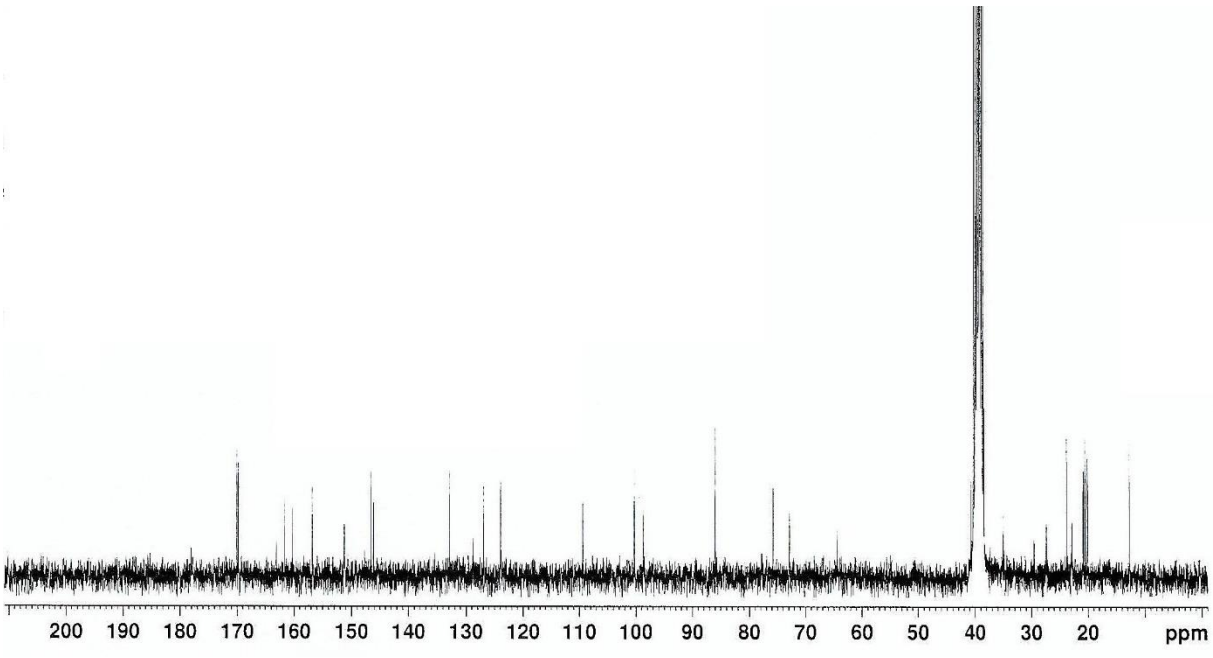

I.16) Similanamide (380)

I.16.1) ^{1}H NMR spectrum (500.13 MHz)

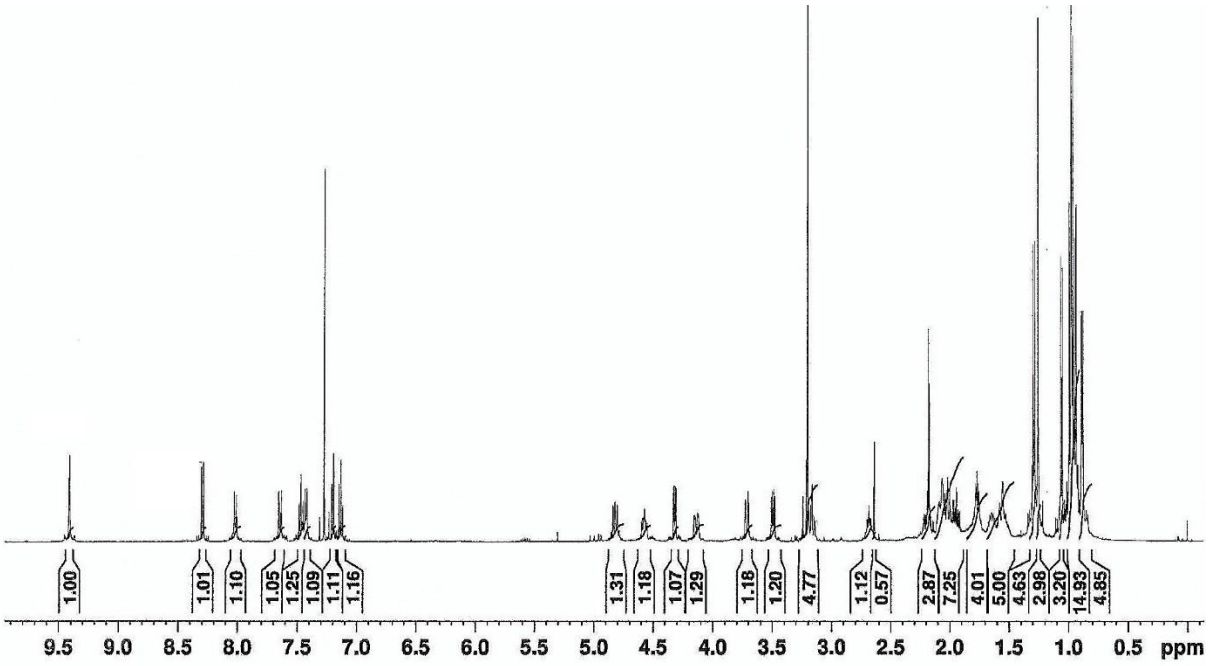

I.16.2) ^{13}C NMR spectrum (125.8 MHz)

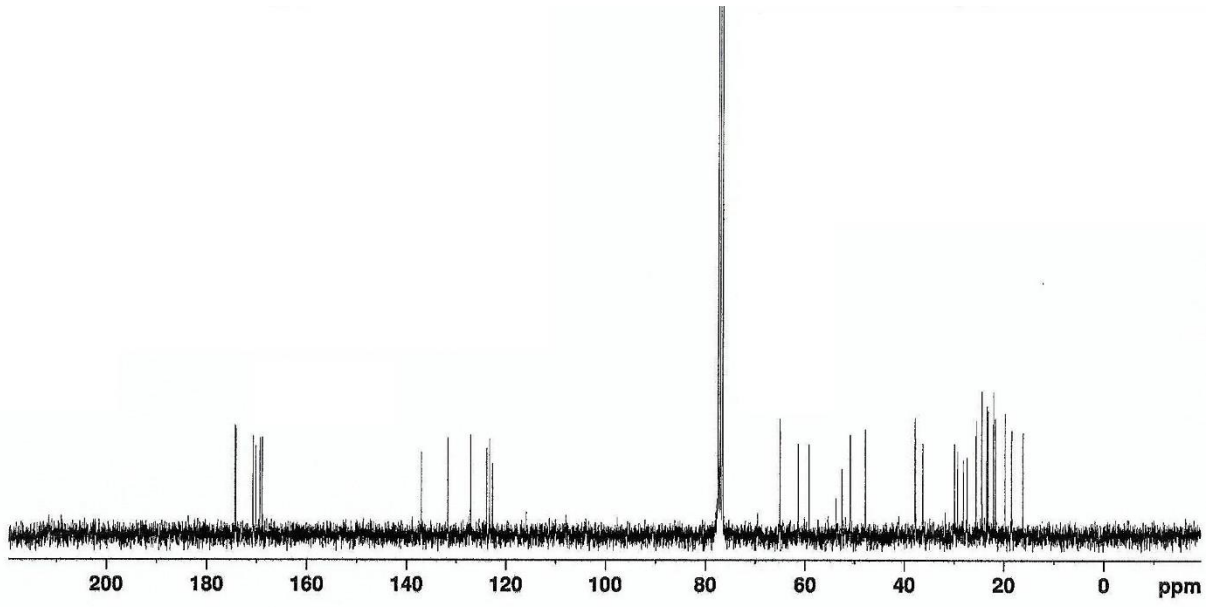

I.17) Quadricinctone A (381)

I.17.1) ^{1}H NMR spectrum (300.13 MHz)

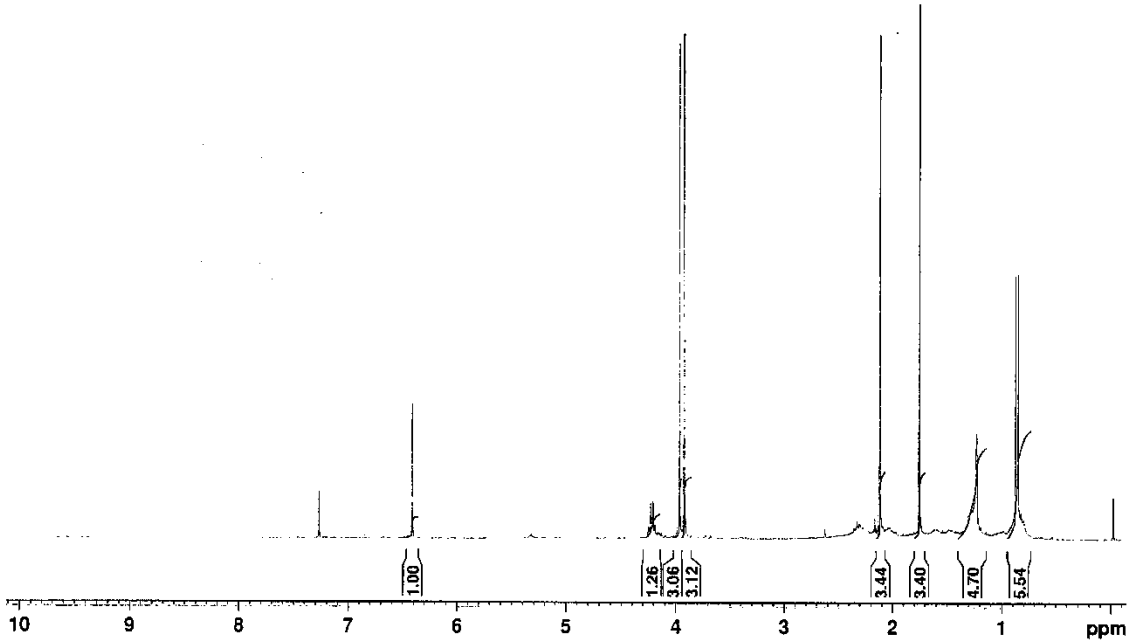

I.17.2) ^{13}C NMR spectrum (75.4 MHz)

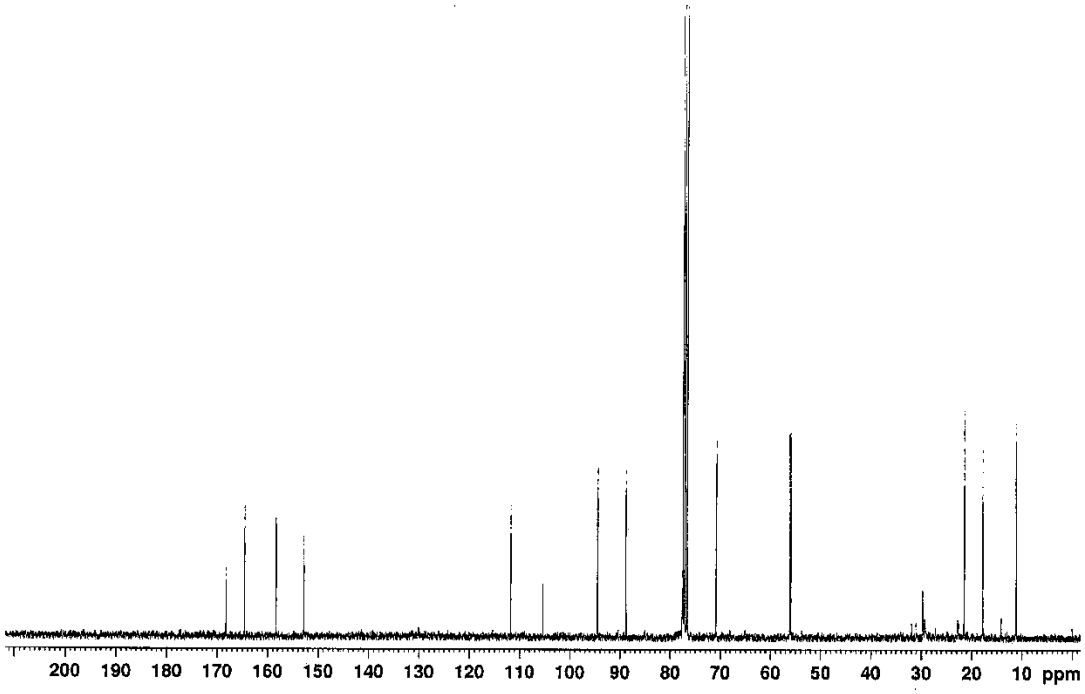

I.18) Quadricinctapyran A (382)

I.18.1) ^{1}H NMR spectrum (300.13 MHz)

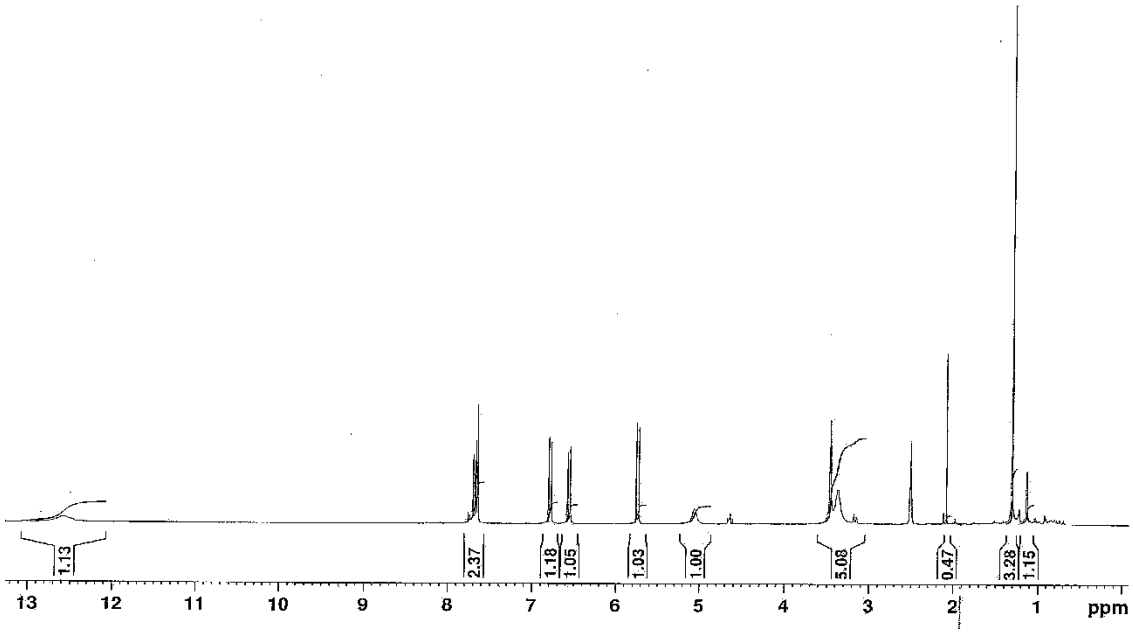

I.18.2) ^{13}C NMR spectrum (75.4 MHz)

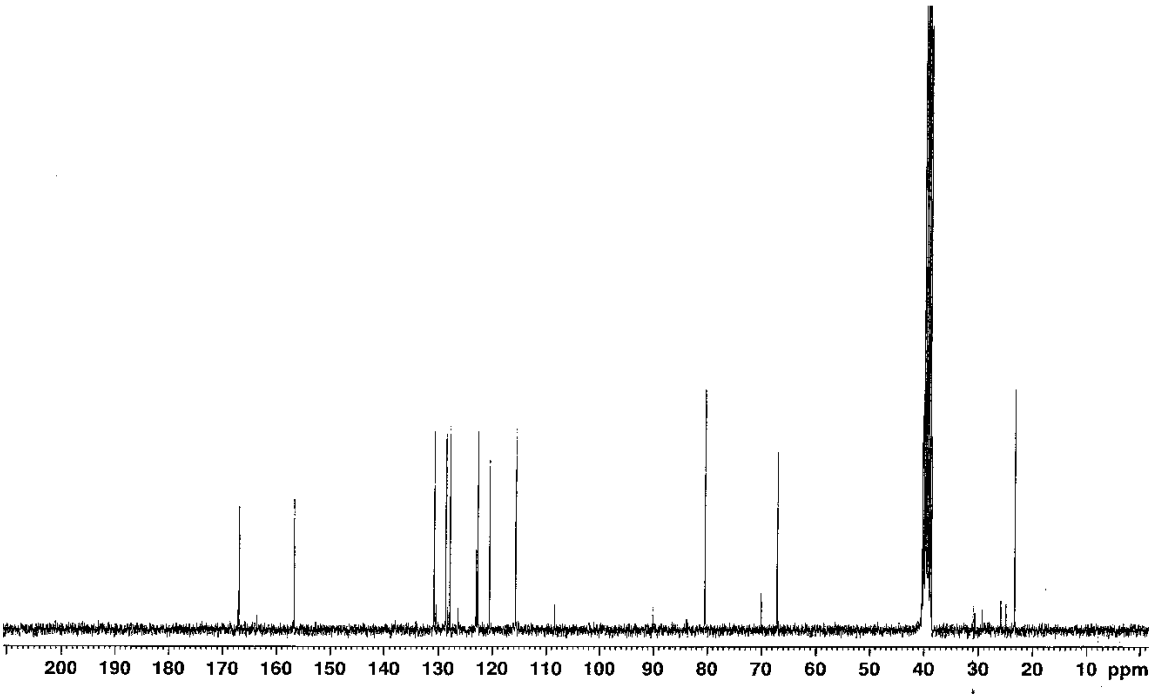

I.19) Quadricinctapyran B (383)

I.19.1) ^{1}H NMR spectrum (300.13 MHz)

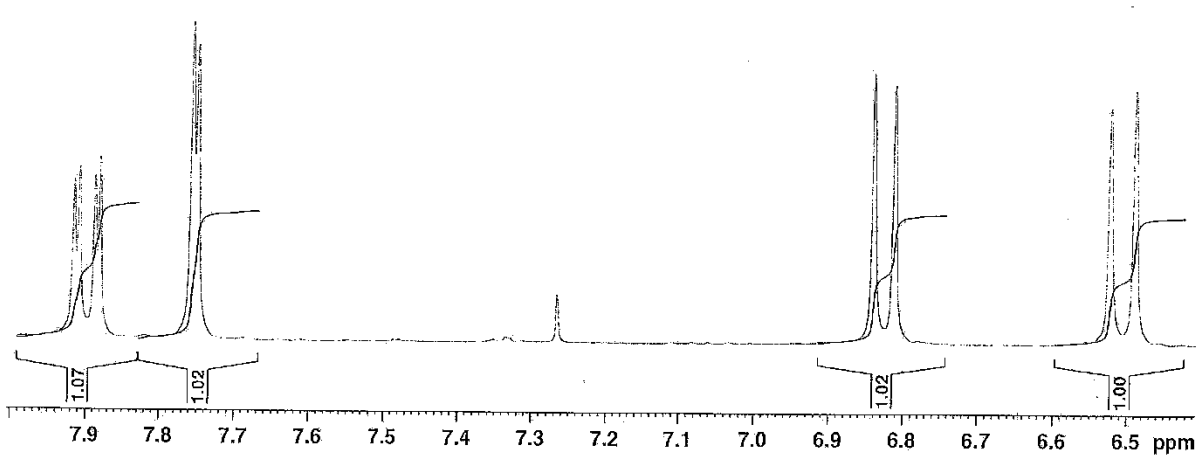

I.19.2) ^{13}C NMR spectrum (75.4 MHz)

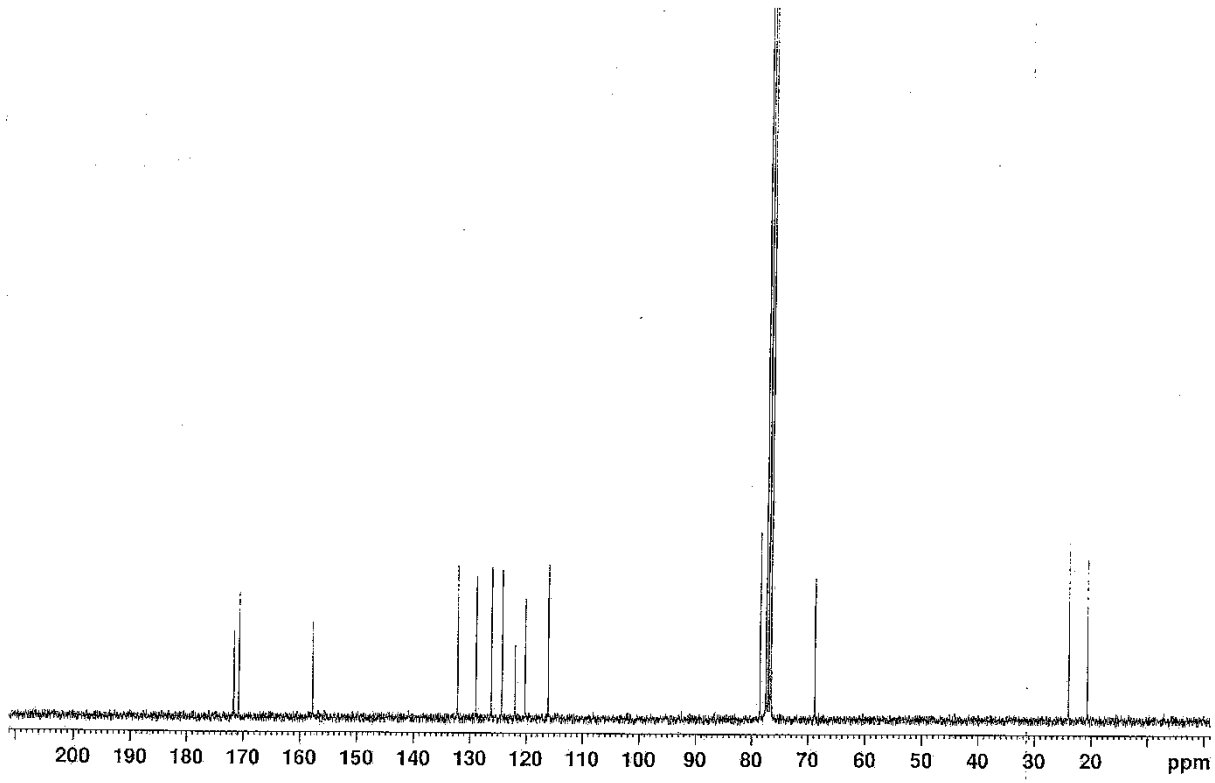

I.20) Quadricinctoxepine (384)

I.20.1) ^{1}H NMR spectrum (300.13 MHz)

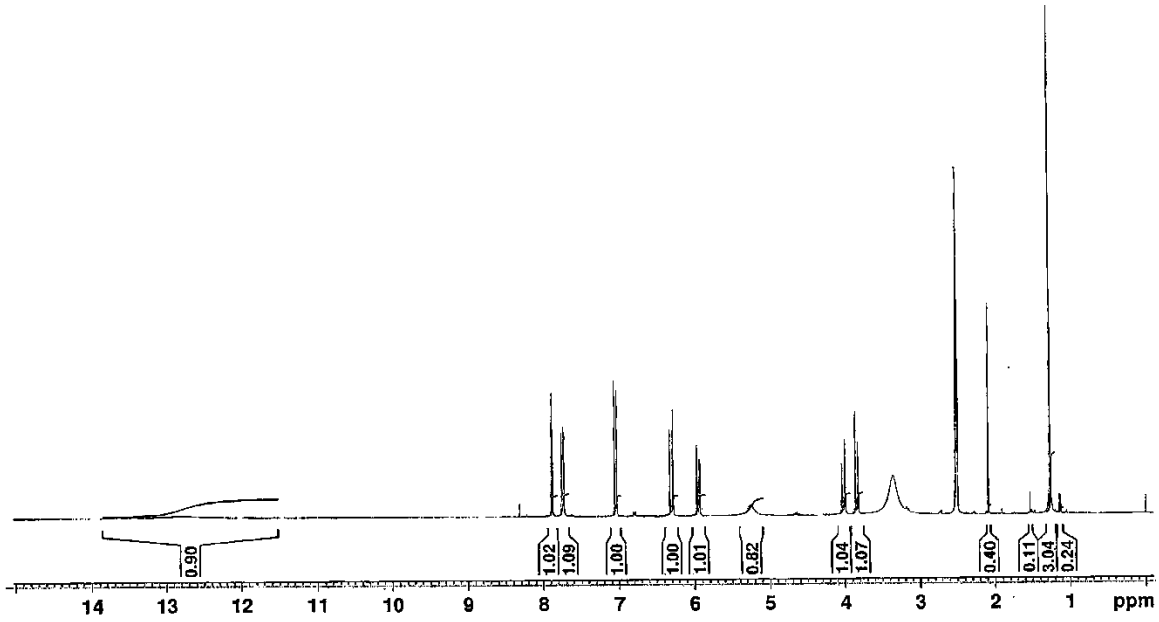

I.20.2) ^{13}C NMR spectrum (75.4 MHz)

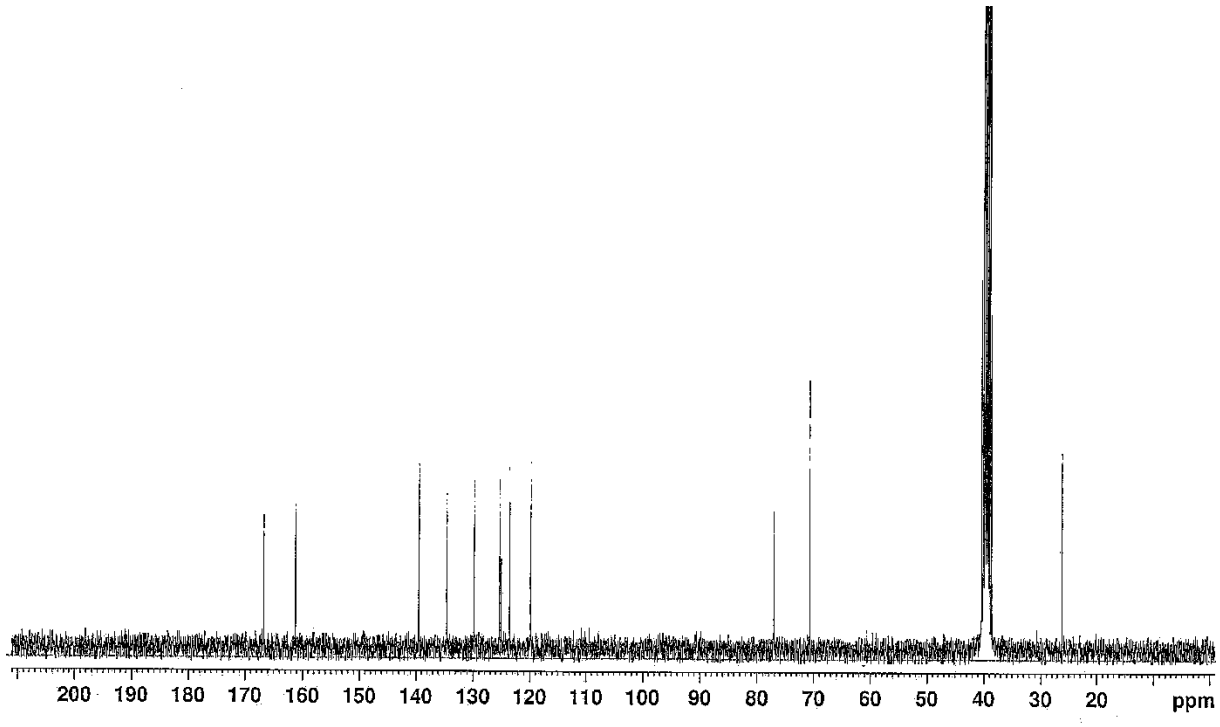

I.21) 6-Hydroxy-2,2-dimethyl-2,3-dihydro-4*H*-chromen-4-one (385)

I.21.1) ^{1}H NMR spectrum (300.13 MHz)

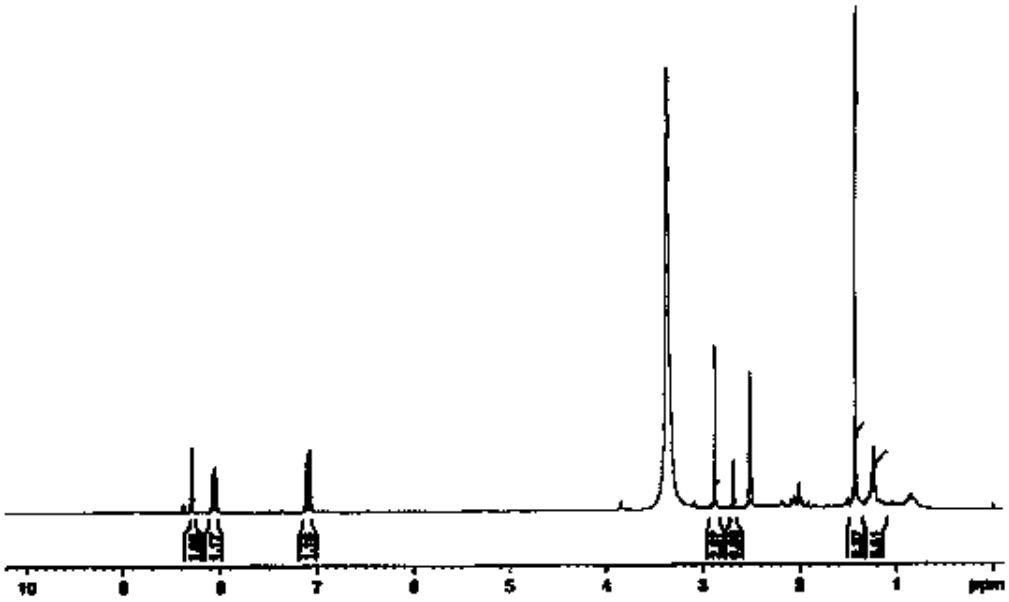

I.21.2) ^{13}C NMR spectrum (75.4 MHz)

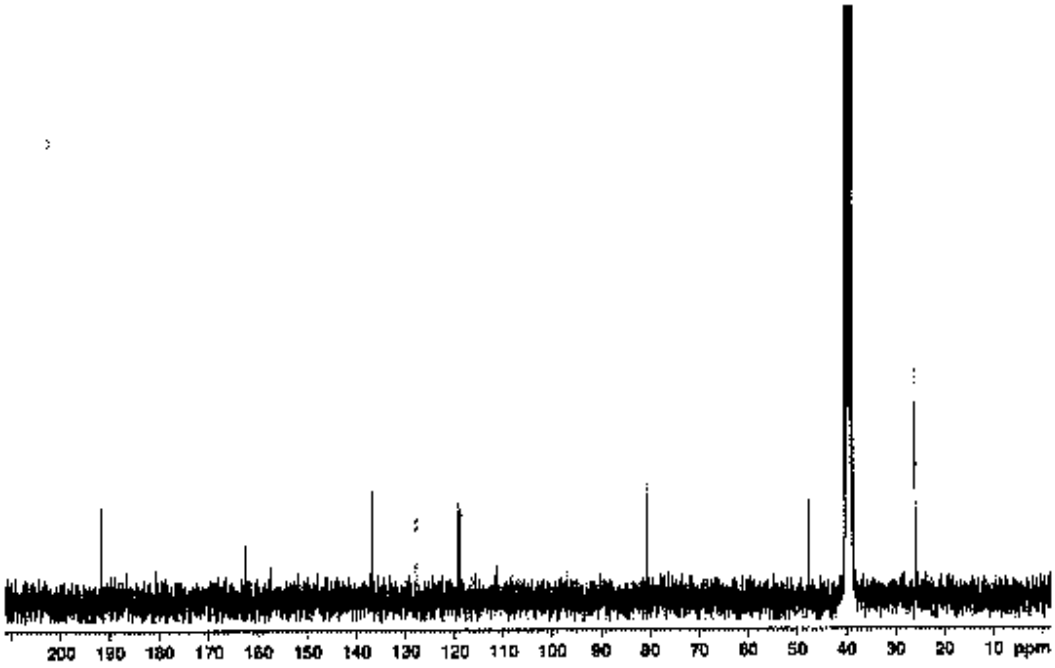

I.22) Quadricinctone B (386)

I.22.1) ^{1}H NMR spectrum (300.13 MHz)

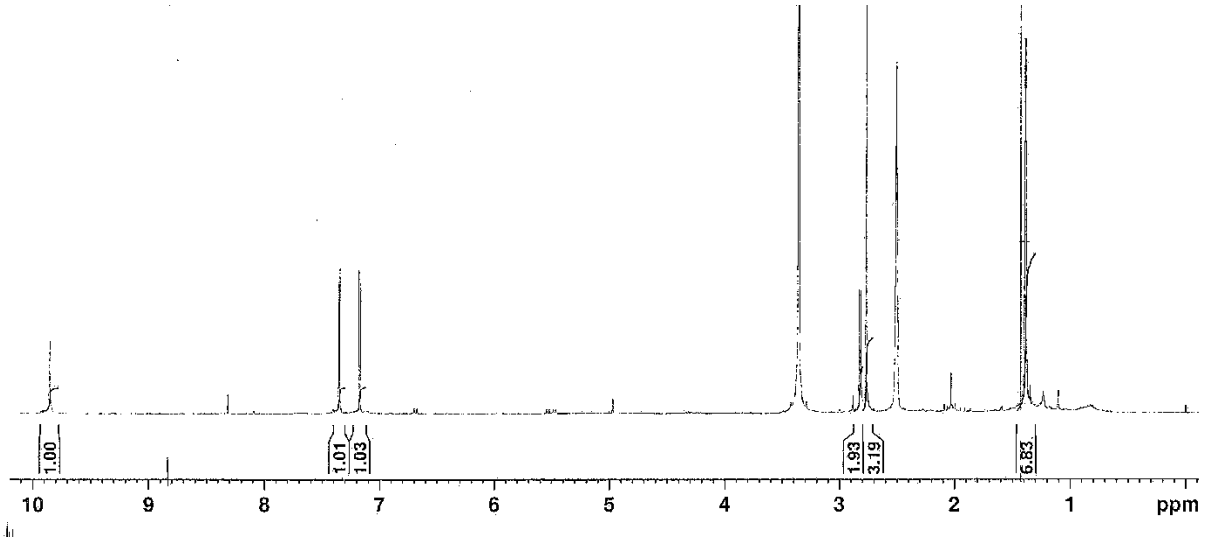

I.22.2) ^{13}C NMR spectrum (75.4 MHz)

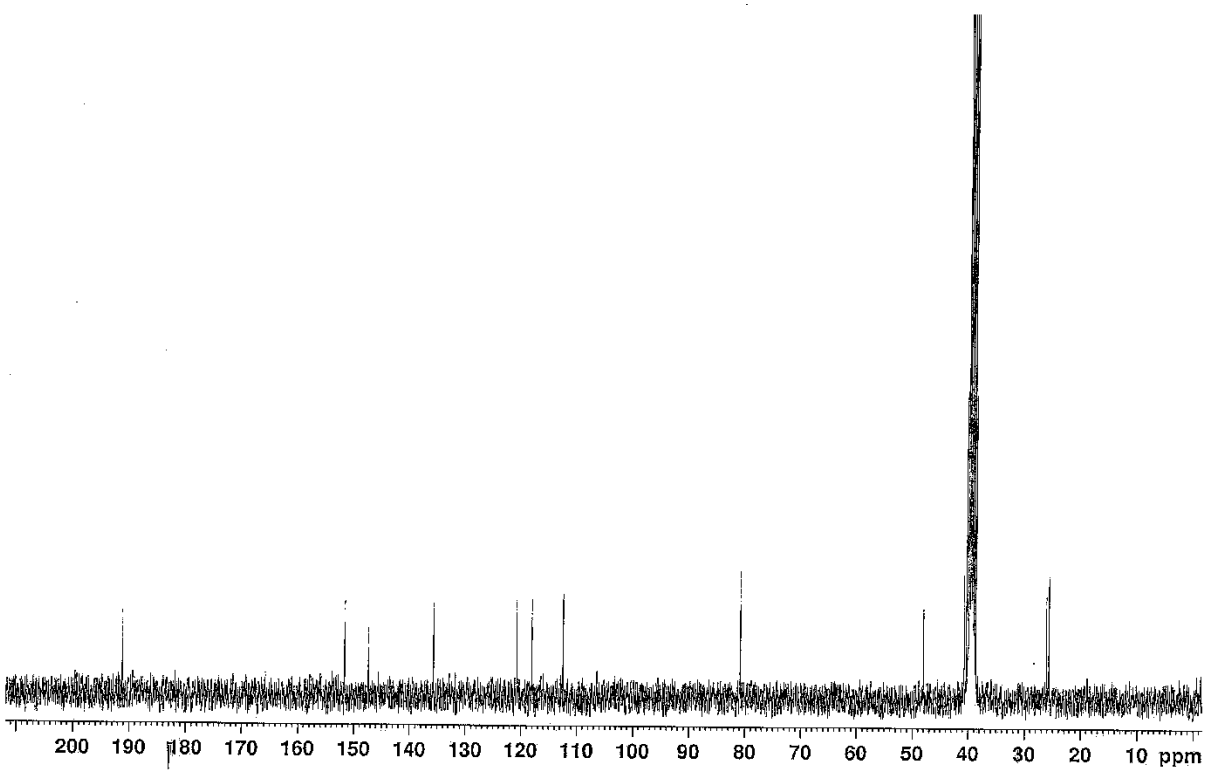

I.23) Quadricinctone C (387)

I.23.1) ^{1}H NMR spectrum (300.13 MHz)

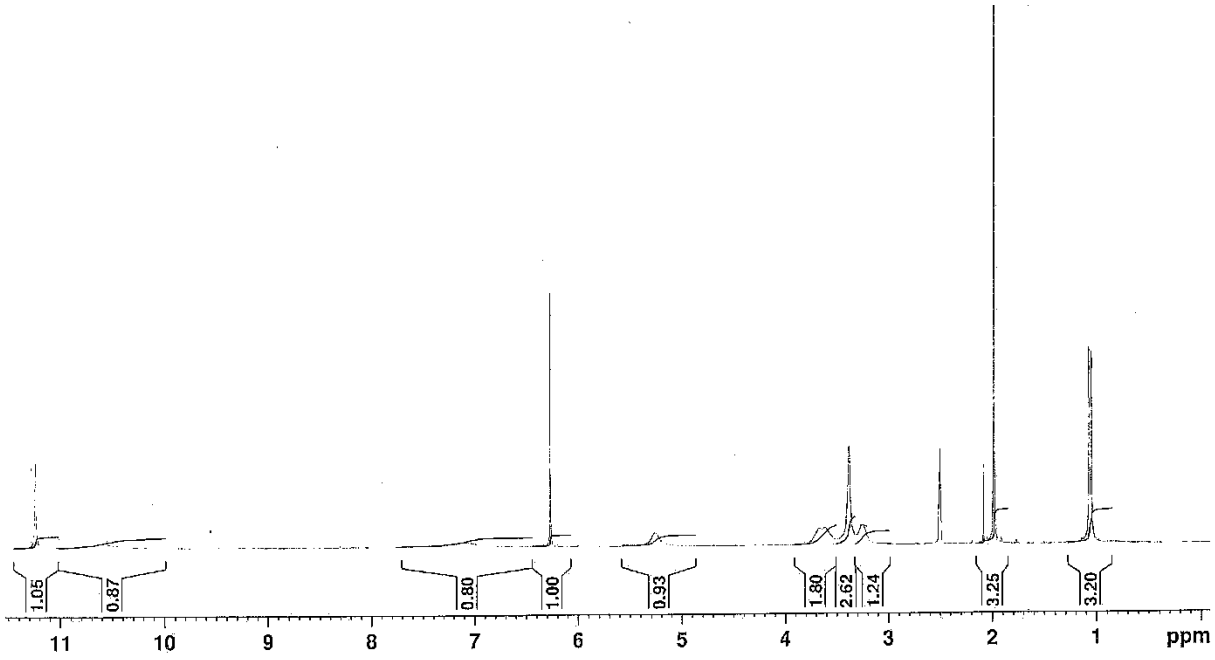

I.23.2) ^{13}C NMR spectrum (75.4 MHz)

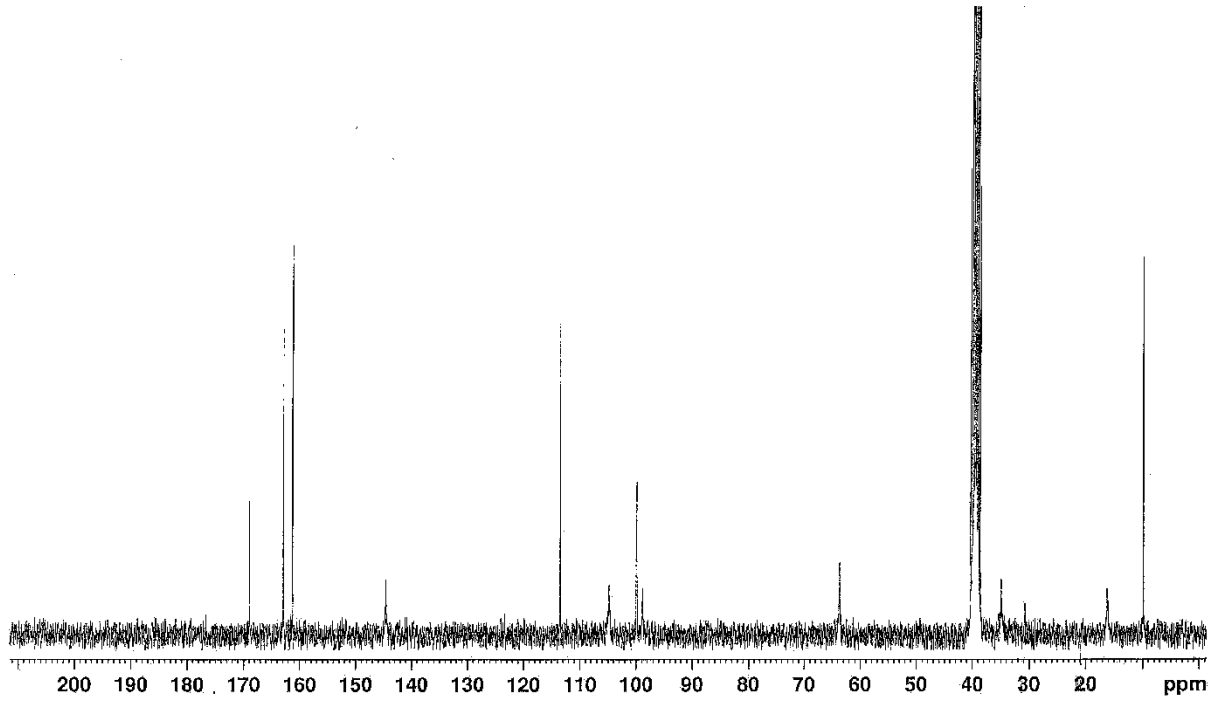

I.24) Quadricinctafuran A (388)

I.24.1) ^{1}H NMR spectrum (300.13 MHz)

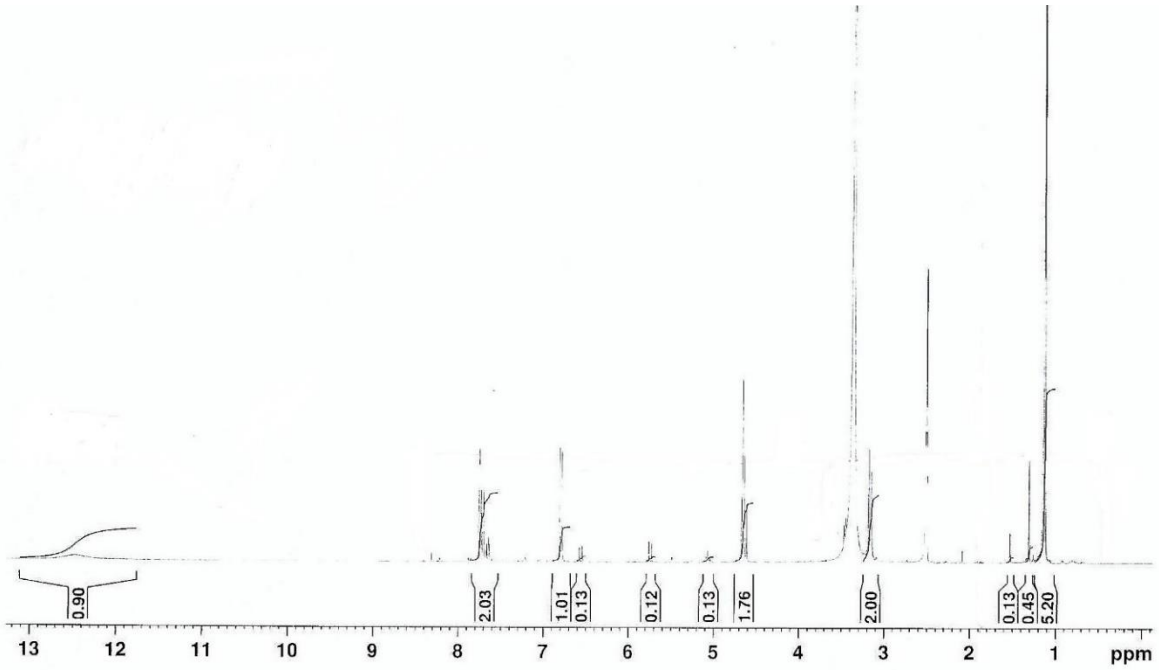

I.24.2) ^{13}C NMR spectrum (75.4 MHz)

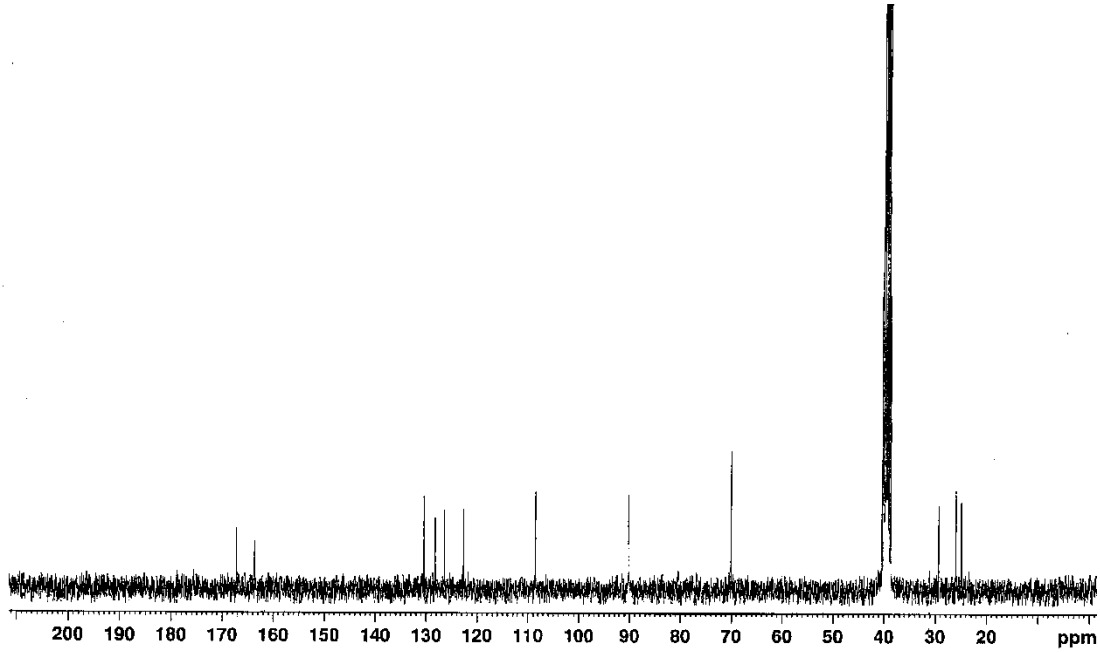

I.25) Quadricinctafuran B (389)

I.25.1) ^{1}H NMR spectrum (300.13 MHz)

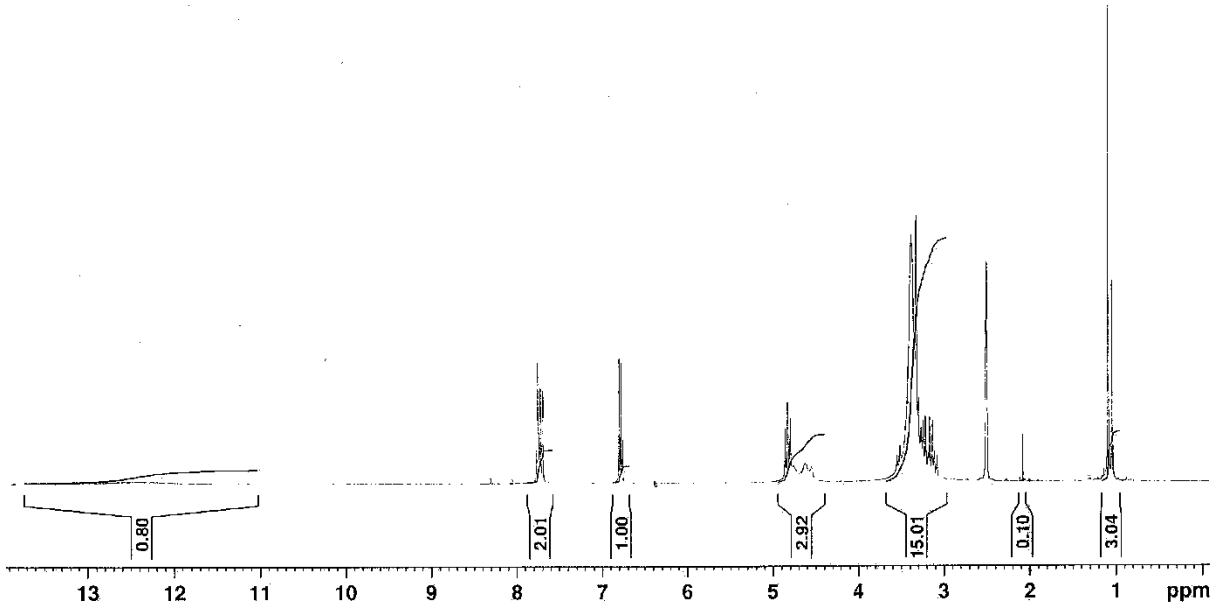

I.25.2) ^{13}C NMR spectrum (75.4 MHz)

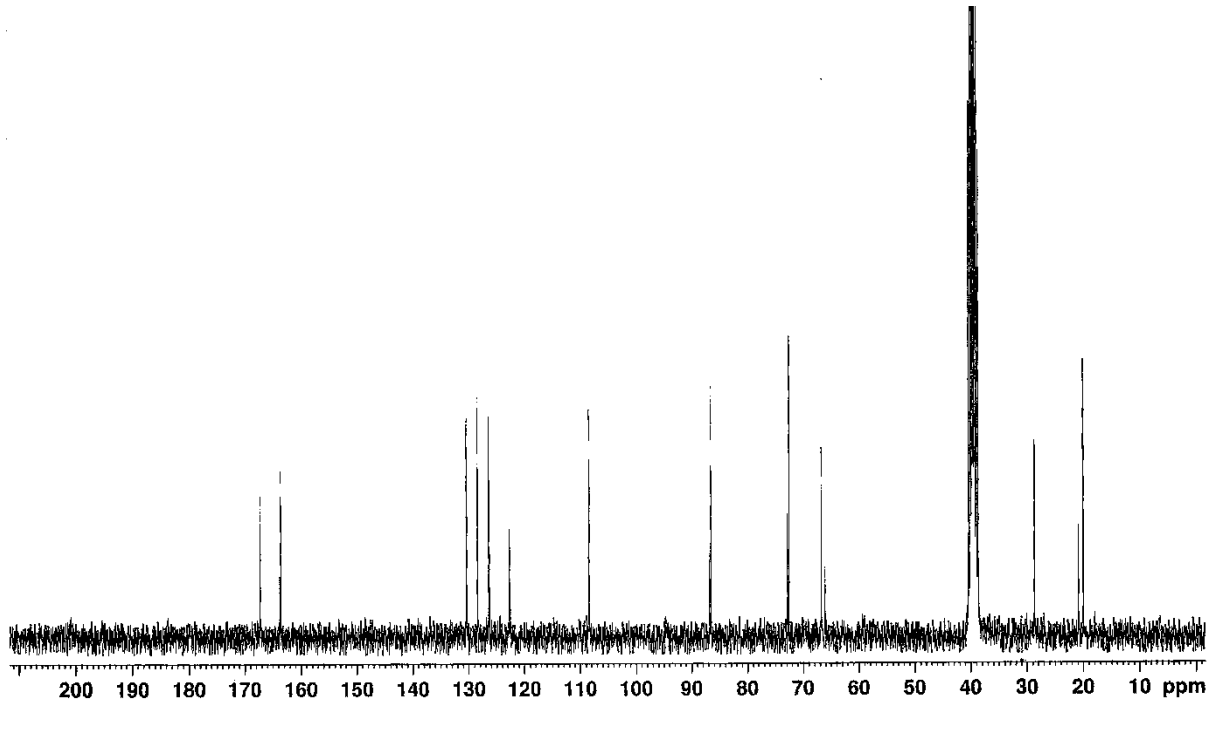

I.26) Quadricinctone D (390)

I.26.1) ^{1}H NMR spectrum (300.13 MHz)

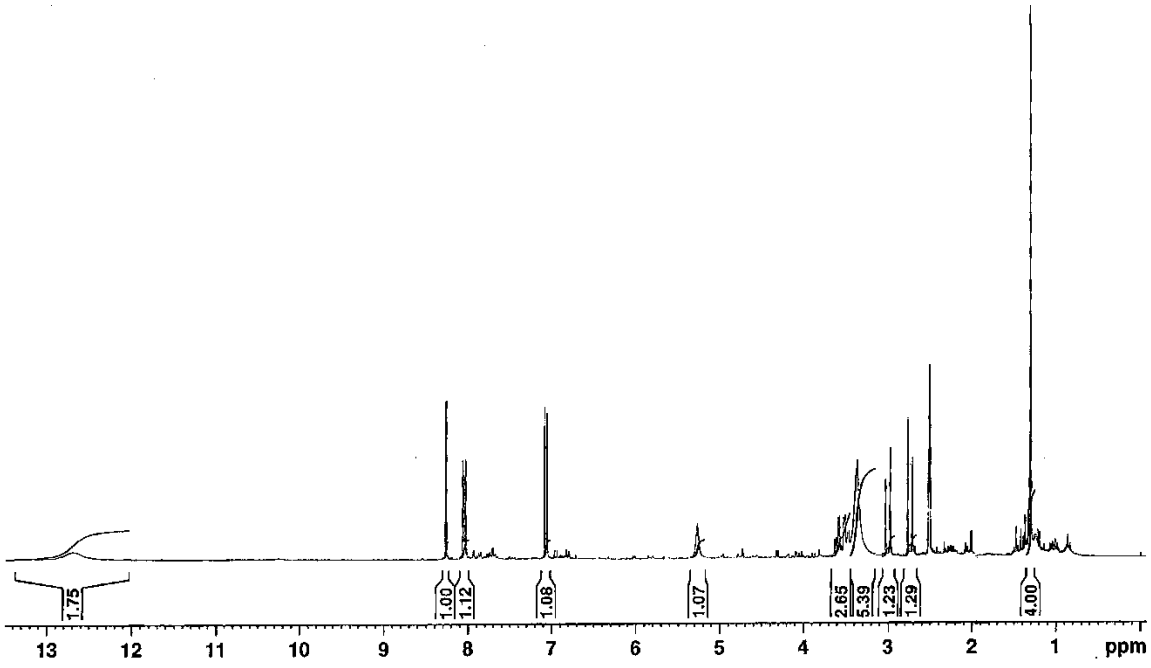

I.26.2) ^{13}C NMR spectrum (75.4 MHz)

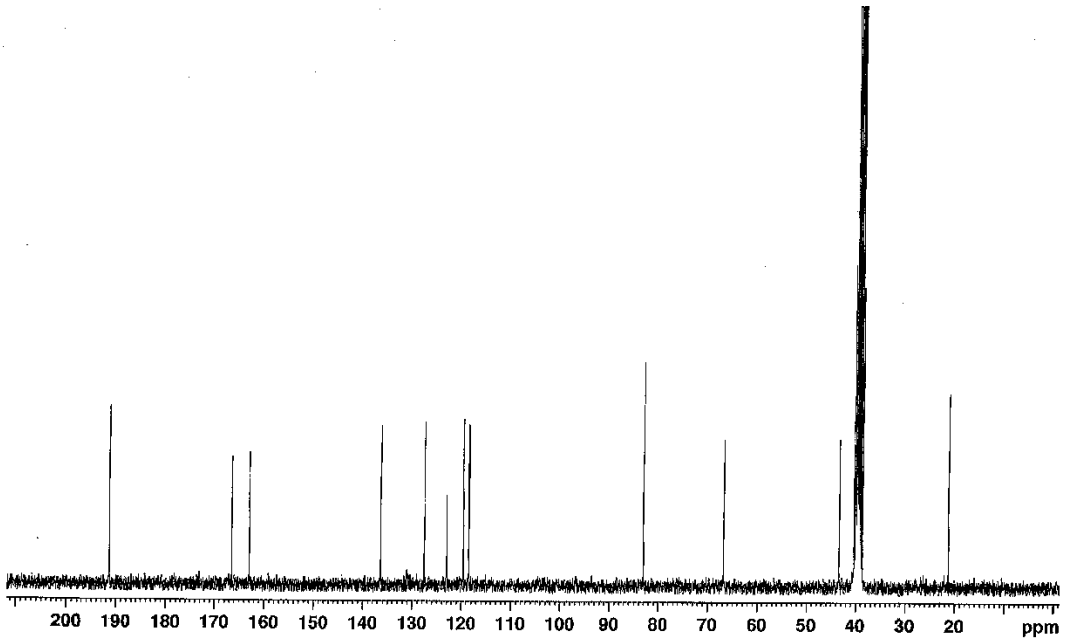

APPENDIX II

Prompanya, C**.**, Dethoup, T., Bessa, L. J., Pinto, M. M., Gales, L., Costa, P. M., Silva, A. M., & Kijjoa, A. (2014). New isocoumarin derivatives and meroterpenoids from the marine sponge-associated fungus *Aspergillus similanensis* sp. nov. KUFA 0013. *Mar. Drugs, 12*, 5160 – 5173. Doi:10.3390/md12105160

Mar. Drugs **2014**, *12*, 5160-5173; doi:10.3390/md12105160

OPEN ACCESS

marine drugs

ISSN 1660-3397

www.mdpi.com/journal/marinedrugs

Article

New Isocoumarin Derivatives and Meroterpenoids from the Marine Sponge-Associated Fungus *Aspergillus similanensis* sp. nov. KUFA 0013

Chadaporn Prompanya [1,2], Tida Dethoup [3], Lucinda J. Bessa [1,2], Madalena M. M. Pinto [2,4], Luís Gales [1,5], Paulo M. Costa [1,2], Artur M. S. Silva [6] and Anake Kijjoa [1,2,*]

1 ICBAS—Instituto de Ciências Biomédicas de Abel Salazar, Universidade do Porto, Rua de Jorge Viterbo Ferreira 228, 4050-313 Porto, Portugal; E-Mails: chadaporn@buu.ac.th (C.P.); lbessa@ciimar.up.pt (L.J.B.); lgales@ibmc.up.pt (L.G.); pmcosta@icbas.up.pt (P.M.C.)

2 Interdisciplinary Centre of Marine and Environmental Research (CIIMAR), Rua dos Bragas 289, 4050-123 Porto, Portugal

3 Department of Plant Pathology, Faculty of Agriculture, Kasetsart University, Bangkok 10240, Thailand; E-Mail: agrtdd@ku.ac.th

4 Centro de Química Medicinal da Universidade do Porto (CEQUIMED-UP) and Laboratório de Química Orgânica e Farmacêutica, Departamento de Ciências Químicas, Faculdade de Farmácia, Universidade do Porto, Rua de Jorge Viterbo 228, 4050-313 Porto, Portugal; E-Mail: madalena@ff.up.pt

5 Instituto de Biologia Celular e Molecular (IBMC), Universidade do Porto, 4099-003 Porto, Portugal

6 Departamento de Química & QOPNA, Universidade de Aveiro, 4810-193 Aveiro, Portugal; E-Mail: artur.silva@ua.pt

* Author to whom correspondence should be addressed; E-Mail: ankijjoa@icbas.up.pt; Tel.: +351-2-2042-8331; Fax: +351-2-2042-8090.

External Editor: Orazio Taglialatela-Scafati

Received: 28 July 2014; in revised form: 24 September 2014 / Accepted: 25 September 2014 / Published: 14 October 2014

Abstract: Two new isocoumarin derivatives, including a new 5-hydroxy-8-methyl-2*H*, 6*H*-pyrano[3,4-*g*]chromen-2,6-dione (**1**) and 6,8-dihydroxy-3,7-dimethylisocoumarin (**2b**), a new chevalone derivative, named chevalone E (**3**), and a new natural product pyripyropene S (**6**) were isolated together with 6, 8-dihydroxy-3-methylisocoumarin (**2a**), reticulol (**2c**), *p*-hydroxybenzaldehyde, chevalone B, chevalone C, S14-95 (**4**), and pyripyropene E (**5**) from the ethyl acetate extract of the undescribed marine sponge-associated fungus

Aspergillus similanensis KUFA 0013. The structures of the new compounds were established based on 1D and 2D NMR spectral analysis, and in the case of compound **3**, X-ray analysis was used to confirm its structure and the absolute configuration of its stereogenic carbons. Compounds **1**, **2a**–**c** and **3**–**6** were evaluated for their antimicrobial activity against Gram-positive and Gram-negative bacteria, *Candida albicans* ATCC 10231, and multidrug-resistant isolates from the environment. Chevalone E (**3**) was found to show synergism with the antibiotic oxacillin against methicillin-resistant *Staphylococcus aureus* (MRSA).

Keywords: *Aspergillus similanensis*; similanpyrones; isocoumarins; meroditerpenes; pyripyropenes; chevalones

1. Introduction

Neosartorya is a teleomorphic (sexual) state of *Aspergillus* section *Fumigati*. Although *Neosartorya* species (Trichocomaceae) have not been as extensively investigated for their secondary metabolites as *Aspergillus*, they have recently been shown to be an interesting source of many bioactive compounds [1–9]. In our ongoing search for new natural products with antibacterial activity produced by the marine-derived fungi of the genus *Neosartorya*, we have investigated the secondary metabolites of a Thai collection of a new species of *Neosartorya*, isolated from the marine sponge *Rhabdermia* sp., collected from the Similan Islands, Phang Nga Province, Southern Thailand. However, in order to comply with the recent "International Code of Nomenclature for algae, fungi and plants (The Melbourne Code)", the strain was renamed *Aspergillus similanensis* (KUFA0013). The ethyl acetate extract of its culture furnished, besides chevalones B and C [9,10], *p*-hydroxybenzaldehyde, reticulol (**2c**) [11], 6,8-dihydroxy-3-methylisocoumarin (**2a**) [12], a meroterpenoid S14-95 (**4**) [13], pyripyropene E (**5**) [14], two new isocoumarins which we have named similanpyrones A (**1**) and B (**2b**), a new chevalone analog (**3**), and a new natural product which we have named pyripyropene S (**6**) [15] (Figure 1). Compounds **1**, **2a**–**c**, **3**–**6** were evaluated for their antimicrobial activity against Gram positive (*Staphylococcus aureus* ATCC 25923 and *Bacillus subtilis* ATCC 6633) and Gram negative (*Escherichia coli* ATCC 25922 and *Pseudomonas aeruginosa* ATCC 27853) bacteria, *Candida albicans* ATCC 10231, as well as multidrug-resistant isolates from the environment.

Figure 1. Secondary metabolites from *Aspergillus similanensis* KUFA0013.

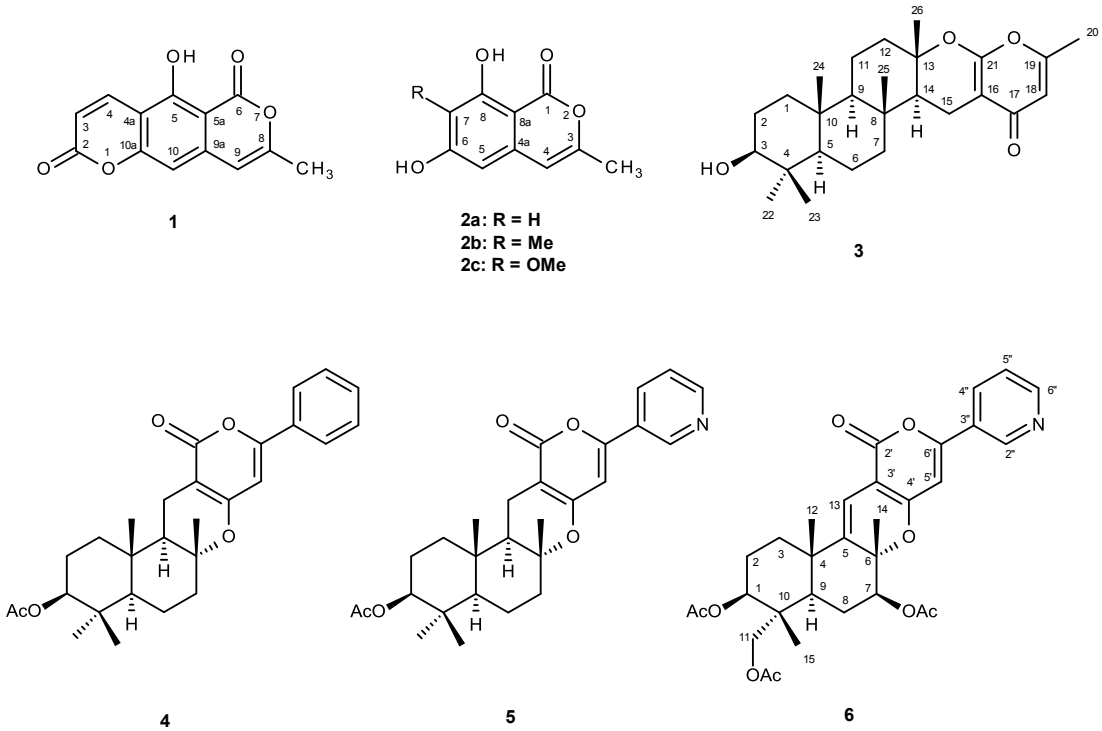

2. Results and Discussion

Compound **1** was isolated as white solid (mp, 322–323 °C), and its molecular formula $C_{13}H_8O_5$ was established on the basis of the (+)-HRESIMS *m/z* 245.0450 $[M + H]^+$, indicating ten degrees of unsaturation. The IR spectrum showed absorption bands for hydroxyl (3446 cm^{-1}), conjugated lactone carbonyl (1748, 1698 cm^{-1}), aromatic (1658 cm^{-1}) and olefin (1634, 1464 cm^{-1}) groups. The ^{13}C NMR (Supplementary Information, Figure S2), DEPTs and HSQC spectra (Table 1, Supplementary Information, Figure S4) revealed the presence of two conjugated ester carbonyls (δ_C 166.3 and 159.7), six quaternary sp^2 (δ_C 101.3, 107.3, 130.0, 140.1, 156.2 and 160.3), four methine sp^2 (δ_C 102.7, 104.6, 114.1, and 137.8) and one methyl (δ_C 19.6) carbons. The ^1H NMR spectrum (Supplementary Information, Figure S1) revealed, besides a singlet of the hydrogen bonded hydroxyl proton at δ_H 11.90, two doublets of the *cis*-olefinic protons at δ_H 8.13 (J = 9.8 Hz) and 6.36 (J = 9.8 Hz), two singlets at δ_H 6.33 and 6.70, and one methyl singlet at δ_H 2.33. The COSY spectrum (Table 1; Supplementary Information, Figure S3) exhibited cross peak between the singlet at δ_H 6.33 (H-9) and the methyl singlet at δ_H 2.33 (Me-8), suggesting that they were allylically coupled. On the other hand, the HMBC spectrum (Table 1; Supplementary Information, Figure S5) showed cross peaks of H-9 to C-8 (δ_C 156.2), C-9a (δ_C 130.3), C-10 (δ_C 102.7), and C-5a (δ_C 101.3), of H-10 (δ_H 6.70, s) to C-5a, C-4a (δ_C 107.3), C-9a and C-10a (δ_C 140.1), of Me-8 to C-8 and C-9 (δ_C 104.6), and of OH-5 (δ_H 11.90) to C-5 (δ_C 160.3), C-5a and C-4a. Taking together the ^1H and ^{13}C chemical shift values and the COSY, HSQC and HMBC correlations (Table 1), the presence of 4a, 10a-disubstituted-5-hydroxy-8-methylisochromen-6-one was corroborated. That the 5-hydroxy-8-methylisochromen-6-one nucleus was fused with a pyran-2-one moiety on C-4a and C-10a was substantiated by the HMBC correlations of H-4 (δ_H 8.13, d, J = 9.8 Hz) to C-10a (δ_C 140.1), and of H-3 (δ_H 6.36, d, J = 9.8 Hz) to C-4a (δ_C 107.3) and C-2 (δ_C 159.7),

respectively. Thus, the structure of compound **1** was established as 5-hydroxy-8-methyl-2*H*, 6*H*-pyrano[3,4-*g*]chromene-2,6-dione. To the best of our knowledge, this is the first report on the isolation of a secondary metabolite with both coumarin and isocoumarin functionalities in the same molecule. Thus, compound **1** is a new compound which we have named similanpyrone A.

Table 1. ^{1}H and ^{13}C NMR ($CDCl_3$, 500.13 MHz and 125.8 MHz) and HMBC assignment for similanpyrone A (**1**).

Position	δ_C, Type	δ_H, (*J* in Hz)	COSY	HMBC
2	159.7, C	-		
3	114.1, CH	6.36, d (9.8)	H-4	10a
4	137.8, CH	8.13, d (9.8)	H-3	C-2, 4a
4a	107.3, C	-		
5	160.3, C	-		
5a	101.3, C	-		
6	166.3, C	-		
8	156.2, C	-		
9	104.6, CH	6.33, s	CH_3-8	C-5a, 8, 10, Me-8
9a	130.0, C	-		
10	102.7, CH	6.70, s		C-4a, 5a, 9a, 10a
10a	140.1, C	-		
CH_3-8	19.6, CH_3	2.33, s	H-9	C-8, 9
OH-5	-	11.90, s		C-4a, 5, 5a

Compound **2b** was also isolated as white solid (mp, 162–163 °C), and its molecular formula $C_{11}H_{10}O_4$ was established on the basis of the (+)-HRESIMS *m/z* 207.0658 $[M + H]^+$, indicating seven degrees of unsaturation. The IR spectrum showed absorption bands for hydroxyl (3243, 3160 cm^{-1}), conjugated carbonyl (1677 cm^{-1}), olefin (1635 cm^{-1}) and aromatic (1617 cm^{-1}) groups. The general feature of the ^{1}H (Supplementary Information, Figure S6), and ^{13}C NMR spectra (Supplementary Information, Figure S7) of **2b** (Table 2) closely resembled those of **1**, except for the absence of the proton and carbon signals of the pyran-2-one moiety. Instead, there were an additional methyl (δ_H 2.00 s; δ_C 8.0) and hydroxyl (δ_H 3.45 brs) groups in the structure of **2b**. That the second methyl group was on C-7 and the second hydroxyl group was on C-6 was corroborated by the HMBC cross peaks of the methyl singlet at δ_H 2.20, s to the signals of C-6 (δ_C 163.7), C-7 (δ_C 109.6) and C-8 (δ_C 106.9). Thus, the structure of compound **2b** was established as 6, 8-dihydroxy-3, 7-dimethylisochromen-1-one. Literature survey revealed that **2b** is a new compound, and therefore we have named it similanpyrone B.

Compound **3** was isolated as white crystals (mp, 262–263 °C), and its molecular formula $C_{26}H_{38}O_4$ was established on the basis of the (+)-HRESIMS *m/z* 415.2851 $[M + H]^+$, indicating eight degrees of unsaturation. The IR spectrum showed absorption bands for hydroxyl (3300 cm^{-1}), conjugated carbonyl (1664 cm^{-1}) and olefin (1607, 1570 cm^{-1}) groups. The ^{13}C NMR (Supplementary Information, Figure S9), DEPTs and HSQC spectra revealed the presence of one conjugated ketone carbonyl (δ_C 180.6), three quaternary sp^2 (δ_C 162.6, 160.5, 98.5), one methine sp^2 (δ_C 111.9), one oxygen bearing quaternary sp^3 (δ_C 84.3), one oxygen bearing methine sp^3 (δ_C 78.7), three quaternary sp^3 (δ_C 37.1, 37.3, 38.9), three methine sp^3 (δ_C 52.3, 55.3, 60.3), seven methylene sp^3 (δ_C 15.2, 17.9, 18.7, 27.2, 38.4, 40.1,

41.1) and six methyl (δ_C 15.4, 16.1, 16.4, 19.2, 20.5, 28.0) carbons. The general feature of the ^1H (Supplementary Information, Figure S8), and ^{13}C NMR spectra of **3** resembled those of chevalone C [9], except for the chemical shift values of the oxygen bearing methine carbon (C-3) which appeared at lower frequencies (δ_C 78.7; δ_H 3.21, dd, J = 11.1, 5.0 Hz) than those of chevalone C [9]. Furthermore, the ^1H and ^{13}C NMR spectra of compound **3** did not exhibit the signals of the acetyl group. Taking together the IR, HRMS and NMR data, it was possible to conclude that compound **3** is a deacetyl analog of chevalone C. Since this is the first report of isolation of this chevalone analog, we have named it chevalone E. Final proof of the structure and the stereochemistry assigned to chevalone E (**3**) was provided by an X-ray analysis (Figure 2), and since the diffraction data were collected with a Gemini PX Ultra equipped with CuKα radiation, it was possible to establish the absolute configuration of C-3, C-5, C-8, C-9, C-10, C-13 and C-14, respectively as 3*S*, 5*R*, 8*R*, 9*R*, 10*R*, 13*S* and 14*S*.

Table 2. ^1H and ^{13}C NMR ($CDCl_3$, 500.13 MHz and 125.8 MHz) and HMBC assignment for similanpyrone B (**2b**).

Position	δ_C, Type	δ_H, (*J* in Hz)	COSY	HMBC
1	166.1, CO	-		
3	153.3, C	-		
4	104.2, CH	6.46, s	CH_3-3	C-5, 8a
4a	136.5, C	-		
5	101.4, CH	6.40, s		C-4, 6, 7, 8a
6	163.7, C	-		
7	109.6, C	-		
8	160.0, C	-		
8a	97.5, C	-		
CH_3-3	18.8, CH_3	2.20, s		C-3, 4
CH_3-7	8.0, CH_3	2.00, s		C-6, 7, 8
OH-6	-	3.45, br		
OH-8	-	11.27, s		C-7, 8, 8a

Figure 2. Ortep view of chevalone E (**3**).

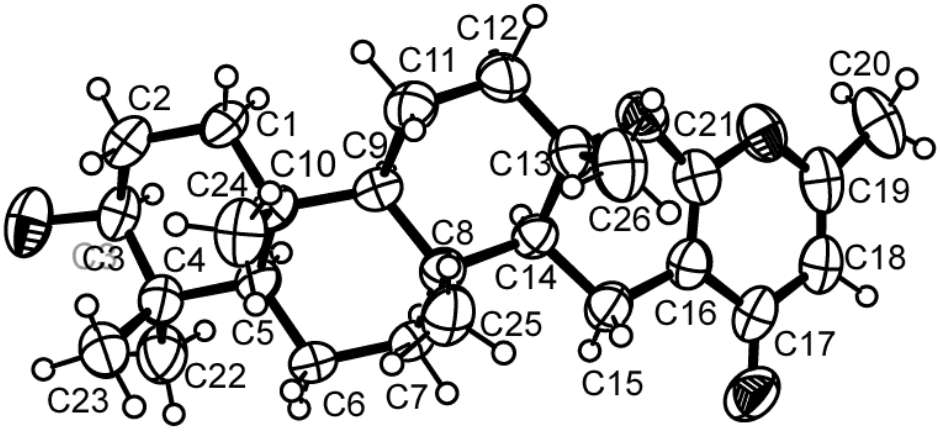

The (+)-HRESIMS of compound **6** indicated the $[M + H]^+$ peak at *m/z* 566.2416, corresponding to $C_{31}H_{36}NO_9$. Thus, the molecular formula of compound **6** was $C_{31}H_{35}NO_9$, indicating fifteen degrees of unsaturation. The IR spectrum showed absorption bands for ester carbonyl (1742 cm^{-1}), conjugated carbonyl (1671 cm^{-1}), aromatic (1586, 1508, 1465 cm^{-1}) and olefin (1625 cm^{-1}) groups. The ^{13}C NMR (Supplementary Information, Figure S11), DEPTs and HSQC spectra (Table 3) revealed the presence of three ester carbonyls (δ_C 171.0, 170.4, 169.8), one conjugated carbonyl (δ_C 161.3), five quaternary sp^2 (δ_C 161.2, 157.2, 144.5, 127.4, 101.1), six methine sp^2 (δ_C 152.1, 146.6, 133.1, 123.8, 111.2, 98.6), one oxyquaternary sp^3 (δ_C 83.9), two oxymethine sp^3 (δ_C 77.7 and 73.2), one oxymethylene sp^3 (δ_C 64.7), two quaternary sp^3 (δ_C 40.6 and 38.8), one methine sp^3 (δ_C 41.1), three methylene sp^3 (δ_C 35.5, 24.3 and 23.2), and six methyl (δ_C 24.2, 21.3, 21.2, 21.2, 20.8 and 13.3) carbons. Analysis of the ^1H (Supplementary Information, Figure S10), ^{13}C, HSQC and HMBC spectra (Table 3) revealed the presence of, besides three acetoxyl groups (δ_C 170.4, 21.2, δ_H 2.05s; δ_C 171.0, 20.8, δ_H 2.10s; δ_C 169.8, 21.2, δ_H 2.17, s), a hexasubstituted decahydronaphthalene ring system. That two of the acetoxyl groups were on C-1 and C-7, and the three methyl groups were on C-4, C-6 and C-10 of the decahydronaphthalene moiety was substantiated by the HMBC cross peaks of the Me-15 singlet (δ_H 0.88, s) to the carbon signals at δ_C 40.6 (C-10), 72.2 (C-1), 64.7 (C-11), of the Me-12 singlet (δ_H 1.26, s) to the carbon signals at δ_C 35.5 (C-3), 38.8 (C-4), 41.1 (C-9), and of the Me-14 singlet (δ_H 1.59, s) to the carbon signals at δ_C 77.7 (C-7), 83.9 (C-6), and 144.5 (C-5). That another substituent on C-10 was the acetoxymethylene group was evidenced by the HMBC cross peaks of H-11 signals (δ_H 3.75, d, J = 11.9 Hz; 3.79, d, J = 11.9 Hz) to C-1, C-9, and the signal of the carbonyl at δ_C 171.0. On the other hand, since Me-14 singlet gave cross peaks to the signals of the oxyquaternary carbon at δ_C 83.9 (C-6) and the quaternary sp^2 carbon at δ_C 144.5 (C-5), the double bond was on C-5, and C-6 was oxygen bearing. This was corroborated by the HMBC cross peaks of the signal of the olefinic proton at δ_H 6.36, s (H-13) to C-4 and C-6. Moreover, the HMBC spectrum also exhibited a cross peak of H-13 signal to the signals of a conjugated carbonyl carbon at δ_C 161.3 (C-2′) and the quaternary sp^2 carbon at δ_C 161.2 (C-4′). On the other hand, there were also HMBC cross peaks of another olefinic proton at δ_H 6.54, s (H-5′) to C-4′ and the signals of another two quaternary sp^2 carbon at δ_C 101.1 (C-3′) and 157.2 (C-6′). Taken together the HMBC correlations, it was clear that the decahydronaphthalene ring system was fused, on C-5 and C-6, with *2H, 5H*-pyrano[4, 3-*b*]pyran-5-one ring system. The COSY and HMBC spectra also indicated the presence of the 3-substituted pyridine ring. That this pyridine ring was connected to the pyranone ring through C-3 of the former and C-6′ of the later was evidenced by the HMBC correlations of the H-5′ singlet to C-3″ (δ_C 127.4), as well as of the signal of H-2″ (δ_H 8.14, dt, J = 7.8, 2.4, 2.4 Hz) to C-6′. Literature search revealed that compound **6** was previously obtained by treatment of pyripyropene A with HCl under anhydrous condition [15]; however, there were neither reports of the ^1H and ^{13}C data nor other description of this compound. Since **6** is a new natural product, we have named it pyripyropene S. It is interesting to point out that **6** is the first natural pyripyropene that lacks a hydroxyl group on C-13.

Table 3. ^{1}H and ^{13}C NMR ($CDCl_3$, 500.13 MHz and 125.8 MHz) and HMBC assignment for pyripyropene S (**6**).

Position	δ_C, Type	δ_H, (*J* in Hz)	COSY	HMBC
1	73.2, CH	4.79, dd (11.7, 4.6)	H-2	
2	23.2, CH_2	1.99, m 1.76, m	H-1	
3	35.5, CH_2	2.09, m	H-2	
4	38.8, C	-		
5	144.5, C	-		
6	83.9, C	-		
7	77.7, CH	5.23, dd (11.9, 5.4)	H-8	C-6
8	24.3, CH_2	1.82, ddd (12.8, 5.1, 1.4) 1.61, m	H-7, H-9	
9	41.1, CH	1.73, brd (12.5)	H-8	
10	40.6, C	-		
11	64.7, CH_2	3.75, d (11.9) 3.79, d (11.9)		C-1, 9, CO (OAc-11)
12	24.2, CH_3	1.26, s		C-3, 4, 9
13	111.2, CH	6.36, s		C-4, 6, 4′
14	21.3, CH_3	1.59,s		C-5, 6, 7
15	13.3, CH_3	0.88, s		C-1, 10, 11
2′	161.3, C	-		
3′	101.1, C	-		
4′	161.2, C	-		
5′	98.6, CH	6.54, s		C-2′, 3′, 6′, 3″
6′	157.2, C	-		
2″	146.6, CH	9.02, brs	H-4″	C-3″, 4″, 6″
3″	127.4, C	-		
4″	133.1, CH	8.14, dt (7.8, 1.4, 1.4)	H-2″, 5″	C-6′, 2″, 6″
5″	123.8, CH	7.42, dd (8.0, 4.9)	H-4″, 6″	C-3″, 6″
6″	151.2, CH	8.68, brd (4.0)	H-5″	C-5″
OAc-1	170.4, CO	-		
	21.2, CH_3	2.05, s		CO (OAc-1)
OAc-7	169.8, CO	-		
	21.2, CH_3	2.17, s		CO (OAc-7)
OAc-11	171.0, CO	-		
	20.8, CH_3	2.10, s		CO (OAc-11)

Compounds **1**, **2a**–**c** and **3**–**6** were tested for their antimicrobial activity against Gram positive (*Staphylococcus aureus* ATCC 25923 and *Bacillus subtilis* ATCC 6633) and Gram negative (*Escherichia coli* ATCC 25922 and *Pseudomonas aeruginosa* ATCC 27853) bacteria, *Candida albicans* ATCC 10231, and multidrug-resistant isolates from the environment. All the compounds tested exhibited neither antibacterial nor antifungal activities, *i.e.*, their MIC values were found to be higher than 256 μg/mL. Like chevalone C, chevalone E (**3**) does not possess the structural requirements for the antibacterial activity of this group of meroditerpenes, *i.e.*, the presence of the β-acetoxyl group on C-3 and the presence of a free 4-hydroxy-6-methyl-2*H*-pyran-2-one ring on C-15 [9]. Therefore, it is not

surprising that chevalone E (**3**) did not exhibit significant antibacterial activity. The fact that chevalone C did not show significant antibacterial activity but demonstrated synergistic effect with the antibiotics against three multidrug-resistant isolates [9] led us explore if some of these compounds could possibly have synergistic effects with antibiotics, *i.e.*, by using a disc diffusion method to assess if, in combination with antibiotics, they could cause an increase in the growth inhibition of multidrug-resistant strains. The results (Table 4) showed that no synergistic effects were observed between the tested compounds and antibiotics for multidrug-resistant *E. coli* and *E. faecalis*; however chevalone E (**3**) was found to exhibit potential synergy with oxacillin and ampicillin against the MRSA strain.

Table 4. Antibacterial efficacy of combined effect of antibiotics with the compounds (15 μg/disc) against three multidrug-resistant isolates, using the disc diffusion method.

Compound	*E. coli* G1				*S. aureus* B1			*E. faecalis* W1		
	Antibiotics									
	CIP	AMP	CTX	S	OX	AMP	CIP	VA	AMP	E
1	−	−	−	−	−	−	−	−	−	−
2a	−	−	−	−	−	++	−	−	−	−
2b	−	−	−	−	−	++	−	−	−	−
2c				−	−	++	−	−	−	−
3	−	−	−	−	+++	+++	−	−	−	−
4			−	−		++	−	−	−	−
5	−	−	−	−	−	++	−	−	−	−
6	−	−	−	−	−	++	−	−	−	−

(−) noneffective; (+) slight efficacy—halo of inhibition or additional increase in the halo of 1 to 2.5 mm around the disc; (++) moderate efficacy—from >2.5 to 5 mm; (+++) good efficacy—from >5 to 8 mm; CIP: ciprofloxacin; AMP: ampicillin; CTX: cefotaxime; S: streptomycin; OX: oxacillin; VA: vancomycin; E: Erythromycin.

In order to verify if the synergism occurred with both antibiotics or with either of them, the checkerboard method was carried out. The results, represented by the fractional inhibitory concentration (FIC) index, shown in Table 5, confirmed the synergy between chevalone E (**3**) and oxacillin, and not between chevalone E (**3**) and ampicillin. It is interesting to note that while chevalone E (**3**) shows synergism with oxacillin against the MRSA isolate, the structurally related meroditerpene aszonapyrone exhibited synergism only with vancomycin against the VRE isolate, and not with oxacillin against the MRSA strain [9].

Table 5. MIC values of chevalone E (**3**) in combination with oxacillin or ampicillin, and the respective FIC index obtained against a MRSA (*S. aureus* B1) using the checkerboard method.

Strain	MIC (μg/mL)				
S. aureus B1	**3** alone	OX alone	**3** with OX	OX with **3**	FIC index
	>1024	128	64	16	<0.188 *
S. aureus B1	**3** alone	AMP alone	**3** with AMP	AMP with **3**	FIC index
	>1024	128	>512	128	>1.5

* FIC index < 0.5 indicates synergy.

3. Experimental Section

3.1. General Procedures

Melting points were determined on a Bock monoscope and are uncorrected. Optical rotations were determined on an ADP410 Polarimeter (Bellingham + Syanley Ltd., Tunbridge Wells, Kent, UK). Infrared spectra were recorded on an ATT Mattson Genesis Series FTIR™ using WinFIRST Software. ^{1}H and ^{13}C NMR spectra were recorded at ambient temperature on a Bruker AMC instrument (Bruker Biosciences Corporation, Billerica, MA, USA) operating at 500.13 and 125.8 MHz, respectively. High resolution mass spectra were measured with a Waters Xevo QToF mass spectrometer (Waters Corporations, Milford, MA, USA) coupled to a Waters Aquity UPLC system. A Merck silica gel GF_{254} was used for preparative TLC, and a Merck Si gel 60 (0.2–0.5 mm) was used for analytical chromatography.

3.2. Extraction and Isolation

The strain KUFA0013 was isolated from the marine sponge *Rhabdermia* sp., which was collected from the coral reef of the Similan Islands, Phang Nga Province, Thailand, by scuba diving at 10 m depth, in April 2010, and the sponge was identified by J. Buaruang (Division of Environmental Science, Faculty of Science, Ramkhamhaeng University, Bangkok 10240, Thailand). Briefly, after rinsing with sterile sea water, the sponge was dried on sterile filter paper and cut into small pieces (5 × 5 mm) and placed on the plates containing malt extract agar [MEA, 30 g of malt extract powder (Himedia, Mumbai, India), 15 g of bacto agar, distilled water 300 mL, sea water 700 mL and adjusted to the final pH at 5.5] with 70% sea water and incubated at 28 °C under 12 h light/12 h dark cycle for seven days. The fungus was identified by one of us (T. Dethoup), by morphological features, including characteristic of ascospores, conidiogenesis and colonies, as well as by DNA sequence analysis of the calmodulin gene described by the previous report [16] (GenBank Accession No. KC 920702). Since the sequence was not identical to that deposited at GenBank, the strain was not identified at species level. The pure cultures were deposited as KUFA0013 at the Department of Plant Pathology, Faculty of Agriculture, Kasetsart University, Bangkok, Thailand. *A. similanensis* (KUFA 0013) was cultured for one week in five 90 mm Petri dishes (i.d. 90 mm) containing 25 mL of MEA with 70% sea water per dish. Thirty 1000 mL Erlenmeyer flasks, each containing white rice (200 g), water (30 mL) and sea water (70 mL), were autoclaved at 121 °C for 15 min, inoculated with ten mycelia plugs of the fungus and incubated at 28 °C for 30 days. The moldy rice was macerated in ethyl acetate (7 L total) for seven days and then filtered by filter paper. The two layers were separated using a separatory funnel, and the ethyl acetate solution was evaporated under reduced pressure to yield 97 g of crude ethyl acetate extract that was dissolved in 500 mL of a 4:1 mixture of EtOAc and $CHCl_3$, and then washed with 5% $NaHCO_3$ aqueous solution (2 × 300 mL) and H_2O (3 × 300 mL). The organic layer was dried with anhydrous Na_2SO_4, filtered and evaporated under reduced pressure to give 75 g of crude extract, which was applied on a column chromatography of silica gel (640 g) and eluted with mixtures of $CHCl_3$–petrol and $CHCl_3$–Me_2CO, 250 mL fractions were collected as follows: Frs 1–18 ($CHCl_3$–petrol, 3:7), 19–53 ($CHCl_3$–petrol, 1:1), 54–114 ($CHCl_3$–petrol, 7:3), 115–215 ($CHCl_3$–petrol, 9:1), 216–395 ($CHCl_3$–Me_2CO, 9:1), 396–443 ($CHCl_3$–Me_2CO, 7:3). Frs 185–196 were combined (654 mg) and purified by TLC (Si gel, $CHCl_3$:Me_2CO:HCO_2H, 97:3:0.01) to

give 4 mg of **1**. Frs 197–221 were combined (1.16 g) and crystallized in a mixture of petrol and $CHCl_3$ to give additional 107.6 mg of yellow solid which was further purified by TLC (Si gel, $CHCl_3$:Me_2CO:HCO_2H, 98:2:0.01) to give 2.5 mg of **1**. Fr 222 (8.06 g) was recrystallized in a mixture of $CHCl_3$ and Me_2CO to give 238 mg of white precipitate, which was further purified by TLC (Si gel, $CHCl_3$:Me_2CO:HCO_2H, 97:3:0.01) to give **2b** (32.7 mg), **4** (4.6 mg) and chevalone B (4.6 mg). The mother liquor was further purified by TLC (Si gel, $CHCl_3$:Me_2CO:HCO_2H, 97:3:0.01) to give **2b** (41.0 mg), **4** (7.2 mg) and chevalone B (70.8 mg). The mother liquor of frs 197–221 and fr 222, and frs 223–224 were combined (9.18 g), applied on the Si gel column (58 g), and eluted with mixtures of petrol–$CHCl_3$ and $CHCl_3$–Me_2CO, wherein 100 mL sfrs were collected as follows: sfrs 1-59 (petrol–$CHCl_3$, 3:7), 60–69 (petrol–$CHCl_3$, 1:9), 70–76 ($CHCl_3$–Me_2CO, 9:1). Sfrs 11–22 were combined (1.97 g) and crystallized in a mixture of petrol and $CHCl_3$ to give additional 16.4 mg of **1**. Sfrs 29–42 were combined (468 mg) and crystallized in a mixture of petrol and $CHCl_3$ to give additional 92.1 mg of **2b**. Frs 225–228 were combined (446 mg) and crystallized in a mixture of petrol and $CHCl_3$ to give 63 mg of a precipitate which was further purified by TLC (Si gel, $CHCl_3$:Me_2CO:HCO_2H, 97:3:0.01) to give **2b** (35.8 mg) and **2a** (35.4 mg). The mother liquor of frs 225–228 and frs 229–330 were combined and chromatographed on a Si gel column (33 g) and eluted with mixtures of petrol–$CHCl_3$ and $CHCl_3$–Me_2CO, wherein 100 mL sub-fractions were collected as follows: sfrs 1–49 (petrol–$CHCl_3$, 3:7), 50–64 (petrol–$CHCl_3$, 1:9), 65–77 ($CHCl_3$–Me_2CO, 9:1). Subfrs 4–5 were combined and recrystallized in a mixture of petrol and $CHCl_3$ to give **1** (2.4 mg). Sfrs 6–10 were combined (160 mg) and recrystallized in a mixture of petrol and $CHCl_3$ to give **2c** (7.6 mg). Sfrs 11–16 were combined (108 mg) and recrystallized in a mixture of petrol to give **2b** (5 mg). Sfrs 27-33 were combined (206 mg) and purified by TLC (Si gel, $CHCl_3$: Me_2CO. 93:7) to give *p*-hydroxybenzaldehyde (36 mg). Frs 231–247 were combined (6.7 g) and recrystallized in a mixture of petrol and Me_2CO to give 1.39 g of chevalone C. Frs 272–294 were combined (1.54 g) and crystallized in a mixture of petrol and Me_2CO to yield **5** (265 mg). Frs 328-335 were combined (296 mg) and applied on a column of Sephadex LH-20 (22 g) and eluted with a mixture of $CHCl_3$–MeOH (9:1) to give **3** (11.2 mg). Frs 354–398 were combined (1.14 g) and purified by TLC (Si gel, $CHCl_3$:MeOH:HCO_2H, 95:5:0.01) to give **6** (27.3 mg).

3.2.1. Similanpyrone A (**1**)

White solid, Mp 322–323 °C (petrol/$CHCl_3$); UV ($CHCl_3$) λ_{max} (log ε) 240 (4.31), 269 (4.31), 295 (3.95), 333 (4.23), 358 (4.16) nm; IR (KBr) ν_{max} 3446, 3010, 2923, 2851, 1748, 1698, 1658, 1634, 1464, 1177, 1151 cm^{-1}; ^1H and ^{13}C NMR (Table 1); HRESIMS *m/z* 245.0455 $(M + H)^+$ (calculated for $C_{13}H_9O_5$, 245.0450).

3.2.2. Similanpyrone B (**2b**)

White crystals, Mp 162–163 °C (petrol/$CHCl_3$); UV ($CHCl_3$) λ_{max} (log ε) 240 (4.35), 277 (3.51), 330 (3.46) nm; IR (KBr) ν_{max} 3243, 3160, 2923, 2851, 1677, 1634, 1617, 1585, 1571, 1455, 1256, 1154, 1110 cm^{-1}; ^1H and ^{13}C NMR (Table 2); HRESIMS *m/z* 207.0658 $(M + H)^+$ (calculated for $C_{11}H_{11}O_4$, 207.0657).

3.2.3. Chevalone E (**3**)

White crystals, Mp 262–263 °C (petrol/$CHCl_3$); $[\alpha]_D^{20}$ −146.3° (*c* 0.04, $CHCl_3$); IR (KBr) ν_{max} 3300, 3016, 2979, 2950, 2871, 1664, 1607, 1570, 1444, 1288 cm^{-1}; ^1H NMR ($CDCl_3$, 500.13 MHz) δ 5.99 (1H, s, H-18), 3.21 (1H, d, *J* = 11.1, 5.0, H-3), 2.55 (1H, dd, *J* = 16.4, 4.9, H_2-15), 2.20 (3H, s, H_3-20), 2.15 (1H, m, H_2-15), 2.14 (1H, m, H_2-12), 1.90 (1H, dt, *J* = 12.8, 3, H_2-7), 1.74 (1H, m, H_2-11), 1.73 (1H, m, H_2-1), 1.71 (1H, m, H_2-12), 1.64 (2H, m, H_2-2), 1.59 (1H, m, H_2-6), 1.50 (1H, dd, *J* = 12.5, 4.7, H-14), 1.45 (1H, m, H_2-6), 1.36 (1H, m, H_2-11), 1.28 (3H, s, H_3-26), 1.05 (1H, m, H_2-7), 1.00 (1H, m, H_2-1), 0.98 (3H, s, H_3-23), 0.93 (1H, brd, *J* = 13.2, H-9), 0.89 (3H, s, H_3-25), 0.84 (3H, s, H_3-24), 0.78 (1H, brd, *J* = 11-6, H-5), 0.78 (3H, s, H_3-22); ^{13}C NMR ($CDCl_3$, 125.8 MHz) δ 180.6 (CO, C-17), 162 (C, C-16), 160.5 (C, C-21), 111.9 (CH, C-18), 98.5 (C, C-19), 84.3 (C, C-13), 78.7 (CH, C-3), 60.3 (CH, C-9), 55.3 (CH, C-5), 52.3 (CH, C-14), 41.1 (CH_2, C-7), 40.1 (CH_2, C-12), 38.9 (C, C-4), 38.4 (CH_2, C-1), 37.3 (C, C-8), 37.1 (C, C-10), 28.0 (CH_3, C-23), 27.2 (CH_2, C-2), 20.5 (CH_3, C-26), 19.2 (CH_3, C-20), 18.7 (CH_2, C-11), 17.9 (CH_2, C-6), 16.4 (CH_3, C-24), 16.1 (CH_3, C-25), 15.4 (CH_3, C-22), 15.2 (CH_3, C-15); HRESIMS *m/z* 415.2851 $(M + H)^+$ (calculated for $C_{26}H_{39}O_4$, 415.2848).

3.2.4. Pyripyropene S (**6**)

Yellow viscous liquid, $[\alpha]_D^{20}$ +116.3 (*c* 0.04, $CHCl_3$); IR (KBr*)* ν_{max} *2*923, 2851, 1742, 1671, 1624, 1586, 1508, 1465, 1374, 1242, 1043 cm^{-1}; ^1H and ^{13}C NMR (Table 3); HRESIMS *m/z* 566.2415 $(M + H)^+$ (calculated for $C_{31}H_{36}NO_9$, 566.2390).

*3.3. X-ray Crystal Structure of Chevalone E (**3**)*

Crystals suitable for X-ray diffraction were obtained by slow evaporation of a solution in petroleum ether/chloroform. They were orthorhombic, space group $P2_12_12_1$, cell volume 2310.9(1) $Å^3$ and unit cell dimensions *a* = 8.2325(2) Å, *b* =11.3341(3) Å and *c* = 24.7665(6) Å. Diffraction data were collected at 293 K with a Gemini PX Ultra equipped with CuK_α radiation (λ = 1.54184 Å). The structures were solved by direct methods using SHELXS-97 and refined with SHELXL-97. Carbon, oxygen and nitrogen atoms were refined anisotropically. Hydrogen atoms were refined freely with isotropic displacement parameters. The refinement converged to *R* (all data) = 6.38% and wR_2 (all data) = 10.21%. Towards the end of refinement the absolute structure parameter *x* (Flack *x* parameter) was refined at the same time as all other parameters, using the TWIN instruction with the default matrix R = (−1 0 0, 0 −1 0, 0 0 −1) and BASF with one parameter (*x*), to reach the final value of *x* = 0.0 (3). The inverted structure, obtained with the instruction MOVE 1 1 1 −1, yielded *x* = 1.5 (3). Tables containing the final fractional coordinates, temperature parameters, bond distances, and bond angles were deposited with the Cambridge Crystallographic Data Centre: CCDC reference number 1002416.

3.4. Antimicrobial Activity Assays

3.4.1. Bacterial Strains

For the antimicrobial assays, the compounds were tested against: bacterial reference strains (*Staphylococcus aureus* ATCC 25923, *Bacillus subtilis* ATCC 6633, *Escherichia coli* ATCC 25922 and

Pseudomonas aeruginosa ATCC 27853), *Candida albicans* ATCC 10231 and multidrug-resistant bacteria isolated from the environment, *S. aureus* B1 (isolated from public bus), *Enterococcus faecalis* W1 (isolated from river water) and *E. coli* G1 (isolated from seagull feces). Bacteria were grown in Mueller-Hinton agar (MH-BioKar diagnostics, Allonne, France) from stock cultures, while *C. albicans* was grown in Sabouraud dextrose agar (SAB-BioKar diagnostics, Allonne, France). MH and SAB plates were incubated at 37 °C prior to obtain fresh cultures for each *in vitro* bioassay.

3.4.2. Determination of Minimum Inhibitory and Bactericidal/Fungal Concentrations

The minimum inhibitory concentrations (MIC) of the compounds were determined using a broth microdilution technique, following the recommendations of the Clinical and Laboratory Standards Institute [17]. Stock solutions of 10 mg/mL, prepared in dimethylsulfoxide (DMSO-Applichem GmbH, Darmstadt, Germany), were serially diluted in Mueller-Hinton broth (MHB-BioKar diagnostics, Allonne, France) to achieve in-test concentrations ranging from 2 to 256 μg/mL. Each bacterial inoculum was prepared in MHB, while *C. albicans* inoculum was prepared in RPMI-1640 with L-glutamine, with MOPS and without $NaHCO_3$ (Lonza, Walkersville, MD, USA). All inocula were standardized in order obtain a concentration of 5×10^5 CFU/mL in each inoculated well of the microtiter plate. The concentration of DMSO in the highest in-test concentration did not affect the microbial growth. The MIC was defined as the lowest concentration of compound that has inhibited the visible growth.

3.4.3. Synergistic Studies

3.4.3.1. Screening of Combined Effect between the Compounds and Antibiotics

A screening susceptibility test to assess the combined effect between the compounds and antibiotics was conducted using the disc diffusion method on MH, according to the procedure already described by Gomes *et al.* [9].

3.4.3.2. Synergy Test: Checkerboard Method

Based on the results of the previous assay, potential synergy between **3** and oxacillin or ampicillin (Sigma-Aldrich, St. Louis, MO, USA) was checked using a broth microdilution checkerboard method and tested in MRSA isolate (*S. aureus* B1), as has been already described [9]. Two independent experiments in duplicate were performed. The fractional inhibitory concentration (FIC) was calculated as follows: FIC of drug A (FIC A) = MIC of drug A in combination/MIC of drug A alone, and FIC of drug B (FIC B) = MIC of drug B in combination/MIC of drug B alone. The FIC index (ΣFIC), calculated as the sum of each FIC, was interpreted as follows: $\Sigma FIC \leq 0.5$, synergy; $0.5 < \Sigma FIC \leq 4$, no interaction; $4 < \Sigma FIC$, antagonism [18].

4. Conclusions

Although several analogs of chevalone have been reported from several members of the genus *Aspergillus*, this is the first report of isolation of isocoumarin derivatives from a member of this genus.

The synergism of chevalone E with the antibiotic oxacillin against MRSA can be considered relevant for anti-infective marine natural products research.

Acknowledgments

This work was partially supported by the Project MARBIOTECH (reference NORTE-07-0124-FEDER-000047) within the SR&TD Integrated Program MARVALOR—Building research and innovation capacity for improved management and valorization of marine resources, supported by the Programa Operacional Regional do Norte (ON.2—O Novo Norte) and by the European Regional Development Fund, and also by FCT—Fundação para a Ciência e a Tecnologia under the project CEQUIMED-PEst-OE/SAU/UI4040/2014, FEDER funds through the COMPETE program under the project FCOMP-01-0124-FEDER-011057. We thank Mick Lee of the Department of Chemistry, Leicester University (UK), for providing the HRESIMS. C.P. thanks the Faculty of Pharmaceutical Sciences, Burapha University, Thailand for her scholarship to the University of Porto. We thank Júlia Bessa and Sara Cravo for technical support.

Author Contributions

Prompanya, C. performed isolation, purification and structure elucidation of some compounds; Kijjoa, A. and Pinto, M.M.M. conceived, designed the research, elucidated the structure of the compounds and wrote the paper; Dethoup, T. isolated, identified, cultured the fungi, and prepared the crude extract; Gales, L. performed X-ray crystallography of compound **3**; Silva, A.M.S. provided the NMR spectra; Bessa, L.J. and Costa, P.M. performed antibacterial activity.

Conflicts of Interest

The authors declare no conflict of interest.

References

1. Asami, Y.; Kakeya, H.; Onose, R.; Yoshida, A.; Matsuzaki, H.; Osada, H. Azaspirene: A novel angiogenesis inhibitor containing a 1-oxa-7-azaspiro[4.4]non-2-ene-4,6-dione skeleton produced by the fungus *Neosartorya* sp. *Org. Lett.* **2002**, *4*, 2845–2848.
2. Asami, Y.; Kakeya, H.; Onose, R.; Chang, Y.H.; Toi, M.; Osada, H. RK-805, an endothelial-cell-growth inhibitor produced by *Neosartorya* sp., and a docking model with methionine aminopeptidase-2. *Tetrahedron* **2004**, *60*, 7085–7091.
3. Jayasuriya, H.; Zink, D.; Basilio, A.; Vicente, F.; Collado, J.; Bills, G.; Goldman, M.L.; Motyl, M.; Huber, J.; Dezeny, G.; *et al*. Discovery and antibacterial activity of glabramycin A–C from *Neosartorya glabra* by an antisense strategy. *J. Antibiotics* **2009**, *62*, 265–269.
4. Yang, S.S.; Wang, G.J.; Cheng, K.F.; Chen, C.H.; Ju, Y.M.; Tsau, Y.J.; Lee, T.H. Bioactive *γ*-lactones from the fermented broth of *Neosartorya* sp. *Planta Med.* **2010**, *76*, 1701–1705.
5. Kijjoa, A.; Santos, S.; Dethoup, T.; Manoch, L.; Almeida, A.P.; Vasconcelos, M.H.; Silva, A.; Gales, L.; Herz, W. Sartoryglabrins, analogs of ardeemins, from *Neosartorya glabra*. *Nat. Prod. Commun.* **2011**, *6*, 807–812.

6. Eamvijarn, A.; Kijjoa, A.; Bruyère, C.; Mathieu, V.; Manoch, V.; LeFranc, F.; Silva, A.; Kiss, R.; Herz, W. Secondary metabolites from a culture of the fungus *Neosartorya pseudofischeri* and their *in vitro* cytostatic activity in human cancer cells. *Planta Med.* **2012**, *78*, 1767–1776.
7. Buttachon, S.; Chandrapatya, A.; Manoch, L.; Silva, A.; Gales, L.; Bruyère, C.; Kiss, R.; Kijjoa, A. Sartorymensin, a new indole alkaloid, and new analogues of tryptoquivaline and fiscalins produced by *Neosartorya siamensis* (KUFC 6349). *Tetrahedron* **2012**, *68*, 3253–3262.
8. Eamvijarn, A.; Gomes, N. M.; Dethoup, T.; Buaruang, J.; Manoch, L.; Silva, A.; Pedro, M.; Marini, I.; Roussis, V.; Kijjoa, A. Bioactive meroditerpenes and indole alkaloids from the soil fungus *Neosartorya fischeri* (KUFC 6344), and the marine-derived fungi *Neosartorya laciniosa* (KUFC 7896) and *Neosartorya tsunodae* (KUFC 9213). *Tetrahedron* **2013**, *69*, 8583–8591.
9. Gomes, N.M.; Bessa, L.J.; Buttachon, S.; Costa, P.M.; Buaruang, J.; Dethoup, T.; Silva, A.M.S.; Kijjoa, A. Antibacterial and Antibiofilm activities of tryptoquivalines and meroditerpenes isolated from the marine-derived fungi *Neosartorya paulistensis*, *N. laciniosa*, *N. tsunodae*, and the Soil Fungi *N. fischeri* and *N. siamensis*. *Mar. Drugs* **2014**, *12*, 822–839.
10. Kanokmedhakul, K.; Kanokmedhakul, S.; Suwannatrai, R.; Soytong, K.; Prabpai, S.; Kongsaeree, P. Bioactive meroterpenoids and alkaloids from the fungus *Eurotium chevalieri*. *Tetrahedron* **2011**, *67*, 5461–5468.
11. Ryoo, I.J.; Xu, G.H.; Km, Y.H.; Choo, S.J.; Ahn, J.S.; Bae, K.; Yoo, I.D. Reticulone, a novel free radical scavenger produced by *Aspergillus* sp. *J. Microbiol. Biotechnol.* **2009**, *12*, 1573–1575.
12. Gallo, M.B.C.; Cavalcanti, B.C.; Barros, F.W.A.; Moraes, M.O.; Costa-Latufo, L.V.; Pessoa, C.; Bastos, J.K.; Pupo, M.T. Chemical constituents of *Papulaspora immersa*, an endophyte from *Smallanthus sonchifolius* (Asteraceae), and their cytotoxic activity. *Chem. Biodivers.* **2010**, *7*, 2941–2950.
13. Erkel, G.; Rether, J.; Anke, T. S14-95, a novel inhibitor of the JAK/STAT pathway from a *Penicillium* species. *J. Antibiotics* **2003**, *56*, 337–343.
14. Tomoda, H.; Tabata, N.; Yang, D.J.; Takaya.naki, H.; Nishida, M.; Omura, S. Pyripyropenes, novel ACAT inhibitors produced by *Aspergillus fumigatus*. III. Structure elucidation of pyripyropenes E to L. *J. Antibiotics* **1995**, *48*, 495–503.
15. Obata, R.; Sunazuka, T.; Tomoda, H.; Harigaya, Y.; Omura, S. Chemical Modification and structure-activity relationships of pyripyropenes, potent, bioavailable inhibitor of acyl-CoA: cholesterol *O*-acyltransferase (ACAT). *Bioorg. Med. Chem. Lett.* **1995**, *5*, 2683–2688.
16. Glass, N.L.; Donaldson, G.C. Development of primer sets designed for use with the PCR to amplify conserved genes from filamentous ascomycetes. *Appl. Environ. Microbiol.* **1995**, *61*, 1323–1330.
17. Franklin, R.; Cockerill, M.D., III. *Performance Standards for Antimicrombial Susceptibility Testing. Twenty-First Informational Supplement M100-S21*; Clinical and Laboratory Standards Institute (CLSI): Wayne, PA, USA, 2011.
18. Odds, F.C. Synergy, antagonism, and what the chequerboard puts between them. *J. Antimicrob. Chemother* **2003**, *52*, 1.

APPENDIX III

Prompanya, C., Fernandes, C., Cravo, S., Pinto, M. M., Dethoup, T., Silva, A. M., & Kijjoa, A. (2015). A new cyclic hexapeptide and a new isocoumarin derivative from the marine sponge-associated fungus *Aspergillus similanensis* KUFA 0013. *Mar. Drugs, 13*, 1432 – 1450. DOI:10.3390/md13031432

Mar. Drugs **2015**, *13*, 1432-1450; doi:10.3390/md13031432

OPEN ACCESS

marine drugs

ISSN 1660-3397

www.mdpi.com/journal/marinedrugs

Article

A New Cyclic Hexapeptide and a New Isocoumarin Derivative from the Marine Sponge-Associated Fungus *Aspergillus similanensis* KUFA 0013

Chadaporn Prompanya [1,2], Carla Fernandes [2,3], Sara Cravo [2,3], Madalena M. M. Pinto [2,3], Tida Dethoup [4], Artur M. S. Silva [5] and Anake Kijjoa [1,2,*]

1 ICBAS-Instituto de Ciências Biomédicas Abel Salazar, Universidade do Porto, Rua de Jorge Viterbo Ferreira, 228, 4050-313 Porto, Portugal; E-Mail: chadaporn@buu.ac.th

2 Interdisciplinary Centre of Marine and Environmental Research (CIIMAR), Rua dos Bragas 289, 4050-123 Porto, Portugal

3 Centro de Química Medicinal da Universidade do Porto (CEQUIMED-UP, Laboratório de Química Orgânica, Departamento de Ciências Químicas, Faculdade de Farmácia, Rua de Jorge Viterbo Ferreira, 228, 4050-313 Porto, Portugal; E-Mails: cfernandes@ff.up.pt (C.F.); scravo@ff.up.pt (S.C.); madalena@ff.up.pt (M.M.M.P.)

4 Department of Plant Pathology, Faculty of Agriculture, Kasetsart University, Bangkok 10240, Thailand; E-Mail: agrtdd@ku.ac.th

5 Departamento de Química & QOPNA, Universidade de Aveiro, 3810-193 Aveiro, Portugal; E-Mail: artur.silva@ua.pt

* Author to whom correspondence should be addressed; E-Mail: ankijjoa@icbas.up.pt; Tel.: +351-2-2042-8331; Fax: +351-2-2042-8090.

Academic Editor: Johannes F. Imhoff

Received: 27 January 2015 / Accepted: 9 March 2015 / Published: 17 March 2015

Abstract: A new isocoumarin derivative, similanpyrone C (**1**), a new cyclohexapeptide, similanamide (**2**), and a new pyripyropene derivative, named pyripyropene T (**3**) were isolated from the ethyl acetate extract of the culture of the marine sponge-associated fungus *Aspergillus similanensis* KUFA 0013. The structures of the compounds were established based on 1D and 2D NMR spectral analysis, and in the case of compound **2** the stereochemistry of its amino acid constituents was determined by chiral HPLC analysis of the hydrolysate by co-injection with the D and L amino acids standards. Compounds **2** and **3** were evaluated for their *in vitro* growth inhibitory activity against MCF-7 (breast adenocarcinoma), NCI-H460 (non-small cell lung cancer) and A373 (melanoma) cell lines,

as well as antibacterial activity against reference strains and the environmental multidrug-resistant isolates (MRS and VRE). Only compound **2** exhibited weak activity against the three cancer cell lines, and neither of them showed antibacterial activity.

Keywords: *Aspergillus similanensis*; cyclic hexapeptide; similanamide; isocoumarin; similanpyrone C; pyripyropene T

1. Introduction

In recent years, there has been an increasing interest in marine-derived fungi as a target source of bioactive marine natural products because many consider them among the world's greatest untapped resources for new biodiversity as well as chemodiversity [1–3]. Moreover, through established culture methods, the compounds can be produced in quantity needed for medicinal chemistry development, clinical trials and even marketing. Among the marine fungal strains investigated, the fungi of the genus *Aspergillus* are the most prolific source of bioactive secondary metabolites, including sterols [4], cerebrosides [5], sesquiterpenoids [6,7], sesterterpenoids [8,9], diterpenoids [10], meroterpenoids [11], anthraquinone derivatives [12,13], nucleoside derivatives [14], indole alkaloids [15–17], prenylated indole alkaloids [18–21], quinazolinone alkaloids [22,23], pyrrolidine alkaloids [8], and cyclic peptides [24–28].

In our ongoing search for new natural products with antibacterial and anticancer activities produced by the marine-derived fungi of the genera *Neosartorya* and *Aspergillus*, we have recently reported the isolation of new isocoumarins similanpyrones A and B, a new chevalone (chevalone E), and a new natural product pyripyrone S; besides the previously reported chevalone B and C, a meroterpenoid S14-95, and pyripyropene E, from the crude ethyl acetate extract of the undescribed marine sponge-associated fungus *Aspergillus similanensis* KUFA 0013 [29]. Reexamination of the fractions remaining from the previous study of this fungus led to the isolation of a new 8-hydroxy-3-methylisocoumarin derivative, which we have named similanpyrone C (**1**), a new cyclic hexapeptide, similanamide (**2**), and a new pyripyropene analog, pyripyropene T (**3**) (Figure 1). Hydrolysis of compound **2**, followed by HPLC analysis of its hydrolysate using a chiral column, led to the elucidation of its amino acid constituents. Compounds **2** and **3** were evaluated for their antibacterial activity as well their cytotoxicity against three human cancer cell lines.

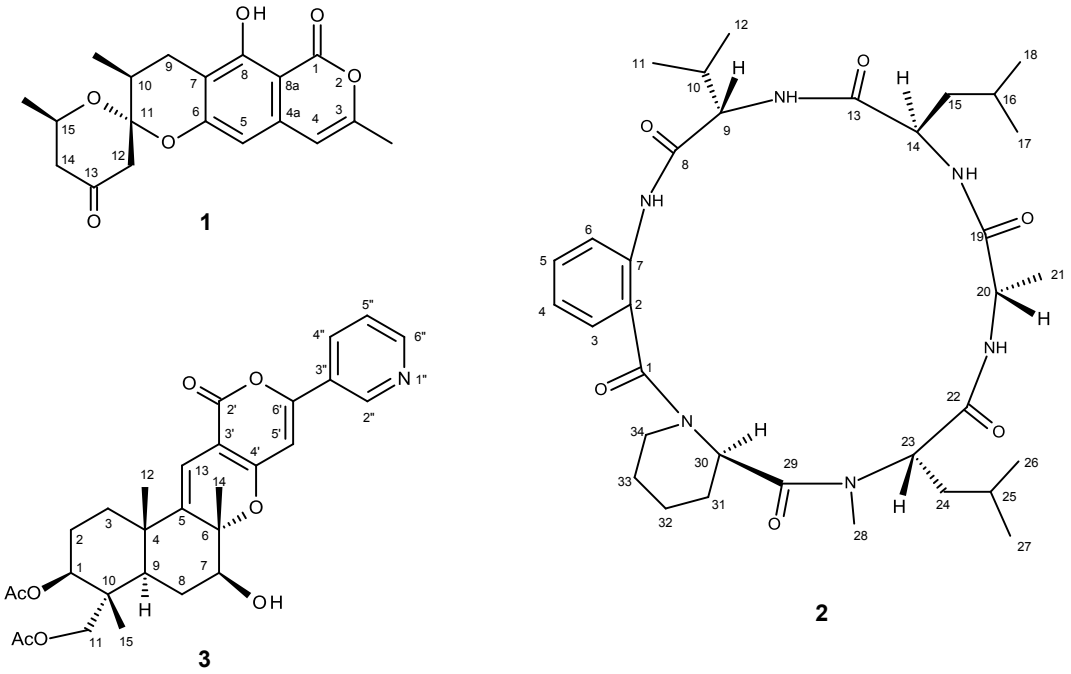

Figure 1. Secondary metabolites from *Aspergillus similanensis* KUFA0013.

2. Results and Discussion

Compound **1** was isolated as pale yellow viscous mass, and its molecular formula $C_{19}H_{20}O_6$ was established on the basis of the (+)-HRESIMS *m/z* 345.1342 $[M + H]^+$, indicating ten degrees of unsaturation. The IR spectrum showed absorption bands for hydroxyl (3443 cm^{-1}), ketone carbonyl (1730 cm^{-1}), conjugated lactone carbonyl (1683 cm^{-1}), olefin (1647 cm^{-1}) and aromatic (1625, 1572 cm^{-1}) groups. The ^{13}C NMR (Supplementary Information, Figure S3), DEPTs and HSQC spectra (Table 1, Supplementary Information, Figure S4) revealed the presence of one ketone carbonyl (δ_C 205.3), one conjugated ester carbonyl (δ_C 166.8), six quaternary sp^2 (δ_C 160.0, 158.3, 153.4, 136.7, 110.0 and 99.6), two methine sp^2 (δ_C 104.4 and 103.0), one ketal (δ_C 102.9), two sp^3 methine (δ_C 67.2 and 33.9), two sp^3 methylene (δ_C 48.3 and 47.2), and three methyl (δ_C 21.6, 19.4 and 15.9) carbons. The ^1H NMR spectrum (Supplementary Information, Figure S1) revealed, besides a singlet of the hydrogen bonded hydroxyl proton at δ_H 11.35, one doublet at δ_H 6.13 (J = 0.9 Hz) and one singlet at δ_H 6.26, two multiplets at δ_H 4.15 and δ_H 1.98, two double double doublets at δ_H 2.48 (J = 14.7, 2.9, 1.9 Hz) and δ_H 2.28 (J = 14.7, 11.3, 0.7 Hz), two double doublets at δ_H 2.81 (J = 16.8, 5.6 Hz) and δ_H 2.55 (14.0, 1.9), two broad doublets at δ_H 2.81 (J = 14.0 Hz) and δ_H 2.57 (J = 16.8 Hz), one methyl singlet at δ_H 2.24, and two methyl doublets at δ_H 1.23 (J = 6.2 Hz) and δ_H 1.21 (J = 6.2 Hz).

Table 1. ^{1}H and ^{13}C NMR ($CDCl_3$, 500.13 MHz and 125.8 MHz) and HMBC assignment for **1**.

Position	δ_C, Type	δ_H, (*J* in Hz)	COSY	HMBC	NOESY
1	166.8, CO	-			
3	153.4, C	-			
4	104.4, CH	6.13, d (0.9)	CH_3-3	C-3, 5, 8a	CH_3-3
4a	136.7, C	-			
5	103.0, CH	6.26, s		C-4, 6, 7, 8a	
6	158.3, C	-			
7	110.0, C	-			
8	160.0, C	-			
8a	99.6, C	-			
9α	23.6, CH_2	2.81, dd (16.8, 5.6)	H-9β, H-10	C-6, 7, 10, 11	H-9β, H-10, CH_3-10
9β		2.57, brd (16.8)	H-9α, H-10	C-7, 10, 11	H-9α, H-10, CH_3-10
10	33.9, CH	1.98, m	H-9α, H-9β, CH_3-10		H-9α,H-9β, CH_3-10
11	102.9, C	-			
12α	47.2, CH_2	2.55, dd (14.0, 1.9)	H-12β	C-10, 11, 13	H-12β
12β		2.81, brd (14.0)	H-12α	C-10, 11, 13	H-12α
13	205.3, CO	-			
14α	48.3, CH_2	2.28, ddd (14.7, 11.3, 0.7)	H-14β, H-15	C-13, 15	H-14β, CH_3-15
14β		2.48, ddd (14.7, 2.9, 1.9)	H-14α, H-15	C-13	H-14β, CH_3-15
15	67.2, CH	4.15, m	H-14α, H-14β, CH_3-15		H-14β, CH_3-15
CH_3-3	19.4, CH_3	2.24, s	H-4	C-3, 4	H-4
CH_3-10	15.9, CH_3	1.23, d (6.2)	H-10	C-9, 10, 11	H-9β, H-10, H-12α, 2β
CH_3-15	21.6, CH_3	1.21, d (6.2)	H-15	C-14, 15	H-14α, H-14β, H-15
OH-8	-	11.35, s		C-7, 8, 8a	

Analysis of the ^{1}H, ^{13}C NMR, HSQC and HMBC spectra (Table 1) revealed the presence of a 6,7-disubstituted 3-methyl-1*H*-isochromen-1-one nucleus, similar to that of similanpyrone B [29]. Thus, another portion of the molecule consisted of one ketone (δ_C 205.3), one ketal (δ_C 102.9), one methine (δ_H 1.98, m; δ_C 33.9), one oxymethine (δ_H 4.15, m; δ_C 67.2), three methylene (δ_H 2.81, dd, J = 16.8, 5.6 Hz and δ_H 2.57, brd, J = 16.8 Hz, δ_C 23.6; δ_H 2.81, brd, J = 14.0 Hz and 2.55, dd, J = 14.0, 1.9 Hz; δ_C 47.2; δ_H 2.48, ddd, J = 14.7, 2.9, 1.9 Hz and 2.28, ddd, J = 14.7, 11.3, 0.7 Hz, δ_C 48.3), two methyl (δ_H 1.21, d, J = 6.2 Hz; δ_C 21.6 and δ_H 1.23, d, J = 6.2 Hz, δ_C 15.9) groups. That this portion was 2,10-dimethyl-1,7-dioxaspiro[5.5]undec-8-en-4-one was evidenced by the COSY correlations (Table 1, Supplementary Information, Figure S2) of H_2-9 (δ_H 2.81, dd, J = 16.8, 5.6 Hz and 2.57, brd, J = 16.8 Hz) to H-10 (δ_H 1.98, m), of H-10 to CH_3-10 (δ_H 1.23, d, J = 6.2 Hz), of H_2-14 (δ_H 2.48, ddd, J = 14.7, 2.9, 1.9 Hz and 2.28, ddd, J = 14.7, 11.3, 0.7 Hz) to H-15 (δ_H 4.15, m), and of H-15 to CH_3-15 (δ_H 1.21, d, J = 6.2 Hz), as well as by the HMBC cross peaks (Table 1, Supplementary Information, Figure S5) of H_2-9 to C-10 and C-11 (δ_C 102.9), of H_2-12 (δ_H 2.81, brd, J = 14.0 Hz and 2.55, dd, J = 14.0, 1.9 Hz) to C-10, 11, 13 (δ_C 205.3), and of H-14 to C-13 and 15, respectively (Figure 2). That the 1,7-dioxaspiro[5.5]undec-8-en-4-one ring system was fused with the 3-methyl-1*H*-isochromen-1-one nucleus, through C-8 and C-9 of the methyldihydropyran ring of the former and C-6 and C-7 of the latter, was supported by the HMBC correlations of H_2-9 to C-6, 7 (Table 1, Supplementary Information, Figure S5). Literature search revealed that **1** is a new compound, and in compliance with our previous work, we have therefore named it similanpyrone C. Since **1** was isolated as viscous mass, it was not possible to obtain suitable crystals for the X-ray analysis. Consequently, the absolute configuration of C-10, C-11 and C-15 is still undetermined.

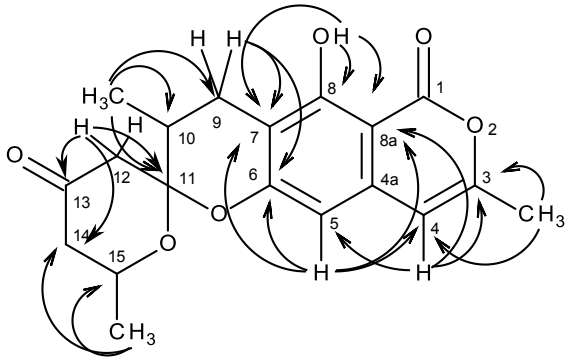

Figure 2. Key HMBC correlations of compound **1**.

In an attempt to determine the stereochemistry of C-10 and C-15, we have sorted out the coupling constants of both H_2-9 and H_2-14. The fact that H_2-9 appeared as a double doublet at δ_H 2.81 with a germinal coupling of 16.8 Hz, and a small coupling at δ_H 5.6 Hz, typical of axial-equatorial coupling, and a broad doublet at δ_H 2.57 with a germinal coupling constant of 16.8 Hz, we concluded that CH_3-10 was in the β-axial position of the half-chair conformation of the tetrahydropyran ring. This was corroborated by the correlations of H-10, which was in α equatorial position, to both H-9β (δ_H 2.57, brd, J = 16.8 Hz) and H-9α (δ_H 2.81, dd, J = 16.8, 5.6 Hz) in the NOESY spectrum (Table 1, Supplementary Information, Figure S6). On the contrary, one of H-14 appeared as a double double doublet at δ_H 2.28, with a germinal coupling of 14.7 Hz and a diaxial coupling of 11.3 Hz, as well as a small coupling (long range) of 0.7 Hz, while another appeared also as a double double doublet at

δ_H 2.48, with a germinal coupling of 14.7 Hz and an axial-equatorial coupling of 2.9 Hz, as well as a small coupling (long range) of 1.9 Hz. These patterns of couplings revealed that CH_3-15 was in α equatorial position of the chair conformation of the tetrahydro-4*H*-pyran-4-one ring. This analysis was corroborated by the NOESY spectrum (Table 1, Supplementary Information, Figure S6), which exhibited a correlation only between H-15 and H-14β (δ_H 2.48, ddd, *J* = 14.7, 2.9, 1.9 Hz) and not between H-15 and H-14α (δ_H 2.28, ddd, *J* = 14.7, 11.3, 0.7 Hz). This assignment was also supported by the higher chemical shift value of H-14β than that of H-14α since the former is under the anisotropic deshielding of the C-13 carbonyl group. Based on the same reasoning, we assigned the broad doublet at δ_H 2.81 *(J* = 14.0 Hz) as H-12β, and the double doublet at δ_H 2.55 *(J* = 14.0, 1.9 Hz) as H-12α. Consequently, the relative configuration of C-10 and C-15 was tentatively assigned as 10*S** and 15*R**. The relative configuration of C-11 was tentatively assigned as 11*S** based on the fact that the NOESY spectrum (Table 1, Supplementary Information, Figure S6) did not exhibit any correlation between H-10 and H-15. According to the molecular model, when the configuration of C-11 is *S**, the substituents on C-11 are arranged in a way that H-10 and H-15 are pointing toward the opposite directions. On the contrary, the *R** configuration of C-11 would have H-10 and H-15 close enough to give a strong NOESY correlation.

Similanpyrone C (**1**) can be assumed to be derived from the acetate-malonate pathway (Scheme 1). Cyclization and enolization of the pentaketide (**I**) leads to the formation of 6,8-dihydroxy-3-methylisocoumarin (**II**), which, after Claisen condensation with the tetraketide (**III**), gives rise to **IV**. Enolization of the side chain, together with a formation of the hemiketal by the phenolic hydroxyl group on C-6 of the isocoumarin nucleus and the ketone carbonyl of the side chain, leads to the formation of a hemiketal **V**. Formation of the ketal and methylation by SAM in the side chain finally gives rise to similanpyrone C (**1**).

Compound **2** was isolated as pale yellow viscous mass, and its molecular formula $C_{34}H_{52}N_6O6$ was established on the basis of the (+)-HRESIMS *m/z* 641.4053 $[M + H]^+$, indicating twelve degrees of unsaturation. The IR spectrum showed absorption bands for amine (3335 cm^{-1}), carbonyl (1682, 1644 cm^{-1}) and aromatic (1594, 1519 cm^{-1}). The ^{13}C NMR (Supplementary Information, Figure S8), DEPTs and HSQC spectra (Table 2, Supplementary Information, Figure S10) revealed the presence of six amide carbonyls (δ_C 174.3, 174.2, 170.7, 170.2, 169.3, 168.9), two quaternary sp^2 (δ_C 137.0, 122.7), four methine sp^2 (δ_C 131.7, 127.1, 123.9, 123.4), eight methine sp^3 (δ_C 65.1, 61.4, 59.3, 50.9, 47.9, 29.9, 25.5, 24.4), six methylene sp^3 (δ_C 52.5, 37.8, 36.2, 28.1, 27.4, 24.5) and eight methyl (δ_C 37.9, 23.3, 23.2, 22.1, 21.7, 19.8, 18.4, 16.2) carbons. The ^1H NMR spectrum (Table 2, Supplementary Information, Figure S7) revealed, besides four NH signals at δ_H 7.43, d (*J* = 7.4 Hz), 7.64, d (*J* = 9.8 Hz), 8.02, d (*J* = 7.9 Hz) and 9.41, brs, the signals of the aromatic protons of the 1,2-disubstituted benzene ring at δ_H 7.20, dd (*J* = 7.7, 1.5 Hz), 7.13, ddd (*J* = 7.9, 7.9, 1.0 Hz), 7.47, ddd, (*J* = 7.9, 7.9, 1.6 Hz) and 8.29, d (*J* = 8.3 Hz). That the 1,2-disubstituted benzene ring belonged to the anthranilic acid residue was corroborated by the HMBC correlations of the NH signal at δ_H 9.41, brs to the carbon signal at δ_C 123.9 (C-6), and of the double doublet at δ_H 7.20 (*J* = 7.7, 1.5 Hz, H-3) to the carbons at δ_C 131.7 (C-5), 137.0 (C-7) and 170.2 (CO-1) (Table 2, Figure 3, Supplementary Information, Figure S11). The anthranilic acid residue was linked to the valine residue, through the amino group of the former and the carboxyl group of the latter, since the HMBC spectrum (Supplementary Information, Figure S11) showed correlations of the NH signal at δ_H 9.41, brs to the

carbonyl carbon at δ_C 170.7 (C-8), of the methine proton at δ_H 4.32 dd, J = 7.4, 3.3 Hz (H-9) to the methine carbon at δ_C 29.9 (C-10), the methyl carbon at δ_C 16.2 (C-12) and C-8, and of the NH signal at δ_H7.43, d (J = 7.5 Hz) to C-9 (δ_C 59.3) and C-10 (Table 2, Figure 3). The presence of the leucine residue was supported by the coupling system from CH-14 (δ_H 4.57, m; δ_C 50.9) through CH_3-17 (δ_H 0.97, d, J = 6.5 Hz; δ_C 23.3) and CH_3-18 (δ_H 0.88, d, J = 6.4 Hz; δ_C 21.1), and of NH at δ_H 8.02 d (J = 7.9 Hz) to H-14, as observed in the COSY spectrum (Table 2, Supplementary Information, Figure S9), as well as by the HMBC correlations of the NH signal at δ_H 8.02 d (J = 7.9 Hz) to C-14 (Table 2, Figure 3). That the valine residue was linked to the leucine residue was supported by the HMBC cross peak between the NH signal of the former (δ_H7.43, d, J = 7.5 Hz) to the signal of the carbonyl carbon (δ_C174.2, C-13) of the latter. In turn, the leucine residue was linked to the alanine residue, as evidenced by the HMBC cross peaks of the NH signal of the former to the carbonyl carbon signal (δ_C174.3, C-19) of the latter, and of the proton signal at δ_H 4.82, dd, J = 9.7, 7.3 Hz (H-20) to C-19 and the methyl carbon at δ_C 18.4 (C-21), as well as by the COSY cross peaks of H-20 to CH_3-21 (δ_H 1.29, d, J = 7.3 Hz), and of H-20 to NH at δ_H 7.64, d (J = 7.9 Hz). The presence of the *N*- methyl leucine moiety was evidenced by the coupling system from H-23 (δ_H 3.49, dd, J = 9.0, 4.7 Hz) through CH_3-26 (δ_H 0.97d, J = 6.5; δ_H 23.2) and CH_3-27 (δ_H 0.99, d, J = 6.5; δ_H 22.1), as observed in the COSY spectrum (Table 2, Supplementary Informatscheion, Figure S9), as well as by the HMBC correlations of H-23 to C-22 (δ_C 169.3) and CH_3-28 (δ_C 37.9). Finally, the presence of the pipecolic acid residue was supported by the coupling system from CH-30 (δ_H 3.71, dd, J = 11.3, 2.5; δ_C 61.4) through CH_2-34 (δ_H 3.16, dd, J = 13.2, 2.3; 4.14, dd, J = 14.4, 2.4; δ_C 52.5), as observed in the COSY spectrum (Table 2, Supplementary Information, Figure S9). Since both H-30 and CH_3-28 gave HMBC cross peaks to C-29 (δ_C 168.9), the pipecolic acid residue was linked to the *N*-methyl leucine residue through the carboxyl group of the former and a nitrogen atom of the latter. Since **2** presents twelve degrees of unsaturation, the nitrogen atom of the piperidine ring of the pipecolic acid residue was linked to the carbonyl of the anthranilic acid residue. The proposed structure was supported by the NOESY correlations which showed cross peaks of NH at δ_H 9.41, brs to H-9, CH_3-12, of NH at δ_H 7.43 (d, J = 7.5 Hz) to H-9, CH_3-11 (δ_H 1.06, d, J = 6.9 Hz), CH_3-12, H-14, of NH at δ_H 8.02 (d, J = 7.9 Hz) to H-14, H-15 (δ_H 2.02, m; 1.77, m), CH_3-17, of NH at δ_H 7.64 (d, J = 7.9 Hz) to CH_3-21, H-23, CH_3-28, of H-3 to H-34β (δ_H 4.14, dd, J = 14.4, 2.4 Hz), and of H-30 to CH_3-28 (Table 2, Supplementary Information, Figure S12). Combining this information, it was possible to conclude that **2** was cyclo (anthranilic acid-Val-Leu-Ala-*N*-methyl-Leu-pipecolic acid).

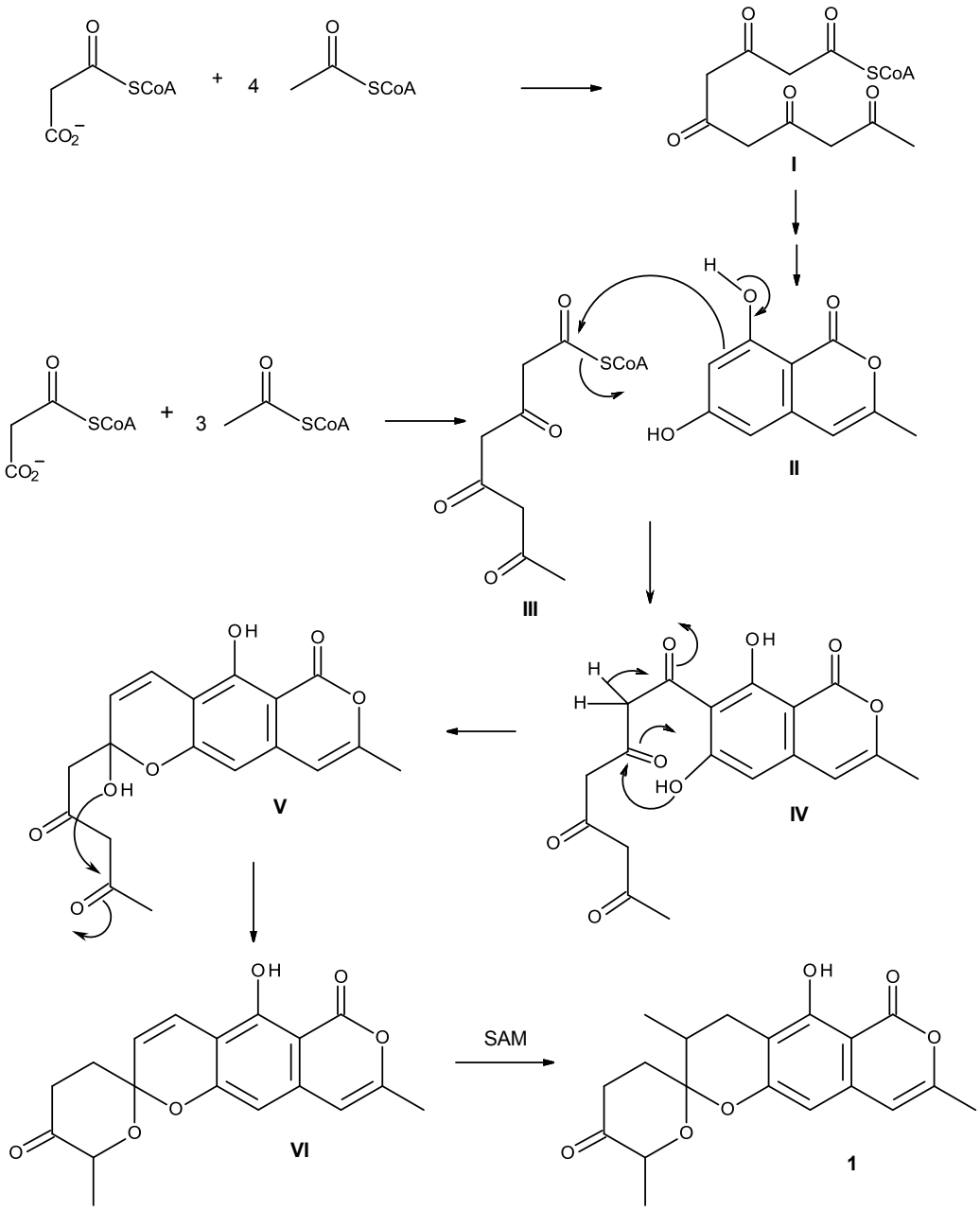

Scheme 1. Proposed biogenesis of similanpyrone C (**1**).

Table 2. ^{1}H and ^{13}C NMR ($CDCl_3$, 500.13 MHz and 125.8 MHz) and HMBC assignment for **2**.

	Position	δ_C, Type	δ_H, (*J* in Hz)	COSY	HMBC	NOESY
Anthranilic acid	1	170.2, CO	-			
	2	122.7, C	-			
	3	127.1, CH	7.20, dd (7.7, 1.5)	H-4	C-1, 5, 7	H-34
	4	123.4, CH	7.13, ddd (7.9, 7.9, 1.0)	H-3, 5	C-2, 6	
	5	131.7, CH	7.47, ddd (7.9, 7.9, 1.6)	H-4, 6	C-3, 7	
	6	123.9, CH	8.29, d (8.3)	H-5	C-2, 4	H-12
	7	137.0, C	-			
	NH	-	9.41, brs		C-6, 7, 8	NH (Val), H-9, 12
Val	8	170.7, CO	-			
	9	59.3, CH	4.32, dd (7.4, 3.3)	H-10, NH	C-8, 10, 11, 12	H-10, 11
	10	29.9, CH	2.68, m	H-9, 11, 12		H-9, 11, 12
	11	19.8, CH_3	1.06, d (6.9)	H-10	C-9, 10, 12	
	12	16.2, CH_3	0.94, d (7.0)	H-10	C-9, 10, 11	
	NH	-	7.43, d (7.5)	H-9	C-9, 10, 13	H-9, 11, 12, 14
Leu	13	174.2, CO	-			
	14	50.9, CH	4.57, m	H-15, NH		H-15, 18
	15	36.2, CH_2	2.02, m; 1.77, m	H-14, 16		
	16	24.4, CH	1.77, m	H-15, 17, 18		
	17	23.3, CH_3	0.97, d (6.5)	H-16	C-15, 16, 18	
	18	21.7, CH_3	0.88, d (6.4)	H-16	C-15, 16, 17	
	NH	-	8.02, d (7.9)	H-14	C-13, 19	NH (Ala), H-14, 15, 17
Ala	19	174.3, CO	-			
	20	47.9, CH	4.82, dd (9.7, 7.3)	H-21, NH	C-19, 21	H-21
	21	18.4, CH_3	1.29, d (7.3)	H-20	C-19, 20	
	NH	-	7.64, d (7.9)	H-20	C-22	C-21, 23, 28

Table 2. *Cont.*

	22	169.3, CO	-			
	23	65.1, CH	3.49, dd (9.0, 4.7)	H-24	C-22, 24, 28, 29	
	24	37.8, CH_2	1.95, m; 2.20, m	H-23, 25		
N-Me Leu	25	25.5, CH	1.65, m	H-24, 26, 27		
	26	23.2, CH_3	0.97, d (6.5)	H-25	C-24, 25, 27	
	27	22.1, CH_3	0.99, d (6.5)	H-25	C-24, 25, 26	
	28	37.9, CH_3	3.20, s		C-23, 29	23, 30, 32, 34α
	29	168.9, CO	-			
	30	61.4, CH	3.71, dd (11.3, 2.5)	H-31	C-1, 29	H-34α
	31	28.1, CH_2	2.05, m	H-30, 32		
Pipecolic acid	32	24.5, CH_2	2.07, m	H-31, 33		
	33	27.4, CH_2	1.56, m	H-32, 34		
	34α	52.5, CH_2	3.16, dd (13.2 2.3)	H-33		H-34β
	34β		4.14, dd (14.4, 2.4)			H-34α

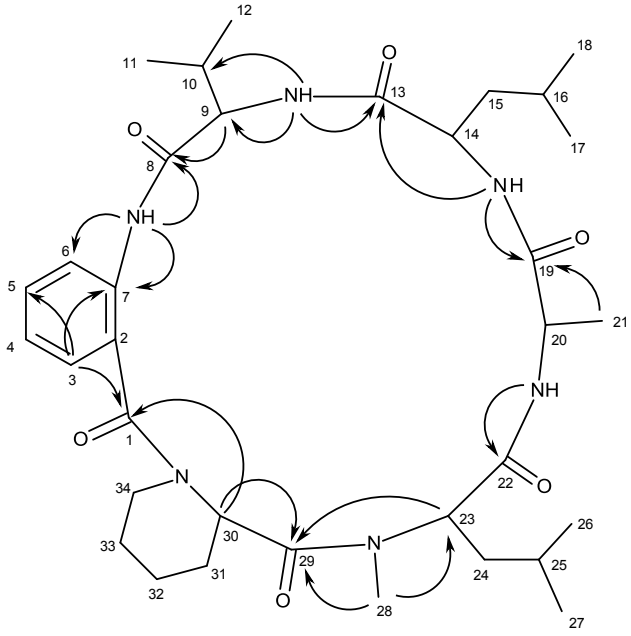

Figure 3. Key HMBC correlations of compound **2**.

The ^{1}H and ^{13}C NMR data of compound **2** resembled those of PF1171C, a cyclic hexapeptide isolated from extracts of the unidentified ascomycete OK-128 fermented with okara by Kai *et al.* [30], and later by a total synthesis by Masuda *et al.* [31]; however, its value of optical rotation was quite different from that of PF1171C [30,31]. Moreover, PF1171C was reported as white solid (mp 138–140 °C) [31], while compound **2** is pale yellow viscous mass. This observation suggested that compound **2** and PF1171C could be diastereomers.

The stereochemistry of the amino acid residues of compound **2** was determined by chiral HPLC analysis of its acidic hydrolysate, using appropriate D and L amino acids standards, according to the previously described method [32]. The enantioseparations of the standard amino acids were successfully performed with the Chirobiotic T column under reversed-phase elution conditions [33]. Actually, the teicoplanin selector of this column has several characteristic features that make it suitable for amino acid analysis [33–35]. The elution order of the enantiomers of all the standard amino acids was confirmed by injecting the solutions of the racemic or enantiomeric mixtures and then each enantiomer separately at a flow rate of 1 mL/min (Supplementary Information, Figure S18). As predicted, the D enantiomer was always more strongly retained than the corresponding L enantiomer on the Chirobiotic T column [33]. Based on mix HPLC analyses of the acidic hydrolysate with standard amino acids (co-injection) (Supplementary Information, Figure S19 and Table S1), compound **2** was elucidated unambiguously as cyclo (anthranilic acid-L-Val-D-Leu-L-Ala-*N*-methyl-L-Leu-D-pipecolic acid). Although the amino acid sequence of compound **2** is the same as that of PF1171C, the stereochemistry of its amino acid constituents is different from that of the amino acids constituent of PF1171C. While PF1171C contains D-Ala, L-Leu, D-Val, and L-pipecolic acid, compound **2** contains L-Ala, D-Leu, L-Val and D-pipecolic acid. Thus compound **2** is a new compound, and we have named it similanamide.

It is interesting to note that Kai *et al.* [30] has firstly assigned the stereochemistry of the amino acid constituents of PF1171C using the reversed phase HPLC analysis of the Marfey derivatives of the amino acids. Since the retention times for the Marfey derivatives of D-Ala (19.4 min) and L-Ala

(20.0 min) were too close for resolution, they had wrongly assigned D-Ala for L-Ala. However, in our chiral HPLC analysis using the Chirobiotic T column under reversed-phase elution conditions, not only the retention time of L-Ala (7.16 min) was very different from that of D-Ala (9.36 min), but also the retention times of the D/L pair of other amino acid constituents (Supplementary Information, Table S1).

So far, only few cyclohexapeptides have been reported from marine-derived microorganisms. Wu *et al.* [36] have isolated two cyclohexapeptides, nocardiamides A and B, from the culture broth of the marine-derived actinomycete *Nocardiopsis* sp. CNX037, isolated from sediment. Cai *et al.* [37] have isolated two anti-*Mycobacterium tuberculosis* cyclohexapeptides from a *Streptomyces hygroscopicus* Strain, while Song *et al.* [38] reported isolation of three new cyclopeptides, desotamides B–D, from the deep South China Sea-derived *Streptomyces scopuliridis* SCSIO ZJ46. To the best of our knowledge, compound **2** is the first cyclopeptide containing D-pipecolic acid residue ever isolated from marine fungi.

Compound **3** was isolated as pale yellow viscous mass, and its molecular formula $C_{29}H_{33}NO_8$ was established on the basis of (+)-HRESIMS *m/z* 524.2287 $[M + H]^+$, indicating fourteen degrees of unsaturation. The IR spectrum showed absorption bands for hydroxyl (3418 cm^{-1}), ester carbonyl (1732 cm^{-1}), conjugated ester carbonyl (1667cm^{-1}), olefin (1643 cm^{-1}), aromatic (1557, 1507 cm^{-1}). The ^{13}C NMR (Supplementary Information, Figure S15), DEPTs and HSQC spectra (Table 3, Supplementary Information, Figure S16) revealed the presence of two ester carbonyl (δ_C 170.1 and 169.8), one conjugated carbonyl (δ_C 161.6), five quaternary sp^2 (δ_C 160.2, 156.8, 146.1, 126.9, 100.3), six methine sp^2 (δ_C 151.3, 146.5, 132.8, 123.9, 109.4, 98.7), one oxyquaternary sp^3 (δ_C 85.9), two oxymethine sp^3 (δ_C 75.7 and 72.8), one oxymethylene sp^3 (δ_C 64.4), two quaternary sp^3 (δ_C 40.3, 38.4), one methine sp^3 (δ_C 40.7), three methylene sp^3 (δ_C 35.2, 27.3, 22.9), and five methyl (δ_C 23.8, 20.8, 20.5, 20.1 and 12.7) carbons. The general feature of ^{13}C and ^1H spectra of compound **3** closely resembled those of pyripyropene S, previously isolated from the same fungus [29]. Analysis of the ^1H (Supplementary Information, Figure S13), ^{13}C, HSQC and HMBC spectra (Table 3, Supplementary Information, Figure S17) revealed the presence of the ring system comprising of the decahydronaphthalene fused, on C-5 and C-6, with the 2*H*,5*H*-pyrano[4,3-*b*]pyran-5-one, which connected to the pyridine ring through C-6′ of the former and C-3″ of the latter, similar to pyripyropene S [29]. However, there were only two acetoxyl groups (δ_C 170.1, CO; δ_C 20.5, CH_3, δ_H 2.00, s and δ_C 169.8, CO; δ_C 20.8, CH_3; δ_H 2.00, s) in compound **3**. That the acetoxyl groups were on C-1 and C-11 was supported by the fact that the chemical shift values of H-1 (δ_H 4.64, t, J = 8.5 Hz) and H-11 (δ_H 3.75, s) were very similar to those of pyripyropene S, whereas the chemical shift of H-7 (δ_H 3.85, dd, J = 10.6, 4.2 Hz) was nearly 1.4 ppm less than that of pyripyropene S. On the other hand, the ^{13}C chemical shift values of C-6 (δ_H 85.9) and C-8 (δ_C 27.4) of compound **3** were 2.00 and 3.00 ppm, respectively, higher than those of the corresponding carbons in pyripyropene S, while the ^{13}C chemical shift value of C-7 (δ_C 75.5) of compound **3** was 2.00 ppm lower than that of C-7 of pyripyropene S. Since H-7 appeared as a double doublet with coupling constants of 10.6 and 4.2 Hz, the position of the hydroxyl group on C-7 was β. Thus, compound **3** is 7-deacetylpyripyropene S. In order to prove the stereochemistry of compound **3**, the NOESY experiment was carried out. As the NOESY spectrum (Table 3) clearly exhibited correlations of CH_3-15 to CH_3-12, but not to H-1 and H-9; of CH_3-12 to CH_3-14 and CH_3-15, and of CH_3-14 to CH_3-12, but not to H-7 (Table 3,

Supplementary Information, Figure S18), the stereochemistry of compound **3** is the same as that of pyripyropene S [29], *i.e.*, 1*S**, 4*R**, 6*S**, 7*S**, 9*R**, 10*R**. Since it is a new compound we have named it pyripyropene T.

Table 3. ^{1}H and ^{13}C NMR (DMSO, 300.13 MHz and 75.47 MHz) and HMBC assignment for **3**.

Position	δ_C, Type	δ_H, (*J* in Hz)	COSY	HMBC	NOESY
1	72.8, CH	4.64, t (8.5)	H-2		
2	22.9, CH_2	1.79, m	H-1, 3		
3	35.2, CH_2	1.98, m	H-2		
4	38.4, C	-			
5	146.1, C	-			
6	85.9, C	-			
7	75.7, CH	3.85, dd (10.6, 4.2)	H-8		
8	27.3, CH_2	1.70, m	H-7		
9	40.7, CH	1.48, m	H-8		
10	40.3, C	-			
11	64.4, CH_2	3.75, s		C-1, 9	H_3-15
12	23.8, CH_3	1.19, s		C-3, 4, 5	H_3-14, 15
13	109.4, CH	6.16, s		C-4, 6, 2″, 4″	
14	20.1, CH_3	1.45, s		C-5, 6, 7	H_3-12
15	12.7, CH_3	0.84, s		C-1, 9, 10, 11	H_2-11, H_3-12
2′	161.6, C	-			
3′	100.3, C	-			
4′	160.2, C	-			
5′	98.7, CH	7.11, s		C-3′, 4′, 6′, 3″	
6′	156.8, C	-			
2″	146.5, CH	9.0, d (1.7)	H-4″	C-3″, 6″	H-5′
3″	126.9, C	-			
4″	132.8, CH	8.25, dt (8.7, 2.2)	H-2″, 5″		H-5′, 5″
5″	123.9, CH	7.54, dd (7.9, 4.8)	H-4″, 6″	C-3″	H-4″, 6″
6″	151.3, CH	8.68, dd (4.8, 1.5)	H-2″, 5″	C-2″, 4″	H-5″
OAc-1	170.1, CO	-			
	20.5, CH_3	2.00, s		CO (Ac)	
OAc-11	169.8, CO	-			
	20.8, CH_3	2.00, s		CO (Ac)	

Since compound **1** was isolated in a very small amount, only compounds **2** and **3** were evaluated for their cytotoxicity and antibacterial activity. Compounds **2** exhibited weak *in vitro* growth inhibitory activity, by Sulforhodamine B (SRB) assay [39], against the MCF-7 (breast adenocarcinoma, GI_{50} = 125 ± 0), NCI-H460 (non-small cell lung cancer, GI_{50} = 117.50 ± 3.55) and A373 (melanoma, GI_{50} = 115 ± 7.07) cell lines. Compounds **2** and **3** were also tested for their antibacterial activity against four reference strains (*Staphylococcus aureus*, *Bacillus subtilis*, *Escherichia coli* and *Pseudomonas aeruginosa*), as well as the environmental multidrug-resistant isolates, according to the previously described method [40], and neither of them showed activity (MIC values higher than 256 μg/mL).

3. Experimental Section

3.1. General Procedure

Melting points were determined on a Bock monoscope and are uncorrected. Optical rotations were determined on an ADP410 Polarimeter (Bellingham + Stanley Ltd., Tunbridge Wells, Kent, UK). Infrared spectra were recorded in a KBr microplate in a FTIR spectrometer Nicolet iS10 from Thermo Scientific (Waltham, MA, USA.) with Smart OMNI-Transmission accessory (Software 188 OMNIC 8.3). ^{1}H and ^{13}C-NMR spectra were recorded at ambient temperature on a Bruker AMC instrument (Bruker Biosciences Corporation, Billerica, MA, USA) operating at 500.13 and 125.8 MHz or at 300.13 and 75.4 MHz, respectively. High-resolution mass spectra were measured with a Waters Xevo QToF mass spectrometer (Waters Corporations, Milford, MA, USA) coupled to a Waters Aquity UPLC system. A Merck (Darmstadt, Germany) silica gel GF254 was used for preparative TLC, and a Merck Si gel 60 (0.2–0.5 mm) was used for analytical chromatography.

3.2. Extraction and Isolation

Isolation and identification of the fungus as well as fractionation of the crude extract of the culture of *A. similanensis* KUFA0013 have been previously described by us [29]. Frs 185–196 were combined (654 mg) and purified by TLC (Si gel, $CHCl_3$:Me_2CO:HCO_2H, 97:3:0.1) to give 7.4 mg of **1**. Frs 310–327 were combined (1.19 g), applied on a Sephadex H-20 column (10 g) and eluted MeOH, wherein ten sfrs of 1 mL were collected. Sfrs 1–7 were combined and purified by TLC (Si gel, $CHCl_3$:Me_2CO:HCO_2H, 19:1:0.01) to give 108 mg of **2**. Frs 336–345 were combined (165 mg) and purified by TLC (Si gel, $CHCl_3$:Me_2CO:HCO_2H, 17:3:0.01) to give additional 60 mg of **2**. Frs 354–398 were combined (1.15 g), applied on a Sephadex LH-20 column (10 g) and eluted with MeOH, wherein thirty four sfrs of 1 mL were collected. Sfrs 7–15 were combined (150 mg) and purified by TLC (Si gel, $CHCl_3$:Me_2CO:HCO_2H, 4:1:0.01) to give 67 mg of pyripyropene S [29]. Frs 435–443 were combined (377 mg), applied on a Sephadex LH-20 column (10 g) and eluted with a mixture of 1:1 v/v of $CHCl_3$: MeOH, wherein fourteen sfrs of 1 mL were collected. Sfrs 8–11 (62 mg) were combined and purified by TLC (Si gel, $CHCl_3$:Me_2CO:HCO_2H, 19:1:0.01) to give 35 mg of **3**.

3.2.1. Similanpyrone C (**1**)

Pale yellow viscous mass; $[\alpha]_D^{20}$ = −80.0 (*c* 0.01, $CHCl_3$); λ_{max} (log ε) 239 (4.57), 245(4.59), 332 (2.10) nm; IR (KBr) ν_{max} 3443, 2923, 2852, 1730, 1683, 1647, 1625, 1572, 1508, 1457, 1429, 1352, 1251 cm^{-1}; ^{1}H and ^{13}C NMR (Table 1); HRESIMS *m/z* 345.1342 $(M + H)^+$ (calculated for $C_{19}H_{21}O_6$, 345.1338).

3.2.2. Similanamide (**2**)

Pale yellow viscous mass; $[\alpha]_D^{20}$ = +30.3 ($CHCl_3$, *c* 0.03), IR (KBr) ν_{max} 3335, 3054, 2958, 2870, 1682, 1644, 1594, 1519, 1449, 1292 cm^{-1}; ^{1}H and ^{13}C NMR (Table 2); HRESIMS *m/z* 641.4053 (calculated for $C_{34}H_{53}N_6O_6$, 641.4027).

3.2.3. Pyripyropene T (**3**)

Pale yellow viscous mass; $[\alpha]_D^{20}$ = +106 ($CHCl_3$, *c* 0.03), IR (KBr) ν_{max} 3418, 2949, 1732, 1667, 1643, 1557, 1507, 1480, 1246, 1028 cm^{-1}; ^1H and ^{13}C NMR (Table 3); HRESIMS *m/z* 524.2287 $(M + H)^+$, calcd for $C_{29}H_{34}NO_8$, 524.2284.

3.3. Amino Acids Analysis of Acidic Hydrolysate of Compound ***2***

3.3.1. Acid Hydrolysis

The stereochemistry of the amino acids was determined by analysis of the acidic hydrolysate from compound **2**. Compound **2** (5.0 mg) was dissolved in 6 N HCl (5 mL) and heated at 110 °C, in a furnace, for 24 h in a sealed glass tube. After cooling to room temperature, the solution was dried under N_2 for 24 h, reconstituted in methanol for HPLC-MS (200 µL), filtered through a 4 mm PTFE Syringe Filter F2504-4 of 0.2 µm pore size (Thermo Scientific, Mumbai, India), and then analyzed by HPLC equipped with a chiral column.

3.3.2. Chiral HPLC Analysis

The HPLC system consisted of Shimadzu LC-20AD pump, equipped with a Shimadzu DGV-20A5 degasser, a Rheodyne 7725i injector fitted with a 20 µL loop, and a SPD-M20A DAD detector (Kyoto, Japan). Data acquisition was performed using Shimadzu LCMS Lab Solutions software, version 3.50 SP2. The chiral column used in this study was Chirobiotic T (15 cm × 4.6 mm I.D., particle size 5 µm) manufactured by ASTEC (Whippany, NJ, USA). The mobile phase composition was MeOH:H_2O:CH_3CO_2H (70:30:0.02, v/v/v), all were LC-MS grade solvents obtained from Sigma-Aldrich Co (St. Louis, MO, USA). The flow rate was 0.5 mL/min and the UV detection wavelength was 210 nm. Analyses were performed at room temperature in an isocratic mode.

All standards of racemic amino acids and pure amino acid enantiomers were purchased from Sigma-Aldrich Co (St. Louis, MO, USA). The elution order of the enantiomers of all the standards amino acids was confirmed by injecting the solutions of the racemic or enantiomeric mixtures, and then each enantiomer separately (or only L- amino acid in the case of *N*-methyl leucine) at a flow rate of 1 mL/min or 0.5 mL/min. Working solutions of single enantiomeric amino acids were prepared by dissolution in MeOH at the concentration of 1 mg/mL (10 µL sample injection), while the enantiomeric mixtures were prepared by mixing equal aliquots of each enantiomer (20 µL sample injection). Mix HPLC analyses of the acidic hydrolysate with standard amino acids (co-injection) confirmed the stereochemistry of the amino acids of compound **2**.

4. Conclusions

Following our first report of the isolation of new isocoumarin derivatives and merotepenoids from the ethyl acetate crude extract of the culture of the undescribed marine sponge-associated fungus *Aspergillus similanensis* KUFA 0013, we have reexamined its remaining column fractions and have isolated a new isocoumarin derivative containing an unusual 1,7-dioxaspiro-undecenone moiety, together with a new cyclohexapeptide and a new pyripyropene analog. Although several cyclopeptides

have been reported from many fungi of the genus *Aspergillus*, this is the first report of isolation of cyclohexapeptide from the marine-derived fungus. The fact that these new cyclohexapeptide and pyripyropene analog did not exhibit relevant antibacterial and the *in vitro* growth inhibitory activities on human cancer cell lines does not mean that they are void of other interesting biological activities. In order to prove this hypothesis, it is necessary to explore their potential in a broader biological or pharmacological assay system.

Acknowledgments

This work was partially supported by the Project MARBIOTECH (reference NORTE-07-0124-FEDER-000047) within the SR&TD Integrated Program MARVALOR—Building research and innovation capacity for improved management and valorization of marine resources, supported by the Programa Operacional Regional do Norte (ON.2—O Novo Norte), the European Regional Development Fund, and FCT-Fundação para a Ciência e a Tecnologia under the project CEQUIMED-PEst-OE/SAU/UI4040/2014. We thank Michael Lee of the Department of Chemistry, Leicester University (UK), for providing the HRESIMS. C.P. thanks the Faculty of Pharmaceutical Sciences, Burapha University, Thailand for her scholarship to the University of Porto. We thank Júlia Bessa for technical support.

Author Contributions

Chadaporn Prompanya performed isolation, purification and structure elucidation of some compounds; Carla Fernandes and Sara Cravo performed HPLC analysis of amino acids by chiral column; Tida Dethoup isolated, identified, cultured the fungi, and prepared the crude extract; Artur M.S. Silva provided 1D and 2D NMR spectra. Madalena M.M. Pinto, and Anake Kijjoa conceived, designed the research, elucidated the structure of the compounds and wrote the paper.

Conflicts of Interest

The authors declare no conflict of interest.

References

1. Bugni, T.S.; Ireland, C.M. Marine-derived fungi: A chemically and biologically diverse group of microorganisms. *Nat. Prod. Rep.* **2004**, *21*, 143–163.
2. Saleem, M.; Ali, M.S.; Hussain, S.; Jabbar, A.; Ashraf, M.; Lee, Y.S. Marine natural products of fungal origin. *Nat. Prod. Rep.* **2007**, *24*, 1142–1152.
3. Rateb, M.E.; Ebel, R. Secondary metabolites of fungi from marine habitats. *Nat. Prod. Rep.* **2011**, *28*, 290–344.
4. Liu, X.-H.; Miao, F.-P.; Liang, X.-R.; Ji, N.-Y. Ergosteroid derivatives from an algicolous strain of *Aspergillus ustus*. *Nat. Prod. Res.* **2014**, *28*, 1182–1186.
5. Yang, G; Sandjo, L.; Yun, K.; Leutou, A.S.; Kim, G.-D.; Choi, H.D.; Kang, S.J.; Hong, J.; Son, B.W. Flavusides A and B, antibacterial cerebrosides from the marine-derived fungus *Aspergillus flavus*. *Chem. Pharm. Bull.* **2011**, *59*, 1174–1177.

6. Sun, L.-L.; Shao, C.-L.; Chen, J. –F.; Guo, Z.-Y.; Fu, X.-M.; Chen, M.; Chen, Y.-Y.; Li, R.; de Voogd, N.J.; She, Z.-G.; Lin, Y.-C.; Wang, C.-Y. New bisabolane sesquiterpenoids from a marine-derived fungus *Aspergillus* sp. isolated from the sponge *Xestospongia testudinaria*. *Bioorg. Med. Chem. Lett*. **2012**, *22*, 1326–1329.
7. Kitano, M.; Yamada, T.; Amagata, T.; Minoura, K.; Tanaka, R.; Numatra, A. Novel pyridino-α-pyrone sesquiterpene type pileotin prduced by a sea urchin-derived *Aspergillus* sp. *Tetrahedron Lett.* **2012**, *53*, 4192–4194.
8. Liu, H.-B.; Edrada-Ebel, R.; Wang, Y.; Schulz, B.; Draeger, S.; Müller, W.E.G.; Wray, V.; Lin, W.-H.; Proksch, P. Ophiobolin sesterterpenoids and pyrrolidine alkaloids from the sponge-derived fungus *Aspergillus ustus*. *Helv. Chim. Acta* **2011**, *94*, 623–631.
9. Zhang, D.; Fukuzawa, S.; Satake, M.; Li, X.; Kuranaga, T.; Niitsu, A.; Yoshizawa, K.; Tachibana, T. Ophiobolin O and 6-*epi*-ophiobolin O, two new cytotoxic sesterterpenes from the marine-derived fungus *Aspergillus* sp. *Nat. Prod. Commun.* **2012**, *7*, 1411–1414.
10. Sun, H.-F.; Li, X.-M.; Cui, C.-M.; Gao, S.-S.; Li, C.-S.; Huang, C.-G.; Wang, B.-G. Asperolides A–C, tetranorlabdane diterpenoids from the marine alga-derived endophytic fungus *Aspergillus wentii* EN-48. *J. Nat. Prod.* **2012**, *75*, 148–152.
11. Zhou, Y.; Debbab, A.; Wray, V.; Lin, W.; Schulz, B.; Trepos, R.; Pile, C.; Hellio, C.; Proksch, P.; Aly, A.H. Marine bacterial inhibitors from the sponge-derived fungus *Aspergillus* sp. *Tetrahedron Lett.* **2014**, *55*, 2789–2792.
12. Zhang, Y.; Li, X.-M.; Wang, B.-G. Anthraquinone derivatives produced by marine-derived fungus *Aspergillus versicolor* EN-7. *Biosci. Biotechnol. Biochem*. **2012**, *76*, 1774–1776.
13. Huang, H.; Wang, F.; Luo, M.; Chen, Y.; Song, Y.; Zhang, W.; Zhang, S.; Ju, J. Halogenated anthraquinones from the marine-derived fungus *Aspergillus* sp. SCSIO F063. *J. Nat. Prod.* **2012**, *75*, 1346–1352.
14. Chen, M.; Fu, X.-M.; Kong, C.-J.; Wang, C.-Y. Nucleoside derivatives from the marine-derived fungus *Aspergillus versicolor*. *Nat. Prod. Res.* **2014**, *28*, 895–900.
15. Cai, S.; Kong, X.; Wang, W.; Zhou, H.; Zhu, T.; Li, D.; Gu, Q. Aspergilazine A, a diketopiperazine dímer with a rare N-1 to C-6 linkage, from a marine-derived fungus *Aspergillus taichungensis*. *Tetrahedron Lett.* **2012**, *53*, 2615–2617.
16. He, F.; Han, Z.; Peng, J.; Qian, P.-Y.; Qi, S.-H. Antifouling indole alkaloids from two marine-derived fungi. *Nat. Prod. Commun.* **2013**, *8*, 329–332.
17. Ji, I.-Y., Liu, Z.-H.; Miao, F.-P.; Qiao, M.-F. Aspeverin, a new alkaloid from algicolous strain of *Aspergillus versicolor*. *Org. Lett.* **2013**, *15*, 2327–2329.
18. Tsukamoto, S.; Umaoka, H.; Yoshikawa, K.; Ikeda, T.; Hirota, H. Notoamide O, a structurally unprecedented prenylated índole alkaloid, and notamides P-R from a marine-derived fungus, *Aspergillus* sp. *J. Nat. Prod.* **2010**, *73*, 1438–1440.
19. Wang, Y.; Lin, C.-L.; Bai, J.; Zhang, L.-M.; Wu, X.; Zhang, L.; Pei, Y.-H.; Jing, Y.-K.; Hua, H.-M. 2,5-Diketopiperazines from the marine-derived fungus *Aspergillus fumigatus* YK-7. *Chem. Biodivers.* **2012**, *9*, 385–393.
20. Song, F.; Liu, X.; Guo, H.; Ren, B.; Chen, C.; Piggott, A.M.; Yu, K.; Gao, H.; Wang, Q.; Liu, M.; *et al.* Brevianamides with antitubercular potential from a marine-derived isolate of *Aspergillus versicolor*. *Org. Lett.* **2012**, *14*, 4770–4773.

21. Chen, M.; Shao, C.-L.; Fu, X.-M.; Xu, R.-F.; Zheng, J.-J.; Zhao, D.-L.; he, Z.-G.; Wang, C.-Y. Bioactive indole alkaloids and phenyl ether derivatives from a marine-derived *Aspergillus* sp. fungus. *J. Nat. Prod.* **2013**, *76*, 547–553.
22. Peng, J.; Zhang, X.-Y.; Tu, Z.-C.; Xu, X.-Y.; Qui, S.-H. Alkaloids from the deep-sea-derived fungus *Aspergillus westerdijkiae* DFFSCS013. *J. Nat. Prod.* **2013**, *76*, 983–987.
23. He, F.; Bao, J.; Zhang, X.-Y.; Tu, Z.-C.; Shi, Y.-M.; Qi, S.-H. Asperterrestide A, a cytotoxic tetrapeptide from the marine-derived fungus *Aspergillus terreus* SCSGAF0162. *J. Nat. Prod.* **2013**, *76*, 1182–1186.
24. Zhou, L.-N.; Gao, H.-Q.; Cai, S.-X.; Zhu, T.-J.; Gu, Q.-Q.; Li, D.-H. Two new cyclic pentapeptides from the marine-derived fungus *Aspergillus versicolor*. *Hel. Chim. Acta* **2011**, *96*, 1065–1070.
25. Zhuang, Y.; Teng, X.; Wang, Y.; Liu, P.; Wang, H.; Li, J.; Li, G.; Zhu, W. Cyclopeptides and polyketides from coral-associated fungus, *Aspergillus versicolor* LCJ-5-4. *Tetrahedron* **2011**, *67*, 7085–7089.
26. Liu, S.; Shen, Y. A new cyclic peptide from the marine fungal strain *Aspergillus* sp. AF119. *Chem. Nat. Compd (Engl. Transl.)* **2011**, *47*, 786–788.
27. Bao, J.; Zhang, X.-Y.; Xu, X.-Y.; He, F.; Nong, X.-H.; Qi, S.-H. New cyclic tripeptides and asteltoxins from gorgonian-derived fungus *Aspergillus* sp. SCSGAF0076. *Tetrahedron* **2013**, *69*, 2113–2117.
28. Ebada, S.S.; Fischer, T.; Hamacher, A.; Du, F.-Y.; Roth, Y.O.; Kassack, M.U.; Wang, B.-G.; Roth, E.H. Psychrophilin E, a new cyclopeptide, from co-fermentation of two marine alga-derived fungi of the genus *Aspergillus*. *Nat. Prod. Res.* **2014**, *28*, 776–781.
29. Prompanya, C.; Dethoup, T.; Bessa, L.J.; Pinto, M.M.M.; Gales, L.; Costa, P.M.; Silva, A.M.S.; Kijjoa, A. New isocoumarin derivatives and meroterpenoids from the marine sponge-associated fungus *Aspergillus similanensis* sp. nov. KUFA 0013. *Mar. Drugs* **2014**, *12*, 5160–5173.
30. Kai, K.; Yoshikawa, H.; Kuo, Y.-H.; Akiyama, K.; Hayashi, H. Determination of absolute structure of cyclic peptides, PF1171A and PF1171C, from unidentified ascomycete OK-128. *Biosci. Biotechnol. Biochem*. **2010**, *74*, 1309–1311.
31. Masuda, Y.; Tanaka, R.; Kai, K.; Ganesan, A.; Doi, T. Total synthesis and biological evaluation of PF1171A, C, F and G, cyclic hxapeptides with insecticidal activity. *J. Org. Chem.* **2014**, *79*, 7844–7853.
32. Huang, H.; She, Z.; Lin, Y.; Vrijmoed, L.L.P.; Lin, W. Cyclic peptide from an endophytic fungus obtained from a mangrove leaf (*Kandelia candel*). *J. Nat. Prod.* **2007**, *70*, 1696–1699.
33. Berthod, A.; Liu, Y.; Bagwill, C.; Armstrong, D.W. Facile liquid chromatographic enantioresolution of native amino acids and peptides using a teicoplanin chiral stationary phase. *J. Chromatogr. A* **1996**, *731*, 123–127.
34. Péter, A.; Török, G.; Armstrong, D.W. High-performance liquid chromatographic separation of enantiomers of unusual amino acids on a teicoplanin chiral stationary phase. *J. Chromatogr. A* **1998**, *793*, 283–296.
35. Kučerová, G.; Vozka, J.; Kalílová, K.; Geryx, R.; Plecita, D.; Pajponova, T.; Tesařová, E. Enantioselective separation of unusual amino acids by high performance liquid chromatography. *Sep. Purif. Technol*. **2013**, *119*, 123–128.

36. Wu, Z.-C.; Li, S.; Nam, S.-J.; Liu, Z.; Zhang, C. Nocardiamides A and B, two cyclohexapeptides from the marine-derived *Actinomycete nocardiopsis* sp. CNX037. *J. Nat. Prod.* **2013**, *76*, 694–701.
37. Cai, G.; Napolitano, J.G.; McAlpine, J.B.; Wang, Y.; Jaki, B.U.; Suh, J.-V.; Yang, S.H.; Lee, I.-A.; Franzblau, S.G.; Pauli, G.F.; Cho, S. Hytramycins V and I, Anti-mycobacterium tuberculosis hexapeptides from a *Streptomyces hygroscopicus* strain. *J. Nat. Prod.* **2013**, *76*, 2009–2018.
38. Song, Y.; Li, Q.; Liu, X.; Chen, Y.; Zhang, Y.; Sun, A.; Zhang, W.; Zhang, J.; Ju, J. Cyclic hexapeptides from the deep South China Sea-derived *Streptomyces scopuliridis* SCSIO ZJ46 active against pathogenic Gram-positive bacteria. *J. Nat. Prod.* **2014**, *77*, 1937–1941.
39. Kijjoa, A.; Wattanadilok, R.; Campos, N.; Maria São José Nascimento, M.S.J.; Pinto, M.; Herz, W. Anticancer activity evaluation of kuanoniamines A and C isolated from the marine sponge *Oceanapia sagittaria*, collected from the Gulf of Thailand. *Mar. Drugs* **2007**, *5*, 6–22.
40. Gomes, N.M.; Bessa, L.J.; Buttachon, S.; Costa, P.M.; Buaruang, J.; Tida Dethoup, T.; Silva, A.M.S.; Kijjoa, A. Antibacterial and antibiofilm activities of tryptoquivalines and meroditerpenes isolated from the marine-derived fungi *Neosartorya paulistensis*, *N. laciniosa*, *N. tsunodae*, and the soil fungi *N. fischeri* and *N. siamensis*. *Mar. Drugs* **2014**, *12*, 822–839.

APPENDIX IV

Prompanya, C., Dethoup, T., Gales, L., Lee, M., Pereira, J. A., Silva, A. M., Pinto, M. M., Kijjoa, A. (2016). New polyketides and new benzoic acid derivatives from the marine sponge-associated fungus *Neosartorya quadricincta* KUFA 0081. *Mar. Drugs, 14*, 134 – 159. Doi:10.3390/md14070134

marine drugs

MDPI

Article

New Polyketides and New Benzoic Acid Derivatives from the Marine Sponge-Associated Fungus *Neosartorya quadricincta* KUFA 0081

Chadaporn Prompanya [1,2], Tida Dethoup [3], Luís Gales [1,4], Michael Lee [5], José A. C. Pereira [1], Artur M. S. Silva [6], Madalena M. M. Pinto [2,7] and Anake Kijjoa [1,2,*]

1 ICBAS—Instituto de Ciências Biomédicas Abel Salazar, Universidade do Porto, Rua de Jorge Viterbo Ferreira, 228, 4050-313 Porto, Portugal; chadaporn@buu.ac.th (C.P.); lgales@ibmc.up.pt (L.G.); jpereira@icbas.up.pt (J.A.P.)

2 Interdisciplinary Centre of Marine and Environmental Research (CIIMAR), Rua dos Bragas 289, 4050-313 Porto, Portugal; madalena@ff.up.pt

3 Department of Plant Pathology, Faculty of Agriculture, Kasetsart University, 10900 Bangkok, Thailand; agrtdd@ku.ac.th

4 Instituto de Biologia Molecular e Celular (IBMC), Universidade do Porto, Rua de Jorge Viterbo Ferreira, 228, 4050-313 Porto, Portugal

5 Department of Chemistry, University of Leicester, University Road, Leicester LE 7 RH, UK; ml34@leicester.ac.uk

6 Departamento de Química & QOPNA, Universidade de Aveiro, 3810-193 Aveiro, Portugal; artur.silva@ua.pt

7 Laboratório de Química Orgânica, Departamento de Ciências Químicas, Faculdade de Farmácia Universidade do Porto, Rua de Jorge Viterbo Ferreira, 228, 4050-313 Porto, Portugal

* Correspondence: ankijjoa@icbas.up.pt; Tel.:+351-22-0428331; Fax: +351-22-2062232

Academic Editor: Russell Kerr

Received: 30 June 2016; Accepted: 12 July 2016; Published: 16 July 2016

Abstract: Two new pentaketides, including a new benzofuran-1-one derivative (**1**) and a new isochromen-1-one (**5**), and seven new benzoic acid derivatives, including two new benzopyran derivatives (**2a**, **b**), a new benzoxepine derivative (**3**), two new chromen-4-one derivatives (**4b**, **7**) and two new benzofuran derivatives (**6a**, **b**), were isolated, together with the previously reported 2,3-dihydro-6-hydroxy-2,2-dimethyl-4*H*-1-benzopyran-4-one (**4a**), from the culture of the marine sponge-associated fungus *Neosartorya quadricincta* KUFA 0081. The structures of the new compounds were established based on 1D and 2D NMR spectral analysis, and in the case of compounds **1**, **2a**, **4b**, **5**, **6a** and **7**, the absolute configurations of their stereogenic carbons were determined by an X-ray crystallographic analysis. None of the isolated compounds were active in the tests for antibacterial activity against Gram-positive and Gram-negative bacteria, as well as multidrug-resistant isolates from the environment (MIC > 256 μg/mL), antifungal activity against yeast (*Candida albicans* ATTC 10231), filamentous fungus (*Aspergillus fumigatus* ATTC 46645) and dermatophyte (*Trichophyton rubrum* FF5) (MIC > 512 μg/mL) and in vitro growth inhibitory activity against the MCF-7 (breast adenocarcinoma), NCI-H460 (non-small cell lung cancer) and A375-C5 (melanoma) cell lines (GI_{50} > 150 μM) by the protein binding dye SRB method.

Keywords: *Neosartorya quadricincta* KUFA 0081; marine-derived fungus; polyketides; pentaketides; benzoic acid derivatives; *Clathria reinwardti*

1. Introduction

Aspergillus section *Fumigati* and its teleomorph *Neosartorya* include many important species because they can be pathogenic or allergenic to man, as well as causing food spoilage and producing mycotoxins. Certain species are also found to produce interesting bioactive secondary metabolites

that can be considered to have potential for drug development [1]. For this reason, we have investigated the bioactive secondary metabolites produced from the cultures of four *Neosartorya* species collected from soil in Thailand, i.e., *Neosartorya glabra* KUFC 6311 [2], *N. pseudofischeri* KUFC 6422 [3], *N. siamensis* KUFC 6349 [4] and *N. fischeri* KUFC 6344 [5], as well as six marine-derived species of *Neosartorya*, including *N. paulistensis* KUFC 7898 [6], *N. laciniosa* KUFC 7896 [5], *N. spinosa* KUFC 8104, *N. tsunodae* KUFC 9213 [5], *N. siamensis* KUFA 0017 and *N. takakii* KUFC 7898 [7], as well as one marine-derived *Aspergillus* species (*Aspergillus similanensis* KUFA 0013) [8,9]. Recently, we have also reported the antifungal activity of the crude extract of *N. quadricincta* KUFA 0064, isolated from an agricultural soil in Southern Thailand, against plant pathogenic fungi, which are causative agents of diseases of economically-important plants of Thailand [10]. So far, the only report on secondary metabolites of *N. quadricincta* was by Ozoe et al., who described the isolation of dihydroisocoumarin derivative, PF1223, from the culture of *N. quadricincta* strain PF1223 (unidentified source). This compound was shown to inhibit the [^{3}H] EBOB binding by 65% [11]. Thus, in our ongoing search for bioactive secondary metabolites from marine-derived fungi from Thai waters, we have investigated the culture of *N. quadricincta* KUFA 0081, isolated from the marine sponge *Clathria reinwardti*, which was collected from the Coral reef at Samae San Island in the Gulf of Thailand. The ethyl acetate extract of the culture of this fungus yielded, besides the previously described 2,3-dihydro-6-hydroxy-2,2-dimethyl-4*H*-1-benzopyran-4-one (**4a**) [12], two new polyketide derivatives (**1**, **5**) and seven new benzoic acid derivatives (**2a**, **2b**, **3**, **4b**, **6a**, **6b** and **7**) (Figure 1). All of the isolated compounds were tested for their antibacterial activity against Gram-positive and Gram-negative bacteria, as well as multidrug-resistant isolates from the environment and for their antifungal activity against yeast (*Candida albicans* ATCC 10231), filamentous fungus (*Aspergillus fumigatus* ATCC 46645) and dermatophyte (*Trichophyton rubrum* FF5). Additionally, these compounds were also evaluated for their in vitro growth inhibitory activity against the MCF-7 (breast adenocarcinoma), NCI-H460 (non-small cell lung cancer) and A375-C5 (melanoma) cell lines by the protein binding dye SRB method.

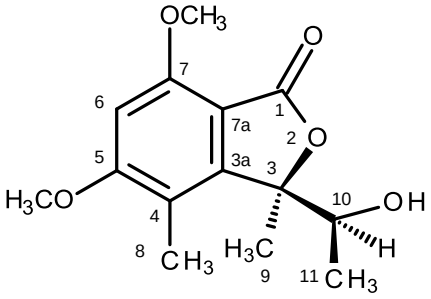

1

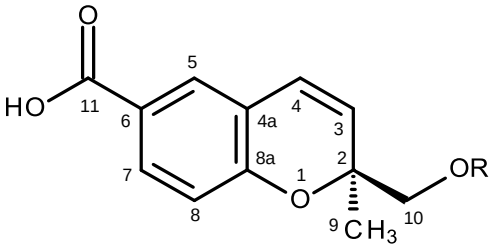

2a: R = H
2b: R = Ac

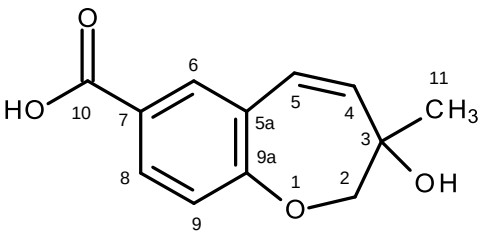

3

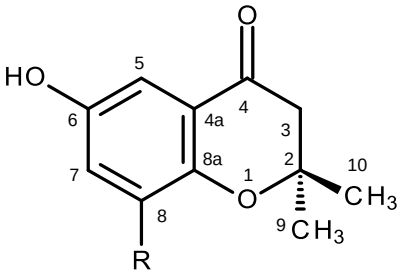

4a: R = H

4b: R =

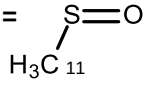

Figure 1. *Cont.*

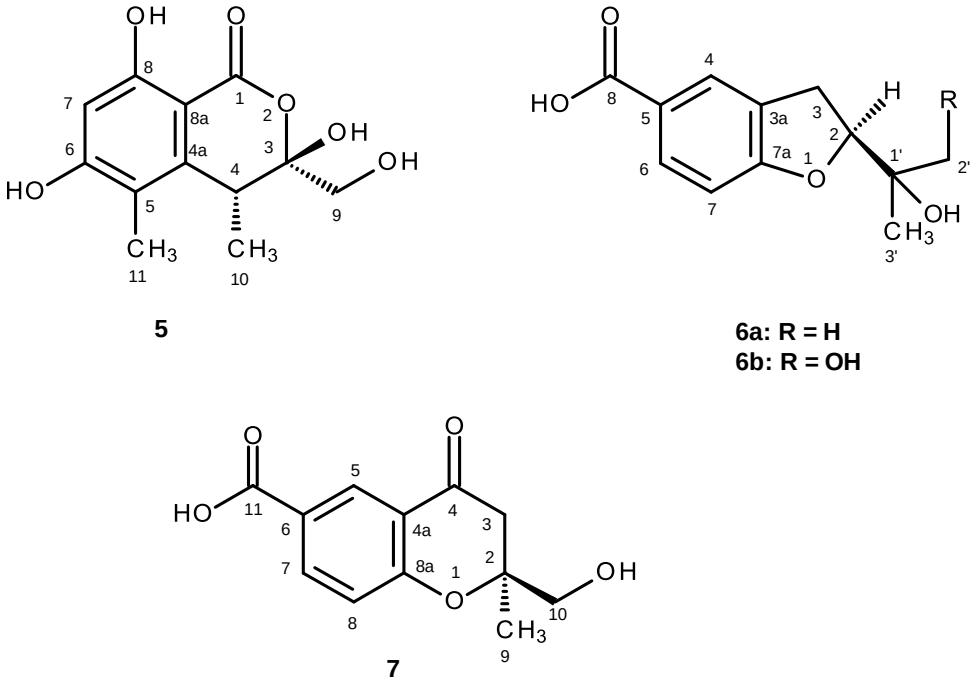

Figure 1. Secondary metabolites of *N. quadricincta* KUFA0081.

2. Results and Discussion

Compound **1** was isolated as white crystals (mp, 176–177 °C), and its molecular formula $C_{14}H_{18}O_5$ was established on the basis of the (+)-HRESIMS *m/z* 267.1243 $[M + H]^+$ (calculated 267.1332), indicating six degrees of unsaturation. The IR spectrum showed absorption bands for hydroxyl (3455 cm^{-1}), conjugated ester carbonyl (1723 cm^{-1}) and aromatic (1612, 1596 cm^{-1}) groups. The ^{13}C NMR, DEPT and HSQC spectra (Table 1, Supplementary Information, Figures S2 and S4) exhibited the signals of one conjugated ester carbonyl (δ_C 168.2), five quaternary sp^2 (δ_C 164.6, 158.3, 152.8, 111.7, 105.5), one methine sp^2 (δ_C 94.5), one oxygen bearing quaternary sp^3 (δ_C 88.8), one oxygen bearing methine sp^3 (δ_C 70.8), two methoxyl (δ_C 56.1 and 56.0) and three methyl (δ_C 21.5, 17.8 and 11.2) groups. The ^1H NMR spectrum (Table 1, Supplementary Information, Figure S1) revealed the presence of, besides a singlet of one aromatic proton at δ_H 6.41, a quartet of the oxymethine proton at δ_H 4.22 (J = 6.4 Hz), two singlets of the methoxyl groups at δ_H 3.97 s and 3.92 s, two methyl singlets at δ_H 2.12 s and 1.76 s, a methyl doublet at δ_H 0.87 (J = 6.4 Hz) and a broad band of the hydroxyl proton at δ_H 2.15. The ^1H and ^{13}C data (Table 1) revealed the presence of a pentasubstituted benzene ring. That this pentasubstituted benzene ring was part of the 5,7-dimethoxy-3,4-dimethyl-2-benzofuran-1(3*H*)-one ring system was corroborated by the HMBC correlations (Table 1, Figure 2a, Supplementary Information, Figure S5) of H-6 (δ_H 6.41, s) to C-7a (δ_C 105.3), C-4 (δ_C 111.7), C-7 (δ_C 158.3), C-5 (δ_C 164.6) and C-1 (δ_C 168.2), of OMe-5 (δ_H 3.92, s) to C-5, of OMe-7 (δ_H 3.97, s) to C-7, of H_3-8 (δ_H 2.12, s) to C-4, C-3a (δ_C 152.8) and C-5, of H_3-9 (δ_H 1.76, s) to C-3a and of the NOESY correlations of H-6 to OMe-5 and OMe-7. That another substituent of C-3 was a 1-hydroxyethyl group was supported by the COSY correlations of H-10 (δ_H 4.22, q, J = 6.4 Hz) to H_3-11 (δ_H 0.87, d, J = 6.4 Hz), by the HMBC correlations of H_3-9 to C-10 (δ_C 70.8), C-3 (δ_C 88.8) and C-3a and of H_3-11 (δ_H 0.87, d, J = 6.4 Hz) to C-3 and C-10 (Table 1, Figure 2a), as well as by the NOESY correlations of H_3-8 to H-10, H_3-9, of H_3-11 to H-10, OH-10 and of H_3-9 to H-10 (Table 1, Figure 2b, Supplementary Information, Figure S6). Final proof of the structure and the stereochemistry assigned to compound **1** was provided by its X-ray analysis (Figure 3), and since the diffraction data were collected with a Gemini PX Ultra equipped with CuKα radiation, it was possible to establish the absolute configurations of C-3 and C-10, respectively, as 3*R* and 10*S*. Since **1** is a new compound, we have named it quadricinctone A.

Table 1. ^{1}H and ^{13}C NMR ($CDCl_3$, 300.13 MHz and 75.4 MHz), HMBC and NOESY assignments for **1**.

Position	δ_C, type	δ_H, (*J* in Hz)	HMBC	NOESY
1	168.2, CO	-		
3	88.8, C	-		
3a	152.8, C	-		
4	111.7, C	-		
5	164.6, C	-		
6	94.5, CH	6.41, s	C-1, 4, 5, 7, 7a	OMe-5, 7
7	158.3, C	-		
7a	105.3, C	-		
8	11.2, CH_3	2.12, s	C-3a, 4, 5, 7	H-9, 10
9	21.5, CH_3	1.76, s	C-3, 3a, 10	H-8, 9
10	70.8, CH	4.22, d (6.4)	C-11	H-8, 9, 10
11	17.8, CH_3	0.87, d (6.4)	C-3, 10	H-10
OMe-5	56.1, CH_3	3.92, s	C-5	H-6
OMe-7	56.0, CH_3	3.97, s	C-7	H-6
OH-10	-	2.15, br	-	H-11

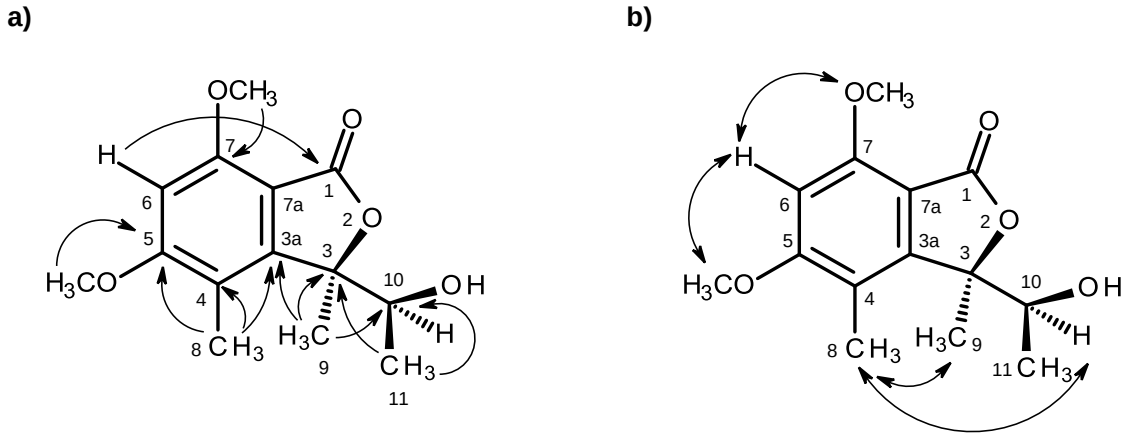

Figure 2. Key HMBC (→) (**a**) and NOESY (↔) (**b**) correlations for compound **1**.

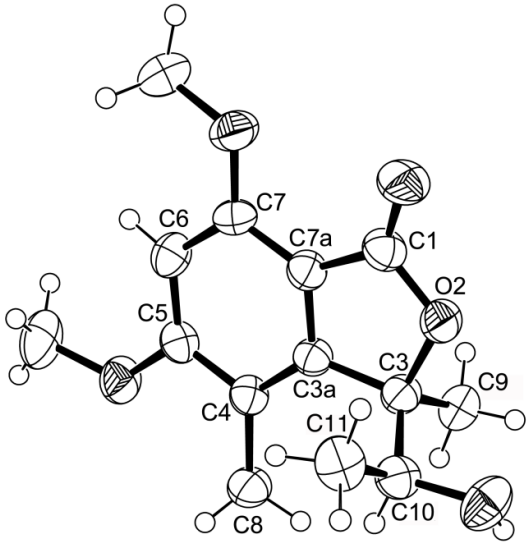

Figure 3. ORTEP diagram of compound **1**.

Compound **2a** was also isolated as white crystals (mp. 147–148 °C), and its molecular formula $C_{12}H_{12}O_4$ was determined based on the (+)-HRESIMS *m/z* 221.0820 $[M + H]^+$ (calculated 221.0814), indicating seven degrees of unsaturation. The IR spectrum showed absorption bands for hydroxyl (3447 cm^{-1}), a conjugated carbonyl (1696 cm^{-1}), aromatic (1609 cm^{-1}) and olefin (1647 cm^{-1}) groups. The ^{13}C NMR, DEPT and HSQC spectra (Table 2, Supplementary Information, Figures S8 and S10) exhibited the signals of one conjugated carboxyl carbonyl (δ_C 167.0), three quaternary sp^2 (δ_C 156.8, 123.0, 120.5), five methine sp^2 (δ_C 130.8, 128.6, 127.9, 122.8, 115.7), one oxy-quaternary sp^3 (δ_C 80.5), one oxymethylene sp^3 (δ_C 67.1) and one methyl (δ_C 23.3) groups. The ^1H NMR spectrum (Table 2, Supplementary Information, Figures S7) revealed, besides the presence of three aromatic protons of the 1,2,4 trisubstituted benzene ring at δ_H 6.79, d (*J* = 8.4 Hz), 7.65, d (*J* = 2.1 Hz) and 7.69, dd (*J* = 8.4, 2.1 Hz), two doublets of the protons of a *cis*-double bond at δ_H 6.56, d (*J* = 10.0 Hz) and 5.74, d (*J* = 10.0 Hz), a methyl singlet at δ_H 1.31, a singlet of two protons at δ_H 3.46 and two broad signals of the hydroxyl protons at δ_H 12.59 and 5.07, respectively. The COSY spectrum (Table 2, Figure 4a, Supplementary Information, Figures S9) exhibited cross-peaks of H-4 (δ_H 6.56, d, *J* = 10.0 Hz) to H-3 (δ_H 5.74, d, *J* = 10.0 Hz), of H-7 (δ_H 7.69, dd, *J* = 8.4, 2.1 Hz) to H-5 (δ_H 7.65, d, *J* = 2.1 Hz) and H-8 (δ_H 6.79, d, *J* = 8.4 Hz), confirming the presence of the 1,2,4 trisubstituted benzene ring and the *cis*-double bond. That the 1,2,4-trisubsituted benzene ring and the *cis*-double bond were part of the 2*H*-chromene-6-carboxylic acid moiety was corroborated by the HMBC correlations (Figure 4a, Supplementary Information, Figures S11) of H-5 to C-4 (δ_C 122.8), C-7 (δ_C 130.8), C-8a (δ_C 156.8) and C-11 (δ_C 167.0), of H-7 to C-5 (δ_C 127.9), C-8a, C-11, of H-8 to C-4a (δ_C 120.5), C-6 (δ_C 123.0) and C-8a, as well as of H-3 to C-4a and of H-4 to C-4a, C-5 and C-8a. As the HMBC spectrum also exhibited correlations of the methyl singlet at δ_H 1.31 (H_3-9) to C-3, C-2 (δ_C 80.5) and C-10 (δ_C 67.1) and of the singlet at δ_H 3.46 (H-10) to C-2, C-3 and CH_3-9 (δ_C 23.3), the methyl and hydroxymethyl groups were placed on C-2. The NOESY correlations (Figure 4b, Supplementary Information, Figures S12) of H-4 to H-3 and H-5, of H-3 to H-4, H_3-9 and H_2-10, of H-8 to H-7, H_2-10 and H_3-9 and of H_3-9 to H-8, H-10 also confirmed this hypothesis. Since compound **2a** was obtained in a suitable crystal, X-ray analysis was carried out, and the ORTEP view shown in Figure 5 revealed that the absolute configuration of C-2 is *S*. A literature search indicated that **2a** has never been previously reported; therefore, it was named quadricinctapyran A.

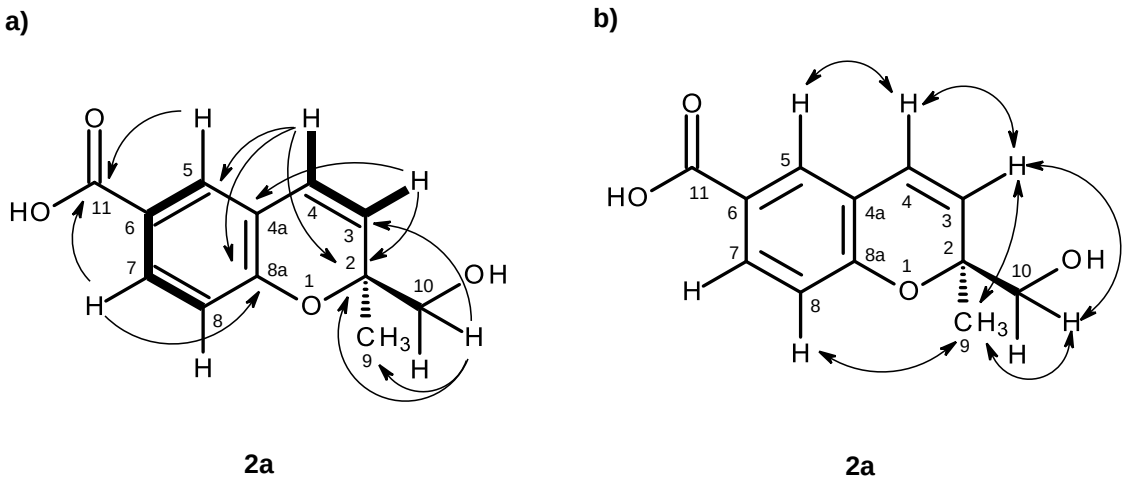

Figure 4. Key COSY (–), HMBC (→) (**a**) and NOESY (↔) (**b**) correlations for compound **2a**.

Table 2. ^{1}H and ^{13}C NMR (DMSO, 300.13 MHz and 75.4 MHz) for **2a** and **2b**.

Position	2a				2b			
	δ_C, type	δ_H, (*J* in Hz)	COSY	HMBC	δ_C, type	δ_H, (*J* in Hz)	COSY	HMBC
2	80.5, C	-			78.5, C	-		
3	128.6, CH	5.74, d (10.0)	H-4	C-2, 4a, 5, 9, 10	126.2, CH	5.59, d (10.0)	H-4	C-2, 4a, 10
4	122.8, CH	6.56, d (10.0)	H-3	C-2, 5, 8a	124.3, CH	6.51, d (10.0)	H-3	C-2, 5, 8a
4a	120.5, C	-			120.2, C	-		
5	127.9, CH	7.65, d (2.1)	H-7	C-4, 8a, 11	128.9, CH	7.75, d (2.1)	H-7	C-4, 7, 8a, 11
6	123.0, C	-			122.0, C	-		
7	139.8, CH	7.69, dd (8.4, 2.1)	H-5, 8	C-5, 8a, 11	132.2, CH	7.90, dd (8.5, 2.1)	H-5, 8	C-5, 8a, 11
8	115.7, CH	6.79, d (8.4)	H-7	C-4a, 6, 8a	116.1, CH	6.83, d (8.5)	H-7	C-4a, 6, 8a
8a	156.8, C	-			157.8, C	-		
9	23.3, CH_3	1.31, s	-	C-2, 3, 10	24.0, CH_3	1.48, s	-	C-2, 3, 10
10	67.1, CH_2	3.45, s	-	C-2, 3, 9	68.8, CH_2	4.13, d (11.7)	H-10	C-2, 3, 9
						4.24, d (11.7)	H-10	C-2, 3, 9
11	167.0, CO	-			171.7, CO	-		
OH-10	-	5.07, br	-		-	-		
OH-11	-	12.59, br	-		-	12.79, br	-	
OAc	-				170.8, CO	-		
					20.7, CH_3	1.98, s	-	CO (Ac)

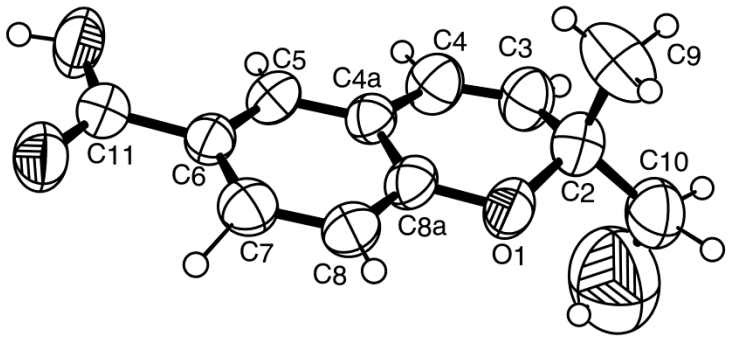

Figure 5. ORTEP diagram of compound **2a**.

Compound **2b** was isolated as a white solid (mp. 118–119 °C), and its molecular formula $C_{14}H_{14}O_5$ was established on the basis of the (+)-HRESIMS *m/z* 263.0971 $[M + H]^+$ (calculated 263.0919), indicating eight degrees of unsaturation. The ^1H and ^{13}C NMR spectral features (Supplementary Information, Figures S13 and S14) of compound **2b** resembled those of compound **2a**, except for an additional carbonyl carbon at δ_C 170.8 and a methyl group at δ_C 20.7 (δ_H 1.98, s), characteristic of the acetoxyl group (Table 2). Moreover, since the signals of the oxymethylene protons (H_2-10) of compound **2b** appeared as two doublets at δ_H 4.13 (J = 11.7 Hz) and 4.24 (J = 11.7 Hz), ca. 0.7 ppm higher than that of H_2-10 in compound **2a**, it was clear that the acetoxyl group was on C-10. This was also corroborated by the HMBC correlations (Table 2, Figure 6a, Supplementary Information, Figure S17) of H_2-10 and the methyl singlet at δ_H 1.98 to the carbonyl of the acetoxyl group (δ_C 170.8). Since Compound **2b** could not be obtained as a suitable crystal for X-ray analysis, the absolute configuration of its C-3 could not be determined with certainty. However, as compound **2b** is the acetate derivative of compound **2a**, it was speculated that the stereochemistry of its C-2 should be the same as that of C-2 of compound **2a**, i.e., 2*S*. In order to confirm this hypothesis, the NOESY experiments were carried out. The NOESY spectrum of compound **2b** showed a weak correlation of H-8 to H_3-9 and not to H_2-10 (Figure 6b, Supplementary Information, Figure S18), similar to what has been observed for compound **2a**. Acid hydrolysis of **2b** gave the product whose structure was confirmed as **2a** by ^1H and ^{13}C NMR data, as well as the optical rotation. Therefore, the absolute configuration of C-2 of **2b** is assigned as 2*S*. Compound **2b** is also a new compound, thus we named it quadricinctapyran B.

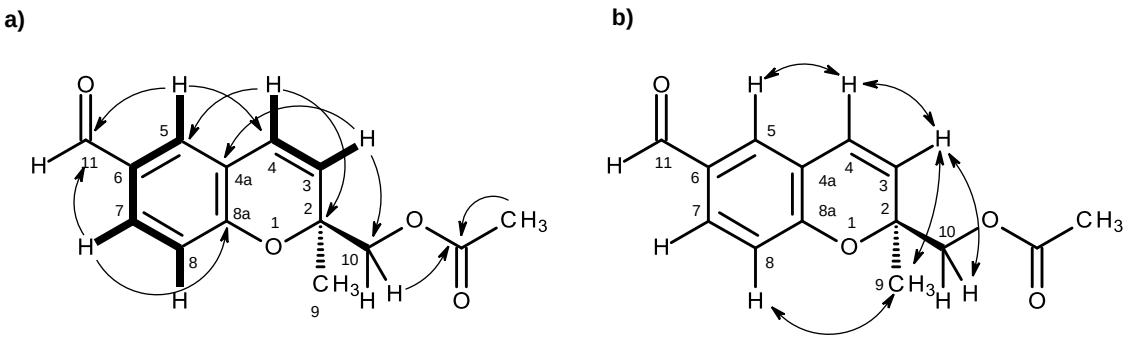

Figure 6. Key COSY (–), HMBC (→) (**a**) and NOESY (↔) (**b**) correlations for compound **2b**.

The molecular formula $C_{12}H_{12}O_4$ of compound **3**, a white solid (mp 189–191 °C), was established based on the (+)-HRESIMS *m/z* 221.0819 $[M + H]^+$ (calculated 221.0814), and thus, it is an isomer of compound **2a**. Furthermore, the general features of its ^1H and ^{13}C NMR spectra resembled those of compound **2a**. However, the chemical shift values of some of the proton and carbon signals were slightly different from those observed in compound **2a**. The ^{13}C NMR, DEPT and HSQC spectra (Table 3, Supplementary Information, Figures S20 and S22) exhibited the signals of one conjugated

carboxyl carbonyl (δ_C 166.7), three quaternary sp^2 (δ_C 161.2, 125.3, 125.0), five methine sp^2 (δ_C 139.5, 134.6, 129.8, 123.5, 119.8), one oxy-quaternary sp^3 (δ_C 70.7), one oxymethylene sp^3 (δ_C 77.0) and one methyl (δ_C 26.1) groups. The ^{1}H NMR spectrum (Table 3, Supplementary Information, Figure S19) revealed the existence of three aromatic protons of the 1,2,4-trisubstituted benzene ring, similar to that of compound **2a**, at δ_H 7.05, d (J = 8.4 Hz), 7.74, dd (J = 8.4, 2.1 Hz), 7.89, d (J = 2.1 Hz), two olefinic protons of the *cis*-double bond at δ_H 5.95, dd (J = 12.0, 1.2 Hz) and 6.31, d (J = 12.0 Hz), two oxymethylene protons at δ_H 3.84, d (J = 11.1 Hz) and 4.02, dd (J = 11.1, 1.6 Hz), and a methyl singlet at δ_H 1.26. That the carboxylic acid functionality was on C-7, and the substituent with a *cis*-double bond was on C-5a was substantiated by the HMBC correlations of H-6 (7.89, d, J = 2.1 Hz) to C-10 (δ_C 166.7), C-9a (δ_C 161.2), C-8 (δ_C 129.8) and C-5 (δ_C 123.5), of H-5 (δ_H 6.31, d, J = 12.0 Hz) to C-6 (δ_C 134.5) and C-9a and of H-4 (δ_H 5.95, dd, d, J = 12.0, 1.2 Hz) to C-5a (δ_C 125.0) (Table 3 and Figure 7a, Supplementary Information, Figure S23). However, contrary to compound **2a**, compound **3** showed the HMBC correlations of H_2-2 (δ_H 3.84, d, J = 11.1 Hz and 4.02, dd, J = 11.1, 1.6 Hz) to not only C-4 (δ_C 139.5), but also to C-9a (Table 3 and Figure 7a). Consequently, the benzoic acid moiety was fused with the 2,3,6,7-tetrahydro-oxepine ring through C-5a and C-9a. That the methyl group and the hydroxyl group were on C-3 of the oxepin ring was confirmed by the HMBC correlations of the methyl singlet at δ_H 1.26 (H-11) to C-3 (δ_C 70.7), C-2 (δ_C 77.0) and C-4, as well as of H_2-2 to C-11 (δ_C 26.1) and C-3 (Table 3 and Figure 7). This was also corroborated by the NOESY correlations of H_3-11 to OH-3 (δ_H 3.39, br), H_2-2 and H-4 (Table 3 and Figure 7b, Supplementary Information, Figure S24). Therefore, Compound **3** was identified as 3-hydroxy-3-methyl-2,3-dihydro-1-benzoxepine-7-carboxylic acid.

Table 3. ^{1}H and ^{13}C NMR (DMSO, 300.13 MHz and 75.4 MHz) and HMBC assignment for **3**.

Position	δ_C, type	δ_H, (J in Hz)	COSY	HMBC	NOESY
2α	77.0, CH_2	3.84, d (11.1)	H-2β	C-3, 4, 9a, 11	H-2β, 4 (w), 11 (w)
β		4.02, dd (11.1, 1.6)	H-2α	C-3, 4, 9a, 11	H-2α, 4 (w), 11 (str)
3	70.7, C	-			
4	139.5, CH	5.95, dd (12.0, 1.2)	H-5	C-2, 5a	H-2α (w), 5, 9 (w), 11
5	123.5, CH	6.31, d (12.0)	H-4	C-3, 5a, 6, 9a	H-4, 6 (str)
5a	125.0, C	-			
6	134.5, CH	7.89, d (2.1)	H-8	C-5, 8, 9a, 10	H-5
7	125.3, C	-			
8	129.8, CH	7.74, dd (8.4, 2.1)	H-6, 9	C-6, 9a	H-9
9	119.8, CH	7.05, d (8.4)	H-8	C-5a, 7, 9a	H-8
9a	161.2, C	-			
10	166.7, C	-			
11	26.1, CH_3	1.26, s	-	C-2, 3, 4	H-2α (w), 2β (str)
OH-3	-	3.39, br	-		H-4, 11
COOH	-	12.79, br	-		

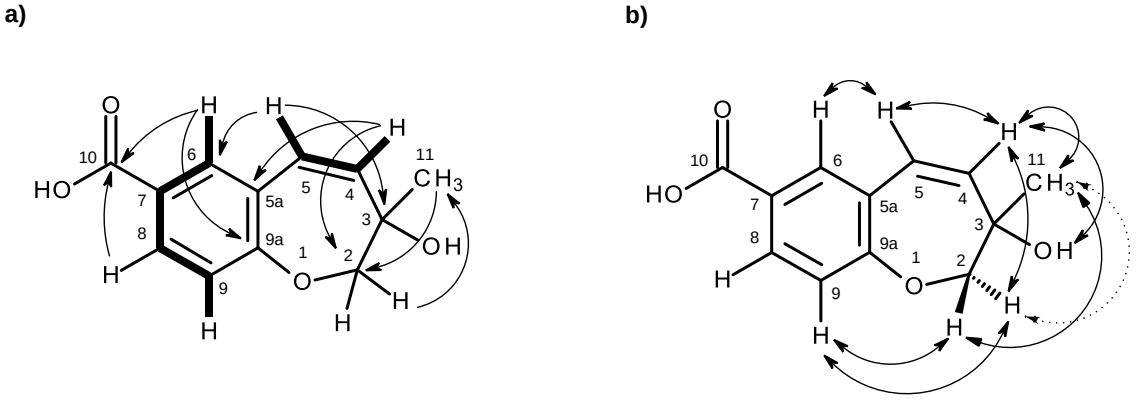

Figure 7. Key COSY (–), HMBC (→) (**a**) and NOESY (↔) (**b**) correlations for compound **3**.

As compound **3** could not be obtained as a suitable crystal for X-ray analysis, an effort to tentatively determine the relative configuration of the stereogenic carbon (C-3) by molecular mechanics conformation analysis and the NOESY experiments was carried out. Stochastic conformational search on the computational models of the structure of **3** with C-3 in *R* configuration, followed by energy minimization, converged to two half-chair conformations for the seven-membered ring C1 and C2, as depicted in Figure 8, regardless of the modelling level of the theory used (MP2/6-311G, PM3, MMFF and MM2). All methods, except for PM3, also agree that conformation C2, with the methyl group in the equatorial position, is more stable by ca. 2 kcal/mol. However, this difference can be attributed to a weak intramolecular hydrogen bond in conformation C2, between HO-3 and O-1, which is not possible in conformation C1. The semi-empirical PM3 method gives less weight to non-ideal intramolecular hydrogen bonds, as compared to the other methods, and assigns virtually the same energy to both conformations of **3**, while still orienting HO-3 towards the seven-membered ring. Since DMSO solvent molecules compete for HO-3 hydrogen bonding, it is more likely that the intramolecular bond is not an important feature of ring conformation C2 and that, in reality, both conformations have approximately the same energy.

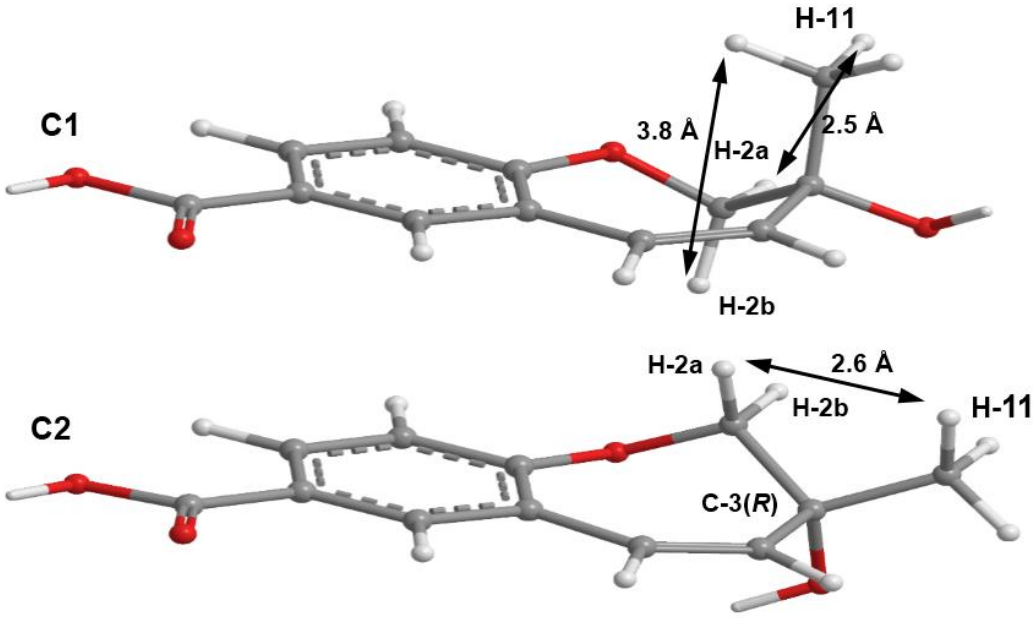

Figure 8. The two minimal energy conformations, C1 and C2, for the structure of **3**, with *R* configuration for C-3. All calculated distances and energies are exactly the same for the pairs 3*R*-C1/3*S*-C2 and 3*R*-C2/3*S*-C1. The shorter predicted inter-hydrogen distances H-2/H-11 are presented; for a discussion of the average, NOE effective distances, please refer to the main text.

Both model conformations of **3** predict hydrogen-hydrogen distances that are similar to within 0.2 Å, with the exception of some distances to the methyl group (H_3-11). The most notable are to the diastereotopic hydrogens (H_2-2), partially presented in Figure 8. While both conformations show almost the same distance between H-2a and H-11, a difference is predicted between H-2b and H-11 if the conformation C1 predominates, which should be apparent in the build-up rate of NOESY cross-peaks for small mixing times. Alternatively, the predominance of the conformation C2 would be indicated by two equal strength cross-peaks for H-2a and H-2b in cross-relaxation with H-11. It is observed that the H-2b (δ_H 3.84, d, J = 11.1 Hz)/H-11 NOESY cross-peak is weak while the H-2a

(δ_H 4.02, dd, J = 11.1, 1.6 Hz)/H-11 is medium, suggesting that the conformation C1 predominates. NOE effective distances, r_{eff}, are calculated by [13] :

$$r_{eff} = \left(\frac{1}{3} \sum_i r_{H-2/H-10_i}^{-6} \right)^{-1/6}$$

The average effective positions of the three methyl H-11$_i$ protons are relative to H-2a or H-2b. The predicted ratio r_{eff} (H-2a/H-11)/r_{eff} (H-2b/H-11) is 1.40 (1.36, if r^{-3} averages are used instead of r^{-6}). Assuming that the cross-relaxation rate is similar in both cases, the NOE intensities should also have a similar ratio [14]. Since the observed intensities ratio is actually closer to two, the evidence points towards the predominance of the conformation C1. Since, as stated previously, both conformations have similar conformational energy, the higher stability of 3*R*-C1 of **3** (or of its stereoisomer 3*S*-C2) must originate from the ready interaction of the equatorial HO-3 with the hydrogen-bonding solvent and also from a higher entropic rotational freedom of the hydroxyl and methyl groups. The NOESY spectrum also revealed the correlations of both H_2-2 to H-9. However, only one of the H_2-2, i.e., the doublet at δ_H 3.84 (J = 11.1 Hz), showed a weak cross-peak to H-4, while the double doublet at δ_H 4.02 (J = 11.1, 1.6 Hz) did not give any cross-peak to H-4. This observation led to the conclusion that the plucked oxepin ring should adopt the conformation in which H-2 at δ_H 3.84 is near H-4, i.e., in the α (axial), while H-2 at δ_H 4.02 is in β (equatorial) positions, which is in agreement with our conformational analysis. A literature search revealed that compound **3** is also a new compound, so we named it quadricinctoxepine.

Compound **4b** was isolated as white crystals (mp, 227–228 °C), and its molecular formula $C_{12}H_{14}O_4S$ was established on the basis of the (+)-HRESIMS *m/z* 255.0694 $[M + H]^+$ (calculated 255.0691). The IR spectrum showed absorption bands for hydroxyl (3442 cm^{-1}), conjugated ketone carbonyl (1690 cm^{-1}) and aromatic (1622 cm^{-1}) groups. The ^{13}C NMR, DEPT and HSQC spectra (Table 4, Supplementary Information, Figures S26 and S28) exhibited the signals of one conjugated ketone carbonyl (δ_C 191.2), four quaternary sp^2 (δ_C 151.6, 147.4, 135.7, 120.8), two methine sp^2 (δ_C 118.0, 112.4), one oxy-quaternary sp^3 (δ_C 80.9), one methylene sp^2 (δ_C 48.0) and three methyl (δ_C 40.8, 26.1 and 25.7) groups. The ^1H NMR spectrum (Table 4, Supplementary Information, Figure S25) exhibited, besides a broad singlet of the phenolic hydroxyl group at δ_H 9.85, the signals of two *meta*-coupled aromatic protons at δ_H 7.17, d (J = 3.1 Hz) and δ_H 7.35, d (J = 3.1 Hz), two geminally-coupled methylene protons at δ_H 2.80, d (J = 16.6 Hz) and 2.82, d (J = 16.6 Hz) and three methyl singlets at δ_H 1.38, s, 1.39, s, and 2.77, s. The chemical shift value of the methyl singlet at δ_H 2.77, s (δ_C 40.8), indicated that it was on the electron-withdrawing moiety. That compound **4b** was a 2,2,6,8-tetrasubstituted 2,3-dihydro-4*H*-chromen-4-one derivative was supported by the HMBC correlations of H-5 (δ_H 7.17, d, J = 3.1 Hz) to C-4 (δ_C 191.2), C-7 (δ_C 118.0) and C-8a (δ_C 147.4), of H-7 (δ_H 7.35, d, J = 3.1 Hz) to C-5 (δ_C 112.4), C-8 (δ_C135.7), C-8a, as well as of H-2 (δ_H 2.80, d, J = 16.6 Hz and 2.82, d, J = 16.6 Hz) to C-3 (δ_C 80.9) and C-4 (Table 4, Figure 9, Supplementary Information, Figure S28). As the HMBC spectrum also exhibited cross-peaks of a broad singlet of the phenolic hydroxyl proton at δ_H 9.85 to C-5, C-6 (δ_C 151.6) and C-7 and of the singlets of the methyl groups at δ_H 1.38 and 1.39 to C-2 (δ_C 48.0) and C-3, the hydroxyl group was placed on C-6, and the two methyl groups were placed on C-2. Since this partial structure accounted for only $C_{11}H_{11}O_3$, another portion of the molecule must contain CH_3SO. That the methyl sulfoxide group was on C-8 was supported by the presence of the deshielded methyl group at δ_H 2.77, s (δ_C 40.8), as well as by the HBMC cross-peak of H_3-11 (δ_H 2.77, s) to C-8. Final proof of the structure of compound **4b** was provided by its X-ray analysis, and its ORTEP view is shown in Figure 10. Moreover, the ORTEP view also revealed that the absolute configuration of the sulfoxide group in compound **4b** is *R*. A literature search showed that compound **4b** is a new compound, and thus, we have named it quadricinctone B.

Table 4. ^{1}H and ^{13}C NMR (DMSO, 300.13 MHz and 75.4 MHz) and HMBC assignment for **4b**.

Position	δ_C, type	δ_H, (*J* in Hz)	COSY	HMBC
2	80.9, C	-		
3	48.0, CH_2	2.80, d (16.6)	H-3	C-2, 4, 9, 10
		2.85, d (16.6)	H-3	C-2, 4, 9, 10
4	191.2, CO	-		
4a	120.8, C	-		
5	112.4, CH	7.17, d (3.1)	H-7	C-4, 6, 7, 8a
6	151.6, C	-		
7	118.7, CH	7.35, d (3.1)	H-5	C-5, 6, 8, 8a
8	135.7, C	-		
8a	147.4, C	-		
9	26.1, CH_3	1.39, s	-	C-2, 3, 10
10	25.7, CH_3	1.38, s	-	C-2, 3, 9
11	40.8, CH_3	2.77, s	-	C-8
OH-6	-	9.85, s		C-5, 6, 7

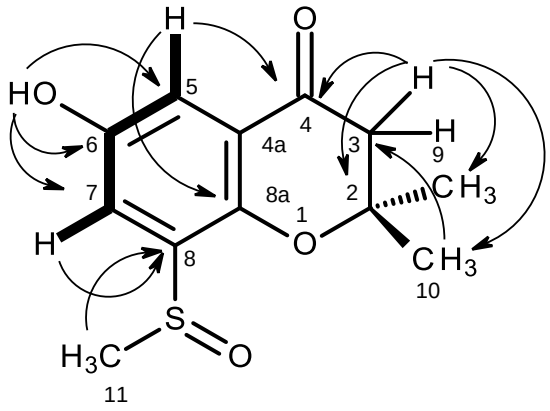

4b

Figure 9. Key COSY (–) and HMBC (→) correlations for compound **4b**.

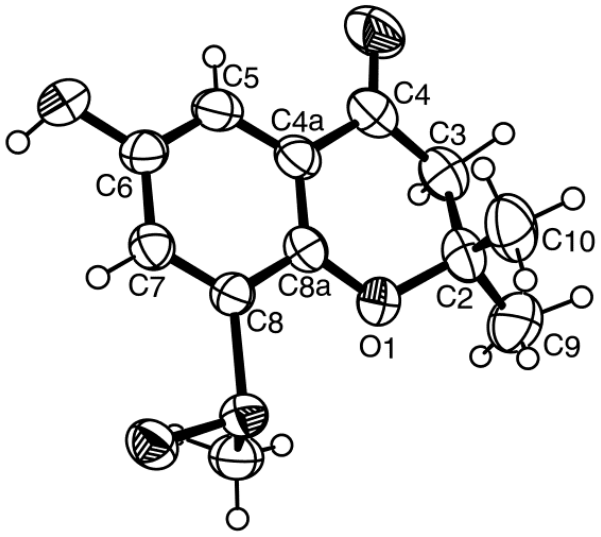

Figure 10. ORTEP diagram of compound **4b**.

The molecular formula $C_{12}H_{14}O_6$ of compound **5** was determined based on the (+)-HRESIMS *m/z* 255.0875 (calculated 255.0869), indicating six degrees of unsaturation. The IR spectrum exhibited absorption bands for hydroxyl (3439 cm^{-1}), conjugated ester carbonyl (1660 cm^{-1}) and aromatic (1643 cm^{-1}) groups. The ^{13}C NMR, DEPT and HSQC spectra (Table 5, Supplementary Information, Figures S31 and S33) exhibited the signals of one conjugated ester carbonyl (δ_C 168.8), five quaternary sp^2 (δ_C 162.9, 161.3, 144.6, 113.5, 98.9), one methine sp^2 (δ_C 99.9), one quaternary sp^3 of a hemiketal (δ_C 104.8), one methine sp^3 (δ_C 34.9), one oxymethylene sp^3 (δ_C 63.7) and two methyl (δ_C 16.3 and 9.8) carbons. The ^1H NMR spectrum (Table 5, Supplementary Information, Figure S30) exhibited, besides a singlet of one aromatic proton at δ_H 6.27, a singlet of a hydrogen-bonded phenolic hydroxyl at δ_H 11.24 and a broad signal of another phenolic hydroxyl at δ_H 10.62, two broad signals of the hydroxyl groups at δ_H 5.26 and 7.07, one broad doublet of two methylene protons at δ_H 3.65 (J = 16.6 Hz), a broad signal of one methine proton at δ_H 3.26, one methyl doublet at δ_H 1.06 (J = 7.2 Hz) and one methyl singlet at δ_H 1.98. That compound **5** was a 3,3,4,5,6,8-hexasubstituted 3,4-dihydro-1*H*-isochromen-1-one was supported by the HBMC correlations of OH-8 (δ_H 11.24, s) to C-8 (δ_C 161.3), C-7 (δ_C 99.9), C-8a (δ_C 98.9) and of H-7 (δ_H 6.27, s) to C-5 (δ_C 113.5), C-6 (δ_C 162.9), C-8 and C-8a (Table 5, Figure 11, Supplementary Information, Figure S34). Since the methyl singlet at δ_H 1.98 gave HMBC cross-peaks to C-5 and the carbons at δ_C 144.6 and 162.9 (Table 5, Figure 11), the methyl group (δ_H 1.98; δ_C 9.8) and another hydroxyl group (δ_H 10.62, br) were placed on C-5 and C-6, respectively, and the carbon signals at δ_C 144.6 and 162.9 were assigned for C-4a and C-6, respectively. On the other hand, the COSY spectrum (Table 5, Supplementary Information, Figure S32) showed cross-peaks of the broad signal at δ_H 3.26 to the methyl doublet at δ_H 1.06 (J = 7.2 Hz) and of the broad signal at δ_H 5.26 to the broad doublet at δ_H 3.65 (J = 16.6 Hz), while the HMBC spectrum (Table 5, Figure 11) gave cross-peaks of the methyl doublet at δ_H 1.06 (J = 7.2 Hz) to C-4a, C-4 (δ_C 34.9), and the signal of the quaternary carbon at δ_C 104.8 (C-3), the methyl and the hydroxymethyl substituents were placed on C-4 and C-3, respectively. Therefore, another hydroxyl group (δ_H 7.07, br) was on C-3. This was supported by the chemical shift value of C-3, which is typical for a hemiketal carbon. Since compound **5** could be obtained as a suitable crystal (mp. 223–224 °C), its X-ray analysis was performed. The ORTEP view of compound **5**, shown in Figure 12, not only confirmed the proposed structure, but also determined the absolute configuration of C-3 and C-4 as 3*S*, 4*R*. Since compound **5** is a new compound, it was named quadricinctone C.

Table 5. ^1H and ^{13}C NMR (DMSO, 300.13 MHz and 75.4 MHz) and HMBC assignment for **5**.

Position	δ_C, type	δ_H, (J in Hz)	COSY	HMBC
1	168.8, C	-		
3	104.8, C	-		
4	34.9, CH	3.26, m	H_3-10	
4a	144.6, C	-		
5	113.5, C	-		
6	162.9, C	-		
7	99.9, CH	6.27, s	-	C-1 (w), 5, 6, 8, 8a
8	161.3, C	-		
8a	98.9, C	-		
9	63.7, CH_2	3.65, brd (16.6)	OH-9	
10	16.3, CH_3	1.06, d (7.2)	H-4	C-3, 4, 4a
11	9.8, CH_3	1.98, s	-	C-4a, 5, 6
OH-3	-	7.07, br	-	
OH-5	-	10.62, br	-	
OH-8	-	11.24, s	-	C-7, 8, 8a
OH-9	-	5.26, br	-	

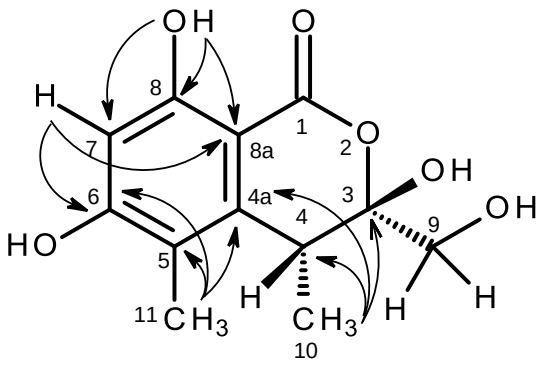

5

Figure 11. Key HMBC (→) correlations for compound **5**.

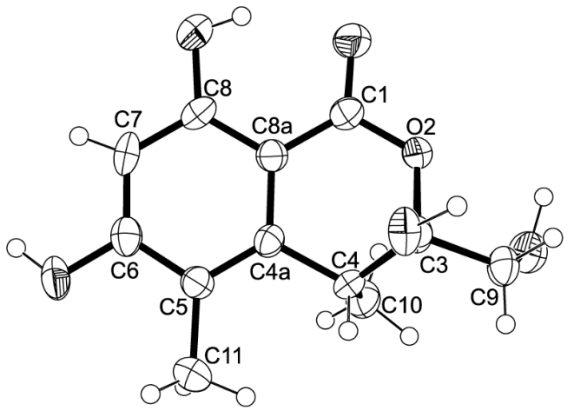

Figure 12. ORTEP diagram of compound **5**.

Compound **6a** was also isolated as white crystals (mp. 149–150 °C), and its molecular formula $C_{12}H_{14}O_4$ was determined based on the (+)-HRESIMS *m/z* 223.9067 $[M + H]^+$ (calculated 223.9070), indicating six degrees of unsaturation. The IR spectrum showed absorption bands for hydroxyl (3417 cm^{-1}), a conjugated carbonyl (1681 cm^{-1}) and aromatic (1634 cm^{-1}) groups. The ^{13}C NMR, DEPT and HSQC spectra (Table 6, Supplementary Information, Figures S36 and S38) exhibited the signals of one conjugated carboxyl carbonyl (δ_C 167.2), two quaternary sp^2 (δ_C 128.2, 122.6), one oxy-quaternary sp^2 (δ_C 163.7), three methine sp^2 (δ_C 130.4, 126.4, 108.4), one oxy-quaternary sp^3 (δ_C 70.0), one oxymethine sp^3 (δ_C 90.2), one methylene sp^2 (δ_C 29.3) and two methyl (δ_C 25.9 and 24.9) carbons. The ^1H NMR spectrum (Table 6, Supplementary Information, Figure S35) showed signals of three aromatic protons of the 1,2,4-trisubstituted benzene ring at δ_H 7.75, d (J = 1.8 Hz), 7.72, dd (J = 8.3, 1.8 Hz), 6.80, d (J = 8.3 Hz), in addition to a broad signal of the hydroxyl proton at δ_H 12.49, a triplet of one proton at δ_H 4.64 (J = 8.9 Hz), a doublet of two protons at δ_H 3.17 (J = 8.9 Hz) and two methyl singlets at δ_H 1.13 and 1.14. That the 1,2,4-trisubstituted benzene ring was part of 2,5-disubstituted 2,3-dihydro-1-benzofuran was supported by the COSY correlations of H-6 (δ_H 7.72, dd, J = 8.3, 1.8 Hz) to H-4 (δ_H 7.75, d, J = 1.8 Hz) and H-7 (δ_H 6.80, d, J = 8.3 Hz) and of H-2 (δ_H 3.17, J = 8.9 Hz) to H-3 (δ_H 4.64, J = 8.9 Hz)(Table 6, Figure 13a, Supplementary Information, Figure S37), as well as of the HMBC correlations of H-4 to C-6 (δ_C 130.4) and C-7a (δ_C 163.7), of H-6 to C-4 (δ_C 126.4), of H-3 to C-2 (δ_C 90.2), C-3a (δ_C 128.2) and C-7a and of H-7 to C-3a, C-7a and C-5 (δ_C 122.6) (Table 6, Figure 13a, Supplementary Information, Figure S39). That the carboxyl group was on C-5 was supported by the HMBC correlations of H-4 and H-6 to the conjugated carbonyl

at δ_C 167.2 (Table 6, Figure 13a), along with the presence of a broad signal at δ_H 12.49, which is characteristic of a hydroxyl group of carboxylic acid. In the same manner, that the 2-hydroxypropyl substituent was placed on C-2 was evidenced by the HMBC correlations of H-2 (δ_H 4.64, J = 8.9 Hz) to C-3 (δ_C 29.3), C-1′ (δ_C 70.0), C-2′ (δ_C 24.9), C-3′ (δ_C 25.9) (Table 6, Figure 13a), as well as by the NOESY correlations of H-2 to H-3, H_3-2′ (δ_H 1.14, s) and H_3-3′ (δ_H 1.13, s)(Figure 13b). Therefore, compound **6a** was identified as 2-(2-hydroxypropan-2-yl)-2,3-dihydro-1-benzofuran-5-carboxylic acid. A literature search revealed that compound **6a** has the same flat structure as anodendroic acid (2-(1-hydroxy-1-methylethyl)-2,3-dihydrobenzofuran-5-carboxylic acid), which was first isolated from the stem of *Anodendron affine* Durce [15]. Anodendroic acid was later synthesized by Yamaguchi et al. [16]; however, its ^{1}H NMR data (DMSO-d_6) were slightly different from those reported by Shima et al. [15]. Anodendroic acid was also obtained by basic hydrolysis of its methyl ester, a constituent of *Eriodictyon sessilifolium* [17], and also by biotransformation of 3-(γ,γ-dimethylallyl)-*p*-coumaric acid [18]. It is interesting to note that, in all of these reports, the identity of anodendroic acid was achieved by comparing its melting point, ^{1}H NMR and MS data with those reported by Shima et al. [15], while no stereochemistry of C-2 was indicated. However, when compared to the ^{1}H NMR and other physical data of compound **6a** with those reported for anodendroic acid by Shima et al. [15], it was found that the ^{1}H NMR data of anodendroic acid (in pyridine-d_6) [15] were slightly different from those of compound **6a** (in DMSO-d_6). Therefore, it was not possible to compare these ^{1}H NMR data, since they were obtained in different solvents. Interestingly, the ^{1}H NMR data, obtained in DMSO-d_6 by Yamaguchi et al. [16], were also slightly different from those of compound **6a**. The obvious differences between anodendroic acid [15] and compound **6a** are their melting points and optical rotations. While anodendroic acid (mp. 212–214 °C) is laevorotatory ($[\alpha]_D^{26}$ −19°, *c* 0.7, EtOH) [15], compound **6a** (mp. 149–150 °C) is dextrorotatory ($[\alpha]_D^{20}$ +74°, *c* 0.03, MeOH). Consequently, we concluded that the structure of compound **6a** is different from that of anodendroic acid. This fact has prompted us to investigate the stereochemistry of compound **6a**. Since Compound **6a** was obtained as a suitable crystal for X-ray diffraction, its X-ray analysis was carried out. The ORTEP view of compound **6a** shown in Figure 14 not only confirmed its proposed structure, but also revealed the absolute configuration for C-2 as 2*R*. Therefore, compound **6a** is a new compound, and we have named it quadricinctafuran A. Since anodendroic acid exhibited the opposite sign of rotation to that of compound **6a**, it is probable that the absolute configuration of its C-2 is 2*S*. This is not unusual, since fomannoxin, another 2,3-dihydrobenzofuran derivative, also showed the opposite optical rotation and has the opposite absolute configuration to tremetone, even though they have very similar structures [16].

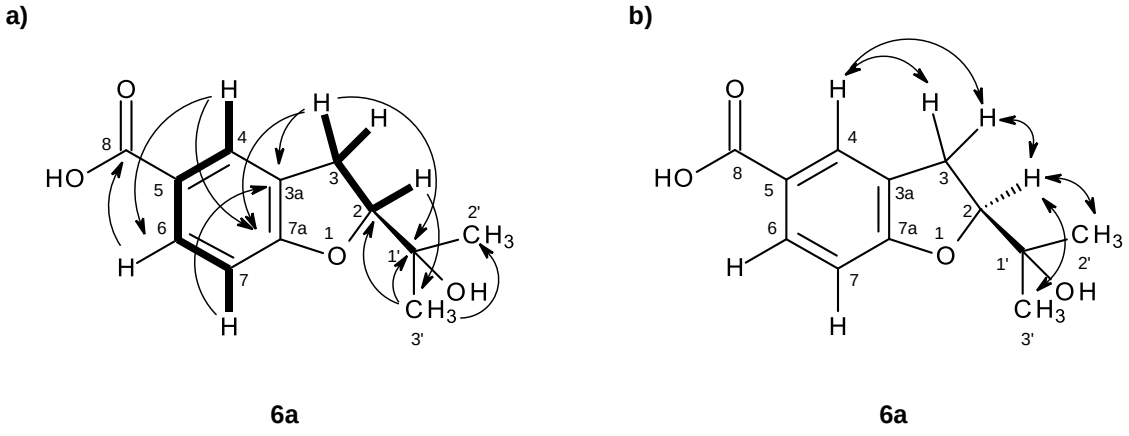

Figure 13. Key COSY (–), HMBC (→) (**a**) and NOESY (↔) (**b**) correlations for compound **6a**.

Table 6. ^{1}H and ^{13}C NMR (DMSO, 300.13 MHz and 75.4 MHz) and HMBC assignment for **6a** and **6b**.

Position	6a				6b			
	δ_C, type	δ_H, (*J* in Hz)	COSY	HMBC	δ_C, type	δ_H, (*J* in Hz)	COSY	HMBC
2	90.2, CH	4.64, t (8.9)	H-3	C-1′, 2′, 3′	86.5, CH	4.83, dd (9.7, 8.1)	H-3	
3	29.3, CH_2	3.17, d (8.9)	H-2	C-1′, 2, 3a, 7a	28.7, CH_2	3.19, m	H-2	C-1′, 3a
3a	128.2, C	-			128.4, C	-		
4	126.4, CH	7.75, d (1.8)	H-6	C-6, 7a, 8	126.4, CH	7.76, d (1.8)	H-6	C-3, 6, 7a
5	122.6, C	-			122.6, C	-		
6	130.4, CH	7.72, dd (8.3, 1.8)	H-4, 7	C-4, 7a, 8	130.8, CH	7.71, dd (8.3, 1.8)	H-4, 7	C-4, 7a, 8
7	108.4, CH	6.80, d (8.3)	H-6	C-3a, 5, 7a	108.4, CH	6.79, d (8.3)	H-6	C-3a, 5, 7a
7a	163.7, C	-			163.6, C	-		
8	167.2, C	-			167.2, C	-		
1′	70.0, C	-			72.5, C	-		
2′	24.9, CH_3	1.14, s	-	C-1′, 2, 3′	66.7, CH_2	3.33, s	-	C-1′, 2, 3′
3′	25.9, CH_3	1.13, s	-	C-1′, 2, 2′	20.0, CH_3	1.09, s		C-1′, 2, 2′
OH-8	-	12.49, br	-		-	12.47, br	-	

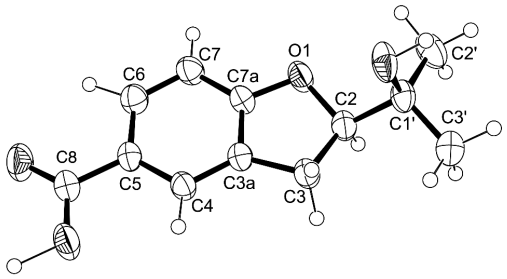

Figure 14. ORTEP diagram of **6a**.

The (+)-HRESIMS of compound **6b** gave the $[M + H]^+$ at *m/z* 239.0919 (calculated 239.0919), indicating its molecular formula $C_{12}H_{14}O_5$ and, therefore, six degrees of unsaturation. The general features of its ^1H and ^{13}C NMR spectra resembled those of compound **6a**. The ^{13}C NMR, DEPT and HSQC spectra (Table 6, Supplementary Information, Figures S42 and S44) exhibited the signals of one conjugated carboxyl carbonyl (δ_C 167.2), two quaternary sp^2 (δ_C 128.4, 122.6), one oxy-quaternary sp^2 (δ_C 163.6), three methine sp^2 (δ_C 130.8, 126.4, 108.4), one oxy-quaternary sp^3 (δ_C 72.5), one oxymethine sp^3 (δ_C 86.5), one methylene sp^2 (δ_C 28.7), one oxymethylene sp^2 (δ_C 66.7) and one methyl (δ_C 20.0) carbons. The ^1H NMR and COSY spectra (Table 6, Supplementary Information, Figures S41 and S43) showed similar proton signals of the 2,3-dihydro-1-benzofuran-5-carboxylic acid nucleus to those of **6a**. However, it exhibited only one methyl singlet at δ_H 1.09 and another singlet of oxymethylene protons at δ_H 3.33, instead of two methyl singlets as in compound **6a**. Therefore, the difference between the structures of compounds **6a** and **6b** resides in the substitutions on C-2. That the substituent on C-2 of compound **6b** was 1,2-dihydroxypropyl was evidenced by not only its molecular formula ($C_{12}H_{14}O_5$), which has one more oxygen atom than that of compound **6a** ($C_{12}H_{14}O_4$), but also the presence of the oxymethylene carbon at δ_C 66.7 (C-2′; δ_H 3.33, s). Moreover, the chemical shift value of C-2 (δ_C 86.5) was nearly 4 ppm lower than that of compound **6a** (δ_C 90.2). Thus, compound **6b** was identified as 2-(1,2-dihydroxypropan-2-yl)-2,3-dihydro-1-benzofuran-5-carboxylic acid. This was confirmed by the HMBC correlations of H_3-3′ (δ_H 1.09) to C-1′ (δ_C 72.5) and C-2′ (δ_C 66.7), as well of H_2-2′ (δ_H 3.33, s) to C-1′ (δ_C 72.5) and C-3′ (δ_C 20.0) (Figure 15, Supplementary Information, Figure S45). Since compound **6b** could not be obtained as suitable crystals for X-ray crystallography, it was not possible to determine the absolute configuration of C-2 by X-ray analysis. Moreover, as compound **6b** also has a tertiary hydroxyl group on C-1′ and a primary hydroxyl group on C-2′, it was not possible to determine the absolute configurations of C-2 and C-1′ by Mosher's method. On the other hand, since the methyl group on C-1 in compound **6a** was replaced by the hydroxymethyl group incompound **6b**, it is legitimate to postulate that compounds **6b** is derived from compound **6a**. Consequently, the absolute configuration of C-2 of compound **6b** should be the same as that of compound **6a**, i.e., 2*R*. However, it is not yet possible to determine the absolute configuration of C-1′. Compound **6b** is also a new compound, and we have named it quadricinctafuran B.

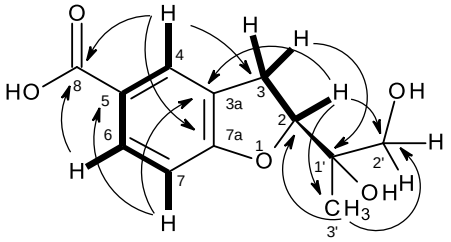

6b

Figure 15. Key COSY (–) and HMBC (→) correlations for compound **6b**.

Compound **7** was also isolated as white crystals (mp. 196–197 °C), and its molecular formula $C_{14}H_{12}O_5$ was established on the basis of the (+)-HRESIMS *m/z* 237.0792 $[M + H]^+$ (calculated 237.0763), indicating seven degrees of unsaturation. The IR spectrum showed absorption bands for hydroxyl (3404 cm^{-1}), conjugated ketone carbonyl (1708 cm^{-1}), conjugated carboxyl carbonyl (1670 cm^{-1}) and aromatic (1558, 1540 cm^{-1}) groups. The ^{13}C NMR, DEPT and HSQC spectra (Table 7, Supplementary Information, Figures S48 and S50) exhibited the signals of one conjugated ketone carbonyl (δ_C 191.1), one conjugated carboxyl carbonyl (δ_C 166.4), one oxy-quaternary sp^2 (δ_C 162.9), two quaternary sp^2 (δ_C 123.0, 119.6), three methine sp^2 (δ_C 136.4, 127.5, 118.5), one oxy-quaternary sp^3 (δ_C 83.0), one oxymethylene sp^2 (δ_C 66.8), one methylene sp^2 (δ_C 43.4) and one methyl (δ_C 21.2) carbons. The ^1H NMR spectra (Table 7, Supplementary Information, Figure S47) exhibited, besides the signals of three aromatic protons of the 1,2,4-trisubstituted benzene ring at δ_H 8.26, d (*J* = 2.3 Hz), 8.04, dd (*J* = 8.7, 2.3 Hz), 7.07, d (*J* = 8.7 Hz), a methyl singlet at δ_H 1.30, two pairs of geminally-coupled methylene protons at δ_H 2.74, d (*J* = 16.7 Hz)/3.00, d (*J* = 16.7 Hz) and δ_H 3.49, dd (*J* = 11.6, 4.5 Hz)/3.59, dd (*J* = 11.6, 4.2 Hz); the latter showed COSY correlations with the broad triplet of the hydroxyl proton at δ_H 5.26 (Table 7, Figure 16a, Supplementary Information, Figure S49). As the HMBC spectrum exhibited correlations of the aromatic proton signal at δ_H 8.26, d (*J* = 2.3 Hz, H-5) to the oxy-quaternary sp^2 carbon at δ_C 162.9 (C-8a), as well as to the conjugated ketone carbonyl carbon at δ_C 191.1 (C-4) and the methine sp^2 at δ_C 136.4 (C-7) (Table 7, Figure 16a, Supplementary Information, Figure S51), the ketone moiety was placed on C-4a. Additionally, the HMBC spectrum also showed correlations of H-8 (δ_H 7.07, d, *J* = 8.7 Hz) to C-8a and the quaternary sp^2 carbons at δ_C 123.0 and 119.6; they were therefore assigned to C-4a and C-6, respectively (Table 7, Figure 16a). The presence of the 1-hydroxy-2-methyl-2-oxypropyl moiety was supported by the HMBC correlations of the methyl singlet at δ_H 1.30 (CH_3-9) to the oxy-quaternary sp^3 carbon at δ_C 83.0 (C-2), the oxymethylene sp^3 carbon at δ_C 66.8 (C-10) and the methylene sp^3 carbon at δ_C 43.4 (C-3), as well as of the H_2-3 (δ_H 2.74, d, *J* = 16.7 Hz/3.00, d, *J* = 16.7 Hz) to C-2, C-9 (δ_C 21.2) and C-10 (Table 7, Figure 16a). Since H_2-3 also gave a HMBC cross-peak to C-4, the 1-hydroxy-2-methyl-2-oxypropyl moiety was linked to C-4. Due to the fact that these two moieties accounted for only $C_{11}H_{12}O_4$, it was concluded that the carboxyl group (δ_C 166.4, δ_H 12.69 br) was on C-6. Therefore, compound **7** was identified as 2-(hydroxymethyl)-2-methyl-4-oxo-3,4-dihydro-2*H*-chromene-6-carboxylic acid. As compound **7** was obtained as a suitable crystal for an X-ray diffraction, its X-ray analysis was carried out. The ORTEP view of compound **7**, shown in Figure 17, revealed the absolute configuration for C-2 as 2*S*. A literature search revealed that compound **7** is also a new compound, so we named it quadricinctone D.

Table 7. ^1H and ^{13}C NMR ($CDCl_3$, 300.13 MHz and 75.47 MHz) and HMBC assignment for **7**.

Position	δ_C, Type	δ_H, (*J* in Hz)	COSY	HMBC	NOESY
2	80.3, C	-			
3α	434, CH_2	2.74, d (16.7)	H-3	C-2, 4, 10, 11	H_3-11 (str)
β		3.00, d (16.7)	H-3	C-2, 4, 10, 11	H_3-11 (w)
4	191.1, CO	-			
4a	123.0, C	-			
5	127.5, CH	8.26, d (2.3)	H-7	C-4, 7, 8a	
6	119.6, C	-			
7	136.4, CH	8.04, dd (8.7, 2.3)	H-5, 8	C-5, 8a	
8	118.5, CH	7.07, d (8.7)	H-7	C-4a, 6, 8	
8a	162.9, C	-			
9	21.2, CH_3	1.30, s	-	C-2, 3, 10	H-3α (str), H3β (w), H-5, 8 (w)
10	66.8, CH_2	3.49, dd (11.6, 4.5)	OH-10		
		3.59, dd (11.6, 4.2)			
11	166.4, CO	-			
OH-10	-	5.26, brt (5.4)	-		
OH-11	-	12.69, br	-		

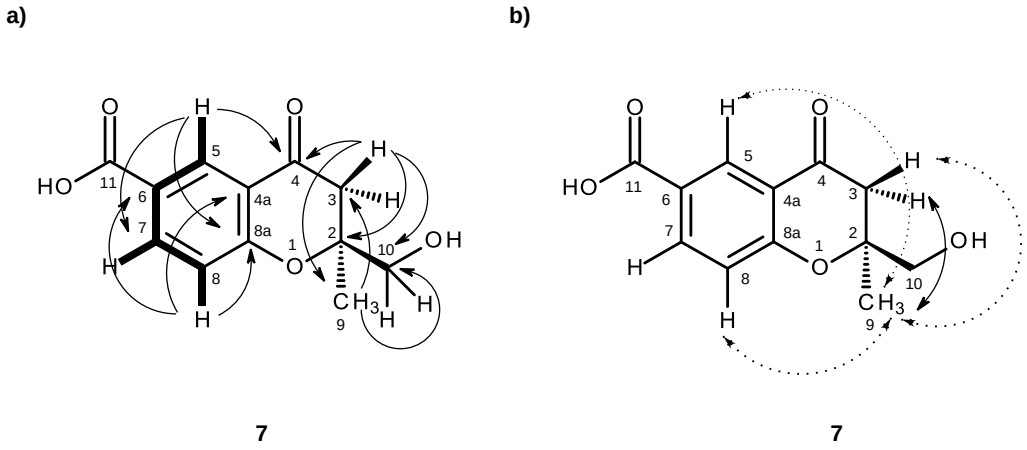

Figure 16. Key COSY (–), HMBC (→) (**a**) and NOESY C-2 (↔) (**b**) C-2 for compound **7**.

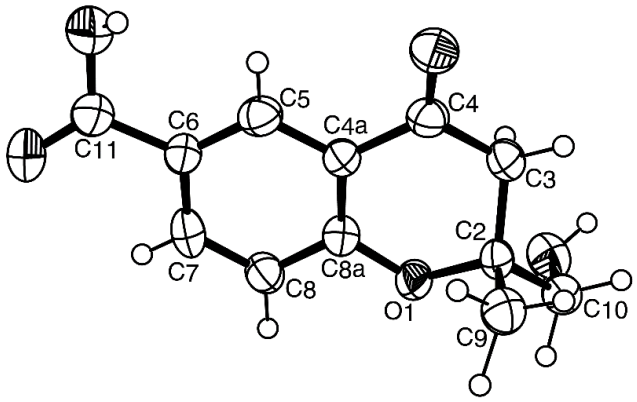

Figure 17. ORTEP diagram of compound **7**.

In order to establish the conformation of the 2,3-dihydro-*4H*-pyran-4-one, analysis of the NOESY correlations was carried out. The NOESY spectrum (Table 7, Figure 16b, Supplementary Information, Figure S52) exhibited not only a strong correlation of H-7 to H-8, but also week correlations of H_3-9 to H-5 and H-8. Therefore, CH_3-9 is in the α-axial position. Additionally, since H_3-9 also exhibited a strong cross-peak with the signal of the methylene proton at δ_H 2.74, d (J = 16.7 Hz), and a weak cross-peak with the proton signal at δ_H 3.00, d (J = 16.7 Hz), the former was assigned to H-3α and the latter to H-3β. It is interesting to observe that the structure of compound **7** is analogous to the structure of compound **3** in that it also exhibits the same methyl-methylene bridge structural feature (at C-9 and C-3), with the same relative intensity of NOESY cross-peaks between the protons of the two groups and with similar conformational energies for the two half-chair conformations of the non-aromatic ring. Therefore, the conclusions drawn for compound **3** are also valid for compound **7**, whose stereochemistry is unequivocally defined by X-ray analysis.

Compounds **1** and **5** can be hypothesized as originating from the pentaketide intermediate (I). Methylation (by SAM) gives II, which undergoes cyclization and enolization to give the intermediate III. Methylation of the phenolic hydroxyl groups and the α-carbon of the carbonyl ketone leads to the intermediate IV. Enolization, followed by a lactonization, originates V, which undergoes hydration to give VI, and oxidation of one of the methyl groups gives rise to compound **5**. Alternatively, oxidation of the α-carbon of the side chain of IV leads to the intermediate VII, which, after lactonization and reduction of the ketone carbonyl, gives rise to compound **1** (Figure 18).

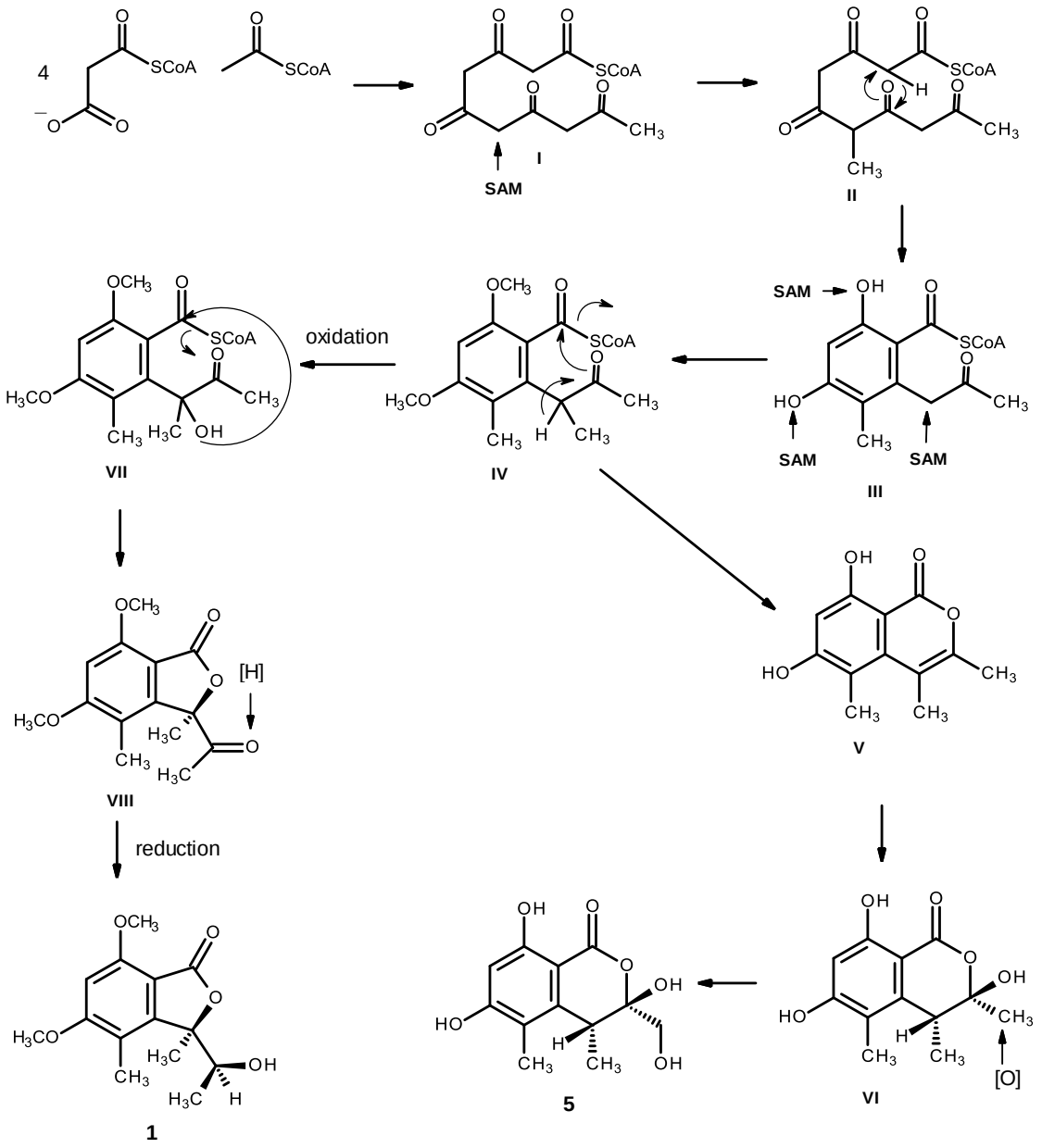

Figure 18. Proposed biosynthetic pathways for compounds **1** and **5**.

Biosynthetically, compounds **2a**, **2b**, **4a**, **4b**, **6a**, **6b** and **7** are of mixed origin, i.e., shikimic acid and mevalonic acid pathways, similar to that proposed for fomannoxin [19], as depicted in Figure 19. Elimination of pyruvate from chorismate (IX) by chorismate pyruvate lyase leads to the formation of *p*-hydroxybenzoic acid (X), which after prenylation by DMAPP (XI), originates the intermediate XII. Epoxidation and cyclization of XII, via Route *a*, leads to a formation of the furan ring in compound **6a** and after oxidation of one of the methyl groups leads to compound **6b**. On the other hand, cyclization via Route *b* leads to the formation of the pyran ring in XIV. Dehydration and oxidation of one of the methyl groups originates compound **2a**, which after acetylation of the primary alcohol function of the side chain will originate compound **2b**. Alternatively, the intermediate XIV can also undergo dehydration, reduction and oxidation to give the ketone function in compound **7**. Oxidative decarboxylation of compound **7** leads to the formation of compound **4a**, which after sulfinylation of the benzene ring originates compound **4b**. However, it is possible that the introduction of the methyl sulfoxide group to the aromatic ring could happen before cyclization.

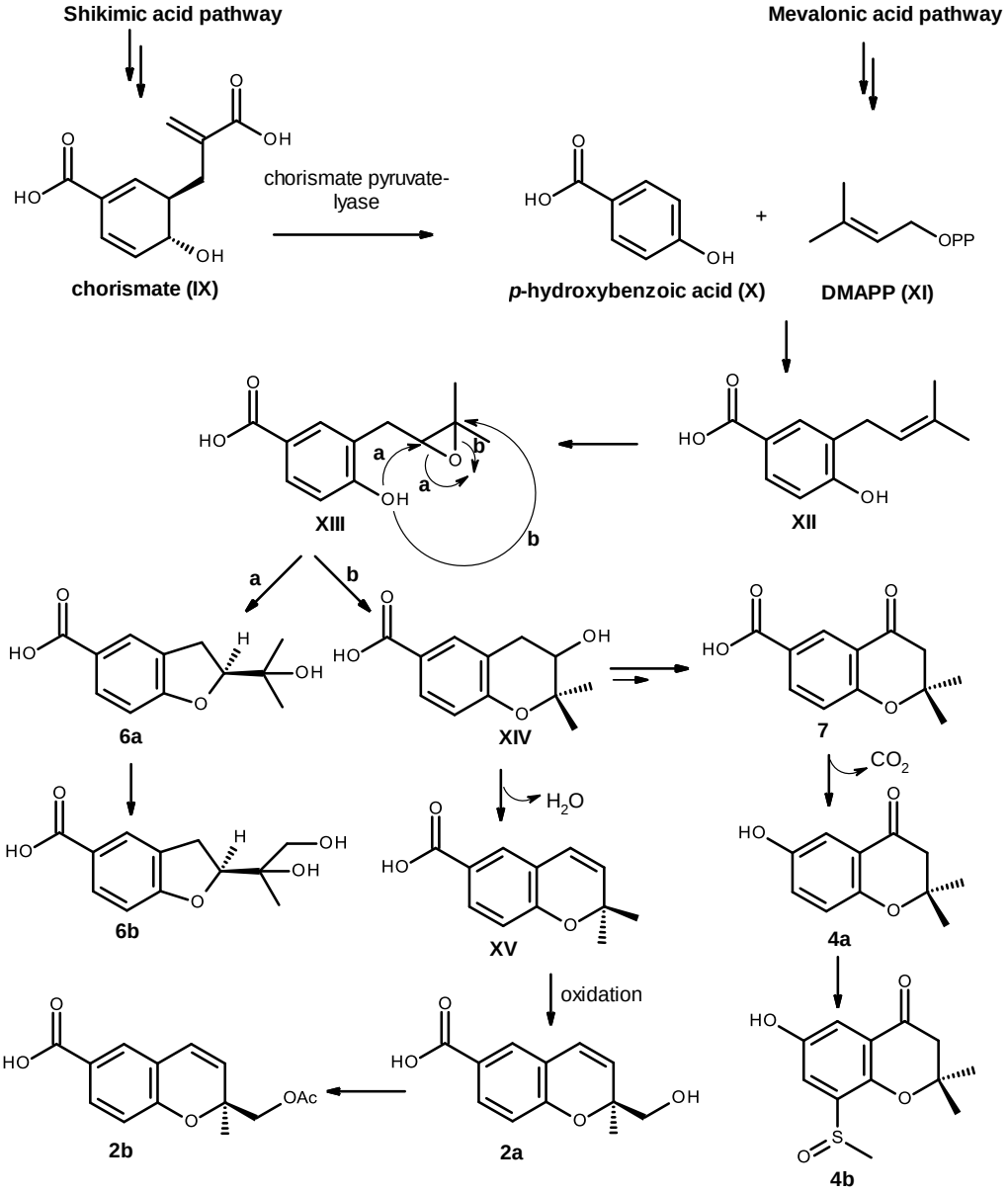

Figure 19. Proposed biosynthetic pathway for compounds **2a**, **2b**, **4a**, **4b**, **6a**, **6b** and **7**.

Compound **3** is also derived from a prenylation of *p*-hydroxybenzoic acid (X); however, it can occur with IPP (XVI) instead of DMAPP (XI). Epoxidation of the double bond of the side chain of XVII, followed by cyclization of XVIII leads to the formation of an oxepin ring in XIX. Oxidation and dehydration of the oxepin ring will lead to the formation of compound **3**, as depicted in Figure 20.

Compounds **1**–**7** were evaluated for their antibacterial activity against Gram-positive and Gram-negative bacteria, as well as multidrug-resistant isolates from the environment, according to the previously described protocol [6], as well as for their antifungal activity against yeast (*Candida albicans* ATCC 10231), filamentous fungus (*Aspergillus fumigatus* ATCC 46645) and dermatophyte (*Trichophyton rubrum* FF5) in the antifungal assay [20]. The results showed that none of the tested compounds exhibited significant antibacterial activity (MIC > 256 μg/mL) or antifungal activity (MIC > 512 μg/mL). These compounds were also evaluated for their in vitro growth inhibitory activity against the MCF-7 (breast adenocarcinoma), NCI-H460 (non-small cell lung cancer) and A375-C5 (melanoma) cell lines by the protein binding dye SRB method [21], and they did not show any activity in this assay (GI_{50} > 150 mM).

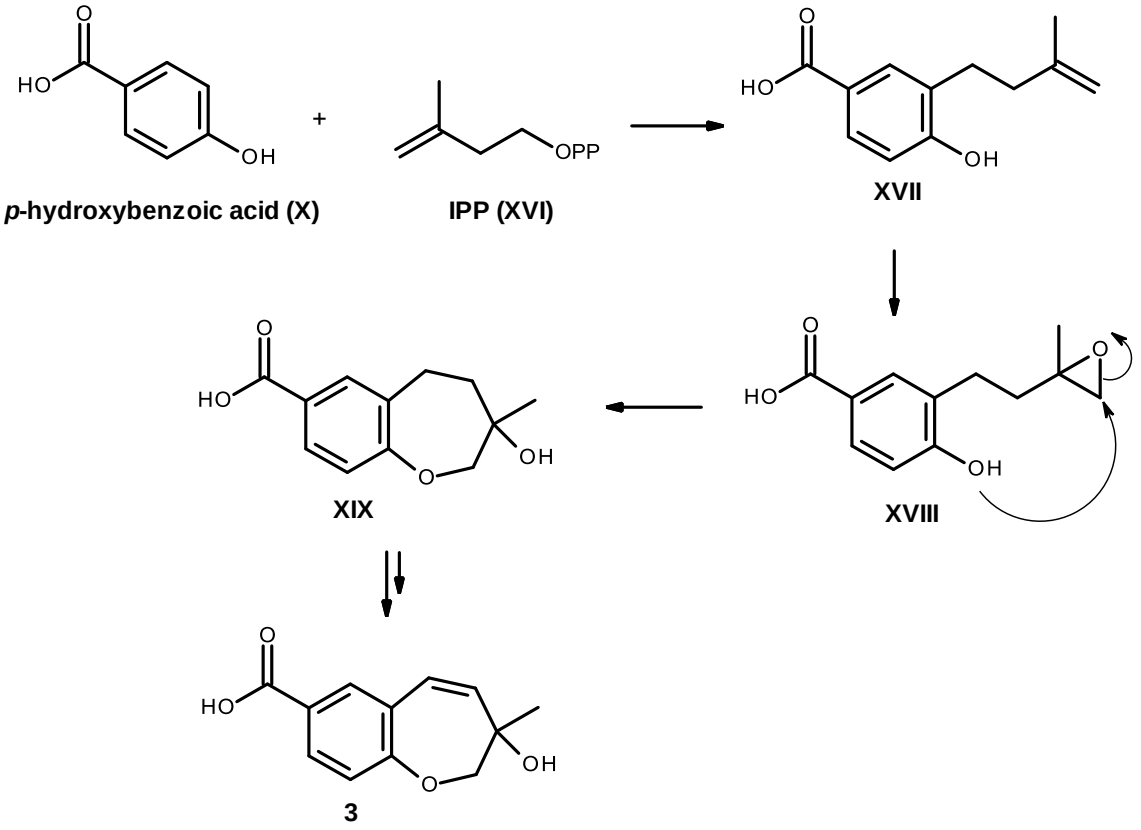

Figure 20. Proposed biosynthetic pathway for compound **3**.

3. Experimental Section

3.1. General Procedure

Melting points were determined on a Bock monoscope and are uncorrected. Optical rotations were measured on an ADP410 Polarimeter (Bellingham + Stanley Ltd., Tunbridge Wells, Kent, U.K.). Infrared spectra were recorded in a KBr microplate in a FTIR spectrometer Nicolet iS10 from Thermo Scientific (Waltham, MA, USA) with the Smart OMNI-Transmission accessory (Software 188 OMNIC 8.3). UV spectra were taken in $CHCl_3$ and were recorded on a Varian CARY 100 spectrophotometer. ^{1}H and ^{13}C NMR spectra were recorded at ambient temperature on a Bruker AMC instrument (Bruker Biosciences Corporation, Billerica, MA, USA) operating at 300.13 and 75.4 MHz, respectively. High resolution mass spectra were measured with a Waters Xevo QToF mass spectrometer (Waters Corporations, Milford, MA, USA) coupled to a Waters Acquity UPLC system. A Merck (Darmstadt, Germany) silica gel GF_{254} was used for preparative TLC, and a Merck Si gel 60 (0.2–0.5 mm) was used for column chromatography.

3.2. Extraction and Isolation

The strain KUFA 0081 was isolated from the marine sponge *Clathria reinwardti*, which was collected, by scuba diving at a depth of 15–20 m, from the coral reef at Samae San Island (12°34′ 36.64″ N 100°56′ 59.69″ E) in the Gulf of Thailand, Chonburi Province, in July 2013. The sponge was washed with 0.06% sodium hypochlorite solution for 1 min, followed by sterilized seawater 3 times and then dried on sterile filter paper, cut into small pieces (5 × 5 mm) and placed on a malt extract agar (MEA) medium containing 70% seawater and 300 mg/L of streptomycin sulphate, then incubated at 28 °C for 7 days, after which the hyphal tips were transferred onto a slant MEA and maintained as pure culture for further identification. The fungus was identified as *Neosartorya quadricincta* (E. Yuill)

Malloch & Cain by one of us (T.D.), based on morphological characteristics, such as colony growth rate and growth pattern on standard media, namely Czapek's agar, Czapek yeast autolysate agar and malt extract agar. Microscopic characteristics, including size, shape and the ornamentation of ascospores, were examined under light and scanning electron microscopes. This identification was supported by sequence analysis of the β-tubulin, calmodulin and actin genes as described in the previous report [22]. *Neosartorya quadricincta* was also confirmed by the analysis sequence of the internal transcribed spacer (ITS) gene according the procedure previously described by us [7]. Its gene sequences were deposited in GenBank with Accession Numbers KM095492 and KT201525, respectively. The pure cultures were deposited as KUFA0081 at Kasetsart University Fungal Collection, Department of Plant Pathology, Faculty of Agriculture, Kasetsart University, Bangkok, Thailand.

The fungus was cultured for one week at 28 °C in 10 Petri dishes (i.d. 90 mm) containing 25 mL of MEA. In order to obtain the mycelial suspension, the mycelial plugs were transferred to two 500-mL Erlenmeyer flasks containing 200 mL of potato dextrose broth and then incubated on a rotary shaker at 120 rpm at 28 °C for 4 days. Fifty 1000-mL Erlenmeyer flasks, each containing 300 g of cooked rice, were autoclaved at 121 °C for 15 min, then inoculated with 20 mL of mycelial suspension of *N. quadricincta* and incubated at 28 °C for 30 days, after which the mouldy rice was macerated in ethyl acetate (25 L total) for 7 days and then filtered. The ethyl acetate solution was concentrated under reduced pressure to yield 176.5 g of crude ethyl acetate extract, which was dissolved in 500 mL of $CHCl_3$ and then washed with H_2O (3 × 500 mL). The organic layers were combined and dried with anhydrous Na_2SO_4, filtered and evaporated under reduced pressure to give 31.1 g of the crude chloroform extract, which was applied on a column of silica gel (440 g) and eluted with mixtures of petrol-$CHCl_3$ and $CHCl_3$-Me_2CO; 250-mL fractions were collected as follows: Frs 1–15 (petrol-$CHCl_3$, 1:1), 16–55 (petrol-$CHCl_3$, 3:7), 56–118 (petrol-$CHCl_3$, 1:9), 119–284 ($CHCl_3$-Me_2CO, 9:1), 285–329 ($CHCl_3$-Me_2CO, 7:1), 330–359 ($CHCl_3$-Me_2CO, 1:1). Frs 175–181 were combined (250 mg) and purified by TLC (silica gel G254, $CHCl_3$-Me_2CO-HCO_2H, 3:2:0.01) to give 86.8 mg of **1** and 15.0 mg of **2b**. Frs 182–197 were combined (565.1 mg) and purified by TLC (silica gel G254, $CHCl_3$-Me_2CO-HCO_2H, 17:3:0.02) to give 35.1 mg of **1** and 14.3 mg of **2b**. Frs 224–235 were combined (249.3 mg) and purified by TLC (silica gel G254, $CHCl_3$-Me_2CO-HCO_2H, 4:1:0.01) to give 11.4 mg of **4a** [12]. Frs 236–285 were combined (1.2 g), applied over a column chromatography of silica gel (42 g) and eluted with mixtures of petrol-$CHCl_3$ and $CHCl_3$-Me_2CO, wherein 100-mL subfractions were collected as follows: sfrs 1–17 (petrol-$CHCl_3$, 1:9), 18–61 ($CHCl_3$-Me_2CO,9:1). Sfrs 24–33 were combined (423.4 mg) and precipitated in a mixture of $CHCl_3$ and Me_2CO to give a white solid (46.2 mg), which was further recrystallized in a mixture of $CHCl_3$ and Me_2CO to give 9.4 mg of white crystals of **6a**, and the mother liquor was purified by TLC (silica gel G254, $CHCl_3$-Me_2CO-HCO_2H, 9:1:0.01) to give 23.2 mg of **6a** and 4.9 mg of **2a**. The mother liquor of sfrs 24–33 (133.0 mg) was purified by TLC (silica gel G254, $CHCl_3$-Me_2CO-HCO_2H, 7: 3:0.01) to give 41.1 mg of **2a** and 12.4 mg of **3**. Sfrs 34–39 were combined (77.7 mg) and purified with TLC (silica gel G254, $CHCl_3$-Me_2CO-HCO_2H, 3: 1:0.01) to give 7.9 mg of **4b** and 17.1 mg of **2a**. Sfrs 40–61 were combined (496.4 mg) and purified by TLC (silica gel G254, $CHCl_3$-Me_2CO-HCO_2H, 4: 1:0.01) to give 22.7 mg of **5**. Frs 307–315 were combined (291.0 mg), applied over a column chromatography of Sephadex LH-20 (10 g) and eluted with a 1:1 mixture of $CHCl_3$: MeOH to give twelve 1-mL sub-fractions. Sfrs 9–12 were combined and purified by TLC (silica gel G254, $CHCl_3$-Me_2CO-HCO_2H, 3: 2:0.01) to give 13.4 mg of **6b** and 9.4 mg of **7**. Frs 316–359 were combined (1.2 g), applied over a column chromatography of Sephadex LH-20 (10 g) and eluted with a 1:1 mixture of $CHCl_3$: MeOH to give twenty-one 1-mL sub-fractions. Sfrs 12–21 were combined (645.7 mg), applied over a column chromatography of Sephadex LH-20 (10 g) and eluted with a 1:1 mixture of $CHCl_3$: MeOH to give sixteen 1-mL fractions. Ssfrs 5–16 were combined (597.5), applied over a column chromatography of silica gel (15 g) and eluted with a mixture of petrol-$CHCl_3$ and $CHCl_3$-Me_2CO, wherein 100-mL fractions were collected as follows: frs 1–8 (petrol-$CHCl_3$, 1:9), 9–28 ($CHCl_3$-Me_2CO, 9:1), 29–41 (($CHCl_3$-Me_2CO, 7:3). Frs 17–18 were combined (47.4 mg) and purified by TLC (silica gel G254, $CHCl_3$-Me_2CO-HCO_2H, 3: 2:0.01) to give 20.8 mg of **6b**.

3.2.1. Quadricinctone A: 3-(1-Hydroxyethyl)-5,7-dimethoxy-3,4-dimethyl-2-benzofuran-1(3*H*)-one (**1**)

White crystals; mp 176–177 °C (petrol/$CHCl_3$); $[\alpha]_D^{20}$ −59° (*c* 0.05, $CHCl_3$); UV (MeOH) λ_{max} (log ε) 233 (4.39), 260 (4.03), 298 (3.78) nm; IR (KBr) υ_{max} 3455, 2981, 2490, 1723, 1612, 1596, 1499, 1467, 1432, 1228 cm^{-1}; ^1H and ^{13}C NMR, see Table 1; HRESIMS *m/z* 267.1243 $[M + H]^+$ (calculated for $C_{14}H_{19}O_5$, 267.1332).

3.2.2. Quadricinctapyran A: 2-(Hydroxymethyl)-2-methyl-2*H*-chromene-6-carboxylic acid (**2a**)

White crystals; mp 147–148 °C ($CHCl_3$/Me_2CO); $[\alpha]_D^{20}$ +30° (*c* 0.03, MeOH); UV (MeOH) λ_{max} (log ε) 237 (4.61) nm; IR (KBr) υ_{max} 3447, 2922, 2359, 2341, 1696, 1647, 1609, 1578, 1490, 143, 1301, 1267 cm^{-1}; ^1H and ^{13}C NMR, see Table 2; HRESIMS *m/z* 221.0820 $[M + H]^+$ (calculated for $C_{12}H_{13}O_4$, 221.0814).

3.2.3. Quadricinctapyran B: 2-[(Acetyloxy)methyl]-2-methyl-2*H*-chromene-6-carboxylic acid (**2b**).

White solid; mp 118–119 °C (petrol/$CHCl_3$); $[\alpha]_D^{20}$ +58° (*c* 0.07, $CHCl_3$); UV (MeOH) λ_{max} (log ε) 201 (4.13), 237 (4.47) nm; IR (KBr) υ_{max} 3441, 2986, 2943, 1745, 1678, 1640, 1607, 1574, 1453, 1419, 1297, 1264, 1228 cm^{-1}; ^1H and ^{13}C NMR, see Table 2; HRESIMS *m/z* 263.0971 $[M + H]^+$ (calculated for $C_{14}H_{15}O_5$, 263.0919).

3.2.4. Quadricinctoxepine: 3-Hydroxy-3-methyl-2,3-dihydro-1-benzoxepine-7-carboxylic acid (**3**)

White solid; mp 189–191 °C ($CHCl_3$/Me_2CO); $[\alpha]_D^{20}$ +21° (*c* 0.07, MeOH); UV (MeOH) λ_{max} (log ε) 234 (4.50) nm; IR (KBr) υ_{max} 3404, 2921, 2359, 2342, 1701, 1606, 1574, 1497, 1384, 1297, 1259, 1117 cm^{-1}; ^1H and ^{13}C NMR, see Table 3; HRESIMS *m/z* 221.0819 $[M + H]^+$ (calculated for $C_{12}H_{13}O_4$, 221.0814).

3.2.5. Quadricinctone B: 6-Hydroxy-2,2-dimethyl-8-(methylsulfinyl)-2,3-dihydro-4*H*-chromen-4-one (**4b**)

White crystals; mp 227–228 °C ($CHCl_3$/Me_2CO); $[\alpha]_D^{20}$ +30° (*c* 0.03, MeOH); UV (MeOH) λ_{max} (log ε) 205 (4.27), 234 (4.22), 358 (3.64) nm; IR (KBr) υ_{max} 3442, 2975, 2922, 1690, 1622, 1484, 1441, 1417, 1326, 1251, 1177 cm^{-1}; ^1H and ^{13}C NMR, see Table 4; HRESIMS *m/z* 255.0694 $[M + H]^+$ (calculated for $C_{12}H_{15}O_4S$, 255.0691).

3.2.6. Quadricinctone C: 3,6,8-Trihydroxy-3-(hydroxymethyl)-4,5-dimethyl-3,4-dihydro-1*H*-isochromen-1-one (**5**)

White crystals; mp 223–224 °C ($CHCl_3$/Me_2CO); $[\alpha]_D^{20}$ +64° (*c* 0.06, MeOH); UV (MeOH) λ_{max} (log ε) 214 (4.23), 271 (3.96), 312 (3.70) nm; IR (KBr) υ_{max} 3439, 3006, 2976, 2360, 2342, 1660, 1644, 1600, 1494, 1472, 1448, 1385, 1157 cm^{-1}; ^1H and ^{13}C NMR, see Table 5; HRESIMS *m/z* 255.0875 $[M + H]^+$ (calculated for $C_{12}H_{15}O_6$, 255.0869).

3.2.7. Quadricinctafuran A: (2*R*)-(2-Hydroxypropan-2-yl)-2,3-dihydro-1-benzofuran-5-carboxylic acid (**6a**)

White crystals; mp 149–150 °C ($CHCl_3$/Me_2CO); $[\alpha]_D^{20}$ +74° (*c* 0.03, MeOH); UV (MeOH) λ_{max} (log ε) 203 (3.40), 254 (3.49) nm; IR (KBr) υ_{max} 3417, 2920, 1681, 1634, 1491, 1261 cm^{-1}; ^1H and ^{13}C NMR, see Table 6; HRESIMS *m/z* 223.9067$[M + H]^+$ (calculated for $C_{12}H_{15}O_4$, 223.0970).

3.2.8. Quadricinctafuran B: (2R)-2-(1,2-Hihydroxypropan-2-yl)-2,3-dihydro-1-benzofuran-5-carboxylic acid (**6b**)

White solid; mp 209–210 °C ($CHCl_3$/Me_2CO); $[\alpha]_D^{20}$ +20° (*c* 0.05, MeOH); UV (MeOH) λ_{max} (log ε) 205 (4.27), 261 (4.03) nm; IR (KBr) υ_{max} 3328, 2984, 2941, 1673, 1610, 1599, 1495, 1362, 1290, 1247 cm^{-1}; ^1H and ^{13}C NMR, see Table 6; HRESIMS *m/z* 239.0919$[M + H]^+$ (calculated for $C_{12}H_{15}O_5$, 239.0919).

3.2.9. Quadricinctone D: 7-Hydroxy-3-(hydroxymethyl)-3-methyl-3,4-dihydro-2-benzoxepine-1, 5-dione (**7**)

White crystals; mp 196–197 °C ($CHCl_3$/Me_2CO); $[\alpha]_D^{20}$ +19° (*c* 0.05, MeOH); UV (MeOH) λ_{max} (log ε) 232 (4.21), 254 (3.84) nm; IR (KBr) υ_{max} 3404, 2934, 2360, 2341, 1708, 1670, 1614, 1492,

1466, 1250 cm^{-1}; ^{1}H and ^{13}C NMR, see Table 7; HRESIMS *m/z* 237.0792 $[M + H]^+$ (calculated for $C_{12}H_{15}O_5$, 237.0763).

*3.3. X-Ray Crystal Structure of Compounds **1**, **2a**, **4b**, **5**, **6a** and **7***

Diffraction data were collected at 293 K with a Gemini PX Ultra equipped with CuK_α radiation (λ = 1.54184 Å). The structures were solved by direct methods using SHELXS-97 and refined with SHELXL-97 [23]. Carbon, oxygen and sulphur atoms were refined anisotropically. Hydrogen atoms were either placed at their idealized positions using appropriate HFIX instructions in SHELXL and included in subsequent refinement cycles or were directly found from difference Fourier maps and were refined freely with isotropic displacement parameters. Full details of the data collection and refinement and tables of atomic coordinates, bond lengths and angles and torsion angles have been deposited with the Cambridge Crystallographic Data Centre.

Quadricinctone A (**1**): Crystals were triclinic, space group P1, cell volume 663.27(7) $Å^3$ and unit cell dimensions *a* = 7.3973(5)Å, *b* =8.4830(6)Å and *c* = 11.2438(6) Å and angles α = 107.541(5)°, β = 92.005(5)° and γ = 98.365(6)° (uncertainties in parentheses). The refinement converged to *R* (all data) = 3.68% and wR_2 (all data) = 9.54%. The absolute structure was established with confidence (flack *x* parameter 0.028(18)). CCDC 1465376.

Quadricinctapyran A (**2a**): Crystals were orthorhombic, space group P*bcn*, cell volume 2189.45(9) $Å^3$ and unit cell dimensions *a* = 21.3981(5)Å, *b* = 14.5017(3)Å and *c* = 7.05561(18)Å. The refinement converged to *R* (all data) = 15.06% and wR_2 (all data) = 40.39%. CCDC 1468869.

Quadricinctone B (**4b**): Crystals were orthorhombic, space group I*ba2*, cell volume 2469.66(11) $Å^3$ and unit cell dimensions *a* = 8.52510(19)Å, *b* = 30.2340(7)Å and *c* = 9.5817(3)Å. The refinement converged to *R* (all data) = 5.90% and wR_2 (all data) = 15.62%. The absolute structure was established with confidence (flack *x* parameter −0.04(4)). CCDC 1468868.

Quadricinctone C (**5**): Crystals were monoclinic, space group $P2_1$, cell volume 1116.25(5) $Å^3$ and unit cell dimensions *a* = 12.1131(3)Å, *b* = 7.0501(2)Å and *c* = 13.2091(3)Å and β = 98.291(2)°. The refinement converged to *R* (all data) = 6.85% and wR_2 (all data) = 17.04%. CCDC 1468170.

Quadricinctafuran A (**6a**): Crystals were monoclinic, space group $P2_1/n$, cell volume 1066.67(10)$Å^3$ and unit cell dimensions *a* = 11.6064(7)Å, *b* = 5.9593(2)Å and *c* = 15.8588(8)Å and β = 103.481(6)°. The refinement converged to *R* (all data) = 11.08% and wR_2 (all data) = 24.01%. CCDC 1468171.

Quadricinctone D (**7**): Crystals were orthorhombic, space group $Pca2_1$, cell volume 1081.35(13) $Å^3$ and unit cell dimensions *a* = 19.5607(13)Å, *b* = 7.4646(5)Å and *c* = 7.4058(5)Å. The refinement converged to *R* (all data) = 3.81% and wR_2 (all data) = 8.57%. CCDC 1468166.

*3.4. Molecular Mechanics Conformation Analysis of **3** and **7***

Molecular simulations for Structures **3** and **7** were carried out in ChemBio3D Ultra 14 (Perkin-Elmer). Molecular mechanics energy minimizations used the MM2 and MMFF force fields with the ChemBio3D most recent default parameters and implementation, adequate for small to medium carbon-based models. Ab initio MP2/6-311G and semi-empirical PM3 molecular modelling was done using CS GAMESS interfaced by ChemBio3D. The conformational search was done by stochastic, dihedral driver and molecular dynamics methods. Around 60 conformations were stochastically created and then minimized using the PM3, MMFF and PM3 methods. The resulting models were then grouped under the resultant two seven-membered ring conformations (exemplified in Figure 8 for **3**). A minimal energy for each model set was found by driving by 360° the dihedral angles of the

single bonds that attach substituent groups to the rings. Molecular dynamics runs were also applied to the models to confirm the convergence to a minimal energy conformation for each model set.

4. Conclusions

Although Ozoe et al. had first reported the isolation of an isocoumarin derivative from the culture of the fungus *N. quadricincta* strain PF1223, using a GABA receptor ligand as a screening target, the source of the fungus was not revealed. Therefore, this is the first report on the secondary metabolites of the culture of a marine-derived *N. quadricincta* (KUFA 0081). Among the nine new isolated compounds, two are polyketide derivatives, and seven are benzoic acid derivatives. The isolation of these structurally-unique, but related, metabolites from this fungus has allowed us to propose the biosynthetic pathways leading to these metabolites. Interestingly, the unprecedented structure of quadricinctone B (**4b**), which possesses a methyl sulfinyl group in the benzopyran nucleus, reflects the capacity of this marine-derived strain to introduce sulphur into the aromatic ring. Therefore, this marine strain of *N. quadricincta* (KUFA 0081) can have potential for biotechnological transformation. Even though the isolated metabolites did not exhibit either antifungal/antibacterial activities or growth inhibitory activity against the three cancer cell lines in our assay protocols, it does not mean that they are devoid of other interesting biological activities. Therefore, it is necessary to investigate these metabolites in other target-based assay protocols.

Supplementary Materials: The supplementary materials are available online at www.mdpi.com/1660-3397/14/7/134/s1.

Acknowledgments: This work was developed in the Natural Products Research Laboratory of the Department of Chemistry, Instituto de Ciências Biomédicas Abel Salazar (ICBAS), of the University of Porto and partially supported through national funds provided by FCT-Foundation for Science and Technology and European Regional Development Fund (ERDF) and COMPETE, under the projects PEst-C/MAR/LA0015/2013, PTDC/MAR-BIO/4694/2014, as well as by the project INNOVMAR (Innovation and Sustainability in the Management and Exploitation of Marine Resources) (Reference NORTE-01-0145-FEDER-000035, within Research Line NOVELMAR/INSEAFOOD/ECOSERVICES), supported by the North Portugal Regional Operational Programme (NORTE 2020), under the PORTUGAL 2020 Partnership Agreement, through the European Regional Development Fund (ERDF). We thank Mrs. Júlia Bessa and Sara Cravo for technical support.

Author Contributions: A. Kijjoa and M. Pinto conceived, designed the experiments and wrote the paper; C. Prompanya performed isolation and purification of the compounds; T. Dethoup collected, isolated, identified and cultured the fungus; L. Gales performed X-ray analysis; J. Pereira performed molecular mechanics conformation analysis; A. Silva provided NMR spectra; M. Lee provided HRMS.

Conflicts of Interest: The authors declare no conflict of interest.

References

1. Hong, S.-B.; Shin, H.-D.; Hong, J.; Frisvad, J.C.; Nielsen, P.V.; Varga, J.; Samson, R.A. New taxa of *Neosartorya* and *Aspergillus* in *Aspergillus* section Fumigati. *Antonie Van Leeuwenhoek* **2008**, *93*, 87–98. [CrossRef] [PubMed]
2. Kijjoa, A.; Santos, S.; Dethoup, T.; Manoch, L.; Almeida, A.P.; Vasconcelos, M.H.; Silva, A.; Gales, L.; Herz, W. Sartoryglabrins, Analogs of the Ardeemins from *Neosartorya glabra*. *Nat. Prod. Commun.* **2011**, *6*, 807–812. [PubMed]
3. Eamvijarn, A.; Anake Kijjoa, A.; Bruyère, C.; Mathieu, V.; Manoch, L.; Lefranc, F.; Silva, A.; Kiss, R.; Herz, W. Secondary Metabolites from a Culture of the Fungus *Neosartorya pseudofischeri* and Their in Vitro Cytostatic Activity in Human Cancer Cells. *Planta Med.* **2012**, *28*, 167–176. [CrossRef] [PubMed]
4. Buttachon, S.; Chandrapatya, A.; Manoch, L.; Silva, A.; Gales, L.; Bruyére, C.; Kiss, R.; Kijjoa, A. Sartorymensin, a New Indole Alkaloid, and New Analogues of Tryptoquivaline and Fiscalins Produced by *Neosartorya siamensis* (KUFC 6349). *Tetrahedron* **2012**, *68*, 3253–3262. [CrossRef]
5. Eamvijarn, A.; Gomes, N.M.; Dethoup, T.; Buaruang, J.; Manoch, L.; Silva, A.; Pedro, M.; Marini, I.; Roussis, V.; Kijjoa, A. Bioactive Meroditerpenes and Indole Alkaloids from the Soil Fungus *Neosartorya fischeri* (KUFC 6344) and the Marine-derived Fungi *Neosartorya laciniosa* (KUFC 7896) and *Neosartorya tsunodae* (KUFC 9213). *Tetrahedron* **2013**, *69*, 8583–8591. [CrossRef]

6. Gomes, N.M.; Bessa, L.J.; Buttachon, S.; Costa, P.M.; Buaruang, J.; Dethoup, T.; Silva, A.M.S.; Kijjoa, A. Antibacterial and Antibiofilm Activity of Tryptoquivalines and Meroditerpenes from Marine-Deived Fungi *Neosartorya paulistensis*, *N. laciniosa*, *N. tsunodae*, and the soil fungi *N. fischeri* and *N. siamensis*. *Mar. Drugs* **2014**, *12*, 822–839. [CrossRef] [PubMed]
7. May Zin, W.W.; Buttachon, S.; Buaruang, J.; Gales, L.; Pereira, J.A.; Pinto, M.M.M.; Silva, A.M.S.; Kijjoa, A. A New Meroditerpene and a New Tryptoquivaline from the Algicolous Fungus *Neosartorya takakii* KUFC 7898. *Mar. Drugs* **2015**, *13*, 3776–3790. [CrossRef] [PubMed]
8. Prompanya, C.; Dethoup, T.; Bessa, L.J.; Pinto, M.M.M.; Gales, L.; Costa, P.M.; Silva, A.M.S.; Kijjoa, A. New Isocoumarin Derivatives and Meroterpenoids from the Marine Sponge-Associated Fungus *Aspergillus similanensis* sp. nov. KUFA 0013. *Mar. Drugs* **2014**, *12*, 5160–5173. [CrossRef] [PubMed]
9. Prompanya, C.; Fernandes, C.; Cravo, S.; Pinto, M.M.; Dethoup, T.; Silva, A.M.; Kijjoa, A. A New Cyclic Hexapeptide and a New Isocoumarin Derivative from the Marine Sponge-Associated Fungus *Aspergillus similanensis* KUFA 0013. *Mar. Drugs* **2015**, *13*, 1432–1450. [CrossRef] [PubMed]
10. Boonsang, N.; Dethoup, T.; Singburaudom, N.; Gomes, N.G.M.; Kijjoa, A. In Vitro Antifungal Activity Screening of Crude Extracts of Soil Fungi against Plant Pathogenic Fungi. *J. Biopest.* **2014**, *7*, 156–166.
11. Ozoe, Y.; Kuriyama, T.; Tachibana, Y.; Harimaya, K.; Takahashi, N.; Yaguchi, T.; Suzuki, E.; Imamura, K.; Oyama, K. Isocoumarin Derivative as a Novel GABA Receptor Ligand from *Neosartorya quadricincta*. *J. Pestic. Sci.* **2004**, *29*, 328–331. [CrossRef]
12. Lourenço, T.O.; Akisue, G.; Roque, N.F. Reduced Acetophenone Derivatives from *Calea cuneifolia*. *Phytochemistry* **1981**, *20*, 773–776. [CrossRef]
13. Fletcher, C.M.; Jones, D.N.M.; Diamond, R.; Neuhaus, D. Treatment of NOE constraints involving equivalent or nonstereoassigned protons in calculations of biomolecular structures. *J. Biomol. NMR* **1996**, *8*, 292–310. [CrossRef] [PubMed]
14. Butts, C.P.; Jones, C.R.; Towers, E.C.; Flynn, J.L.; Appleby, L.; Barron, N. Interproton distance determinations by NOE—Surprising accuracy and precision in a rigid organic molecule. *J. Org. Biomol. Chem.* **2011**, *9*, 177–184. [CrossRef] [PubMed]
15. Shima, K.; Hisada, S.; Inagaki, I. Studies on the constituents of *Anodendron affine* Durce. V. Isolation and structure of two new constituents. *Yakugaku Zasshi* **1972**, *92*, 1410–1414. [PubMed]
16. Yamaguchi, S.; Kondo, S.; Shimokawa, K.; Inoue, O.; Sannomiya, M.; Kawase, Y. The synthesis of racemic fomannoxin, anodendroic acid, and 5-acetyl-2-[1-(hydroxymethyl)vinyl]-2,3-dihydrobenzofuran. *Bull. Chem. Soc. Jpn.* **1982**, *55*, 2500–2503. [CrossRef]
17. Arriaga-Giner, F.J.; Wollenweber, E.; Schober, I.; Yatskievych, G. Three New Benzoic Acid Derivatives from the Glandular Excretion of *Eriodictyon sessilifolium* (Hydrophyllaceae). *Z. Naturforch.* **1988**, *43c*, 337–340.
18. Bisogno, F.; Mascoti, L.; Sanchez, C.; Garibotto, F.; Giannini, F.; Kurina-Sanz, M.; Enriz, R. Structure-antifungal activity relationship of cinnamic acid derivatives. *J. Agric. Food Chem.* **2007**, *55*, 10635–10640. [CrossRef] [PubMed]
19. Hansson, D.; Menkis, A.; Olson, Å.; Stenlid, J.; Broberg, A.; Karlsson, M. Biosynthesis of fomannoxin in the root rotting pathogen *Heterobasidion occidentale*. *Phytochemistry* **2012**, *84*, 31–39. [CrossRef] [PubMed]
20. Wattanadilok, R.; Sawangwong, P.; Rodrigues, C.; Cidade, H.; Pinto, M.; Pinto, E.; Silva, A.; Kijjoa, A. Antifungal activity evaluation of the constituents of *Haliclona baeri* and *H. cymaeformis*, collected from the Gulf of Thailand. *Mar. Drugs* **2007**, *5*, 40–51. [CrossRef] [PubMed]
21. Cidade, H.M.; Nascimento, M.S.J.; Pinto, M.M.M.; Kijjoa, A.; Silva, A.M.S.; Herz, W. Artelastocarpin and carpelastofuran, two new flavones, and cytotoxicities of prenyl flavonoids from *Artocarpus elasticus* against three cancer cell lines. *Planta Med.* **2001**, *67*, 867–870. [CrossRef] [PubMed]
22. Matsuzawa, T.; Horie, Y.; Abliz, P.; Gonoi, T.; Yaguchi, T. *Aspergillus huiyaniae* sp. nov., a new teleomorphic species in Aspergillus section *Fumigati* isolated from desert soil in China, and described using polyphasic approach. *Mycoscience* **2014**, *55*, 213–220. [CrossRef]
23. Sheldrick, G.M.A. A short history of SHELX. *Acta Cryst.* **2008**, *A64*, 112–122. [CrossRef] [PubMed]